frontiers | Research Topics

Genetic insights and diagnostic innovations in cerebrovascular and cerebrospinal fluid disorders

Edited by
Hao Yu, Haipeng Liu and Linfang Lan

Coordinated by
Ling Li

Published in
Frontiers in Neurology

ISSN 1664-8714
ISBN 978-2-8325-7101-9
DOI 10.3389/978-2-8325-7101-9

Generative AI statement
Any alternative text (Alt text) provided alongside figures in the articles in this ebook has been generated by Frontiers with the support of artificial intelligence and reasonable efforts have been made to ensure accuracy, including review by the authors wherever possible. If you identify any issues, please contact us.

About Frontiers

Frontiers is more than just an open access publisher of scholarly articles: it is a pioneering approach to the world of academia, radically improving the way scholarly research is managed. The grand vision of Frontiers is a world where all people have an equal opportunity to seek, share and generate knowledge. Frontiers provides immediate and permanent online open access to all its publications, but this alone is not enough to realize our grand goals.

Frontiers journal series

The Frontiers journal series is a multi-tier and interdisciplinary set of open-access, online journals, promising a paradigm shift from the current review, selection and dissemination processes in academic publishing. All Frontiers journals are driven by researchers for researchers; therefore, they constitute a service to the scholarly community. At the same time, the *Frontiers journal series* operates on a revolutionary invention, the tiered publishing system, initially addressing specific communities of scholars, and gradually climbing up to broader public understanding, thus serving the interests of the lay society, too.

Dedication to quality

Each Frontiers article is a landmark of the highest quality, thanks to genuinely collaborative interactions between authors and review editors, who include some of the world's best academicians. Research must be certified by peers before entering a stream of knowledge that may eventually reach the public - and shape society; therefore, Frontiers only applies the most rigorous and unbiased reviews. Frontiers revolutionizes research publishing by freely delivering the most outstanding research, evaluated with no bias from both the academic and social point of view. By applying the most advanced information technologies, Frontiers is catapulting scholarly publishing into a new generation.

What are Frontiers Research Topics?

Frontiers Research Topics are very popular trademarks of the *Frontiers journals series*: they are collections of at least ten articles, all centered on a particular subject. With their unique mix of varied contributions from Original Research to Review Articles, Frontiers Research Topics unify the most influential researchers, the latest key findings and historical advances in a hot research area.

Find out more on how to host your own Frontiers Research Topic or contribute to one as an author by contacting the Frontiers editorial office: frontiersin.org/about/contact

Genetic insights and diagnostic innovations in cerebrovascular and cerebrospinal fluid disorders

Topic editors
Hao Yu — Zhejiang University, China
Haipeng Liu — Coventry University, United Kingdom
Linfang Lan — The First Affiliated Hospital of Sun Yat-sen University, China

Topic coordinator
Ling Li — Zhoushan Hospital, China

Citation
Yu, H., Liu, H., Lan, L., Li, L., eds. (2025). *Genetic insights and diagnostic innovations in cerebrovascular and cerebrospinal fluid disorders*. Lausanne: Frontiers Media SA. doi: 10.3389/978-2-8325-7101-9

Table of contents

frontiers | Frontiers in Neurology

TYPE Editorial
PUBLISHED 21 October 2025
DOI 10.3389/fneur.2025.1691759

OPEN ACCESS

EDITED AND REVIEWED BY
Huifang Shang,
Sichuan University, China

*CORRESPONDENCE
Hao Yu
haoyuzju@zju.edu.cn

RECEIVED 24 August 2025
ACCEPTED 22 September 2025
PUBLISHED 21 October 2025

CITATION
Li L, Liu H, Lan L and Yu H (2025) Editorial: Genetic insights and diagnostic innovations in cerebrovascular and cerebrospinal fluid disorders. *Front. Neurol.* 16:1691759. doi: 10.3389/fneur.2025.1691759

Editorial: Genetic insights and diagnostic innovations in cerebrovascular and cerebrospinal fluid disorders

Ling Li[1], Haipeng Liu [2,3], Linfang Lan[4] and Hao Yu[5]*

[1]Department of Neurology, Zhoushan Hospital, Wenzhou Medical University, Zhoushan, Zhejiang, China, [2]Centre for Intelligent Healthcare, Coventry University, Coventry, United Kingdom, [3]National Medical Research Association, Leicester, United Kingdom, [4]Department of Neurology, The First Affiliated Hospital of Sun Yat-sen University, Guangzhou, China, [5]Department of Medical Genetics and Center for Rare Diseases, Second Affiliated Hospital, Zhejiang University School of Medicine and Zhejiang Key Laboratory of Rare Diseases for Precision Medicine and Clinical Translation, Hangzhou, Zhejiang, China

KEYWORDS

cerebrovascular diseases (CVDs), neuroimaging, multi-omics data analysis, molecular genetics, artificial intelligence

Editorial on the Research Topic
Genetic insights and diagnostic innovations in cerebrovascular and cerebrospinal fluid disorders

Genetics-centered precision neurology is reshaping both research and clinical practice in cerebrovascular disease and cerebrospinal fluid-related disorders. Technological advancements in multimodal neuroimaging, standardized laboratory testing, next-generation sequencing, transcriptomics, and extracellular-vesicle analytics are collectively accelerating the acquisition, management, processing, and interpretation of novel biomarkers for clinical practice. The impact is evident in earlier etiologic clarification, finer-grained risk stratification, and biomarker-informed monitoring that spans the acute phase through rehabilitation. Within this Research Topic, Genetic Insights and Diagnostic Innovations in Cerebrovascular and Cerebrospinal Fluid Disorders, we assembled 13 contributions—reviews, bioinformatics analyses, clinical cohort studies, neuroimaging investigations, and preclinical experimentation—that collectively illustrate how genetics and novel biomarkers are being applied to cerebrovascular and cerebrospinal fluid-related diseases. Taken together, these studies provide up-to-date examples of how molecular insights can be translated into implementable diagnostic tools and mechanism-informed therapeutic strategies. The details are summarized in Supplementary Table 1.

We observed that multiple low-cost and readily obtainable blood biomarkers show promise for risk stratification and outcome prediction. Building on a randomized study, Mitra et al. showed that Short Message Service–guided exercise improved post-stroke six-minute walk test (6MWT) performance and attenuated the decline in brain-derived neurotrophic factor (BDNF). Changes in choline acetyltransferase (ChAT) activity and in the ChAT/butyrylcholinesterase (ChAT/BChE) index correlated with the 6MWT outcomes, with stronger signals observed in women for ChAT activity. This synchronized acquisition of biomarker and behavioral endpoints highlights the potential of peripheral markers as tools for monitoring treatment response.

In an observational analysis of 1,470 older adults with acute ischemic stroke (AIS), Huang et al. identified a non-linear inverse association between a lower hemoglobin-to-red blood cell distribution width ratio (HRR) and a higher risk of unfavorable 3-month outcomes. Restricted cubic spline modeling revealed an optimal inflection point at 10.70, with an area under the curve of approximately 0.64. Lower HRR values signaled greater risk. As a zero-additional-cost index derived from routine hematology tests, the HRR may offer practical value for bedside risk stratification.

In a cohort of AIS patients treated with intravenous thrombolysis, Li et al. evaluated the etiology-dependent prognostic value of lymphocyte-related ratios. The neutrophil-to-lymphocyte ratio (NLR) consistently predicted 90-day outcomes across the Trial of Org 10,172 in Acute Stroke Treatment (TOAST) subtypes with subtype-specific cutoffs and was associated with adverse outcomes in each category, whereas the lymphocyte-to-monocyte ratio (LMR) showed predictive value primarily in the large-artery atherosclerosis subtype.

Using a large United States adult cohort and multivariable logistic regression, Ye et al. examined the neutrophil percentage-to-albumin ratio (NPAR) in relation to stroke prevalence and found that a higher NPAR was associated with greater prevalence. These findings provide new insights for primary prevention and support the NPAR as a practical tool for estimating stroke likelihood.

Drawing on a clinical database of critically ill patients with acute brain injury, Wang J. et al. assessed the stress hyperglycemia ratio (SHR) and showed that it independently predicts both short- and long-term mortality. When combined with the Glasgow Coma Scale (GCS) and ventilation status, the SHR further improved risk stratification, supporting its use as a practical and feasible quantitative metric in intensive care settings.

In a large cross-sectional analysis of the National Health and Nutrition Examination Survey (NHANES), Xu H. et al. used weighted multivariable models with stratified interaction testing and provided the first population-level evidence of an independent inverse association between the serum klotho and stroke risk. The association was consistent across most subgroups. These results suggest that anti-aging endocrine pathways may modulate cerebrovascular risk, indicating the possibility of developing hormone biomarker panels for risk stratification.

With respect to genetics and large-vessel structural phenotypes, Wang J.-W. et al. examined the association between the apolipoprotein E (APOE) genotype and extracranial carotid artery (ECA) tortuosity in a Chinese cohort and found that the ε2 allele may be associated with the increased tortuosity of the ECA, whereas the ε4 allele might be a protective factor. These observations suggest that lipid-metabolism genotypes may influence the geometry of cerebral arteries.

By integrating peripheral blood transcriptomes from multiple Gene Expression Omnibus cohorts, Wang and Liu further identified ABCA1, CLEC4E, and IRS2 as potential key biomarkers and therapeutic targets for cardioembolic stroke and ischemic stroke, serving as shared feature genes. Their expression correlates closely with neutrophil infiltration and autophagy activation, and a nomogram based on these markers demonstrates potential clinical applicability. This progression from single-gene signals to systems-level networks suggests translatable diagnostic and therapeutic targets.

In symptomatic intracranial atherosclerotic stenosis (sICAS), Xu X. et al. linked cerebral perfusion patterns to infarct topography and early neurological outcomes. Specific perfusion abnormality profiles were associated with cortical and subcortical infarct distributions, as well as short-term clinical trajectories, underscoring the central role of hemodynamic compromise in the risk stratification of sICAS and identifying the candidates for intensified hemodynamic management. The penumbra-infarct core mismatch volume in CT perfusion, with a Tmax of >4s defining the penumbra, was associated with early neurological outcomes in patients with sICAS.

On the translational front, using a murine transient middle cerebral artery occlusion model, Wang L.-P. et al. evaluated the anti-inflammatory and blood–brain barrier (BBB)–protective effects of oligodendrocyte precursor cell (OPC) transplantation. OPCs reduced neuroinflammation, preserved BBB integrity, decreased infarct volume, and improved neurobehavioral outcomes, with benefits associated with Wnt/β-catenin signaling. These findings indicate a promising therapeutic strategy for ischemic stroke.

From a phytochemistry perspective, Yu et al. reviewed natural compounds derived from traditional Chinese medicine (TCM) that regulate microglial polarization to achieve neuroprotection after ischemic stroke. Multiple classes of compounds inhibit pro-inflammatory polarization and/or promote protective polarization, thereby exerting neuroprotective effects within a multitarget network. The review systematically catalogs candidate molecules and pathways, summarizes delivery innovations, and emphasizes the need for standardized pharmacology, pharmacokinetics, and quality control to advance standardized and personalized TCM treatment and management of ischemic stroke.

Liang et al. presented a comprehensive synthesis of blood-based biomarkers in ischemic stroke, covering coagulation and fibrinolysis pathways, endothelial dysfunction markers, inflammatory mediators, neuronal and axonal injury markers, and extracellular vesicles with their circular RNAs. The review also surveys contemporary detection platforms and assay methodologies, providing critical guidance for clinical implementation. Across these categories, many candidates show promise for etiologic subtyping, early neurological deterioration, and prognostic assessment, thereby bridging molecular mechanisms with deployable diagnostic assays.

Abbreviations: AI, artificial intelligence; APOE, apolipoprotein E; CFD, computational fluid dynamics; ChAT, choline acetyltransferase; CTP, computed tomography perfusion; FSI, fluid–structure interaction; HRR, hemoglobin-to-red blood cell distribution width ratio; QC, quality control; NLR, neutrophil-to-lymphocyte ratio; NPAR, neutrophil percentage-to-albumin ratio; SHR, stress hyperglycemia ratio; sICAS, symptomatic intracranial atherosclerotic stenosis; OPC, oligodendrocyte precursor cell.

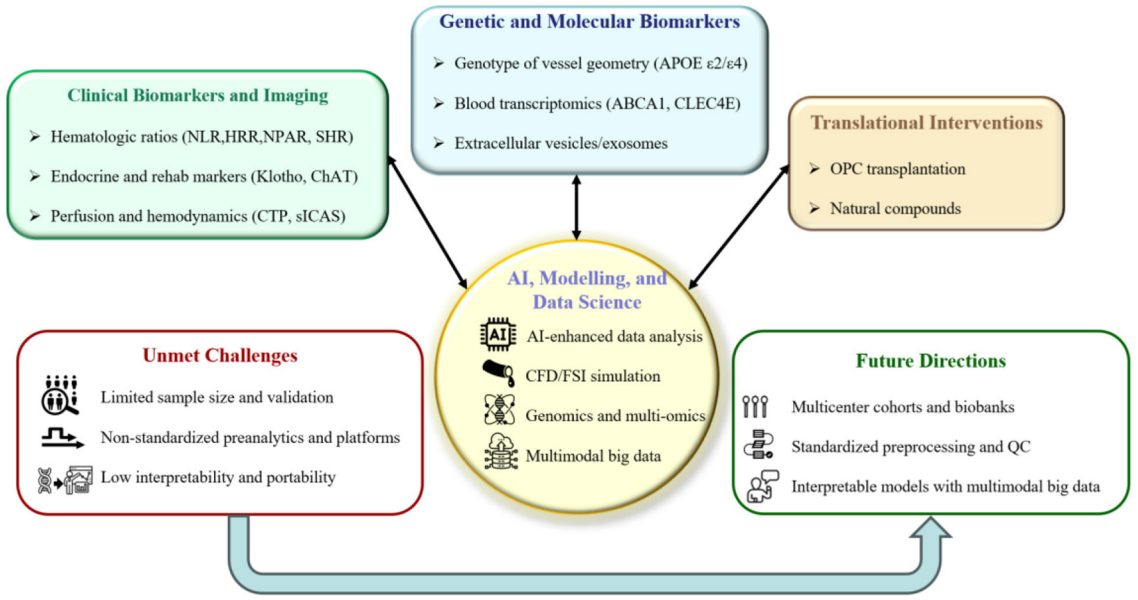

FIGURE 1
Overview of this Research Topic. The top colored panels summarize the Research Topics represented by the selected contributions: (i) clinical biomarkers and imaging; (ii) genetic and molecular biomarkers; and (iii) translational interventions. The central hub depicts AI, modeling, and data science, which are also prioritized as future directions. The bottom outline panels synthesize the limitations of the current state of the art and the corresponding priorities for future research.

Using bibliometric methods, Ding et al. comprehensively appraised exosome research in ischemic stroke, focusing on endogenous and therapeutic exosomes, engineered cargo, and delivery across the BBB. This data-driven landscape provides valuable references and resources to guide further exploration of exosome-based diagnostics and therapeutics.

This Research Topic delineates some research hotspots of genetics in cerebral circulation and relevant diseases. The Research Topic spans bibliometric analysis and methodological reviews (Liang et al.; Ding et al.), low-cost hematologic ratios for risk stratification and prognosis (Huang et al.; Li et al.; Ye et al.; Wang J. et al.), endocrine and rehabilitation-related markers (Mitra et al.; Xu H. et al.), genetic and molecular biomarkers (Wang J.-W. et al.; Wang and Liu; Liang et al.; Ding et al.), and perfusion-based imaging phenotypes linked to early clinical outcomes (Xu X. et al.). The cell-based and natural-product interventions establish a foundation for mechanism-guided therapies (Wang L.-P. et al.; Yu et al.). These contributions also advance clinical decision support by integrating inexpensive hematologic indexes with imaging and transcriptomic information, aiming to enhance diagnostic precision for acute management, etiologic classification, prognostic stratification, and rehabilitation follow-up.

Not with standing this progress, several challenges remain: insufficient availability of high-quality specimens and multicenter external validation (Mitra et al.; Huang et al.; Li et al.; Ye et al.; Wang J. et al.; Xu H. et al.; Wang J.-W. et al.; Xu X. et al.), lack of standardization in pre-analytical workflows and analytical platforms (Wang and Liu; Liang et al.; Ding et al.), limited interpretability and portability of multimodal models (Wang and Liu; Ding et al.), constraints in clinical integration and turnaround time (Liang et al.; Ding et al.), incomplete translational and regulatory pathways (Wang L.-P. et al.; Yu et al.), and ethics concerns regarding equity and accessibility (Ye et al.; Xu H. et al.). Figure 1 provides an overview of the selected contributions and maps current limitations and future research directions. Future research priorities include establishing multicenter prospective cohorts and biobanks, refining standardized preprocessing and quality-control frameworks, and developing computational models based on multimodal big data. Current efforts could be coupled with advanced computational modeling—such as computational fluid dynamics (CFD), fluid–structure interaction (FSI), and multiphysics simulation—to reconstruct cerebral and cerebrospinal fluid dynamics (1–4). Genomics and multi-omics can delineate risk loci and pathways for pathological analysis (5–8). Furthermore, interpretable artificial intelligence (AI) approaches that integrate neuroimaging, biochemical, genetic, and hemodynamic features, along with large-scale multimodal clinical data, can improve diagnostic accuracy and prognostic performance (9–13). In parallel, mechanism-anchored early-phase translation should be accelerated to support the development and evaluation of targeted interventions. Taken together, these computational and data-driven approaches will enable mechanistic elucidation, early diagnosis, and the optimization of interventions toward individualized therapy and precise medicine.

Author contributions

LLi: Methodology, Visualization, Conceptualization, Writing – original draft, Investigation, Writing – review & editing. HL:

Writing – original draft, Writing – review & editing, Investigation, Validation, Visualization, Supervision, Conceptualization. LLa: Validation, Writing – review & editing, Formal analysis. HY: Visualization, Formal analysis, Writing – original draft, Writing – review & editing, Supervision.

Funding

The author(s) declare that financial support was received for the research and/or publication of this article. This work was supported by the National Natural Science Foundation of China (82201513).

Acknowledgments

We appreciate the contributors to this Research Topic.

Conflict of interest

The authors declare that the research was conducted in the absence of any commercial or financial relationships that could be construed as a potential conflict of interest.

Generative AI statement

The author(s) declare that no Gen AI was used in the creation of this manuscript.

Any alternative text (alt text) provided alongside figures in this article has been generated by Frontiers with the support of artificial intelligence and reasonable efforts have been made to ensure accuracy, including review by the authors wherever possible. If you identify any issues, please contact us.

Publisher's note

Supplementary material

The Supplementary Material for this article can be found online at: https://www.frontiersin.org/articles/10.3389/fneur.2025.1691759/full#supplementary-material

References

1. Liu Y, Li S, Liu H, Tian X, Liu Y, Li Z, et al. Clinical implications of haemodynamics in symptomatic intracranial atherosclerotic stenosis by computational fluid dynamics modelling: a systematic review. *Stroke Vasc Neurol.* (2025) 10:16–24. doi: 10.1136/svn-2024-003202

2. Liu H, Zheng D, Wang D, Shi L, Leng X, Wong LKS, et al. State-of-the-art computational models of circle of willis with physiological applications: a review. *IEEE Access.* (2020) 8:156261–73. doi: 10.1109/ACCESS.2020.3007737

3. Fillingham P, Levendovszky SR, Andre J, Bindschadler M, Friedman S, Kurt M, et al. Noninvasive, patient-specific computational fluid dynamics simulations of dural venous sinus pressures in idiopathic intracranial hypertension. *Brain Multiphys.* (2023) 5:100081. doi: 10.1016/j.brain.2023.100081

4. Liu H, Pan F, Lei X, Hui J, Gong R, Feng J, et al. Effect of intracranial pressure on photoplethysmographic waveform in different cerebral perfusion territories: a computational study. *Front Physiol.* (2023) 14:1085871. doi: 10.3389/fphys.2023.1085871

5. Li W, Shao C, Zhou H, Du H, Chen H, Wan H, et al. Multi-omics research strategies in ischemic stroke: a multidimensional perspective. *Ageing Res Rev.* (2022) 81:101730. doi: 10.1016/j.arr.2022.101730

6. Montaner J, Ramiro L, Simats A, Tiedt S, Makris K, Jickling GC, et al. Multilevel omics for the discovery of biomarkers and therapeutic targets for stroke. *Nat Rev Neurol.* (2020) 16:247–64. doi: 10.1038/s41582-020-0350-6

7. Debette S, Paré G. Stroke genetics, genomics, and precision medicine. *Stroke.* (2024) 55:2163–8. doi: 10.1161/STROKEAHA.123.044212

8. Bordes C, Sargurupremraj M, Mishra A, Debette S. Genetics of common cerebral small vessel disease. *Nat Rev Neurol.* (2022) 18:84–101. doi: 10.1038/s41582-021-00592-8

9. Bonkhoff AK, Grefkes C. Precision medicine in stroke: towards personalized outcome predictions using artificial intelligence. *Brain.* (2022) 145:457–75. doi: 10.1093/brain/awab439

10. Czap AL, Sheth SA. Overview of imaging modalities in stroke. *Neurology.* (2021) 97(20 Suppl 2):S42–51. doi: 10.1212/WNL.0000000000012794

11. Heo J, Yoon JG, Park H, Kim YD, Nam HS, Heo JH. Machine learning-based model for prediction of outcomes in acute stroke. *Stroke.* (2019) 50:1263–5. doi: 10.1161/STROKEAHA.118.024293

12. Akay EMZ, Hilbert A, Carlisle BG, Madai VI, Mutke MA, Frey D. Artificial intelligence for clinical decision support in acute ischemic stroke: a systematic review. *Stroke.* (2023) 54:1505–16. doi: 10.1161/STROKEAHA.122.041442

13. Haller S. AI-accelerated MRI for acute stroke: faster acquisitions, faster diagnoses. *Radiology.* (2024) 310:e240099. doi: 10.1148/radiol.240099

frontiers | Frontiers in Neurology

TYPE Original Research
PUBLISHED 28 January 2025
DOI 10.3389/fneur.2025.1520298

OPEN ACCESS

EDITED BY
Haipeng Liu,
Coventry University, United Kingdom

REVIEWED BY
Xintian Cai,
People's Hospital of Xinjiang Uygur Autonomous Region, China
Zhen Hu,
Anthem, United States

*CORRESPONDENCE
Jun Yan
✉ yanjun@gxmu.edu.cn
Guozhong Zhang
✉ zhanggz456@126.com

†These authors have contributed equally to this work

RECEIVED 01 November 2024
ACCEPTED 14 January 2025
PUBLISHED 28 January 2025

CITATION
Ye C, Mo Y, Su T, Huang G, Lu J, Tang S, Huang Q, Li Q, Jiang Q, Guo F, Wu P, Zhang G and Yan J (2025) Cross-sectional study on the association between neutrophil-percentage-to-albumin ratio (NPAR) and prevalence of stroke among US adults: NHANES 1999–2018.
Front. Neurol. 16:1520298.
doi: 10.3389/fneur.2025.1520298

Cross-sectional study on the association between neutrophil-percentage-to-albumin ratio (NPAR) and prevalence of stroke among US adults: NHANES 1999–2018

Chenglin Ye[1†], Yong Mo[1†], Tiansheng Su[1], Guangxiang Huang[1], Jiachao Lu[1], Shuling Tang[1], Qianrong Huang[1], Qiuyun Li[2], Qian Jiang[1], Fangzhou Guo[1], Pinghua Wu[1], Guozhong Zhang[3]* and Jun Yan[1]*

[1]Department of Neurosurgery, Guangxi Medical University Cancer Hospital, Nanning, China, [2]Department of Breast Surgery, Guangxi Medical University Cancer Hospital, Nanning, China, [3]Department of Neurosurgery, Institute of Brain Diseases, Nanfang Hospital of Southern Medical University, Guangzhou, China

The neutrophil-to-albumin ratio (NPAR) is a relatively novel composite biomarker of inflammation, which has been used for prognostication in cardiovascular diseases and may also be associated with stroke. A cross-sectional analysis was conducted using data from the National Health and Nutrition Examination Survey (NHANES) 1999–2018, including 48,734 individuals with complete NPAR and stroke data. The association between stroke prevalence and NPAR values was assessed through multivariate regression analysis. The relationship between these variables was further visualized using restricted cubic splines (RCS). Additionally, potential factors influencing this relationship were explored through subgroup analysis. The regression model revealed a significant association between NPAR and stroke prevalence, even after adjusting for other covariates [1.06 (1.04, 1.08)]. Stroke prevalence was 62% higher in the highest NPAR group compared to the lowest [1.62 (1.40, 1.89)]. The RCS analysis further confirmed this positive correlation. Subgroup analysis showed that this association was not significantly influenced by other factors. This study establishes a strong association between NPAR and stroke prevalence. However, further studies are needed to clarify the underlying mechanisms and establish a direct causal link.

KEYWORDS

NPAR, stroke, NHANES, a cross-sectional study, restricted cubic

1 Introduction

Cerebrovascular disorders, such as stroke, are characterized by the blockage of blood vessels (1). SStroke is the third leading cause of mortality and disability globally and the second leading cause of death worldwide. Between 1990 and 2019, stroke incidence increased by 70%, and its global prevalence rose by 85% (2). This growing trend is largely attributable to the aging population (3). Stroke remains a major public health challenge, as it is responsible for high rates of morbidity, mortality, and disability. Moreover, the global annual economic burden of stroke exceeds $89.1 billion, placing a significant strain on healthcare systems (4). Moreover,

the global annual economic burden of stroke exceeds $89.1 billion, placing a significant strain on healthcare systems (5). Identifying and managing controllable and preventable risk factors is therefore crucial in reducing stroke incidence. The development of novel biomarkers facilitates early detection of stroke risk (6, 7), thereby helping to lower stroke rates within the population.

The pathogenesis of stroke is closely linked to inflammation, with acute ischemic stroke involving endothelial activation, blood–brain barrier disruption, the release of inflammatory mediators, oxidants, and cytokines, and infiltration by platelets and leukocytes (8, 9). Inflammation is one of the first responses to cerebral injury following a stroke, and it also plays a key role in tissue repair during the recovery phase (10). Evaluating peripheral leukocytes, particularly neutrophils, offers a cost-effective and accessible approach to assess inflammation (11). Neutrophil activation in stroke-damaged brain tissue attracts immune cells, which in turn produce a variety of substances that exacerbate inflammation (12).

Albumin, a protein constituting over half of the serum's protein content, is an intermediate-sized protein with a molecular weight ranging between 66 and 69 kDa (13). It performs essential roles in osmoregulation, antioxidation, and anti-inflammatory processes (14). NPAR, which combines both neutrophil percentage and albumin levels, is an emerging biomarker used to assess immune and systemic inflammatory conditions (15). Reduced albumin levels have been strongly associated with poor outcomes in stroke patients (16). Previous studies have shown that elevated neutrophil counts in the early stages of stroke are associated with greater stroke severity (17). NPAR is increasingly utilized in research on disease risk and outcomes. For example, myocardial infarction patients with elevated NPAR have been found to have higher hospital mortality (18). A prior retrospective study indicated that NPAR is independently associated with stroke recurrence within 3 months following the first acute stroke, suggesting that NPAR might be a better predictor of acute ischemic stroke recurrence than albumin levels or neutrophil percentage alone (19). A recent investigation further revealed that NPAR was associated with ICU hospitalization in ischemic stroke patients (20). Collectively, these findings suggest a potential link between NPAR and stroke. However, the existing data on this relationship remain limited, highlighting the need for more comprehensive research. This study aims to investigate the association between NPAR and stroke within the National Health and Nutrition Examination Survey (NHANES) cohort.

2 Materials and methods

2.1 Survey description

Data for this study were collected through the NHANES, conducted across the United States. The survey employed a stratified multistage random sampling design, which provided a robust framework for assessing the health and nutritional status of the U.S. population (21). Participants underwent a range of assessments, including laboratory tests, home interviews, physical examinations, and additional evaluations. Written informed consent was obtained from all participants prior to their inclusion in the study (22). NHANES, with its extensive database, serves as a comprehensive and reliable tool for deriving population-level insights.

2.2 Study population

Data from 10 cycles of NHANES, spanning from 1999 to 2018, were analyzed in this study, providing broad population coverage and a large sample size. After applying the inclusion and exclusion criteria, 48,734 individuals were enrolled (Figure 1). The exclusion criteria were as follows: (1) individuals under 20 years of age, (2) those with incomplete stroke data, and (3) participants missing NPAR data.

2.3 Assessment of NPAR

The Coulter VCS system was used to determine the white blood cell (WBC) differential. NPAR was calculated using the following formula: (Percentage of neutrophils among total white blood cell count) × 100 ÷ Albumin (g/dL) (23). The same blood sample was used for both the WBC differential and albumin measurement. NPAR values were used as the primary exposure variable in this study.

2.4 Diagnosis of stroke

To assess stroke occurrence, a medical conditions questionnaire was administered. Participants were classified as having experienced a stroke if they answered "yes" to the question: "Has a doctor or other health professional ever informed you that you had a stroke?" Previous studies have demonstrated the reliability of self-reported stroke data (24). In this study, stroke was considered the primary outcome variable.

2.5 Data processing for covariates

Based on existing literature, several factors related to stroke and NPAR were identified as covariates. These included age, gender, ethnicity, educational level, poverty-to-income ratio (PIR), physical activity (PA), body mass index (BMI), tobacco and alcohol consumption, hypertension, and diabetes status. Upon examining the NHANES dataset, we noted the presence of missing data for several key variables. Multiple imputation (MI) was employed to handle the missing data.

The rationale for selecting MI over alternative methods, such as full case analysis or single imputation, is multifaceted. MI preserves the inherent variability and structure of the dataset by generating multiple plausible datasets, where missing values are estimated based on observed data. This approach mitigates the bias inherent in single imputation methods, which can underestimate variability and lead to overly confident results. By incorporating uncertainty from the missing data, MI produces more reliable and efficient estimates and standard errors, offering more accurate statistical conclusions compared to methods that fail to address this uncertainty adequately. Furthermore, MI can improve model performance by accounting for missing data-related uncertainty, thereby enhancing the accuracy and precision of parameter estimates. This contributes to more dependable findings and predictions. MI also helps stabilize estimates, reducing potential bias caused by missing data, which in turn improves the consistency and generalizability of the results.

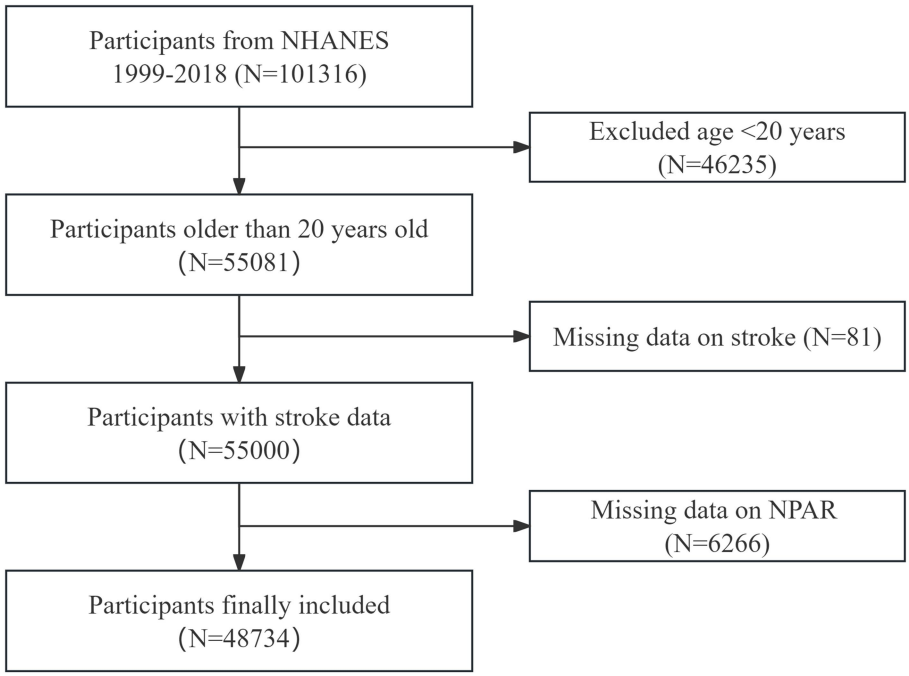

FIGURE 1
Flowchart of participant selection. This flowchart illustrates the process used to select participants for the study, from initial screening to final inclusion. The figure shows the number of participants excluded at each stage and the final cohort included in the analysis.

2.6 Statistical analysis

All statistical analyses were conducted using R and EmpowerStats software. Participants' characteristics were compared across NPAR quartiles using chi-square tests for categorical variables and t-tests for continuous variables. Multivariate logistic regression was employed in three separate models to explore the linear relationship between NPAR and stroke. These models were as follows: Model 1: No covariates were adjusted. Model 2: Adjustments were made for age, gender, ethnicity, and education. Model 3: A broader set of covariates was included, such as age, gender, ethnicity, education, alcohol consumption, smoking, diabetes, hypertension, PA, and PIR. After converting NPAR scores into quartiles, trend tests were performed to evaluate the linear association between NPAR and stroke prevalence. Subgroup analyses were then conducted to examine this relationship further, using various stratifying factors. Additionally, RCS analysis was performed to assess the potential for nonlinear relationships between NPAR and stroke occurrence.

3 Results

3.1 Baseline characteristics of participants

The study included 48,734 participants with a mean age of 46.93 years (SD = 16.90). Of the participants, 48.24% were male and 51.76% were female. The overall stroke prevalence was 3.76%, with rates increasing progressively across higher NPAR quartiles. The baseline characteristics of the participants are summarized in Table 1, which organizes the data by NPAR quartiles. The mean NPAR for the entire cohort was 13.93 ± 2.86, with quartile cutoffs as follows: Quartile 1: <12.11; Quartile 2: 12.11–13.76; Quartile 3: 13.76–15.48; Quartile 4: >15.48. Participants in the higher NPAR quartiles were more likely to be older, predominantly female, have lower educational attainment, and have a higher prevalence of smoking. They also exhibited a greater prevalence of diabetes, hypertension, and stroke compared to the general population. Additionally, higher NPAR values were associated with increased levels of BMI, waist circumference (WC), body weight, triglycerides, LDL-C, and total cholesterol (TC), while PIR and HDL-C levels were relatively lower. This pattern suggests a possible link between unhealthy lifestyle choices and elevated NPAR levels. Further analysis of stroke prevalence across various demographics (Table 2). The findings indicated that older age, female gender, obesity, low educational attainment, poverty, smoking, hypertension, and diabetes were associated with a greater prevalence of stroke. Stroke patients have elevated levels of CRP, FPG, HbA1c, TG, and NPAR.

3.2 Association between the NPAR and stroke

The relationship between NPAR and stroke incidence is presented in Table 3. In both the unadjusted model [OR 1.11 (1.09, 1.12)] and the partially adjusted model [OR 1.08 (1.07, 1.10)], a significant positive association was observed between NPAR and stroke. After applying full adjustments, the association remained statistically significant, with each unit increase in NPAR corresponding to a 6% increase in stroke prevalence [OR 1.06 (1.04, 1.08)]. The correlation remained robust even when NPAR was divided into quartiles, with

TABLE 1 Baseline characteristics according to NPAR quartiles.

Characteristics	Total (*N* = 48,734)	Quartiles of NPAR				
		Q1 (<12.11)	Q2(12.11–13.76)	Q3(13.76–15.48) (2.54–3.43)	Q4 (> 15.48)	*p* value
Age (years)	46.93 ± 16.90	43.76 ± 16.30	45.61 ± 16.13	48.22 ± 16.58	50.41 ± 17.94	<0.0001
Gender (%)						<0.0001
Male	48.24	57.61	51.9	45.98	36.5	
Female	51.76	42.39	48.1	54.02	63.5	
Race (%)						<0.0001
Mexican American	8.19	7.69	8.72	8.47	7.79	
Other Hispanic	5.67	5.75	6.17	5.46	5.22	
Non-Hispanic White	68.62	62.22	69.19	71.51	71.58	
Non-Hispanic Black	10.65	16.4	8.83	8.13	9.41	
Other	6.88	7.94	7.09	6.43	6	
Education (%)						<0.0001
Less than high school	17.23	17.14	16.56	16.95	18.39	
High school grade	23.97	22.4	23.88	24.42	25.28	
Some college or above	58.8	60.46	59.57	58.63	56.33	
PIR (%)						<0.0001
Low	21.25	20.82	19.95	20.67	23.87	
Moderate	36.03	35.47	35.31	35.56	37.97	
High	42.72	43.71	44.74	43.77	38.16	
Drinking status (%)						<0.0001
Never	19.06	17.55	17.88	18.91	22.34	
Moderate	39.59	39.64	40.59	40.01	37.83	
Heavy	41.36	42.81	41.53	41.08	39.83	
Smoking Status (%)						<0.0001
No	53.8	55.39	55.13	53.34	51.06	
Yes	46.2	44.61	44.87	46.66	48.94	
PA level (%)						<0.0001
Low	26.35	22.78	23.25	27.36	32.62	
Moderate	38.37	36.61	38.21	38.04	40.81	
High	35.28	40.61	38.54	34.6	26.57	
Hypertension (%)						<0.0001
No	62.38	67.76	65.46	60.99	54.59	
Yes	37.62	32.24	34.54	39.01	45.41	
Diabetes (%)						<0.0001
No	87.82	91.58	90.44	87.31	81.35	
Yes	12.18	8.42	9.56	12.69	18.65	
BMI (kg/m^2)	28.76 ± 6.72	27.30 ± 5.58	28.12 ± 5.99	29.07 ± 6.58	30.75 ± 8.15	<0.0001
CRP (mg/L)	0.41 ± 0.80	0.24 ± 0.41	0.29 ± 0.49	0.39 ± 0.64	0.78 ± 1.31	<0.0001
WAIST (cm)	98.33 ± 16.26	94.66 ± 14.44	96.96 ± 15.18	99.35 ± 16.21	102.87 ± 18.18	<0.0001
FPG (mg/dL)	105.23 ± 31.11	101.15 ± 23.31	103.40 ± 26.84	106.50 ± 33.41	110.28 ± 38.59	<0.0001
HbA1c (%)	5.57 ± 0.91	5.48 ± 0.79	5.51 ± 0.83	5.59 ± 0.92	5.71 ± 1.09	<0.0001
HDL (mg/dL)	53.19 ± 16.26	53.76 ± 16.73	52.98 ± 16.07	52.77 ± 15.93	53.30 ± 16.29	<0.0001
LDL (mg/dL)	115.69 ± 35.38	117.53 ± 36.28	117.38 ± 34.81	117.30 ± 35.07	110.15 ± 34.79	<0.0001
TC (mg/dL)	196.06 ± 41.32	197.79 ± 42.30	197.87 ± 40.87	196.33 ± 40.32	191.82 ± 41.56	<0.0001
TG (mg/dL)	131.5 ± 103.95	125.8 ± 107.49	131.79 ± 103.62	134.48 ± 100.53	134.23 ± 103.81	<0.0001

10.3389/fneur.2025.1520298

TABLE 2 Baseline characteristics according to stroke.

Characteristics	Total (*N* = 48,734)	Non-stroke (*N* = 46,904)	Stroke (*N* = 1830)	*p* value
Age (years)	46.93 ± 16.90	46.43 ± 16.70	64.69 ± 14.36	<0.0001
Gender (%)				<0.0001
Male	48.24	48.40	42.67	
Female	51.76	51.60	57.33	
Race (%)				<0.0001
Mexican American	8.19	8.30	4.28	
Other Hispanic	5.67	5.73	3.22	
Non-Hispanic White	68.62	68.53	71.65	
Non-Hispanic Black	10.65	10.56	13.90	
Other	6.88	6.88	6.95	
Education (%)				<0.0001
Less than high school	17.23	16.90	28.84	
High school grade	23.97	23.82	29.42	
Some college or above	58.8	59.28	41.74	
PIR (%)				<0.0001
Low	21.25	20.94	32.21	
Moderate	36.03	35.80	43.93	
High	42.72	43.25	23.86	
Drinking status (%)				<0.0001
Never	19.06	18.67	35.83	
Moderate	39.59	39.58	39.87	
Heavy	41.36	41.75	24.30	
Smoking Status (%)				<0.0001
No	53.8	54.14	41.81	
Yes	46.2	45.86	58.19	
PA level (%)				<0.0001
Low	26.35	25.71	49.05	
Moderate	38.37	38.49	34.07	
High	35.28	35.80	16.88	
Hypertension (%)				<0.0001
No	62.38	63.58	20.51	
Yes	37.62	36.42	79.49	
Diabetes (%)				<0.0001
No	87.82	88.45	65.47	
Yes	12.18	11.55	34.53	
BMI(kg/m^2)	28.76 ± 6.72	28.73 ± 6.71	29.90 ± 6.88	<0.0001
CRP(mg/L)	0.41 ± 0.80	0.41 ± 0.79	0.65 ± 1.10	<0.0001
WAIST(cm)	98.33 ± 16.26	98.20 ± 16.25	103.50 ± 16.03	<0.0001
FPG(mg/dL)	105.23 ± 31.11	104.84 ± 30.56	118.64 ± 43.96	<0.0001
HbA1c (%)	5.57 ± 0.91	5.56 ± 0.90	6.05 ± 1.27	<0.0001
HDL(mg/dL)	53.19 ± 16.26	53.24 ± 16.24	51.70 ± 16.61	0.0007
LDL(mg/dL)	115.69 ± 35.38	115.89 ± 35.20	108.87 ± 40.60	<0.0001
TC(mg/dL)	196.06 ± 41.32	196.23 ± 41.16	189.96 ± 46.07	<0.0001
TG(mg/dL)	131.5 ± 103.95	131.20 ± 104.21	143.38 ± 94.25	<0.0001
NPAR	13.82 ± 2.63	13.79 ± 2.62	14.79 ± 2.79	<0.0001

TABLE 3 Association of NPAR with stroke.

Exposure	OR (95%CI), *p* value		
	Model 1[a]	Model 2[b]	Model 3[c]
NPAR	1.11 (1.09, 1.12) <0.0001	1.08 (1.07, 1.10) <0.0001	1.06 (1.04, 1.08) <0.0001
NPAR quartile			
Q1 (<12.11)	1	1	1
Q2 (12.11–13.76)	1.30 (1.11, 1.52) 0.0011	1.29 (1.10, 1.52) 0.0019	1.26 (1.07, 1.48) 0.0063
Q3 (13.76–15.48)	1.80 (1.55, 2.09) <0.0001	1.54 (1.32, 1.79) <0.0001	1.44 (1.23, 1.68) <0.0001
Q4 (> 15.48)	2.55 (2.21, 2.94) <0.0001	1.89 (1.63, 2.19) <0.0001	1.62 (1.40, 1.89) <0.0001
AIC	12105.22	10578.38	10106.73
BIC	12123.38	10631.63	10225.08
Pseudo R^2	0.013	0.139	0.179
AUC	0.602	0.794	0.826

[a]No-adjusted model: adjusted for none.
[b]Minimally adjusted model: adjusted for age, gender, race, and education.
[c]Fully adjusted model: adjusted for age, gender, race, education, PIR, BMI, HbA1c, smoking status, drinking status, physical activity, hypertension, and diabetes.

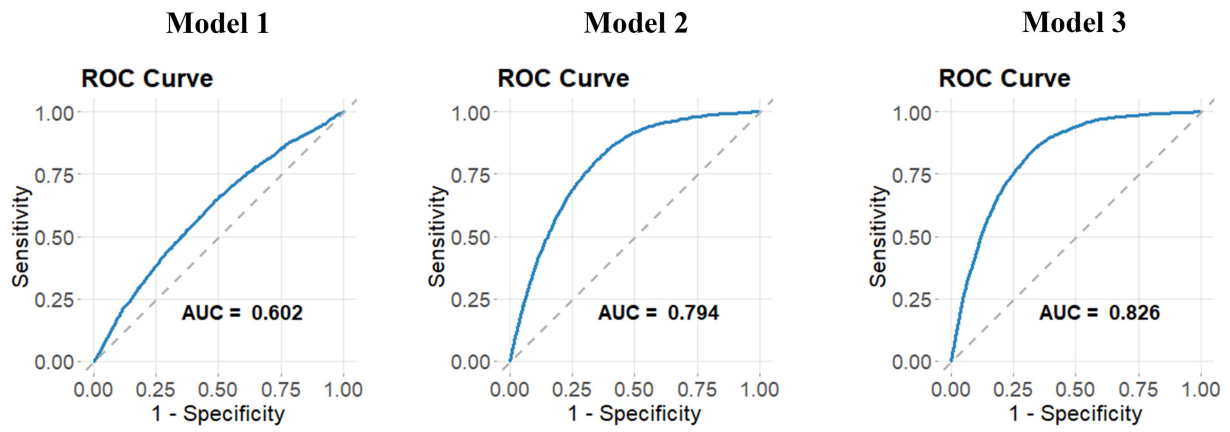

FIGURE 2
ROC curves for three models. ROC curves for three models are presented to assess their ability to discriminate between different outcomes. The curves plot sensitivity against 1-specificity, demonstrating the performance of each model in classifying stroke prevalence. Higher AUC values indicate better model performance in distinguishing stroke cases.

stroke prevalence 62% higher in the highest NPAR quartile compared to the lowest. In comparison to the previous models, Model 3 showed lower Akaike Information Criterion (AIC), Bayesian Information Criterion (BIC), and pseudo-R^2 values. Furthermore, the Receiver Operating Characteristic (ROC) curve analysis indicated that Model 3 had the highest area under the curve (AUC) value (Figure 2), with an AUC of 0.826, demonstrating excellent model performance.

The RCS curve further illustrated the relationship between NPAR and stroke odds ratios (OR; Figure 3). The red solid line represents the estimated OR, while the shaded blue region indicates the 95% confidence interval (CI) around the OR. The overall relationship between NPAR and stroke was statistically significant (P-overall <0.001). Additionally, the analysis suggested a nonlinear association between NPAR and stroke prevalence (P-non-linear = 0.013). Low NPAR Values (<10): In this range, the OR remained close to 1, indicating no significant relationship between NPAR and stroke incidence. Medium NPAR Values (10–20): A slight upward trend was observed in the curve, suggesting a modest increase in stroke prevalence with rising NPAR values. High NPAR Values (>20): Above this threshold, the curve steepened significantly, accompanied by a wider CI, indicating a marked increase in stroke prevalence with higher NPAR values. Additionally, we calculated the Variance Inflation Factors (VIFs) for all covariates in the model, which ranged from 1.07 to 1.41. These values suggest that multicollinearity among the covariates is minimal, as VIFs below 2 are generally considered acceptable. Thus, multicollinearity was not a significant concern in our analysis.

3.3 Subgroup analysis

Subgroup analyses and interaction testing were performed to examine whether the association between NPAR and stroke varied across different demographic groups. A forest plot was used to

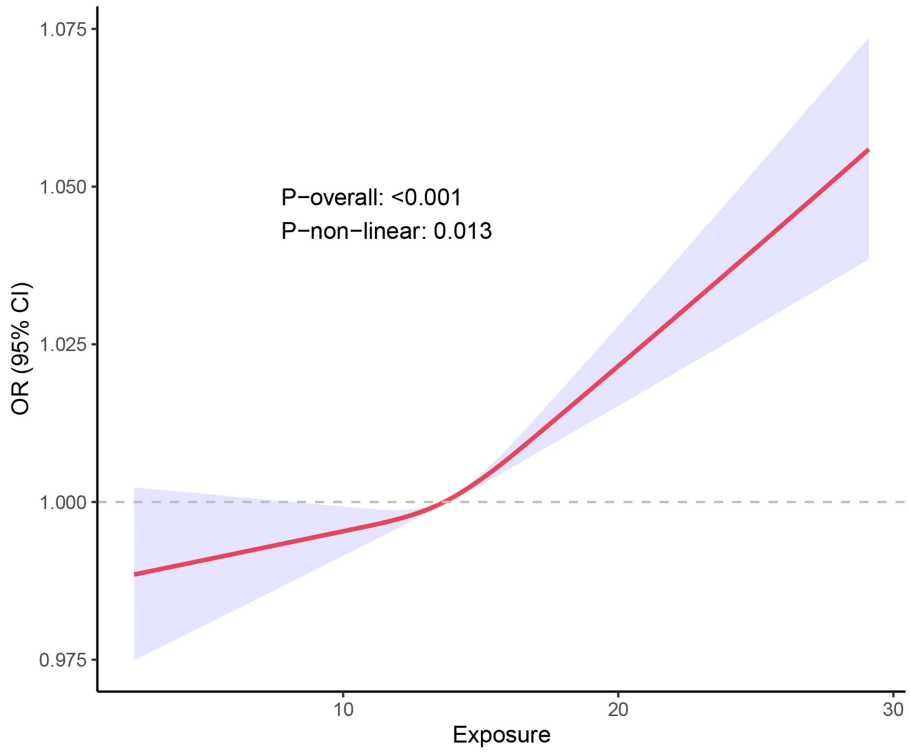

FIGURE 3
RCS fitting curve illustrated the association between NPAR and stroke incidence. X-axis (Exposure): Represents the range of NPAR values. Y-axis [OR (95% CI)]: Depicts the OR for stroke incidence along with its 95% CI. Red Curve Illustrates the trend in stroke incidence as the NPAR value increases. The shape of this curve indicates a complex, non-linear relationship rather than a simple linear correlation. Blue Shaded Area: Represents the 95% confidence interval for the red curve. A narrower shaded region indicates higher precision of the estimate, while a wider region indicates more uncertainty.

visualize these results (Figure 4). Our findings showed that the relationship between NPAR and stroke remained consistent across various subgroups, with all interaction *p*-values exceeding 0.05. This indicates that the association is independent of the stratifying factors, suggesting that NPAR may be a broadly applicable biomarker for stroke risk across diverse populations.

4 Discussion

Our study identified a significant association between stroke prevalence and NPAR in a large, community-representative cohort of 48,734 participants. Elevated NPAR levels were linked to higher stroke rates, and this positive correlation was consistently observed across various demographic subgroups. Subgroup analyses and interaction tests further supported the robustness of this association, suggesting that NPAR could serve as a valuable marker in stroke assessment. Notably, an inflection point was observed around an NPAR value of 14, indicating a threshold effect where stroke prevalence increases more sharply beyond this point. These findings underscore the potential importance of NPAR in stroke prevention and management, highlighting that elevated NPAR may be associated with an increased risk of stroke.

Research on stroke biomarkers has advanced to enhance the early detection of stroke prevalence. Following a literature review, we identified that stroke biomarkers mostly include the below categories: Lipid indicators, including TC and non-HDL, may more accurately predict stroke incidence than LDL (25); Inflammatory markers, especially IL-6, shown significant correlations with stroke risk (26); Hemodynamic indicators such as midregional proatrial natriuretic peptide and N-terminal pro-B-type natriuretic peptide shown promise in differentiating stroke subtypes (27, 28); Particular microRNAs (miR-125a-5p, miR-125b-5p, miR-143-3p) shown upregulation in acute ischemic stroke (29); Metabolomic investigations discovered new markers, including tetradecanedioate and hexadecanedioate, associated with cardioembolic stroke (30); Neurodegenerative indicators, such as total-tau and neurofilament light chain, were correlated with heightened stroke risk (31).

Neutrophil levels upon hospital admission have been associated with early neurological deterioration and poorer outcomes, especially in patients with intracerebral hemorrhage (ICH) (32). Albumin levels have been recognized as reliable biomarkers for predicting mortality and functional recovery in stroke patients (33, 34). There is a correlation between high albumin levels and improved functional recovery and decreased mortality in stroke patients, which suggests that some neuroprotective effects may be present (35). Albumin's role as a major plasma antioxidant is crucial, contributing to delayed neuronal death phases (36), while reduced serum albumin can increase oxidative stress and lower antioxidant defenses. Inflammatory responses in ICH involve both neutrophils and albumin, and hypoalbuminemia, often seen in

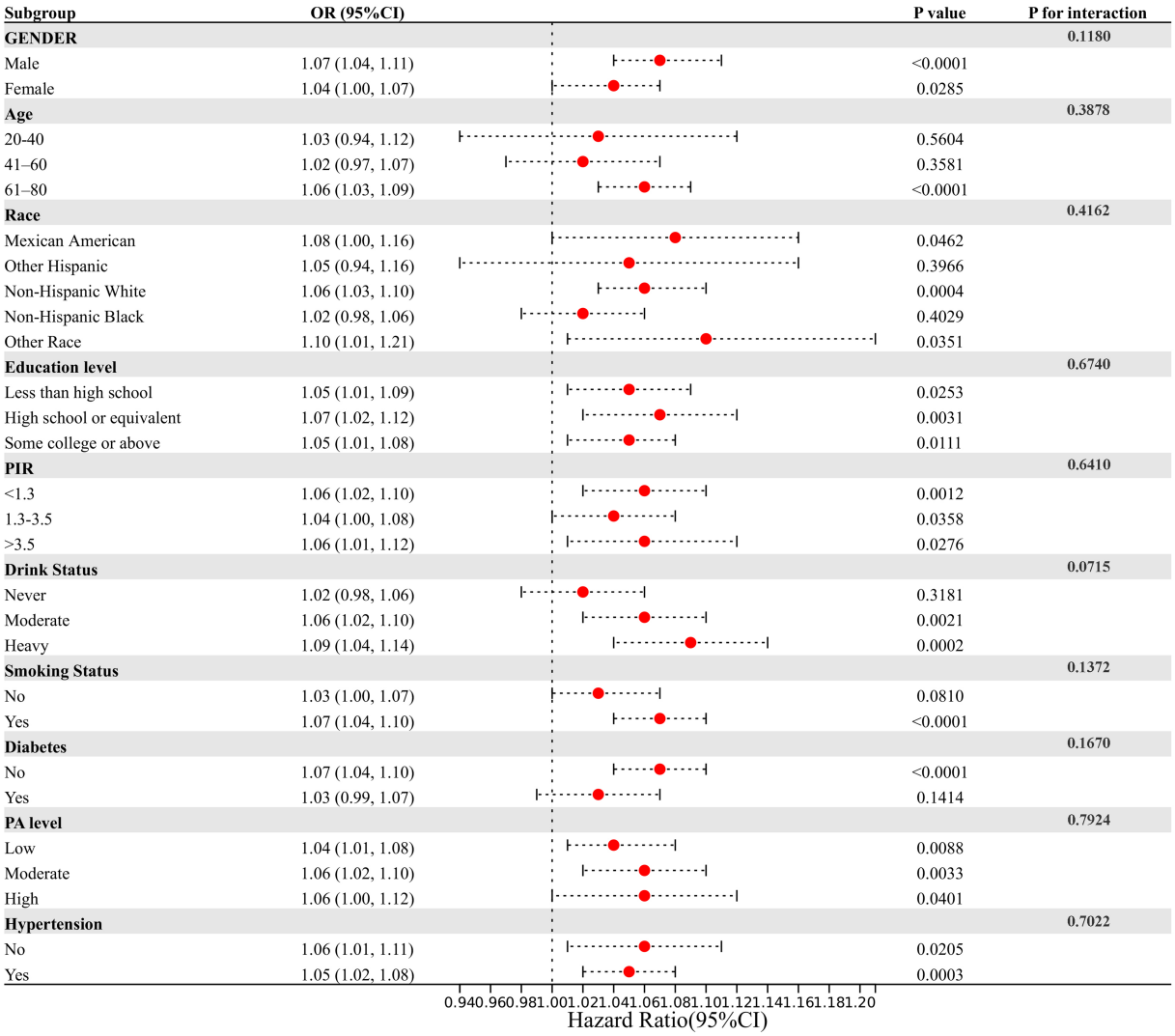

FIGURE 4
Assessment of the correlation between NPAR and stroke by subgroup analysis. This figure assesses the relationship between NPAR and stroke incidence across various demographic and clinical subgroups. Each row represents a specific subgroup, showing the OR and 95% CI for stroke incidence in relation to NPAR within that subgroup. The lack of significant interaction effects (P for interaction) in most subgroups suggests that the impact of NPAR on stroke prevalence is consistent across different demographic and clinical characteristics. However, certain subgroups—such as those defined by drinking status and age—may show slight differences in the NPAR-stroke relationship, though these interactions are not strongly significant.

malnutrition, renal or hepatic issues, is linked to poorer health outcomes and greater frailty. Furthermore, albumin has been shown to independently predict pneumonia risk after acute ischemic stroke (37).

The combined use of neutrophil count and albumin levels has shown potential in improving the accuracy of stroke outcome predictions, integrating both acute inflammatory responses and nutritional status. Several studies have also highlighted the connection between NPAR and stroke-related outcomes. A 2021 retrospective study found that NPAR outperformed other biomarkers, such as albumin and neutrophil-to-leukocyte ratios, in predicting stroke-associated pneumoni (38). Chen et al. found that stroke patients with elevated NPAR had a higher risk of mortality (39), and Cui et al. reported worse outcomes in acute ICH patients with higher NPAR levels (40). Additionally, Lv and colleagues showed that increased NPAR was independently associated with adverse outcomes in both stroke-associated pneumonia and spontaneous ICH (41). These studies reinforce the strong link between NPAR and stroke, and our research provides further clarification of this relationship, suggesting that NPAR could serve as a novel biomarker for stroke risk assessment.

This is, to our knowledge, the first study to specifically investigate the relationship between NPAR and stroke prevalence. Previous research has primarily focused on NPAR's association with cardiovascular diseases. For example, Zhang et al. found that high NPAR levels independently predicted coronary slow flow in patients with myocardial ischemia (42). Elevated NPAR levels in individuals with hypertension have also been associated with increased

cardiovascular disease risk and overall mortality (43). Moreover, NPAR has been shown to correlate with coronary atherosclerosis in patients with chronic renal disease, accurately predicting the severity of the condition (44). These findings emphasize NPAR's role as a marker of systemic inflammation and suggest that it may also reflect the severity of brain damage and post-stroke complications.

This study has notable strengths. The analysis was based on data from 48,734 U.S. adults, with sample weights adjusted to ensure representativeness of the broader U.S. population. However, several limitations must be acknowledged. As a cross-sectional study, we cannot establish a direct causal relationship between NPAR and stroke. Selection bias may also have influenced the results. To further explore the dynamics of NPAR in stroke progression, longitudinal studies with larger sample sizes are needed. Additionally, the absence of information on medication history and stroke subtype classification in the dataset introduces the potential for recall bias. Stroke diagnoses were based on self-reported questionnaires, which may further contribute to this bias. Future clinical investigations are necessary to validate these findings and explore the broader applicability of NPAR in stroke detection and management.

5 Conclusion

Our study demonstrates that elevated NPAR levels are associated with increased stroke prevalence. This finding offers new insights for primary stroke prevention, suggesting that NPAR could serve as a practical tool for assessing stroke likelihood. By incorporating NPAR into clinical decision-making, healthcare providers could implement timely preventive measures for individuals with higher NPAR levels, ultimately optimizing stroke prevention strategies and improving patient outcomes.

Data availability statement

The original contributions presented in the study are included in the article/supplementary material, further inquiries can be directed to the corresponding authors.

Ethics statement

Ethical review and approval were not required for the study on human participants in accordance with the local legislation and institutional requirements. Written informed consent from the patients/participants or patients/participants' legal guardian/next of kin was not required to participate in this study in accordance with the national legislation and the institutional requirements.

Author contributions

CY: Conceptualization, Data curation, Formal analysis, Investigation, Methodology, Project administration, Software, Supervision, Validation, Writing – original draft, Writing – review & editing. YM: Data curation, Methodology, Project administration, Supervision, Validation, Writing – original draft, Writing – review & editing. TS: Investigation, Methodology, Resources, Software, Supervision, Writing – review & editing. GH: Data curation, Investigation, Methodology, Software, Writing – review & editing. JL: Data curation, Methodology, Writing – review & editing. ST: Formal analysis, Project administration, Writing – review & editing. QH: Investigation, Software, Writing – review & editing. QL: Data curation, Methodology, Writing – review & editing. QJ: Formal analysis, Project administration, Writing – review & editing. FG: Investigation, Software, Writing – review & editing. PW: Resources, Visualization, Writing – review & editing. GZ: Data curation, Formal analysis, Funding acquisition, Project administration, Resources, Validation, Visualization, Writing – original draft, Writing – review & editing. JY: Formal analysis, Funding acquisition, Methodology, Project administration, Resources, Supervision, Visualization, Writing – original draft, Writing – review & editing.

Funding

The author(s) declare that financial support was received for the research, authorship, and/or publication of this article. This study was supported by grants from Guangxi Natural Science Foundation (nos. 2023GXNSFDA026028, 2020GXNSFAA297154 and 2018GXNSFAA281151), National Natural Science Foundation of China (nos. 82260239 and 82060225), and the Scientific Research Project of Guangxi Health Commission (No. S2018020) to JY.

Acknowledgments

We would like to express our gratitude to all the NHANES staff and participants for their valuable contributions.

Conflict of interest

The authors declare that the research was conducted in the absence of any commercial or financial relationships that could be construed as a potential conflict of interest.

Generative AI statement

The author(s) declare that no Gen AI was used in the creation of this manuscript.

Publisher's note

References

1. Kuriakose D, Xiao Z. Pathophysiology and treatment of stroke: present status and future perspectives. *Int J Mol Sci*. (2020) 21. doi: 10.3390/ijms21207609

2. GBD 2019 Stroke Collaborators. Global, regional, and national burden of stroke and its risk factors, 1990-2019: a systematic analysis for the global burden of disease study 2019. *Lancet Neurol*. (2021) 20:795–820. doi: 10.1016/S1474-4422(21)00252-0

3. Roth GA, Mensah GA, Johnson CO, Addolorato G, Ammirati E, Baddour LM, et al. Global burden of cardiovascular diseases and risk factors, 1990-2019: update from the GBD 2019 study. *J Am Coll Cardiol*. (2020) 76:2982–3021. doi: 10.1016/j.jacc.2020.11.010

4. Feigin VL, Brainin M, Norrving B, Martins S, Sacco RL, Hacke W, et al. World stroke organization (WSO): global stroke fact sheet 2022. *Int J Stroke*. (2022) 17:18–29. doi: 10.1177/17474930211065917

5. Owolabi MO, Thrift AG, Mahal A, Ishida M, Martins S, Johnson WD, et al. Primary stroke prevention worldwide: translating evidence into action. *Lancet Public Health*. (2022) 7:e74–85. doi: 10.1016/S2468-2667(21)00230-9

6. Cai X, Hu J, Wen W, Wang M, Zhu Q, Liu S, et al. Association between the geriatric nutritional risk index and the risk of stroke in elderly patients with hypertension: a longitudinal and cohort study. *Front Nutr*. (2022) 9:1048206. doi: 10.3389/fnut.2022.1048206

7. Cai X, Hu J, Zhu Q, Wang M, Liu S, Dang Y, et al. Relationship of the metabolic score for insulin resistance and the risk of stroke in patients with hypertension: a cohort study. *Front Endocrinol (Lausanne)*. (2022) 13:1049211. doi: 10.3389/fendo.2022.1049211

8. Anrather J, Iadecola C. Inflammation and stroke: an overview. *Neurotherapeutics*. (2016) 13:661–70. doi: 10.1007/s13311-016-0483-x

9. Chamorro Á, Dirnagl U, Urra X, Planas AM. Neuroprotection in acute stroke: targeting excitotoxicity, oxidative and nitrosative stress, and inflammation. *Lancet Neurol*. (2016) 15:869–81. doi: 10.1016/S1474-4422(16)00114-9

10. Danton GH, Dietrich WD. Inflammatory mechanisms after ischemia and stroke. *J Neuropathol Exp Neurol*. (2003) 62:127–36. doi: 10.1093/jnen/62.2.127

11. Mortaz E, Alipoor SD, Adcock IM, Mumby S, Koenderman L. Update on neutrophil function in severe inflammation. *Front Immunol*. (2018) 9:2171. doi: 10.3389/fimmu.2018.02171

12. Strecker JK, Schmidt A, Schäbitz WR, Minnerup J. Neutrophil granulocytes in cerebral ischemia - evolution from killers to key players. *Neurochem Int*. (2017) 107:117–26. doi: 10.1016/j.neuint.2016.11.006

13. Arques S. Human serum albumin in cardiovascular diseases. *Eur J Intern Med*. (2018) 52:8–12. doi: 10.1016/j.ejim.2018.04.014

14. Roche M, Rondeau P, Singh NR, Tarnus E, Bourdon E. The antioxidant properties of serum albumin. *FEBS Lett*. (2008) 582:1783–7. doi: 10.1016/j.febslet.2008.04.057

15. He X, Dai F, Zhang X, Pan J. The neutrophil percentage-to-albumin ratio is related to the occurrence of diabetic retinopathy. *J Clin Lab Anal*. (2022) 36:e24334. doi: 10.1002/jcla.24334

16. Famakin B, Weiss P, Hertzberg V, McClellan W, Presley R, Krompf K, et al. Hypoalbuminemia predicts acute stroke mortality: Paul Coverdell Georgia stroke registry. *J Stroke Cerebrovasc Dis*. (2010) 19:17–22. doi: 10.1016/j.jstrokecerebrovasdis.2009.01.015

17. Kang L, Yu H, Yang X, Zhu Y, Bai X, Wang R, et al. Neutrophil extracellular traps released by neutrophils impair revascularization and vascular remodeling after stroke. *Nat Commun*. (2020) 11:2488. doi: 10.1038/s41467-020-16191-y

18. Cui H, Ding X, Li W, Chen H, Li H. The neutrophil percentage to albumin ratio as a new predictor of in-hospital mortality in patients with ST-segment elevation myocardial infarction. *Med Sci Monit*. (2019) 25:7845–52. doi: 10.12659/MSM.917987

19. Yang D, Niu C, Li P, Du X, Zhao M, Jing W. Study of the neutrophil percentage-to-albumin ratio as a biomarker for predicting recurrence of first-episode ischemic stroke. *J Stroke Cerebrovasc Dis*. (2024) 33:107485. doi: 10.1016/j.jstrokecerebrovasdis.2023.107485

20. Zawiah M, Khan AH, Farha RA, Usman A, Al-Ashwal FY, Akkaif MA. Assessing the predictive value of neutrophil percentage to albumin ratio for ICU admission in ischemic stroke patients. *Front Neurol*. (2024) 15:1322971. doi: 10.3389/fneur.2024.1322971

21. Curtin LR, Mohadjer LK, Dohrmann SM, Kruszon-Moran D, Mirel LB, Carroll MD, et al. National Health and nutrition examination survey: sample design, 2007-2010. *Vital Health Stat*. (2013) 2:1–23.

22. Xie R, Zhang Y. Association between 19 dietary fatty acids intake and rheumatoid arthritis: results of a nationwide survey. *Prostaglandins Leukot Essent Fat Acids*. (2023) 188:102530. doi: 10.1016/j.plefa.2022.102530

23. Liu CF, Chien LW. Predictive role of neutrophil-percentage-to-albumin ratio (NPAR) in nonalcoholic fatty liver disease and advanced liver fibrosis in nondiabetic US adults: evidence from NHANES 2017-2018. *Nutrients*. (2023) 15:1892. doi: 10.3390/nu15081892

24. Yang L, Chen X, Cheng H, Zhang L. Dietary copper intake and risk of stroke in adults: a case-control study based on National Health and nutrition examination survey 2013-2018. *Nutrients*. (2022) 14:409. doi: 10.3390/nu14030409

25. Harshfield EL, Markus HS. Association of Baseline Metabolomic Profiles with Incident Stroke and Dementia and with imaging markers of cerebral small vessel disease. *Neurology*. (2023) 101:e489–501. doi: 10.1212/WNL.0000000000207458

26. Jenny NS, Callas PW, Judd SE, McClure LA, Kissela B, Zakai NA, et al. Inflammatory cytokines and ischemic stroke risk: the REGARDS cohort. *Neurology*. (2019) 92:e2375–84. doi: 10.1212/WNL.0000000000007416

27. Bustamante A, López-Cancio E, Pich S, Penalba A, Giralt D, García-Berrocoso T, et al. Blood biomarkers for the early diagnosis of stroke: the stroke-Chip study. *Stroke*. (2017) 48:2419–25. doi: 10.1161/STROKEAHA.117.017076

28. Katan M, Moon YP, Paik MC, Mueller B, Huber A, Sacco RL, et al. Procalcitonin and Midregional Proatrial natriuretic peptide as markers of ischemic stroke: the northern Manhattan study. *Stroke*. (2016) 47:1714–9. doi: 10.1161/STROKEAHA.115.011392

29. Tiedt S, Prestel M, Malik R, Schieferdecker N, Duering M, Kautzky V, et al. RNA-Seq identifies circulating miR-125a-5p, miR-125b-5p, and miR-143-3p as potential biomarkers for acute ischemic stroke. *Circ Res*. (2017) 121:970–80. doi: 10.1161/CIRCRESAHA.117.311572

30. Sun D, Tiedt S, Yu B, Jian X, Gottesman RF, Mosley TH, et al. A prospective study of serum metabolites and risk of ischemic stroke. *Neurology*. (2019) 92:e1890–8. doi: 10.1212/WNL.0000000000007279

31. Heshmatollah A, Fani L, Koudstaal PJ, Ghanbari M, Ikram MA, Ikram MK. Plasma β-amyloid, Total-tau, and Neurofilament light chain levels and the risk of stroke: a prospective population-based study. *Neurology*. (2022) 98:e1729–37. doi: 10.1212/WNL.0000000000200004

32. Lattanzi S, Cagnetti C, Provinciali L, Silvestrini M. Neutrophil-to-lymphocyte ratio predicts the outcome of acute intracerebral hemorrhage. *Stroke*. (2016) 47:1654–7. doi: 10.1161/STROKEAHA.116.013627

33. Artero A, Zaragoza R, Camarena JJ, Sancho S, González R, Nogueira JM. Prognostic factors of mortality in patients with community-acquired bloodstream infection with severe sepsis and septic shock. *J Crit Care*. (2010) 25:276–81. doi: 10.1016/j.jcrc.2009.12.004

34. Park JE, Chung KS, Song JH, Kim SY, Kim EY, Jung JY, et al. The C-reactive protein/albumin ratio as a predictor of mortality in critically ill patients. *J Clin Med*. (2018) 7:333. doi: 10.3390/jcm7100333

35. Idicula TT, Waje-Andreassen U, Brogger J, Naess H, Thomassen L. Serum albumin in ischemic stroke patients: the higher the better. *The Bergen Stroke Study Cerebrovasc Dis*. (2009) 28:13–7. doi: 10.1159/000215938

36. Halliwell B. Albumin—An important extracellular antioxidant? *Biochem Pharmacol*. (1988) 37:569–71. doi: 10.1016/0006-2952(88)90126-8

37. Dziedzic T, Pera J, Klimkowicz A, Turaj W, Slowik A, Rog TM, et al. Serum albumin level and nosocomial pneumonia in stroke patients. *Eur J Neurol*. (2006) 13:299–301. doi: 10.1111/j.1468-1331.2006.01210.x

38. Zhang H, Wu T, Tian X, Lyu P, Wang J, Cao Y. High neutrophil percentage-to-albumin ratio can predict occurrence of stroke-associated infection. *Front Neurol*. (2021) 12:705790. doi: 10.3389/fneur.2021.705790

39. Chen Z, Xie D, Li Y, Dai Z, Xiang S, Chen Z, et al. Neutrophil albumin ratio is associated with all-cause mortality in stroke patients: a retrospective database study. *Int J Gen Med*. (2022) 15:1–9. doi: 10.2147/IJGM.S323114

40. Cui T, Wang C, Zhu Q, Li S, Yang Y, Wang A, et al. Association between neutrophil percentage-to-albumin ratio and 3-month functional outcome in acute ischemic stroke patients with reperfusion therapy. *Front Neurol*. (2022) 13:898226. doi: 10.3389/fneur.2022.898226

41. Lv XN, Shen YQ, Li ZQ, Deng L, Wang ZJ, Cheng J, et al. Neutrophil percentage to albumin ratio is associated with stroke-associated pneumonia and poor outcome in patients with spontaneous intracerebral hemorrhage. *Front Immunol*. (2023) 14:1173718. doi: 10.3389/fimmu.2023.1173718

42. Zang SW, Long JJ, Wang Y. Neutrophil percentage to albumin ratio as a predictor for coronary slow flow phenomenon in patients with myocardial ischemia with no obstructive coronary arteries. *Int J Gen Med*. (2024) 17:3511–9. doi: 10.2147/IJGM.S477431

43. Liu Z, Dong L, Shen G, Sun Y, Liu Y, Mei J, et al. Associations of neutrophil-percentage-to-albumin ratio level with all-cause mortality and cardiovascular disease-cause mortality among patients with hypertension: evidence from NHANES 1999-2010. *Front Cardiovasc Med*. (2024) 11:1397422. doi: 10.3389/fcvm.2024.1397422

44. Zhao M, Huang X, Zhang Y, Wang Z, Zhang S, Peng J. Predictive value of the neutrophil percentage-to-albumin ratio for coronary atherosclerosis severity in patients with CKD. *BMC Cardiovasc Disord*. (2024) 24:277. doi: 10.1186/s12872-024-03896-x

frontiers | Frontiers in Neurology

TYPE Review
PUBLISHED 24 February 2025
DOI 10.3389/fneur.2025.1488726

OPEN ACCESS

EDITED BY
Haipeng Liu,
Coventry University, United Kingdom

REVIEWED BY
Xiaoyan Lan,
Affiliated Central Hospital of Dalian University of Technology, China
Oscar Salvador Barrera-Vázquez,
National Autonomous University of Mexico, Mexico
Gita Vita Soraya,
Hasanuddin University, Indonesia

*CORRESPONDENCE
Yuan Xu
✉ yuanxwh2024@126.com
Shimin Wu
✉ mintyrain@126.com

RECEIVED 30 August 2024
ACCEPTED 10 February 2025
PUBLISHED 24 February 2025

CITATION
Liang Y, Chen J, Chen Y, Tong Y, Li L, Xu Y and Wu S (2025) Advances in the detection of biomarkers for ischemic stroke.
Front. Neurol. 16:1488726.
doi: 10.3389/fneur.2025.1488726

Advances in the detection of biomarkers for ischemic stroke

Ying Liang[1], Juan Chen[1], Yue Chen[1], Yaoyao Tong[1], Linhao Li[1], Yuan Xu[2]* and Shimin Wu[1]*

[1]Center for Clinical Laboratory, General Hospital of the Yangtze River Shipping, Wuhan Brain Hospital, Wuhan, Hubei, China, [2]Center for Clinical Laboratory, Wuhan Hospital of Traditional Chinese Medicine, Wuhan, Hubei, China

Ischemic stroke is a leading cause of mortality and morbidity globally. Prompt intervention is essential for arresting disease progression and minimizing central nervous system damage. Although imaging studies play a significant role in diagnosing ischemic stroke, their high costs and limited sensitivity often result in diagnostic and treatment delays. Blood biomarkers have shown considerable promise in the diagnosis and prognosis of ischemic stroke. Serum markers, closely associated with stroke pathophysiology, aid in diagnosis, subtype identification, prediction of disease progression, early neurological deterioration, and recurrence. Their advantages are particularly pronounced due to their low cost and rapid results. Despite the identification of numerous candidate blood biomarkers, their clinical application requires rigorous research and thorough validation. This review focuses on various blood biomarkers related to ischemic stroke, including coagulation and fibrinolysis-related factors, endothelial dysfunction markers, inflammatory biomarkers, neuronal and axonal injury markers, exosomes with their circular RNAs and other relevant molecules. It also summarizes the latest methods and techniques for stroke biomarker detection, aiming to provide critical references for the clinical application of key stroke biomarkers.

KEYWORDS

stroke, biomarkers, inflammatory factors, axonal injury markers, clinical testing

1 Introduction

Stroke remains one of the leading causes of disability and mortality worldwide. According to the World Health Organization (WHO), stroke is the second leading cause of death globally, accounting for approximately 5.5 million deaths annually, with about half of the survivors experiencing long-term disability (1, 2). Among these, ischemic stroke constitutes approximately 80% of all stroke cases, primarily caused by the obstruction of cerebral blood vessels, leading to ischemia and hypoxia of brain tissue, and resulting in irreversible neuronal damage (3). Early diagnosis and timely treatment are crucial for reducing the disability and mortality rates among ischemic stroke patients (4, 5). Currently, the primary clinical treatment strategy for ischemic stroke is intravenous thrombolysis within the "golden window" to restore blood perfusion. However, some patients present with subtle or atypical symptoms, and the specificity of imaging-based assessments remains limited, leading to misdiagnosis, missed diagnoses, and delays in clinical decision-making. Therefore, there is an urgent need to establish novel laboratory-based rapid auxiliary diagnostic strategies (6).

Biomarkers are defined as measurable indicators that objectively reflect normal or pathological physiological processes or predict and assess responses to therapeutic interventions. In the context of ischemic stroke, biomarkers can provide insights into the pathophysiological mechanisms triggered by cerebrovascular occlusion, including inflammation, oxidative stress, and neuronal injury. They not only facilitate early diagnosis and subtype differentiation but also

serve as crucial tools for disease assessment, prognosis prediction, and individualized therapeutic decision-making (7). Compared to traditional imaging-based diagnostics, biomarker detection in blood or other bodily fluids is generally more cost-effective, technically less complex, and offers the potential for dynamic monitoring, making it an indispensable tool in clinical practice (8).

The study of stroke biomarkers has been extensively discussed in multiple reviews, yet existing literature often lacks a comprehensive evaluation of their clinical applications and associated challenges. This review aims to systematically summarize the currently identified biomarkers for ischemic stroke, evaluate their research status and detection methodologies, and explore unresolved critical issues and future research directions.

2 Pathogenesis of ischemic stroke

Acute ischemic stroke (AIS) primarily results from atherosclerosis, cardioembolism, small vessel disease, and other rare causes, such as hypercoagulable states, arterial dissection, and genetic disorders. Among these, atherosclerosis is the most common mechanism, characterized by lipid deposition, chronic inflammation, and endothelial dysfunction, leading to the formation of atherosclerotic plaques. Plaque rupture can trigger platelet aggregation and coagulation cascade reactions, ultimately leading to thrombosis and acute occlusion of cerebral arteries, resulting in symptoms such as cerebral ischemia, neuronal necrosis, and functional impairment (9).

The pathogenesis of ischemic stroke involves multiple pathological processes, among which thrombosis is a key mechanism (10). The rupture of atherosclerotic plaques exposes the subendothelial matrix, leading to platelet activation and coagulation factor recruitment, thereby triggering the coagulation cascade. This process results in thrombus formation and vascular occlusion. The coordinated interaction between platelet activation and fibrin formation is a critical pathological event, along with abnormal activation of the coagulation system. Glial cells also play a crucial role in cerebral ischemia (11). The activation of microglia and astrocytes exhibits spatiotemporal specificity. In the early phase, microglia predominantly exhibit a pro-inflammatory phenotype (M1), concurrently inducing astrocytes to transition into a pro-inflammatory subtype (A1). As the disease progresses, microenvironmental signals drive these cells toward an anti-inflammatory phenotype (M2 and A2), thereby facilitating tissue repair and neuronal functional recovery. During neuronal injury, astrocytes release glial fibrillary acidic protein (GFAP), which is closely associated with the severity of neuronal damage.

Within hours following a stroke, the ischemic brain tissue rapidly initiates an inflammatory response. Perivascular microglia and macrophages release various cytokines, including tumor necrosis factor-alpha (TNF-α) and interleukin-6. Neutrophil infiltration occurs within minutes of ischemic stroke onset and peaks between 24 and 72 h. Within 48 h, monocytes and lymphocytes are also recruited to the brain (12). Subsequently, activated microglia, macrophages, and infiltrating leukocytes release additional inflammatory mediators, including TNF-α and interleukins (IL-1β, IL-6), thereby initiating a sustained inflammatory response through the secretion of IL-8 and IL-6. This inflammatory cascade leads to increased levels of fibrinogen and C-reactive protein (CRP), as well as the upregulation of adhesion molecules, including members of the immunoglobulin superfamily such as intercellular adhesion molecule-1 (ICAM-1) and vascular cell adhesion molecule-1 (VCAM-1) (13). Additionally, pro-inflammatory factors enhance matrix metalloproteinase (MMP) activity, further disrupting the blood–brain barrier (BBB), exacerbating cerebral edema, and promoting neuronal damage. Notably, MMP-9 levels significantly increase following stroke, contributing to extracellular matrix degradation and leukocyte infiltration, thereby amplifying the inflammatory response (Figure 1).

Thus, the pathogenesis of ischemic stroke involves multiple pathological pathways and bioactive molecules, many of which can serve as diagnostic and prognostic biomarkers. Based on their respective pathophysiological roles, these biomarkers can be broadly categorized into coagulation and fibrinolysis-related factors, endothelial dysfunction markers, inflammatory biomarkers, neuronal and axonal injury markers, and other relevant molecules (Table 1).

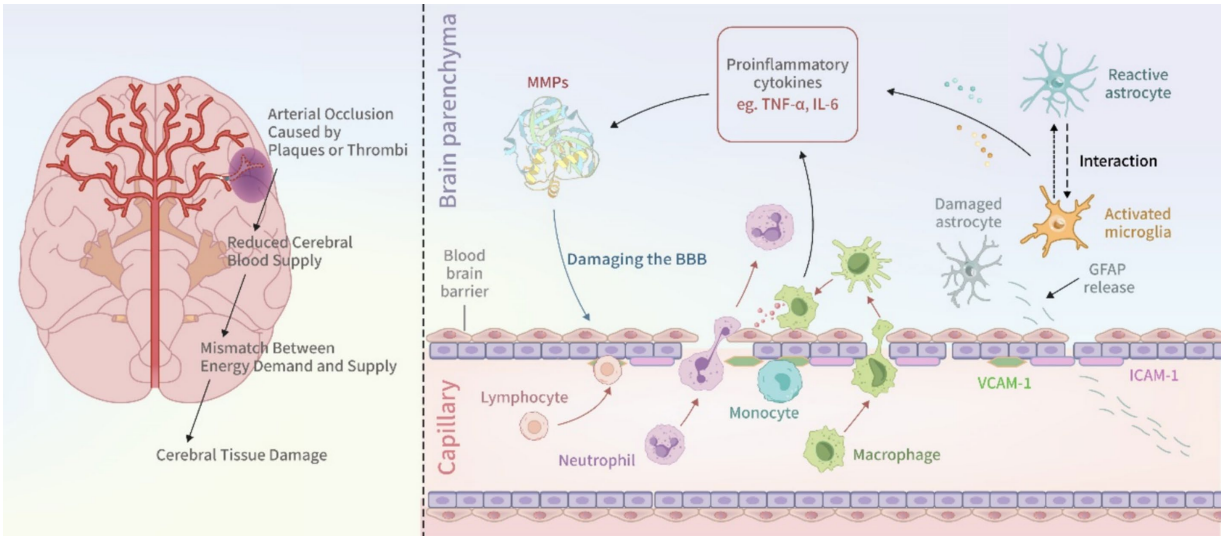

FIGURE 1
Pathogenesis of ischemic stroke.

TABLE 1 Biomarkers for stroke detection.

Mechanism	Biomarker	Sample size	Clinical significance	Current clinical validation stage	References
Coagulation and fibrinolysis-related factors	Prothrombin, plasminogen, fibrinogen alpha-chain, and histidine-rich glycoprotein	95	Diagnostic	Prothrombin and plasminogen have been widely used for routine testing, while others are still under exploratory research	(19)
	Ceruloplasmin, α-1-antitrypsin (SERPINA1), vWF, and coagulation factor XIII B chain (F13B)	60	Diagnostic		(20)
Endothelial dysfunction-related biomarkers	ICAM-1, VCAM-1	131	Diagnostic	Exploratory research stage	(23)
	ICAM-1	69	Diagnostic		(24)
		286	Prognosis		(25)
		118	Prognosis		(27)
		113	Prognosis		(28)
	VCAM-1	38	Prognosis		(29)
	VWF	90	Diagnostic		(30)
		40	Diagnostic		(31)
Inflammatory markers	hsCRP	9,438	Prognosis	MMP-9 and HGMB-1are still under exploratory research, while others have been widely used for routine testing.	(35)
	IL-6, IL-1 β, IL-8, TNF-α, and hsCRP	680	Diagnosis and prognosis		(36)
	IL-6, CRP, WBC	138	Prognosis		(37)
	hsCRP, IL-6, Ferritin, ESR, and WBC	321	Prognosis		(38)
	hs-CRP,IL-6,TNF-α	588	Diagnostic and Prognostic		(39)
	MMP-9	60	Diagnostic		(41)
		62	Diagnostic		(42)
		3,186	Prognosis		(43)
	HGMB-1	183	Prognosis		(46)
		42	Prognosis		(47)
		544	Prognosis		(48)
Neuronal and axonal injury markers	GFAP, UCH-L1	251	Diagnostic	Exploratory research stage	(21)
	RBP-4, NT-proBNP, and GFAP	189	Diagnostic		(52)
	GFAP	155	Diagnostic		(53)
	GFAP and NT-proBNP	200	Diagnostic		(55)
	NfL	595	Prognosis		(55)
		211	Prognosis		(56)
		30	Prognosis		(57)
	MBP	83	Diagnostic		(60)
Exosomes and their circular RNA	lnc-CRKL-2, lnc-NTRK3-4, RPS6KA2-AS1and lnc-CALM1-7	200	Diagnostic	Exploratory research stage	(59)
	circFUNDC1	30	Diagnostic		(60)
	Exosomal circ_0043837 and circ_0001801	621	Diagnostic		(61)
	Exosomal Mir-134	10,172	Diagnostic		(62)
	Exosomal microRNA-21-5p and microRNA-30a-5p	167	Diagnostic		(63)
	exo-lnc_000048, exo-lnc_001350 and exo-lnc_016442	602	Diagnostic		(64)
Others	NETs	243	Prognosis	Exploratory research stage	(70)
		95	Diagnostic		(17)
		54	Prognosis		(71)
		101	Prognosis		(72)
		235	Prognosis		(73)

It is important to note that the pathophysiological processes of ischemic stroke exhibit distinct temporal dynamics. Specifically, in the hyperacute phase (<6 h), acute phase (6–72 h), and subacute phase (>72 h), different blood biomarkers display varying sensitivities and specificities (14). Therefore, the temporal dependency of biomarker expression must be carefully considered in both research and clinical applications to achieve more precise diagnostic and prognostic evaluations. For example, IL-6 levels begin to rise within hours after stroke onset, and persistently elevated IL-6 levels in the subacute phase may indicate ongoing inflammatory injury (15, 16). Similarly, GFAP is released progressively within 12 h post-stroke, making it a valuable biomarker for predicting intracranial pathology in both the hyperacute and acute phases. Furthermore, neutrophil extracellular traps (NETs) exhibit rapid fluctuations following thrombolysis or mechanical thrombectomy, providing insights into reperfusion status and aiding in the identification of futile recanalization (17).

3 Biomarkers associated with ischemic stroke

3.1 Coagulation and fibrinolysis-related factors

The coagulation and fibrinolysis systems are pivotal in the pathophysiology of stroke. Detecting related factors is vital for the early diagnosis and treatment of stroke. Biomarkers such as thrombin-antithrombin complex (TAT), tissue plasminogen activator inhibitor complex (t-PAIC), activated partial thromboplastin time (APTT), prothrombin time (PT), fibrinogen (FIB), D-dimer, and fibrin degradation products (FDP) reflect dynamic changes in thrombosis and fibrinolytic activity, aiding clinical decision-making. Elevated D-dimer levels indicate active fibrinolysis, commonly used to assess thrombus burden and prognosis in stroke patients. Ohara et al. highlighted that serum D-dimer assists in diagnosing cryptogenic stroke and secondary prevention, with continuous monitoring enhancing the efficacy of antithrombotic treatment in cryptogenic stroke (18). Lee et al., through proteomics, identified four candidate biomarkers—prothrombin, plasminogen, fibrinogen alpha chain, and histidine-rich glycoprotein—with AUC values over 0.9, confirming their diagnostic value related to coagulation mechanisms (19). Misra et al. used SWATH-MS-based proteomics to identify ceruloplasmin, α-1-antitrypsin (SERPINA1), von Willebrand factor (vWF), and coagulation factor XIII B chain (F13B) as effective biomarkers for distinguishing total stroke, ischemic stroke, and intracerebral hemorrhage (ICH) from healthy controls (20). Bioinformatics suggested common pathways in stroke cases, including complement and coagulation cascades, platelet degranulation, immune processes, and acute phase reactions (21).

3.2 Endothelial dysfunction-related biomarkers

Endothelial dysfunction can lead to dysregulation of vascular endothelial cell function, further exacerbating cerebral blood flow reduction and tissue damage.

3.2.1 ICAM-1 and VCAM-1

ICAM-1 and VCAM-1 belong to the immunoglobulin superfamily and are primarily expressed on the surface of endothelial cells. Following ischemic injury, elevated levels of pro-inflammatory cytokines induce the expression of ICAM-1 and VCAM-1 in the endothelial cells of the blood–brain barrier (BBB), thereby mediating neuroinflammation (22). Elevated levels of ICAM-1 and VCAM-1 have been detected in the blood and infarct regions of stroke patients (23). Studies suggest that ICAM-1 may serve as a potential prognostic biomarker for AIS. Nielsen et al. evaluated ICAM-1 levels in AIS patients and found that they were significantly elevated within <8 h of stroke onset, whereas S100B and E-selectin levels showed no significant changes (24). Additionally, Wang et al. reported that the sensitivity and specificity of serum ICAM-1 in predicting AIS were 74 and 76%, respectively (25). Moreover, the rs5498 polymorphism of ICAM-1 has been associated with an increased risk of ischemic stroke in Caucasian populations (26). Furthermore, the combined detection of ICAM-1 and CRP has been shown to predict the 3-month prognosis of AIS patients (27). However, some studies have failed to establish a significant correlation between soluble ICAM-1 and stroke prognosis (28). In contrast, VCAM-1 levels have been proposed as a predictor of stroke prognosis, although they do not correlate with infarct volume or disability severity (29). Overall, the diagnostic and prognostic value of ICAM-1 and VCAM-1 in ischemic stroke remains incompletely understood, necessitating further research and clinical validation.

3.2.2 von Willebrand factor

VWF is a multimeric glycoprotein secreted by endothelial cells and megakaryocytes, primarily involved in platelet adhesion and blood coagulation. Sabbah et al. found that serum VWF levels were significantly elevated in patients with AIS compared to control groups. Elevated plasma VWF levels were observed in patients with acute ischemic atherosclerotic stroke, suggesting that serum VWF levels could serve as a biomarker for AIS, particularly for the atherosclerotic subtype (30).

Sharma et al., through proteomic studies, also identified VWF as useful in distinguishing total stroke, ischemic stroke, and intracerebral hemorrhage (ICH) from healthy controls. Changes in its concentration may lead to endothelial dysfunction and are associated with inflammation and endothelial dysfunction in AIS patients, making it a novel candidate protein (31). Steliga et al. also summarized that VWF could serve as a diagnostic biomarker for AIS (32). Baez et al. included 12 articles involving blood combinations of stroke protein biomarkers and proposed a new biomarker combination model (NR2 + GFAP + MMP-9 + VWF + S100β) involving VWF for the early diagnosis of ischemic stroke subtypes (33). Moreover, VWF is considered an effective biomarker for predicting the risk of death in ischemic stroke patients. Kawano et al. found that elevated VWF levels are an independent predictor of mortality within 1 year after stroke onset (34). Further research on these biomarkers and their roles in the pathophysiology of ischemic stroke is crucial for improving patient prognosis and developing targeted therapeutic strategies.

3.3 Inflammatory markers

C-reactive protein (CRP), as an acute-phase protein, serves not only as an indicator of systemic inflammation but also as a

crucial biomarker for evaluating prognosis post-stroke. Elevated CRP levels are associated with poor outcomes in stroke patients and reflect the systemic inflammatory state (35). IL-6 plays a key role in immune regulation within the central nervous system, while TNF-α exacerbates brain tissue damage by inducing apoptosis and promoting inflammatory responses (36).

Lasek-Bal et al. reported that IL-6 levels on the first day after stroke could predict acute neurological and functional status, while increased CRP and leukocyte counts were associated with worse acute stroke prognosis (37). Reiche et al. studied two composite indices reflecting inflammation levels—INFLAM Index 1 (comprising the z-scores of hsCRP, IL-6, ferritin, ESR, and WBC) and INFLAM Index 2 (derived by subtracting the z-score of 25(OH) D from INFLAM Index 1 and adding the z-scores of iron and TSP). These indices demonstrated significant predictive value for AIS in both healthy volunteers and AIS patients, with AUC values of 0.851 and 0.870, respectively. They also identified redox imbalance related to IL-6 signaling as a potential target for preventing short-term mortality in AIS (38). Ma et al. developed diagnostic and prognostic models for ischemic stroke using inflammatory markers such as hs-CRP, IL-6, and TNF-α, which were validated in additional cohorts (39).

Matrix metalloproteinase-9 (MMP-9) plays a crucial role in degrading components of the extracellular matrix, activating pro-inflammatory cytokines, and compromising the integrity of the blood–brain barrier (BBB). The activation of M1-polarized microglia has been shown to upregulate MMP-9 expression, leading to BBB disruption and ischemic brain injury (40). Abdelnaseer et al. reported that serum MMP-9 levels within 24 h of stroke onset were significantly correlated with clinical stroke severity (41). Similarly, Weekman et al. demonstrated a positive association between MMP-9 levels and infarct volume, with the strongest correlation observed within the first 6 hours post-stroke. Notably, MMP-9 is considered the only biomarker capable of precisely predicting the final infarct volume, where higher MMP-9 expression is linked to larger infarct areas (42). Further research by Zhong et al. revealed that elevated serum MMP-9 levels in the acute phase of ischemic stroke were positively correlated with mortality and severe disability within 3 months post-stroke (43). These findings suggest that targeted inhibition of MMP-9 activity may serve as a promising therapeutic strategy to mitigate brain injury and improve stroke prognosis (44).

High mobility group box 1 (HMGB1) has been identified as a potential diagnostic and prognostic biomarker for ischemic stroke (45). A study by Tsukagawa demonstrated that serum and plasma HMGB1 levels were significantly elevated in patients with ischemic stroke (46). Moreover, Sapojnikova et al. reported a strong correlation between MMP-9 and HMGB1 levels in stroke patients, with both biomarkers closely associated with poor prognosis (47). Similarly, Shen et al. found that elevated serum HMGB1 levels served as a reliable predictor of AIS recurrence (48). However, it is important to note that HMGB1 exhibits a complex biphasic role in the pathogenesis and progression of ischemic stroke. In the hyperacute and acute phases (within 4–5 days post-stroke), HMGB1 functions as a pro-inflammatory mediator, exacerbating neuronal death and blood–brain barrier disruption. Conversely, in the late acute, subacute, and chronic phases (>3 weeks post-stroke), HMGB1 contributes to vascular remodeling and neurofunctional recovery (49).

3.4 Neuronal and axonal injury markers

Ischemic stroke leads to increased blood–brain barrier permeability and the release of neuronal and axonal injury biomarkers, such as GFAP, neurofilament light chain protein (NFL), and S100 proteins. These markers are rapidly released into the blood following brain tissue injury, with their levels accurately reflecting the extent of brain damage and providing crucial prognostic information. Luger et al. conducted a study to assess the diagnostic accuracy of serum GFAP and ubiquitin carboxy-terminal hydrolase L1 (UCH-L1) concentrations, measured using ELISA, in differentiating between acute cerebral hemorrhage and ischemic stroke. The results indicated that the area under the curve (AUC) for GFAP was 0.866, surpassing the 0.590 AUC for UCH-L1 (21). Bustamante et al. validated a panel of blood biomarkers, including RBP-4, NT-proBNP, and GFAP, which distinguished IS from ICH with moderate accuracy at 100% specificity (50). Kalra et al. tested the diagnostic accuracy of GFAP in a prospective cohort of stroke patients in India. Using the highly sensitive SIMOA technology, GFAP concentrations were measured within 12 h of admission in acute stroke patients. ROC analysis identified an optimal GFAP threshold of 0.57 μg/L for distinguishing intracerebral hemorrhage from ischemic stroke and stroke mimic conditions (AUC 0.871 [95% CI 0.810–0.933], $p < 0.001$) (51). Recently, a systematic review confirmed the high diagnostic accuracy of blood GFAP levels as a discriminative test for cerebral hemorrhage and ischemic stroke (52). Additionally, Lee et al. developed a time-resolved fluorescence lateral flow immunoassay (TRF-LFIA) utilizing europium nanoparticle (EuNP)-conjugated specific monoclonal antibodies targeting NT-proBNP and GFAP for simultaneous quantification. The combination of GFAP and NT-proBNP was determined to be the most effective biomarker pair for differentiating IS from HS based on an algorithm (53). In summary, the use of blood biomarkers, particularly GFAP, holds promise for the diagnosis and differentiation of ischemic stroke and cerebral hemorrhage. Further research is necessary to validate these findings and establish standardized protocols for measuring acute stroke biomarkers.

Neurofilament light chain (NfL) levels have been shown to be a robust biomarker in cerebrospinal fluid (CSF) for neuronal damage and neurodegeneration. Several studies have demonstrated the potential of NfL as a blood biomarker for ischemic stroke. Sanchez et al. conducted a systematic review and meta-analysis, including 19 studies that reported serum/plasma NfL values from a total of 4,237 different stroke patients, to evaluate the utility of blood NfL as a diagnostic, prognostic, and monitoring biomarker for stroke. They found that blood NfL levels varied significantly across three different time periods: acute (0–7 days), subacute (9–90 days), and chronic (>90 days) phases of stroke, with a sharp peak observed in the early subacute phase, 14 to 21 days post-stroke. Additionally, blood NfL can serve as a diagnostic biomarker for differentiating AIS from transient ischemic attacks and other cerebrovascular subtypes (54). Pedersen et al. included 595 ischemic stroke cases in their study to investigate the correlation between serum NfL concentrations at different time points post-stroke. They found that NfL could predict neurological and functional outcomes in both the acute phase (range 1–14 days, median 4 days) and the long-term (cases followed up after 3 months) (55). Uphaus et al. also highlighted NfL as a biomarker for predicting cerebrovascular function 90 days post-ischemic stroke (56). Barba et al. explored the relationship between

serum NfL concentrations and clinical outcomes in patients with AIS, finding that patients with higher NfL levels showed less clinical improvement post-treatment. In patients with moderate to severe AIS, serum NfL levels were correlated with clinical and radiological scores at different time points and were predictive of short-term and intermediate-term clinical outcomes (57).

Myelin basic protein (MBP) is a membrane protein synthesized by oligodendrocytes that plays a crucial role in stabilizing myelin structure and is highly specific to neural tissue. In cases of brain injury, myelin damage leads to the release of MBP into the bloodstream, resulting in elevated serum levels. The concentration of MBP in the blood serves as an indicator of central nervous system injury. Studies have shown that serum MBP levels in patients with AIS are positively correlated with infarct volume, suggesting its potential as a biomarker for brain injury assessment (58).

3.5 Exosomes and their circular RNA

Exosomes are nanoscale extracellular vesicles secreted by most cells, capable of crossing the blood–brain barrier and transferring various bioactive molecules between cells. They facilitate intercellular communication and are closely associated with the occurrence and progression of various diseases. Exosomes, particularly the functional substances they carry, play a crucial role in the pathogenesis and recovery process of ischemic stroke by affecting the neurovascular unit. Following an ischemic stroke event, various types of cells, including peripheral blood cells, endothelial cells, and brain cells, release exosomes. These exosomes can traverse the blood–brain barrier and be detected in cerebrospinal fluid and peripheral blood. Consequently, exosomes are increasingly recognized as potential biomarkers for the early diagnosis and prognosis of IS.

Xu et al. demonstrated that long non-coding RNAs (lncRNAs) such as lnc-CRKL-2, lnc-NTRK3-4, RPS6KA2-AS1, and lnc-CALM1-7, isolated from the serum of acute stroke patients, are significantly elevated (59). Bai et al. isolated exosomes from serum samples of IS patients and normal controls, finding elevated expression of circFUNDC1 in exosomes derived from IS patients' serum. Receiver operating characteristic (ROC) analysis revealed an area under the curve (AUC) of 0.882 for circFUNDC1, indicating its high sensitivity and specificity as a diagnostic biomarker for IS (60). Xiao et al., through exosome circular RNA sequencing, large-sample validation, and diagnostic model construction, identified exosomal circ-0043837 and circ-0001801 as independent predictors of large-artery atherosclerosis (LAA) stroke. These circular RNAs showed significantly higher expression levels compared to controls, with diagnostic accuracies of AUC = 0.89 and AUC = 0.91, respectively, surpassing the diagnostic performance of plasma circular RNAs (61). Zhou et al. found that levels of miR-134 and miR-223 in exosomes from IS patients were significantly higher than those in non-ischemic stroke patients. Additionally, these levels correlated positively with NIHSS scores ($r = 0.65$, $p < 0.01$) and infarct volume ($r = 0.68$, $p < 0.01$), suggesting that miR-134 and miR-223 have potential diagnostic value for assessing the occurrence and severity of IS (62).

Exosomes are not only useful for the early diagnosis of IS but also help distinguish between different stages of the disease. Wang et al. found that, compared to controls, plasma exosomes in subacute and recovery-phase stroke patients showed significantly elevated levels of miRNA-21-5p, while exosomal miR-30a-5p was significantly higher in ultra-early stroke patients but lower than in controls during the acute phase. Furthermore, early diagnosis of large-artery atherosclerosis (LAA), which is associated with the worst prognosis, is particularly crucial (63). Zhang et al. observed significant increases in exosomal lnc_000048, lnc_001350, and lnc_016442 in LAA patients, with levels rising with stroke severity and showing better predictive capability for prognosis than NIHSS scores (64).

In recent years, multiple studies have demonstrated significant alterations in the expression of specific exosomal miRNAs in patients with AIS. Several miRNAs exhibit upregulated expression in AIS, including exosomal miR-212/132, miR-21, miR-9, miR-124, miR-134, and miR-223. In contrast, the expression level of exosomal miR-126 is downregulated in AIS patients (62, 65–68). These distinct miRNA expression patterns not only provide insights into the pathophysiological mechanisms of AIS but also hold potential clinical value as biomarkers for early diagnosis and disease assessment.

3.6 Other biomolecules

NETs are web-like structures released by neutrophils, primarily composed of free DNA, nucleosomes, and citrullinated histone H3 (citH3). NETs play a crucial role in the onset and progression of AIS. Studies have shown that NETs exacerbate early blood–brain barrier (BBB) disruption in AIS, increasing its permeability and potentially facilitating inflammatory cell infiltration, thereby aggravating neuronal damage (69). Research by Vallés et al. revealed that plasma NET levels in AIS patients were significantly higher than those in healthy individuals (70). Similarly, Lim et al. reported a marked increase in NET levels in AIS patients, and receiver operating characteristic (ROC) curve analysis demonstrated that the area under the curve (AUC) for double-stranded DNA (dsDNA) in early AIS diagnosis reached 0.859, suggesting its potential as an early diagnostic biomarker for AIS (17). Beyond its diagnostic implications, NETs are also closely associated with AIS severity and prognosis. Studies indicate that NET levels in thrombi and peripheral blood can reflect stroke severity and effectively predict short-term patient outcomes (71). Additionally, NETs may influence treatment responses in AIS. Evidence suggests that NETs could serve as prognostic biomarkers for futile recanalization following intravenous thrombolysis or mechanical thrombectomy. Arnaud et al. found that NETs were universally present in AIS thrombi, with all patients exhibiting NET-containing clots. High NET content in thrombi was correlated with failed recanalization, prolonged procedure time, and poorer stroke outcomes as assessed by the National Institutes of Health Stroke Scale (NIHSS) and modified Rankin Scale (mRS) scores (72). Moreover, analysis by Chen et al. demonstrated that the enrichment of NETs affects thrombus mechanical properties, potentially influencing the success rate of mechanical thrombectomy. Lower NET levels were significantly associated with higher rates of initial vascular recanalization (73).

To provide a more intuitive overview of these biomarkers and their roles, we present a summary table outlining their specific functions and recent research progress in ischemic stroke (Table 1).

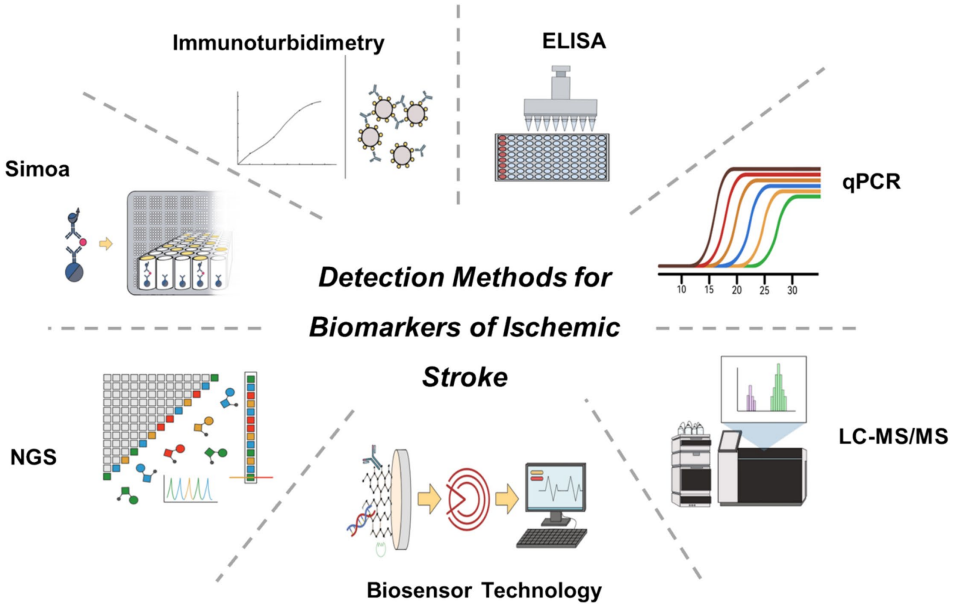

FIGURE 2
Common detection methods for ischemic stroke-related biomarkers.

4 Detection methods for ischemic stroke-related biomarkers

Currently, common diagnostic methods for stroke biomarkers in clinical practice include enzyme-linked immunosorbent assay (ELISA), quantitative real-time PCR (qPCR), liquid chromatography-tandem mass spectrometry (LC-MS/MS), immunoturbidimetry, next-generation sequencing (NGS), single-molecule array (Simoa), and biosensing technologies (Figure 2). This paper summarizes the advantages, disadvantages, and clinical applications of various detection methods (Table 2).

4.1 Enzyme-linked immunosorbent assay

ELISA is a widely used method for detecting protein levels in body fluids, characterized by high sensitivity and specificity. It utilizes antigen–antibody reactions, with enzyme-labeled antibodies to detect target proteins. ELISA is suitable for detecting various stroke-related biomarkers, such as CRP (74–76), IL-6 (43, 74, 75), TNF-α (75, 76), ICAM-1, MMP-9 (43, 75), VCAM-1 (77, 78), GFAP[53] (79, 80), and S100[53] (81). The advantages of ELISA include simplicity of operation, good reproducibility, and the ability to detect multiple samples simultaneously. However, its disadvantages are longer detection time and higher costs.

4.2 Quantitative real-time PCR

qPCR is a technique used to quantify RNA levels by labeling PCR amplification products with fluorescent dyes and monitoring the fluorescence signal changes in real-time. It is suitable for detecting genetic biomarkers like miRNA and lncRNA. The advantages of qPCR include high sensitivity, strong specificity, and accurate quantification, capable of detecting low-abundance RNA molecules (82–84). However, qPCR requires high-quality RNA samples, is complex to operate, and has high costs.

4.3 Liquid chromatography-mass spectrometry

LC–MS/MS combines the separation capabilities of liquid chromatography with the high sensitivity of mass spectrometry. It is used to detect metabolites such as fatty acid derivatives, amino acids, and oxidative stress markers like 3-nitrotyrosine nitrated fibrinogen (85), 8-iso-PGF2α (86), and MDA (87). The advantages of LC–MS/MS are high sensitivity, strong specificity, and the ability to detect multiple metabolites simultaneously, making it a key tool in metabolomics research. However, LC–MS/MS equipment is expensive, the operation is complex, and it requires professional technicians.

4.4 Immunoturbidimetry

Immunoturbidimetry measures the turbidity changes in a solution due to antigen–antibody complex formation, quantifying protein biomarkers in blood. It is suitable for detecting coagulation and fibrinolysis system-related factors such as D-dimer, FIB, TAT, t-PAIC, APTT, PT, FDP, and SAA (88, 89). The advantages of immunoturbidimetry include rapid detection, ease of operation, and lower costs, but its sensitivity and specificity are relatively lower.

TABLE 2 Comparison of detection methods for ischemic stroke-related biomarkers.

Detection method	Advantages	Limitations	Clinical significance	Clinical application status
ELISA	High sensitivity and specificity; simple operation; capable of detecting multiple biomarkers simultaneously.	Long detection time; high cost.	Commonly used for detecting inflammatory biomarkers such as CRP, IL-6, and TNF-α; suitable for large-scale studies and clinical validation.	Widely applied in clinical practice.
qPCR	High sensitivity; suitable for detecting low-abundance RNA molecules; accurate quantification.	High sample quality requirements; complex operation; relatively high cost.	Used for detecting genetic biomarkers such as miRNA and lncRNA; an essential tool in molecular biology research.	
LC–MS/MS	High sensitivity and specificity; capable of detecting multiple metabolites simultaneously.	Expensive equipment; complex operation; requires specialized technical support.	Widely used in metabolomics research (e.g., oxidative stress biomarker MDA detection); limited clinical translation.	
Immunoturbidimetry	Simple and rapid operation; relatively low cost.	Lower sensitivity and specificity.	Commonly used for rapid detection of coagulation and fibrinolysis system biomarkers (e.g., D-dimer); suitable for preliminary clinical screening.	
Simoa	Ultra-high sensitivity; simultaneous detection of multiple biomarkers; capable of detecting femtomolar concentrations.	High cost; requires specialized equipment.	Suitable for detecting neuronal injury biomarkers such as GFAP and NFL; plays an important role in early stroke diagnosis and prognosis assessment.	
NGS	High sensitivity and specificity; high throughput; automated; applicable to various biological samples.	High cost limits widespread application; complex data analysis; risk of false positives/negatives.	Used for detecting genetic mutations, vascular injury biomarkers, and epigenetic factors (e.g., miRNA, circRNA); facilitates precision diagnosis, classification, and novel biomarker discovery.	
Biosensors	High sensitivity; real-time detection; highly portable; suitable for point-of-care testing.	Susceptible to environmental interference; complex readout technology.	Has potential for on-site diagnosis of acute stroke; suitable for rapid detection of biomarkers such as GFAP.	Still in preclinical research stage.

10.3389/fneur.2025.1488726

4.5 Next-generation sequencing

NGS is a high-throughput DNA sequencing technology used for comprehensive analysis of genomes, transcriptomes, and epigenomes. It can detect DNA methylation states and RNA expression profiles, suitable for studying complex genetic biomarkers (90, 91). The advantages of NGS include high throughput, strong sensitivity, and specificity, and the ability to detect thousands of genes and their regulatory elements simultaneously. However, NGS equipment and operating costs are high, data analysis is complex, and it requires professional bioinformatics support.

4.6 Single-molecule array

Simoa is a breakthrough in biomarker detection due to its extremely high sensitivity and specificity. This technology combines single-molecule immunocapture with fluorescence detection, capable of detecting extremely low concentrations of biomarkers, making it advantageous in stroke biomarker detection. Simoa's core lies in its ability to capture and detect single target molecules in each reaction well, significantly enhancing detection sensitivity. Compared to traditional ELISA, Simoa can detect biomarkers at femtomolar levels. Simoa has been used to detect neuronal injury markers such as GFAP, NFL, and S100, which are rapidly released into the blood after brain tissue injury, providing crucial information for prognosis assessment (92–94).

Recent research has expanded the application of Simoa in stroke biomarker detection, developing multiplex detection platforms for simultaneous detection of multiple inflammatory and neuronal injury markers, improving detection efficiency and data reliability. Onatsu et al. utilized Simoa to analyze the NfL levels in 136 patients with AIS, discovering that the presence and extent of axonal injury estimated by NfL were correlated with the final infarct volume (95). Mattila et al. measured the GFAP levels and release rates in patients with acute cerebral ischemia using the Simoa method, finding that for patients with acute cerebral ischemia, prehospital sampling within 3 h combined with a specific rule (prehospital GFAP >410 pg./mL or prehospital GFAP 90–410 pg./mL combined with GFAP release >0.6 pg./mL/min) exhibited high specificity (NPV 98.4%) in 68% of acute cerebral ischemia patients (96).

4.7 Advances in biosensing technologies for stroke biomarker detection

Recent years have seen significant progress in the application of biosensing technologies for stroke biomarker detection, showing great potential and prospects. Biosensors combine biological recognition elements with physical sensors, converting biological molecules into detectable signals, enabling high sensitivity, rapid, and on-site detection, playing a key role in early diagnosis, condition monitoring, and personalized treatment of stroke.

4.7.1 Electrochemical biosensors

Electrochemical biosensors detect biological molecules' interactions with electrode surfaces to produce electrical signals, achieving high sensitivity detection. Rodríguez-Penedo et al. (97) developed a method for on-site GFAP detection using microcentrifuge tubes through electrochemical means, enabling rapid detection of hemorrhagic stroke biomarkers. These electrochemical biosensors provide high accuracy results in a short time, suitable for on-site acute stroke diagnosis.

4.7.2 Optical biosensors

Optical biosensors leverage optical signal transduction mechanisms to enhance the sensitivity and specificity of biomarker detection. These sensors employ fluorescence detection, surface plasmon resonance (SPR), or colorimetric analysis to convert biomolecular interactions into quantifiable optical signals, significantly improving detection accuracy and real-time monitoring capabilities. Due to their high sensitivity and rapid response characteristics, optical biosensors are particularly suitable for early diagnosis of ischemic stroke and continuous biomarker monitoring.

4.7.3 Microfluidic biosensors

Microfluidic biosensors use microfluidic technology to achieve biomarker detection. Sayad et al. developed a magneto-impedance-based microfluidic platform for detecting GFAP in blood, classifying acute stroke subtypes (98). This platform integrates microfluidic technology and magneto-impedance biosensors, providing high sensitivity and specificity in GFAP detection, offering a new method for early stroke diagnosis and classification.

4.7.4 Comparison of biosensing technologies for AIS

To provide a clearer comparison of biosensing technologies used for detecting biomarkers in AIS, we have summarized the detection mechanisms, readout methods, and diagnostic performance of various biosensors (Table 3).

5 Conclusion

Biomarkers play a crucial role in the diagnosis, prognostic assessment, and therapeutic monitoring of ischemic stroke. However, despite extensive research identifying numerous stroke-related biomarkers, their clinical application remains limited by several challenges, including insufficient specificity, complex dynamic variations, labor-intensive detection methods, and a lack of standardization. An ideal stroke biomarker should possess characteristics similar to cardiac troponin T (cTnT) in myocardial infarction—accurately reflecting pathophysiological changes while being detectable through rapid, efficient, and precise methods suitable for clinical use.

Currently, ischemic stroke biomarkers primarily include inflammatory factors, neuronal injury proteins, and coagulation and fibrinolysis-related factors. However, these biomarkers typically represent only specific aspects of the pathological process rather than the entire disease course. Additionally, individual variations in stroke etiology limit the clinical applicability of single biomarkers. One promising future research direction is the integration of multi-omics data to identify core biomarkers that dynamically reflect stroke progression. Furthermore, the development of multiplex biomarker panels combining inflammatory, coagulation, neuronal injury, and

TABLE 3 Comparison of biosensors for AIS diagnosis.

Sensor	Biomarker	Detection range	Limit of detection (LOD)	Core mechanism	References
Electrochemical biosensors	CRP	0.01–5.0 μg/mL	0.008 μg/mL	Dual Magnetic Antibody Capture	(99)
	GFAP	10–1,000 pg/mL	3 pg/mL	Antibody Capture	(100)
	S100β	0.05–1 ng/mL	0.35 pg/mL	Au@AgNPs-Modified Antibody Capture	(101)
Optical biosensors	CRP	0.889–20.7 μg/mL	1.2 μg/mL	Aptamer-mediated gold nanoparticle (AuNP) aggregation	(102)
	GFAP	1 pg/mL to 50 ng/mL	1 pg/mL	Thionin acetate as a Raman reporter gene, AuNRs as a SERS probe	(103)
	MMP-9	0.05-20 μg/mL	0.05 ng/mL	Optical Interference-Free Surface-Enhanced Raman Scattering CO-Nanotags	(104)
	TNF-α/GFAP	/	0.023 pg/mL; 0.018 pg/mL	Gold nanorod array substrate based on surface-enhanced Raman scattering	(105)
	TNF-α	/	1 pg/mL	A magnetic bead pull-down assay with purified and highly Raman-active gold nanoparticle clusters	(106)
	MMP-9, IL-6, GFAP, IL-1β, TNF-α	/	0.21 pg/mL, 0.153 pg/mL, 0.106 pg/mL, 0.125 pg/mL, 0.15 pg/mL	5,5′-dithiobis-2-nitrobenzoic acid (DTNB) antibody-modified gold nanoparticles (AuNPs) on SERS devices as SERS probes	(107)
Microfluidic biosensors	GFAP	0.15–0.59 ng/mL	0.01 ng/mL	Magnetic labeling to capture GFAP	(98)
	CRP	/	0.1–50 mg/L	Integrated with Field-effect transistor (FET) sensor	(108)
	IL-6, GFAP, IL-8	/	437 pg/mL; 125 pg/mL; 2 pg/mL	Microbead-Based Quantum Dot-Linked Immunosorbent Assay	(109)

metabolic markers may enhance diagnostic sensitivity and specificity. Incorporating imaging modalities and clinical scoring systems, such as the National Institutes of Health Stroke Scale (NIHSS), could further improve the clinical utility of biomarkers.

Beyond biomarker discovery, advancements in detection technologies will be critical for their successful clinical implementation. Current methodologies, including ELISA, qPCR, and LC–MS/MS, are widely used in research but face challenges such as complexity, lengthy processing times, and high equipment requirements, making them less suitable for the rapid diagnosis of this time-sensitive condition. In recent years, ultra-sensitive detection technologies, such as Simoa and biosensors, have achieved significant breakthroughs, with progressively lower detection limits. If these platforms can be further optimized to meet the needs of portable and point-of-care testing (POCT), the clinical translation of stroke biomarkers could be significantly accelerated. Additionally, the integration of artificial intelligence (AI) and machine learning algorithms may enhance diagnostic accuracy.

At present, most stroke biomarkers remain in the clinical research phase and have yet to be widely implemented in routine diagnostics. Future studies should focus on large-scale, multicenter cohort investigations with rigorous study designs, including prospective cohort studies, to establish clear reference ranges, specificity, and clinically relevant cutoff values for various biomarkers.

Overall, only by simultaneously advancing our understanding of the pathogenesis of AIS and enhancing the sensitivity, specificity, stability, and resistance to interference of detection technologies can stroke biomarkers truly support early diagnosis, disease monitoring, and personalized treatment strategies.

Author contributions

YL: Writing – original draft. JC: Writing – review & editing. YC: Writing – review & editing. YT: Writing – review & editing. LL: Writing – review & editing. YX: Writing – review & editing. SW: Writing – review & editing.

Funding

The author(s) declare that financial support was received for the research, authorship, and/or publication of this article. The present study is supported by the Funding for Scientific Research Projects from Wuhan Municipal Health Commission (WX23A57).

Conflict of interest

The authors declare that the research was conducted in the absence of any commercial or financial relationships that could be construed as a potential conflict of interest.

Publisher's note

References

1. Krishnamurthi RV, Ikeda T, Feigin VL. Global, regional and country-specific burden of Ischaemic stroke, intracerebral Haemorrhage and subarachnoid Haemorrhage: A systematic analysis of the global burden of disease study 2017. *Neuroepidemiology*. (2020) 54:171–9. doi: 10.1159/000506396

2. Owolabi MO, Thrift AG, Martins S, Johnson W, Pandian J, Abd-Allah F, et al. The state of stroke services across the globe: report of world stroke organization–World Health Organization surveys. *J Int J Stroke*. (2021) 16:889–901. doi: 10.1177/17474930211019568

3. Murphy SJ, Werring DJ. Stroke: causes and clinical features. *Medicine*. (2020) 48:561–6. doi: 10.1016/j.mpmed.2020.06.002

4. Herpich F, Rincon F. Management of Acute Ischemic Stroke. *Crit Care Med*. (2020) 48:1654–63. doi: 10.1097/CCM.0000000000004597

5. Saini V, Guada L, Yavagal DR. Global epidemiology of stroke and access to acute ischemic stroke interventions. *Neurology*. (2021) 97:S6–S16. doi: 10.1212/WNL.0000000000012781

6. Hasan TF, Hasan H, Kelley RE. Overview of Acute Ischemic Stroke Evaluation and Management. *Biomedicines*. (2021) 9:1486. doi: 10.3390/biomedicines9101486

7. Kamtchum-Tatuene J, Jickling GC. Blood biomarkers for stroke diagnosis and management. *NeuroMolecular Med*. (2019) 21:344–68. doi: 10.1007/s12017-019-08530-0

8. Montellano FA, Ungethüm K, Ramiro L, Nacu A, Hellwig S, Fluri F, et al. Role of blood-based biomarkers in ischemic stroke prognosis a systematic review. *Stroke*. (2021) 52:543–51. doi: 10.1161/strokeaha.120.029232

9. Tuo QZ, Zhang ST, Lei P. Mechanisms of neuronal cell death in ischemic stroke and their therapeutic implications. *Med Res Rev*. (2022) 42:259–305. doi: 10.1002/med.21817

10. Staessens S, De Meyer SF. Thrombus heterogeneity in ischemic stroke. *Platelets*. (2021) 32:331–9. doi: 10.1080/09537104.2020.1748586

11. Li J, Pan Y, Xu J, Li S, Wang M, Quan K, et al. Residual inflammatory risk predicts poor prognosis in acute ischemic stroke or transient ischemic attack patients. *Stroke*. (2021) 52:2827–36. doi: 10.1161/STROKEAHA.120.033152

12. Li Z, Bi R, Sun S, Chen S, Chen J, Hu B, et al. The role of oxidative stress in acute ischemic stroke-related thrombosis. *Oxid Med Cell Longev*. (2022) 2022:1–19. doi: 10.1155/2022/8418820

13. Maida CD, Norrito RL, Daidone M, Tuttolomondo A, Pinto A. Neuroinflammatory mechanisms in ischemic stroke: focus on Cardioembolic stroke, background, and therapeutic approaches. *Int J Mol Sci*. (2020) 21:6454. doi: 10.3390/ijms21186454

14. van Putten MJ, Fahlke C, Kafitz KW, Hofmeijer J, Rose CR. Dysregulation of astrocyte ion homeostasis and its relevance for stroke-induced brain damage. *Int J Mol Sci*. (2021) 22:5679. doi: 10.3390/ijms22115679

15. Zhou X, Chen H, Wang L, Lenahan C, Lian L, Ou Y, et al. Mitochondrial dynamics: A potential therapeutic target for ischemic stroke. *Front Aging Neurosci*. (2021) 13:721428. doi: 10.3389/fnagi.2021.721428

16. Mo Y, Sun Y-Y, Liu K-Y. Autophagy and inflammation in ischemic stroke. *Neural Regen Res*. (2020) 15:1388–96. doi: 10.4103/1673-5374.274331

17. Lim HH, Jeong IH, An GD, Woo KS, Kim KH, Kim JM, et al. Evaluation of neutrophil extracellular traps as the circulating marker for patients with acute coronary syndrome and acute ischemic stroke. *J Clin Lab Anal*. (2020) 34:e23190. doi: 10.1002/jcla.23190

18. Ohara T, Farhoudi M, Bang OY, Koga M, Demchuk AM. The emerging value of serum D-dimer measurement in the work-up and Management of Ischemic Stroke. *Int J Stroke*. (2020) 15:122–31. doi: 10.1177/1747493019876538

19. Lee J, Mun S, Park A, Kim D, Lee YJ, Kim HJ, et al. Proteomics reveals plasma biomarkers for ischemic stroke related to the coagulation Cascade. *J Mol Neurosci*. (2020) 70:1321–31. doi: 10.1007/s12031-020-01545-4

20. Misra S, Singh P, Nath M, Bhalla D, Sengupta S, Kumar A, et al. Blood-based protein biomarkers for the diagnosis of acute stroke: A discovery-based Swath-Ms proteomic approach. *Front Neurol*. (2022) 13:989856. doi: 10.3389/fneur.2022.989856

21. Luger S, Jæger HS, Dixon J, Bohmann FO, Schaefer J, Richieri SP, et al. Diagnostic accuracy of glial fibrillary acidic protein and ubiquitin Carboxy-terminal hydrolase-L1 serum concentrations for differentiating acute intracerebral hemorrhage from ischemic stroke. *Neurocrit Care*. (2020) 33:39–48. doi: 10.1007/s12028-020-00931-5

22. Haydinger CD, Ashander LM, Tan ACR, Smith JR. Intercellular adhesion molecule 1: more than a leukocyte adhesion molecule. *Biology*. (2023) 12:743. doi: 10.3390/biology12050743

23. Blann A, Kumar P, Krupinski J, McCollum C, Beevers DG, Lip GYH. Soluble intercellular adhesion Molecule-1, E-selectin, vascular cell adhesion Molecule-1 and Von Willebrand factor in stroke. *Blood Coagul Fibrinolysis*. (1999) 10:277–84. doi: 10.1097/00001721-199907000-00009

24. Nielsen HH, Soares CB, Hogedal SS, Madsen JS, Hansen RB, Christensen AA, et al. Acute Neurofilament light chain plasma levels correlate with stroke severity and clinical outcome in ischemic stroke patients. *Front Neurol*. (2020) 11:448. doi: 10.3389/fneur.2020.00448

25. Wang L, Chen Y, Feng D, Wang X. Serum Icam-1 as a predictor of prognosis in patients with acute ischemic stroke. *Biomed Res Int*. (2021) 2021:5539304. doi: 10.1155/2021/5539304

26. Gao H, Zhang XH. Associations of intercellular adhesion Molecule-1 Rs5498 polymorphism with ischemic stroke: A Meta-analysis. *Mol Genet Genomic Med*. (2019) 7:e643. doi: 10.1002/mgg3.643

27. Rakhimbaeva GS, kizi Abdurakhmonova KB. Icam-1 and Crp as biomarkers of 3-month outcome in acute Ischaemic stroke. *BMJ Neurol Open*. (2023) 5:e000516. doi: 10.1136/bmjno-2023-000516

28. Orion D, Schwammenthal Y, Reshef T, Schwartz R, Tsabari R, Merzeliak O, et al. Interleukin-6 and soluble intercellular adhesion Molecule-1 in acute brain Ischaemia. *Eur J Neurol*. (2008) 15:323–8. doi: 10.1111/j.1468-1331.2008.02066.x

29. Bitsch A, Klene W, Murtada L, Prange H, Rieckmann P. A longitudinal prospective study of soluble adhesion molecules in acute stroke. *Stroke*. (1998) 29:2129–35. doi: 10.1161/01.Str.29.10.2129

30. Sabbah AS, Elkattan MM, Labib DM, Hamdy MSE, Wahdan NS, Aboulfotoh ASM. Role of Von Willebrand factor level as a biomarker in acute ischemic stroke. *Egypt J Neurol Psychiatry Neurosurg*. (2024) 60:63. doi: 10.1186/s41983-024-00837-5

31. Sharma R, Gowda H, Chavan S, Advani J, Kelkar D, Kumar GS, et al. Proteomic signature of endothelial dysfunction identified in the serum of acute ischemic stroke patients by the Itraq-based Lc-Ms approach. *J Proteome Res*. (2015) 14:2466–79. doi: 10.1021/pr501324n

32. Steliga A, Kowiański P, Czuba E, Waśkow M, Moryś J, Lietzau G. Neurovascular unit as a source of ischemic stroke biomarkers—limitations of experimental studies and perspectives for clinical application. *Transl Stroke Res*. (2020) 11:553–79. doi: 10.1007/s12975-019-00744-5

33. SdlC B, García del Barco D, Hardy-Sosa A, Guillen Nieto G, Bringas-Vega ML, Llibre-Guerra JJ, et al. Scalable bio marker combinations for early stroke diagnosis: A systematic review. *Front Neurol*. (2021) 12:638693. doi: 10.3389/fneur.2021.638693

34. Kawano T, Gon Y, Sakaguchi M, Yamagami H, Abe S, Hashimoto H, et al. Von Willebrand factor antigen levels predict poor outcomes in patients with stroke and

Cancer: findings from the multicenter, prospective, observational Scan study. *J Am Heart Assoc*. (2024) 13:e032284. doi: 10.1161/JAHA.123.032284

35. Wang Y, Li J, Pan Y, Wang M, Meng X, Wang Y. Association between high-sensitivity C-reactive protein and prognosis in different periods after ischemic stroke or transient ischemic attack. *J Am Heart Assoc*. (2022) 11:e025464. doi: 10.1161/JAHA.122.025464

36. Coveney S, Murphy S, Belton O, Cassidy T, Crowe M, Dolan E, et al. Inflammatory cytokines, high-sensitivity C-reactive protein, and risk of one-year vascular events, death, and poor functional outcome after stroke and transient ischemic attack. *Int J Stroke*. (2022) 17:163–71. doi: 10.1177/1747493021995595

37. Lasek-Bal A, Jedrzejowska-Szypulka H, Student S, Warsz-Wianecka A, Zareba K, Puz P, et al. The importance of selected markers of inflammation and blood-brain barrier damage for short-term ischemic stroke prognosis. *J Physiol Pharmacol*. (2019) 70:209–17. doi: 10.26402/jpp.2019.2.04

38. Reiche EMV, Gelinksi JR, Alfieri DF, Flauzino T, Lehmann MF, de Araújo MCM, et al. Immune-inflammatory, oxidative stress and biochemical biomarkers predict short-term acute ischemic stroke death. *Metab Brain Dis*. (2019) 34:789–804. doi: 10.1007/s11011-019-00403-6

39. Ma Z, Yue Y, Luo Y, Wang W, Cao Y, Fang Q. Clinical utility of the inflammatory factors combined with lipid markers in the diagnostic and prognostic assessment of ischemic stroke: based on logistic regression models. *J Stroke Cerebrovasc Dis*. (2020) 29:104653. doi: 10.1016/j.jstrokecerebrovasdis.2020.104653

40. Gkantzios A, Tsiptsios D, Karatzetzou S, Kitmeridou S, Karapepera V, Giannakou E, et al. Stroke and emerging blood biomarkers: A clinical prospective. *Neurol Int*. (2022) 14:784–803. doi: 10.3390/neurolint14040065

41. Abdelnaseer M, Elfayomi N, Hassan E, Kamal M, Hamdy A, Elsawy E. Serum matrix Metalloproteinase-9 in acute ischemic stroke and its relation to stroke severity. *Egypt J Neurol Psychiatry Neurosurg*. (2015) 52:274. doi: 10.4103/1110-1083.170661

42. Weekman EM, Wilcock DM. Matrix metalloproteinase in blood-brain barrier breakdown in dementia. *J Alzheimers Dis*. (2016) 49:893–903. doi: 10.3233/jad-150759

43. Zhong CK, Yang JY, Xu T, Xu T, Peng YB, Wang AL, et al. Serum matrix Metalloproteinase-9 levels and prognosis of acute ischemic stroke. *Neurology*. (2017) 89:805–12. doi: 10.1212/wnl.0000000000004257

44. Mathias K, Machado RS, Stork S, dos Santos D, Joaquim L, Generoso J, et al. Blood-brain barrier permeability in the ischemic stroke: An update. *Microvasc Res*. (2024) 151:151. doi: 10.1016/j.mvr.2023.104621

45. Jayaraj RL, Azimullah S, Beiram R, Jalal FY, Rosenberg GA. Neuroinflammation: friend and foe for ischemic stroke. *J Neuroinflammation*. (2019) 16:142. doi: 10.1186/s12974-019-1516-2

46. Tsukagawa T, Katsumata R, Fujita M, Yasui K, Akhoon C, Ono K, et al. Elevated serum high-mobility group Box-1 protein level is associated with poor functional outcome in ischemic stroke. *J Stroke Cerebrovasc Dis*. (2017) 26:2404–11. doi: 10.1016/j.jstrokecerebrovasdis.2017.05.033

47. Sapojnikova N, Kartvelishvili T, Asatiani N, Zinkevich V, Kalandadze I, Gugutsidze D, et al. Correlation between Mmp-9 and extracellular cytokine Hmgb1 in prediction of human ischemic stroke outcome. *BBA-Mol Basis Dis*. (2014) 1842:1379–84. doi: 10.1016/j.bbadis.2014.04.031

48. Shen LP, Yang JS, Zhu ZF, Li WZ, Cui JY, Gu LY. Elevated serum Hmgb1 levels and their association with recurrence of acute Ischaemic stroke. *J Inflamm Res*. (2024) 17:6887–94. doi: 10.2147/jir.S477415

49. Li JM, Wang ZX, Li JM, Zhao HP, Ma QF. Hmgb1: A new target for ischemic stroke and hemorrhagic transformation. *Transl Stroke Res*. (2024). 514:05. doi: 10.1007/s12975-024-01258-5

50. Bustamante A, Penalba A, Orset C, Azurmendi L, Llombart V, Simats A, et al. Blood biomarkers to differentiate ischemic and hemorrhagic strokes. *Neurology*. (2021) 96:e1928–39. doi: 10.1212/WNL.0000000000011742

51. Kalra LP, Khatter H, Ramanathan S, Sapehia S, Devi K, Kaliyaperumal A, et al. Serum Gfap for stroke diagnosis in regions with limited access to brain imaging (be fast India). *Eur Stroke J*. (2021) 6:176–84. doi: 10.1177/23969873211010069

52. Perry LA, Lucarelli T, Penny-Dimri JC, McInnes MD, Mondello S, Bustamante A, et al. Glial fibrillary acidic protein for the early diagnosis of intracerebral hemorrhage: systematic review and Meta-analysis of diagnostic test accuracy. *Int J Stroke*. (2019) 14:390–9. doi: 10.1177/1747493018806167

53. Lee M, Rafiq Sayyed D, Kim H, Sanchez JC, Sik Hong S, Choi S, et al. A comprehensive Exdia Trf-Lfia for simultaneous quantification of Gfap and Nt-Probnp in distinguishing ischemic and hemorrhagic stroke. *Clin Chim Acta*. (2024) 557:117872. doi: 10.1016/j.cca.2024.117872

54. Sanchez JD, Martirosian RA, Mun KT, Chong DS, Llorente IL, Uphaus T, et al. Temporal patterning of Neurofilament light as a blood-based biomarker for stroke: A systematic review and Meta-analysis. *Front Neurol*. (2022) 13:841898. doi: 10.3389/fneur.2022.841898

55. Pedersen A, Stanne TM, Nilsson S, Klasson S, Rosengren L, Holmegaard L, et al. Circulating Neurofilament light in ischemic stroke: temporal profile and outcome prediction. *J Neurol*. (2019) 266:2796–806. doi: 10.1007/s00415-019-09477-9

56. Uphaus T, Bittner S, Gröschel S, Steffen F, Muthuraman M, Wasser K, et al. Nfl (Neurofilament light chain) levels as a predictive marker for Long-term outcome after ischemic stroke. *Stroke*. (2019) 50:3077–84. doi: 10.1161/STROKEAHA.119.026410

57. Barba L, Vollmuth C, Abu-Rumeileh S, Halbgebauer S, Oeckl P, Steinacker P, et al. Serum B-Synuclein, Neurofilament light chain and glial fibrillary acidic protein as prognostic biomarkers in moderate-to-severe acute ischemic stroke. *Sci Rep*. (2023) 13:20941. doi: 10.1038/s41598-023-47765-7

58. O'Connell GC, Smothers CG, Gandhi SA. Newly-identified blood biomarkers of neurological damage are correlated with infarct volume in patients with acute ischemic stroke. *J Clin Neurosci*. (2021) 94:107–13. doi: 10.1016/j.jocn.2021.10.015

59. Xu X, Zhuang C, Chen L. Exosomal Long non-coding Rna expression from serum of patients with acute minor stroke. *Neuropsychiatr Dis Treat*. (2020) 16:153–60. doi: 10.2147/NDT.S230332

60. Bai X, Liu X, Wu H, Feng J, Chen H, Zhou D. Circfundc1 knockdown alleviates oxygen-glucose deprivation-induced human brain microvascular endothelial cell injuries by inhibiting Pten via Mir-375. *Neurosci Lett*. (2022) 770:136381. doi: 10.1016/j.neulet.2021.136381

61. Xiao Q, Hou R, Li H, Zhang S, Zhang F, Zhu X, et al. Circulating Exosomal circRNAs contribute to potential diagnostic value of large artery atherosclerotic stroke. *Front Immunol*. (2022) 12:830018. doi: 10.3389/fimmu.2021.830018

62. Zhou J, Chen L, Chen B, Huang S, Zeng C, Wu H, et al. Increased serum Exosomal Mir-134 expression in the acute ischemic stroke patients. *BMC Neurol*. (2018) 18:198. doi: 10.1186/s12883-018-1196-z

63. Wang W, Li D-B, Li R-Y, Zhou X, Yu D-J, Lan X-Y, et al. Diagnosis of Hyperacute and acute Ischaemic stroke: the potential utility of Exosomal Microrna-21-5p and Microrna-30a-5p. *Cerebrovasc Dis*. (2018) 45:204–12. doi: 10.1159/000488365

64. Zhang S, Wang X, Yin R, Xiao Q, Ding Y, Zhu X, et al. Circulating Exosomal Lncrnas as predictors of risk and unfavorable prognosis for large artery atherosclerotic stroke. *Clin Transl Med*. (2021) 11:e555. doi: 10.1002/ctm2.555

65. Chen F, Du Y, Esposito E, Liu Y, Guo SZ, Wang XY, et al. Effects of focal cerebral ischemia on Exosomal versus serum Mir126. *Transl Stroke Res*. (2015) 6:478–84. doi: 10.1007/s12975-015-0429-3

66. Burek M, König A, Lang M, Fiedler J, Oerter S, Roewer N, et al. Hypoxia-induced Microrna-212/132 Alter blood-brain barrier integrity through inhibition of tight junction-associated proteins in human and mouse brain microvascular endothelial cells. *Transl Stroke Res*. (2019) 10:672–83. doi: 10.1007/s12975-018-0683-2

67. Tan KS, Armugam A, Sepramaniam S, Lim KY, Setyowati KD, Wang CW, et al. Expression profile of Micrornas in young stroke patients. *PLoS One*. (2009) 4:e7689. doi: 10.1371/journal.pone.0007689

68. Chen YJ, Song YY, Huang J, Qu MJ, Zhang Y, Geng JL, et al. Increased circulating Exosomal Mirna-223 is associated with acute ischemic stroke. *Front Neurol*. (2017) 8:8. doi: 10.3389/fneur.2017.00057

69. Kang LJ, Yu HL, Yang X, Zhu YB, Bai XF, Wang RR, et al. Neutrophil extracellular traps released by neutrophils impair revascularization and vascular remodeling after stroke. *Nature. Communications*. (2020) 11:2488. doi: 10.1038/s41467-020-16191-y

70. Vallés J, Lago A, Santos MT, Latorre AM, Tembl JI, Salom JB, et al. Neutrophil extracellular traps are increased in patients with acute ischemic stroke: prognostic significance. *Thromb Haemost*. (2017) 117:1919–29. doi: 10.1160/th17-02-0130

71. Denorme F, Portier I, Rustad JL, Cody MJ, de Araujo CV, Hoki C, et al. Neutrophil extracellular traps regulate ischemic stroke brain injury. *J Clin Invest*. (2022) 132:e154225. doi: 10.1172/jci154225

72. Lapostolle A, Loyer C, Elhorany M, Chaigneau T, Bielle F, Alamowitch S, et al. Neutrophil extracellular traps in ischemic stroke thrombi are associated Wth poor clinical outcome. *Stroke*. (2023) 3:e000639. doi: 10.1161/SVIN.122.000639

73. Chen X, Wang L, Jiang ML, Lin L, Ba ZJ, Tian H, et al. Leukocytes in cerebral Thrombus respond to large-vessel occlusion in a time-dependent manner and the Association of Nets with collateral flow. *Front Immunol*. (2022) 13:13. doi: 10.3389/fimmu.2022.834562

74. Pawluk H, Grzesk G, Kolodziejska R, Kozakiewicz M, Wozniak A, Grzechowiak E, et al. Effect of Il-6 and Hscrp serum levels on functional prognosis in stroke patients undergoing iv-thrombolysis: retrospective analysis. *Clin Interv Aging*. (2020) 15:1295–303. doi: 10.2147/CIA.S258381

75. Fang C, Lou B, Zhou J, Zhong R, Wang R, Zang X, et al. Blood biomarkers in ischemic stroke: role of biomarkers in differentiation of clinical phenotype. *Eur J Inflamm*. (2018) 16:2058739218780058. doi: 10.1177/2058739218780058

76. Sun C, Ma C, Sun Y, Ma L. Effect of Edaravone combined with anticoagulant therapy on the serum Hs-Crp, Il-6, and Tnf-alpha levels and activity of daily living in patients with acute cerebral infarction. *J Healthc Eng*. (2022) 2022:8603146. doi: 10.1155/2022/8603146

77. Zhang X, Wang L, Han Z, Dong J, Pang D, Fu Y, et al. Klf4 alleviates cerebral vascular injury by ameliorating vascular endothelial inflammation and regulating tight junction protein expression following ischemic stroke. *J Neuroinflammation*. (2020) 17:1–16. doi: 10.1186/s12974-020-01780-x

78. Zhang J, Yang J, Hu J, Zhao W. Clinical value of serum Jkap in acute ischemic stroke patients. *J Clin Lab Anal*. (2022) 36:e24270. doi: 10.1002/jcla.24270

79. Amalia L. Glial fibrillary acidic protein (Gfap): Neuroinflammation biomarker in acute ischemic stroke. *J Inflamm Res*. (2021) 14:7501–6. doi: 10.2147/JIR.S342097

80. Puspitasari V, Gunawan PY, Wiradarma HD, Hartoyo V. Glial fibrillary acidic protein serum level as a predictor of clinical outcome in ischemic stroke. *Open Access Maced J Med Sci*. (2019) 7:1471–4. doi: 10.3889/oamjms.2019.326

81. Bhatia R, Warrier AR, Sreenivas V, Bali P, Sisodia P, Gupta A, et al. Role of blood biomarkers in differentiating ischemic stroke and intracerebral hemorrhage. *Neurol India*. (2020) 68:824–9. doi: 10.4103/0028-3886.293467

82. Sun Y, Wang J, Han B, Meng K, Han Y, Ding Y. Elucidating the molecular mechanism of ischemic stroke using integrated analysis of Mirna, Mrna, and Lncrna expression profiles. *Front Integr Neurosci*. (2021) 15:638114. doi: 10.3389/fnint.2021.638114

83. Xiang Y, Zhang Y, Xia Y, Zhao H, Liu A, Chen Y. Lncrna Meg3 targeting Mir-424-5p via Mapk signaling pathway mediates neuronal apoptosis in ischemic stroke. *Aging (Albany NY)*. (2020) 12:3156–74. doi: 10.18632/aging.102790

84. Tian J, Liu Y, Wang Z, Zhang S, Yang Y, Zhu Y, et al. Lncrna Snhg8 attenuates microglial inflammation response and blood-brain barrier damage in ischemic stroke through regulating Mir-425-5p mediated Sirt1/Nf-Kappab signaling. *J Biochem Mol Toxicol*. (2021) 35:e22724. doi: 10.1002/jbt.22724

85. Medeiros R, Sousa B, Rossi S, Afonso C, Bonino L, Pitt A, et al. Identification and relative quantification of 3-Nitrotyrosine residues in fibrinogen nitrated in vitro and fibrinogen from ischemic stroke patient plasma using Lc-Ms/Ms. *Free Radic Biol Med*. (2021) 165:334–47. doi: 10.1016/j.freeradbiomed.2021.01.049

86. Kamal FZ, Lefter R, Jaber H, Balmus IM, Ciobica A, Iordache AC. The role of potential oxidative biomarkers in the prognosis of acute ischemic stroke and the exploration of antioxidants as possible preventive and treatment options. *Int J Mol Sci*. (2023) 24:6389. doi: 10.3390/ijms24076389

87. Rattanawong W, Ongphichetmetha T, Hemachudha T, Thanapornsangsuth P. Neurofilament light is associated with clinical outcome and hemorrhagic transformation in moderate to severe ischemic stroke. *J Cent Nerv Syst Dis*. (2023) 15:11795735221147212. doi: 10.1177/11795735221147212

88. Jiang W, Niu J, Gao H, Dang Y, Qi M, Liu Y. A retrospective study of immunoglobulin E as a biomarker for the diagnosis of acute ischemic stroke with carotid atherosclerotic plaques. *PeerJ*. (2022) 10:e14235. doi: 10.7717/peerj.14235

89. Donkel SJ, Benaddi B, Dippel DW, Ten Cate H, de Maat MP. Prognostic hemostasis biomarkers in acute ischemic stroke: A systematic review. *Arterioscler Thromb Vasc Biol*. (2019) 39:360–72. doi: 10.1161/ATVBAHA.118.312102

90. Cuadrat RR, Kratzer A, Arnal HG, Rathgeber AC, Wreczycka K, Blume A, et al. Cardiovascular disease biomarkers derived from circulating cell-free DNA methylation. *NAR genomics. Bioinformatics*. (2023) 5:lqad061. doi: 10.1093/nargab/lqad061

91. Shu Y, Guo Y, Zheng Y, He S, Shi Z. Rna methylation in vascular disease: A systematic review. *J Cardiothorac Surg*. (2022) 17:323. doi: 10.1186/s13019-022-02077-1

92. Pujol-Calderon F, Zetterberg H, Portelius E, Lowhagen Henden P, Rentzos A, Karlsson JE, et al. Prediction of outcome after endovascular embolectomy in anterior circulation stroke using biomarkers. *Transl Stroke Res*. (2022) 13:65–76. doi: 10.1007/s12975-021-00905-5

93. Ferrari F, Rossi D, Ricciardi A, Morasso C, Brambilla L, Albasini S, et al. Quantification and prospective evaluation of serum Nfl and Gfap as blood-derived biomarkers of outcome in acute ischemic stroke patients. *J Cereb Blood Flow Metab*. (2023) 43:1601–11. doi: 10.1177/0271678X231172520

94. Traub J, Grondey K, Gassenmaier T, Schmitt D, Fette G, Frantz S, et al. Sustained increase in serum glial fibrillary acidic protein after first St-elevation myocardial infarction. *Int J Mol Sci*. (2022) 23:10304. doi: 10.3390/ijms231810304

95. Onatsu J, Vanninen R, Jäkälä P, Mustonen P, Pulkki K, Korhonen M, et al. Serum Neurofilament light chain concentration correlates with infarct volume but not prognosis in acute ischemic stroke. *J Stroke Cerebrovasc Dis*. (2019) 28:2242–9. doi: 10.1016/j.jstrokecerebrovasdis.2019.05.008

96. Mattila OS, Ashton NJ, Blennow K, Zetterberg H, Harve-Rytsälä H, Pihlasviita S, et al. Ultra-early differential diagnosis of acute cerebral ischemia and hemorrhagic stroke by measuring the prehospital release rate of Gfap. *Clin Chem*. (2021) 67:1361–72. doi: 10.1093/clinchem/hvab128

97. Rodríguez-Penedo A, Costa-Rama E, Fernández B, García-Cabo C, Benavente L, Calleja S, et al. Palladium nanoclusters as a label to determine Gfap in human serum from donors with stroke by bimodal detection: inductively coupled plasma-mass spectrometry and linear sweep voltammetry. *Microchim Acta*. (2023) 190:493. doi: 10.1007/s00604-023-06059-5

98. Sayad A, Uddin SM, Yao S, Wilson H, Chan J, Zhao H, et al. A Magnetoimpedance biosensor microfluidic platform for detection of glial fibrillary acidic protein in blood for acute stroke classification. *Biosens Bioelectron*. (2022) 211:114410. doi: 10.1016/j.bios.2022.114410

99. Molinero-Fernández A, Moreno-Guzmán M, Arruza L, López MA, Escarpa A. Toward early diagnosis of late-onset Sepsis in preterm neonates: dual Magnetoimmunosensor for simultaneous Procalcitonin and C-reactive protein determination in diagnosed clinical samples. *ACS Sens*. (2019) 4:2117–23. doi: 10.1021/acssensors.9b00890

100. Salahandish R, Hassani M, Zare A, Haghayegh F, Sanati-Nezhad A. Autonomous electrochemical biosensing of glial fibrillary acidic protein for point-of-care detection of central nervous system injuries. *Lab Chip*. (2022) 22:1542–55. doi: 10.1039/d2lc00025c

101. Sun JY, Zhao Y, Hou YJ, Li HX, Yang MF, Wang Y, et al. Multiplexed electrochemical and Sers dual-mode detection of stroke biomarkers: rapid screening with high sensitivity. *New J Chem*. (2019) 43:13381–7. doi: 10.1039/c9nj01598a

102. António M, Ferreira R, Vitorino R, Daniel-da-Silva AL. A simple aptamer-based colorimetric assay for rapid detection of C-reactive protein using gold nanoparticles. *Talanta*. (2020) 214:120868. doi: 10.1016/j.talanta.2020.120868

103. Sun JY, Gao F, Song YA, Wang MY, Wang C, Ni QB, et al. Paper lateral flow strips based on gold Nanorods for ultrasensitive detection of traumatic brain injury biomarkers. *ACS Appl Nano Mater*. (2023) 6:18729–38. doi: 10.1021/acsanm.3c00178

104. Gong TX, Hong ZY, Chen CH, Tsai CY, Liao LD, Kong KV. Optical interference-free surface-enhanced Raman scattering co-Nanotags for logical multiplex detection of vascular disease related biomarkers. *ACS Nano*. (2017) 11:3365–75. doi: 10.1021/acsnano.7b00733

105. Li JQ, Wu JG, Chen JX, Huang S, Liu J, Gao F, et al. Dual detection of spinal cord injury biomarkers in rat model using gold Nanorod Array substrate based on surface-enhanced Raman scattering. *Surf Interfaces*. (2022) 34:102400. doi: 10.1016/j.surfin.2022.102400

106. Lai YM, Schlücker S, Wang YL. Rapid and sensitive Sers detection of the cytokine tumor necrosis factor alpha (Tnf-A) in a magnetic bead pull-down assay with purified and highly Raman-active gold nanoparticle clusters. *Anal Bioanal Chem*. (2018) 410:5993–6000. doi: 10.1007/s00216-018-1218-0

107. Wang MY, Wan HY, Wang YJ, Yuan H, Ni QB, Sun BL, et al. A microfluidics-based multiplex Sers immunoassay device for analysis of acute ischemic stroke biomarkers. *Transl Stroke Res*. (2023). 1124:10. doi: 10.1007/s12975-023-01204-x

108. Sinha A, Tai TY, Li KH, Gopinathan P, Chung YD, Sarangadharan I, et al. An integrated microfluidic system with field-effect-transistor sensor arrays for detecting multiple cardiovascular biomarkers from clinical samples. *Biosens Bioelectron*. (2019) 129:155–63. doi: 10.1016/j.bios.2019.01.001

109. Krausz AD, Korley FK, Burns MA. A variable height microfluidic device for multiplexed immunoassay analysis of traumatic brain injury biomarkers. *Biosensors (Basel)*. (2021) 11:320. doi: 10.3390/bios11090320

frontiers | Frontiers in Neurology

TYPE Original Research
PUBLISHED 11 March 2025
DOI 10.3389/fneur.2025.1534564

OPEN ACCESS

EDITED BY
Haipeng Liu,
Coventry University, United Kingdom

REVIEWED BY
Mohammed Ahmed Akkaif,
QingPu Branch of Zhongshan Hospital Affiliated to Fudan University, China
Sarawut Krongsut,
Department of Internal Medicine, Thailand

*CORRESPONDENCE
Ming Yu
yuming609800@163.com
Lei Xu
xl1588@sns120.com

†These authors have contributed equally to this work and share first authorship

‡These authors have contributed equally to this work

RECEIVED 11 December 2024
ACCEPTED 17 February 2025
PUBLISHED 11 March 2025

CITATION
Huang L, Li L, Ouyang Q-r, Chen P, Yu M and Xu L (2025) Association between the hemoglobin-to-red cell distribution width ratio and three-month unfavorable outcome in older acute ischemic stroke patients: a prospective study.
Front. Neurol. 16:1534564.
doi: 10.3389/fneur.2025.1534564

Association between the hemoglobin-to-red cell distribution width ratio and three-month unfavorable outcome in older acute ischemic stroke patients: a prospective study

Luwen Huang[1†], Linlin Li[1†], Qing-rong Ouyang[1], Ping Chen[2], Ming Yu[1*‡] and Lei Xu[1*‡]

[1]Department of Neurology, Suining Central Hospital, Suining, Sichuan Province, China, [2]Department of Pharmacy, Suining Central Hospital, Suining, Sichuan Province, China

Objective: Acute ischemic stroke (AIS) is a prevalent acute condition among older individuals. This study is the first investigation of the link between the HRR and unfavorable three-month outcome in older AIS patients.

Methods: This secondary research used data from a sample of 1,470 older AIS patients collected from a South Korean hospital between January 2010 and December 2016. Multiple imputation was applied to account for absent values. Binary logistic regression analysis was used to examine the relationship between the baseline HRR and adverse outcome at three-month. Restricted cubic spline analysis was employed to evaluate the correlation between HRR levels and adverse outcome. Interaction tests were performed to discern variations among subgroups.

Results: At 3 months, the overall incidence of adverse events was 31.43%, with a median HRR of 9.49. Compared to those with a lower HRR (Q1), the adjusted odds ratios (ORs) for the HRR in Q2, Q3, and Q4 were 0.61 (95% CI: 0.41–0.92, $p = 0.017$), 0.49 (95% CI: 0.31–0.78, $p = 0.003$), and 0.54 (95% CI: 0.31–0.92, $p = 0.025$), respectively. The correlation between the HRR and adverse outcome was non-linear ($p < 0.05$). An inflection point threshold of 10.70 was established via RCS analysis. Each 1-unit increase in HRR on the left side of the infection point was associated with a 24.0% decrease in the likelihood of adverse outcomes (OR = 0.76, 95% CI: 0.66–0.86, $p < 0.001$). ROC analysis revealed that HRR had the highest AUC (0.64, 95% CI: 0.61–0.67), followed by hs-CRP (0.60, 95% CI: 0.57–0.63), FPG/HbA1c (0.59, 95% CI: 0.55–0.63), and WBC (0.55, 95% CI: 0.51–0.58).

Conclusion: A lower HRR was correlated with a higher risk for adverse outcome in older AIS patients.

KEYWORDS

acute ischemic stroke, hemoglobin-to-red cell distribution width ratio, prognosis, association, older participants

1 Introduction

Stroke is the second leading cause of mortality worldwide and the third major contributor to disability in non-communicable diseases; acute ischemic stroke (AIS) constituted approximately 62.4 to 67.7% of all stroke incidents in 2021 (1). AIS is a common illness among the older population. Between 1990 and 2019, the prevalence of ischemic stroke among older adults was markedly greater than that among younger adults worldwide (2). Consequently, it is imperative to determine appropriate and effective clinical indicators to predict AIS prognosis in geriatric patients, guide clinical care, and improve treatment outcome.

Red blood cell distribution width (RDW), which reflects the variability in red blood cell volume, has traditionally been used for the diagnosis and differential diagnosis of anemia (3). Clinical studies have demonstrated that RDW is increasingly acknowledged as an independent risk factor for recurrence, hemorrhagic transformation, in-hospital mortality, and poststroke fatigue in patients with AIS (4–7). Moreover, recent research has identified RDW as a potential inflammatory marker significantly associated with stroke-associated pneumonia (SAP) and as a valuable tool for enhancing SAP risk stratification in thrombolyzed AIS patients when integrated into established prediction models (8). Nevertheless, a study including 1,504 patients indicated that RDW could not predict the severity or functional results of AIS (9). Therefore, novel and dependable markers are needed to predict AIS outcome. These limitations underscore the urgent need for novel, dependable biomarkers to improve AIS outcome prediction.

The hemoglobin-to-red blood cell distribution width ratio (HRR) is a novel biomarker first introduced by Peng et al. in their research on the progression of esophageal squamous cell cancer (10). HRR has demonstrated a strong correlation with inflammatory levels and has been associated with adverse outcomes in various diseases (10–16). Compared to single inflammatory markers such as WBC or hs-CRP, HRR offers a unique advantage by simultaneously reflecting red blood cell metabolism and systemic inflammation. As a simple and easily obtainable parameter, HRR may provide a more comprehensive prediction of unfavorable outcomes in AIS patients. Importantly, studies have also shown a negative association between HRR and poor outcome in AIS patients (17–19).

Nonetheless, the correlation between HRR and negative outcome in elderly AIS patients remains unclear. This study aimed to address this gap by investigating the correlation between HRR and unfavorable outcome. The ultimate goal is to establish HRR as a simple and accessible biomarker that can aid clinicians in early risk stratification, thereby improving patient management and enhancing quality of life.

2 Materials and methods

2.1 Data sources

This research performed a secondary analysis of a prospective cohort study. Data were gathered from January 2010 to December 2016 through a single-center prospective registry in South Korea (20). The research was approved by the Institutional Review Board of Seoul National University Hospital (IRB No. 1009–062-332, 20). All data were anonymized to protect patient privacy, and the requirement for informed consent was waived by the board. The study methodology conformed to the standards set by the Declaration of Helsinki. The following data were acquired from the subsequent study: Kang et al. (20). The material is freely available and may be used, disseminated, and reproduced in any format, depending on appropriate attribution to the original authors and source. This is authorized under the Creative Commons Attribution License (20).

2.2 Study population

The initial trial included 2,084 individuals with AIS admitted within 7 days of initial symptoms, based on a prospective registry approach (20). The exclusion criteria were as follows: (1) absence of laboratory data or dysphagia assessment within 24 h of admission; (2) lack of modified 3-month Rankin scale (mRS) score information posthospitalization; and (3) age under 60 years. In total, 1,470 patients were included in this study (Figure 1). Patients without dysphagia assessment within 24 h were excluded to prevent bias, as early dysphagia evaluation is crucial for preventing complications and improving prognosis in ischemic stroke (21).

2.3 Variables and covariates

The HRR was calculated by dividing hemoglobin (Hb; g/L) by the red cell distribution width (RDW; %) (17, 18). The covariates included the following: (1) continuous variables such as white blood cell count (WBC), red blood cell count (RBC), hemoglobin (Hb), red cell distribution width (RDW), platelet count (PLT), low-density lipoprotein cholesterol (LDL-C), blood urea nitrogen (BUN), serum creatinine (Scr), alanine aminotransferase (ALT), fasting blood glucose (FBG), hemoglobin A1c (HbA1c), high-sensitivity C-reactive protein (hs-CRP), fibrinogen (FIB), and body mass index (BMI) (20). (2) The categorical factors included sex, age, hypertension, diabetes mellitus (DM), hyperlipidemia, smoking status, atrial fibrillation (AF), coronary heart disease (CHD), National Institutes of Health Stroke Scale (NIHSS) score, and stroke etiology. Laboratory data collected within 24 h of admission were retrieved from electronic healthcare records (20). Body mass index (BMI) was calculated by dividing weight in kilograms by the square of height in meters (kg/m^2). Stress hyperglycemia was evaluated using the following formula: FBG (mg/dl)/HbA1c (%).

2.4 Endpoints

The primary outcome was characterized as an unfavorable AIS result after 3 months, evaluated using the mRS score (22). Patient follow-up was primarily conducted through outpatient visits or structured telephone interviews, both performed by neurologists (20). An unfavorable outcome is defined by an mRS score of 3 or higher, while a favorable outcome is defined by an mRS score of 2 or lower (22).

2.5 Statistical analysis

Continuous variables are expressed as the mean ± standard deviation (SD) or median (interquartile range). Student's t-test or the

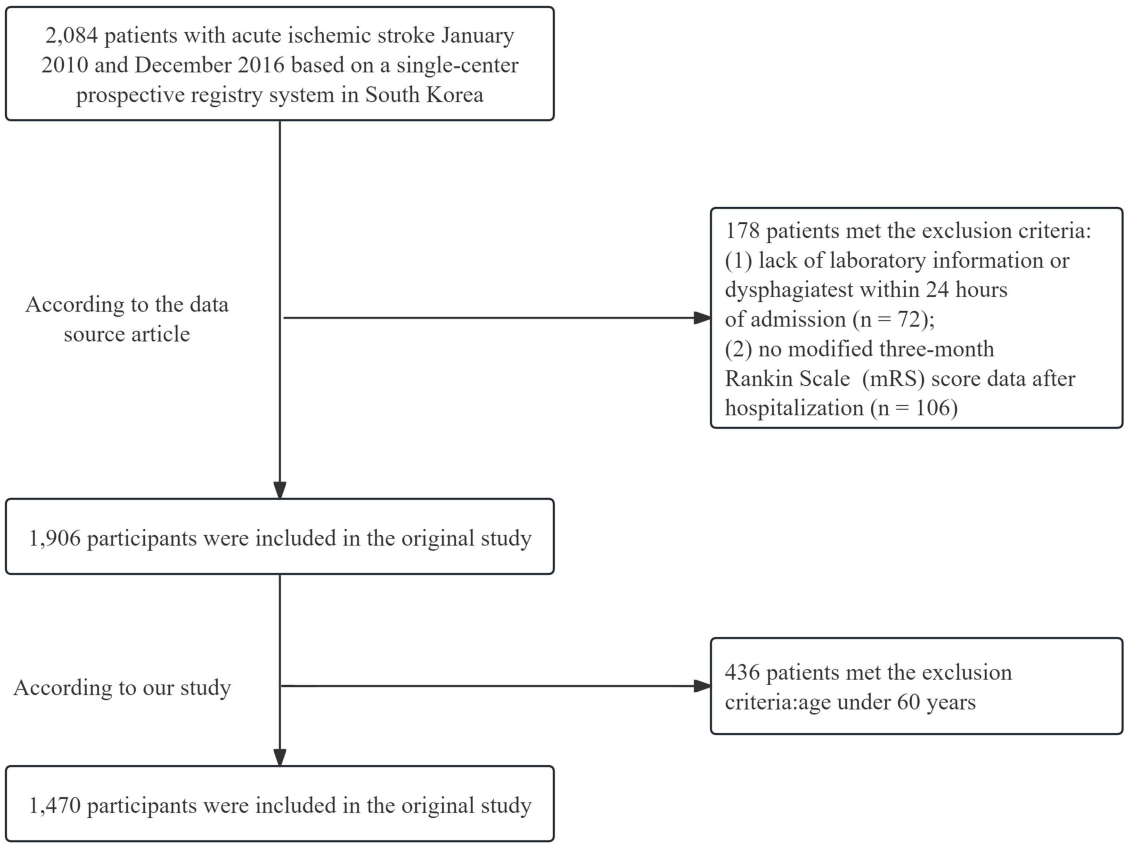

FIGURE 1
Flow chart.

Mann–Whitney U test was utilized on the basis of the normality of the distribution. Categorical variables are expressed as counts (%), and the chi-square test (or Fisher's exact test) was employed to examine differences among the four HRR quartiles (23).

Binary logistic regression analyses, both univariate and multivariate, were conducted to minimize the influence of different variables on adverse outcomes. Confounders were determined according to the following criteria: (1) The factor exerted a substantial influence (>10%) on the research variable. (2) Certain factors had a documented influence on the outcome variable according to previous studies (17, 18). (3) In the univariate analysis, factors with a *p*-value less than 0.05 were deemed significant. In multivariate analysis, various statistical models are employed to guarantee the stability of the results. No variables were adjusted in the crude model. Model I was adjusted for age and sex, while Model II included adjustments for 17 additional variables: WBC, RBC, PLT, LDL-C, BUN, FBG, ALT, hs-CRP, BMI, hypertension, DM, hyperlipidemia, CHD, AF, smoking status, NIHSS score at admission, and previous mRs. To control for the false discovery rate (FDR) in multiple hypothesis testing, we applied the Benjamini-Hochberg (BH) procedure.

Restricted cubic spline (RCS) analysis was employed to evaluate the potential nonlinear association between the HRR and adverse outcome. If a non-linear association was identified, a two-piecewise regression model would be conducted to calculate the threshold effect of HRR on poor outcomes, based on the smoothing plot. The HRR turning point was determined via exploratory analysis, wherein trial turning points were evaluated over predefined intervals, ultimately selecting the one with the highest model likelihood. A log-likelihood ratio test (LRT) was employed to identify the optimal model characterizing the association between the HRR and 3-month adverse outcome in senior AIS patients (24).

Furthermore, interaction and stratified analyses were conducted based on age, sex, hypertension status, DM status, hyperlipidemia status, smoking status, CHD status, BMI, and NIHSS score upon admission. Missing values were addressed by multiple imputations. Information on the missing data is shown in Supplementary Table 1. The area under the receiver operating characteristic (ROC) curve (AUC) and the corresponding 95% confidence intervals (CI) were calculated to evaluate and compare the predictive performance of HRR, hs-CRP, FPG/HbA1c, and WBC for unfavorable outcomes in older adults with AIS.

The data were analyzed via R (The R Foundation; version 4.2.0)[1] and EmpowerStats (X&Y Solutions, Inc., Boston, MA)[2] (24).

1 http://www.r-project.org
2 www.empowerstats.net

A two-sided p value below 0.05 was considered statistically significant.

3 Results

3.1 Baseline characteristics of the study patients

Following screening, 1,470 population with AIS were included in the data analysis. The baseline characteristics of the population individuals by HRR quartiles are presented in Table 1 (Q1: <8.96, Q2: 8.96–10.30, Q3: 10.31–11.30, and Q4: >11.30). The participants were categorized into the following age groups: 60 to <70 years (n = 505, 34.35%); 70 to <80 years (n = 670, 45.58%); and ≥ 80 years (n = 295, 20.07%). Supplementary Table 2 presents the demographics, laboratory variables, comorbidities, and other pertinent data categorized by HRR quartiles. Supplementary Table 2 illustrates notable disparities in age; sex; WBC, RBC, Hb, RDW, LDL-C, BUN, Scr, ALT, FBG, and hs-CRP levels; BMI; DM; smoking status; the National Institutes of Health Stroke Scale (NIHSS) score at admission; and stroke etiology.

Supplementary Table 3 indicates that 462 participants experienced unfavorable consequences. The group with poor outcome at 3 months presented a decreased HRR (mean: 9.49 vs. 10.23, $p < 0.001$). Univariate analysis indicated that age, sex, WBC, RDW, BUN, LDL-C, FBG, hs-CRP, hypertension, DM, and AF were correlated with worse outcome (all $p < 0.05$; Supplementary Table 4). Adverse outcome in AIS patients were strongly correlated with an undetermined cause (OR = 2.46, 95% CI: 1.58–3.82; $p < 0.001$).

3.2 Associations between the baseline HRR and unfavorable outcome

Table 1 displays the unadjusted and multivariable-adjusted correlations between the HRR and adverse outcome. Analysis of the HRR as a continuous variable revealed an inverse correlation with adverse outcome (non-adjusted model: OR = 0.82, 95% CI: 0.77–0.87, $p < 0.001$; Model I: OR = 0.85, 95% CI: 0.80–0.91, $p < 0.001$; Model II: OR = 0.80, 95% CI: 0.71–0.90, $p < 0.001$). The likelihood of adverse outcome in AIS patients decreased with each 1-unit increase in the HRR. Additionally, when the HRR was examined as a categorical variable, patients with decreased HRR levels had a markedly elevated risk of adverse outcome in AIS patients. In comparison to the reference group (Q1), the adjusted ORs for participants in Q2, Q3, and Q4 were 0.61 (95% CI: 0.41–0.92, $p = 0.017$), 0.49 (95% CI: 0.31–0.78, $p = 0.003$), and 0.54 (95% CI: 0.31–0.92, $p = 0.025$), respectively (p for trend = 0.01). After employing multiple imputations to address missing data, the results remained consistent with prior findings (Table 2). After applying the Benjamini-Hochberg correction to control for false discovery rate, all tests for HRR (both continuous and categorical variables), including the HRR quartiles (Q2, Q3, Q4) and the trend test, remained statistically significant. Sensitivity analysis evaluated the HRR values as continuous and categorical variables before and following multiple imputations, consistently yielding similar results for adverse outcome.

As shown in Supplementary Table 5, hemoglobin (Hb) was classified into quartiles, and these categorical Hb values were integrated into the model. The multivariate-adjusted model results demonstrated that hemoglobin levels between 134 and 145 g/L were inversely correlated with adverse outcome (OR = 0.58, 95% CI: 0.34–0.99, $p = 0.047$). None of the RDW quartiles exhibited a significant correlation with adverse outcome after controlling for all covariates (Q2: OR = 0.83, 95% CI: 0.56–1.21, $p = 0.321$; Q3: OR = 1.04, 95% CI: 0.71–1.53, $p = 0.841$; Q4: OR = 1.35, 95% CI: 0.91–1.98, $p = 0.133$; Supplementary Table 6).

3.3 Analysis of the nonlinear relationship between the baseline HRR and unfavorable outcome

After adjusting for factors in Model II, a curve-fitting equation for the baseline HRR and adverse outcomes was derived via RCS analysis. We identified a nonlinear correlation between the HRR and adverse outcome (Figure 2). A two-piecewise model was employed in the threshold analysis to evaluate the correlation between the baseline HRR and adverse outcome. The inflection point was determined to be 10.70 (Table 3). To the left of the inflection point, the OR for the HRR was 0.76 (95% CI: 0.66–0.86, $p < 0.001$), indicating a 24% decrease in the likelihood of adverse outcome with each 1-unit increase in the HRR. To the right of the inflection point, the OR was 1.04 (95% CI: 0.82–1.31, $p = 0.755$), indicating that the

TABLE 1 Relationship between HRR and unfavorable outcome 3 months after AIS in different models.

Variable	Crude model (OR, 95%CI)	p-value	Model I (OR, 95%CI)	p-value	Model II (OR, 95%CI)	p-value
HRR	0.82 (0.77, 0.87)	<0.001*	0.85 (0.80, 0.91)	<0.001*	0.81 (0.72, 0.91)	<0.001*
HRR (Quartiles)						
Q1 (<8.96)	Ref		Ref		Ref	
Q2 (8.96–10.30)	0.59 (0.44, 0.80)	<0.001*	0.59 (0.44, 0.81)	<0.001*	0.65 (0.44, 0.97)	0.028*
Q3 (10.30–11.30)	0.43 (0.31, 0.59)	<0.001*	0.51 (0.37, 0.70)	<0.001*	0.53 (0.33, 0.84)	0.007*
Q4 (>11.3)	0.43 (0.32, 0.59)	<0.001*	0.57 (0.41, 0.79)	<0.001*	0.58 (0.34, 0.96)	0.039*
p for trend	0.81 (0.75, 0.87)	<0.001*	0.86 (0.80, 0.92)	<0.001*	0.87 (0.76, 0.98)	0.024*

Crude mode1: we did not adjust for other covariates; Model I: we adjusted for sex and age; Model II: Model I + WBC, RBC, PLT, LDL-C, BUN, FBG, ALT, hs-CRP, BMI, hypertension, DM, hyperlipidemia, CHD, AF, smoking status, NIHSS score at admission, and previous mRs. *Indicates statistical significance after Benjamini-Hochberg.

TABLE 2 Relationship between HRR and unfavorable outcome 3 months after AIS in different models by using multiple imputation.

Variable	Crude model (OR, 95%CI)	*p*-value	Model I (OR, 95%CI)	*p*-value	Model II (OR, 95%CI)	*p*-value
HRR	0.82 (0.77, 0.87)	<0.001	0.85 (0.80, 0.91)	<0.001	0.80 (0.71, 0.90)	<0.001
HRR (Quartiles)						
Q1 (<8.96)	Ref		Ref		Ref	
Q2 (8.96–10.30)	0.59 (0.44, 0.80)	<0.001	0.59 (0.44, 0.81)	<0.001	0.65 (0.45, 0.95)	0.026
Q3 (10.30–11.30)	0.43 (0.31, 0.59)	<0.001	0.51 (0.37, 0.70)	<0.001	0.52 (0.34, 0.80)	0.003
Q4 (>11.3)	0.43 (0.32, 0.59)	<0.001	0.57 (0.41, 0.79)	<0.001	0.60 (0.36, 1.00)	0.049
p for trend	0.81 (0.75, 0.87)	<0.001	0.86 (0.80, 0.92)	<0.001	0.87 (0.77, 0.98)	0.024

Crude mode 1: we did not adjust for other covariates; Model I: We adjusted for sex and age; Model II: Model I + WBC, RBC, PLT, LDL-C, BUN, FBG, ALT, hs-CRP, BMI, hypertension, DM, hyperlipidemia, CHD, smoking status, and previous mRs.

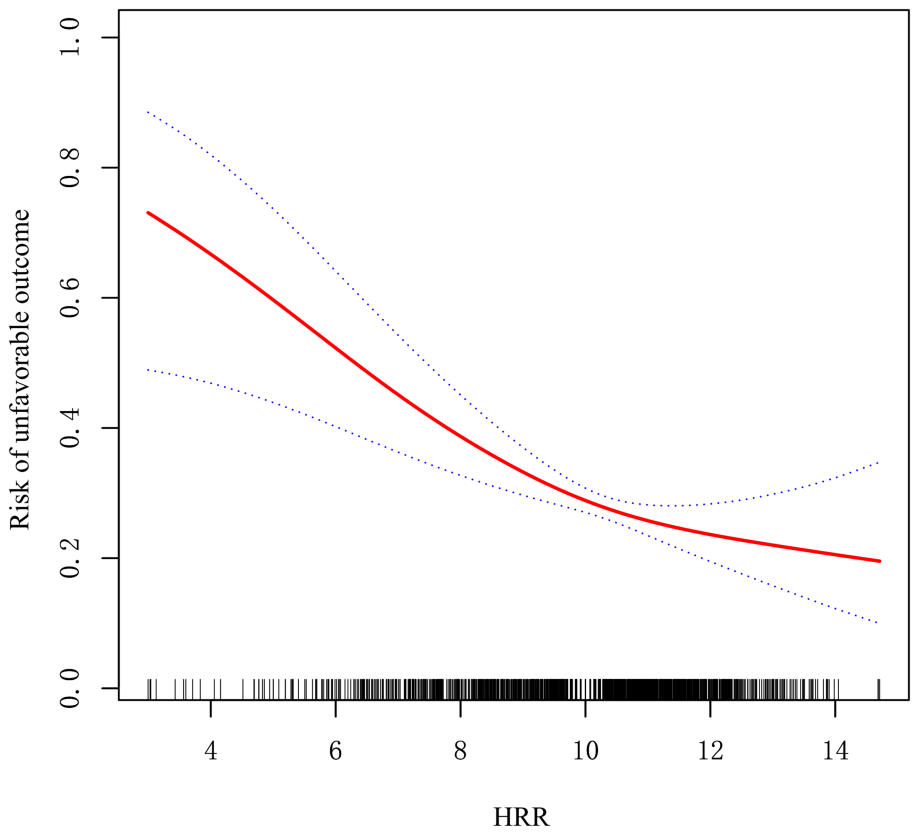

FIGURE 2
Non-linear relationship observed between the baseline HRR level and the risk of unfavorable outcome. The solid red line represents the smooth curve fit between variables. Blue bands present the 95% confidence interval. The data were adjusted for the variables in Model II.

correlation between the HRR and adverse outcome was not statistically significant when the HRR exceeded 10.71. This finding suggests that the likelihood of adverse outcome decreases with increasing HRR. The *p*-value for the LRT in our research was 0.022.

3.4 Subgroup analysis

Subgroup analysis was performed to investigate the association between the HRR and unfavorable outcome across multiple variables, including age, sex, hypertension, DM, hyperlipidemia, smoking status, CHD, BMI, and NIHSS score at admission. The findings are illustrated in Figure 3. The analysis of the interaction between the HRR and each subgroup variable indicated no significant interactions (*p* for interaction >0.05).

3.5 Comparative predictive value of HRR and other inflammatory biomarkers for 3-month unfavorable outcomes in older AIS patients

In the Crude Model, white blood cell count (WBC) was significantly associated with unfavorable outcomes 3 months after

TABLE 3 Threshold-effect analysis of the relationship between the baseline HRR level and unfavorable outcome 3 months after AIS.

Models	Per-unit increase		
	OR	95%CI	*p*-value
Model I	0.81	0.721–0.91	<0.001
One line effect			
Model II			
Turning point (K)	10.70		
Baseline HRR levels < K	0.76	0.66–0.86	<0.001
Baseline HRR levels > K	1.04	0.82–1.31	0.755
p-value for LRT test*			0.022

Model I, one-line linear regression model; Model II, two-piece wise linear regression model. Adjusted for WBC, RBC, PLT, LDL-C, BUN, FBG, ALT, hs-CRP, BMI, hypertension, DM, hyperlipidemia, CHD, AF, smoking status, NIHSS score at admission, and previous mRs. OR, Odd Ratio; CI, confidence interval; LRT, logarithm likelihood ratio test. *$p < 0.05$ indicates that Model II is significantly different from Model I.

acute ischemic stroke (AIS; OR = 1.07, 95%CI: 1.03–1.11, $p < 0.001$; Supplementary Table 7). This significant association persisted in Model I after adjusting for sex and age (OR = 1.07, 95%CI: 1.03–1.11, $p = 0.001$). However, in the fully adjusted Model II, the association between WBC and unfavorable outcomes was no longer significant (OR = 1.02, 95%CI: 0.97–1.07, $p = 0.556$). Hs-CRP was significantly associated with unfavorable outcomes across all models (Supplementary Table 8). In the Crude Model, each unit increase in hs-CRP was associated with a 14% higher risk of unfavorable outcomes (OR = 1.14, 95%CI: 1.09–1.18, $p < 0.001$). This association remained significant in Model I (OR = 1.12, 95%CI: 1.08–1.17, $p < 0.001$) and Model II (OR = 1.10, 95%CI: 1.05–1.16, $p < 0.001$). For the FPG/HbA1c ratio, a significant association with unfavorable outcomes was observed in the Crude Model (OR = 1.08, 95%CI: 1.05–1.11, p < 0.001) and Model I (OR = 1.09, 95%CI: 1.06–1.12, $p < 0.001$; Supplementary Table 9). However, this association became nonsignificant in the fully adjusted Model II (OR = 1.05, 95%CI: 0.99–1.12, $p = 0.111$).

To further evaluate the predictive value of HRR compared with other inflammatory biomarkers, including hs-CRP, FPG/HbA1c, and WBC, ROC curves and the corresponding AUC values were calculated (Supplementary Figure 1). For unfavorable outcomes within 3 months, the AUCs (95% confidence intervals) were as follows: HRR, 0.64 (0.61–0.67); hs-CRP, 0.60 (0.57–0.63); FPG/HbA1c, 0.59 (0.55–0.63); and WBC, 0.55 (0.51–0.58).

4 Discussion

This retrospective observational study investigated the correlation between baseline heart rate recovery (HRR) levels and three-month unfavorable outcome in older patients with AIS, yielding several significant findings. First, the HRR exhibited an inverse relationship with unfavorable outcome after controlling for potential confounders. Second, a threshold effect was identified: when the HRR fell below 10.71, the risk of adverse outcome decreased as the HRR increased. However, in older patients with HRR levels exceeding this threshold, no further reduction in the risk of unfavorable outcome was observed over 3 months. Third, no significant interaction was found between the baseline HRR and adverse outcome in AIS patients, suggesting that the HRR was independently associated with unfavorable outcome across various subgroups. Fourth, the HRR demonstrated better predictive performance for unfavorable outcome. This study bridges the gap in understanding the role of HRR as a composite hematological biomarker derived from Hb and RDW, offering a novel perspective for integrating these routinely available parameters into clinical risk stratification for AIS.

Researchers have proposed several hypotheses to explain why older people with AIS experience negative outcome due to a lower HRR. Initially, elevated RDWs within normal limits may signify enhanced red blood cell breakdown, inefficient erythropoiesis, or a greater quantity of immature red blood cells (25, 26). Concurrently, red blood cells possess significant antioxidant capacity, and abnormalities in these cells might result in diminished cell survival rates (27, 28). Oxidative stress and microcirculatory impairment also exert considerable influence. Moreover, extensive recognition links inflammation to AIS. Inflammatory responses can exacerbate cerebral edema, hinder healing, and lead to an unfavorable prognosis (29, 30). RDW is positively related to plasma inflammatory biomarkers such as C-reactive protein (31, 32), the erythrocyte sedimentation rate (ESR) (33), soluble tumor necrosis factor-α (TNF-α) (34), and interleukin-6 (34, 35). An increased RDW, even within the normal limits, may signify an underlying inflammatory condition, potentially intensifying inflammation and worsening results following AIS. Research has indicated that elevated RDWs correlate with adverse functional outcome in AIS patients at discharge and at the three-month follow-up (26, 36). Second, decreased hemoglobin levels indicate a reduced ability for oxygen transport, resulting in inadequate oxygen supply and an energy deficit in the ischemic penumbra (37). Reduced hemoglobin levels can diminish muscle strength, induce cognitive impairment, and increase fatigue, thereby increasing the risk of frailty in older individuals (38). Moreover, anemia can induce the release of inflammatory mediators, including TNF-α (30). Bullock et al. reported that inadequate nutritional status and a weakened immune response may adversely affect patient prognosis (39).

While hemoglobin and red cell distribution width exhibit predictive significance in AIS patients, they are influenced by numerous factors. Our investigation revealed no significant associations between Hb or RDW and adverse outcome in AIS patients. Since Hb and RDW combine to form the HRR, it could offer a more stable and effective evaluation than individual Hb or RDW measurements do. HRR objectively indicates inflammatory and microcirculatory conditions, potentially functioning as a superior biomarker. The HRR, derived from routine hematological parameters, provides a practical and cost-effective tool for early risk stratification in older AIS patients, enabling timely and targeted therapeutic interventions in real-world clinical settings. Prior research has indicated that a lower HRR is correlated with unfavorable outcome in multiple malignant conditions (10, 40–44). Recently, the HRR has become a vital predictor of mortality and prognosis in cardiovascular disease patients (45). A study with 1,816 older participants indicated that an elevated HRR in heart failure patients decreased the likelihood of 3-month readmission by approximately 30% (46). Yuan et al. reported a negative correlation between the HRR and the incidence of severe adverse cardiovascular events in older adults with CHD (47). According to Qu et al., there is an inverse relationship between a low HRR (<9.76) and the likelihood of frailty in older people with CHD (48). These findings indicate that the HRR is a better predictor of frailty than the RDW or Hb level (48). Research using the MIMIC-IV database also revealed that a lower HRR

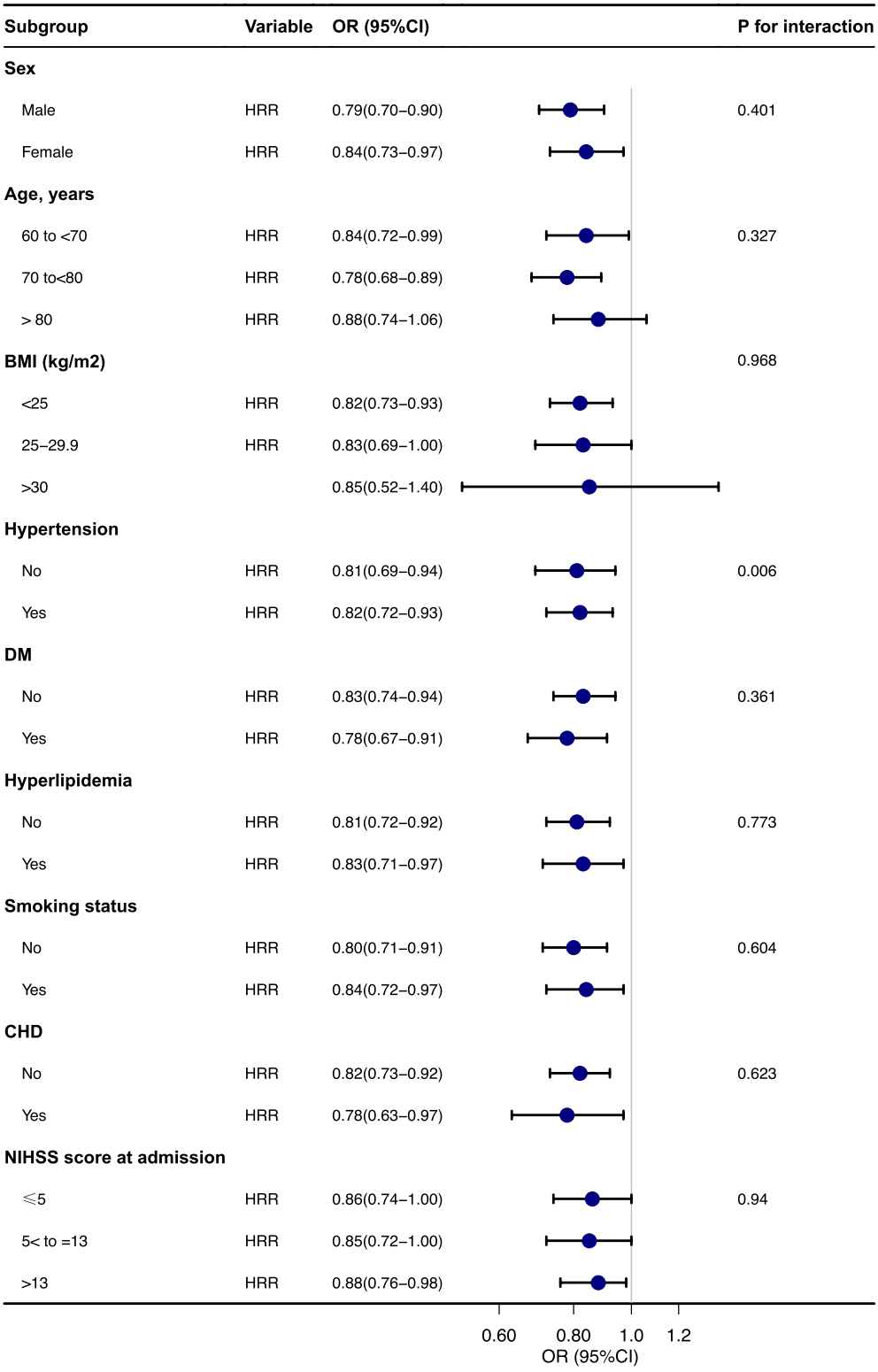

FIGURE 3
Subgroup analyses of the effect of unfavorable outcomes.

(HRR <9.74) was linked to a lower risk of mortality from any cause in people with AIS and atrial fibrillation (19). In patients with AIS receiving intravenous thrombolysis or mechanical thrombectomy, a decreased HRR is correlated with an increased risk of adverse outcome and mortality (49, 50). Lin et al. reported a significant correlation between a decreased HRR and increased mortality risk in older patients suffering from cerebral hemorrhage (51). Our study corroborates prior research and examines the influence of low HRR values on negative outcome in senior AIS patients after 3 months. When the HRR was ≤10.71, we noted a 26% reduction in the likelihood of unfavorable

outcome for older AIS patients with each 1-unit increase in the HRR. These findings suggest that a decreased HRR is correlated with poorer outcome than an elevated HRR. We hypothesize that lower HRR may elevate the risk of adverse outcomes in older individuals with AIS. Additional research is needed to substantiate this notion.

Previous studies have reported that hs-CRP is associated with unfavorable outcome in AIS (51, 52), which is consistent with our findings. Additionally, stress-induced hyperglycemia (FPG/HbA1c) has been linked to increased short-and long-term mortality in AIS, as well as early neurological deterioration (53–55). Traditional inflammatory biomarkers, such as WBC and the Neutrophil-to-Lymphocyte Ratio, have also been associated with poor prognosis in AIS (56, 57). However, in our study, no significant correlations were found between FPG/HbA1c or WBC and unfavorable outcome in AIS. In the ROC prediction model, HRR demonstrated the highest AUC, suggesting that this indicator could potentially offer a more comprehensive and stable prognostic marker for AIS outcome.

Our study has numerous strengths: (1) This is the first investigation into the correlation between baseline HRR levels and adverse outcome in older patients with AIS. (2) The research employed empirical data and included a broad, heterogeneous population. The absence of HRR values likely reduced selection bias. (3) Multiple imputations were used to mitigate statistical bias and improve the reliability of the results. (4) We utilized a two-piecewise logistic regression analysis to examine the threshold influence of the HRR on poor outcome.

However, this study has several limitations. First, the study cohort was derived from a single Korean center, which may not fully represent a broader patient population. Variations in healthcare resources, baseline patient characteristics, and treatment strategies across different regions may influence the association between HRR and unfavorable outcomes. Therefore, future studies should be conducted in multicenter and multi-regional settings to validate these findings and enhance their generalizability. Additionally, we only performed Hb and RDW tests at admission and did not repeat them throughout the hospital stay, thus failing to assess their dynamic changes over time. Previous studies recently highlighted that serial assessments of the Alberta Stroke Program Early CT Score (ASPECTS) may be useful predictors of mortality and poor functional outcomes following thrombolytic therapy (49, 58, 59). The development of a novel clinical prediction model integrating established predictors, serial ASPECTS evaluations, and dynamic HRR changes to predict adverse functional outcomes in elderly patients with AIS remains a significant focus for future research. Futhermore, the study's results were only assessed via the mRS score. Although the mRS extensively evaluates post-stroke performance, it covers only specific aspects of patient rehabilitation. Lastly, comorbid conditions such as heart failure, chronic kidney disease, malnutrition, iron deficiency, vitamin B12 deficiency, folate deficiency, anemia of chronic disease, and thalassemia can significantly impact red blood cell production and lifespan. These effects may alter hemoglobin (Hb) levels and red cell distribution width (RDW), which are critical hematological parameters. Additionally, thrombolysis and endovascular thrombectomy are essential therapeutic interventions that can substantially influence post-stroke outcomes. However, as this study is based on secondary data analysis, the dataset provided by the original authors did not include these variables, limiting our ability to adjust for potential confounding factors. Future multi-center, prospective studies incorporating these variables are necessary to further validate and refine the observed.

5 Conclusion

This study demonstrated a nonlinear association between the HRR and adverse functional outcome in older individuals with AIS. We identified a substantial inverse correlation between elevated HRR and adverse outcome in older people with AIS when the HRR was less than 10.71. Consequently, the HRR predicts favorable clinical outcome in older patients with AIS and may function as an accessible and affordable prognostic biomarker. Timely care for older patients with increased HRR may mitigate adverse AIS outcome.

Data availability statement

The datasets presented in this study can be found in online repositories. The names of the repository/repositories and accession number(s) can be found in the article/Supplementary material.

Ethics statement

The studies involving humans were approved by Institutional Review Board of Seoul National University Hospital (IRB No. 1009–062-332). The studies were conducted in accordance with the local legislation and institutional requirements. The participants provided their written informed consent to participate in this study.

Author contributions

LH: Conceptualization, Formal analysis, Methodology, Writing – original draft. LL: Conceptualization, Formal analysis, Methodology, Writing – original draft. Q-rO: Conceptualization, Methodology, Writing – original draft. PC: Conceptualization, Writing – original draft. MY: Conceptualization, Formal analysis, Supervision, Validation, Writing – review & editing. LX: Conceptualization, Formal analysis, Supervision, Validation, Writing – review & editing.

Funding

The author(s) declare that no financial support was received for the research, authorship, and/or publication of this article.

Acknowledgments

Since this is a secondary analysis, the primary sources of the data and method explanations are as follows: Kang et al. (20). Every researcher who contributed to the original study is deeply appreciated.

Conflict of interest

The authors declare that the research was conducted in the absence of any commercial or financial relationships that could be construed as a potential conflict of interest.

Generative AI statement

The authors declare that no Gen AI was used in the creation of this manuscript.

Publisher's note

All claims expressed in this article are solely those of the authors and do not necessarily represent those of their affiliated organizations, or those of the publisher, the editors and the reviewers. Any product that may be evaluated in this article, or claim that may be made by its manufacturer, is not guaranteed or endorsed by the publisher.

Supplementary material

The Supplementary material for this article can be found online at: https://www.frontiersin.org/articles/10.3389/fneur.2025.1534564/full#supplementary-material

References

1. Valery LF, Melsew DA, Ohannes HA, Samar AE, Foad AA, Hmed A, et al. Global, regional, and national burden of stroke and its risk factors, 1990-2021: a systematic analysis for the Global Burden of Disease Study 2021. *Lancet Neurol.* (2024) 23:973–1003. doi: 10.1016/S1474-4422(24)00369-7

2. Li XY, Kong XM, Yang CH, Cheng ZF, Lv JJ, Guo H, et al. Global, regional, and national burden of ischemic stroke, 1990-2021: an analysis of data from the global burden of disease study 2021. *EClinicalMedicine*. (2024) 75:102758. doi: 10.1016/j.eclinm.2024.102758

3. Salvagno GL, Sanchis-Gomar F, Picanza A, Lippi G. Red blood cell distribution width: a simple parameter with multiple clinical applications. *Crit Rev Cl Lab Sci*. (2015) 52:86–105. doi: 10.3109/10408363.2014.992064

4. Shen Z, Huang Y, Zhou Y, Jia J, Zhang X, Shen T, et al. Association between red blood cell distribution width and ischemic stroke recurrence in patients with acute ischemic stroke: a 10-years retrospective cohort analysis. *Aging (Albany NY)*. (2023) 15:3052–63. doi: 10.18632/aging.204657

5. Li M, Wang L, Zhu X, Huang J, Zhang Y, Gao B, et al. Dose-response relationship between red blood cell distribution width and in-hospital mortality in oldest old patients with acute ischemic stroke. *Gerontology*. (2023) 69:379–85. doi: 10.1159/000527504

6. Peng M, Chen Y, Chen Y, Feng K, Shen H, Huang H, et al. The relationship between red blood cell distribution width at admission and post-stroke fatigue in the acute phase of acute ischemic stroke. *Front Neurol*. (2022) 13:922823. doi: 10.3389/fneur.2022.922823

7. Wang C, Wang L, Zhong D, Deng L, Qiu S, Li Y, et al. Association between red blood cell distribution width and hemorrhagic transformation in acute ischemic stroke patients. *Cerebrovasc Dis*. (2019) 48:193–9. doi: 10.1159/000504742

8. Krongsut S, Na-Ek N, Soontornpun A, Anusasnee N. Integrating the A2DS2 score with 24-hour ASPECTS and red cell distribution width for enhanced prediction of stroke-associated pneumonia following intravenous thrombolysis: model development and internal validation. *Eur J Med Res*. (2025) 30:28. doi: 10.1186/s40001-025-02282-3

9. Ntaios G, Gurer O, Faouzi M, Aubert C, Michel P. Red cell distribution width does not predict stroke severity or functional outcome. *Int J Stroke*. (2012) 7:2–6. doi: 10.1111/j.1747-4949.2011.00609.x

10. Sun P, Zhang F, Chen C, Bi X, Yang H, An X, et al. The ratio of hemoglobin to red cell distribution width as a novel prognostic parameter in esophageal squamous cell carcinoma: a retrospective study from southern China. *Oncotarget*. (2016) 7:42650–60. doi: 10.18632/oncotarget.9516

11. Chen JL, Wu JN, Lv XD, Yang QC, Chen JR, Zhang DM. The value of red blood cell distribution width, neutrophil-to-lymphocyte ratio, and hemoglobin-to-red blood cell distribution width ratio in the progression of non-small cell lung cancer. *PLoS One*. (2020) 15:e0237947. doi: 10.1371/journal.pone.0237947

12. Yuan X, Zeng W, Wang H, Shu G, Wu C, Nie M, et al. Predictive value of the early postoperative hemoglobin-to-red blood cell distribution width ratio for acute kidney injury in elderly intertrochanteric fracture patients. *BMC Musculoskelet Disord*. (2024) 25:630. doi: 10.1186/s12891-024-07745-y

13. Xi L, Fang F, Zhou J, Xu P, Zhang Y, Zhu P, et al. Association of hemoglobin-to-red blood cell distribution width ratio and depression in older adults: a cross sectional study. *J Affect Disord*. (2024) 344:191–7. doi: 10.1016/j.jad.2023.10.027

14. Liu S, Zhang H, Zhu P, Chen S, Lan Z. Predictive role of red blood cell distribution width and hemoglobin-to-red blood cell distribution width ratio for mortality in patients with COPD: evidence from NHANES 1999-2018. *BMC Pulm Med*. (2024) 24:413. doi: 10.1186/s12890-024-03229-w

15. Sun X, Zhang R, Fan Z, Liu Z, Hua Q. Predictive value of hemoglobin-to-red blood cell distribution width ratio for contrast-induced nephropathy after emergency percutaneous coronary intervention. *Perfusion*. (2023) 38:1511–8. doi: 10.1177/02676591221119422

16. Wu F, Yang S, Tang X, Liu W, Chen H, Gao H. Prognostic value of baseline hemoglobin-to-red blood cell distribution width ratio in small cell lung cancer: a retrospective analysis. *Thorac cancer*. (2020) 11:888–97. doi: 10.1111/1759-7714.13330

17. Krongsut S, Piriyakhuntorn P. Unlocking the potential of HB/RDW ratio as a simple marker for predicting mortality in acute ischemic stroke patients after thrombolysis. *J Stroke Cerebrovasc*. (2024) 33:107874. doi: 10.1016/j.jstrokecerebrovasdis.2024.107874

18. Liu J, Wang J. Association between hemoglobin-to-red blood cell distribution width ratio and hospital mortality in patients with non-traumatic subarachnoid hemorrhage. *Front Neurol*. (2023) 14. doi: 10.3389/fneur.2023.1180912

19. Qin Z, Liao N, Lu X, Duan X, Zhou Q, Ge L. Relationship between the hemoglobin-to-red cell distribution width ratio and all-cause mortality in ischemic stroke patients with atrial fibrillation: An analysis from the MIMIC-IV database. *Neuropsychiatr Dis Treat*. (2022) 18:341–54. doi: 10.2147/NDT.S350588

20. Kang MK, Kim TJ, Kim Y, Nam KW, Jeong HY, Kim SK, et al. Geriatric nutritional risk index predicts poor outcomes in patients with acute ischemic stroke - automated undernutrition screen tool. *PLoS One*. (2020) 15:e0228738. doi: 10.1371/journal.pone.0228738

21. Sørensen RT, Rasmussen RS, Overgaard K, Lerche A, Johansen AM, Lindhardt T. Dysphagia screening and intensified oral hygiene reduce pneumonia after stroke. *J Neurosci Nurs*. (2013) 45:139–46. doi: 10.1097/JNN.0b013e31828a412c

22. Le Bouc R, Clarençon F, Meseguer E, Lapergue B, Consoli A, Turc G, et al. Efficacy of endovascular therapy in acute ischemic stroke depends on age and clinical severity. *Stroke*. (2018) 49:1686–94. doi: 10.1161/STROKEAHA.117.020511

23. Wang J, Chen Z, Yang H, Li H, Chen R, Yu J. Relationship between the hemoglobin-to-red cell distribution width ratio and all-cause mortality in septic patients with atrial fibrillation: based on propensity score matching method. *J Cardiovasc Dev Dis*. (2022) 9:400. doi: 10.3390/jcdd9110400

24. Lin L, Chen CZ, Yu XD. The analysis of threshold effect using empower stats software. *Zhonghua Liu Xing Bing Xue Za Zhi*. (2013) 34:1139–41.

25. Song SY, Hua C, Dornbors D, Kang RJ, Zhao XX, Du X, et al. Baseline red blood cell distribution width as a predictor of stroke occurrence and outcome: a comprehensive Meta-analysis of 31 studies. *Front Neurol*. (2019) 10:1237. doi: 10.3389/fneur.2019.01237

26. Turcato G, Cappellari M, Follador L, Dilda A, Bonora A, Zannoni M, et al. Red blood cell distribution width is an independent predictor of outcome in patients undergoing thrombolysis for ischemic stroke. *Semin Thromb Hemost*. (2017) 43:30–5. doi: 10.1055/s-0036-1592165

27. Lippi G, Plebani M. Red blood cell distribution width (RDW) and human pathology. One size fits all. *Clin Chem Lab Med*. (2014) 52:1247–9. doi: 10.1515/cclm-2014-0585

28. Emans ME, van der Putten K, van Rooijen KL, Kraaijenhagen RJ, Swinkels D, van Solinge WW, et al. Determinants of red cell distribution width (RDW) in cardiorenal patients: RDW is not related to erythropoietin resistance. *J Card Fail*. (2011) 17:626–33. doi: 10.1016/j.cardfail.2011.04.009

29. Zhao X, Ting SM, Liu CH, Sun G, Kruzel M, Roy-O'Reilly M, et al. Neutrophil polarization by IL-27 as a therapeutic target for intracerebral hemorrhage. *Nat Commun*. (2017) 8:602. doi: 10.1038/s41467-017-00770-7

30. Esposito E, Zhang F, Park JH, Mandeville ET, Li W, Cuartero MI, et al. Diurnal differences in immune response in brain, blood and spleen after focal cerebral ischemia in mice. *Stroke*. (2022) 53:e507–11. doi: 10.1161/STROKEAHA.122.040547

31. Karabuga B, Gemcioglu E, Konca Karabuga E, Baser S, Ersoy O. Comparison of the predictive values of CRP, CRP/albumin, RDW, neutrophil/lymphocyte, and platelet/lymphocyte levels in determining the severity of acute pancreatitis in patients with acute pancreatitis according to the BISAP score. *Bratisl Med J*. (2022) 123:129–35. doi: 10.4149/BLL_2022_020

32. Crook JM, Horgas AL, Yoon SL, Grundmann O, Johnson-Mallard V. Vitamin C plasma levels associated with inflammatory biomarkers, CRP and RDW: results from the NHANES 2003-2006 surveys. *Nutrients*. (2022) 14:1254. doi: 10.3390/nu14061254

33. Kc S, Kc R, Yadav BK, Basnet B, Basnet A. The role of TLC, RDW, and ESR in predicting short-term prognosis among admitted patients with acute ischemic stroke: insights from a cross-sectional study. *Health Sci Rep*. (2024) 7:e2168. doi: 10.1002/hsr2.2168

34. He Y, Liu C, Zeng Z, Ye W, Lin J, Ou Q. Red blood cell distribution width: a potential laboratory parameter for monitoring inflammation in rheumatoid arthritis. *Clin Rheumatol*. (2018) 37:161–7. doi: 10.1007/s10067-017-3871-7

35. Dai M, Wei Q, Zhang Y, Fang C, Qu P, Cao L. Predictive value of red blood cell distribution width in Poststroke depression. *Comput Math Method*. (2021) 2021:1–6. doi: 10.1155/2021/8361504

36. Pinho J, Marques SA, Freitas E, Araújo J, Taveira M, Alves JN, et al. Red cell distribution width as a predictor of 1-year survival in ischemic stroke patients treated with intravenous thrombolysis. *Thromb Res*. (2018) 164:4–8. doi: 10.1016/j.thromres.2018.02.002

37. Desai A, Oh D, Rao EM, Sahoo S, Mahajan UV, Labak CM, et al. Impact of anemia on acute ischemic stroke outcomes: a systematic review of the literature. *PLoS One*. (2023) 18:e0280025. doi: 10.1371/journal.pone.0280025

38. Kang JY, Kim CH, Sung EJ, Shin HC, Shin WJ, Jung KH. The association between frailty and cognition in elderly women. *Korean J Fam Med*. (2016) 37:164–70. doi: 10.4082/kjfm.2016.37.3.164

39. Bullock AF, Greenley SL, McKenzie GAG, Paton LW, Johnson MJ. Relationship between markers of malnutrition and clinical outcomes in older adults with cancer: systematic review, narrative synthesis and meta-analysis. *Eur J Clin Nutr*. (2020) 74:1519–35. doi: 10.1038/s41430-020-0629-0

40. Zhai Z, Gao J, Zhu Z, Cong X, Lou S, Han B, et al. The ratio of the hemoglobin to red cell distribution width combined with the ratio of platelets to lymphocytes can predict the survival of patients with gastric Cancer liver metastasis. *Biomed Res Int*. (2021) 2021:8729869. doi: 10.1155/2021/8729869

41. Petrella F, Casiraghi M, Radice D, Cara A, Maffeis G, Prisciandaro E, et al. Prognostic value of the hemoglobin/red cell distribution width ratio in resected lung adenocarcinoma. *Cancers (Basel)*. (2021) 13:710. doi: 10.3390/cancers13040710

42. Mirili C. The ratio of hemoglobin-to-red cell distribution width could predict survival in advanced pancreatic adenocarcinoma. *Leuk Res*. (2019) 85:S74. doi: 10.1016/S0145-2126(19)30391-1

43. Bozkaya Y, Kurt B, Gürler F. A prognostic parameter in advanced non-small cell lung cancer: the ratio of hemoglobin-to-red cell distribution width. *Int J Clin Oncol*. (2019) 24:798–806. doi: 10.1007/s10147-019-01417-x

44. Tham T, Olson C, Wotman M, Teegala S, Khaymovich J, Coury J, et al. Evaluation of the prognostic utility of the hemoglobin-to-red cell distribution width ratio in head and neck cancer. *Eur Arch Oto-Rhino-L*. (2018) 275:2869–78. doi: 10.1007/s00405-018-5144-8

45. Rahamim E, Zwas DR, Keren A, Elbaz-Greener G, Ibrahimli M, Amir O, et al. The ratio of hemoglobin to red cell distribution width: a strong predictor of clinical outcome in patients with heart failure. *J Clin Med*. (2022) 11:886. doi: 10.3390/jcm11030886

46. Song J, Yu T, Yan Q, Zhang Q, Wang L. Association of Hemoglobin to red blood cell distribution width-standard deviation (RDW-SD) ratio and 3-month readmission in elderly Chinese patients with heart failure: a retrospective cohort study. *Int J Gen Med*. (2023) 16:303–15. doi: 10.2147/IJGM.S396805

47. Yuan X, Lv C, Wu S, Wang H, Liu X. The predictive value of hemoglobin to red cell blood distribution width ratio combined with serum sodium for MACE of acute heart failure with preserved ejection fraction in elderly patients. *Int J Gen Med*. (2024) 17:863–70. doi: 10.2147/IJGM.S453538

48. Qu J, Zhou T, Xue M, Sun H, Shen Y, Chen Y, et al. Correlation analysis of hemoglobin-to-red blood cell distribution width ratio and frailty in elderly patients with coronary heart disease. *Front Cardiovasc Med*. (2021) 8:728800. doi: 10.3389/fcvm.2021.728800

49. Krongsut S, Srikaew S, Anusasnee N. Prognostic value of combining 24-hour ASPECTS and hemoglobin to red cell distribution width ratio to the THRIVE score in predicting in-hospital mortality among ischemic stroke patients treated with intravenous thrombolysis. *PLoS One*. (2024) 19:e0304765. doi: 10.1371/journal.pone.0304765

50. Feng X, Zhang Y, Li Q, Wang B, Shen J. Hemoglobin to red cell distribution width ratio as a prognostic marker for ischemic stroke after mechanical thrombectomy. *Front Aging Neurosci*. (2023) 15:1259668. doi: 10.3389/fnagi.2023.1259668

51. Lin Q, Liao J, Dong W, Zhou F, Xu Y. The relationship between hemoglobin/red blood cell distribution width ratio and mortality in patients with intracranial hemorrhage: a possible protective effect for the elderly? *Intern Emerg Med*. (2023) 18:2301–10. doi: 10.1007/s11739-023-03431-4

52. Gu HQ, Yang KX, Lin JX, Jing J, Zhao XQ, Wang YL, et al. Association between high-sensitivity C-reactive protein, functional disability, and stroke recurrence in patients with acute ischaemic stroke: A mediation analysis. *EBioMedicine*. (2022) 80:104054. doi: 10.1016/j.ebiom.2022.104054

53. Liu Y, Wang J, Zhang L, Wang C, Wu J, Zhou Y, et al. Relationship between C-reactive protein and stroke: a large prospective community based study. *PLoS One*. (2014) 9:e107017. doi: 10.1371/journal.pone.0107017

54. Mi D, Li Z, Gu H, Jiang Y, Zhao X, Wang Y, et al. Stress hyperglycemia is associated with in-hospital mortality in patients with diabetes and acute ischemic stroke. *CNS Neurosci Ther*. (2022) 28:372–81. doi: 10.1111/cns.13764

55. Roberts G, Sires J, Chen A, Thynne T, Sullivan C, Quinn S, et al. A comparison of the stress hyperglycemia ratio, glycemic gap, and glucose to assess the impact of stress-induced hyperglycemia on ischemic stroke outcome. *J Diabetes*. (2021) 13:1034–42. doi: 10.1111/1753-0407.13223

56. Adiguzel A, Arsava EM, Topcuoglu MA. Temporal course of peripheral inflammation markers and indexes following acute ischemic stroke: prediction of mortality, functional outcome, and stroke-associated pneumonia. *Neurol Res*. (2022) 44:224–31. doi: 10.1080/01616412.2021.1975222

57. Xue J, Huang W, Chen X, Li Q, Cai Z, Yu T, et al. Neutrophil-to-Lymphocyte Ratio Is a Prognostic Marker in Acute Ischemic Stroke. *J Stroke Cerebrovasc*. (2017) 26:650–7. doi: 10.1016/j.jstrokecerebrovasdis.2016.11.010

58. Krongsut S, Naraphong W, Srikaew S, Anusasnsee N. Performance of serial CT ASPECTS for predicting stroke outcomes in patients with thrombolyzed acute ischemic stroke. *J Neurosci Rural Pra*. (2023) 14:671–80. doi: 10.25259/JNRP_57_2023

59. Kong WY, Tan BYQ, Ngiam NJH, Tan DYC, Yuan CH, Holmin S, et al. Validation of serial Alberta stroke program early CT score as an outcome predictor in Thrombolyzed stroke patients. *J Stroke Cerebrovasc*. (2017) 26:2264–71. doi: 10.1016/j.jstrokecerebrovasdis.2017.05.009

frontiers | Frontiers in Neurology

TYPE Original Research
PUBLISHED 08 April 2025
DOI 10.3389/fneur.2025.1567902

OPEN ACCESS

EDITED BY
Haipeng Liu,
Coventry University, United Kingdom

REVIEWED BY
Xiaoyan Lan,
Affiliated Central Hospital of Dalian University of Technology, China
Yun-Xiang Zhou,
The First Affiliated Hospital of Shaoyang University, China
Danyang Li,
The Second Affiliated Hospital of Harbin Medical University, China

*CORRESPONDENCE
Xueyuan Liu
✉ Liuxy@tongji.edu.cn

RECEIVED 28 January 2025
ACCEPTED 24 March 2025
PUBLISHED 08 April 2025

CITATION
Wang X and Liu X (2025) Exploration of the shared gene signatures and molecular mechanisms between cardioembolic stroke and ischemic stroke.
Front. Neurol. 16:1567902.
doi: 10.3389/fneur.2025.1567902

Exploration of the shared gene signatures and molecular mechanisms between cardioembolic stroke and ischemic stroke

Xuan Wang[1,2] and Xueyuan Liu[2,3]*

[1]Department of Neurology, Shanghai Tenth People's Hospital, Tongji University School of Medicine, Shanghai, China, [2]School of Medicine, Tongji University, Shanghai, China, [3]Department of Neurology, Tongren Hospital, Shanghai Jiao Tong University School of Medicine, Shanghai, China

Introduction: This study aimed to investigate the shared molecular mechanisms underlying cardioembolic stroke (CS) and ischemic stroke (IS) using integrated bioinformatics analysis.

Methods: Microarray datasets for the CS (GSE58294, blood samples from CS and controls) and IS (GSE16561, blood from IS and controls; GSE22255, peripheral blood mononuclear cells from IS and matched controls) were acquired from the Gene Expression Omnibus database. Differential expression analysis and weighted gene co-expression network analysis were utilized to identify shared genes between the two diseases. Protein-protein interaction (PPI) network and topology analyses were conducted to identify the core shared genes. Three machine learning algorithms were employed to detect biomarkers from the core shared genes, and the diagnostic value of the hub genes was evaluated by establishing a predictive nomogram. Immune infiltration was evaluated using single-sample gene set enrichment analysis (ssGSEA), and pathways were analyzed with gene set enrichment analysis.

Results: There were 125 shared up-regulated genes and 2 shared down-regulated between CS and IS, which were mainly involved in immune inflammatory response-related biological functions. The Maximum Clique Centrality algorithm identified 25 core shared genes in the PPI network constructed using the shared genes. ABCA1, CLEC4E, and IRS2 were identified as biomarkers for both CS and IS and performed well in predicting the onset risk of CS and IS. All three biomarkers were highly expressed in both CS and IS compared to their corresponding controls. These biomarkers significantly correlated with neutrophil infiltration and autophagy activation in both CS and IS. Particularly, all three biomarkers were associated with the activation of neutrophil extracellular trap formation, but only in the IS.

Conclusion: ABCA1, CLEC4E, and IRS2 were identified as potential key biomarkers and therapeutic targets for CS and IS. Autophagy and neutrophil infiltration may represent the common mechanisms linking these two diseases.

KEYWORDS

cardioembolic stroke, ischemic stroke, biomarker, autophagy, neutrophil

1 Introduction

Stroke is one of the leading causes of death worldwide, placing a heavy burden on both individuals and society, particularly as population aging has become a key feature of demographic development (1, 2). The stroke burden has increased substantially (70% and 102% increase in incidence and prevalence, and 43% increase in deaths) from 1990 to 2019, based on the Global Stroke Fact Sheet 2022 published by the World Stroke Organization (3). In China, the incidence and mortality rates of stroke increased by 86.0% and 32.3%, respectively, from 1990 to 2019 (4). Ischemic stroke (IS) is the most common type of stroke, accounting for 87% of all strokes (5). IS can be caused by an interruption of cerebral blood flow from multiple events, such as embolism of cardiac origin, occlusion of small vessels in the brain, and atherosclerosis, which initiate a series of pathophysiological processes, including immune cell infiltration and neuronal death (6). Despite current advances in medical intervention, treatment options for IS remain limited (7, 8), emphasizing the need to illustrate the mechanisms of IS and develop new therapeutic targets.

Cardiogenic cerebral embolism, also termed cardioembolic stroke (CS), refers to the clinical syndrome of cerebral artery embolism caused by cardioembolic embolism from the heart and aortic arch through circulation (9). CS is a major subtype of IS, which accounts for approximately 20%-30% of all IS cases worldwide (10, 11). Compared with IS caused by other etiologies, CS is more severe, has a worse prognosis, and has a higher recurrence rate (12). However, it is worth noting that CS has a missed diagnosis rate as high as 10%−15% (13). In addition, differences in etiology and embolus composition across different stroke subtypes determine the differences in treatment methods (9, 14). For example, patients with CS often requires oral anticoagulants to prevent recurrent events (15, 16). Therefore, illustrating the similarities and differences in the molecular expression and regulatory mechanisms between CS and other IS is of great significance in the clinical management of stroke. Nevertheless, this issue has rarely been investigated.

In this study, genes associated with CS and IS were screened independently using differential analysis and weighted gene co-expression network analysis (WGCNA), followed by screening for shared genes between these two stroke subtypes. Next, three machine learning algorithms were employed to identify core biomarkers for these two diseases. Subsequently, the associations of these biomarkers with immune infiltration and biological pathways as well as the molecular drug regulatory network for biomarkers were explored in both CS and IS. This study revealed inherent connections between the CS and IS, which may contribute to the clinical management of stroke.

Abbreviations: CS, cardioembolic stroke; IS, ischemic stroke; DEGs, differentially expressed genes; WGCNA, weighted gene co-expression network analysis; PPI, protein-protein interaction; GSEA, gene set enrichment analysis; MCC, Maximum Clique Centrality; NETs, neutrophil extracellular traps.

2 Materials and methods

2.1 Data acquisition and preprocessing

The gene expression profiles of CS (GSE58294) and IS (GSE16561 and GSE22255) used in this analysis were downloaded from the Gene Expression Omnibus database using the R package GEOquery (version 2.66.0). Dataset GSE58294 for CS comprised of 90 blood samples from 69 CS patients and 23 normal controls. Dataset GSE16561 for IS contained 63 blood samples from 39 patients with IS and 24 healthy controls and was used as the discovery dataset. Dataset GSE22255 for IS contained 40 peripheral blood mononuclear cells samples from 20 patients with IS and 20 healthy controls; 15 IS samples and 17 control samples were retained after eliminating outlier samples. This dataset was used as the validation dataset for IS. No additional dataset for CS was retrieved from the GEO database, and therefore no external validation dataset was utilized for CS in this study. The raw microarray data were pre-processed individually for quality control (including background adjustment and normalization) by robust multi-array average (RMA). The count value was converted to log2 (cpm+1) expression data for analysis. Probes ID were converted into gene symbol based on the corresponding annotation file of the platform, and the probes matched no gene symbol were removed.

2.2 Differential expression analysis

Differentially expressed genes (DEGs) between the CS and control samples in the GSE58294 dataset and between the IS and control samples in the GSE16561 dataset were screened using the R package Limma (version 3.54.2), followed by Benjamini & Hochberg corrections for multiple tests. The cut-off values of $|\log FC| > 0.263$ and adjusted $P < 0.05$ were utilized for screening of DEGs.

2.3 WGCNA

The R package WGCNA (version 1.72-1) was run to identify the CS- and IS-associated gene modules. The top 5,000 genes ranked by the median absolute deviation in the discovery dataset were selected for analysis. To remove outliers from the sample, hierarchical clustering analysis was conducted utilizing the "hclust" function, coupled with "method = average" as parameter for calculating distance. Next, a soft-threshold power was determined (the scale-free topological fit index R^2 reached 0.8 for the first time) to establish an unsupervised co-expression matrix that approached a scale-free network. A gene hierarchical clustering dendrogram and dynamic tree cutting were conducted to identify highly correlated gene modules. Finally, Pearson correlations were performed to identify CS and IS-associated gene modules.

2.4 Shared genes between CS and IS

The DEGs of CS and IS, as well as the corresponding module genes, were intersected to obtain the shared genes across the two diseases. Gene ontology and Kyoto Encyclopedia of Genes and Genomes (KEGG) pathway enrichment analysis were performed utilizing R package clusterProfiler (version 4.6.2) to explore potential biological functions and signaling pathways associated with these shared genes, with Benjamini and Hochberg method employed for multiple-testing correction. The adjusted $P < 0.05$ and count ≥ 2 was utilized as cut-off values. Protein–protein interactions (PPI) among these shared genes were predicted utilizing the Search Tool for the Retrieval of Interacting Genes/Proteins (STRING) database, and the PPI network was visualized using Cytoscape software (version 3.10.2). The Maximum Clique Centrality (MCC) method of the CytoHubba plug-in was applied to screen the top 25 genes in the PPI network.

2.5 Machine learning for identifying diagnostic biomarkers

Three machine learning algorithms, lasso-logistic, Boruta, and Support Vector Machine-Recursive Feature Elimination (SVM-REF), were employed to select potential diagnostic biomarkers from shared genes. Specifically, lasso-logistic analysis was conducted utilizing the R package glmnet (version 4.1-8) with 5-fold cross-validation, while Boruta analysis was conducted using the R packages Boruta (version 8.0.0). SVM-RFE is a feature selection method based on SVM, which was carried out with 10-fold cross validation by using R package e1071 (version 1.7-14). The feature genes identified by each algorithm were merged to obtain candidate diagnostic biomarkers. The expression of these candidate biomarkers in both discovery and validation datasets was analyzed. The predictive power of these candidate biomarkers was assessed by plotting receiver operating characteristic (ROC) and precision-recall (PR) curves. Only those with consistent differential expression in both discovery and validation datasets and an area under the ROC curve (AUROC) and PR curve (AUPRC) over 0.6 were finally selected as biomarkers. To facilitate the clinical use of these identified biomarkers, a predictive Nomogram was established using the R package "rms" (version 6.7-1). The accuracy and clinical value of the Nomogram model was further evaluated through calibration curve and decision curve analysis, which were plotted utilizing the calibrate method provided in "rms" package and the R package rmda (version 1.6), respectively.

2.6 Evaluation of immune infiltration

The infiltration fractions of 28 types of immune cells in tissue samples were inferred using single-sample gene set enrichment analysis (ssGSEA), which was conducted through the R package GSVA (version 1.46.0). In addition, differences in the infiltration fractions of each immune cell type across the disease and control groups were assessed using *t*-tests ($P < 0.05$). Pearson's correlation analysis was performed to determine the relationship between biomarkers and infiltrating immune cells.

2.7 Construction of regulatory networks

The interacting genes and their functions in the identified biomarkers were further analyzed using the GeneMANIA database (http://genemania.org/). Transcription factors and microRNA (miRNAs) that may target biomarkers were predicted utilizing the online tool NetworkAnalyst.

2.8 Small molecule drug prediction and molecular docking

Small molecule drugs that may target biomarkers were predicted using the dgidb database. To gain insight into how the drugs bind to key genes, we performed a molecular docking analysis. Briefly, the three-dimensional (3D) structures of the drugs were acquired from the PubChem database, and the protein structures corresponding to the biomarkers were predicted using the R package AlphaFold (version 2.0). Subsequently, CB-Dock (version 1.0) was employed to simulate molecular docking, and the results were visualized using the PyMOL software (version 3.0).

2.9 Gene set enrichment analysis

To illustrate the biological functions of biomarkers, disease samples were categorized into high- and low-expression groups based on the median value, and the deregulated pathways across the expression groups were explored through GSEA. Briefly, with the KEGG gene set as an enrichment reference, GSEA analysis was performed utilizing the R package clusterProfiler, and the threshold values were adjusted to $P < 0.05$ and |normalized enrichment Score (NES)| > 1.

3 Results

3.1 Screening of key dysregulated genes in CS and IS

In the GSE58294 dataset, there were 4,591 DEGs between the CS and control samples. Of which, the expression of 2,272 genes increased, whereas the expression of 2,319 genes decreased in the CS samples (Figure 1A). Gene modules highly associated with CS were further screened utilizing WGCNA, and a soft-threshold power of 10 was selected to balance the relationship between mean connectivity and scale independence (Figure 1B). A total of 15 gene modules were identified, with a minimum of 50 genes per gene module, and 10 modules were determined when merging the modules with 75% correlation (Figure 1C). Heatmap of module–trait relationships showed that "blue" module was positively correlated with CS ($r = 0.66$, $P = 5e\text{-}13$, Figure 1D). Therefore, the 817 genes in this "blue" module were regarded as CS-associated module genes.

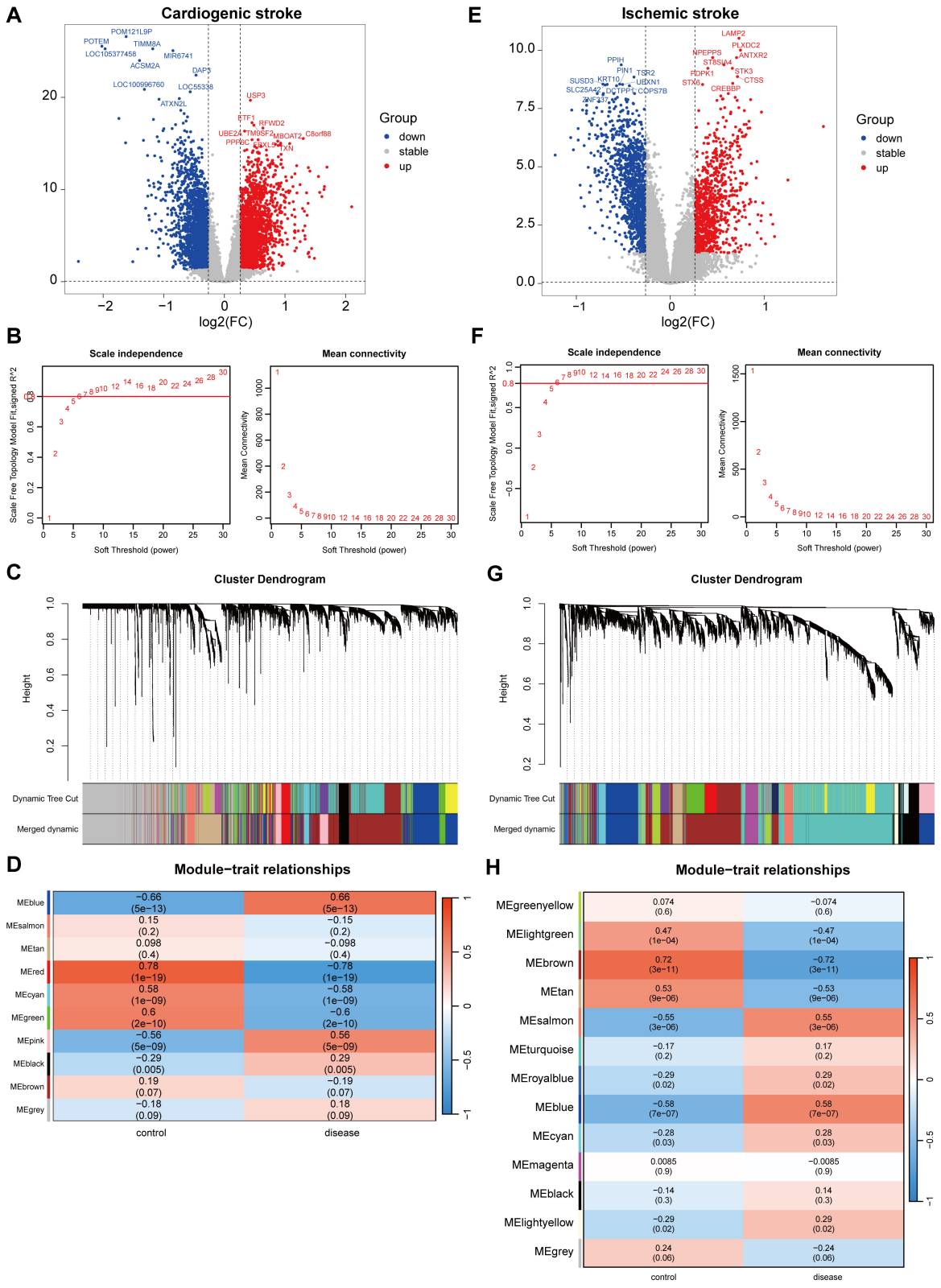

FIGURE 1
Identification of gene modules associated with cardioembolic stroke (CS) and ischemic stroke (IS). **(A, E)** Volcano plots showing the differentially expressed genes (DEGs) between CS and control samples or between IS and control samples. The red and blue dots refer to the up-regulated and down-regulated genes, and the gray dots refer the genes with no significant changes on their expression; **(B, F)** calculation of soft threshold (power) in weighted gene co-expression network analysis (WGCNA); **(C, G)** cluster dendrogram generated through hierarchical clustering based on dissimilarity measures of genes; **(D, H)** heatmaps of module-trait relationships.

In the GSE16561 dataset, there were 2,473 DEGs between the IS and control samples, including 1,069 upregulated and 1,404 downregulated genes (Figure 1E). WGCNA was conducted to identify gene modules highly associated with IS, and a soft threshold power of 7 was selected (Figure 1F). A total of 21 gene modules were identified, with the minimum number of genes per gene module set to 50, and 13 modules were determined when merging the modules with 75% correlation (Figure 1G). Among the 13 modules, "blue" module was positively correlated with IS (r=0.58, P = 7e-07, Figure 1H), and 673 genes in this module were obtained.

3.2 Shared hub genes in CS and IS

Among the upregulated DEGs for CS (n = 2,272) and IS (n = 1,069), as well as the module genes for CS (n = 817) and IS (n = 673), 125 shared genes were screened (Figure 2A). These genes were significantly enriched in biological processes related to the immune inflammatory response, such as leukocyte activation, negative regulation of immune effector processes, and inflammatory responses. Consistently, these genes were also markedly enriched in the molecular function terms of immune receptor activity (Figure 2B), indicating their involvement in immune inflammation-related functions. Only KEGG pathway of inflammatory bowel disease was enriched with the cut-off values of adjusted $P < 0.05$ and count ≥ 2 (Supplementary Table 1). Two shared genes were further screened from the downregulated DEGs for CS (n = 2,319) and IS (n = 1,404), as well as the module genes for CS (n = 817) and IS (n = 673), as shown in Figure 2C. The enrichment results of these two genes (ZNF83 and THOC1) are displayed in Supplementary Table 1. However, no significant enrichment terms were determined under the cut-off values of adjusted $P < 0.05$ and count ≥ 2 owing to the limited gene number. Interestingly, we found that THOC1 was enriched in multiple immune-related terms such as negative regulation of immunoglobulin-mediated immune response, negative regulation of B cell activation, and negative regulation of lymphocyte-mediated immunity (Supplementary Table 1). We further investigated the interactions between 127 shared genes and constructed a PPI network (Figure 2D). From this network, the top 25 genes were determined using the MCC algorithm, and close interactions were observed among these 25 hub genes (Figure 2D). These 25 genes were selected for subsequent analysis.

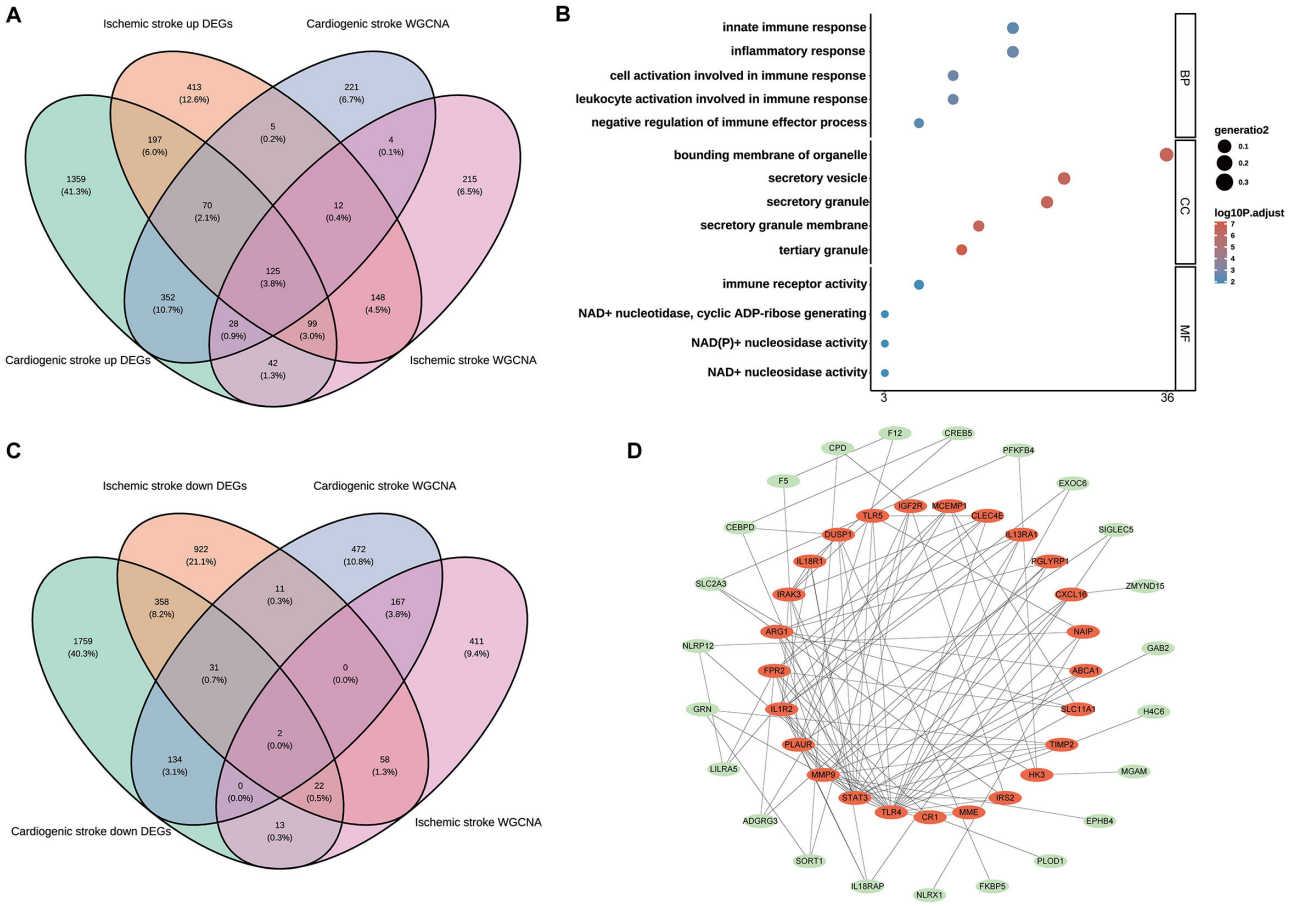

FIGURE 2
Identification of the shared genes in cardioembolic stroke (CS) and ischemic stroke (IS). **(A)** Venn diagram showing the shared upregulated genes between CS and IS; **(B)** the top five terms of three gene ontology categorizations; **(C)** Venn diagram depicting the shared downregulated genes between CS and IS; **(D)** the PPI network of the shared genes, in which the red nodes represent the top 25 hub genes identified from the PPI network using the Maximum Clique Centrality (MCC) method.

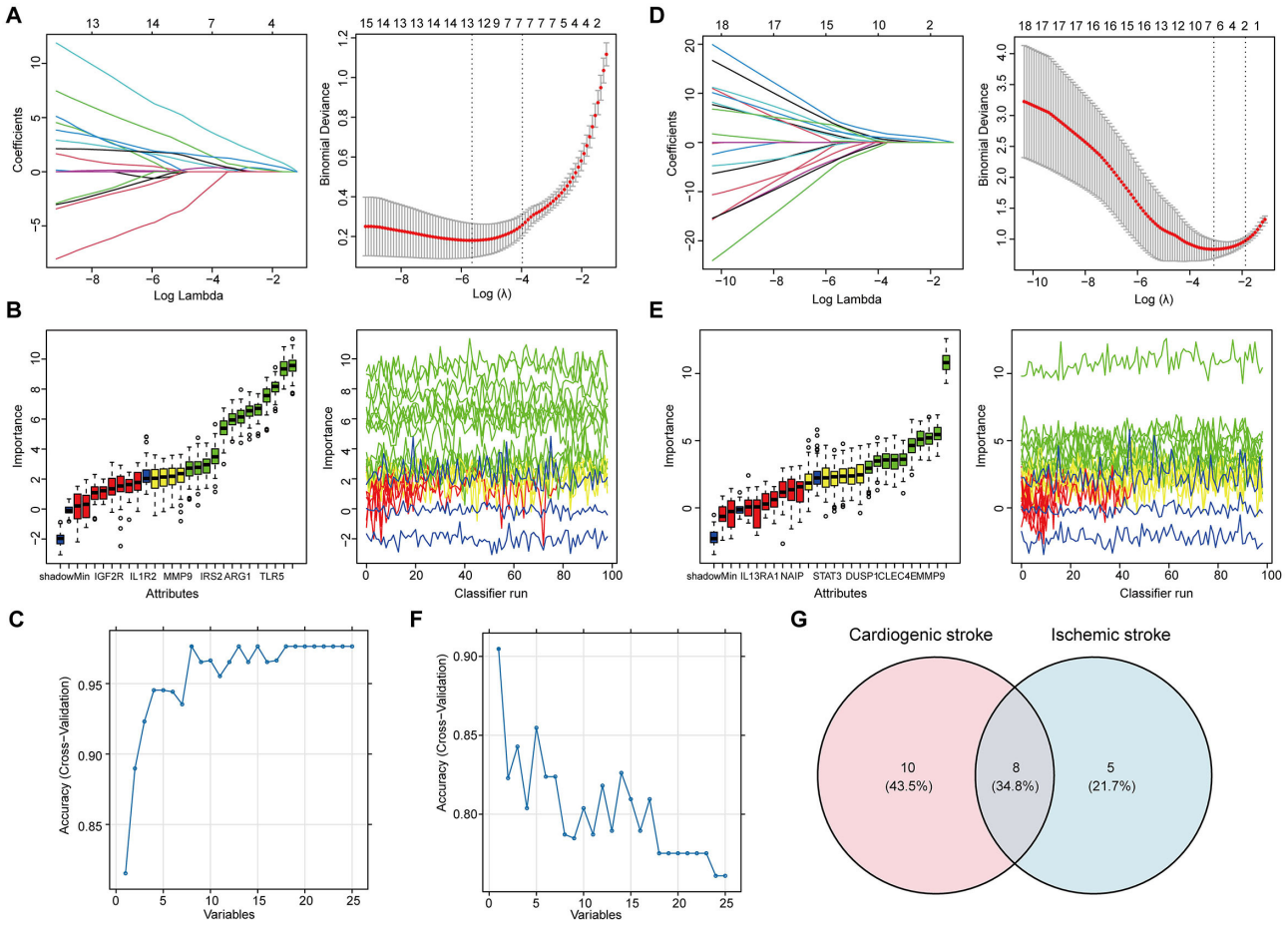

FIGURE 3
Determination of the shared feature genes in cardioembolic stroke (CS) and ischemic stroke (IS). **(A, D)** Parameter selection for the LASSO regression. (left) Cross-validation to select the optimal parameter lambda, and (right) distribution of the LASSO coefficient for feature genes; **(B, E)** results of the Boruta algorithm for identifying feature genes by assessing their importance; **(C, F)** results of SVM-RFE algorithm for screening feature genes with the highest accuracy, in which the horizontal coordinate refers to the number of genes, and the vertical coordinate refers to the accuracy under 10-fold cross-validation; **(G)** Venn diagram showing the eight shared feature genes between CS and IS.

3.3 Determination of candidate biomarkers through machine learning

Feature selection from the 25 shared hub genes was conducted using three machine learning algorithms. In the context of CS, LASSO logistic regression (Figure 3A) and Boruta analysis (Figure 3B) each identified 13 feature genes. SVM-RFE identified eight feature genes with the highest accuracy of 0.976 in 10-fold cross-validation (Figure 3C). In total, 18 genes that were considered candidate biomarkers in CS were obtained through these three algorithms after removing redundancies (Supplementary Table 2).

For feature gene screening in the context of IS, LASSO regression determined seven genes (Figure 3D), and Boruta analysis identified 10 genes (Figure 3E). Among the 25 hub genes, only one was identified as a key feature gene for IS using the SVM-RFE algorithm, with the highest accuracy of 0.9 (Figure 3F). Following the union of the genes obtained from the three algorithms, 13 feature genes were determined in the IS (Supplementary Table 2). Ultimately, eight candidate biomarkers shared between CS and IS were screened: IGF2R, IRAK3, TLR4, ABCA1, CXCL16, CLEC4E, ARG1, and IRS2 (Figure 3G).

3.4 Determination of diagnostic biomarkers by assessing expression and predictive performance

Further screening of the eight candidate biomarkers was performed to identify additional weighted diagnostic biomarkers. As described above, only those with consistent differential expression in both the discovery and validation datasets and an AUC over 0.6 were finally selected. This screening step was conducted in the IS but not in the CS because there was only one CS dataset. In both the training set GSE16561 and validation set GSE22255, the expression of ABCA1, CLEC4E, and IRS2 was elevated in IS samples compared to that in normal controls (Figures 4A, B). In addition, these three genes performed well in

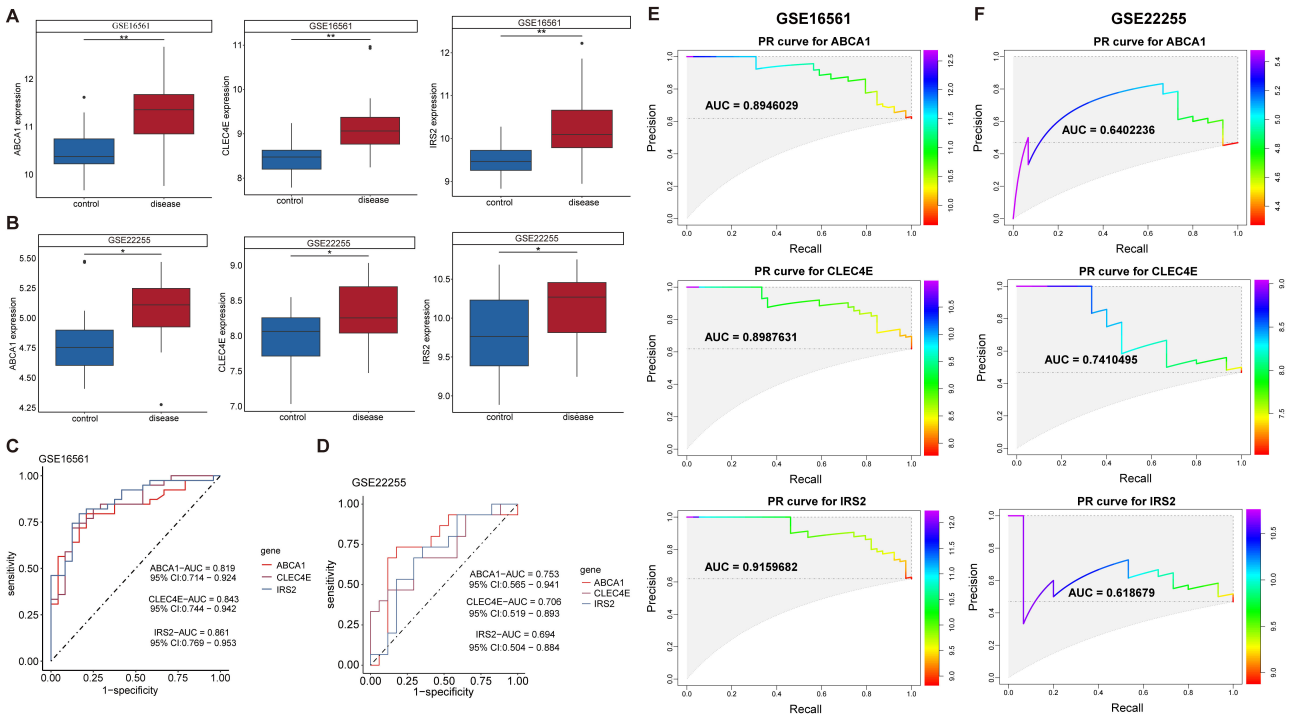

FIGURE 4
Expression and predictive performance of diagnostic biomarkers in ischemic stroke (IS). Expression of the three biomarkers in training set GSE16561 **(A)** and validation set GSE22255 **(B)**; Receiver operating characteristic (ROC) curves showing the predictive power of the three biomarkers for IS in training set GSE16561 **(C)** and validation set GSE22255 **(D)**. Precision-recall (PR) curves showing the predictive power of the three biomarkers for IS in training set GSE16561 **(E)** and validation set GSE22255 **(F)**. $^{*}P < 0.05$; $^{**}P < 0.01$.

distinguishing IS samples, with AUROC of 0.819, 0.843, and 0.861 for ABCA1, CLEC4E, and IRS2, respectively, in the training set GSE16561 (Figure 4C). Similarly, in the validation set GSE22255, the AUROC for ABCA1, CLEC4E, and IRS2 were 0.753, 0.706, and 0.694 (Figure 4D), respectively, indicating moderate predictive power for IS. The predictive performance of these three genes were also assessed by PR curves. In the training set GSE16561, the AUPRC for ABCA1, CLEC4E, and IRS2 were 0.895, 0.899, and 0.916, respectively (Figure 4E). In the validation set GSE22255, the AUPRC for ABCA1, CLEC4E, and IRS2 were 0.640, 0.741, and 0.619 (Figure 4F). The AUROC and AUPRC were all over 0.6 for these three genes in both training and validation sets. Therefore, ABCA1, CLEC4E, and IRS2 were identified as potential diagnostic biomarkers.

3.5 Construction of clinical predictive nomogram for CS and IS

To facilitate the clinical use of the identified biomarkers, a predictive nomogram was established for CS and IS based on the three identified biomarkers, ABCA1, CLEC4E, and IRS2 (Figures 5A, B). In the Nomogram for both CS and IS, CLEC4E harbored the highest weight among the three genes (Figures 5A, B). The high conformance of the predicted dotted line with the actual calibration curve suggested that the nomogram had outstanding accuracy in predicting the onset risk of CS and IS (Figures 5C, D). The greatest net benefit of the model with all three genes compared with that with a single characteristic gene in the decision curve further demonstrated the high accuracy of the predictive nomogram in predicting the risk of CS and IS (Figures 5E, F). The clinical impact curve further confirmed the conformance between the predicted and actual probabilities in CS and IS (Figures 5G, H), implying the clinical applicability of the nomogram.

3.6 Biomarkers expression correlated with immune cell abundance in CS and IS

Immune cells in the samples were inferred using ssGSEA based on gene expression profiles. In the CS samples, there were 19 immune cells with an abundance markedly different from that in the normal controls (Figure 6A). For instance, CS samples harbored a lower abundance of activated/immature B cells and effector memory CD4+/CD8+ T cells and a higher abundance of macrophages, mast cells, and neutrophils (Figure 6A). The correlations between biomarker expression and immune cell abundance were analyzed. All three biomarkers positively correlated with the levels of multiple cells, such as neutrophils, macrophages, and regulatory T cells (Tregs) and negatively correlated with cells including activated/immature B cells and effector memory CD4+/CD8+ T cells (Figure 6B, Supplementary Figure 1A).

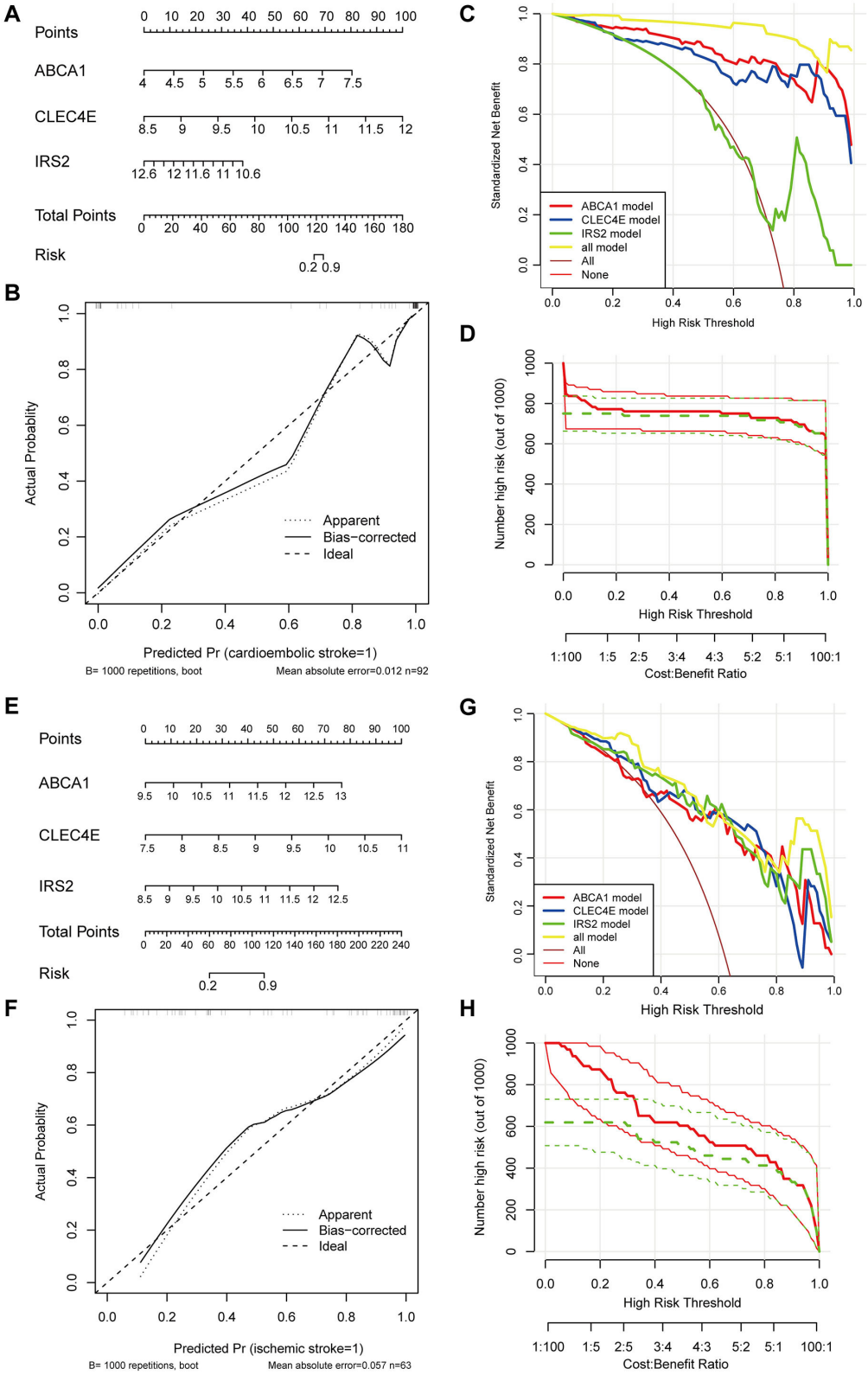

FIGURE 5
Establishment and evaluation of predictive Nomogram. Nomogram established using three biomarkers for predicting the onset risk of cardioembolic stroke (CS) **(A)** and ischemic stroke (IS) **(E)**; calibration curve for assessing the accuracy of nomogram in predicting CS **(B)** and IS **(F)**; decision curve for evaluating the clinical benefit of nomogram in CS **(C)** and IS **(G)**; clinical impact curve for evaluating the clinical benefit of nomogram in CS **(D)** and IS **(H)**.

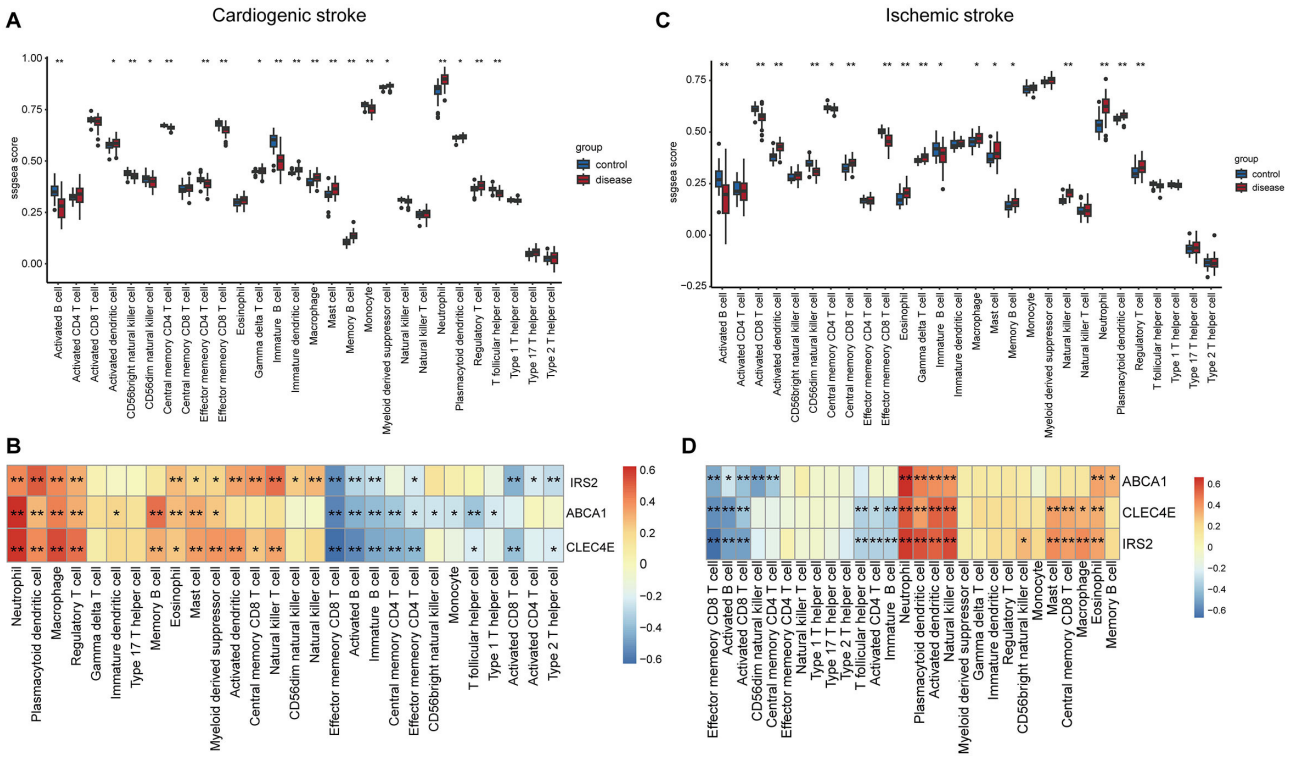

FIGURE 6
Correlations of biomarkers with immune cells. Boxplots showing the differences in the infiltration levels of 28 immune cells between disease and control samples in cardioembolic stroke (CS) **(A)** and ischemic stroke (IS) **(C)**. The comparisons between disease and control groups were conducted using *t*-tests; correlation heatmaps revealing the relationships between the three biomarkers and the immune cells in CS **(B)** and IS **(D)**. $^{*}P < 0.05$; $^{**}P < 0.01$.

In the context of IS, there were 17 immune cells, with their abundance markedly differing between IS and normal controls (Figure 6C). Consistently, the IS samples also exhibited a lower abundance of activated/immature B cells and effector memory CD8+ T cells and a higher abundance of macrophages, mast cells, and neutrophils (Figure 6C). Correlation analysis suggested that the three biomarkers were positively correlated with the levels of neutrophils, plasmacytoid/activated dendritic cells, and natural killer cells and negatively correlated with effector memory CD8+ T cells, activated B cells, and activated CD8+ T cells (Figure 6D, Supplementary Figure 1B).

3.7 Biomarker-associated pathways in CS and IS

To discover the KEGG pathways probably affected by biomarkers expression, we performed GSEA for each biomarker in both diseases. In the context of CS, pathways such as antigen processing and presentation, NK cell-mediated cytotoxicity, lipids, and atherosclerosis were activated, with increased ABCA1 expression (Figure 7A). Elevated expression of CLEC4E and IRS2 was activated through the activation of autophagy and the B-cell receptor signaling pathway (Figures 7B, C). However, multiple pathways related to metabolism and nucleotide excision repair were inhibited (Supplementary Figures 2A–C). Interestingly, the elevated expression of biomarkers was accompanied by the activation of autophagy in the IS. In addition, neutrophil extracellular trap (NET) formation was observed (Figures 7D–F). Ribosome biogenesis-related pathways were inhibited with the expression of these three biomarkers (Supplementary Figures 2D–F). Overall, autophagy was a common pathway activated in both CS and IS.

3.8 Regulatory networks for biomarkers

A potential molecular regulatory mechanism was identified to provide a comprehensive understanding of the three biomarkers. GeneMANIA analysis revealed that ABCA1, CLEC4E, IRS2, and their interacting genes were mainly involved in the cellular response to insulin stimulus, cellular response to peptide hormones, and regulation of cholesterol efflux (Figure 8A). Regarding molecular regulation, both ABCA1 and IRS2 were likely targeted by multiple miRNAs and transcription factors (Figure 8B), indicating the potential of these two genes as therapeutic targets. Therefore, we predicted the drugs that could target these three genes. Sixteen drugs were predicted for ABCA1, while four and five drugs were predicted for IRS2 and CLEC4E, respectively (Figures 9A–C). Molecular docking was conducted to confirm the binding of the genes to predicted representative drug molecules. For ABCA1, docking was conducted for ABCA1 and the top

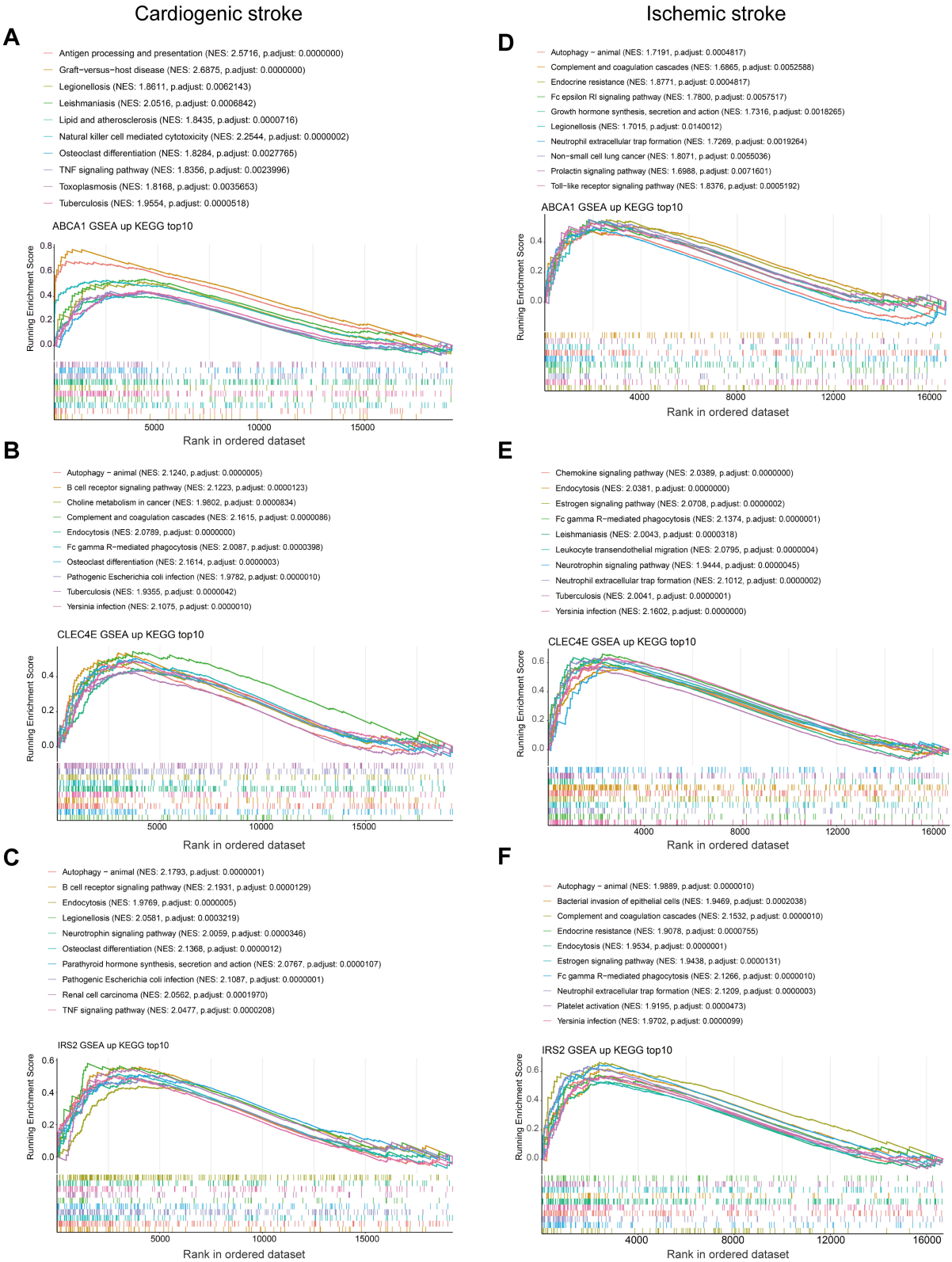

FIGURE 7
Gene set enrichment analysis. Top 10 activated KEGG pathways with ABCA1 expression in cardioembolic stroke (CS) **(A)** and ischemic stroke (IS) **(D)**; top 10 activated KEGG pathways with CLEC4E expression in CS **(B)** and IS **(E)**; top 10 activated KEGG pathways with IRS2 expression in CS **(C)** and IS **(F)**.

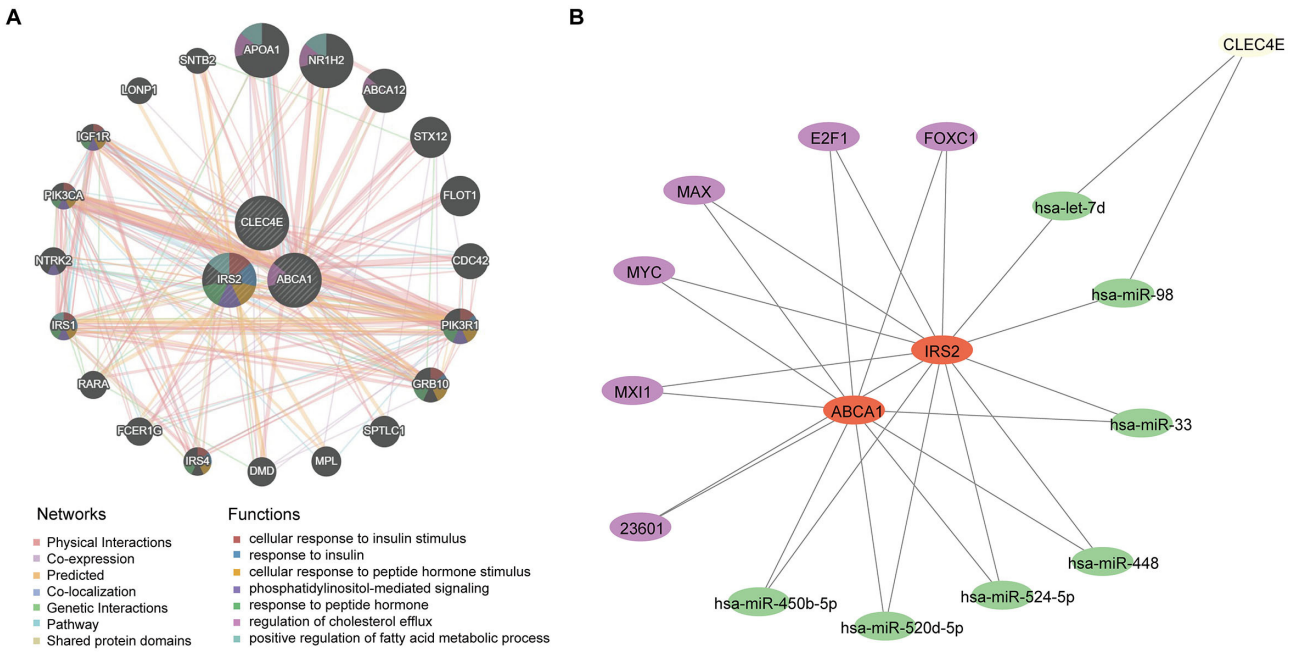

FIGURE 8
Regulatory network for biomarkers. **(A)** Interaction network and involved functions of ABCA1, CLE4E, and IRS2 using GeneMANIA; **(B)** microRNAs and transcription factors for ABCA1, CLE4E, and IRS2, in which the purple nodes represent transcription factors and the green nodes indicate miRNAs.

three drugs: probucol, mefloquine, and istradefylline. Five docking models were obtained, and the model with the lowest binding energy (best affinity) was selected. The binding energy of ABCA1 with probucol, mefloquine, and istradefylline were −8.8, −8.8, and −7.5 kcal/mol, respectively (Figure 9D, Supplementary Table 3). For the five drugs predicted for IRS2, docking was only conducted for aspirin and dexamethasone (Figure 9E) because of the unavailability of 3D structures of the other three drugs. The binding energy of IRS2 with aspirin and dexamethasone were −5.4 and −6.7 kcal/mol (Supplementary Table 3). Similarly, docking was conducted for CLEC4E with Cianidanol and Tetradioxin (Figure 9F), and the binding energy was −6.4 and −6.0 kcal/mol, respectively (Supplementary Table 3). The docking results confirmed the binding of these genes to the predicted drugs with high affinity.

4 Discussion

CS is the major IS subtype. The etiology and pathogenesis of different stroke subtypes are diverse, leading to variations in their treatment. Therefore, illustrating the similarities and differences in the molecular mechanisms of different stroke subtypes can contribute to an accurate early diagnosis and a more targeted therapeutic schedule for patients with stroke. In this study, we revealed the overlapping molecular mechanisms across the two stroke subtypes through integrated bioinformatics analyses.

Based on differential analysis and WGCNA, we identified 127 shared differential genes between CS and IS. These genes were mainly implicated in biological processes related to immune inflammatory responses, such as leukocyte activation and negative regulation of immune effector processes. Immune-inflammatory response exerts vital and bidirectional roles in the pathological process of IS (17, 18). Immune cell infiltration is the core mechanism involved in the modulation of nerve injury and repair after stroke (19). In stroke brain tissue, some types of infiltrated T cells promote inflammatory responses to aggravate tissue injury, while T cells contribute to protecting neurons from ischemic injury by inducing immunosuppression (20–23). Currently, immunological mechanisms are a hotspot of research in the field of IS, and targeting the immune-inflammatory response has been proposed as a promising therapeutic strategy to improve the injury post stroke (18, 23). A previous study demonstrated that FOXP3+ macrophages are beneficial for stroke outcomes by inhibiting IS-induced neural inflammation (24). Therefore, exploring alterations in the immune status of IS may provide novel insights into its management and treatment.

Machine learning is a burgeoning field in medicine that provides superior predictive power in comparison with conventional statistical models, capturing non-linear relations across predictive factors and outcomes and complex interactions within predictive factors (25, 26). Given their high accuracy, machine learning approaches are increasingly being applied in the medical field, particularly in stroke (27, 28). In this study, three machine-learning algorithms, LASSO-logistic, Boruta, and SVM-RFE, were employed to identify more weighted feature genes from shared genes. Eight feature genes were identified, which were considered candidate biomarkers for the two diseases. Further expression and predictive power assessments determined three diagnostic biomarkers—ABCA1, CLEC4E, and IRS2.

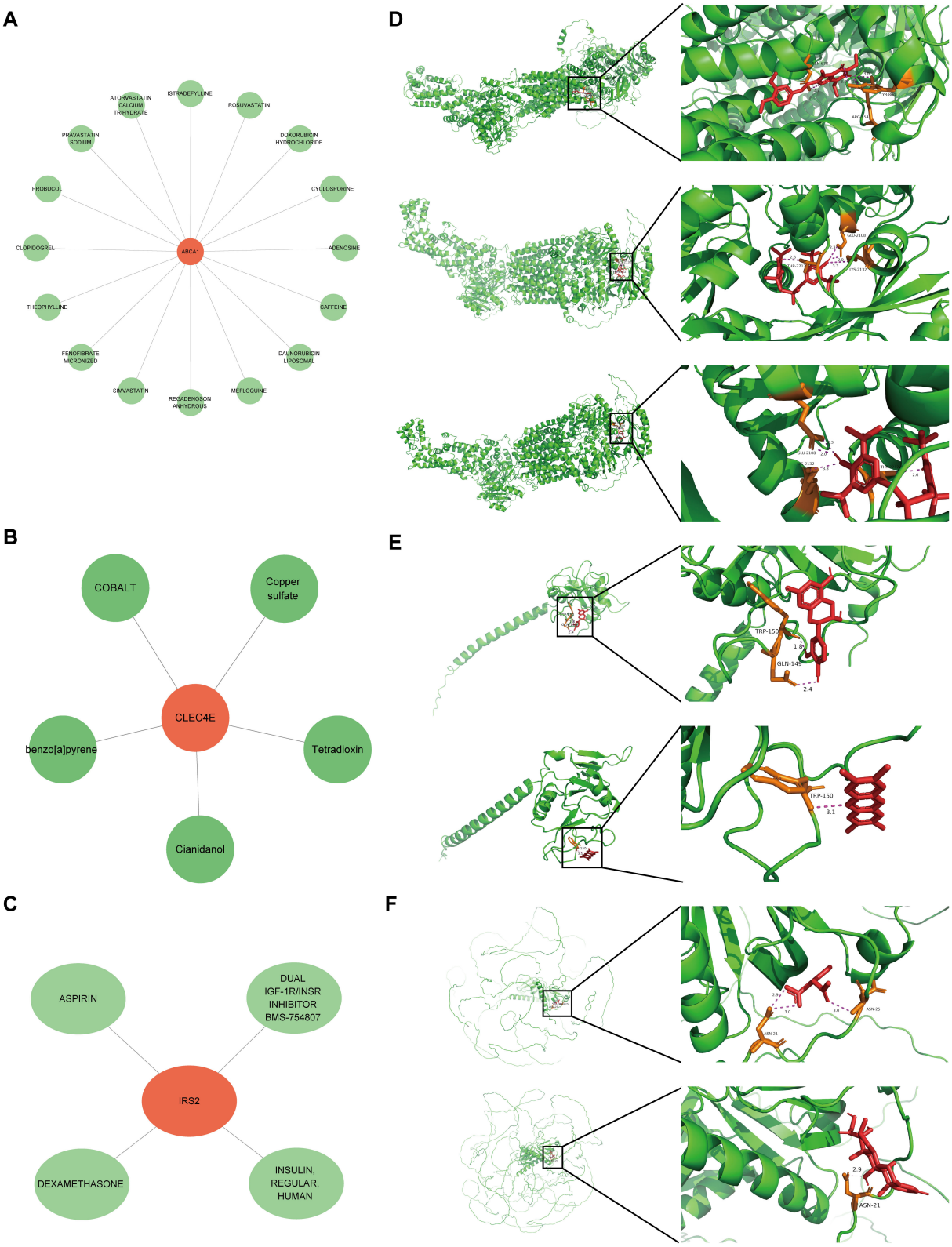

FIGURE 9
Small molecular drugs for targeting biomarkers. Small molecular drug network for ABCA1 **(A)**, CLE4E **(B)** and IRS2 **(C)**, in which the green nodes refer to the drugs; **(D)** results of molecular docking for ABCA1 and the corresponding top three drugs probucol, mefloquine, and istradefylline; **(E)** results of molecular docking for CLEC4E and drugs Cianidanol and Tetradioxin; **(F)** results of molecular docking for IRS2 and drugs aspirin and dexamethasone.

Cholesterol plays important structural and functional roles in both the gray and white matter. ABCA1, an ATP-binding cassette transporter A1, is a major membrane transporter that functions as a cholesterol efflux pump to mediate cholesterol homeostasis in the brain, particularly the efflux of cholesterol from astrocytes (29, 30). Excessive cholesterol causes fat to build up in the arteries, forming atherosclerosis and increasing the risk of cerebrovascular disease, one of the main causes of stroke (31, 32). Besides, ABCA1 modulates a variety of brain functions, such as neuroinflammation (a crucial process following stroke) and blood-brain barrier leakage, and both these two are key factors to worsen stroke outcomes (30, 33). Genetic variants of ABCA1 have been implicated in etiology and the onset risk of IS (34, 35). ABCA1 expression is implicated in the neurorestoration post stroke. For instance, specific deletion of brain-ABCA1 could reduce the density of white matter and gray matter in the ischemic brain and harm post stroke functional outcomes (29). Upregulation of ABCA1 is involved in the effects of LXR agonists in decreasing neuroinflammation, facilitating neuroprotection, and improving neurological functional-outcomes post stroke (36, 37).

CLEC4E encodes a member of the C-type lectin superfamily, which modulates immune and inflammatory responses, as well as cell-to-cell adhesion (38, 39). Although CLEC4E has not been reported in patients with stroke, other members of this superfamily have been shown to play important roles. For example, CLEC14A deficiency can exacerbate the neuronal loss post stroke by enhancing the pro-inflammatory response and blood-brain barrier permeability (40). Particularly, C-Type lectin receptor 2 has been recognized as a biomarker of platelet activation and is associated with pathological features and prognosis of strokes (41, 42). IRS2 encodes insulin receptor substrate (IRS) 2; ISR signaling mediates cardiac energy metabolism and heart failure (43) and is associated with CS (44). Gene polymorphism of IRS1 has been proposed as a risk factor for IS (45). IRS proteins are key molecular that regulates insulin signaling pathways and is strongly associated with the development of diabetes (46), while diabetes has been shown to be a risk factor for a significantly increased risk of stroke (47, 48). Nevertheless, the exact role of IRS2 in strokes remains unclear. We found that IRS2 and CLEC14A were overexpressed in both CS and IS and that their expression was associated with the risk of disease onset.

Neutrophil targeting has been proposed as a promising strategy for IS therapy (49–51). Specifically, there was a rapid increase of neutrophils in peripheral blood and in the peri-infarct cortex during all stages of IS, with enhanced neutrophil frequency linked to poor clinical outcomes (50, 52). NETs induce thrombosis by activating the clotting pathway and endothelium by acting as a scaffold for tissue factors and platelets, resulting in a procoagulant state (53). In addition, NETs released by neutrophils can mediate cerebral injury after IS. For instance, NETs facilitate thrombus formation (54) and repress vascular remodeling post-IS (52). Treatment with NET-inhibitory factors reduce cerebral infarcts and improve overall outcomes in a stroke mouse model (51). In this study, we found that all three biomarkers, ABCA1, CLEC4E, and IRS2, were associated with the activation of NET formation and infiltration levels of neutrophils in the IS, implying their importance in stroke. Autophagy was found to be a shared pathway associated with biomarkers of both diseases. Autophagy is an adaptive mechanism of the cell response to stroke and plays a vital role in maintaining cell homeostasis and survival by clearing damaged cell components via autophagic lysosomal degradation. During IS, the lack of oxygen and glucose supply caused by cerebral ischemia leads to activation of the AMPK pathway, activating autophagy in various cell types in the brain (55). Autophagy appears to play a "double-edged sword" role in the pathogenesis of IS, and its exact role in IS remains controversial, despite extensive study (56, 57). These findings further highlight the close involvement of the three identified biomarkers in stroke.

Despite the above findings, several limitations in this study should be admitted. First at all, since there was only one CS dataset, the determination of diagnostic biomarkers by assessing expression and predictive performance was conducted based solely on the IS datasets. The sample size of the dataset analyzed in this study is not large enough, which may reduce statistical power and generalizability, thus leading to certain unrobustness of the results. Second, we observed an association between the expression of three biomarkers and the activity of NET pathway, but this association appears to be observed only in IS. Such differences might be explained by the differential expression pattern of genes in the context of these two strokes. In future, the NET levels in serum/plasma samples should be tested in large number of patients to further discover whether there are differences on NETs levels between CS and IS. Besides, the causal relationship of the dysregulated status of biomarkers and NET activity should be investigated by functional experiments. Third, functional experiments are required to further confirm exact role of these three genes in stroke, mainly the similarities and differences of the actions of these three genes in the CS and IS. The last one, the drug molecules that may target these tree key genes were predicted, and the binding of the genes to predicted representative drug molecules were confirmed by molecular docking. In future, binding assays are required to confirm such drug-target interactions, and the potential applications of these drugs in strokes need to be further explored.

In summary, the current study discovered the similarities and differences in gene expression and molecular mechanisms between the two stroke subtypes to illustrate their associations. ABCA1, CLEC4E, and IRS2 were identified as common diagnostic biomarkers of both CS and IS, and their expression was associated with neutrophil infiltration and autophagy activation.

Data availability statement

The original contributions presented in the study are included in the article/Supplementary material, further inquiries can be directed to the corresponding author.

Ethics statement

Ethical review and approval was not required for the study on human participants in accordance with the local legislation and institutional requirements. Written informed consent from the

patients/participants or patients/participants' legal guardian/next of kin was not required to participate in this study in accordance with the national legislation and the institutional requirements.

Author contributions

XW: Data curation, Formal analysis, Investigation, Methodology, Software, Validation, Visualization, Writing – original draft, Writing – review & editing. XL: Conceptualization, Funding acquisition, Methodology, Project administration, Resources, Supervision, Writing – review & editing.

Funding

The author(s) declare that financial support was received for the research and/or publication of this article. This work was supported by grants from the Shanghai Science and Technology Commission (No. 22Y31900204) and Shanghai Health Commission (No. 20234Y001).

Acknowledgments

The authors express sincere gratitude for the invaluable data support extended by the GEO databases.

Conflict of interest

The authors declare that the research was conducted in the absence of any commercial or financial relationships that could be construed as a potential conflict of interest.

Generative AI statement

The author(s) declare that no Gen AI was used in the creation of this manuscript.

Publisher's note

Supplementary material

The Supplementary Material for this article can be found online at: https://www.frontiersin.org/articles/10.3389/fneur.2025.1567902/full#supplementary-material

References

1. Markus HS, Michel P. Treatment of posterior circulation stroke: acute management and secondary prevention. *Int J Stroke.* (2022) 17:723–32. doi: 10.1177/17474930221107500

2. Gil-Garcia C-A, Flores-Alvarez E, Cebrian-Garcia R, Mendoza-Lopez A-C, Gonzalez-Hermosillo L-M, Garcia-Blanco M-C, et al. Essential topics about the imaging diagnosis and treatment of hemorrhagic stroke: a comprehensive review of the 2022 AHA guidelines. *Curr Probl Cardiol.* (2022) 47:101328. doi: 10.1016/j.cpcardiol.2022.101328

3. Feigin VL, Brainin M, Norrving B, Martins S, Sacco RL, Hacke W, et al. World Stroke Organization (WSO): global stroke fact sheet 2022. *Int J Stroke.* (2022) 17:18–29. doi: 10.1177/17474930211065917

4. Ma Q, Li R, Wang L, Yin P, Wang Y, Yan C, et al. Temporal trend and attributable risk factors of stroke burden in China, 1990–2019: an analysis for the Global Burden of Disease Study 2019. *Lancet Public Health.* (2021) 6:e897–906. doi: 10.1016/S2468-2667(21)00228-0

5. Barthels D, Das H. Current advances in ischemic stroke research and therapies. *Biochimica Biophys Acta.* (2020) 1866:165260. doi: 10.1016/j.bbadis.2018.09.012

6. Feske SK. Ischemic stroke. *Am J Med.* (2021) 134:1457–64. doi: 10.1016/j.amjmed.2021.07.027

7. Shen Z, Xiang M, Chen C, Ding F, Wang Y, Shang C, et al. Glutamate excitotoxicity: potential therapeutic target for ischemic stroke. *Biomed Pharmacother.* (2022) 151:113125. doi: 10.1016/j.biopha.2022.113125

8. Romano JG, Rundek T. Expanding treatment for acute ischemic stroke beyond revascularization. *New Engl J Med.* (2023) 388:2095–6. doi: 10.1056/NEJMe2303184

9. Yu MY, Caprio FZ, Bernstein RA. Cardioembolic stroke. *Neurol Clin.* (2024) 42:651–61. doi: 10.1016/j.ncl.2024.03.002

10. Chen Y, He Y, Jiang Z, Xie Y, Nie S. Ischemic stroke subtyping method combining convolutional neural network and radiomics. *J X-Ray Sci Technol.* (2022) 31:223–35. doi: 10.3233/XST-221284

11. Yaghi S. Diagnosis and management of cardioembolic stroke. *Continuum: Lifelong Learn Neurol.* (2023) 29:462–85. doi: 10.1212/CON.0000000000001217

12. Wang Y-J, Li Z-X, Gu H-Q, Zhai Y, Jiang Y, Zhao X-Q, et al. China Stroke Statistics 2019: A Report From the National Center for Healthcare Quality Management in Neurological Diseases, China National Clinical Research Center for Neurological Diseases, the Chinese Stroke Association, National Center for Chronic and Non-communicable Disease Control and Prevention, Chinese Center for Disease Control and Prevention and Institute for Global Neuroscience and Stroke Collaborations. *Stroke Vasc Neurol.* (2020) 5:211–39. doi: 10.1136/svn-2020-000457

13. Yang Y, Zhang M, Li Z, He S, Ren X, Wang L, et al. Identification and cross-validation of autophagy-related genes in cardioembolic stroke. *Front Neurol.* (2023) 14. doi: 10.3389/fneur.2023.1097623

14. Shoamanesh A, Mundl H, Smith EE, Masjuan J, Milanov I, Hirano T, et al. Factor XIa inhibition with asundexian after acute non-cardioembolic ischaemic stroke (PACIFIC-Stroke): an international, randomised, double-blind, placebo-controlled, phase 2b trial. *Lancet.* (2022) 400:997–1007. doi: 10.1016/S0140-6736(22)01588-4

15. Kato Y, Tsutsui K, Nakano S, Hayashi T, Suda S. Cardioembolic stroke: past advancements, current challenges, and future directions. *Int J Mol Sci.* (2024) 25:5777. doi: 10.3390/ijms25115777

16. Kernan WN, Ovbiagele B, Black HR, Bravata DM, Chimowitz MI, Ezekowitz MD, et al. Guidelines for the prevention of stroke in patients with stroke and transient ischemic attack. *Stroke.* (2014) 45:2160–236. doi: 10.1161/STR.0000000000000024

17. DeLong JH, Ohashi SN, O'Connor KC, Sansing LH. Inflammatory responses after ischemic stroke. *Semin Immunopathol.* (2022) 44:625–48. doi: 10.1007/s00281-022-00943-7

18. Simats A, Liesz A. Systemic inflammation after stroke: implications for post-stroke comorbidities EMBO. *Molec Med.* (2022) 14:e16269. doi: 10.15252/emmm.202216269

19. Wang H, Ye J, Cui L, Chu S, Chen N. Regulatory T cells in ischemic stroke. *Acta Pharmacol Sin.* (2021) 43:1–9. doi: 10.1038/s41401-021-00641-4

20. Zhang D, Ren J, Luo Y, He Q, Zhao R, Chang J, et al. T Cell response in ischemic stroke: from mechanisms to translational insights. *Front Immunol.* (2021) 12:707972. doi: 10.3389/fimmu.2021.707972

21. Wang Y-R, Cui W-Q, Wu H-Y, Xu X-D, Xu X-Q. The role of T cells in acute ischemic stroke. *Brain Res Bull.* (2023) 196:20–33. doi: 10.1016/j.brainresbull.2023.03.005

22. Wu F, Liu Z, Zhou L, Ye D, Zhu Y, Huang K, et al. Systemic immune responses after ischemic stroke: from the center to the periphery. *Front Immunol.* (2022) 13:911661. doi: 10.3389/fimmu.2022.911661

23. Zhu L, Huang L, Le A, Wang TJ, Zhang J, Chen X, et al. Interactions between the autonomic nervous system and the immune system after stroke. *Compr Physiol.* (2022) 12:3665–704. doi: 10.1002/cphy.c210047

24. Cai W, Hu M, Li C, Wu R, Lu D, Xie C, et al. FOXP3+ macrophage represses acute ischemic stroke-induced neural inflammation. *Autophagy.* (2022) 19:1144–63. doi: 10.1080/15548627.2022.2116833

25. Greener JG, Kandathil SM, Moffat L, Jones DT. A guide to machine learning for biologists. *Nat Rev Molec Cell Biol.* (2021) 23:40–55. doi: 10.1038/s41580-021-00407-0

26. Lo Vercio L, Amador K, Bannister JJ, Crites S, Gutierrez A, MacDonald ME, et al. Supervised machine learning tools: a tutorial for clinicians. *J Neural Eng.* (2020) 17:062001. doi: 10.1088/1741-2552/abbff2

27. Sheth SA, Giancardo L, Colasurdo M, Srinivasan VM, Niktabe A, Kan P. Machine learning and acute stroke imaging. *J Neurointerv Surg.* (2022) 15:195–9. doi: 10.1136/neurintsurg-2021-018142

28. Schwartz L, Anteby R, Klang E, Soffer S. Stroke mortality prediction using machine learning: systematic review. *J Neurol Sci.* (2023) 444:120529. doi: 10.1016/j.jns.2022.120529

29. Wang X, Li R, Zacharek A, Landschoot-Ward J, Wang F, Wu K-HH, et al. Administration of downstream ApoE attenuates the adverse effect of brain ABCA1 deficiency on stroke. *Int J Mol Sci.* (2018) 19:3368. doi: 10.3390/ijms19113368

30. Paseban T, Alavi MS, Etemad L, Roohbakhsh A. The role of the ATP-Binding Cassette A1 (ABCA1) in neurological disorders: a mechanistic review. *Expert Opin Ther Targets.* (2023) 27:531–52. doi: 10.1080/14728222.2023.2235718

31. Hackam DG, Hegele RA. Cholesterol lowering and prevention of stroke. *Stroke.* (2019) 50:537–41. doi: 10.1161/STROKEAHA.118.023167

32. Li W, Huang Z, Fang W, Wang X, Cai Z, Chen G, et al. Remnant cholesterol variability and incident ischemic stroke in the general population. *Stroke.* (2022) 53:1934–41. doi: 10.1161/STROKEAHA.121.037756

33. Candelario-Jalil E, Dijkhuizen RM, Magnus T. Neuroinflammation, stroke, blood-brain barrier dysfunction, and imaging modalities. *Stroke.* (2022) 53:1473–86. doi: 10.1161/STROKEAHA.122.036946

34. Au A, Griffiths LR, Irene L, Kooi CW, Wei LK. The impact of APOA5, APOB, APOC3 and ABCA1 gene polymorphisms on ischemic stroke: evidence from a meta-analysis. *Atherosclerosis.* (2017) 265:60–70. doi: 10.1016/j.atherosclerosis.2017.08.003

35. Yang S, Jia J, Liu Y, Li Z, Li Z, Zhang Z, et al. Genetic variations in ABCA1/G1 associated with plasma lipid levels and risk of ischemic stroke. *Gene.* (2022) 823:146343. doi: 10.1016/j.gene.2022.146343

36. Cui X, Chopp M, Zacharek A, Cui Y, Roberts C, Chen J. The neurorestorative benefit of GW3965 treatment of stroke in mice. *Stroke.* (2013) 44:153–61. doi: 10.1161/STROKEAHA.112.677682

37. Morales JR, Ballesteros I, Deniz JM, Hurtado O, Vivancos J, Nombela F, et al. Activation of liver X receptors promotes neuroprotection and reduces brain inflammation in experimental stroke. *Circulation.* (2008) 118:1450–9. doi: 10.1161/CIRCULATIONAHA.108.782300

38. Kingeter LM, Lin X. C-type lectin receptor-induced NF-κB activation in innate immune and inflammatory responses. *Cell Molec Immunol.* (2012) 9:105–12. doi: 10.1038/cmi.2011.58

39. Zelensky AN, Gready JE. The C-type lectin-like domain superfamily. *FEBS J.* (2005) 272:6179–217. doi: 10.1111/j.1742-4658.2005.05031.x

40. Kim Y, Lee S, Zhang H, Lee S, Kim H, Kim Y, et al. CLEC14A deficiency exacerbates neuronal loss by increasing blood-brain barrier permeability and inflammation. *J Neuroinflam.* (2020) 17:48. doi: 10.1186/s12974-020-1727-6

41. Uchiyama S, Suzuki-Inoue K, Wada H, Okada Y, Hirano T, Nagao T, et al. Soluble C-type lectin-like receptor 2 in stroke (CLECSTRO) study: protocol of a multicentre, prospective cohort of a novel platelet activation marker in acute ischaemic stroke and transient ischaemic attack. *BMJ Open.* (2023) 13:e073708. doi: 10.1136/bmjopen-2023-073708

42. Zhang X, Zhang W, Wu X, Li H, Zhang C, Huang Z, et al. Prognostic significance of plasma CLEC-2 (C-Type Lectin-Like Receptor 2) in patients with acute ischemic stroke. *Stroke.* (2019) 50:45–52. doi: 10.1161/STROKEAHA.118.022563

43. Guo CA, Guo S. Insulin receptor substrate signaling controls cardiac energy metabolism and heart failure. *J Endocrinol.* (2017) 233:R131–43. doi: 10.1530/JOE-16-0679

44. Kelley RE, Kelley BP. Heart–brain relationship in stroke. *Biomedicines.* (2021) 9:1835. doi: 10.3390/biomedicines9121835

45. Syahrul, Wibowo S, Haryana SM, Astuti I, Nurwidya F. The role of insulin receptor substrate 1 gene polymorphism Gly972Arg as a risk factor for ischemic stroke among Indonesian subjects. *BMC Res Notes.* (2018) 11:718. doi: 10.1186/s13104-018-3823-6

46. Lavin DP, White MF, Brazil DP. IRS proteins and diabetic complications. *Diabetologia.* (2016) 59:2280–91. doi: 10.1007/s00125-016-4072-7

47. Sacco S, Foschi M, Ornello R, De Santis F, Pofi R, Romoli M. Prevention and treatment of ischaemic and haemorrhagic stroke in people with diabetes mellitus: a focus on glucose control and comorbidities. *Diabetologia.* (2024) 67:1192–205. doi: 10.1007/s00125-024-06146-z

48. Lau L, Lew J, Borschmann K, Thijs V, Ekinci EI. Prevalence of diabetes and its effects on stroke outcomes: a meta-analysis and literature review. *J Diabetes Invest.* (2018) 10:780–792. doi: 10.1111/jdi.12932

49. Dhanesha N, Patel RB, Doddapattar P, Ghatge M, Flora GD, Jain M, et al. PKM2 promotes neutrophil activation and cerebral thromboinflammation: therapeutic implications for ischemic stroke. *Blood.* (2022) 139:1234–45. doi: 10.1182/blood.2021012322

50. Cai W, Liu S, Hu M, Huang F, Zhu Q, Qiu W, et al. Functional dynamics of neutrophils after ischemic stroke. *Transl Stroke Res.* (2019) 11:108–21. doi: 10.1007/s12975-019-00694-y

51. Denorme F, Portier I, Rustad JL, Cody MJ, de Araujo CV, Hoki C, et al. Neutrophil extracellular traps regulate ischemic stroke brain injury. *J Clin Investig.* (2022) 132:154225. doi: 10.1172/JCI154225

52. Kang L, Yu H, Yang X, Zhu Y, Bai X, Wang R, et al. Neutrophil extracellular traps released by neutrophils impair revascularization and vascular remodeling after stroke. *Nat Commun.* (2020) 11:2488. doi: 10.1038/s41467-020-16191-y

53. Liaptsi E, Merkouris E, Polatidou E, Tsiptsios D, Gkantzios A, Kokkotis C, et al. Targeting neutrophil extracellular traps for stroke prognosis: a promising path. *Neurol Int.* (2023) 15:1212–26. doi: 10.3390/neurolint15040076

54. Laridan E, Denorme F, Desender L, François O, Andersson T, Deckmyn H, et al. Neutrophil extracellular traps in ischemic stroke thrombi. *Ann Neurol.* (2017) 82:223–232. doi: 10.1002/ana.24993

55. Shi Q, Cheng Q, Chen C. The role of autophagy in the pathogenesis of ischemic stroke. *Curr Neuropharmacol.* (2021) 19:629–40. doi: 10.2174/1570159X18666200729101913

56. Peng L, Hu G, Yao Q, Wu J, He Z, Law BY-K, et al. Microglia autophagy in ischemic stroke: a double-edged sword. *Front Immunol.* (2022) 13:1013311. doi: 10.3389/fimmu.2022.1013311

57. Ajoolabady A, Wang S, Kroemer G, Penninger JM, Uversky VN, Pratico D, et al. Targeting autophagy in ischemic stroke: from molecular mechanisms to clinical therapeutics. *Pharmacol Therapeut.* (2021) 225:107848. doi: 10.1016/j.pharmthera.2021.107848

frontiers | Frontiers in Neurology

TYPE Original Research
PUBLISHED 28 April 2025
DOI 10.3389/fneur.2025.1552462

OPEN ACCESS

EDITED BY
Haipeng Liu,
Coventry University, United Kingdom

REVIEWED BY
Jeremy Man Ho Hui,
The University of Hong Kong, Hong Kong SAR, China
Ahmad Sabry Saleh,
Alhayat Clinic, Egypt
Kassu Mehari Beyene,
Barrow Neurological Institute (BNI), United States

*CORRESPONDENCE
Chun-Hua Hang
hang_neurosurgery@163.com
Wei Li
wei.li@nju.edu.cn

†These authors have contributed equally to this work

RECEIVED 28 December 2024
ACCEPTED 07 April 2025
PUBLISHED 28 April 2025

CITATION
Wang J, Ding P-f, Peng Z, Hang C-H and Li W (2025) The stress hyperglycemia ratio as a predictor of short- and long-term mortality in patients with acute brain injury: a retrospective cohort study. *Front. Neurol.* 16:1552462. doi: 10.3389/fneur.2025.1552462

The stress hyperglycemia ratio as a predictor of short- and long-term mortality in patients with acute brain injury: a retrospective cohort study

Juan Wang[1,2,3†], Peng-fei Ding[2,3†], Zheng Peng[1,2,3†], Chun-Hua Hang[1,2,3*] and Wei Li[1,2,3*]

[1]Department of Neurosurgery, Nanjing Drum Tower Hospital, Clinical College of Nanjing University of Chinese Medicine, Nanjing, China, [2]Department of Neurosurgery, Nanjing Drum Tower Hospital, Clinical College of Nanjing Medical University, Nanjing, China, [3]Neurosurgical Institute, Nanjing University, Nanjing, China

Background: This study examines the Stress Hyperglycemia Ratio (SHR) as a predictor of mortality in acute brain injury (ABI) patients using the MIMIC-IV v3.1 database.

Methods: In this retrospective cohort study of 2,423 ABI patients, SHR was calculated as SHR = [Admission blood glucose (mg/dL)] / [28.7 × HbA1c (%) − 46.7]. Mortality outcomes included ICU, in-hospital, 30, 60, 90, and 365-day mortality. Cox regression models adjusted for covariates assessed the association between SHR and mortality risk, with restricted cubic splines confirming linearity. Predictive performance was evaluated using ROC curves, incorporating SHR, Glasgow Coma Scale (GCS), and first-day ventilation status.

Results: SHR was significantly associated with mortality across all outcomes, showing a linear relationship. Adjusted hazard ratios (HR) for in-hospital and ICU mortality were 1.18 (95% CI: 1.06–1.32, $p = 0.003$) and 1.16 (95% CI: 1.02–1.32, $p = 0.029$), respectively. Dichotomized SHR indicated increased in-hospital mortality risk (HR: 1.44, 95% CI: 1.13–1.83, $p = 0.003$). Combining SHR with GCS and ventilation status improved predictive accuracy, achieving AUCs of 0.817 for ICU mortality and 0.788 for in-hospital mortality. Robustness was supported by E-values of 2.24 and 2.37 for in-hospital and ICU mortality.

Conclusion: SHR independently predicts short- and long-term mortality in ABI patients, with enhanced utility when combined with GCS and ventilation status, supporting its role in clinical risk stratification.

KEYWORDS

acute brain injury, stress hyperglycemia ratio (SHR), linear association, short-term and long-term mortality, ROC curve

Introduction

Acute brain injury (ABI), including traumatic brain injury (TBI), intracerebral hemorrhage (ICH), and ischemic stroke, is a critical condition characterized by high mortality and prolonged recovery, posing significant challenges in critical care (1). The neuroendocrine stress response in ABI often results in transient hyperglycemia. Unlike chronic hyperglycemia, stress-induced hyperglycemia reflects an immediate response to

injury and is associated with poorer outcomes in critically ill patients (2). Traditional measures, such as admission blood glucose (ABG), have limited predictive value as they do not distinguish baseline glycemic control from acute hyperglycemia, especially in patients with diabetes.

To address these limitations, the stress hyperglycemia ratio (SHR) has been introduced as a specific indicator of hyperglycemia resulting from physiological stress. SHR is calculated by adjusting acute blood glucose levels relative to baseline glycemic control, specifically taking into account both the patient's current glucose levels and long-term glycemic status (as indicated by HbA1c) (2, 3). Our preliminary work suggested a U-shaped relationship between glucose variability and all-cause mortality in ABI patients, with significant interactions involving age and diabetes status, indicating the potential value of a reliable predictor that can capture the impact of hyperglycemia on ABI prognosis.

This study investigates SHR as a predictor of primary outcomes (in-hospital, ICU, and 365-day mortality) and secondary outcomes (30, 60, and 90-day mortality) in ABI patients. Recognizing the Glasgow Coma Scale (GCS) as an established neurological assessment in neurosurgical populations and the significant impact of mechanical ventilation on ABI prognosis, we further evaluate the predictive power of SHR in conjunction with GCS scores and ICU ventilation on day one. By analyzing SHR alongside these clinical parameters, we aim to enhance risk stratification in ABI and offer insights for future management strategies.

Methods

Database source

This study utilized data from the Medical Information Mart for Intensive Care version 3.1 (MIMIC-IV v3.1), a comprehensive clinical dataset from the Beth Israel Deaconess Medical Center in Boston, Massachusetts, covering the period from 2008 to 2022. The MIMIC-IV v3.1 database contains 94,458 admissions, providing detailed clinical information on demographics, vital signs, laboratory results, comorbidities, treatments, and discharge outcomes. Renowned for its rigor and depth, MIMIC-IV v3.1 is extensively used in clinical research, particularly for critical care data. Access to this publicly available dataset was granted with ethical approval, with author Juan Wang certified to utilize the data (certification number: 13313422). All analyses adhered to the Strengthening the Reporting of Observational Studies in Epidemiology (STROBE) guidelines to ensure transparency and reproducibility (4).

Data collection

Inclusion and exclusion criteria

Inclusion criteria were first ICU admission during initial hospitalization to ensure unique patient records, age ≥18 years, documented diagnosis of ABI including traumatic brain injury, spontaneous intracranial hemorrhage, and ischemic stroke, and availability of both glucose and glycated hemoglobin (HbA1c) measurements for calculating the SHR. Exclusion criteria included missing glucose or HbA1c data, ICU stays of <24 h, and ABI resulting from secondary etiologies such as tumors, infections, metabolic disorders, or toxic causes. After applying these criteria, 2,423 patients were included in the final analysis.

Data extraction and definitions

Data were extracted from the MIMIC-IV v3.1 database using Navicat Premium (version 17) and SQL queries. Variables were categorized as follows, based on established methodologies in the MIMIC database and SHR research (3, 5, 6). These variables are detailed in Supplementary Table 1. Demographic: age, sex, and weight; Vital signs: baseline measurements recorded within the first 24 h of ICU admission, including heart rate (HR, beats per minute), mean blood pressure (MBP, mmHg), respiratory rate (RR, breaths per minute), temperature (°C), and oxygen saturation (SpO_2, %); Laboratory tests: hemoglobin (g/dL), platelets ($\times 10^9$/L), red blood cell count (RBC, $\times 10^{12}$/L), white blood cell count (WBC, $\times 10^9$/L), blood urea nitrogen (BUN, mg/dL), creatinine (mg/dL), sodium (mmol/L), potassium (mmol/L), and aspartate aminotransferase (AST, U/L);Medical history and comorbidities: smoking status and conditions such as dementia, Cerebrovascular disease (CBD), cancer, rheumatic disease, liver disease, hyperlipidemia, diabetes, hypertension, myocardial infarction (MI), congestive heart failure (CHF), and sepsis, as defined by Sepsis-3 criteria; Organ dysfunction and severity: Charlson Comorbidity Index (CCI), Glasgow Coma Scale (GCS), and Simplified Acute Physiology Score II (SAPS II);In-hospital procedures: mechanical ventilation on the first ICU day, craniotomy, percutaneous cerebral arterial embolization (Pe), ventricular drainage (Vd), and the use of diuretics and β-blockers.

Exposure definition

The SHR was calculated to quantify stress-induced hyperglycemia, adjusting for baseline glycemic control. The formula used was SHR = [Admission blood glucose (mg/dL)] / [28.7 × HbA1c (%) – 46.7]. This formula is commonly applied in critical care research, as it standardizes the assessment of acute hyperglycemia by considering both current and chronic glucose levels (3, 7).

Outcome measures

The primary outcomes of this study included in-hospital and ICU mortality as short-term indicators, and 365-day mortality as a long-term indicator. Additionally, 30, 60, and 90-day mortality were assessed as secondary short-term outcomes. These outcomes collectively provide a comprehensive evaluation of both short- and long-term mortality risks (8, 9).

Statistical analyses

Statistical analyses were performed using R Statistical Software (version 4.2.2) and the Free Statistics analysis platform (version 2.0, Beijing, China). Cox regression analysis was conducted using the coxph function from the survival package, and

ROC curves were generated using the roc function from the pROC package in R. The Kolmogorov-Smirnov test assessed the normality of continuous variables. Normally distributed continuous variables were reported as mean ± standard deviation (SD), while non-normally distributed variables were reported as median and interquartile range (IQR). Categorical variables were summarized as frequencies and percentages. Group comparisons used the independent samples *t*-test or Mann-Whitney U-test for continuous variables, and the chi-square or Fisher's exact test for categorical variables. Bonferroni adjustments were applied where necessary to reduce Type I error due to multiple comparisons, with statistical significance set at a two-sided p-value < 0.05.

Baseline characteristics for the two exposure groups (high and low SHR) were presented before and after imputation ensuring robust comparisons across exposure categories.

Cox proportional hazards regression models were used to evaluate the association between SHR and mortality outcomes, including in-hospital, ICU, 365, 30, 60, and 90-day mortality. SHR was analyzed as a continuous variable and dichotomized to assess mortality risk across SHR levels. The proportional hazards assumption was tested with log-log survival plots and Schoenfeld residuals. Kaplan-Meier survival curves were generated for SHR categories to depict survival probabilities, with statistical differences across groups assessed via the log-rank test.

To account for potential confounders, three progressively adjusted Cox regression models were developed: (1) Model 1: unadjusted; (2) Model 2: adjusted for demographic and clinical variables; (3) Model 3: further adjusted for additional covariates, including Clinical Severity Scores and In-hospital Procedures. These variables were selected based on univariate analysis ($p < 0.1$) and their clinical relevance. Additionally, stepwise regression analysis, as part of a sensitivity analysis, identified the final set of predictors for mortality outcomes, which were incorporated into the models.

Receiver operating characteristic (ROC) curves were generated to evaluate the predictive performance of SHR for mortality outcomes, assessed both independently and in combination with GCS scores and mechanical ventilation on the first ICU-day (10, 11). As part of a sensitivity analysis, LASSO regression was conducted to perform variable selection and further validate the predictive value of SHR for mortality outcomes. The area under the curve (AUC) was calculated to compare the predictive power of models for short- and long-term mortality, covering in-hospital, ICU, 30, 60, 90, and 365-day mortality. For each model, performance metrics including specificity, sensitivity, accuracy, precision, and recall were reported.

Subgroup analyses explored potential effect modifications by variables such as age, hypertension, diabetes, sepsis, and craniotomy status, using interaction terms with SHR to evaluate group heterogeneity. To examine the consistency of the association between SHR and mortality outcomes, we categorized SHR as a continuous, dichotomized, variable, with dichotomization based on the median value of SHR observed in our cohort, and restricted cubic splines confirmed the linear association between SHR and mortality outcomes.

To ensure robustness, the primary and secondary outcomes of this study, including in-hospital, ICU, and 365-day mortality as long-term indicators, and 30, 60, and 90-day mortality for short-term assessment, were analyzed. Sevenfold multiple imputation applied to address missing data using the "mice" package in R. *E*-values were calculated to estimate the minimum strength of association required for an unmeasured confounder to explain the observed association between SHR and mortality outcomes. The *E*-value represents the smallest effect size that an unmeasured confounder would need to havein order to fully account for the observed relationship.

Results

Supplementary Figure 1 presents the screening process of 94,458 ICU admissions from the MIMIC-IV v3.1 database. After applying inclusion criteria to select only first ICU admissions, 6,824 patients with complete data for SHR calculation were identified. Additional exclusions based on age, ICU stay duration, and ABI diagnosis resulted in a final cohort of 2,423 patients.

Cohort characteristics

Baseline characteristics of the cohort are summarized in Table 1, with patients categorized into two SHR groups: Group 1 (SHR 0.185–1.021) and Group 2 (SHR 1.022–15.041). The cohort had a mean age of 69.7 years, with 52.2% male patients. Common comorbidities included hypertension (79.3%), diabetes (31.4%), congestive heart failure (18.8%), and sepsis (35.0%). Compared to Group 1, Group 2 patients exhibited significantly higher heart and respiratory rates, as well as elevated white blood cell counts and urea nitrogen levels, indicating greater physiological stress. Additionally, Group 2 had higher rates of liver disease and hyperlipidemia, suggesting a greater burden of underlying health conditions. Notably, in-hospital procedures differed significantly between the two groups: Group 2 patients had higher rates of mechanical ventilation initiated on the first ICU-day (27.4% vs. 16.4%, $P < 0.001$), craniotomy (9.9% vs. 4.3%, $P < 0.001$), and ventricular drainage (2.8% vs. 1.1%, $P = 0.002$), indicating more intensive treatment. Baseline characteristics were consistent before and after imputation, indicating that the imputation process did not influence overall group comparisons or key variables, thus supporting the robustness of the dataset for further analysis.

Clinical outcomes

After baseline assessment, associations between SHR and various mortality outcomes were analyzed in the cohort of 2,423 ABI patients. As shown in Supplementary Figure 2, the proportional hazards assumption was tested and confirmed using log-log survival plots and Schoenfeld residuals. The test for SHR yielded a chi-square of 0.587 ($p = 0.444$), validating the use of Cox regression models to explore the relationship between SHR and mortality outcomes. Kaplan-Meier survival curves for short- and long-term mortality outcomes (in-hospital, ICU, 30, 60, 90, and

TABLE 1 Characteristics and outcomes of participants by SHR category, before and after imputation.

Characteristic	Before Imputation				After Imputation			
	Total ($N = 2,423$)	Group 1 ($N = 1,211$)	Group 2 ($N = 1,212$)	*P*-value	Total ($N = 2,423$)	Group 1 ($N = 1,211$)	Group 1 ($N = 1,212$)	*P*-value
Demographic								
Sex (Male)	1,265 (52.2)	633 (52.3)	632 (52.1)	0.951	1,265 (52.2)	633 (52.3)	632 (52.1)	0.951
Age	69.7 ± 15.4	70.6 ± 15.2	68.8 ± 15.5	0.004	69.7 ± 15.4	70.6 ± 15.2	68.8 ± 15.5	0.004
Weight*	80.2 ± 30.4	79.5 ± 36.9	80.9 ± 22.1	0.244	80.2 ± 30.4	79.4 ± 36.9	81.0 ± 22.1	0.217
Vital signs								
HR (bpm)*	80.0 ± 14.7	77.6 ± 13.7	82.5 ± 15.2	<0.001	80.0 ± 14.7	77.6 ± 13.7	82.5 ± 15.2	<0.001
MBP*	88.2 ± 11.4	89.4 ± 11.4	87.1 ± 11.3	<0.001	88.2 ± 11.4	89.4 ± 11.4	87.1 ± 11.3	<0.001
RR (bpm)*	18.9 ± 3.0	18.5 ± 2.8	19.2 ± 3.2	<0.001	18.9 ± 3.0	18.5 ± 2.8	19.2 ± 3.2	<0.001
Temperature*	37.0 ± 0.4	37.0 ± 0.4	37.0 ± 0.4	0.001	37.0 ± 0.4	37.0 ± 0.4	37.0 ± 0.4	0.001
SpO_2 (%)*	97.0 ± 1.8	96.8 ± 1.8	97.2 ± 1.8	<0.001	97.0 ± 1.8	96.8 ± 1.8	97.2 ± 1.8	<0.001
Laboratory tests								
Hemoglobin*	11.9 ± 2.2	12.1 ± 2.0	11.7 ± 2.3	<0.001	11.9 ± 2.2	12.1 ± 2.0	11.7 ± 2.3	<0.001
Platelets*	208.6 ± 77.3	215.6 ± 74.4	201.6 ± 79.5	<0.001	208.6 ± 77.3	215.6 ± 74.4	201.7 ± 79.4	<0.001
RBC*	3.9 ± 1.0	4.0 ± 1.0	3.8 ± 0.9	<0.001	3.9 ± 1.0	4.0 ± 1.0	3.8 ± 0.9	<0.001
WBC*	12.0 ± 7.0	10.7 ± 7.7	13.3 ± 6.0	<0.001	12.0 ± 7.0	10.7 ± 7.7	13.3 ± 6.0	<0.001
Urea nitrogen*	21.4 ± 14.4	20.1 ± 12.3	22.7 ± 16.2	<0.001	21.4 ± 14.4	20.1 ± 12.3	22.7 ± 16.2	<0.001
Creatinine#*	0.9 (0.8, 1.2)	0.9 (0.8, 1.2)	1.0 (0.8, 1.2)	0.093	0.9 (0.8, 1.2)	0.9 (0.8, 1.2)	1.0 (0.8, 1.2)	0.103
Sodium*	138.1 ± 4.4	138.5 ± 4.0	137.7 ± 4.7	<0.001	138.1 ± 4.4	138.5 ± 4.0	137.7 ± 4.7	<0.001
Potassium*	3.8 ± 0.5	3.9 ± 0.5	3.8 ± 0.5	0.009	3.8 ± 0.5	3.9 ± 0.5	3.8 ± 0.5	0.005
AST#*	19.0 (14.0, 30.0)	18.0 (13.0, 28.0)	21.0 (14.0, 32.0)	<0.001	19.0 (14.0, 29.0)	18.0 (13.0, 28.0)	20.5 (14.0, 32.0)	<0.001
Glucose	142.5 ± 71.1	112.8 ± 33.0	172.1 ± 85.2	<0.001	142.5 ± 71.1	112.8 ± 33.0	172.1 ± 85.2	<0.001
HbA1c	6.2 ± 1.5	6.3 ± 1.5	6.1 ± 1.4	<0.001	6.2 ± 1.5	6.3 ± 1.5	6.1 ± 1.4	<0.001
Medical history								
Smoke	756 (31.2)	393 (32.5)	363 (30)	0.184	756 (31.2)	393 (32.5)	363 (30)	0.184
Organ dysfunction								
Dementia	169 (7.0)	88 (7.3)	81 (6.7)	0.573	169 (7.0)	88 (7.3)	81 (6.7)	0.573
CBD	2,316 (95.6)	1,174 (96.9)	1,142 (94.2)	0.001	2,316 (95.6)	1,174 (96.9)	1,142 (94.2)	0.001
Cancer	152 (6.3)	67 (5.5)	85 (7)	0.133	152 (6.3)	67 (5.5)	85 (7)	0.133
Rheumatic	45 (1.9)	19 (1.6)	26 (2.1)	0.293	45 (1.9)	19 (1.6)	26 (2.1)	0.293
Liver disease	104 (4.3)	32 (2.6)	72 (5.9)	< 0.001	104 (4.3)	32 (2.6)	72 (5.9)	<0.001
Hyperlipidemia	1,139 (47.0)	609 (50.3)	530 (43.7)	0.001	1,139 (47.0)	609 (50.3)	530 (43.7)	0.001
Diabetes	762 (31.4)	359 (29.6)	403 (33.3)	0.056	762 (31.4)	359 (29.6)	403 (33.3)	0.056
HBP	1,921 (79.3)	955 (78.9)	966 (79.7)	0.609	1,921 (79.3)	955 (78.9)	966 (79.7)	0.609
MI	293 (12.1)	140 (11.6)	153 (12.6)	0.422	293 (12.1)	140 (11.6)	153 (12.6)	0.422
CHF	455 (18.8)	227 (18.7)	228 (18.8)	0.966	455 (18.8)	227 (18.7)	228 (18.8)	0.966
Sepsis3	849 (35.0)	329 (27.2)	520 (42.9)	< 0.001	849 (35.0)	329 (27.2)	520 (42.9)	< 0.001
Score								
CCI	6.1 ± 2.7	6.2 ± 2.7	6.1 ± 2.8	0.523	6.1 ± 2.7	6.2 ± 2.7	6.1 ± 2.8	0.523

(Continued)

TABLE 1 (Continued)

Characteristic	Before Imputation				After Imputation			
	Total ($N = 2,423$)	Group 1 ($N = 1,211$)	Group 2 ($N = 1,212$)	*P*-value	Total ($N = 2,423$)	Group 1 ($N = 1,211$)	Group 1 ($N = 1,212$)	*P*-value
GCS	11.1 ± 3.5	11.8 ± 3.2	10.5 ± 3.7	<0.001	11.1 ± 3.5	11.8 ± 3.2	10.5 ± 3.7	<0.001
SAPS II	32.5 ± 11.3	30.9 ± 10.5	34.1 ± 11.9	<0.001	32.5 ± 11.3	30.9 ± 10.5	34.1 ± 11.9	<0.001
In-hospital procedures								
Vent1day	530 (21.9)	198 (16.4)	332 (27.4)	<0.001	530 (21.9)	198 (16.4)	332 (27.4)	<0.001
Craniotomy	172 (7.1)	52 (4.3)	120 (9.9)	<0.001	172 (7.1)	52 (4.3)	120 (9.9)	<0.001
Pe	357 (14.7)	162 (13.4)	195 (16.1)	0.06	357 (14.7)	162 (13.4)	195 (16.1)	0.06
Vd	47 (1.9)	13 (1.1)	34 (2.8)	0.002	47 (1.9)	13 (1.1)	34 (2.8)	0.002
Diuretic	818 (33.8)	346 (28.6)	472 (38.9)	<0.001	818 (33.8)	346 (28.6)	472 (38.9)	<0.001
β_blocker	1653 (68.2)	759 (62.7)	894 (73.8)	<0.001	1653 (68.2)	759 (62.7)	894 (73.8)	<0.001

SHR, Stress Hyperglycemia Ratio; ABI, acute brain injury; ICU, intensive care unit; HR, heart rate (beats per minute, bpm); MBP, mean blood pressure (mmHg); RR, respiratory rate (breaths per minute, bpm); SpO_2, oxygen saturation (%); WBC, white blood cell count (10^9/L); RBC, red blood cell count (10^12/L); Hemoglobin (g/dL); Platelets (10^9/L); Creatinine (mg/dL); Urea nitrogen (mg/dL); Sodium (mmol/L); Potassium (mmol/L); AST, aspartate aminotransferase (U/L); MI, myocardial infarction; CHF, congestive heart failure; CBD, Cerebrovascular disease; HBP, hypertension; Sepsis3, Sepsis clinical criteria from The Third International Consensus Definitions for Sepsis and Septic Shock; CCI, Charlson comorbidity index; SAPS II, simplified acute physiological score II; GCS, Glasgow coma scale; Vent1day, ventilation on the first day of ICU admission; Pe, percutaneous cerebral arterial embolization; Vd, ventricular drainage.
Values are presented as mean ± standard deviation (SD), median [interquartile range, IQR], or number (%). *Variables with <5% missing data include Heart rate, MBP, Respiratory rate, SpO_2, Temperature, Weight, WBC, Hemoglobin, Platelets, Urea nitrogen, Creatinine, Potassium and Sodium. Variables with 20–30% missing data include AST. #Due to non-normal distribution, Creatinine and AST values are presented as median [IQR]. Group comparisons were assessed with appropriate statistical tests, with p-values < 0.05 indicating statistical significance.

365-day) demonstrated significantly lower survival probabilities in the higher SHR group (Group 2) compared to the lower SHR group (Group 1). Log-rank tests confirmed significant differences across all outcomes ($p < 0.001$; Figure 1, Supplementary Figure 3).

Cox regression analysis was performed, incorporating variables with $p < 0.1$ from univariate analysis and clinically significant covariates (Supplementary Table 2), with multiple imputation used to address missing data. As shown in Table 2 and Supplementary Table 3, higher SHR levels were significantly associated with increased risks for both short- and long-term mortality outcomes. When analyzed as a continuous variable, SHR consistently demonstrated a significant positive association with in-hospital (HR: 1.18, 95% CI: 1.06–1.32, $P = 0.003$), ICU (HR: 1.16, 95% CI: 1.02–1.32, $P = 0.029$), and 365-day mortality (HR: 1.14, 95% CI: 1.05–1.23, $P = 0.002$) in fully adjusted models (Model 3). When dichotomized, higher SHR (Group 2 vs. Group 1) was associated with increased mortality risks for in-hospital (HR: 1.44, 95% CI: 1.13–1.83, $P = 0.003$), ICU (HR: 1.50, 95% CI: 1.10–2.04, $P = 0.009$), and 365-day mortality (HR: 1.33, 95% CI: 1.14–1.56, P<0.001).

For other secondary endpoints, including 30, 60, and 90-day mortality, similar patterns were observed, with higher SHR consistently associated with increased risks. For example, as a continuous variable, SHR demonstrated significant associations with 30-day mortality (HR: 1.16, 95% CI: 1.07–1.27, $P = 0.001$), 60-day mortality (HR: 1.16, 95% CI: 1.06–1.26, $P = 0.001$), and 90-day mortality (HR: 1.15, 95% CI: 1.05–1.25, $P = 0.002$). Dichotomized SHR analysis similarly showed elevated risks across these endpoints. Stepwise regression analysis, as part of a sensitivity analysis, identified relevant predictors of mortality outcomes and adjusted for them in the final models, as presented in Supplementary Tables 4, 5. These consistent findings across multiple outcomes underscore the robustness of the observed association between SHR and mortality, further supporting the reliability of the study conclusions.

Restricted cubic spline analyses (Figure 2 and Supplementary Figure 4) confirmed a linear relationship between SHR and mortality outcomes, reinforcing SHR's predictive value. The fitted hazard ratios (HR) with 95% confidence intervals consistently indicated higher mortality risks with increasing SHR values, with no evidence of non-linearity (P for non-linearity > 0.05 across all mortality outcomes).

Subgroup analysis

Subgroup analyses supported the primary findings, as part of our sensitivity analysis, further validating the relationship between SHR and mortality across various patient subgroups (Figure 3). Stratifications by age, diabetes status, hypertension, sepsis, and craniotomy provided comprehensive insights into SHR's predictive capacity in different clinical settings. Across all subgroups, higher SHR values were consistently linked to increased risks of in-hospital, ICU, 30, 60, 90, and 365-day mortality.

For in-hospital, ICU, and 365-day mortality (Figure 3A), the association between elevated SHR and higher mortality risk was most pronounced in older and non-diabetic patients, with odds ratios slightly higher than those observed in younger or diabetic patients. Interaction p-values exceeded 0.05, reinforcing the stability of the linear relationship between SHR and mortality across these subgroups. Similarly, for 30, 60, and 90-day mortality (Figure 3B), the association remained consistent across all subgroups, further confirming SHR's robustness as a predictor of mortality across different patient characteristics.

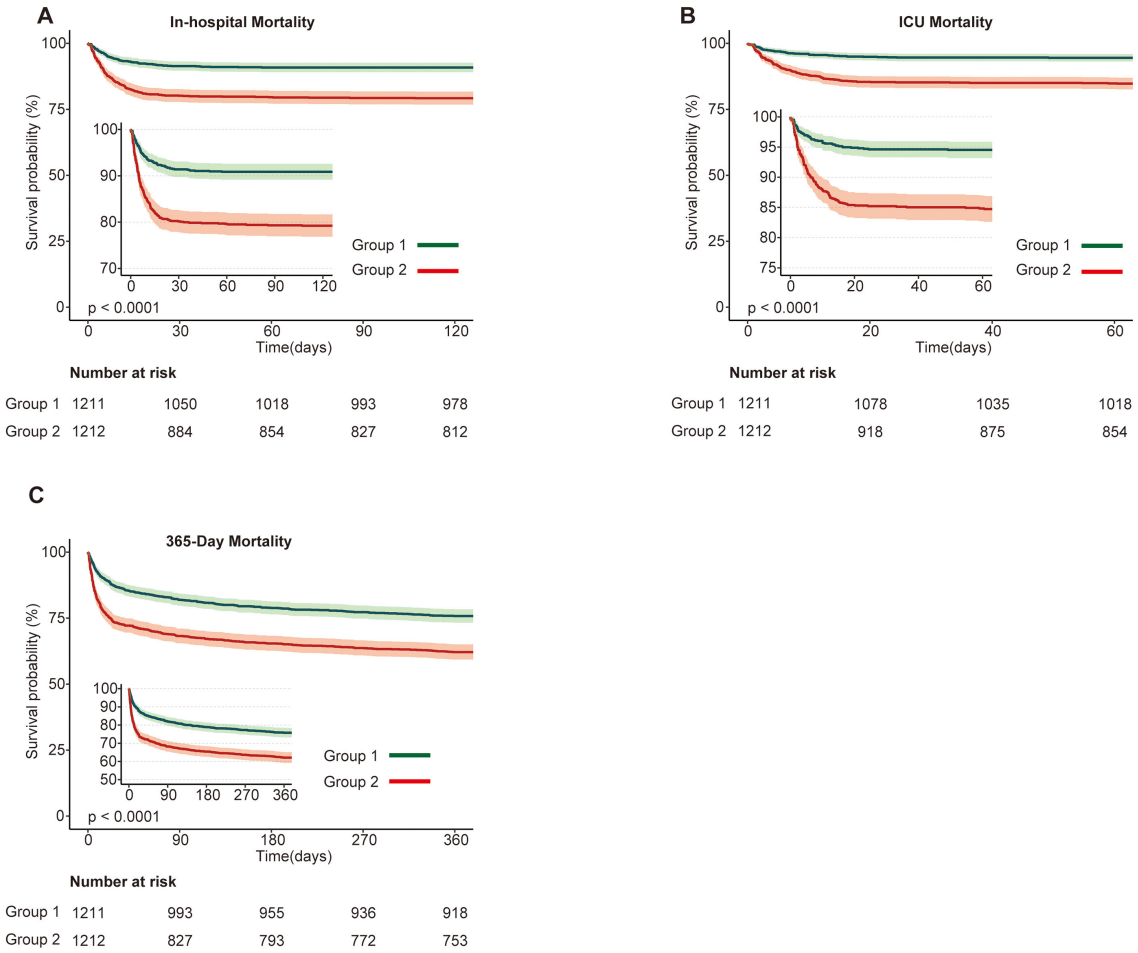

FIGURE 1
Kaplan-Meier survival curves for primary mortality outcomes stratified by SHR groups in patients with acute brain injury. **(A)** In-hospital mortality; **(B)** ICU mortality; **(C)** 365-day mortality. Survival probabilities are compared between Group 1 (green) and Group 2 (red), with Group 1 showing higher survival probabilities across all outcomes. The number at risk at each time point is displayed below the plots. Statistically significant differences in survival are observed between the groups ($p < 0.0001$).

SHR and its combined use with GCS and Vent1day in predicting mortality in ABI patients

As shown in Table 3, SHR demonstrated strong independent predictive value across all mortality outcomes. GCS and Vent1day were selected based on their clinical significance and their established role in predicting mortality, especially in critically ill neurosurgical patients (10, 11). Model 1 (SHR alone) achieved high AUC values, surpassing both the GCS-based (Model 2) and Vent1day-based (Model 3) models. For in-hospital mortality, Model 1 achieved an AUC of 0.673 (95% CI: 0.642–0.705), outperforming Model 2 (AUC: 0.647) and Model 3 (AUC: 0.661). Combining SHR with GCS and Vent1day further enhanced predictive accuracy, as evidenced by the highest AUC values in Model 6 across both short- and long-term mortality outcomes. For instance, Model 6 achieved an AUC of 0.817 (95% CI: 0.792–0.842) for ICU mortality and 0.788 (95% CI: 0.764–0.812) for in-hospital mortality, underscoring the enhanced predictive power of integrating multiple markers. The ROC curves in Figure 4 and Supplementary Figure 5 visually confirmed this pattern, with Model 6 consistently exhibiting superior discriminatory power across various mortality endpoints in ABI patients. To clarify, we have revised the original manuscript to include the following statement: Model 1 (SHR alone) shows moderate performance with accuracy of 0.657, specificity of 0.669, and sensitivity of 0.590. When SHR is combined with GCS and Vent1day in Model 6, accuracy increases to 0.695, and specificity rises to 0.819, with sensitivity also improving to 0.819. These improvements demonstrate that combining these variables enhances predictive accuracy for mortality outcomes. All key performance metrics—accuracy, specificity, and sensitivity—are shown for each model across different mortality outcomes in Table 3. As part of a sensitivity analysis, LASSO regression was performed to further validate the variable selection, ensuring that the identified variables, including SHR, GCS, and Vent1day, were robust and critical predictors for mortality outcomes (shown in Supplementary Figure 6). Additionally, Time-dependent AUC analysis for predicting in-hospital mortality was performed as a sensitivity analysis (Supplementary Figure 7)

TABLE 2 Association of SHR with short-term and long-term mortality risk.

Categories	Model1		Model2		Model3	
	HR (95%CI)	*P*-value	HR (95%CI)	*P*-value	HR (95%CI)	*P*-value
In-hospital mortality						
SHR (continuous variable)	1.25 (1.17–1.34)	<0.001	1.23 (1.11–1.36)	<0.001	1.18 (1.06–1.32)	0.003
SHR (dichotomized)						
Group1	Ref	Ref	Ref	Ref	Ref	Ref
Group2	1.79 (1.43–2.24)	<0.001	1.58 (1.25–2.01)	<0.001	1.44 (1.13–1.83)	0.003
ICU mortality						
SHR (continuous variable)	1.21 (1.11–1.31)	<0.001	1.24 (1.1–1.39)	<0.001	1.16 (1.02–1.32)	0.029
SHR (dichotomized)						
Group1	Ref	Ref	Ref	Ref	Ref	Ref
Group2	1.86 (1.4–2.48)	<0.001	1.65 (1.22–2.22)	0.001	1.5 (1.1–2.04)	0.009
365-day mortality						
SHR (continuous variable)	1.31 (1.24–1.38)	<0.001	1.19 (1.11–1.29)	<0.001	1.14 (1.05–1.23)	0.002
SHR (dichotomized)						
Group1	Ref	Ref	Ref	Ref	Ref	Ref
Group2	1.77 (1.53–2.05)	<0.001	1.45 (1.24–1.7)	<0.001	1.33 (1.14–1.56)	<0.001
30-day mortality						
SHR (continuous variable)	1.31 (1.24–1.38)	<0.001	1.22 (1.13–1.33)	<0.001	1.16 (1.07–1.27)	0.001
SHR (dichotomized)						
Group1	Ref	Ref	Ref	Ref	Ref	Ref
Group2	2.24 (1.85–2.7)	<0.001	1.79 (1.46–2.18)	<0.001	1.61 (1.31–1.97)	<0.001
60-day mortality						
SHR (continuous variable)	1.31 (1.24–1.38)	<0.001	1.22 (1.13–1.32)	<0.001	1.16 (1.06–1.26)	0.001
SHR (dichotomized)						
Group1	Ref	Ref	Ref	Ref	Ref	Ref
Group2	2.05 (1.72–2.45)	<0.001	1.66 (1.37–1.99)	<0.001	1.49 (1.23–1.8)	<0.001
90-day mortality						
SHR (continuous variable)	1.31 (1.24–1.38)	<0.001	1.21 (1.11–1.3)	<0.001	1.15 (1.05–1.25)	0.002
SHR (dichotomized)						
Group1	Ref	Ref	Ref	Ref	Ref	Ref
Group2	1.97 (1.67–2.32)	<0.001	1.58 (1.32–1.88)	<0.001	1.43 (1.2–1.71)	<0.001

SHR, Stress hyperglycemia ratio; HR, hazard ratio; CI, confidence interval; ABI, acute brain injury; ICU, intensive care unit; MBP, mean blood pressure; SpO_2, oxygen saturation; RBC, red blood cell; WBC, white blood cell; BUN, blood urea nitrogen; SAPS II, simplified acute physiological score II; GCS, Glasgow coma scale. Model Descriptions: Model 1, unadjusted; Model 2, adjusted for admission age, weight, heart rate, MBP, respiratory rate, SpO_2, hemoglobin, platelets, RBC, WBC, BUN, creatinine, sodium, liver disease, hypertension, diabetes, and Sepsis3; Model 3, adjusted for Model 2 covariates plus Charlson comorbidity index, GCS, SAPS II, ventilation on the first ICU day, craniotomy, and diuretic use in the ICU.

to further validate the incremental predictive value of SHR.

Supplementary Figure 8 presents the *E*-values from Table 4, demonstrating SHR's resilience to unmeasured confounding across all mortality outcomes. The *E*-value represents the minimum strength of association that an unmeasured confounder would need to have with both SHR and the mortality outcome to fully explain the observed relationship. For ICU mortality, SHR had an *E*-value of 2.37 (lower CI: 1.43), indicating that even a moderate unmeasured confounder would need a strong association with both SHR and ICU mortality to nullify the observed association. Similarly, for in-hospital mortality, the *E*-value was 2.24 (lower CI: 1.51). Additional results include 30-day mortality (E-value: 2.60, lower CI: 1.95), 60-day mortality (E-value: 2.34, lower CI: 1.76), 90-day mortality (E-value: 2.21, lower CI: 1.69), and 365-day mortality (E-value: 1.99, lower CI: 1.54), further reinforcing SHR's predictive strength across both short-term and long-term outcomes. These findings highlight that the association between SHR and mortality

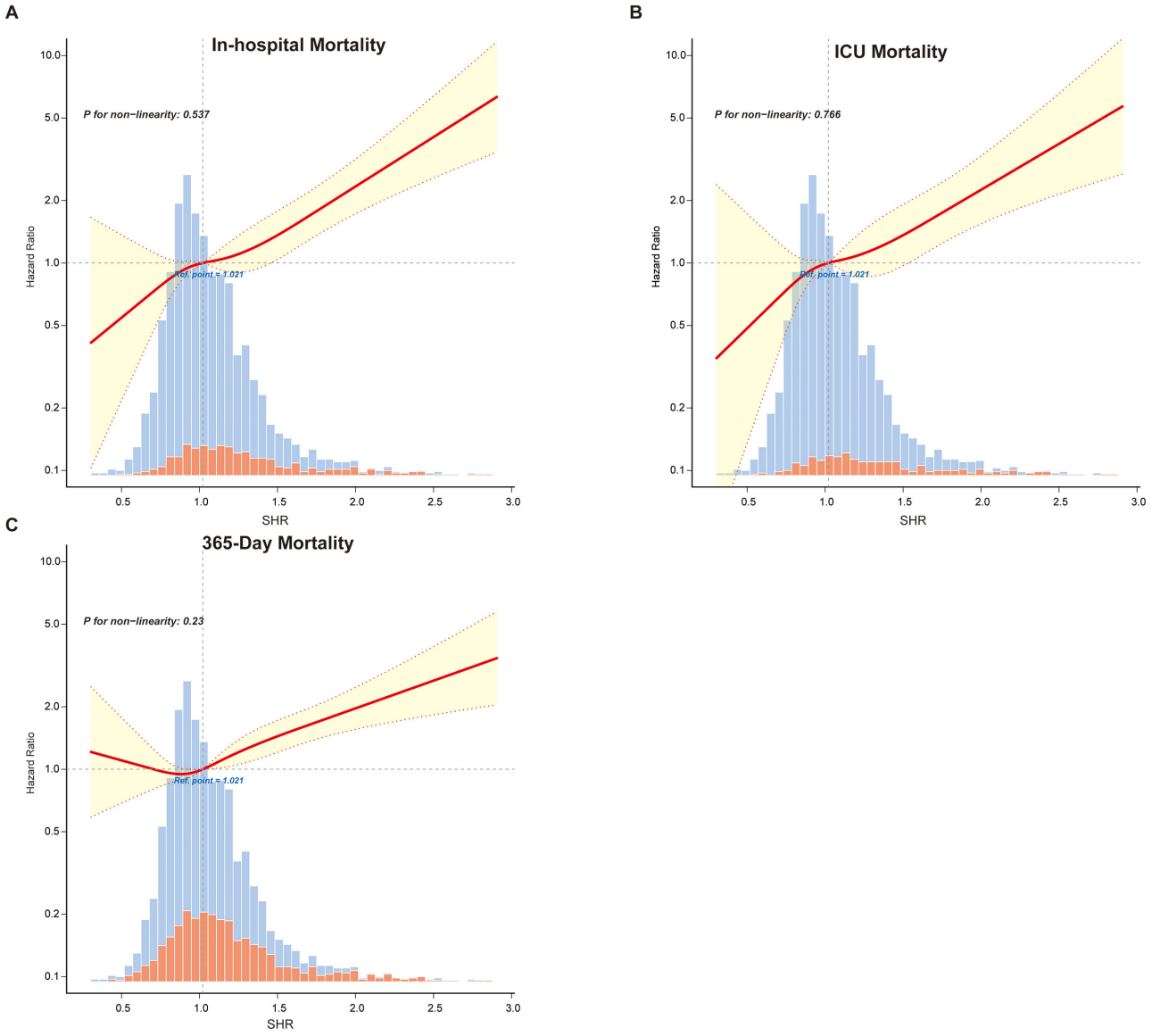

FIGURE 2
Restricted cubic spline curves illustrating the linear relationship between SHR and primary outcomes: **(A)** in-hospital mortality, **(B)** ICU mortality and **(C)** 365-Day mortality. Vertical dashed lines indicate reference points, the red line represents fully adjusted hazard ratios, and the shaded yellow area shows the 95% confidence interval.

is robust and not likely to be significantly impacted by unmeasured confounding.

Discussion

In this study, we demonstrated that the SHR is a reliable, independent predictor of mortality at various time points: in-hospital, ICU, 30, 60, 90, and 365-day outcomes in patients with ABI. The linear association between SHR and mortality, consistent across various patient subgroups, highlights SHR's stability and its potential utility as a robust biomarker for mortality risk stratification with ABI. These findings support and extend previous studies, further validating SHR's role in reflecting acute metabolic stress in critically ill brain-injured patients. The consistency of SHR's association with mortality across subgroups, combined with its linear relationship to mortality, indicates its reliable predictive capacity, distinguishing it from other glycemic metrics.

Our results build on the findings of Rau et al. and Pan et al., who associated stress hyperglycemia with increased mortality in traumatic brain injury and ischemic stroke, highlighting SHR's superior predictive ability compared to conventional glucose metrics (8, 12). In contrast to these studies, our analysis expands the prognostic utility of SHR by covering a diverse ABI cohort that includes both stroke and trauma cases. Similar ABI cohorts have been utilized in high-impact studies, which further underscores the relevance of our cohort (1). Comparative studies have revealed the diverse relationships between SHR and mortality in different critical populations (13, 14). For example, in acute myocardial infarction (AMI) patients, a J-shaped association was observed

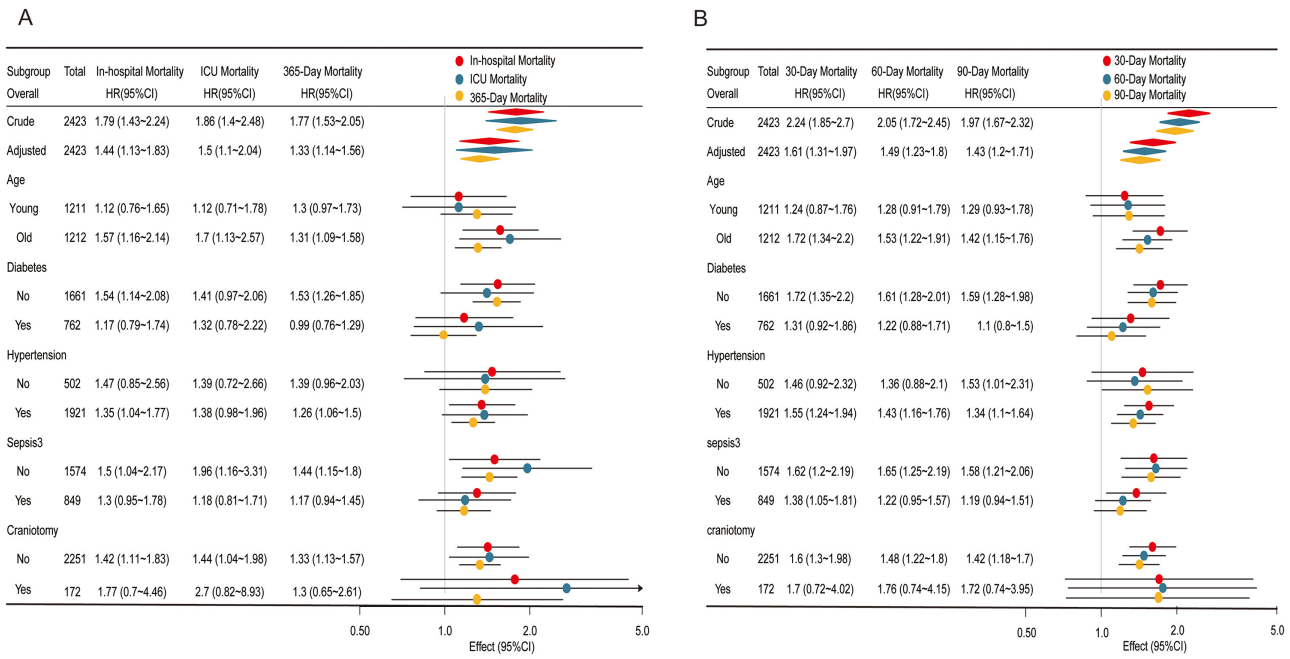

FIGURE 3
Subgroup analyses of the association between the stress hyperglycemia ratio (SHR) and mortality outcomes. **(A)** Association of SHR with in-hospital mortality, ICU mortality, and 365-day mortality. **(B)** Association of SHR with 30, 60, and 90-day mortality. Each subgroup analysis displays the Hazard ratios (HR) and 95% confidence intervals (CI) for different mortality outcomes, stratified by age, diabetes status, hypertension, sepsis, and craniotomy status. Colored markers represent mortality types: red for in-hospital/30-day mortality, blue for ICU/60-day mortality, and yellow for 365-day/90-day mortality. Significant associations are highlighted, with effect estimates plotted on a logarithmic scale for clarity.

between SHR and all-cause mortality, with both high and low SHR values associated with elevated risk, particularly in non-diabetic individuals (7). Likewise, Zhang et al. observed a clearly non-linear, potentially J-shaped, association in patients with acute coronary syndrome and triple-vessel disease, with elevated SHR posing a significant cardiovascular mortality risk, especially among diabetic patients (15). In contrast to this, Le Li's study on sepsis reported a U-shaped association between SHR and 1-year mortality, with an SHR of 0.99 as the inflection point; both high and low SHR values were associated with increased mortality risk, improving the predictive accuracy of conventional severity scores (16). In a similar vein, Climent et al. reported that higher acute-to-chronic glycemic ratio (ACR) values were associated with worse outcomes in ischemic stroke patients, indicating a steady increase in risk without the non-linear patterns observed in AMI and coronary disease (17).

Our study highlights a stable linear association between the SHR and mortality across multiple time points in ABI patients, with no significant interaction effects across subgroups. This finding supports SHR as a consistent and independent predictor of mortality risk in ABI. In contrast, our previous research demonstrated a U-shaped association between GV and mortality in non-diabetic patients, with both high and low GV levels elevating mortality risk, emphasizing the need for population-specific glycemic assessment. This underscores the importance of population-specific assessment in glycemic monitoring, as different glycemic metrics may have varying implications depending on patient characteristics (8, 18, 19). Consistent with our findings, several studies have repeatedly demonstrated SHR's prognostic value across diverse critical conditions and populations. For example, Ding et al. found that SHR is significantly associated with all-cause and cardiovascular mortality in diabetic and prediabetic patients, reinforcing its predictive value in glucose-sensitive populations (20). Additionally, research on coronary artery disease patients showed that combined assessment of SHR and GV provided superior prognostic accuracy, with non-diabetic individuals experiencing the greatest risk of in-hospital and 1-year mortality when both SHR and GV were elevated (6). Furthermore, a study in acute myocardial infarction (AMI) patients demonstrated that elevated fasting SHR strongly correlated with in-hospital mortality in both diabetic and non-diabetic groups, highlighting SHR's value as a robust risk stratification tool across glucose metabolism statuses (3).

ABI is associated with high incidence and poor prognosis, driving significant research efforts to develop more effective prognostic models (21, 22). The Glasgow Coma Scale (GCS) and early mechanical ventilation are among the most accessible ICU indicators for ABI outcomes (23, 24). Previous studies have demonstrated that combining multiple monitoring parameters can enhance predictive accuracy; however, these models often rely on complex metrics, which may limit their clinical applicability (25–28). By contrast, our model, which combines the SHR with GCS and Vent1day, achieves strong predictive performance using readily available indicators. This approach provides a practical and feasible tool for routine use in ABI prognosis, supporting its broader adoption in critical care settings (29, 30).

10.3389/fneur.2025.1552462

TABLE 3 Performance of SHR, GCS, and Vent1day models in predicting short-term and long-term mortality.

Models	Specificity	Sensitivity	Accuracy	Precision	Recall	AUC
In-hospital mortality						
Model 1	0.669	0.590	0.657	0.234	0.590	0.673 (0.642–0.705)
Model 2	0.797	0.551	0.761	0.317	0.551	0.647 (0.608–0.686)
Model 3	0.828	0.494	0.780	0.330	0.494	0.661 (0.634–0.689)
Model 4	0.736	0.675	0.727	0.304	0.675	0.734 (0.704–0.764)
Model 5	0.683	0.729	0.690	0.282	0.729	0.751 (0.723–0.779)
Model 6	0.674	0.819	0.695	0.301	0.819	0.788 (0.764–0.812)
ICU mortality						
Model 1	0.657	0.638	0.655	0.172	0.638	0.700 (0.663–0.736)
Model 2	0.856	0.510	0.822	0.284	0.510	0.641 (0.592–0.691)
Model 3	0.820	0.568	0.795	0.260	0.568	0.694 (0.662–0.726)
Model 4	0.762	0.642	0.750	0.232	0.642	0.747 (0.712–0.783)
Model 5	0.751	0.708	0.747	0.241	0.708	0.785 (0.755–0.815)
Model 6	0.713	0.819	0.724	0.241	0.819	0.817 (0.792–0.842)
365-day mortality						
Model 1	0.616	0.560	0.599	0.396	0.560	0.612 (0.587–0.637)
Model 2	0.712	0.612	0.681	0.489	0.612	0.673 (0.648–0.698)
Model 3	0.831	0.329	0.675	0.466	0.329	0.580 (0.560–0.599)
Model 4	0.770	0.563	0.705	0.524	0.563	0.710 (0.688–0.733)
Model 5	0.724	0.512	0.658	0.455	0.512	0.643 (0.619–0.668)
Model 6	0.697	0.636	0.678	0.485	0.636	0.722 (0.700–0.743)
30-day mortality						
Model 1	0.609	0.624	0.612	0.287	0.624	0.655 (0.627–0.682)
Model 2	0.814	0.524	0.756	0.416	0.524	0.659 (0.627–0.691)
Model 3	0.831	0.417	0.748	0.385	0.417	0.624 (0.601–0.648)
Model 4	0.717	0.667	0.707	0.373	0.667	0.733 (0.708–0.758)
Model 5	0.715	0.624	0.697	0.356	0.624	0.709 (0.682–0.735)
Model 6	0.613	0.812	0.653	0.347	0.812	0.764 (0.742–0.786)
60-day mortality						
Model 1	0.610	0.601	0.608	0.312	0.601	0.641 (0.614–0.668)
Model 2	0.689	0.652	0.681	0.382	0.652	0.669 (0.639–0.699)
Model 3	0.832	0.392	0.732	0.408	0.392	0.612 (0.590–0.634)
Model 4	0.740	0.639	0.717	0.420	0.639	0.730 (0.706–0.754)
Model 5	0.713	0.597	0.686	0.380	0.597	0.690 (0.664–0.716)
Model 6	0.696	0.701	0.697	0.404	0.701	0.754 (0.732–0.776)
90-day mortality						
Model 1	0.676	0.529	0.639	0.351	0.529	0.633 (0.607–0.660)
Model 2	0.697	0.647	0.685	0.415	0.647	0.675 (0.647–0.703)
Model 3	0.834	0.377	0.720	0.428	0.377	0.605 (0.584–0.626)
Model 4	0.748	0.620	0.717	0.450	0.620	0.727 (0.703–0.750)
Model 5	0.719	0.569	0.681	0.401	0.569	0.679 (0.653–0.704)
Model 6	0.667	0.723	0.681	0.418	0.723	0.748 (0.727–0.770)

ABI, acute brain injury; ICU, intensive care unit; HR, hazard ratio; CI, confidence interval; AUC, area under the curve.
Model descriptions: Model 1: based on SHR; Model 2: based on Glasgow Coma Scale (GCS); Model 3: based on ventilation on the first ICU day (Vent1day); Model 4: combined SHR and GCS; Model 5: combined SHR and Vent1day; Model 6: combined SHR, GCS, and Vent1day.

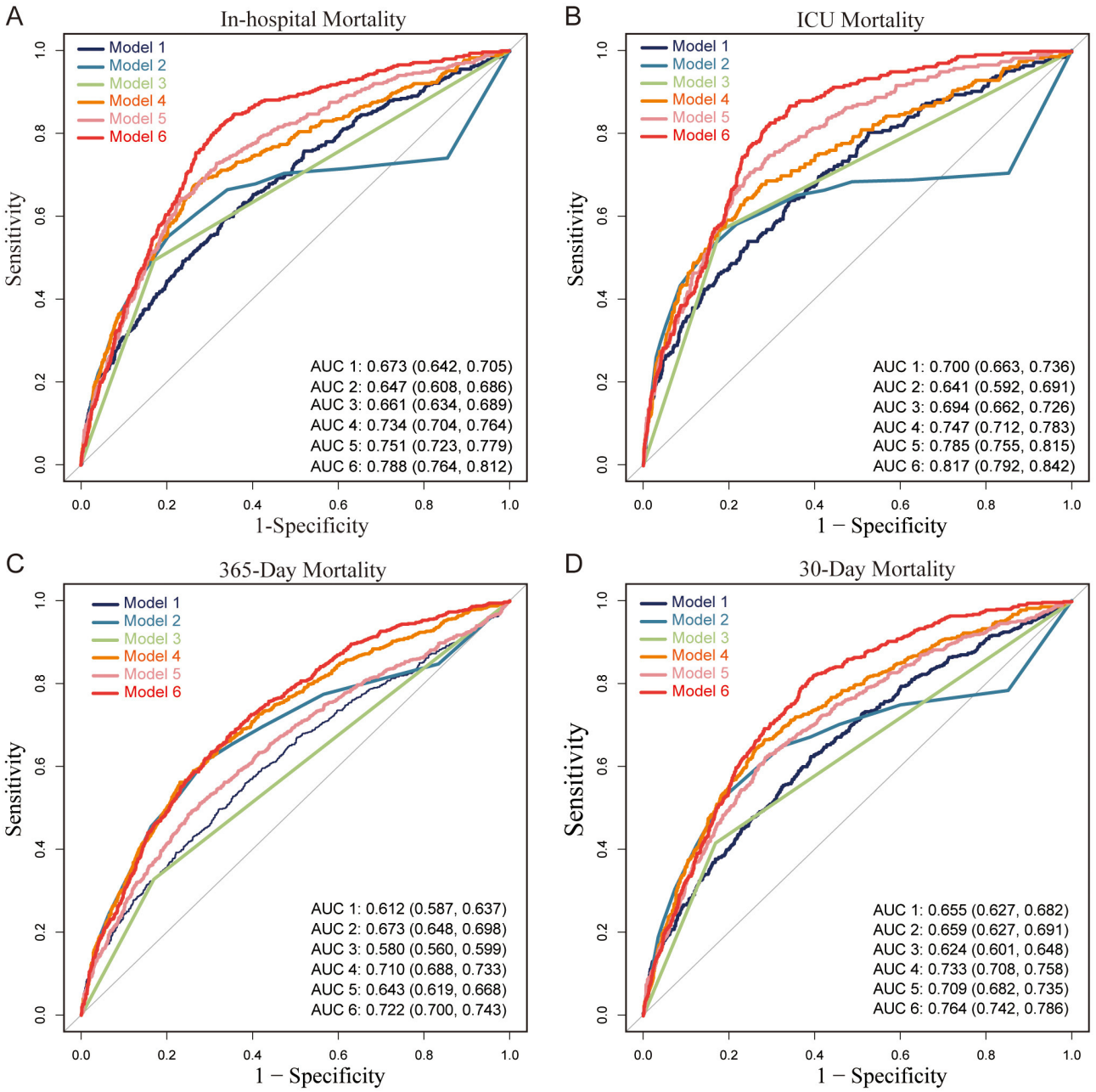

FIGURE 4
Receiver Operating Characteristic (ROC) curves for predictive models of mortality in patients with acute brain injury (ABI). **(A)** In-hospital mortality, **(B)** ICU mortality, **(C)** 365-day mortality, and **(D)** 30-day mortality. Abbreviations: ABI, acute brain injury; ICU, intensive care unit; AUC, area under the curve; SHR, stress hyperglycemia ratio; GCS, Glasgow Coma Scale; Vent1day, ventilation initiated on the first ICU admission. Model Descriptions: Model 1: SHR only; Model 2: GCS only; Model 3: Vent1day only; Model 4: SHR and GCS combined; Model 5: SHR and Vent1day combined; Model 6: SHR, GCS, and Vent1day combined. Notes: Each ROC curve illustrates the sensitivity and specificity of six predictive models for different mortality outcomes in ABI patients. The AUC value indicates each model's discriminatory ability, with higher values reflecting better predictive performance. Model 6 consistently achieves the highest AUC across all mortality outcomes, indicating the strongest predictive accuracy.

The observed linear relationship between SHR and mortality in ABI patients suggests a direct impact of stress-induced hyperglycemia on adverse outcomes, potentially mediated through neuroendocrine activation (31), oxidative stress (32), and inflammation (22, 33). Glucose is critical for brain function (34), supporting ATP production and neurotransmitter synthesis. However, stress disrupts normal metabolism, increasing reliance on glycolysis and the pentose phosphate pathway, which may intensify oxidative damage and neuroinflammation (2, 35). The hypothalamus-sympathetic-liver (HSL) axis rapidly mobilizes glucose in response to stress, independent of adrenal activity, providing an immediate energy supply. However, potentially

TABLE 4 E-values for SHR as a predictor of short-term and long-term mortality.

Outcomes	In-hospital mortality	ICU mortality	365-day mortality	30-day mortality	60-day mortality	90-day mortality
E-value (Lower CI)	2.24 (1.51)	2.37 (1.43)	1.99 (1.54)	2.60 (1.95)	2.34 (1.76)	2.21 (1.69)

exacerbating neuroinflammation and endothelial dysfunction when prolonged (36). Additionally, glucose-sensing alterations to non-diabetic patients may modify the threshold for detecting glycemic extremes, amplifying the impact of hyperglycemia on ABI outcomes (37). Together, these mechanisms underscore SHR's prognostic value and highlight the importance of tailored glycemic management in ABI.

Strengths and limitations

Although our study provides compelling evidence for the prognostic utility of SHR in ABI, several limitations should be acknowledged. The retrospective design and reliance on a single-center database may limit the generalizability of our study's findings (5, 38). Prospective, multi-center studies are essential to validate the predictive capability of SHR and its influence on clinical decision-making in various clinical settings. Furthermore, further exploration of the mechanistic pathways linking SHR to ABI outcomes is warranted, as this could uncover novel therapeutic targets to mitigate hyperglycemia-induced damage in this patient population.

Conclusion

In conclusion, our study confirms SHR as a reliable and independent predictor of mortality in ABI patients, offering a novel approach to mortality risk stratification that incorporates baseline glycemic status. The linear association between SHR and mortality across multiple time points and subgroups further highlights its potential as a stable biomarker in neurocritical care. Integrating SHR into clinical risk assessment may enable clinicians to better identify high-risk patients early and optimize glycemic management strategies. Prospective studies are needed to validate these findings and investigate SHR-guided interventions aimed at improving patient outcomes in ABI, ultimately enhancing survival and recovery in this vulnerable population.

Data availability statement

The datasets presented in this study can be found in online repositories. The names of the repository/repositories and accession number(s) can be found below: https://physionet.org/content/mimiciv/3.1/.

Ethics statement

Ethical review and approval was not required for the study on human participants in accordance with the local legislation and institutional requirements. Written informed consent from the patients/participants or patients/participants' legal guardian/next of kin was not required to participate in this study in accordance with the national legislation and the institutional requirements.

Author contributions

JW: Conceptualization, Data curation, Writing – original draft, Writing – review & editing. P-fD: Data curation, Writing – review & editing. ZP: Data curation, Writing – review & editing. C-HH: Funding acquisition, Writing – review & editing. WL: Funding acquisition, Writing – review & editing.

Funding

The author(s) declare that financial support was received for the research and/or publication of this article. This work was supported by funding's for Clinical Trials from the Affiliated Drum Tower Hospital, Medical School of Nanjing University (No. LCYJ-MS-37 for C-HH, No. LCYJ-PY-38 for WL) and Nanjing Health Commission Project (No. ZKX23025 for WL).

Conflict of interest

The authors declare that the research was conducted in the absence of any commercial or financial relationships that could be construed as a potential conflict of interest.

Generative AI statement

The author(s) declare that no Gen AI was used in the creation of this manuscript.

Publisher's note

Supplementary material

The Supplementary Material for this article can be found online at: https://www.frontiersin.org/articles/10.3389/fneur.2025.1552462/full#supplementary-material

References

1. Dahyot-Fizelier C, Lasocki S, Kerforne T, Perrigault PF, Geeraerts T, Asehnoune K, et al. Ceftriaxone to prevent early ventilator-associated pneumonia in patients with acute brain injury: a multicentre, randomised, double-blind, placebo-controlled, assessor-masked superiority trial. *Lancet Respir Med.* (2024) 12:375–85. doi: 10.1016/S2213-2600(23)00471-X

2. Kivimäki M, Bartolomucci A, Kawachi I. The multiple roles of life stress in metabolic disorders. *Nat Rev Endocrinol.* (2023) 19:10–27. doi: 10.1038/s41574-022-00746-8

3. Cui K, Fu R, Yang J, Xu H, Yin D, Song W, et al. The impact of fasting stress hyperglycemia ratio, fasting plasma glucose and hemoglobin A1c on in-hospital mortality in patients with and without diabetes: findings from the China acute myocardial infarction registry. *Cardiovasc Diabetol.* (2023) 22:165. doi: 10.1186/s12933-023-01868-7

4. Johnson AE, Bulgarelli L, Shen L, Gayles A, Shammout A, Horng S, et al. MIMIC-IV, a freely accessible electronic health record dataset. *Sci Data.* (2023) 10:1. doi: 10.1038/s41597-023-02136-9

5. Wu WT, Li YJ, Feng AZ, Li L, Huang T, Xu AD, et al. Data mining in clinical big data: the frequently used databases, steps, and methodological models. *Mil Med Res.* (2021) 8:44. doi: 10.1186/s40779-021-00338-z

6. He HM, Zheng SW, Xie YY, Wang Z, Jiao SQ, Yang FR, et al. Simultaneous assessment of stress hyperglycemia ratio and glycemic variability to predict mortality in patients with coronary artery disease: a retrospective cohort study from the MIMIC-IV database. *Cardiovasc Diabetol.* (2024) 23:61. doi: 10.1186/s12933-024-02146-w

7. Liu J, Zhou Y, Huang H, Liu R, Kang Y, Zhu T, et al. Impact of stress hyperglycemia ratio on mortality in patients with critical acute myocardial infarction: insight from american MIMIC-IV and the chinese CIN-II study. *Cardiovasc Diabetol.* (2023) 22:281. doi: 10.1186/s12933-023-02012-1

8. Pan H, Xiong Y, Huang Y, Zhao J, Wan H. Association between stress hyperglycemia ratio with short-term and long-term mortality in critically ill patients with ischemic stroke. *Acta Diabetol.* (2024) 61:859–68. doi: 10.1007/s00592-024-02259-4

9. Bai W, Hao B, Xu L, Qin J, Xu W, Qin L. Frailty index based on laboratory tests improves prediction of short-and long-term mortality in patients with critical acute myocardial infarction. *Front Med.* (2022) 9:1070951. doi: 10.3389/fmed.2022.1070951

10. Lang L, Wang T, Xie L, Yang C, Skudder-Hill L, Jiang J, et al. An independently validated nomogram for individualised estimation of short-term mortality risk among patients with severe traumatic brain injury: a modelling analysis of the CENTER-TBI China Registry Study. *EClinicalMedicine.* (2023) 59:101975. doi: 10.1016/j.eclinm.2023.101975

11. Meyfroidt G, Bouzat P, Casaer MP, Chesnut R, Hamada SR, Helbok R, et al. Management of moderate to severe traumatic brain injury: an update for the intensivist. *Intensive Care Med.* (2022) 48:649–66. doi: 10.1007/s00134-022-06702-4

12. Rau CS, Wu SC, Chen YC, Chien PC, Hsieh HY, Kuo PJ, et al. Stress-induced hyperglycemia, but not diabetic hyperglycemia, is associated with higher mortality in patients with isolated moderate and severe traumatic brain injury: analysis of a propensity score-matched population. *Int J Environ Res Public Health.* (2017) 14:1340 doi: 10.3390/ijerph14111340

13. Yan F, Chen X, Quan X, Wang L, Wei X, Zhu J. Association between the stress hyperglycemia ratio and 28-day all-cause mortality in critically ill patients with sepsis: a retrospective cohort study and predictive model establishment based on machine learning. *Cardiovasc Diabetol.* (2024) 23:163. doi: 10.1186/s12933-024-02265-4

14. Liu Q, You N, Pan H, Shen Y, Lu P, Wang J, et al. Glycemic trajectories and treatment outcomes of patients with newly diagnosed tuberculosis: a prospective study in Eastern China. *Am J Respir Crit Care Med.* (2021) 204:347–56. doi: 10.1164/rccm.202007-2634OC

15. Zhang Y, Guo L, Zhu H, Jiang L, Xu L, Wang D, et al. Effects of the stress hyperglycemia ratio on long-term mortality in patients with triple-vessel disease and acute coronary syndrome. *Cardiovasc Diabetol.* (2024) 23:143. doi: 10.1186/s12933-024-02220-3

16. Li L, Ding L, Zheng L, Wu L, Hu Z, Liu L, et al. Relationship between stress hyperglycemia ratio and acute kidney injury in patients with congestive heart failure. *Cardiovasc Diabetol.* (2024) 23:29. doi: 10.1186/s12933-023-02105-x

17. Climent Biescas E, Rodríguez-Campello A, Jiménez-Balado J, Fernández Miró M, Jimenez-Conde J, Llauradó Cabot G, et al. Acute-to-chronic glycemic ratio as an outcome predictor in ischemic stroke in patients with and without diabetes mellitus. *Cardiovasc Diabetol.* (2024) 23:206. doi: 10.1186/s12933-024-02260-9

18. McCrimmon RJ. Consequences of recurrent hypoglycaemia on brain function in diabetes. *Diabetologia.* (2021) 64:971–7. doi: 10.1007/s00125-020-05369-0

19. Chun KH, Oh J, Lee CJ, Park JJ, Lee SE, Kim MS, et al. In-hospital glycemic variability and all-cause mortality among patients hospitalized for acute heart failure. *Cardiovasc Diabetol.* (2022) 21:291. doi: 10.1186/s12933-022-01720-4

20. Ding L, Zhang H, Dai C, Zhang A, Yu F, Mi L, et al. The prognostic value of the stress hyperglycemia ratio for all-cause and cardiovascular mortality in patients with diabetes or prediabetes: insights from NHANES 2005-2018. *Cardiovasc Diabetol.* (2024) 23:84. doi: 10.1186/s12933-024-02172-8

21. Wafa HA, Marshall I, Wolfe CD, Xie W, Johnson CO, Veltkamp R, et al. Burden of intracerebral haemorrhage in Europe: forecasting incidence and mortality between 2019 and 2050. *Lancet Reg Health Eur.* (2024) 38:100842. doi: 10.1016/j.lanepe.2024.100842

22. Garcia-Bonilla L, Shahanoor Z, Sciortino R, Nazarzoda O, Racchumi G, Iadecola C, et al. Analysis of brain and blood single-cell transcriptomics in acute and subacute phases after experimental stroke. *Nat Immunol.* (2024) 25:357–70. doi: 10.1038/s41590-023-01711-x

23. Olasveengen TM, Stocchetti N. Prehospital ventilation targets in severe traumatic brain injury. *Intensive Care Med.* (2023) 49:554–5. doi: 10.1007/s00134-023-07044-5

24. Teasdale G, Maas A, Lecky F, Manley G, Stocchetti N, Murray G. The Glasgow Coma Scale at 40 years: standing the test of time. *Lancet Neurol.* (2014) 13:844–54. doi: 10.1016/S1474-4422(14)70120-6

25. Oddo M, Taccone FS, Petrosino M, Badenes R, Blandino-Ortiz A, Bouzat P, et al. The Neurological Pupil index for outcome prognostication in people with acute brain injury (ORANGE): a prospective, observational, multicentre cohort study. *Lancet Neurol.* (2023) 22:925–33. doi: 10.1016/S1474-4422(23)00271-5

26. Gugger JJ, Sinha N, Huang Y, Walter AE, Lynch C, Kalyani P, et al. Structural brain network deviations predict recovery after traumatic brain injury. *Neuroimage Clin.* (2023) 38:103392. doi: 10.1016/j.nicl.2023.103392

27. Perkins GD, Callaway CW, Haywood K, Neumar RW, Lilja G, Rowland MJ, et al. Brain injury after cardiac arrest. *Lancet.* (2021) 398:1269–78. doi: 10.1016/S0140-6736(21)00953-3

28. Rzechorzek NM, Thrippleton MJ, Chappell FM, Mair G, Ercole A, Cabeleira M, et al. A daily temperature rhythm in the human brain predicts survival after brain injury. *Brain.* (2022) 145:2031–48. doi: 10.1093/brain/awab466

29. Langouche L, Vanhorebeek I, Van den Berghe G. Therapy insight: the effect of tight glycemic control in acute illness. *Nat Clin Pract Endocrinol Metab.* (2007) 3:270–8. doi: 10.1038/ncpendmet0426

30. Guo JY, Chou RH, Kuo CS, Chao TF, Wu CH, Tsai YL, et al. The paradox of the glycemic gap: Does relative hypoglycemia exist in critically ill patients? *Clin Nutr.* (2021) 40:4654–61. doi: 10.1016/j.clnu.2021.06.004

31. von Rauchhaupt E, Rodemer C, Kliemank E, Bulkescher R, Campos M, Kopf S, et al. Glucose load following prolonged fasting increases oxidative stress- linked response in individuals with diabetic complications. *Diabetes Care.* (2024) 47:1584–92. doi: 10.2337/dc24-0209

32. Wei Y, Miao Q, Zhang Q, Mao S, Li M, Xu X, et al. Aerobic glycolysis is the predominant means of glucose metabolism in neuronal somata, which protects against oxidative damage. *Nat Neurosci.* (2023) 26:2081–9. doi: 10.1038/s41593-023-01476-4

33. Banks WA, Reed MJ, Logsdon AF, Rhea EM, Erickson MA. Healthy aging and the blood-brain barrier. *Nat Aging.* (2021) 1:243–54. doi: 10.1038/s43587-021-00043-5

34. Fan S, Xu Y, Lu Y, Jiang Z, Li H, Morrill JC, et al. A neural basis for brain leptin action on reducing type 1 diabetic hyperglycemia. *Nat Commun.* (2021) 12:2662. doi: 10.1038/s41467-021-22940-4

35. Dienel GA. Brain glucose metabolism: integration of energetics with function. *Physiol Rev.* (2019) 99:949–1045. doi: 10.1152/physrev.00062.2017

36. Liu L, Huang Z, Zhang J, Wang M, Yue T, Wang W, et al. Hypothalamus-sympathetic-liver axis mediates the early phase of stress-induced hyperglycemia in the male mice. *Nat Commun.* (2024) 15:8632. doi: 10.1038/s41467-024-52815-3

37. Schwartz MW, Krinsley JS, Faber CL, Hirsch IB, Brownlee M. Brain glucose sensing and the problem of relative hypoglycemia. *Diabetes Care.* (2023) 46:237–44. doi: 10.2337/dc22-1445

38. Sarkar R, Martin C, Mattie H, Gichoya JW, Stone DJ, Celi LA. Performance of intensive care unit severity scoring systems across different ethnicities in the USA: a retrospective observational study. *Lancet Digit Health.* (2021) 3:e241–9. doi: 10.1016/S2589-7500(21)00022-4

frontiers | Frontiers in Neurology

TYPE Original Research
PUBLISHED 08 May 2025
DOI 10.3389/fneur.2025.1542889

OPEN ACCESS

EDITED BY
Haipeng Liu,
Coventry University, United Kingdom

REVIEWED BY
Wang Miao,
First Affiliated Hospital of Zhengzhou University, China
Yun-Xiang Zhou,
The First Affiliated Hospital of Shaoyang University, China
Sushma Jaiswal,
Guru Ghasidas Vishwavidyalaya, India
Muhana Fawwazy Ilyas,
Sebelas Maret University, Indonesia
Adalet Göçmen,
Harran University, Türkiye

*CORRESPONDENCE
Chunyan Lei
leichunyan328@163.com

RECEIVED 25 February 2025
ACCEPTED 22 April 2025
PUBLISHED 08 May 2025

CITATION
Li Y, Chen K, Wang L, Zhao L, Lei C, Gu Y, Zhu X and Deng Q (2025) Values of lymphocyte-related ratios in predicting the clinical outcome of acute ischemic stroke patients receiving intravenous thrombolysis based on different etiologies.
Front. Neurol. 16:1542889.
doi: 10.3389/fneur.2025.1542889

Values of lymphocyte-related ratios in predicting the clinical outcome of acute ischemic stroke patients receiving intravenous thrombolysis based on different etiologies

Yongyu Li, Keyang Chen, Lu Wang, Linhu Zhao, Chunyan Lei*, Yu Gu, Xiaoyan Zhu and Qionghua Deng

The First Department of Neurology, First Affiliated Hospital of Kunming Medical University, Kunming, Yunnan, China

Background: While neutrophil-to-lymphocyte ratio (NLR), lymphocyte-to-monocyte ratio (LMR), and platelet-to-lymphocyte ratio (PLR) have been associated with acute ischemic stroke (AIS) outcomes, their differential predictive value across etiological subtypes (TOAST classification) in thrombolysis-treated patients remains underexplored.

Methods: In this retrospective cohort study, we analyzed 381 AIS patients receiving intravenous thrombolysis. Hematological indices were calculated from pre-thrombolysis. Using multivariable logistic regression adjusted for age, NIHSS, and comorbidities, we assessed associations between baseline ratios and 90-day unfavorable outcomes (mRS 3–6). Receiver operating characteristic (ROC) analysis was used to determine optimal cutoffs stratified by TOAST subtypes.

Results: A total of 381 patients were included in the study. NLR showed superior predictive performance: large-artery atherosclerosis: AUC = 0.702 (aOR = 1.35, 95%CI = 1.14–1.61, p = 0.001), small-artery occlusion: AUC = 0.750 (aOR = 1.51, 95%CI = 1.08–2.10, p = 0.015), cardioembolic stroke: AUC = 0.679 (aOR = 1.82, 95%CI = 1.07–3.10, p = 0.028). LMR showed predictive value only in large-artery atherosclerosis (AUC = 0.632, p = 0.004). Optimal NLR cutoffs: 3.19 (large-artery), 3.94 (small-artery), 3.17 (cardioembolic stroke).

Conclusion: NLR emerged as a robust, subtype-specific predictor of post-thrombolysis outcomes, particularly in atherosclerotic stroke variants. These findings supported NLR's clinical utility for risk stratification in thrombolysis-eligible AIS patients.

KEYWORDS

stroke, etiology, thrombolysis, neutrophil, lymphocyte, outcome

Introduction

Stroke was the second leading cause of mortality globally, with acute ischemic stroke (AIS) representing up to 84% of all stroke types (1). AIS resulted in a high incidence of disability, with a prevalence of 20 to 25%, and a mortality rate of 10% (2). These figures impose substantial burdens on society and families. The prognosis of each type of AIS was associated with underlying etiology. The current internationally recognized classification system for AIS based on etiology was derived from a multicenter clinical trial called the Trial of Org 10,172 in Acute Stroke Treatment (TOAST) (3).

A meta-analysis of the literature confirmed that intravenous thrombolysis was the most effective treatment for AIS, which significantly reduced disability and mortality rates (4). Alteplase (rt-PA) has been demonstrated to be an efficacious and widely utilized thrombolytic agent. However, administration of rt-PA is within 4.5 h of symptom onset (5), and its efficacy varies according to the etiology of AIS (4, 6). The rapid and objective identification of ineffective thrombolysis or potential side effects is of the utmost importance for the long-term quality of life of patients.

Animal studies indicate that humoral factors released by dying neurons may trigger inflammation in the injured cerebral area, which may result in the recruitment of peripheral immune cells, including neutrophils, lymphocytes, and monocytes, into the infarcted tissue. This may exacerbate neuronal damage and result in disruption of the blood–brain barrier (7, 8). Neutrophils are the initial inflammatory cells to respond following the onset of AIS, with an increase occurring within 30 min of the initial event, followed by monocytes and lymphocytes (9). These inflammatory responses product a considerable number of inflammatory factors, including interleukins, nitric oxide, interferon gamma, and tumor necrosis factor-alpha (8). The elevated levels of inflammatory factors may induce oxidative stress reactions, which can damage brain tissue cells and result in neurological deficits. The level of platelet monocyte aggregation in patients with a stroke is markedly elevated (10). Platelets, together with these inflammatory cells, participate in the inflammatory development process of cerebral infarction, which lead to microvascular occlusion and exacerbate brain damage (11).

Previous study indicated that higher circulating white cell counts and neutrophil to lymphocyte ratio (NLR) were associated with symptomatic intracerebral hemorrhage (sICH) and poor prognosis in AIS patients receiving intravenous thrombolysis. In addition, some studies had also shown that the NLR, lymphocyte to monocyte ratio (LMR), and platelet to lymphocyte ratio (PLR) at admission were associated with neurological deterioration during hospitalization in AIS patients receiving intravenous thrombolysis treatment (12–14). A recent meta-analysis confirmed a higher level of NLR was associated with adverse outcomes 3 months after thrombolytic therapy in AIS patients (15).

NLR, LMR, and PLR had become effective indicators for evaluating the prognosis of AIS. However, the predictive ability of these inflammatory cell ratios for the prognosis of AIS patients with different etiologies receiving thrombolytic therapy was not clear. This study provided the first direct comparison of NLR, LMR and PLR in functional outcome prediction using standardized modified Rankin Scale (mRS) scores. Values exceeding these cutoffs may justify intensified monitoring or adjuvant anti-inflammatory therapies in specific TOAST subtypes, particularly when combined with higher NIHSS scores or atrial fibrillation.

Methods

Study population

This study was a single-center retrospective cohort study. Patients within 4.5 h of AIS onset were enrolled after being admitted to the First Affiliated Hospital of Kunming Medical University, Kunming, China from September 2018 to September 2023, who received intravenous rt-PA treatment. The study protocol was approved by the Scientific Research Department of the First Affiliated Hospital of Kunming Medical University and was designed in accordance with local ethics criteria for human research.

Inclusion criteria: (1) Age ≥18 years old; (2) Onset to treatment time within 4.5 h; (3) Patients receiving rt-PA intravenous treatment. Exclusion criteria: (1) Patients with inflammatory lesions or infectious diseases before admission. The diagnostic criteria for infection require meeting at least two of the following four parameters: (a) Temperature >38°C or <36°C; (b) Heart rate >90 beats per minute; (c) Respiratory rate >20 breaths per minute or hyperventilation ($PaCO_2$ < 32 mmHg); (d) White blood cell count >12 × 10^9/L or <4 × 10^9/L (or immature granulocytes >10%) (16). (2) Patients with absolute contraindications to intravenous thrombolytic therapy; (3) Patients who had not undergone CT or MRI examinations after admission; (4) Those who were unable to get data.

Data collection

At admission, demographic characteristics, vascular risk factors, past medical history, vital signs, laboratory indicators, thrombolytic therapy-related indicators and imaging indicators before thrombolysis were obtained. National Institutes of Health Stroke Scale (NIHSS) was assessed before thrombolysis. All patients underwent brain Computed Tomography (CT) or Magnetic Resonance Imaging (MRI) scan to exclude intracranial hemorrhage at admission and then received thrombolytic therapy. All patients underwent multimodal CT, MRI, pulmonary CT, carotid ultrasound and echocardiography evaluation to assess etiology, and infarct location.

The etiology classification of all included patients was evaluated by two professional neurologists. All patients underwent standardized etiological workup per the TOAST criteria. Specifically, suspected CE strokes received: ≥24-h cardiac telemetry; transthoracic echocardiography when thrombus was suspected. According to the TOAST criteria to determine the etiology classification of AIS (3). TOAST categorized AIS into five subtypes: large-artery atherosclerosis, cardioembolism, small-vessel occlusion, other determined etiology, and undetermined etiology, and each subtype had specific diagnostic criteria (3).

Treatment method

Intravenous rt-PA treatment (dosage: 0.9 mg per kg body weight, maximum dose of 90 mg, 10% of the dose given at the first 1 min, the remaining 90% administered as a continuous intravenous infusion within an hour), during thrombolysis and 24 h after intravenous thrombolysis, and no antiplatelet therapy within 24 h after intravenous thrombolysis treatment.

Neuroimaging assessment

According to the European Cooperative Acute Stroke Study (ECASS) II criteria (17), sICH was defined as any intracranial bleeding within 7 days after thrombolysis that led to clinical deterioration or an increase in the NIHSS score by more than 4 points in any intracranial location.

Clinical outcomes

Long-term outcomes were assessed using mRS, with telephone follow-ups conducted at 90 days post-onset. Each patient's mRS score was evaluated by two experienced neurologists without knowledge of the patients' baseline data. An mRS score of 0–2 at 90 days was classified as a favorable functional outcome, while a score of 3–6 at 90 days was classified as an unfavorable functional outcome.

Statistical analysis

All statistical analyses were performed using the Windows version of IBM SPSS Statistics 26 and GraphPad Prism 10.1.2 statistical package. Count data were presented as percentages, normally distributed data were presented as mean ± standard deviation, and non-normally distributed data were presented as median and interquartile range (IQR), i.e., the 25th to 75th percentile. Chi-square test was used to compare categorical variables among groups. For continuous variables, comparison of variance between groups was used for normally distributed data, and the Mann–Whitney U test was used for non-normally distributed data. According to the expected statistical analysis methods, the baseline characteristics of various types of AIS patients included in the study were firstly analyzed. Then the 90-day mRS scores and sICH were grouped and analyzed for their demographic and clinical characteristics. Predictive factors for the prognosis of each subtype of AIS were analyzed using binary logistic regression analysis, with Odds Ratio (OR) and 95% Confidence Interval (CI) obtained from univariate model regression analysis. Variables with a p value < 0.05 in the univariate model were selected as covariates for the multivariate model to obtain adjusted Odds Ratio (aOR) and 95%CI. Finally, receiver operating characteristic (ROC) curve analysis was conducted for variables demonstrating statistical significance ($p < 0.05$) in the multivariable logistic regression model, using the ROC curves to determine the Area Under Curve (AUC), sensitivity and specificity of the prediction, the best cutoff value for the ratio of inflammatory cells was determined using AUC and 95% confidence intervals, with an AUC of 0.70 or higher considered to indicate good predictive ability (18). A two-sided $p < 0.05$ was considered statistically significant.

Results

Baseline characteristics

From September 2018 to September 2023, of the 473 patients enrolled in our study, 34 (0.7%) patients were excluded because data were lost owing to update in the record system; 21 (4.4%) patients received endovascular intervention after thrombolytic therapy; 9 (1.9%) patients had severe infectious diseases before admission. Finally, 409 patients were included. At the follow-up period of 3 months, a total of 28 (5.9%) patients were lost to follow-up. Finally, 381 patients who met the criteria were included in this study (Figure 1).

Among the 381 included patients, the most common etiology was large-artery atherosclerosis ($n = 158$, 41.5%), followed by small-artery occlusion ($n = 72$, 18.9%), cardioembolism ($n = 62$, 16.3%), other determined etiology ($n = 35$, 9.2%), and undetermined etiology ($n = 54$, 14.2%). The demographic and clinical characteristics were compared according to TOAST classification (Table 1). The age was higher in cardioembolism, while younger in undetermined etiology ($p < 0.001$). The cardioembolism had higher proportions of history of atrial fibrillation ($p < 0.001$) and coronary heart disease ($p = 0.021$), and also had a higher NIHSS score ($p < 0.001$) on admission compared to other etiologies. Moreover, cardioembolism showed lower LMR values compared to other etiologies ($p = 0.046$). Regarding the location of infarction, large-artery atherosclerosis stroke was more likely to occur in the anterior circulation, while small-artery occlusion stroke was most commonly observed in the posterior circulation. The cardioembolism was more likely to lead to infarction involving both anterior and posterior circulations ($p < 0.001$).

In terms of clinical outcomes, large-artery atherosclerosis stroke (7.6%) had the highest proportion of in-hospital mortality, followed by cardioembolism (4.8%; $p = 0.002$). The cardioembolism was more likely to result in hemorrhagic transformation compared to other etiologies ($p < 0.001$). Among patients with favorable functional outcomes, the small-artery occlusion stroke had the highest proportion (84.7%; $p < 0.001$). The cardioembolism had the highest proportion of unfavorable functional outcomes (53.2%; $p < 0.001$).

Lymphocyte-related ratios and sICH

The demographic and clinical characteristics were compared in positive sICH group and negative sICH group (Table 2). The patients with positive sICH had advanced age ($p = 0.009$) and a higher rate of history of atrial fibrillation ($p < 0.001$), and a higher baseline NIHSS score [14.0 (9.0–17.8) vs. 5.0 (3.0–9.0); $p < 0.001$]. Anterior circulation infarcts or anterior–posterior circulation infarcts were more likely to develop sICH compared to posterior circulation infarcts ($p < 0.001$). For etiologies, cardioembolism was more likely to develop sICH compared to other etiologies of stroke ($p < 0.001$). However, there was no statistical difference between lymphocyte-related ratios and sICH.

90-day clinical outcomes

Comparison of the clinical characteristics and lymphocyte ratio between AIS patients with favorable functional outcome and those with unfavorable functional outcome at 90 days (Table 3). Male patients were more likely to have favorable functional outcome at 90 days after onset ($p = 0.014$). The patients in unfavorable functional outcome group were associated with advanced age ($p < 0.001$), a history of atrial fibrillation ($p < 0.001$), and higher NIHSS scores at admission [9.0 (6.0–14.0) vs. 4.0 (2.0–6.0); $p < 0.001$]. For the laboratory results, higher neutrophil counts [6.3 (4.6–8.5) vs. 4.5 (3.4–6.1); $p < 0.001$] and NLR [4.0 (2.7–6.3) vs. 2.4 (1.8–3.7);

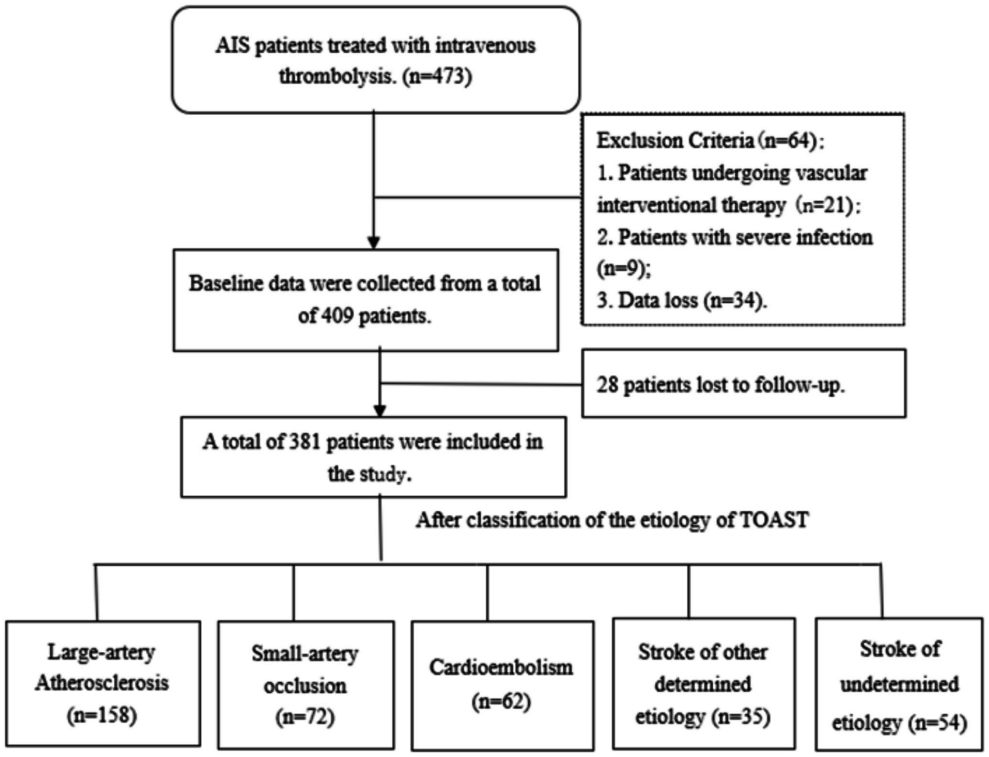

FIGURE 1
Flowchart of patient recruitment for inclusion in the study cohort.

$p < 0.001$], lower lymphocyte counts [1.6 (1.1–2.1) vs. 1.7 (1.3–2.3); $p = 0.005$] and LMR [3.4 (2.2–4.5) vs. 3.8 (2.9–5.0); $p < 0.001$], and shorter APTT [33.5 (31.3–37.2) vs. 35.0 (33.2–38.6); $p = 0.003$] were more likely to result in unfavorable functional outcome at 90 days. Additionally, hemorrhage transformation ($p < 0.001$), anterior circulation stroke or anterior–posterior circulation stroke ($p = 0.001$), and large-artery atherosclerosis stroke or cardioembolic stroke ($p < 0.001$) were also more likely to result in an unfavorable functional outcome. In Figure 2, we graphically analyzed the influence of NLR on the 90-day mRS scores for TOAST subtypes, and found that higher NLR was associated with poor functional outcome patients with large-artery atherosclerosis stroke ($p < 0.0001$), small-artery occlusion stroke ($p < 0.01$), and cardioembolic stroke ($p < 0.01$).

Univariable logistic regression analysis of 90-day clinical outcomes

Univariate logistic regression analysis indicated that male (OR, 0.585; 95%CI, 0.381–0.898; $p = 0.014$), age (OR, 1.032; 95%CI, 1.015–1.050; $p < 0.001$), history of atrial fibrillation (OR, 4.294; 95%CI, 2.390–7.715; $p < 0.001$), hemorrhage transformation (OR, 4.866; 95%CI, 2.331–10.159; $p < 0.001$), and baseline NIHSS score (OR, 1.291; 95%CI, 1.215–1.372; $p < 0.001$) were associated with adverse functional outcome at 90 days (Table 4). When using posterior circulation infarction as the reference, both anterior circulation infarction (OR, 2.189; 95%CI, 1.361–3.518; $p = 0.001$) and anterior–posterior circulation infarction (OR, 3.800; 95%CI, 1.741–8.292; $p = 0.001$) were associated with unfavorable functional outcome. In the TOAST classification, when using small-artery occlusion as the reference, large-artery atherosclerosis (OR, 5.011; 95%CI, 2.454–10.232; $p < 0.001$) and cardioembolic (OR, 6.310; 95%CI, 2.799–14.229; $p < 0.001$) strokes were associated with unfavorable functional outcome. Additionally, in the laboratory results, neutrophil count (OR, 1.413; 95%CI, 1.275–1.565; $p < 0.001$), lymphocyte count (OR, 0.684; 95%CI, 0.522–0.898; $p = 0.006$), monocyte count (OR, 3.423; 95%CI, 1.357–8.634; $p = 0.009$), NLR (OR, 1.217; 95%CI, 1.127–1.313; $p < 0.001$), and LMR (OR, 0.784; 95%CI, 0.691–0.890; $p < 0.001$) were associated with adverse functional outcome.

Multivariable logistic regression analysis of 90-day clinical outcomes

After adjusting for sex, age, history of atrial fibrillation, hemorrhage transformation, infarction location, and admission NIHSS score as confounding factors, the multivariable model (Table 5) suggested that NLR before thrombolysis (aOR, 1.261; 95% CI, 1.148–1.384; $p < 0.001$) and LMR (aOR, 0.735; 95% CI, 0.622–0.868; $p < 0.001$) were independent predictors of unfavorable functional outcome in AIS patients after intravenous thrombolysis treatment. Among them, NLR could be regarded as an independent predictor of poor functional outcome in patients with large-artery atherosclerotic stroke (aOR, 1.354; 95% CI, 1.142–1.606; $p = 0.001$), small-artery occlusion stroke (aOR, 1.505; 95% CI, 1.081–2.096; $p = 0.015$), and cardioembolic stroke (aOR, 1.871; 95% CI, 1.065–3.101; $p = 0.028$). LMR was only an independent predictor of unfavorable functional

TABLE 1 Baseline characteristics of AIS patients according to TOAST classification subtypes.

Variable	Large-artery atherosclerosis	Small-artery occlusion	Cardioembolism	Stroke of other determined etiology	Stroke of undetermined etiology	*p*-value
	(*n* = 158)	(*n* = 72)	(*n* = 62)	(*n* = 35)	(*n* = 54)	
Demography						
Male (%)	108 (68.4)	42 (58.3)	32 (51.6)	25 (71.4)	35 (64.8)	0.125
Age [Y, *M* (P_{25}, P_{75})]	69.5 (58.8–78.0)	65.0 (54.0–74.8)	75.5 (66.0–80.0)	68.0 (53.0–75.0)	63.5 (51.8–72.3)	<0.001
Risk factors (%)						
Hypertension	104 (65.8)	43 (59.7)	40 (64.5)	19 (54.3)	29 (53.7)	0.443
Diabetes	39 (24.7)	23 (31.9)	13 (21.0)	6 (17.1)	9 (16.7)	0.252
Hyperlipidemia	40 (25.3)	22 (30.6)	15 (24.2)	8 (22.9)	19 (35.2)	0.551
Atrial fibrillation	11 (7.0)	0 (0.0)	48 (77.4)	0 (0.0)	1 (1.9)	<0.001
Coronary heart disease	24 (15.2)	5 (6.9)	12 (19.4)	5 (14.3)	1 (1.9)	0.021
Previous TIA	7 (4.4)	2 (2.8)	4 (6.5)	2 (5.7)	0 (0.0)	0.210
Previous stroke	35 (22.2)	12 (16.7)	12 (19.4)	7 (20.0)	7 (13.0)	0.634
Current smoking	55 (34.8)	21 (29.2)	14 (22.6)	13 (37.1)	22 (40.7)	0.240
SBP (mmHg, $\bar{X} \pm S$)	143.7 ± 20.9	145.8 ± 17.0	145.7 ± 19.4	142.4 ± 17.7	147.4 ± 22.5	0.701
Admission NIHSSS [*M* (P_{25}, P_{75})]	6.0 (3.0–10.0)	4.0 (2.3–6.0)	8.5 (4.8–14.0)	4.0 (3.0–7.0)	5.0 (3.0–8.0)	<0.001
OTT [h, *M* (P_{25}, P_{75})]	2.8 (2.0–3.5)	2.8 (2.0–3.9)	3.0 (2.2–3.8)	3.0 (1.9–3.5)	3.0 (2.4–3.8)	0.411
OBD [h, *M* (P_{25}, P_{75})]	2.0 (1.0–2.5)	2.0 (1.0–3.0)	1.8 (1.0–2.7)	1.5 (1.0–2.9)	2.9 (1.5–2.7)	0.297
Lab results						
Neutrophil counts [$\times 10^9$/L, *M* (P_{25}, P_{75})]	5.1 (3.8–6.7)	4.2 (3.4–6.1)	5.4 (3.9–7.3)	5.5 (4.1–7.3)	5.3 (3.4–7.5)	0.124
Lymphocyte counts [$\times 10^9$/L, *M* (P_{25}, P_{75})]	1.6 (1.2–2.3)	1.7 (1.2–2.2)	1.6 (1.1–2.0)	1.9 (1.5–2.4)	1.7 (1.1–2.3)	0.097
Monocyte counts [$\times 10^9$/L, *M* (P_{25}, P_{75})]	0.4 (0.4–0.6)	0.4 (0.3–0.6)	0.5 (0.3–0.6)	0.5 (0.3–0.7)	0.5 (0.4–0.6)	0.304
Platelet counts [$\times 10^9$/L, *M* (P_{25}, P_{75})]	209.0 (165.8–255.0)	210.0 (166.0–238.0)	191.0 (152.8–228.0)	206.0 (182.0–242.0)	192.5 (171.3–218.5)	0.171
NLR [*M* (P_{25}, P_{75})]	3.0 (2.0–5.1)	2.6 (1.8–4.1)	3.3 (2.4–5.3)	2.9 (1.7–4.6)	3.1 (2.0–6.2)	0.241
LMR [*M* (P_{25}, P_{75})]	3.9 (2.8–4.9)	3.6 (2.7–5.8)	3.4 (2.4–4.1)	4.4 (2.9–5.8)	3.6 (2.5–4.6)	0.046
PLR [*M* (P_{25}, P_{75})]	437.9 (325.9–647.0)	447.3 (336.8–741.1)	398.1 (289.8–507.0)	394.1 (296.8–590.2)	404.5 (289.9–530.4)	0.101
APTT [s, *M* (P_{25}, P_{75})]	34.4 (32.1–37.9)	34.9 (33.0–38.5)	33.9 (30.9–37.1)	34.1 (31.5–37.8)	35.5 (31.3–39.1)	0.379
PT [s, *M* (P_{25}, P_{75})]	13.1 (12.6–13.8)	13.2 (12.4–13.8)	13.1 (12.7–13.8)	13.1 (12.6–13.9)	13.4 (12.5–13.8)	0.966
INR [*M* (P_{25}, P_{75})]	1.0 (1.0–1.1)	1.0 (1.0–1.1)	1.0 (1.0–1.1)	1.0 (1.0–1.1)	1.0 (1.0–1.1)	0.901
Blood glucose [mmol/L, *M* (P_{25}, P_{75})]	7.2 (6.2–9.3)	6.9 (5.9–8.9)	7.0 (6.3–7.7)	7.1 (6.0–9.6)	6.8 (6.0–8.1)	0.382
LDL (mmol/L, $\overline{X} \pm S$)	2.8 ± 0.9	2.6 ± 0.8	2.6 ± 0.9	2.8 ± 1.0	2.7 ± 0.7	0.639

(Continued)

TABLE 1 (Continued)

Variable	Large-artery atherosclerosis	Small-artery occlusion	Cardioembolism	Stroke of other determined etiology	Stroke of undetermined etiology	*p*-value
	(*n* = 158)	(*n* = 72)	(*n* = 62)	(*n* = 35)	(*n* = 54)	
Hemorrhage transformation (%)	17 (10.8)	1 (1.4)	17 (27.4)	0 (0.0)	3 (5.6)	<0.001
SICH	6 (3.8)	0 (0.0)	9 (14.5)	0 (0.0)	1 (1.9)	
aSICH	11 (7.0)	1 (1.4)	8 (12.9)	0 (0.0)	2 (3.7)	
mRS score of 0–2 (%)	83 (52.5)	61 (84.7)	29 (46.8)	27 (77.1)	39 (72.2)	<0.001
mRS score of 3–6 (%)	75 (47.5)	11 (15.3)	33 (53.2)	8 (22.9)	15 (27.8)	<0.001
Death in hospital (%)	12 (7.6)	0 (0.0)	3 (4.8)	0 (0.0)	0 (0.0)	0.002
Infarction location (%)						<0.001
Anterior circulation	110 (69.6)	20 (27.8)	33 (53.2)	20 (57.1)	28 (51.9)	
Posterior circulation	44 (27.8)	51 (70.8)	12 (19.4)	7 (20.0)	22 (40.7)	
Anterior–posterior circulation	4 (2.5)	1 (1.4)	17 (27.4)	8 (22.9)	4 (7.4)	

outcome in patients with large-artery atherosclerosis stroke (aOR, 0.693; 95% CI, 0.541–0.886; $p = 0.004$).

Predictive ability of NLR and LMR

The abilities of NLR and LMR to predict 90-day unfavorable functional outcome according to TOAST subtypes are summarized in Table 6, and presented the ROC curves with good results in Figure 3. The ROC values of NLR and LMR were well differentiated among the TOAST subtypes. Table 6 and Figure 3 indicated that the AUC values of NLR for all AIS patients, large-artery atherosclerosis stroke, small-artery occlusion stroke and cardioembolic stroke were 0.701, 0.702, 0.750, and 0.679 respectively, the sensitivities were 0.662, 0.653, 0.727 and 0.727 respectively, the specificities were 0.707, 0.733, 0.787 and 0.690, respectively. The cutoff values of NLR for predicting unfavorable functional outcome in all AIS patients, large-artery atherosclerosis stroke, small-artery occlusion stroke and cardioembolic stroke were 3.281, 3.193, 3.937 and 3.172, respectively. LMR had poor predictive ability for unfavorable functional outcome in large-artery atherosclerosis stroke with an AUC of 0.591, and its predictive ability for other subtypes were not statistically significant.

Discussion

Our study involving 381 AIS patients underwent intravenous thrombolysis, there was significant differences in the clinical characteristics of AIS patients receiving intravenous thrombolysis based on TOAST classification. Admission higher NLR and lower LMR as peripheral inflammatory markers were associated with unfavorable functional outcomes at 90 days, but not with sICH. Otherwise, based on TOAST classification, NLR was associated with unfavorable functional outcomes in large-artery atherosclerosis stroke, small-artery occlusion stroke, and cardioembolic stroke, while LMR was only associated with unfavorable functional outcome in large-artery atherosclerosis stroke. The accuracy of NLR in predicting unfavorable functional outcomes in large-artery atherosclerotic stroke and small-artery occlusive stroke were good, but its accuracy in predicting prognosis for other etiologies were poor.

Previous studies have shown that a high NLR combined with a low LMR measured 24 h after thrombolysis was related with poor functional outcome at 90 days in AIS patients (19). A recent meta-analysis also suggested that a higher NLR was associated with poor functional outcome at 3 months, however, the time at which NLR was obtained was not specified before or after thrombolysis (15). Another large retrospective study of patients undergoing mechanical thrombectomy showed that the admission NLR was associated with 3-month mortality and sICH in patients with large-artery atherosclerosis stroke (20). Within 30 min of onset, the inflammation began to respond and neutrophils increased in circulating (9). A large prospective study suggested that elevated levels of plasma neutrophil elastase obtained upon admission were associated with adverse neurological outcomes at 3 months after receiving intravenous thrombolysis for AIS, which was released by neutrophils (21). Intravenous thrombolysis therapy could partially restore blood flow in ischemic penumbra and minimized brain tissue damage, while the immune system may still maintain an inflammatory response after vascular recanalization (22). The interaction between thrombolysis and inflammatory mechanisms drove the progression of neural damage in AIS (23). These lymphocyte-related ratios obtained before or after thrombolysis may be associated with adverse functional outcomes, and differed in their relationship with different etiologies of stroke. In our study, the baseline characteristics and prognostic factors of AIS with different etiologies showed significant differences. Rapid evaluation of prognosis of various etiological AIS before intravenous thrombolysis can provide clinical decision-making guidance.

Neutrophils played a role in releasing cytokines and inflammatory mediators, infiltrating and releasing oxygen free radicals, expressing elastase to disrupt the blood–brain barrier, and causing capillary stasis and neuronal ischemia and hypoxia, which resulted in neurological

TABLE 2 Analysis of symptomatic intracerebral hemorrhage.

Variable	SICH		*p*-value
	Positive (n = 16)	Negative (n = 365)	
Demography			
Male (%)	8 (50.0)	234 (64.1)	0.251
Age [Y, M (P_{25}, P_{75})]	74.5 (71.0–84)	68.0 (57.0–77.0)	0.009
Risk factors (%)			
Hypertension	9 (56.3)	226 (61.9)	0.648
Diabetes	5 (31.3)	85 (23.3)	0.665
Hyperlipidemia	4 (25.0)	100 (27.4)	0.833
Atrial fibrillation	9 (56.3)	51 (14.0)	<0.001
Coronary heart disease	2 (12.5)	45 (12.3)	0.984
Previous TIA	0 (0.0)	15 (4.1)	0.865
Previous stroke	3 (18.8)	70 (19.2)	0.966
Current smoking	1 (6.3)	124 (34.0)	0.021
SBP (mmHg, $\bar{x} \pm s$)	153.5 ± 28.0	144.5 ± 19.4	0.219
Admission NIHSSS [M (P_{25}, P_{75})]	14.0 (9.0–17.8)	5.0 (3.0–9.0)	0.001
OTT [h, M(P_{25},P_{75})]	2.3 (1.8–3.2)	3.0 (2.0–3.6)	0.168
Lab results			
Neutrophil counts [×10^9/L, M (P_{25}, P_{75})]	6.2 (4.1–7.3)	5.0 (3.7–6.7)	0.143
Lymphocyte counts [×10^9/L, M (P_{25}, P_{75})]	1.8 (1.1–2.2)	1.6 (1.2–2.2)	0.878
Monocyte counts [×10^9/L, M (P_{25}, P_{75})]	0.5 (0.3–0.6)	0.5 (0.3–0.6)	0.786
Platelet counts [×10^9/L, M (P_{25}, P_{75})]	170.5 (153.5–226.3)	203 (167.5–241.0)	0.116
NLR [M (P_{25}, P_{75})]	3.2 (2.0–6.7)	3.0 (2.0–4.9)	0.526
LMR [M (P_{25}, P_{75})]	4.1 (2.8–5.3)	3.7 (2.7–4.9)	0.592
PLR [M (P_{25}, P_{75})]	389.9 (298.3–491.2)	430.1 (322.5–642.1)	0.426
APTT [s, M (P_{25}, P_{75})]	34.0 (32.1–37.7)	34.6 (31.9–38.2)	0.944
PT [s, M (P_{25}, P_{75})]	13.2 (12.6–13.6)	13.2 (12.6–13.8)	0.674
INR [M (P_{25}, P_{75})]	1.0 (1.0–1.1)	1.0 (1.0–1.1)	0.393
Blood glucose [mmol/L, M (P_{25}, P_{75})]	6.9 (5.9–7.9)	7.0 (6.1–8.8)	0.570
LDL (mmol/L, $\bar{x} \pm s$)	2.7 ± 0.9	2.7 ± 0.9	0.863
Infarction location (%)			0.001
Anterior circulation	14 (87.5)	197 (54.0)	
Posterior circulation	0 (0.0)	136 (37.3)	
Anterior–posterior circulation	2 (12.5)	32 (8.8)	
TOAST classification (%)			<0.001
Large-artery Atherosclerosis	6 (37.5)	152 (41.6)	
Small-artery occlusion	0 (0.0)	72 (19.7)	
Cardioembolism	9 (56.3)	53 (14.5)	
Other determined etiology	0 (0.0)	35 (9.6)	
Undetermined etiology	1 (6.3)	53 (14.5)	

deterioration (11, 24, 25). Animal models of stroke suggested that the depletion of γδT cells had a damaging role post-stroke, meanwhile, CD8 + T cells aggregated in the necrotic area mediating cytotoxic reactions to disrupt the blood–brain barrier (11). Monocytes increased within hours after infarction, releasing deleterious inflammatory mediators that caused inflammation in the infarct area and promoted platelet-monocyte aggregate formation, which lead to thrombus formation and vascular occlusion (11, 26).

TABLE 3 Analysis of mRS scores at 90 days.

Variable	Neurological functional outcomes at 90 days		*p*-value
	mRS score of 0~2	mRS score of 3~6	
	(*n* = 239)	(*n* = 142)	
Demography			
Male (%)	163 (68.2)	79 (55.6)	0.014
Age [Y, *M* (P_{25}, P_{75})]	66.0 (54.0–75.0)	72.5 (61.8–80.0)	<0.001
Risk factors (%)			
Hypertension	142 (59.4)	93 (65.5)	0.238
Diabetes	58 (24.3)	32 (22.5)	0.700
Hyperlipidemia	67 (28.0)	37 (26.1)	0.675
Atrial fibrillation	20 (8.4)	40 (28.2)	<0.001
Coronary heart disease	32 (13.4)	15 (10.6)	0.417
Previous TIA	13 (5.4)	2 (1.4)	0.050
Previous stroke	40 (16.7)	33 (23.2)	0.119
Current smoking	87 (36.4)	38 (26.8)	0.053
SBP (mmHg,$\overline{X} \pm S$)	143.6 ± 19.9	146.9 ± 19.9	0.119
Admission NIHSSS [*M* (P_{25}, P_{75})]	4.0 (2.0–6.0)	9.0 (6.0–14.0)	<0.001
OTT [h, *M*(P_{25},P_{75})]	3.0 (2.0–3.6)	3.0 (2.2–3.5)	0.777
Lab results			
Neutrophil counts [×10^9/L, *M* (P_{25}, P_{75})]	4.5 (3.4–6.1)	6.3 (4.6–8.5)	<0.001
Lymphocyte counts [×10^9/L, *M* (P_{25}, P_{75})]	1.7 (1.3–2.3)	1.6 (1.1–2.1)	0.005
Monocyte counts [×10^9/L, *M* (P_{25}, P_{75})]	0.5 (0.3–0.6)	0.5 (0.4–0.6)	0.071
Platelet counts [×10^9/L, *M* (P_{25}, P_{75})]	201.0 (169.0–237.0)	155.0 (143.0–165.0)	0.795
NLR [*M* (P_{25}, P_{75})]	2.4 (1.8–3.7)	4.0 (2.7–6.3)	<0.001
LMR [*M* (P_{25}, P_{75})]	3.8 (2.9–5.0)	3.4 (2.2–4.5)	<0.001
PLR [*M* (P_{25}, P_{75})]	434.1 (333.3–643.6)	398.1 (287.6–620.0)	0.162
APTT [s, *M* (P_{25}, P_{75})]	35.0 (33.2–38.6)	33.5 (31.3–37.2)	0.003
PT [s, *M* (P_{25}, P_{75})]	13.2 (12.6–13.8)	13.2 (12.6–13.8)	0.974
INR [*M* (P_{25}, P_{75})]	1.0 (1.0–1.1)	1.0 (1.0–1.1)	0.702
Blood glucose [mmol/L, *M* (P_{25}, P_{75})]	6.9 (6.0–8.6)	7.2 (6.1–8.9)	0.27
LDL (mmol/L, $\overline{X} \pm S$)	2.7 ± 0.9	2.8 ± 0.9	0.215
Hemorrhage transformation (%)	11 (4.6)	27 (19.0)	<0.001
SICH	0 (0.0)	16 (11.3)	
aSICH	11 (4.6)	11 (7.7)	
Infarction location (%)			<0.001
Anterior circulation	122 (51.0)	89 (62.7)	
Posterior circulation	102 (42.7)	34 (23.9)	
Anterior–posterior circulation	15 (6.3)	19 (13.4)	
TOAST classification (%)			<0.001
Large-artery Atherosclerosis	83 (34.7)	75 (52.8)	
Small-artery occlusion	61 (25.5)	11 (7.7)	
Cardioembolism	29 (12.1)	33 (23.2)	
Other determined etiology	27 (11.3)	8 (5.6)	
Undetermined etiology	39 (16.3)	15 (10.6)	

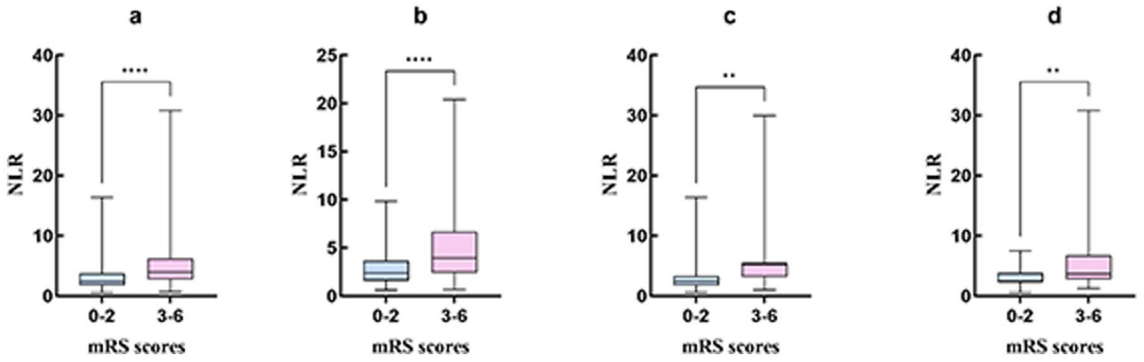

FIGURE 2
The graphical analysis of NLR and the 90-day mRS score of 3–6 for TOAST subtypes. **(A)** Included patients; **(B)** Large-artery atherosclerosis stroke; **(C)** Small-artery occlusion stroke; **(D)** Cardioembolic stroke. **$p < 0.01$; ****$p < 0.0001$. ***indicates statistical significance at $p < 0.001$.

Chronic inflammation of the arterial wall also played a key role in the occurrence and development of atherosclerosis (27). The plaque rupture was caused by infiltration of neutrophils and increased neutrophil–platelet adhesion. Animal studies have shown that neutrophils infiltrated into arterial plaques, leading to chronic inflammation; additionally, neutrophils may also damage plaques by releasing proteolytic enzymes. Even within the normal range of white blood cell count, a higher NLR was still associated with atherosclerotic events (27). This may be one of the mechanisms by which a higher admission NLR can predict unfavorable neurological outcome at 90 days in large-artery atherosclerosis stroke and small-artery occlusion stroke. Moreover, high admission NLR has been shown to have predictive value for cerebral infarction progression during hospitalization in large-artery atherosclerosis stroke (28). In cardioembolic stroke, although high NLR was an independent predictor for adverse neurological outcome at 90 days post onset, its predictive value was limited. Other studies have suggested that higher NLR within 24 h of admission was predictive of the hemorrhage transformation in patients with atrial fibrillation-related AIS, and the relationship with poor neurological outcomes remained to be further confirmed (29).

In large-artery atherosclerotic stroke, exposure of the lipid-rich necrotic core within unstable plaques triggered T-lymphocyte infiltration, while systemic inflammation exacerbated lymphocyte apoptosis, leading to a reduction in peripheral blood lymphocyte absolute counts and consequently elevating the NLR (11, 27). This pathophysiological cascade justified the higher NLR cutoff observed in large-artery atherosclerotic stroke patients. In cardioembolic stroke, tissue factors released from cardiac thrombi or injured myocardium activated thromboinflammatory cascades (11), the absence of chronic arterial inflammation resulted in a milder decline in lymphocytes and thus a lower NLR cutoff compared to large-artery atherosclerotic stroke. In small-artery occlusion stroke, chronic blood–brain barrier leakage promoted peripheral lymphocyte migration into brain parenchyma (11), which may stabilize peripheral lymphocyte counts despite localized neuroinflammation, this unique mechanism likely contributed to the distinctively higher NLR cutoff compared to other subtypes.

Although low LMR obtained within 24 h of admission was associated hemorrhage transformation in AIS patients (30). NLR, LMR, and PLR at admission were not found to be related to sICH in AIS patients after receiving intravenous thrombolysis treatment in our study, and similar findings had been reported in other studies (31).

Furthermore, platelet-monocyte activation in stroke patients was significantly higher than in healthy individuals, leading to spontaneous platelet aggregation. After stroke onset, platelets were activated and aggregated, which caused neuronal damage (22, 32). In cardioembolic stroke, platelets played a pivotal role in the pathophysiological processes of cerebral infarction through activation of the coagulation cascade and microcirculatory obstruction. These mechanisms exacerbated inflammatory responses and propagated thrombus formation, thereby hindering stroke recovery and contributing to adverse clinical outcomes (33), which may result higher PLR obtained before thrombolysis has been found to be associated with early neurological deterioration in patients with AIS (13). However, in our study, we did not find evidence that pre-thrombolysis PLR was associated with sICH or poor neurological outcomes. This may be related with the lack of significant early changes in platelets, and similar findings have been reported in other studies (34). The limited predictive utility of LMR and PLR may relate to monocyte/platelet dynamics being more influenced by acute-phase responses rather than chronic vascular inflammation. Future studies should evaluate serial measurements of these ratios in conjunction with advanced imaging biomarkers to clarify their pathophysiological roles.

There were several limitations to this study. Firstly, it was a study with a relatively small sample size from a single center, the predictive performance for large-artery atherosclerotic stroke marginally exceeded the predefined threshold (AUC = 0.70), suggesting suboptimal discriminative capacity. Especially with fewer cases in other determined etiological stroke, there were only 35 cases were included in the multiple regression analysis, which substantially diminishes the statistical power to detect outcomes within this subtype. Thus, multivariate regression models analyzing this subgroup may yield imprecise OR with disproportionately wide CI, reducing the reliability of predictive inferences. While this limitation inherently reflected fundamental challenges in current etiological research on AIS, it simultaneously delineates actionable pathways for future investigations. Furthermore, establishing multicenter collaborative cohorts may prove particularly valuable

TABLE 4 Univariate analysis of characteristics of patients with AIS to identify predictors of 90-day unfavorable neurological outcome.

Variable	mRS score of 3~6 at 90 days.		
	OR	95%CI	*p*-value
Demography			
Male	0.585	0.381–0.898	0.014
Age (y)	1.032	1.015–1.050	<0.001
Risk factors			
Hypertension	1.296	0.842–1.996	0.238
Diabetes	0.908	0.555–1.485	0.700
Hyperlipidemia	0.905	0.566–1.446	0.675
Atrial fibrillation	4.294	2.390–7.715	<0.001
Coronary heart disease	0.764	0.398–1.466	0.418
Previous TIA	0.248	0.055–1.117	0.069
Previous stroke	1.506	0.898–2.525	0.12
Current smoking	0.638	0.405–1.007	0.053
SBP (mmHg)	1.008	0.998–1.019	0.119
Admission NIHSSS	1.291	1.215–1.372	<0.001
OTT (h)	1.020	0.830–1.254	0.853
Lab results			
Neutrophil counts ($\times10^9$/L)	1.413	1.275–1.565	<0.001
Lymphocyte counts ($\times10^9$/L)	0.684	0.522–0.898	0.006
Monocyte counts ($\times10^9$/L)	3.423	1.357–8.634	0.009
Platelet counts ($\times10^9$/L)	1.002	0.998–1.005	0.358
NLR	1.217	1.127–1.313	<0.001
LMR	0.784	0.691–0.890	<0.001
PLR	1.000	0.999–1.001	0.671
APTT (s)	0.984	0.954–1.016	0.323
PT (s)	1.096	0.983–1.223	0.098
INR	0.975	0.823–1.156	0.773
Blood glucose (mmol/L)	1.027	0.964–1.093	0.413
LDL (mmol/L)	1.163	0.916–1.477	0.215
Hemorrhage transformation	4.866	2.331–10.159	<0.001
Infarction location			
Anterior circulation	2.189	1.361–3.518	0.001
Posterior circulation	Reference	Reference	
Anterior–posterior circulation	3.800	1.741–8.292	0.001
TOAST classification			
Large-artery Atherosclerosis	5.011	2.454–10.232	<0.001
Small-artery occlusion	Reference	Reference	
Cardioembolism	6.310	2.799–14.229	<0.001
Other determined etiology	1.643	0.594–4.544	0.339
Undetermined etiology	2.133	0.889–5.120	0.090

for augmenting statistical power while preserving clinical heterogeneity across diverse populations. Importantly, our multivariate models did not adjust for post-thrombolysis interventions (e.g., antiplatelet timing) and complications (e.g., infections), which may confound inflammatory marker trajectories. While our cohort followed institutional protocols for standard care, residual confounding from unmeasured clinical decisions cannot be excluded. Future prospective studies should integrate real-time monitoring of both baseline and in-hospital variables to disentangle these effects. Secondly, we obtained

TABLE 5 Multivariable analysis was used to investigate the effects of NLR and LMR on the 90-day unfavorable neurological outcomes based on TOAST classification.

TOAST	NLR			LMR		
	aOR*	95%CI	*p*-value	aOR*	95%CI	*p*-value
All included patients	1.261	1.148–1.384	<0.001	0.735	0.622–0.868	<0.001
Large-artery atherosclerosis	1.354	1.142–1.606	0.001	0.693	0.541–0.886	0.004
Small-artery occlusion	1.505	1.081–2.096	0.015	0.641	0.373–1.101	0.107
Cardioembolism	1.817	1.065–3.101	0.028	0.700	0.359–1.365	0.296
Other determined etiology	1.047	0.738–1.486	0.796	0.939	0.490–1.799	0.849
Undetermined etiology	1.053	0.857–1.293	0.623	0.736	0.395–1.373	0.335

*Adjusted for gender, age, history of atrial fibrillation, admission NIHSS score, location of infarct and hemorrhage transformation.

TABLE 6 ROC curves were used to analyze the prognostic value of unfavorable neurological outcomes at 90 days.

TOAST	NLR			LMR		
	AUC	95%CI	*p*-value	AUC	95%CI	*p*-value
All included patients	0.701	0.646–0.755	<0.001	0.615	0.555–0.674	<0.001
Large-artery Atherosclerosis	0.702	0.620–0.784	<0.001	0.591	0.502–0.679	0.049
Small-artery occlusion	0.750	0.572–0.928	0.009	0.656	0.463–0.850	0.100
Cardioembolism	0.679	0.565–0.829	0.008	0.606	0.464–0.748	0.152
Other determined etiology	0.685	0.508–0.862	0.116	0.708	0.482–0.934	0.077
Undetermined etiology	0.667	0.515–0.818	0.060	0.639	0.451–0.827	0.116

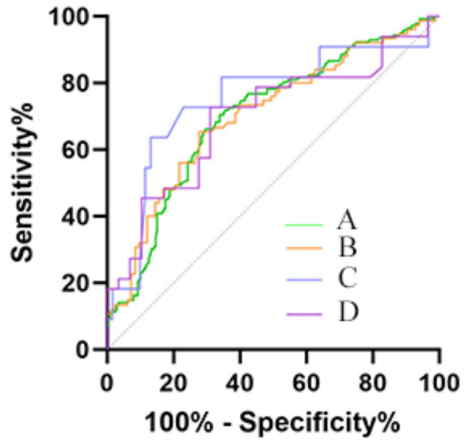

FIGURE 3
ROC curves were depicted for significant predictive value of mRS score 0f 3–6. **(A)** Included patients (Sensitivity: 0.662; Specificity: 0.707; Cutoff: 3.281); **(B)** Large-artery atherosclerosis subtype (Sensitivity: 0.653; Specificity: 0.733; Cutoff: 3.193); **(C)** Small-artery occlusion subtype (Sensitivity: 0.727; Specificity: 0.787; Cutoff: 3.937); **(D)** Cardioembolic subtype (Sensitivity: 0.727; Specificity: 0.690; Cutoff: 3.172).

lymphocyte-related ratios at admission, which was a single time point and restricted the evaluation of dynamic changes in inflammation after thrombolysis. Our reliance on baseline NLR/LMR precluded conclusions about the role of post-thrombolysis inflammatory dynamics. Prior studies had suggested that higher NLR within 24 h of admission was predictive of the hemorrhage transformation in patients with atrial fibrillation-related AIS, and the relationship with poor neurological outcomes remained to be further confirmed (29). Future prospective studies should integrate serial biomarker measurements to disentangle acute vs. secondary inflammatory effects on stroke outcomes. Finally, there was limited research on the relationship between NLR at admission and sICH after receiving intravenous thrombolysis for AIS. Furthermore, the observed AUC differences should be interpreted cautiously due to sample heterogeneity. Future studies with larger, overlapping cohorts are needed to rigorously validate subtype-specific performance differences.

Our study provided the first evidence on the prognostic utility of pre-thrombolysis lymphocyte-related ratios (e.g., NLR) in AIS patients with distinct etiological subtypes following intravenous thrombolysis. By focusing on pre-intervention biomarkers, we isolated early inflammatory responses inherent to the index stroke, thereby minimizing confounding effects from post-stroke complications (e.g., hospital-acquired infections) or secondary systemic inflammation. Notably, admission NLR emerged as an etiology-specific prognostic indicator, with validated cutoffs offering clinical utility for risk stratification and personalized therapeutic decision-making. Further investigations should elucidate the pathophysiological interplay between pre-thrombolysis inflammatory profiles and stroke subtypes, while expanding biomarker panels to include cytokines and neutrophil elastase for precise outcome prediction.

Conclusion

NLR had a borderline adequate predictive capacity for adverse neurological outcomes in large-artery atherosclerosis stroke and a

reasonable predictive performance for small-artery occlusion stroke, the NLR may serve as an important prognostic marker for AIS, assisting in evaluating therapeutic efficacy and selecting treatment modalities in clinical decision-making through cut-off values.

Data availability statement

The raw data supporting the conclusions of this article will be made available by the authors, without undue reservation.

Ethics statement

The studies involving humans were approved by the Medical Ethics Committee of the First Affiliated Hospital of Kunming Medical University. The studies were conducted in accordance with the local legislation and institutional requirements. The participants provided their written informed consent to participate in this study.

Author contributions

YL: Investigation, Writing – original draft, Writing – review & editing. KC: Investigation, Methodology, Software, Writing – review & editing. LW: Data curation, Formal analysis, Writing – original draft. LZ: Formal analysis, Resources, Validation, Writing – review & editing. CL: Conceptualization, Funding acquisition, Resources, Supervision, Visualization, Writing – review & editing. YG: Data curation, Software, Writing – review & editing. XZ: Software, Writing – review & editing. QD: Writing – review & editing.

Funding

The author(s) declare that financial support was received for the research and/or publication of this article. This work was supported by the Joint Research Fund of Yunnan Province (202301AY070001-200), Nervous System Disease Clinical Diagnosis and Treatment Center of Yunnan Province (ZX2022-09-01), Yunnan Clinical Medical Center for Neurological and Cardiovascular Diseases (YWLCYXZX2023300077), and Key Clinical Specialty of Neurology in Yunnan Province (300064).

Conflict of interest

The authors declare that the research was conducted in the absence of any commercial or financial relationships that could be construed as a potential conflict of interest.

Generative AI statement

The authors declare that no Gen AI was used in the creation of this manuscript.

Publisher's note

References

1. Song S, Liang L, Fonarow GC, Smith EE, Bhatt DL, Matsouaka RA, et al. Comparison of clinical care and in-hospital outcomes of Asian American and white patients with acute ischemic stroke. *JAMA Neurol*. (2019) 76:430–9. doi: 10.1001/jamaneurol.2018.4410

2. Morotti A, Poli L, Costa P. Acute Stroke. *Semin Neurol*. (2019) 39:61–72. doi: 10.1055/s-0038-1676992

3. Adams HP Jr, Bendixen BH, Kappelle LJ, Biller J, Love BB, Gordon DL, et al. Classification of subtype of acute ischemic stroke. Definitions for use in a multicenter clinical trial. TOAST. Trial of org 10172 in acute stroke treatment. *Stroke*. (1993) 24:35–41. doi: 10.1161/01.STR.24.1.35

4. Mendelson SJ, Prabhakaran S. Diagnosis and Management of Transient Ischemic Attack and Acute Ischemic Stroke: a review. *JAMA*. (2021) 325:1088–98. doi: 10.1001/jama.2020.26867

5. Hacke W, Kaste M, Bluhmki E, Brozman M, Dávalos A, Guidetti D, et al. Thrombolysis with alteplase 3 to 4.5 hours after acute ischemic stroke. *N Engl J Med*. (2008) 359:1317–29. doi: 10.1056/NEJMoa0804656

6. Emberson J, Lees KR, Lyden P, Blackwell L, Albers G, Bluhmki E, et al. Effect of treatment delay, age, and stroke severity on the effects of intravenous thrombolysis with alteplase for acute ischaemic stroke: a meta-analysis of individual patient data from randomised trials. *Lancet*. (2014) 384:1929–35. doi: 10.1016/S0140-6736(14)60584-5

7. Macrez R, Ali C, Toutirais O, Le Mauff B, Defer G, Dirnagl U, et al. Stroke and the immune system: from pathophysiology to new therapeutic strategies. *Lancet Neurol*. (2011) 10:471–80. doi: 10.1016/S1474-4422(11)70066-7

8. Atik İ, Kozacı N, Beydilli İ, Avcı M, Ellidağ H, Keşaplı M. Investigation of oxidant and antioxidant levels in patients with acute stroke in the emergency service. *Am J Emerg Med*. (2016) 34:2379–83. doi: 10.1016/j.ajem.2016.08.062

9. Xu X, Jiang Y. The Yin and Yang of innate immunity in stroke. *Biomed Res Int*. (2014) 2014:807978:1–8. doi: 10.1155/2014/807978

10. Sarejloo S, Kheradjoo H, Haghi SE, Hosseini S, Gargari MK, Azarhomayoun A, et al. Neutrophil-to-lymphocyte ratio and early neurological deterioration in stroke patients: a systematic review and Meta-analysis. *Biomed Res Int*. (2022) 2022:8656864. doi: 10.1155/2022/8656864

11. Iadecola C, Anrather J. The immunology of stroke: from mechanisms to translation. *Nat Med*. (2011) 17:796–808. doi: 10.1038/nm.2399

12. Liu YL, Lu JK, Yin HP, Xia PS, Qiu DH, Liang MQ, et al. High neutrophil-to-lymphocyte ratio predicts hemorrhagic transformation in acute ischemic stroke patients treated with intravenous thrombolysis. *Int J Hypertens*. (2020) 2020:1–6. doi: 10.1155/2020/5980261

13. Gong P, Liu Y, Gong Y, Chen G, Zhang X, Wang S, et al. The association of neutrophil to lymphocyte ratio, platelet to lymphocyte ratio, and lymphocyte to monocyte ratio with post-thrombolysis early neurological outcomes in patients with acute ischemic stroke. *J Neuroinflammation*. (2021) 18:51. doi: 10.1186/s12974-021-02090-6

14. Zhang YX, Shen ZY, Jia YC, Guo X, Guo XS, Xing Y, et al. The Association of the Neutrophil-to-Lymphocyte Ratio, platelet-to-lymphocyte ratio, lymphocyte-to-monocyte ratio and systemic inflammation response index with short-term functional outcome in patients with acute ischemic stroke. *J Inflamm Res*. (2023) 16:3619–30. doi: 10.2147/JIR.S418106

15. Wang C, Zhang Q, Ji M, Mang J, Xu Z. Prognostic value of the neutrophil-to-lymphocyte ratio in acute ischemic stroke patients treated with intravenous thrombolysis: a systematic review and meta-analysis. *BMC Neurol*. (2021) 21:191. doi: 10.1186/s12883-021-02222-8

16. Bone RC, Balk RA, Cerra FB, Dellinger RP, Fein AM, Knaus WA, et al. Definitions for sepsis and organ failure and guidelines for the use of innovative therapies in sepsis. The ACCP/SCCM consensus conference committee. American College of Chest Physicians/Society of Critical Care Medicine. *Chest*. (1992) 101:1644–55. doi: 10.1378/chest.101.6.1644

17. Hacke W, Kaste M, Fieschi C, Toni D, Lesaffre E, von Kummer R, et al. Intravenous thrombolysis with recombinant tissue plasminogen activator for acute hemispheric stroke. The European Cooperative Acute Stroke Study (ECASS). *JAMA*. (1995) 274:1017–25. doi: 10.1001/jama.1995.03530130023023

18. Hosmer DW, Lemeshow S. Applied Logistic Regression. 2nd edn. eds. Hosmer, W. David and S Lemeshow. Wiley (2000).

19. Sadeghi F, Sarkady F, Zsóri KS, Szegedi I, Orbán-Kálmándi R, Székely EG, et al. High neutrophil-lymphocyte ratio and low lymphocyte-monocyte ratio combination after thrombolysis is a potential predictor of poor functional outcome of acute ischemic stroke. *J Pers Med*. (2022) 12:1221. doi: 10.3390/jpm12081221

20. Goyal N, Tsivgoulis G, Chang JJ, Malhotra K, Pandhi A, Ishfaq MF, et al. Admission neutrophil-to-lymphocyte ratio as a prognostic biomarker of outcomes in large vessel occlusion strokes. *Stroke*. (2018) 49:1985–7. doi: 10.1161/STROKEAHA.118.021477

21. Li L, Han Z, Wang R, Fan J, Zheng Y, Huang Y, et al. Association of admission neutrophil serine proteinases levels with the outcomes of acute ischemic stroke: a prospective cohort study. *J Neuroinflammation*. (2023) 20:70. doi: 10.1186/s12974-023-02758-1

22. Alawieh AM, Langley EF, Feng W, Spiotta AM, Tomlinson S. Complement-dependent synaptic uptake and cognitive decline after stroke and reperfusion therapy. *J Neurosci*. (2020) 40:4042–58. doi: 10.1523/JNEUROSCI.2462-19.2020

23. Nieswandt B, Kleinschnitz C, Stoll G. Ischaemic stroke: a thrombo-inflammatory disease? *J Physiol*. (2011) 589:4115–23. doi: 10.1113/jphysiol.2011.212886

24. Fann DY, Lee SY, Manzanero S, Chunduri P, Sobey CG, Arumugam TV. Pathogenesis of acute stroke and the role of inflammasomes. *Ageing Res Rev*. (2013) 12:941–66. doi: 10.1016/j.arr.2013.09.004

25. Petrovic-Djergovic D, Goonewardena SN, Pinsky DJ. Inflammatory disequilibrium in stroke. *Circ Res*. (2016) 119:142–58. doi: 10.1161/CIRCRESAHA.116.308022

26. Oberheiden T, Nguyen XD, Fatar M, Elmas E, Blahak C, Morper N, et al. Platelet and monocyte activation in acute ischemic stroke--is there a correlation with stroke etiology? *Clin Appl Thromb Hemost*. (2012) 18:87–91. doi: 10.1177/1076029611412359

27. Eriksson EE, Xie X, Werr J, Thoren P, Lindbom L. Direct viewing of atherosclerosis in vivo: plaque invasion by leukocytes is initiated by the endothelial selectins. *FASEB J*. (2001) 15:1149–57. doi: 10.1096/fj.00-0537com

28. Weiping Pang BaW. The predictive value of neutrophil-to-lymphocyte ratio, platelet-to-lymphocyte ratio, and platelet-to-neutrophil ratio for the progression of large-artery atherosclerotic ischemic stroke. *Chin Med J*. (2023) 20:93–7. doi: 10.20047/j.issn1673-7210.2023.32.20

29. Yuexia Ma JG, Liu G, Ma X, Zhu C. Clinical significance of neutrophil/lymphocyte ratio in acute Aschemic stroke patients with atrial fibrillation related hemorrhagic transformation. *J Brain Nerve Disord*. (2022) 30:495–9.

30. Song Q, Pan R, Jin Y, Wang Y, Cheng Y, Liu J, et al. Lymphocyte-to-monocyte ratio and risk of hemorrhagic transformation in patients with acute ischemic stroke. *Neurol Sci*. (2020) 41:2511–20. doi: 10.1007/s10072-020-04355-z

31. Ören O, Haki C, Kaya H, Yüksel M. Predictive value of admission neutrophil/lymphocyte ratio in symptomatic intracranial hemorrhage after stroke thrombolysis. *Neurol Sci*. (2022) 43:435–40. doi: 10.1007/s10072-021-05326-8

32. Franks ZG, Campbell RA, Weyrich AS, Rondina MT. Platelet-leukocyte interactions link inflammatory and thromboembolic events in ischemic stroke. *Ann N Y Acad Sci*. (2010) 1207:11–7. doi: 10.1111/j.1749-6632.2010.05733.x

33. Cuartero MI, Ballesteros I, Moraga A, Nombela F, Vivancos J, Hamilton JA, et al. N2 neutrophils, novel players in brain inflammation after stroke: modulation by the PPARγ agonist rosiglitazone. *Stroke*. (2013) 44:3498–508. doi: 10.1161/STROKEAHA.113.002470

34. Sun YY, Wang MQ, Wang Y, Sun X, Qu Y, Zhu HJ, et al. Platelet-to-lymphocyte ratio at 24h after thrombolysis is a prognostic marker in acute ischemic stroke patients. *Front Immunol*. (2022) 13:1000626. doi: 10.3389/fimmu.2022.1000626

Glossary

AIS - Acute ischemic stroke

aOR - Adjusted odds ratio

APTT - Activated partial thromboplastin time

aSICH - Asymptomatic intracerebral hemorrhage

AUC - Area under the receiver operating characteristic curve

CI - Confidence interval

INR - International normalized ratio

LDL - Low density lipoprotein

LMR - Lymphocyte to monocyte ratio

M - Median

mRS - modified Rankin Scale

NIHSS - National Institutes of Health Stroke Scale

NLR - Neutrophil to lymphocyte ratio

ODB - Onset to draw blood

OR - Odds ratio

OTT - Onset to thrombolysis time

PT - Prothrombin time

PLR - Platelet to lymphocyte ratio

ROC - Receiver operating characteristic curve

SICH - Symptomatic intracerebral hemorrhage

TOAST - Trial of Org 10,172 in Acute Stroke Treatment

TIA - Transient ischemic attack

Y - Years old

frontiers | Frontiers in Neurology

TYPE Original Research
PUBLISHED 09 May 2025
DOI 10.3389/fneur.2025.1498613

OPEN ACCESS

EDITED BY
Haipeng Liu,
Coventry University, United Kingdom

REVIEWED BY
Jose Wagner Leonel Tavares Junior,
Federal University of Ceara, Brazil
Marly Da Silva,
Federal Technological University of Paraná, Brazil
Irwan Ary Dharmawan,
Universitas Padjadjaran, Indonesia

*CORRESPONDENCE
Ge Jin
wysnjg@163.com

RECEIVED 20 September 2024
ACCEPTED 25 April 2025
PUBLISHED 09 May 2025

CITATION
Wang J-W, Li X, Lu L-X, Chen J-L, Yang Y-T and Jin G (2025) Association between Apolipoprotein E gene polymorphism and the tortuosity of extracranial carotid artery. *Front. Neurol.* 16:1498613. doi: 10.3389/fneur.2025.1498613

Association between Apolipoprotein E gene polymorphism and the tortuosity of extracranial carotid artery

Jun-Wei Wang, Xin Li, Liu-Xi Lu, Jun-Lin Chen, Yong-Tao Yang and Ge Jin*

Department of Neurology, The Fifth People's Hospital of Chongqing, Chongqing, China

Background: It is widely recognized that the Apolipoprotein E (ApoE) exhibits a significant association with dyslipidemia and atherosclerotic cardiovascular disease (ASCVD). The tortuous extracranial carotid artery (ECA) is a frequently encountered vascular morphological anomaly that may be associated to ischemic cerebrovascular disease. The purpose of this study was to investigate the association between ApoE gene polymorphism and the tortuosity of ECA.

Methods: The clinical data and ApoE genetic test of inpatients who underwent head and neck DSA or CTA at our department between June 2020 and January 2024, were retrospectively analyzed. The tortuosity index (TI) of the ECA was measured and calculated. The included patients were analyzed using two grouping methods based on TI of the ECA: three groups determined by the tertile distribution and two groups based on the median distribution. Multivariate logistic regression analysis and Spearman rank correlation analysis were employed to investigate the correlation between ApoE genotypes and ECA tortuosity.

Results: A total of 238 patients were included in the study. The lowest tertile, the middle tertile and the highest tertile of TI distribution encompassed 91 cases (38.2%), 65 cases (27.3%) and 82 cases (34.5%) respectively. On the other hand, there were 127 cases (53.4%) in the low median group and 111 cases (46.6%) in the high median group. Due to the rarity of the three genotypes (ε2/ε2, $n = 4$; ε2/ε4, $n = 1$; ε4/ε4, $n = 1$), they were excluded for further statistical analysis. After adjusting for all covariates, the genotype ε3/ε4 continued to show an independent correlation with ECA tortuosity in the tertile groups (adjusted odds ratio = 0.469, 95% confidence interval: 0.242–0.969, $p = 0.025$). The Spearman's rank correlation analysis revealed a significant negative correlation between the TI of ECA and ApoE gene polymorphism (in sequential order: ε2/ε3, ε3/ε3, and ε3/ε4) ($r_S = -0.149$, $p = 0.023$).

Conclusion: Our study suggested that the ε2 allele may be associated with the increased tortuosity of ECA, whereas the ε4 allele may leads to be a protective factor. The ε3 allele, as the most prevalent wild-type in human, has not exert a significant influence on ECA tortuosity.

KEYWORDS

ApoE, gene polymorphism, tortuosity, extracranial carotid artery, correlation

Introduction

Apolipoprotein E (ApoE) is expressed primarily by the liver parenchymal cells in the human body and is a major apolipoprotein found in plasma. It exhibits genetic polymorphism, consisting of three alleles (ε2, ε3, and ε4), which combine to form six different genotypes (ε2/ε2, ε2/ε3, ε2/ε4, ε3/ε3, ε3/ε4, and ε4/ε4) (1, 2). The above three alleles (ε2, ε3, and ε4) encode three ApoE isoforms (E2, E3, and E4), which play different roles in maintaining cholesterol metabolic balance. ApoE4 is associated with various diseases, including hyperlipidemia (3), atherosclerosis (4), Alzheimer's disease (5, 6) coronary atherosclerotic heart disease, and ischemic stroke (7). Extracranial carotid artery (ECA) tortuosity is considered an age-related degenerative change, but its underlying mechanism is still incompletely clear. Previous study has shown severe ECA tortuosity is associated with hemodynamic changes and transient ischemic attack, which commonly arisen from atherosclerotic stenosis (8). Furthermore, the obvious ECA tortuosity increases the challenge of endovascular treatment (9), and may leads to poor prognosis of anterior circulation ischemic stroke patients who without undergoing interventional procedure (10).

Although ECA tortuosity and ApoE are both associated with cerebrovascular disease, the causal relationship between them is currently unknow yet. The aim of this study is to investigate the relationship between ECA tortuosity and ApoE gene polymorphism, and to providing more clues and evidence for the pathogenesis of ECA tortuosity.

Materials and methods

Patients

The clinical data and ApoE gene tests of inpatients, who underwent the head and neck digital subtraction angiography (DSA) or computed tomography angiography (CTA) in our department from June 2020 to January 2024, were retrospectively analyzed. The clinical data comprised demographic information and the cerebrovascular disease's common risk factors. The tortuosity index (TI) of ECA for each patient were measured and calculated. Referring to the methods in previous literatures (11, 12), the included patients were divided into three groups based on the tertile distribution of ECA TI and two groups based on the median distribution. We compared the differences in clinical data and ApoE genotypes between these groups.

The inclusion criteria for this study were hospitalized patients who had completed both head and neck CTA/DSA and ApoE genotyping, without restriction based on disease entities. The exclusion criteria were defined as follows. (1) patients with poor imaging quality of CTA or DSA which could not complete the measure and calculate for the tortuosity index. (2) patients with the bilateral ECA occlusion. (3) patient is under 18 years old. This study was designed for retrospective research, and the formal consent from patients was not required. All research procedures involving human participants adhered to the ethical standards of the Declaration of Helsinki of 1964 and its subsequent amendments or similar ethical standards.

Acquisition of ECA imaging

The DSA was performed using an Allura xper FD20 X-ray system (Philips, Netherlands), while the CTA was performed using a Brilliance 64 row 128 slice spiral CT (Philips, Netherlands). The three-dimensional volume rendering of the head and neck arteries were achieved using the Philips Extended Brilliance™ workstation (Philips, Netherlands). Both DSA and CTA procedures were all using non-ionic contrast agents (iohexol, iopamidol or iodixanol) for imaging. The informed consent form for DSA or CTA procedures were signed by the enrolled patients or their next of kin.

Quantification of tortuosity index

The DICOM document of CTA and DSA images were downloaded and collected from picture archiving and communication system (PACS). The tortuosity index of the ECA was measured and calculated by two independent experts in cerebrovascular disease imaging using Sante DICOM Viewer 3D software (Sante soft LTD, Nicosia, Cyprus). After loading DICOM files or selected JPEG format images into the Sante DICOM Viewer software, the anteroposterior view of 3D volume-rendered images for bilateral ECA were choose to measure. The proximal end for measure was the bifurcation point of the aortic arch in the left ECA or the brachiocephalic trunk in the right ECA. The distal end of measurement was the ECA located at the entrance of the carotid canal. A line measurement tool was used to measure the actual length from the proximal end to the distal end along the curvature of the ECA, and a linear distance tool was used to measure the straight length between the two points. The calculation formula for the TI of ECA is as follows. TI = [actual length/straight length−1] × 100. Since relative numbers cannot be averaged, the higher value obtained from the bilateral ECA calculations was taken to represent the TI of the patient. The specific measurement and calculation methods refer to the previously published literature (13, 14) (Figure 1).

Detection of ApoE genotype

After extracting DNA from venous blood of patients, the ApoE genotypes was detected and analyzed by Fascan-48E Multichannel Fluorescence Quantitative Analyzer and SNP-U4 Human ApoE Gene PCR Detection Kit (TIANLONG Technology Ltd., Xi'an city, CHN). The genotype of each subject was one of six possible results: three homozygotes (ε2/ε2, ε3/ε3, ε4/ε4) or three heterozygotes (ε2/ε3, ε2/ε4, ε3/ε4).

Statistical analysis

All the data were statistically processed by using SPSS software (version 20.0, IBM Corporation, Armonk, NY). The Kolmogorov Smirnov test and Shapiro Wilk test was used to examine the normal distribution of continuous variables, and the Levene test is used to test the homogeneity of variance. The continuous variables that follow a normal distribution were described as Mean (SD), and inter group comparisons were performed by using the analysis of variance or the student's t test. The continuous variables with skewed distribution were described as Median (IQR), and intergroup comparisons were performed by using Kruskal Wallis rank-sum test or Mann Whitney U test. The categorical variables were described as *n* (%), and inter group comparisons were conducted by using chi-square test, Fisher's

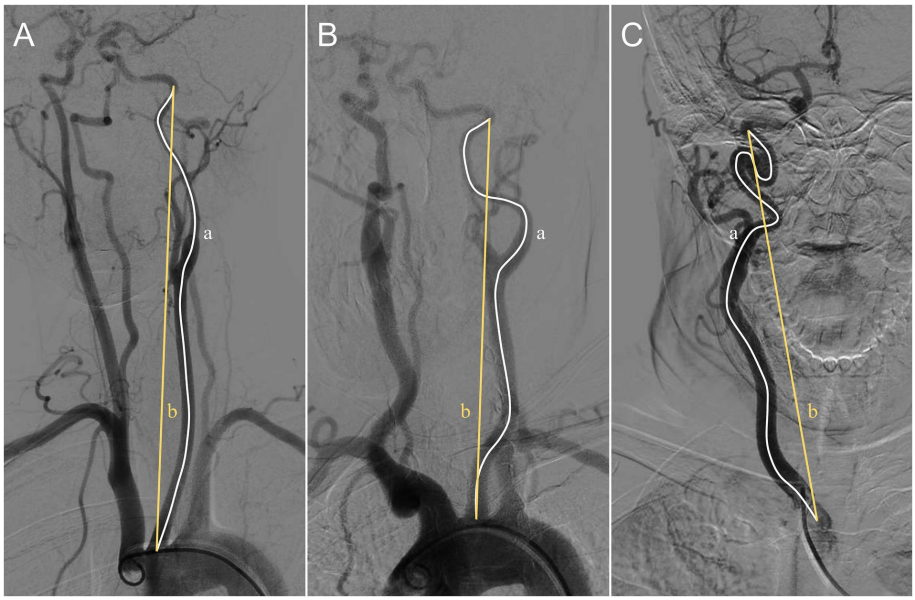

FIGURE 1
The actual length (white line) and straight length (yellow line) of the left ECA **(A,B)** and the right one **(C)**. Based on the calculations using the formula (TI = [a/b−1] × 100), the tortuosity of ECA in **A** is mild (TI = 4), while that in **B** is moderate (TI = 15), and that in **C** is severe (TI = 36). ECA, extracranial carotid artery; TI, tortuosity index.

exact test, or Kruskal Wallis rank-sum test. The multivariate analysis was performed by using the ordinal logistic regression and binary logistic regression. The odds ratio (OR) and 95% confidence interval (CI) were calculated to analyze the independent risk factors for ECA tortuosity. The spearman correlation coefficient (r_s) was used to analyze the correlation between ApoE gene polymorphism and the degree of ECA tortuosity. $p < 0.05$ indicates the statistically significant.

Results

Univariate analysis

A total of 238 patients with ischemic cerebrovascular disease or those with its risk factors were included in this study. According to the tertile distribution of ECA TI, there were 91 cases (38.2%) in the TI < 13 group, 65 cases (27.3%) in the TI 13–19 group, and 82 cases (34.5%) in the TI > 19 group. According to the median distribution of ECA TI, there were 127 cases (53.4%) in the TI ≤ 15 group and 111 cases (46.6%) in the TI > 15 group. The age, sex, hypertension, diabetes, total cholesterol (TC), triglyceride (TG), low-density lipoprotein cholesterol (LDL-C), atrial fibrillation, smoking history, drinking history, and previous stroke history were analyzed and compared.

Among the 238 patients included, the distribution of ApoE genotypes is as follows: 4 cases of ε2/ε2 (1.68%), 40 cases of ε2/ε3 (16.8%), 1 case of ε2/ε4 (0.42%), 143 cases of ε3/ε3 (60.1%), 49 cases of ε3/ε4 (20.58%), and 1 case of ε4/ε4 (0.42%). Due to the rarity of genotypes ε2/ε2, ε2/ε4, and ε4/ε4, the six cases were excluded for further statistical analysis as refer to a previous research (15).

There were significant differences ($p < 0.05$) in age, female gender, and smoking history between the tertile groups and the median groups. In addition, there were significant differences in alcohol consumption between the median groups and in atrial fibrillation between the tertile groups. As for the genotypes of ApoE, ε3/ε4 ($p = 0.029$) showed statistically difference in the tertile groups for ECA TI. In contrast, no statistically significant differences were observed in either grouping methods for ε2/ε3 and ε3/ε3 (Table 1).

Multivariate logistic regression analysis

The variables demonstrated with statistical differences in univariate analysis, including age, gender, smoking history, alcohol consumption history, and the two target independent variables (ApoE genotype ε2/ε3 and ε3/ε4), were utilized into ordinal multiclassification logistic regression and binary logistic regression analyses to investigate the risk factors associated with ECA tortuosity.

After adjusting for age, female gender, and smoking, the ordinal multiclassification logistic regression for the tertile groups revealed that ε2/ε3 (OR = 1.116, 95% CI 0.550–2.264; $p = 0.76$) did not emerge as an independent risk factor, while ε3/ε4 (OR = 0.469, 95% CI 0.242–0.909; $p = 0.025$) demonstrated as a protective factor for ECA tortuosity. Neither ε2/ε3 (OR = 1.374, 95% CI 0.609–3.102; $p = 0.444$) nor ε3/ε4 (OR = 0.6, 95% CI 0.282–1.273; $p = 0.183$) showed the significant independent relationship to ECA tortuosity after adjusting for age, female gender, smoking, and alcohol consumption in binary logistic regression (Table 2).

Correlation analysis between ApoE gene polymorphism and ECA tortuosity

The distribution of the ECA tortuosity index in ApoE genotypes (ε2/ε3, ε3/ε3, and ε3/ε4) is displayed in Figure 2. The Spearman's rank

10.3389/fneur.2025.1498613

TABLE 1 The characteristics of clinical data and ApoE genotypes between the tertile and the median groups for ECA TI.

Factors	The tertile groups of TI			*p* value	The median groups of TI		*p* value
	TI < 13	TI 13–19	TI > 19		TI ≤ 15	TI > 15	
	(*n* = 91)	(*n* = 65)	(*n* = 82)		(*n* = 127)	(*n* = 111)	
Age in years, mean (SD)	63.9 (11.1)	69.4 (10.6)	71.7 (10.6)	<0.001	65.2 (11.1)	71.4 (10.5)	<0.001
Female, *n*(%)	18 (19.8)	21 (32.3)	57 (69.5)	<0.001	29 (22.8)	67 (60.4)	<0.001
Hypertension, *n*(%)	70 (76.9)	54 (83.1)	67 (81.7)	0.585	100 (78.7)	91 (82.0)	0.531
Diabetes mellitus, *n*(%)	34 (37.4)	32 (49.2)	27 (32.9)	0.121	53 (41.7)	40 (36.0)	0.369
TG, median (IQR)	1.33 (1.43)	1.3 (1.17)	1.29 (0.8)	0.923	1.30 (1.20)	1.29 (0.85)	0.710
TC, median (IQR)	4.46 (1.65)	4.28 (1.69)	4.42 (1.8)	0.214	4.46 (1.66)	4.36 (1.57)	0.966
LDL-C, median (IQR)	2.78 (0.97)	2.71 (1.34)	2.68 (1.44)	0.348	2.76 (1.00)	2.69 (1.23)	0.934
Atrial fibrillation, *n*(%)	7 (7.7)	0 (0)	5 (6.1)	0.048	7 (5.5)	5 (4.5)	0.775
Smoking, *n*(%)	51 (56.0)	25 (38.5)	13 (15.9)	<0.001	66 (52.0)	23 (20.7)	<0.001
Alcohol drinking, *n*(%)	23 (25.3)	15 (23.1)	7 (8.5)	0.978	32 (25.2)	13 (11.7)	0.008
Stroke history, *n*(%)	11 (12.1)	7 (10.8)	8 (9.8)	0.965	15 (11.8)	11 (9.9)	0.682
ApoE genotype, *n*(%)							
ε2/ε2	0 (0)	3 (4.6)	1 (1.2)	/	1 (0.8)	3 (2.7)	/
ε2/ε3	12 (13.2)	9 (13.8)	19 (23.2)	0.177	16 (12.6)	24 (21.6)	0.082
ε2/ε4	1 (1.1)	0 (0)	0 (0)	/	1 (0.8)	0 (0)	/
ε3/ε3	54 (59.3)	37 (56.9)	52 (63.4)	0.715	78 (61.4)	65 (58.6)	0.653
ε3/ε4	24 (26.4)	16 (24.6)	9 (11)	0.029	31 (24.4)	18 (16.2)	0.148
ε4/ε4	0 (0)	0 (0)	1 (1.2)	/	0 (0)	1 (0.9)	/

SD, standard deviation; IQR, interquartile range; CA, carotid artery; TI, tortuosity index; TG, triglyceride; TC, total cholesterol; LDL-C, low-density lipoprotein cholesterol; ApoE, Apolipoprotein E.

TABLE 2 Multivariate logistic regression for ECA tortuosity.

Factors	The tertile groups of TI			The median groups of TI		
	OR	95% CI	*p* value	OR	95% CI	*p* value
Age	1.059	1.033–1.085	<0.001	1.059	1.029–1.090	<0.001
Female	4.345	2.286–8.258	<0.001	3.989	1.933–8.230	<0.001
Smoking	1.829	0.961–3.481	0.066	2.370	1.047–5.367	0.039
Alcoholism	/	/	/	0.570	0.227–1.432	0.231
ApoE genotype						
ε2/ε3	1.116	0.550–2.264	0.760	1.374	0.609–3.102	0.444
ε3/ε4	0.469	0.242–0.909	0.025	0.600	0.282–1.273	0.183

OR, odds ratio and CI, confidence interval.

correlation analysis revealed a significant negative correlation between the TI of ECA and ApoE genotypes (in sequential order: ε2/ε3, ε3/ε3, and ε3/ε4) ($r_S = -0.149$, $p = 0.023$).

Discussion

In this study, we have demonstrated a potential association between the ApoE gene polymorphism and the tortuosity of ECA in adult patients. Our findings indicated that individuals with the ApoE genotype ε3/ε4 exhibit an independent protective factor for ECA tortuosity. Furthermore, we have revealed a significant negative correlation between ECA tortuosity and three genotypes of ApoE (in sequential order: ε2/ε3, ε3/ε3, and ε3/ε4). Specifically, these results suggest that the ε4 allele may exert a protective effect on the tortuosity of ECA, while as for the ε3 allele, the most common wild-type of ApoE, has no significant influence on ECA tortuosity. Although the ε2 allele did not show the statistical significance in the multivariate

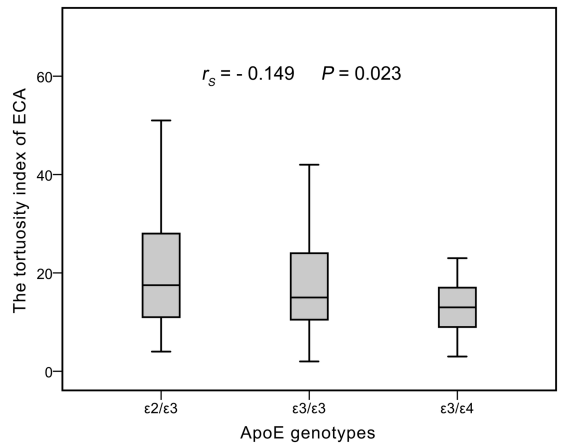

FIGURE 2
The distribution of ECA tortuosity index in ApoE genotypes and suggested a significant negative correlation. ECA, extracranial carotid artery; r_s, spearman correlation coefficient.

analysis, according to the Spearman correlation analysis, the ε2 allele carriers still may exist a potential promotive mechanism for ECA tortuosity.

Apolipoprotein E, a basic protein rich in arginine, is one of the main apolipoproteins in plasma. ApoE gene can lead to a variety of diseases by affecting the metabolism of lipids in serum (16). The ε4 allele carriers have higher levels of cholesterol and low-density lipoprotein, while the ε2 allele carriers have lower levels of cholesterol and low-density lipoprotein. The ApoE2 isoform can reduce the level of low-density lipoprotein in plasma, so it is considered to play a protective role in atherosclerotic cardiovascular disease (ASCVD) (4). In addition, ApoE participates in regulating multiple information pathways in the central nervous system, including cholesterol/lipid homeostasis, synaptic function, glucose metabolism, neurogenesis, mitochondrial function, tau protein phosphorylation, neuronal atrophy, etc., thereby affecting cognitive function (17–19). The prevailing consensus suggests that ApoE4 serves as a critical genetic risk factor in the pathogenesis of neurodegenerative disorders, notably Alzheimer's disease. On the contrary, ApoE2 is a genetic protective factor for Alzheimer's disease (AD), and its exact mechanism is not yet clear (20). Furthermore, some previous studies related to neurodegenerative diseases suggest that ApoE2 may increases the risk of progressive supranuclear palsy (21, 22). In summary, the ApoE4 may plays an important role in the development of Aging process, while ApoE2 is a protective isoform for ASCVD and AD.

Although the pathogenesis is currently unclear, there are evidences to suggest the ECA tortuosity may association with ischemic stroke (23, 24), arterial dissection (25, 26), white matter hyperintensities (27, 28), connective tissue disease (29), and intracranial aneurysm (30). Considering the significant relationship between ECA tortuosity and age, it may be classified as a type of vascular morphological anomaly attributed to the process of aging. However, our research results surprisingly showed that ECA tortuosity seems to be positively correlated with the ε2 allele, a protective genetic gene for atherosclerosis and AD, and be negatively correlated with the ε4 allele, which is considered as a risk gene. Although whether arterial tortuosity is an independent risk factor for ischemic stroke or related to atherosclerosis remains controversial (31–33), our research results also found that common risk factors of stroke, such as dyslipidemia, hypertension, diabetes, smoking and alcohol consumption, could not be confirmed as the independent risk factors of ECA tortuosity. Apart from the factor of age, female participants exhibited a more pronounced tortuosity of the ECA, which may be attributed to their comparatively shorter average height when compared to males. Furthermore, although some genetic arterial diseases, such as Loeys-Dietz syndrome, Marfan syndrome, Aneurysm-osteoarthritis syndrome, can manifest as aortic or carotid artery tortuosity through the remodeling of vascular connective tissue (34), there are currently a lack of reports linking ApoE gene polymorphisms to these genetic connective tissue disorders. Overall, even though ECA tortuosity is considered to be associated with degenerative changes, there is still a significant discrepancy in the mechanism between ECA tortuosity and atherosclerosis. The underlying genetic factors and remodeling of vascular wall may both be involved in the pathogenesis of ECA tortuosity. However, it is still unclear how ApoE gene polymorphism affects ECA tortuosity, and further in-depth research is needed to explore the pathogenesis of vascular tortuosity.

There are several limitations in our study. First of all, there is a possibility of congenital bias due to this study is retrospective. Second, our research is a single center study and did not include the race factor of participants. It is uncertain whether there are differences in the results between different racial populations. Finally, the proportion of patients with ApoE genotype ε2/ε3 and ε3/ε4 were relatively small, which leads to certain difference in sample size between the groups, and it is necessary to increase the sample size, preferably through further research on big data.

Conclusion

Our study suggested that the ApoE ε2 allele may be associated with increased tortuosity of ECA, whereas the ε4 allele may leads to be the protective factor. The ε3 allele, as the most prevalent wild-type in human, has not shown a significant influence on ECA tortuosity. The pathogenesis of ECA tortuosity may be associated with genetics and age-related vascular degenerative changes. In further research, we aim to verify the association between ApoE gene polymorphism and ECA tortuosity by expanding the sample size, conducting big data analysis, and including participants from diverse regions and ethnic backgrounds. Additionally, we anticipate more fundamental studies to elucidate the mechanisms underlying these research findings.

Data availability statement

The original contributions presented in the study are included in the article/supplementary material, further inquiries can be directed to the corresponding author.

Ethics statement

The studies involving humans were approved by the Ethics Committee of Chongqing Fifth People's Hospital. The studies were conducted in accordance with the local legislation and institutional

requirements. The ethics committee/institutional review board waived the requirement of written informed consent for participation from the participants or the participants' legal guardians/next of kin due to the retrospective nature of this study.

Author contributions

J-WW: Writing – original draft. XL: Data curation, Writing – original draft. L-XL: Data curation, Writing – original draft. J-LC: Data curation, Writing – original draft. Y-TY: Data curation, Writing – review & editing. GJ: Funding acquisition, Methodology, Writing – review & editing.

Funding

The author(s) declare that financial support was received for the research and/or publication of this article. This study was supported by grant from the Chongqing Nan'an District Science and Health Joint Medical Research Project (grant no. 2021-27) and the Medical Research Project of Chongqing Health Commission (grant no. 2015MSXM113).

Conflict of interest

The authors declare that the research was conducted in the absence of any commercial or financial relationships that could be construed as a potential conflict of interest.

Publisher's note

All claims expressed in this article are solely those of the authors and do not necessarily represent those of their affiliated organizations, or those of the publisher, the editors and the reviewers. Any product that may be evaluated in this article, or claim that may be made by its manufacturer, is not guaranteed or endorsed by the publisher.

References

1. Lanfranco MF, Sepulveda J, Kopetsky G, Rebeck GW. Expression and secretion of apoE isoforms in astrocytes and microglia during inflammation. *Glia*. (2021) 69:1478–93. doi: 10.1002/glia.23974

2. Iannucci J, Sen A, Grammas P. Isoform-specific effects of apolipoprotein E on markers of inflammation and toxicity in brain glia and neuronal cells in vitro. *Curr Issues Mol Biol*. (2021) 43:215–25. doi: 10.3390/cimb43010018

3. Lumsden AL, Mulugeta A, Zhou A, Hyppönen E. Apolipoprotein E (APOE) genotype-associated disease risks: a phenome-wide, registry-based, case-control study utilising the UK biobank. *EBioMedicine*. (2020) 59:102954. doi: 10.1016/j.ebiom.2020.102954

4. Pereira LC, Nascimento JCR, Rêgo JMC, Canuto KM, Crespo-Lopez ME, Alvarez-Leite JI, et al. Apolipoprotein E, periodontal disease and the risk for atherosclerosis: a review. *Arch Oral Biol*. (2019) 98:204–12. doi: 10.1016/j.archoralbio.2018.11.009

5. Yang LG, March ZM, Stephenson RA, Narayan PS. Apolipoprotein E in lipid metabolism and neurodegenerative disease. *Trends Endocrinol Metab*. (2023) 34:430–45. doi: 10.1016/j.tem.2023.05.002

6. Serrano-Pozo A, Das S, Hyman BT. APOE and Alzheimer's disease: advances in genetics, pathophysiology, and therapeutic approaches. *Lancet Neurol*. (2021) 20:68–80. doi: 10.1016/S1474-4422(20)30412-9

7. Li L, Li R, Zacharek A, Wang F, Landschoot-Ward J, Chopp M, et al. ABCA1/ApoE/HDL signaling pathway facilitates myelination and Oligodendrogenesis after stroke. *Int J Mol Sci*. (2020) 21:4369. doi: 10.3390/ijms21124369

8. Milic DJ, Jovanovic MM, Zivic SS, Jankovic RJ. Coiling of the left common carotid artery as a cause of transient ischemic attacks. *J Vasc Surg*. (2007) 45:411–3. doi: 10.1016/j.jvs.2006.10.002

9. Koge J, Tanaka K, Yoshimoto T, Shiozawa M, Kushi Y, Ohta T, et al. Internal carotid artery tortuosity: impact on mechanical Thrombectomy. *Stroke*. (2022) 53:2458–67. doi: 10.1161/STROKEAHA.121.037904

10. Jin G, Li Q, Zheng P, Cao D, Zhu D, Zou D, et al. Association between extracranial carotid artery tortuosity and clinical outcomes in anterior circulation acute ischemic stroke without undergoing endovascular treatment. *J Stroke Cerebrovasc Dis*. (2020) 29:104512. doi: 10.1016/j.jstrokecerebrovasdis.2019.104512

11. Shiba M, Kato T, Morimoto T, Yaku H, Inuzuka Y, Tamaki Y, et al. Serum cholinesterase as a prognostic biomarker for acute heart failure. *Eur Heart J Acute Cardiovasc Care*. (2021) 10:335–42. doi: 10.1093/ehjacc/zuaa043

12. Botezatu SB, Tzolos E, Kaiser Y, Cartlidge TRG, Kwiecinski J, Barton AK, et al. Serum lipoprotein(a) and bioprosthetic aortic valve degeneration. *Eur Heart J Cardiovasc Imaging*. (2023) 24:759–67. doi: 10.1093/ehjci/jeac274

13. Morris SA, Orbach DB, Geva T, Singh MN, Gauvreau K, Lacro RV. Increased vertebral artery tortuosity index is associated with adverse outcomes in children and young adults with connective tissue disorders. *Circulation*. (2011) 124:388–96. doi: 10.1161/CIRCULATIONAHA.110.990549

14. de Vries EE, Pourier VEC, van Laarhoven CJHCM, Vonken EJ, van Herwaarden JA, de Borst GJ. Comparability of semiautomatic tortuosity measurements in the carotid artery. *Neuroradiology*. (2019) 61:147–53. doi: 10.1007/s00234-018-2112-3

15. Montag C, Kunz L, Axmacher N, Sariyska R, Lachmann B, Reuter M. Common genetic variation of the APOE gene and personality. *BMC Neurosci*. (2014) 15:64. doi: 10.1186/1471-2202-15-64

16. Almeida FC, Patra K, Giannisis A, Niesnerova A, Nandakumar R, Ellis E, et al. APOE genotype dictates lipidomic signatures in primary human hepatocytes. *J Lipid Res*. (2024) 65:100498. doi: 10.1016/j.jlr.2024.100498

17. Rantalainen V, Lahti J, Kajantie E, Tienari P, Eriksson JG, Raikkonen K. APOE ε4, rs405509, and rs440446 promoter and intron-1 polymorphisms and dementia risk in a cohort of elderly Finns-Helsinki birth cohort study. *Neurobiol Aging*. (2019) 73:230.e5–8. doi: 10.1016/j.neurobiolaging.2018.09.005

18. Paradela RS, Justo AFO, Paes VR, Leite REP, Pasqualucci CA, Grinberg LT, et al. Association between APOE-ε4 allele and cognitive function is mediated by Alzheimer's disease pathology: a population-based autopsy study in an admixed sample. *Acta Neuropathol Commun*. (2023) 11:205. doi: 10.1186/s40478-023-01681-z

19. Nichols E, Brickman AM, Casaletto KB, Dams-O'Connor K, George KM, Kumar RG, et al. AD and non-AD mediators of the pathway between the APOE genotype and cognition. *Alzheimers Dement*. (2023) 19:2508–19. doi: 10.1002/alz.12885

20. Twohig D, Rodriguez-Vieitez E, Sando SB, Berge G, Lauridsen C, Møller I, et al. The relevance of cerebrospinal fluid α-synuclein levels to sporadic and familial Alzheimer's disease. *Acta Neuropathol Commun*. (2018) 6:130. doi: 10.1186/s40478-018-0624-z

21. Jabbari E, Holland N, Chelban V, Jones PS, Lamb R, Rawlinson C, et al. Diagnosis across the Spectrum of progressive Supranuclear palsy and Corticobasal syndrome. *JAMA Neurol*. (2020) 77:377–87. doi: 10.1001/jamaneurol.2019.4347

22. Sabir MS, Blauwendraat C, Ahmed S, Serrano GE, Beach TG, Perkins M, et al. Assessment of APOE in atypical parkinsonism syndromes. *Neurobiol Dis*. (2019) 127:142–6. doi: 10.1016/j.nbd.2019.02.016

23. Weibel J, Fields WS. Tortuosity, coiling, and kinking of the internal carotid artery. II. Relationship of morphological variation to cerebrovascular insufficiency. *Neurology*. (1965) 15:462–8. doi: 10.1212/wnl.15.5.462

24. Benson JC, Brinjikji W, Messina SA, Lanzino G, Kallmes DF. Cervical internal carotid artery tortuosity: a morphologic analysis of patients with acute ischemic stroke. *Interv Neuroradiol*. (2020) 26:216–21. doi: 10.1177/1591019919891295

25. Venturini G, Vuolo L, Pracucci G, Picchioni A, Failli Y, Benvenuti F, et al. Association between carotid artery dissection and vascular tortuosity: a case-control study. *Neuroradiology*. (2022) 64:1127–34. doi: 10.1007/s00234-021-02848-y

26. Zhang L, Liu X, Gong B, Li Q, Luo T, Lv F, et al. Increased internal carotid artery tortuosity is a risk factor for spontaneous Cervicocerebral artery dissection. *Eur J Vasc Endovasc Surg*. (2021) 61:542–9. doi: 10.1016/j.ejvs.2020.11.046

27. Liu J, Ke X, Lai Q. Increased tortuosity of bilateral distal internal carotid artery is associated with white matter hyperintensities. *Acta Radiol*. (2021) 62:515–23. doi: 10.1177/0284185120932386

28. Chen YC, Wei XE, Lu J, Qiao RH, Shen XF, Li YH. Correlation between internal carotid artery tortuosity and imaging of cerebral small vessel disease. *Front Neurol*. (2020) 11:567232. doi: 10.3389/fneur.2020.567232

29. Welby JP, Kim ST, Carr CM, Lehman VT, Rydberg CH, Wald JT, et al. Carotid artery tortuosity is associated with connective tissue diseases. *AJNR Am J Neuroradiol*. (2019) 40:1738–43. doi: 10.3174/ajnr.A6218

30. van Laarhoven CJHCM, Willemsen SI, Klaassen J, de Vries EE, van der Vliet QMJ, Hazenberg CEVB, et al. Carotid tortuosity is associated with extracranial carotid artery aneurysms. *Quant Imaging Med Surg*. (2022) 12:5018–29. doi: 10.21037/qims-22-89

31. Nagata T, Masumoto K, Hayashi Y, Watanabe Y, Kato Y, Katou F. Three-dimensional computed tomographic analysis of variations of the carotid artery. *J Craniomaxillofac Surg*. (2016) 44:734–42. doi: 10.1016/j.jcms.2016.02.011

32. Del Corso L, Moruzzo D, Conte B, Agelli M, Romanelli AM, Pastine F, et al. Tortuosity, kinking, and coiling of the carotid artery: expression of atherosclerosis or aging. *Angiology*. (1998) 49:361–71. doi: 10.1177/000331979804900505

33. Daitoku S, Yuasa T, Tsunenari H, Maenohara S, Mine K, Tamatsu Y, et al. Angle between the common and internal carotid arteries detected by ultrasound is related to intima-media thickness among those with atherosclerotic disease. *Environ Health Prev Med*. (2015) 20:216–23. doi: 10.1007/s12199-015-0453-7

34. Ciurică S, Lopez-Sublet M, Loeys BL, Radhouani I, Natarajan N, Vikkula M, et al. Arterial Tortuosity. *Hypertension*. (2019) 73:951–60. doi: 10.1161/HYPERTENSIONAHA.118.11647

frontiers | Frontiers in Neurology

TYPE Original Research
PUBLISHED 16 May 2025
DOI 10.3389/fneur.2025.1573027

OPEN ACCESS

EDITED BY
Haipeng Liu,
Coventry University, United Kingdom

REVIEWED BY
Senthil Kumaran Satyanarayanan,
Hong Kong Institute of Innovation and Technology, Hong Kong SAR, China
Leiluo Geng,
The University of Hong Kong, Hong Kong SAR, China
Natalia Campos-obando,
Erasmus Medical Center, Netherlands

*CORRESPONDENCE
Cunfu Wang
✉ 81298573@qq.com
Shunliang Xu
✉ slxu@live.com

†These authors have contributed equally to this work

RECEIVED 11 February 2025
ACCEPTED 25 April 2025
PUBLISHED 16 May 2025

CITATION
Xu H, Ding Y, Zhang Y, Li J, Zhou S, Wang D, Xing X, Ma X, Wang C and Xu S (2025) The association between serum klotho protein and stroke: a cross-sectional study from NHANES 2007–2016.
Front. Neurol. 16:1573027.
doi: 10.3389/fneur.2025.1573027

The association between serum klotho protein and stroke: a cross-sectional study from NHANES 2007–2016

Hongjia Xu[1†], Yiming Ding[2,3†], Ye Zhang[1], Jianwen Li[1], Shiyue Zhou[1], Dewei Wang[1], Xinyue Xing[1], Xiaoyu Ma[1], Cunfu Wang[1*] and Shunliang Xu[1,4*]

[1]Department of Neurology, The Second Hospital, Cheeloo College of Medicine, Shandong University, Jinan, China, [2]Department of Pediatric Surgery, Qilu Hospital of Shandong University, Jinan, China, [3]Cheeloo College of Medicine, Shandong University, Jinan, China, [4]Department of Human Genetics, School of Medicine, Emory University, Atlanta, GA, United States

Objective: Serum klotho protein is a protein with anti-aging effects. Since the relationship between serum klotho and Stroke remains rather ambiguous, this research probed into the potential correlation between serum klotho concentration and Stroke.

Methods: This study employed a cross-sectional design and incorporated population data from the NHANES from 2007 to 2016. Weighted univariate and multivariate logistic regression models were utilized to inspect the relationship between klotho and Stroke. Stratified analyses and interaction tests were carried out to explore the latent correlation between klotho and Stroke. Finally, a fitted smooth curve was adopted to depict the non-linear relationship.

Results: In this study, after excluding all the missing data, a total of 12,414 participants were encompassed, including 450 Stroke individuals. After adjusting for all covariates, higher klotho was associated with a lower prevalence of Stroke. According to the subgroup analyses and interaction tests, age, gender, race, BMI, hypertension, diabetes mellitus, family members, drinker and smoker were not significantly correlated with the influence of klotho and Stroke. After adjusting for all covariates, higher klotho was associated with a lower prevalence of stroke [OR: 0.68, 95% CI: 0.47–0.99].

Conclusion: This study disclosed the negative correlation between serum klotho protein levels and the prevalence of Stroke. Further prospective studies are requisite to investigate the impact of serum klotho protein levels on Stroke and determine the causal relationship.

KEYWORDS

klotho, stroke, atherosclerosis, cross-sectional study, NHANES

1 Introduction

Stroke represents the second leading global cause of mortality, surpassed only by acute ischemic heart disease (1). This severe acute cerebrovascular disease not only threatens survival but frequently induces debilitating sequelae including motor deficits, cognitive impairment, and affective disorders, imposing substantial socioeconomic burdens and quality-of-life deterioration (2). With the current development of an aging population, the prevalence rate of stroke is continuously rising (3). Furthermore, stroke is currently emerging gradually among the young

population (attributed to factors including patent foramen ovale, dyslipidemia, hormonal therapies, and genetic predisposition) (4, 5). Since stroke is a global public health problem, researchers have never stopped their research on the specific etiology, pathogenesis, predictive means and treatment measures of stroke. And they have been endeavoring to prevent the occurrence of stroke and handle it in a timely manner through some laboratory test indicators and other approaches.

The klotho gene, first identified through longevity studies in murine models (1997), has emerged as a pleiotropic regulator of aging processes. In mice, the overexpression of the klotho gene prolongs lifespan, while its mutation reduces it (6). The human klotho gene is situated at chromosome 13q12. It demonstrates effects such as anti-aging and anti-inflammation and is correlated with numerous age-related diseases (7, 8). The klotho protein encoded by the klotho gene is predominantly a single-channel transmembrane protein, and its soluble component can be cleaved to form α-klotho and dissolve in the blood, featuring three distinct functional types: membrane-bound α-klotho, truncated soluble α-klotho, and secreted α-klotho (6). Unless otherwise specified, the term "klotho" specifically refers to α-klotho. In previous studies, it has been found to be associated with kidney diseases (9), cardiovascular diseases (10, 11), and diabetes mellitus (12). Additionally, in the field of neurology, it has also been discovered that its reduction might be related to Alzheimer's disease and other degenerative disorders (13). In 2014, Dubal and colleagues discovered that mice with higher serum klotho levels exhibited stronger cognitive function across all age groups, independent of the aging process (14). Subsequently, the team of Castner demonstrated through experiments in rodents and primates that klotho enhances synaptic plasticity and cognitive capacity. Notably, their research revealed that a single low-dose (but not high-dose) administration of klotho could improve memory function in aged non-human primates (15). Emerging evidence from animal studies has demonstrated that beyond its well-documented cardiovascular effects, klotho protein plays a significant role in mediating ischemic preconditioning mechanisms. This endogenous neuroprotective function not only reduces stroke prevalence but also exhibits therapeutic potential through multifaceted cerebroprotective actions, including attenuation of oxidative stress and modulation of apoptotic pathways (16, 17).

Despite these advances, critical knowledge gaps persist regarding klotho's clinical relevance in cerebrovascular disease. Whether serum klotho levels demonstrate an independent association with stroke risk beyond traditional cardiovascular risk factors. The number of related clinical studies is limited, and the sample sizes therein are relatively small. We hypothesize that: Serum klotho concentration inversely correlates with stroke prevalence in adults. This association remains significant after comprehensive adjustment for confounders including lipid profiles and metabolic comorbidities. Hence, we carried out this research, conducting a large-sample study in the NHANES, which is representative of the national population, in the hope of testing these hypotheses between serum klotho and the prevalence of Stroke in the clinical setting.

2 Materials and methods

2.1 Study population

The data for this article were derived from the National Health and Nutrition Examination Survey (NHANES), which is a nationwide cross-sectional examination carried out by the National Center for Health Statistics (NCHS) of the US Centers for Disease Control and Prevention (CDC) to evaluate the health and nutrition status of the US population. The complete research design and data can be accessed on the NCHS website.[1] All participants provided written informed consent. The Research Ethics Review Board of the CDC and NCHS sanctioned the survey protocol.

We collected data from 50,588 participants in the NHANES database between 2007 and 2016. After excluding participants with missing Stroke data (n = 21,388) and klotho data (n = 15,436). Since klotho protein is primarily secreted by the kidneys, we excluded participants with chronic kidney disease (CKD), defined as an estimated glomerular filtration rate (eGFR) < 60 ml/min. As the NHANES database does not directly provide eGFR values, we calculated eGFR using established formulas from previous literature (18).

The CKD-EPI equations for estimating the GFR are as follows:

$$eGFR = a \times (SCr / b)c \times (0.993)Age$$

where SCr is μmol/L. ① a-values: 166 for black females and 163 for black males; 144 for white females of other races and 141 for white males of other races; ② b-values: 0.7 for females and 0.9 for males; and ③ c-values: −0.329 for females with SCr ≤ 0.7 mg/dl and −1.209 for females with SCr > 0.7 mg/dl; −0.411 for males with SCr ≤ 0.9 mg/dl and −1.209 for males with SCr > 0.9 mg/dl.

12,414 participants were ultimately encompassed in the current study. A total of 450 participants were defined as Stroke. The NHANES data utilized in this study were gathered in accordance with standard operating procedures. By conducting repeated measurements under the same conditions, intra-batch variability can be minimized, while inter-batch variability can be reduced through standardized procedures and periodic equipment calibration. We also employed sample weighting and multiple imputation methods in the analysis to further augment the reliability of the results (Figure 1).

2.2 Assessment of stroke

The definition of Stroke is based on previous studies (19–21). Stroke was defined by self-reported previous diagnosis by a physician. "Have you ever been told by a physician or a health professional that you had stroke?" If you answered yes, you were considered having stroke. Given that previous studies have shown the relatively high prevalence of ischemic stroke among stroke patients and its closer association with the klotho gene, despite the lack of information on stroke types in the NHANES database, it is highly likely that the majority of stroke participants included in this study were ischemic stroke cases (22).

2.3 Exposure

According to prior research, klotho measurements can be directly obtained from NHANES with established validity (23). All

1 www.cdc.gov/nchs/nhanes/

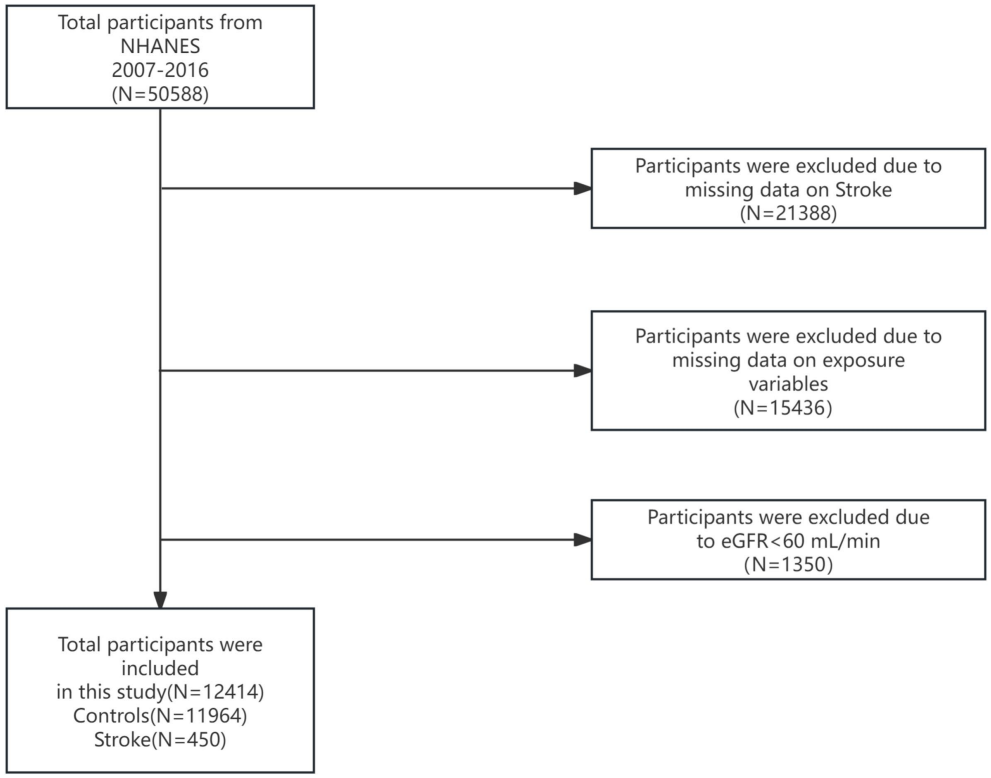

FIGURE 1
Flow chart of participants selection. NHANES, National Health and Nutrition Examination Survey.

participants' blood samples were collected and preserved at −80°C. Then klotho concentration in each participant was determined by enzyme-linked immunosorbent assay (ELISA) kit provided by IBL International. Each sample underwent duplicate testing, and the validation results were shared with the study investigators. The final value was calculated as the average of the two results. In order to more clearly define the relationship between klotho and stroke, we discussed the relationship between every 1,000 pg./ml increase in klotho protein and the prevalence rate of stroke in this article. The specific laboratory measurement process and standards for exposure variables can be traced at the NHANES.[2]

2.4 Assessment of covariates

Our analysis incorporated multiple covariates across three domains: sociodemographic characteristics, biochemical parameters, and chronic comorbidities. Sociodemographic data including age, gender, race, and family members were collected through standardized questionnaires. Weight (kg) divided by height squared (m^2) was used to determine BMI. Biochemical measurements comprised serum phosphorus levels and lipid profile components: high-density lipoprotein (HDL), total cholesterol (TC), triglycerides (TG), and low-density lipoprotein (LDL). "Have you smoked at least 100 cigarettes in your entire life?" If you answered yes, you were defined as a smoker. "Had at least 12 alcohol drinks/1 year?" If you answered yes, you were defined as a drinker. Chronic comorbidities encompass hypertension (HBP) and diabetes mellitus (DM). Hypertension was defined as having an average systolic blood pressure of ≥ 140 mmHg or an average diastolic blood pressure of ≥ 90 mmHg and a prior diagnosis of hypertension by a physician. The diabetes mellitus was defined by fasting glucose (mmol/L) ≥ 7.0 and a prior diagnosis of diabetes mellitus by a physician. Moreover, as previous studies have demonstrated associations between phosphorus/phosphate and cardiovascular mortality, but phosphate data are unavailable in NHANES, we adjusted for phosphorus in the covariates (24). All detailed measurement procedures for these variables can be accessed at www.cdc.gov/nchs/nhanes/.

2.5 Statistical analyses

R software (version 4.2) and EmpowerStats (version 4.2) were employed for data analysis, and all calculations were weighted in accordance with the guidelines of NHANES. In the stage of demographic analysis, the data were categorized into Stroke and HC groups. For continuous variables, characteristics were described as mean ± standard error (SE), while for categorical variables, they were described as proportions. Categorical variables were analyzed by means of chi-square test, and continuous variables were analyzed via t-test. A multivariate logistic regression analysis was utilized to explore the association between klotho and Stroke. In Model 1, no covariates were

2 See footnote 1.

incorporated for adjustment. In Model 2, adjustment variables encompassed age, gender, race, and education. In Model 3, all factors were taken into consideration and adjusted, and a weighted generalized additive model was adopted. Additionally, the smoothed curve fits were generated to examine potential nonlinear relationships. Finally, further stratified analyses and interaction tests were conducted to determine the association between klotho and Stroke. Statistical significance was determined if the two-sided *p*-value was less than 0.05.

3 Result

3.1 Participants characteristics at baseline

The baseline of all participants characteristics are presented in the Table 1. In total of 12,414 participants were comprised in our research, of which 450 were stroke patients. The average age of the Stroke cohort was 61.79 years, with 49.19% being male and 50.81% female. And the average klotho/1000 was 0.81. Notably, comparative analysis revealed significantly lower klotho values in the stroke group compared with HC ($p < 0.05$). Significant intergroup differences were observed in established biomarkers including TC, LDL, and AGE (all $p < 0.05$). Furthermore, the stroke cohort demonstrated significant disparities in multiple categorical variables: race ($p < 0.05$), family members ($p < 0.05$), smoker ($p < 0.05$), HBP ($p < 0.05$), and DM ($p < 0.05$) all showed statistically meaningful variations compared to the control group.

3.2 Association between klotho and stroke

Table 2 summarizes our comprehensive analysis examining the inverse association between klotho/1000 and stroke risk. Using multivariate logistic regression with three progressively adjusted models, we consistently observed statistically significant negative correlations across all analytical frameworks. The fully adjusted model (Model 3) revealed that each unit increase in klotho/1000 was associated with a 32% reduction in stroke risk (OR: 0.68; 95% CI: 0.47–0.99).

When stratifying stroke risk into quartiles, significant associations were identified in Quartiles 2 and 4 of the crude model (Model 1). However, these quartile-based associations attenuated to non-significance in the fully adjusted model. Model calibration was confirmed through Hosmer-Lemeshow testing ($\chi^2 = 14.6928$, df = 12, $p = 0.1437$), with the non-significant *p*-value indicating adequate goodness-of-fit when data were stratified into 12 quantile groups (Table 3).

Complementary analyses using generalized additive models (GAM) with smooth curve fitting (Figure 2) reinforced the consistent inverse relationship pattern across all models. This multimodal analytical approach substantiates the robustness of the observed negative correlation between klotho/1000 expression and stroke susceptibility.

3.3 Subgroup analysis

As delineated in Table 4, we conducted stratified subgroup analyses and multiplicative interaction testing across clinically relevant demographic and lifestyle parameters (age, gender, race, BMI, hypertension status, diabetes mellitus, family members, alcohol consumption patterns, and smoking status) to evaluate the robustness of the klotho-stroke association and identify potential effect modifiers. Notably, likelihood ratio tests revealed non-significant interaction effects ($p > 0.05$) across all pre-specified subgroups. This pattern of null heterogeneity suggests the observed association exhibits stability independent of these demographic stratifications, with no evidence of differential effects modulated by subgroup-level characteristics.

4 Discussion

In this research, we selected a total of 12,414 eligible participants from the NHANES from 2007 to 2016, among whom 450 were stroke patients, and explored the correlation between serum klotho and the prevalence of stroke. Notably, this represents the first large-scale epidemiological study establishing an independent negative correlation between serum klotho levels and stroke risk using nationally representative data. Even after eliminating all possible confounding factors, this negative correlation remained highly significant in the fully adjusted model ($p < 0.05$), with a 32% reduction in the risk of having stroke for every 1,000 pg./ml increase in klotho concentration. When comparing continuous variables and quartile-based categorical variables, the continuous variables show significance while the quartile variables do not. This discrepancy may arise due to the following reasons: (1) Information loss during variable categorization: Converting continuous variables into categorical variables (e.g., quartiles) may lead to information loss. For instance, the original linear relationship of the continuous variable could become obscured after categorization, as internal variations are averaged out and original trends are disrupted. Categorical variables may fail to capture subtle changes inherent in continuous variables, thereby reducing statistical power and resulting in a larger *p*-value. (2) Sample size limitations: Although the study includes 450 patients, this sample size may still be insufficient relative to the broader population. When categorized into quartiles, the number of stroke patients within each subgroup becomes smaller, further diminishing the statistical power of hypothesis testing. This reduction in power may hinder the detection of true differences or trends, even if they exist in the population. Finally, through subgroup analysis, we discovered that in the majority of subgroups, the negative correlation between serum klotho levels and the prevalence of stroke was remarkable.

Stroke is a globally prevalent public health concern. It is not only the second leading cause of death globally but also the third major cause of death and disability, and incurs substantial costs during the rehabilitation process following a stroke (1). Numerous researchers have been persistently dedicated to investigations in the direction of identifying the specific pathogenic mechanisms and are constantly in pursuit of effective clinical therapeutic approaches for alleviating or preventing Stroke (25, 26). As the population structure changes and the trend of younger strokes emerges, more effective diagnostic and preventive measures, as well as novel and efficacious treatment approaches, are required.

The klotho protein is a significant co-carrier of fibroblast growth factor 23 (FGF23), and their combination exhibits a certain degree of stability. The klotho protein participates in the regulation of calcium and phosphorus, as well as numerous metabolic regulations such as

TABLE 1 Basic characteristics of participants (n = 12,414) in NHANES 2007–2016.

Variable	HC (n = 11,964)	Stroke (n = 450)	p-value
Age	55.06 (54.74, 55.38)	61.79 (60.55, 63.04)	<0.0001
BMI	29.39 (29.19, 29.59)	30.33 (29.38, 31.28)	0.0544
HDL	1.41 (1.39, 1.42)	1.36 (1.30, 1.42)	0.1634
TC	5.23 (5.19, 5.26)	4.83 (4.69, 4.97)	<0.0001
TG	1.41 (1.39, 1.43)	1.39 (1.31, 1.48)	0.6890
LDL	3.09 (3.07, 3.10)	2.89 (2.82, 2.96)	<0.0001
KLOTHO/1000	0.86 (0.85, 0.87)	0.81 (0.79, 0.84)	0.0061
Phosphorus	1.20 (1.20, 1.21)	1.20 (1.17, 1.22)	0.6898
Drinker			0.8181
No	26.88 (25.32, 28.51)	27.42 (22.82, 32.55)	
Yes	73.12 (71.49, 74.68)	72.58 (67.45, 77.18)	
Gender (%)			0.7937
Male	48.33 (47.31, 49.34)	49.19 (42.90, 55.51)	
Female	51.67 (50.66, 52.69)	50.81 (44.49, 57.10)	
Race (%)			<0.0001
Mexican American	6.97 (5.58, 8.67)	5.85 (4.12, 8.24)	
Other Hispanic	4.87 (3.88, 6.11)	3.70 (2.45, 5.54)	
Non-Hispanic White	72.61 (69.43, 75.58)	65.68 (59.61, 71.28)	
Non-Hispanic Black	8.86 (7.56, 10.37)	14.45 (11.48, 18.03)	
Other Race	6.68 (5.78, 7.72)	10.32 (6.67, 15.65)	
Family members (%)			0.0007
1	14.02 (13.14, 14.94)	20.09 (15.52, 25.59)	
2	39.42 (37.40, 41.47)	45.69 (39.54, 51.99)	
3	16.68 (15.38, 18.06)	15.17 (11.12, 20.36)	
4	16.25 (14.96, 17.62)	9.07 (6.25, 13.00)	
5	7.69 (6.94, 8.52)	5.47 (3.56, 8.31)	
6	3.01 (2.55, 3.56)	2.41 (1.18, 4.86)	
7 or more	2.94 (2.40, 3.59)	2.10 (1.06, 4.12)	
Smoker (%)			<0.0001
No	52.54 (51.13, 53.94)	34.21 (29.06, 39.77)	
Yes	47.46 (46.06, 48.87)	65.79 (60.23, 70.94)	
DM (%)			<0.0001
No	86.39 (85.41, 87.31)	71.25 (65.20, 76.63)	
Yes	13.61 (12.69, 14.59)	28.75 (23.37, 34.80)	
HBP (%)			<0.0001
No	55.67 (54.38, 56.95)	22.52 (17.30, 28.77)	
Yes	44.33 (43.05, 45.62)	77.48 (71.23, 82.70)	

Mean ± SD for continuous variables: the p value was calculated by the weighted linear regression model; (%) for categorical variables: the p value was calculated by the weighted chi-square test. BMI, body mass index.

oxidative stress, through the FGF-klotho axis, and is likely to exert a crucial role in senile diseases (27, 28). klotho protein can be generated by ependymal cells of the choroid plexus, Purkinje EC cells, and hippocampal neurons and exists abundantly in the brain (29). In the field of neurology, especially in diseases associated with cognition, overexpressed klotho protein is capable of ameliorating cognitive impairments represented by Alzheimer's disease. Furthermore, artificial injection of klotho protein is also able to enhance synaptic plasticity and cognitive capacity in non-human primates (13, 15). In another study in 2023, klotho protein can treat sarcopenia by inhibiting transforming growth factor β through binding to ligands and type I and type II serine/threonine kinase receptors (30). An increasing amount of evidence suggests that klotho exerts a neuroprotective effect in the central nervous system and plays a

TABLE 2 Association between klotho and stroke.

Exposure	Model 1		Model 2		Model 3	
	OR (95%CI)	*p*-value	OR (95%CI)	*p*-value	OR (95%CI)	*p*-value
KLOTHO.1000	0.59 (0.39, 0.89)	0.0142	0.67 (0.45, 0.99)	0.0472	0.68 (0.47, 0.99)	0.0492
KLOTHO Ln quartile						
Quartile 1	1.0		1.0		1.0	
Quartile 2	0.73 (0.56, 0.95)	0.0201	0.78 (0.60, 1.02)	0.0671	0.76 (0.51, 1.14)	0.1924
Quartile 3	0.85 (0.66, 1.10)	0.2176	0.93 (0.72, 1.20)	0.5858	0.86 (0.58, 1.25)	0.4292
Quartile 4	0.75 (0.58, 0.98)	0.0338	0.96 (0.88, 1.05)	0.1780	0.73 (0.50, 1.09)	0.1294

Model 1: no covariates were adjusted. Model 2: Age, Gender, Race, Family members have been adjusted. Model 3: Age, Gender, Race, BMI, Family members, DM, HBP, HDL, LDL, Phosphorus, TC, TG, Drinker, and Smoker were adjusted.

TABLE 3 Hosmer-Lemeshow test.

Model	HL χ^2 value	df	*p*-value	Conclusion
Extended model	14.6928	12	0.1437	Adequate fit

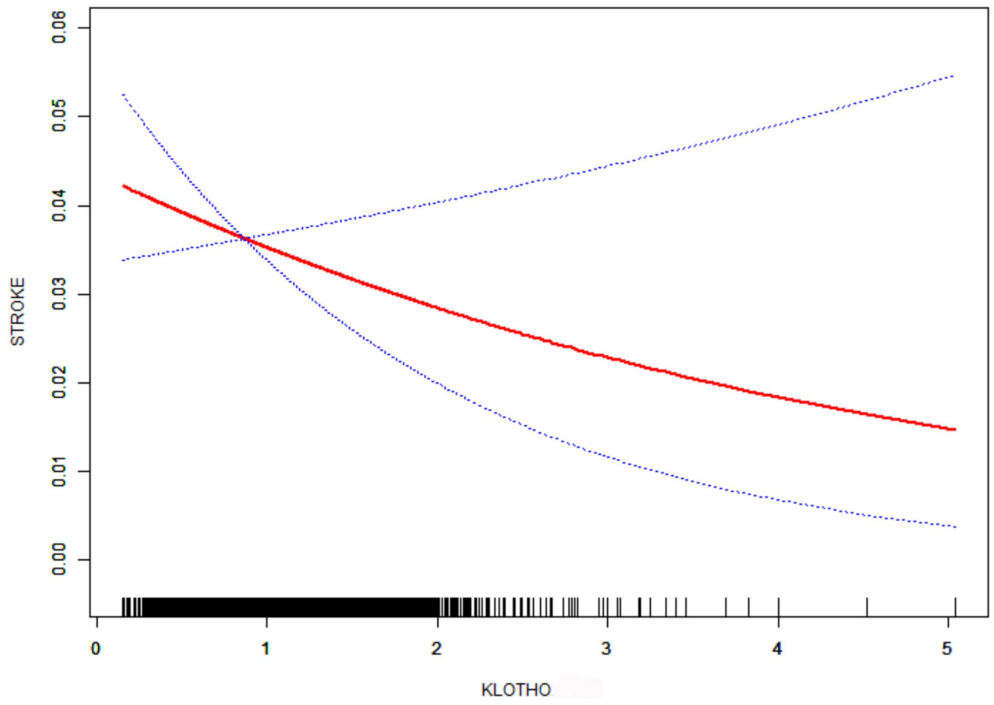

FIGURE 2
Smooth curve fitting. Age, Gender, Race, BMI, Family members, DM, HBP, HDL, LDL, Phosphorus, TC, TG, Drinker, and Smoker were adjusted.

significant role in neurological disorders. Then, with regard to stroke, the most common disorder in the field of neurology, whether klotho plays a significant role in its pathogenesis and offers a certain degree of neuroprotection, or whether klotho can act as a predictive factor or contribute to the rehabilitation of stroke patients, are the issues that researchers aim to address.

In an analysis of a large-scale database, it was also discovered that the reduction of klotho levels has a certain correlation with the high prevalence of hyperlipidemia. It is considered that the potential mechanisms underlying this negative correlation may include three possibilities: anti-inflammatory action, insulin resistance, and antioxidant effects (31). klotho protein is capable of participating in and influencing lipid metabolism, and elevated blood lipids (particularly the increase of LDL) constitute a crucial factor for atherosclerosis and cerebral artery stenosis, which subsequently give rise to stroke. Cerebral ischemic preconditioning (CIP) is capable of inducing cerebral ischemic tolerance and protecting neurons against potential ischemic damage (32, 33). Previous studies have revealed that the upregulation of klotho is capable of preventing ischemic injury in the brain (34, 35). Consequently, two animal experiments conducted in 2022 and 2024 revealed that the upregulation of klotho was capable of suppressing apoptosis and was conducive to the neuroprotection induced by CIP (16, 17). This could also be the reason why klotho contributes to neuroprotection and the prevention of stroke, and there may exist a

TABLE 4 Subgroups analysis.

Subgroup	klotho [OR (95%CI)]	P
Gender		0.5058
Male	0.89 (0.56, 1.39)	
Female	0.71 (0.45, 1.12)	
Age		0.0630
≤60	0.52 (0.30, 0.92)	
>60	1.00 (0.67, 1.47)	
Race		0.1173
Mexican American	1.20 (0.59, 2.43)	
Other Hispanic	0.27 (0.08, 0.92)	
Non-Hispanic White	0.76 (0.44, 1.33)	
Non-Hispanic Black	1.04 (0.62, 1.74)	
Other Race	0.29 (0.06, 1.40)	
Family members		0.8289
1	0.63 (0.31, 1.28)	
2	0.91 (0.55, 1.53)	
3	0.93 (0.42, 2.06)	
4	0.74 (0.28, 2.01)	
5	0.43 (0.10, 1.83)	
6	1.65 (0.25, 11.11)	
7 or more	0.27 (0.02, 3.80)	
HBP		0.9660
No	0.81 (0.38, 1.73)	
Yes	0.80 (0.56, 1.13)	
DM		0.6148
No	0.74 (0.49, 1.11)	
Yes	0.88 (0.52, 1.49)	
Smoker		0.3693
No	0.96 (0.58, 1.58)	
Yes	0.71 (0.46, 1.08)	
Drinker		0.5382
No	0.69 (0.40, 1.19)	
Yes	0.85 (0.57, 1.27)	
BMI		0.7833
≤18.5	2.58 (0.10, 69.21)	
>18.5, ≤24	0.86 (0.36, 2.04)	
>24	0.78 (0.55, 1.11)	

Age, Gender, Race, BMI, Family members, DM, HBP, HDL, LDL, Phosphorus, TC, TG, Drinker, and Smoker were adjusted.

potential therapeutic approach. Ferroptosis is a type of cell death where iron overload results in the accumulation of lethal levels of lipid hydroperoxides, thereby causing cell death (36, 37). Previous studies have also indicated that following cerebral ischemia, inflammation promptly occurs in the vascular system, generating pro-inflammatory signals and activating immune cells, thereby aggravating neuronal injury (38, 39). However, the augmented expression of klotho is capable of regulating energy metabolism within the brain, mitigating ferroptosis of neurons, and suppressing inflammatory responses, etc. (40–42). The klotho protein, functioning as a coreceptor for fibroblast growth factor 21 (FGF21), plays a critical role in modulating cellular aging processes mediated by human cerebral vascular smooth muscle cells. This cooperative interaction enhances mitochondrial pathway activity while suppressing p53 signaling, ultimately contributing to reduced prevalence of stroke and other neurological disorders (43). Emerging evidence from these investigations and subsequent human studies reveals that klotho's unique neuroprotective mechanism against stroke pathogenesis appears to be multifactorial. The protein primarily exerts its effects through coordinated suppression of oxidative stress and inflammatory cascades (44–47). Specifically, klotho demonstrates the capacity to regulate endothelial cell homeostasis and attenuate reactive oxygen species (ROS) generation, and inhibit apoptotic signaling while downregulating the expression of adhesion molecules and pro-inflammatory cytokines through multiple intercellular pathways.

However, whether serum klotho protein can act as a clinically applicable indicator for predicting Stroke, or whether the artificial and rational overexpression of klotho protein can prevent, treat or ameliorate the sequelae brought about by Stroke, these are issues that might require resolution in subsequent clinical studies. Compared to previous studies, our research presents several advantages in the following aspects: (1) This is the first clinical data study based on a large sample size from the NHANES database. As a comprehensive dataset collected over an extended period, NHANES encompasses objective health data from all racial groups within the U.S. population, ensuring representativeness and mitigating selection bias. Furthermore, we have thoroughly considered sample design and weighting in our data analysis. This enhances the representativeness and credibility of our research findings. (2) Due to the influence of potential confounding factors in observational studies, we employed a multivariable logistic regression model in our data analysis. This approach allowed us to control for a range of relevant covariates and comprehensively elucidate the correlation between serum klotho levels and the prevalence of stroke. (3) We also conducted stratified and interaction effect analyses, which yielded consistent conclusions regarding the correlation between serum klotho levels and stroke prevalence across different subgroups. This demonstrates the robustness of the results in the present investigation. However, our study does have certain limitations: (1) This study has limitations as a non-prospective investigation. The detection method employed for klotho was not the gold standard (immunoprecipitation immunoblotting), thus introducing potential measurement bias (48). Due to the cross-sectional design of the research, we can only establish a correlation between serum klotho levels and the prevalence of stroke, without being able to determine a causal relationship. Further prospective studies with larger sample sizes are needed to clarify this causality. (2) The selection of stroke patients was limited by the absence of stroke subtype classification in the NHANES database, resulting in potential heterogeneity of cerebrovascular pathology that precluded definitive confirmation of ischemic stroke diagnoses, thereby introducing potential selection bias. (3) The limitations of the data included in the database prevent us from accounting for all potential confounding variables that may influence the results, as well as other possible contributing factors. (4) Given that NHANES primarily relies on data from the U.S. population and its ethnic groups, further investigations are required to ascertain whether our findings are applicable to specific circumstances in other countries and among different ethnicities.

5 Conclusion

In summary, our research indicates a significant negative correlation between serum klotho levels and the prevalence of stroke. Furthermore, lower serum klotho levels are independently associated with a higher prevalence of stroke. This raises the possibility that supplementation with klotho protein may prevent or treat stroke. However, it is important to note that the current findings only demonstrate correlation and do not establish causation. Therefore, further large-scale, multi-ethnic prospective studies are needed to confirm the causal relationship between serum klotho levels and stroke prevalence.

Data availability statement

The original contributions presented in the study are included in the article/supplementary material, further inquiries can be directed to the corresponding authors.

Ethics statement

The studies involving humans were approved by National Center for Health Statistics (NCHS) of the US Centers for Disease Control and Prevention (CDC). The studies were conducted in accordance with the local legislation and institutional requirements. The participants provided their written informed consent to participate in this study.

Author contributions

HX: Conceptualization, Data curation, Formal analysis, Investigation, Methodology, Writing – original draft, Writing – review & editing. YD: Data curation, Formal analysis, Validation, Writing – review & editing. YZ: Conceptualization, Data curation, Investigation, Writing – original draft. JL: Data curation, Writing – original draft. SZ: Software, Writing – original draft. DW: Formal analysis, Writing – review & editing. XX: Supervision, Writing – review & editing. XM: Validation, Writing – review & editing. CW: Data curation, Supervision, Writing – original draft. SX: Data curation, Formal analysis, Supervision, Writing – review & editing.

Funding

The author(s) declare that no financial support was received for the research and/or publication of this article.

Conflict of interest

The authors declare that the research was conducted in the absence of any commercial or financial relationships that could be construed as a potential conflict of interest.

Generative AI statement

The author(s) declare that no Gen AI was used in the creation of this manuscript.

Publisher's note

All claims expressed in this article are solely those of the authors and do not necessarily represent those of their affiliated organizations, or those of the publisher, the editors and the reviewers. Any product that may be evaluated in this article, or claim that may be made by its manufacturer, is not guaranteed or endorsed by the publisher.

References

1. Feigin VL, Brainin M, Norrving B, Martins S, Sacco RL, Hacke W, et al. World stroke organization (WSO): global stroke fact sheet 2022. *Int J Stroke*. (2022) 17:18–29. doi: 10.1177/17474930211065917

2. Herpich F, Rincon F. Management of Acute Ischemic Stroke. *Crit Care Med*. (2020) 48:1654–63. doi: 10.1097/ccm.0000000000004597

3. Ekker MS, Verhoeven JI, Vaartjes I, van Nieuwenhuizen KM, Klijn CJM, de Leeuw F-E. Stroke incidence in young adults according to age, subtype, sex, and time trends. *Neurology*. (2019) 92:7533. doi: 10.1212/wnl.0000000000007533

4. Bhatt N, Malik AM, Chaturvedi S. Stroke in young adults. *Neurol Clin Pract*. (2018) 8:501–6. doi: 10.1212/cpj.0000000000000522

5. Potter TBH, Tannous J, Vahidy FS. A contemporary review of epidemiology, risk factors, etiology, and outcomes of premature stroke. *Curr Atheroscler Rep*. (2022) 24:939–48. doi: 10.1007/s11883-022-01067-x

6. Xu Y, Sun Z. Molecular basis of klotho: from gene to function in aging. *Endocr Rev*. (2015) 36:174–93. doi: 10.1210/er.2013-1079

7. Makoto Kuro-o YM, Aizawa H, Kawaguchi H, Suga T, Utsugi T, Ohyama Y, et al. Mutation of the mouse klotho gene leads to a syndrome resembling ageing. *Nature*. (1997) 390:45–51. doi: 10.1038/36285

8. Yutaka Matsumura HA, Shiraki-Iida T, Kuro-o M, Nabeshima Y-i. HumanklothoGene and its two transcripts encoding membrane and SecretedklothoProtein. *Biochem Biophys Res Commun*. (1997) 242:626–30. doi: 10.1006/bbrc.1997.8019

9. Neyra JA, Hu MC, Moe OW. klotho in clinical nephrology. *Clin J Am Soc Nephrol*. (2021) 16:162–76. doi: 10.2215/cjn.02840320

10. Cai J, Zhang L, Chen C, Ge J, Li M, Zhang Y, et al. Association between serum klotho concentration and heart failure in adults, a cross-sectional study from NHANES 2007–2016. *Int J Cardiol*. (2023) 370:236–43. doi: 10.1016/j.ijcard.2022.11.010

11. Lanzani C, Citterio L, Vezzoli G. klotho: a link between cardiovascular and non-cardiovascular mortality. *Clin Kidney J*. (2020) 13:926–32. doi: 10.1093/ckj/sfaa100

12. Tang A, Zhang Y, Wu L, Lin Y, Lv L, Zhao L, et al. klotho's impact on diabetic nephropathy and its emerging connection to diabetic retinopathy. *Front Endocrinol*. (2023) 14:1180169. doi: 10.3389/fendo.2023.1180169

13. Zhao Y, Zeng CY, Li XH, Yang TT, Kuang X, Du JR. klotho overexpression improves amyloid-β clearance and cognition in the APP/PS1 mouse model of Alzheimer's disease. *Aging Cell*. (2020) 19:e13239. doi: 10.1111/acel.13239

14. Dubal DB, Yokoyama JS, Zhu L, Broestl L, Worden K, Wang D, et al. Life extension factor klotho enhances cognition. *Cell Rep*. (2014) 7:1065–76. doi: 10.1016/j.celrep.2014.03.076

15. Castner SA, Gupta S, Wang D, Moreno AJ, Park C, Chen C, et al. Longevity factor klotho enhances cognition in aged nonhuman primates. *Nat Aging*. (2023) 3:931–7. doi: 10.1038/s43587-023-00441-x

16. Liu X-Y, Zhang L-Y, Wang X-Y, Li S-C, Hu Y-Y, Zhang J-G, et al. STAT4-mediated klotho up-regulation contributes to the brain ischemic tolerance by cerebral ischemic preconditioning via inhibiting neuronal pyroptosis. *Mol Neurobiol*. (2023) 61:2336–56. doi: 10.1007/s12035-023-03703-2

17. Zhang L-Y, Liu X-Y, Su AC, Hu Y-Y, Zhang J-G, Xian X-H, et al. klotho upregulation via PPARγ contributes to the induction of brain ischemic tolerance by cerebral ischemic preconditioning in rats. *Cell Mol Neurobiol*. (2022) 43:1355–67. doi: 10.1007/s10571-022-01255-y

18. Zhu M, Wang X, Peng Z, Yan W, Deng Q, Li M, et al. The role of the estimated glomerular filtration rate and body roundness index in the risk assessment of uric acid-lowering therapy-resistant gout in U.S. adults: evidence from the National Health and nutrition examination survey (2007–2018). *Ren Fail*. (2025) 47:1398. doi: 10.1080/0886022x.2024.2441398

19. Jiang YA, Shen J, Chen P, Cai J, Zhao Y, Liang J, et al. Association of triglyceride glucose index with stroke: from two large cohort studies and Mendelian randomization analysis. *Int J Surg*. (2024) 110:5409–16. doi: 10.1097/js9.0000000000001795

20. Shi R, Tian Y, Tian J, Liu Q, Zhang J, Zhang Z, et al. Association between the systemic immunity-inflammation index and stroke: a population-based study from NHANES (2015–2020). *Sci Rep*. (2025) 15:381. doi: 10.1038/s41598-024-83073-4

21. Zheng Y, Huang C, Jin J, Zhao Y, Cui H, Wei C. Association between stroke and relative fat mass: a cross-sectional study based on NHANES. *Lipids Health Dis*. (2024) 23:354. doi: 10.1186/s12944-024-02351-2

22. Mao Y, Weng J, Xie Q, Wu L, Xuan Y, Zhang J, et al. Association between dietary inflammatory index and stroke in the US population: evidence from NHANES 1999–2018. *BMC Public Health*. (2024) 24:50. doi: 10.1186/s12889-023-17556-w

23. Jiang L, Guo T, Zhong X, Cai Y, Yang W, Zhang J. Serum protein α-klotho mediates the association between lead, mercury, and kidney function in middle-aged and elderly populations. *Environ Health Prev Med*. (2025) 30:10–0. doi: 10.1265/ehpm.24-00296

24. Campos-Obando N, Lahousse L, Brusselle G, Stricker BH, Hofman A, Franco OH, et al. Serum phosphate levels are related to all-cause, cardiovascular and COPD mortality in men. *Eur J Epidemiol*. (2018) 33:859–71. doi: 10.1007/s10654-018-0407-7

25. Han Z, Song Y, Qin C, Zhou H, Han D, Yan S, et al. S-Nitrosylation of Dexras1 controls post-stroke recovery via regulation of neuronal excitability and dendritic remodeling. *CNS Neurosci Ther*. (2025) 31:e70199. doi: 10.1111/cns.70199

26. Sun E, Torices S, Osborne OM, Toborek M. Microvascular dysfunction, mitochondrial reprogramming, and inflammasome activation as critical regulators of ischemic stroke severity induced by chronic exposure to prescription opioids. *J Neurosci*. (2025) 45:e0614242024. doi: 10.1523/jneurosci.0614-24.2024

27. Chen G, Liu Y, Goetz R, Fu L, Jayaraman S, Hu M-C, et al. α-klotho is a non-enzymatic molecular scaffold for FGF23 hormone signalling. *Nature*. (2018) 553:461–6. doi: 10.1038/nature25451

28. Sun F, Liang P, Wang B, Liu W. The fibroblast growth factor–klotho axis at molecular level. *Open Life Sci*. (2023) 18:655. doi: 10.1515/biol-2022-0655

29. Wang X, Sun Z. RNAi silencing of brain klotho potentiates cold-induced elevation of blood pressure via the endothelin pathway. *Physiol Genomics*. (2010) 41:120–6. doi: 10.1152/physiolgenomics.00192.2009

30. Ohsawa Y, Ohtsubo H, Munekane A, Ohkubo K, Murakami T, Fujino M, et al. Circulating α-klotho counteracts transforming growth factor-β–induced sarcopenia. *Am J Pathol*. (2023) 193:591–607. doi: 10.1016/j.ajpath.2023.01.009

31. Yan S, Luo W, Lei L, Zhang Q, Xiu J. Association between serum klotho concentration and hyperlipidemia in adults: a cross-sectional study from NHANES 2007–2016. *Front Endocrinol*. (2023) 14:1280873. doi: 10.3389/fendo.2023.1280873

32. Gidday JM. Cerebral preconditioning and ischaemic tolerance. *Nat Rev Neurosci*. (2006) 7:437–48. doi: 10.1038/nrn1927

33. Steiger HJ, Hänggi D. Ischaemic preconditioning of the brain, mechanisms and applications. *Acta Neurochir*. (2006) 149:1–10. doi: 10.1007/s00701-006-1057-1

34. Karizmeh MS, Shabani M, Shabani M, Sardari M, Babaei JF, Nabavizadeh F, et al. Preconditioning exercise reduces hippocampal neuronal damage via increasing klotho expression in ischemic rats. *Brain Res Bull*. (2022) 188:133–42. doi: 10.1016/j.brainresbull.2022.07.022

35. Long F-Y, Shi M-Q, Zhou H-J, Liu D-L, Sang N, Du J-R. klotho upregulation contributes to the neuroprotection of ligustilide against cerebral ischemic injury in mice. *Eur J Pharmacol*. (2018) 820:198–205. doi: 10.1016/j.ejphar.2017.12.019

36. Gowtham A, Chauhan C, Rahi V, Kaundal RK. An update on the role of ferroptosis in ischemic stroke: from molecular pathways to neuroprotection. *Expert Opin Ther Targets*. (2024) 28:1149–75. doi: 10.1080/14728222.2024.2446319

37. Wu X, Li Y, Zhang S, Zhou X. Ferroptosis as a novel therapeutic target for cardiovascular disease. *Theranostics*. (2021) 11:3052–9. doi: 10.7150/thno.54113

38. Alsbrook DL, Di Napoli M, Bhatia K, Biller J, Andalib S, Hinduja A, et al. Neuroinflammation in acute ischemic and hemorrhagic stroke. *Curr Neurol Neurosci Rep*. (2023) 23:407–31. doi: 10.1007/s11910-023-01282-2

39. He Y, Wang J, Ying C, Xu KL, Luo J, Wang B, et al. The interplay between ferroptosis and inflammation: therapeutic implications for cerebral ischemia-reperfusion. *Front Immunol*. (2024) 15:1482386. doi: 10.3389/fimmu.2024.1482386

40. Orellana AM, Mazucanti CH, dos Anjos LP, de Sá Lima L, Kawamoto EM, Scavone C. klotho increases antioxidant defenses in astrocytes and ubiquitin–proteasome activity in neurons. *Sci Rep*. (2023) 13:15080. doi: 10.1038/s41598-023-41166-6

41. Roig-Soriano J, Griñán-Ferré C, Espinosa-Parrilla JF, Abraham CR, Bosch A, Pallàs M, et al. AAV-mediated expression of secreted and transmembrane αklotho isoforms rescues relevant aging hallmarks in senescent SAMP8 mice. *Aging Cell*. (2022) 21:e13581. doi: 10.1111/acel.13581

42. Xu T, Zhu Q, Huang Q, Gu Q, Zhu Y, Tang M, et al. FGF21 prevents neuronal cell ferroptosis after spinal cord injury by activating the FGFR1/β-klotho pathway. *Brain Res Bull*. (2023) 202:110753. doi: 10.1016/j.brainresbull.2023.110753

43. Wang X-M, Xiao H, Liu L-L, Cheng D, Li X-J, Si L-Y. FGF21 represses cerebrovascular aging via improving mitochondrial biogenesis and inhibiting p53 signaling pathway in an AMPK-dependent manner. *Exp Cell Res*. (2016) 346:147–56. doi: 10.1016/j.yexcr.2016.06.020

44. Chen O, Woo HG, Chang Y, Ryu D-R, Song T-J. Plasma klotho concentration is associated with the presence, burden and progression of cerebral small vessel disease in patients with acute ischaemic stroke. *PLoS One*. (2019) 14:796. doi: 10.1371/journal.pone.0220796

45. Cui W, Leng B, Liu W, Wang G. Suppression of apoptosis in human umbilical vein endothelial cells (HUVECs) by klotho protein is associated with reduced endoplasmic reticulum oxidative stress and activation of the PI3K/AKT pathway. *Med Sci Monit*. (2018) 24:8489–99. doi: 10.12659/msm.911202

46. Rakugi H, Matsukawa N, Ishikawa K, Yang J, Imai M, Ikushima M, et al. Anti-oxidative effect of klotho on endothelial cells through cAMP activation. *Endocrine*. (2007) 31:82–7. doi: 10.1007/s12020-007-0016-9

47. Wei H, Li H, Song X, Du X, Cai Y, Li C, et al. Serum klotho: a potential predictor of cerebrovascular disease in hemodialysis patients. *BMC Nephrol*. (2019) 20:63. doi: 10.1186/s12882-019-1232-2

48. Drew DA, Ix JH, Sarnak MJ, Sidhu SS, Gianella F, Pastor J, et al. Performance of soluble klotho assays in clinical samples of kidney disease. *Clin Kidney J*. (2020) 13:235–44. doi: 10.1093/ckj/sfz085

frontiers | Frontiers in Neurology

TYPE Original Research
PUBLISHED 29 May 2025
DOI 10.3389/fneur.2025.1551364

OPEN ACCESS

EDITED BY
Leonard Yeo,
National University Health System, Singapore

REVIEWED BY
Ali Reza Malek,
St. Mary's Medical Center, United States
Qazi Zeeshan,
University of Pittsburgh Medical Center, United States

*CORRESPONDENCE
Xinyi Leng
✉ xinyi_leng@cuhk.edu.hk
Yuhua Fan
✉ fanyuhua@mail.sysu.edu.cn

†These authors have contributed equally to this work and share first authorship

RECEIVED 03 January 2025
ACCEPTED 30 April 2025
PUBLISHED 29 May 2025

CITATION
Xu X, Lan L, Li Z, Zhou W, Yang J, Leng X and Fan Y (2025) Associations of cerebral perfusion with infarct patterns and early neurological outcomes in symptomatic intracranial atherosclerotic stenosis. *Front. Neurol.* 16:1551364. doi: 10.3389/fneur.2025.1551364

Associations of cerebral perfusion with infarct patterns and early neurological outcomes in symptomatic intracranial atherosclerotic stenosis

Xiangming Xu[1†], Linfang Lan[1†], Zhuhao Li[2], Wenli Zhou[1], Jing Yang[1], Xinyi Leng[3*] and Yuhua Fan[1*]

[1]Department of Neurology, The First Affiliated Hospital of Sun Yat-sen University, Guangzhou, China, [2]Department of Radiology, The First Affiliated Hospital, Sun Yat-sen University, Guangzhou, China, [3]Department of Medicine and Therapeutics, Prince of Wales Hospital, The Chinese University of Hong Kong, Hong Kong, Hong Kong SAR, China

Objectives: Intracranial atherosclerotic stenosis (ICAS) is a major cause of ischemic stroke, with various infarct patterns. We aimed to investigate the cerebral perfusion features underlying different infarct patterns and the relationship between cerebral perfusion and early neurological outcomes in symptomatic ICAS (sICAS).

Methods: Patients with 50%–99% sICAS in the anterior circulation were enrolled. Cerebral perfusion measures were obtained from computed tomography (CT) perfusion images, including infarct core volumes, penumbra defined with Tmax values > 6 s and > 4 s, and penumbra-core mismatch. Infarct patterns on diffusion-weighted magnetic resonance imaging (MRI) were categorized into four categories: borderzone, perforator, territorial, and mixed patterns. A favorable early neurological outcome was a decrease in the National Institutes of Health Stroke Scale (NIHSS) of ≥1 point at discharge compared with admission.

Results: We recruited 144 patients (median age: 66 years; 61.8% male patients). Significant perfusion compromise was observed in patients with borderzone or territorial infarcts compared to those with perforator infarct patterns. Patients with a favorable early neurological outcome exhibited smaller volumes of penumbra and penumbra-core mismatch at baseline. A multivariate logistic regression analysis revealed that penumbra (defined by Tmax of >4 s)-core mismatch volume of >15 mL was independently associated with a lower chance of achieving a favorable early neurological outcome (adjusted odds ratio, 0.323; 95% confidence interval, 0.121–0.866; $p = 0.03$).

Conclusion: Hemodynamic compromise likely underlies borderzone and territorial cortical/subcortical infarcts in patients with sICAS. The penumbra-infarct core mismatch volume in CT perfusion, with Tmax of >4 s defining the penumbra, was associated with early neurological outcomes of sICAS patients.

KEYWORDS

intracranial atherosclerotic stenosis, cerebral perfusion, infarct patterns, neurological outcome, computed tomography perfusion

Introduction

Intracranial atherosclerotic stenosis (ICAS) represents a major cause of ischemic stroke and transient ischemic attack, particularly in the Chinese population (1, 2). Perfusion failure and artery-to-artery embolism are standard stroke mechanisms in ICAS (3). It has been reported that hemodynamic compromise and artery-to-artery embolism often interact, particularly in the borderzone regions of middle cerebral artery (MCA) stenosis, where impaired washout of emboli occurs (4, 5). Previous studies have also demonstrated perfusion impairment as an independent predictor for the risk of recurrent stroke in patients with symptomatic ICAS (sICAS). For example, the Vertebrobasilar Flow Evaluation and Risk of Transient Ischaemic Attack and Stroke (VERiTAS) study associated distal blood flow compromise, as measured by quantitative magnetic resonance angiography, with an increased risk of subsequent stroke in patients with sICAS in vertebrobasilar arteries (6).

In patients with extracranial or intracranial arterial occlusive disease, cerebral perfusion has been investigated for a long time using various imaging methods and parameters, such as oxygen extraction fraction in positron emission tomography (7) or cerebral vasoreactivity by transcranial Doppler (8). The above-mentioned earlier methods were unable to quantify the volume of brain tissue with ischemia or at risk of ischemia; however, there have been emerging methods for this purpose in recent years. For instance, the volume of tissue with time to the maximum of residue function (Tmax) of >6 s on computed tomography (CT)/magnetic resonance (MR) perfusion imaging has been used to quantify the penumbra tissue volume in recent studies (9, 10). Moreover, the penumbra-to-infarct core mismatch ratio has been used to gauge the amount of salvageable tissue that may benefit from reperfusion therapy (10). The clinical significance of these quantitative perfusion measures has been more often investigated in studies on hyperacute reperfusion therapy in ischemic stroke. However, there is limited evidence available on ICAS patients. A small-scale study ($n = 26$) found that a mismatch of ≥15 mL between penumbra (defined either by Tmax > 6 s or > 8 s) and infarct core was associated with neurological deterioration at 30 days in patients with anterior-circulation sICAS (11).

In the current study, we aimed to reveal the characteristics of cerebral perfusion in acute ischemic stroke patients with sICAS in the anterior circulation. We used quantitative perfusion measures in CT perfusion (CTP) to investigate their associations with the infarct topology and the early neurological outcomes.

Methods

Study design and subjects

This observational study was approved by the First Affiliated Hospital of Sun Yat-sen University Clinical Research Ethics Committee. Written informed consent was waived due to the retrospective study design. Patients with acute ischemic stroke were recruited from January 2017 to May 2022 at the First Affiliated Hospital of Sun Yat-sen University, based on the following inclusion criteria: (1) admission to the stroke unit within 14 days of symptom onset; (2) ischemic stroke attributable to 50–99% atherosclerotic stenosis of the intracranial portion of internal carotid artery (ICA) or M1 segment of MCA, as observed in computed tomography angiography (CTA); and (3) completion of a patient who underwent brain CTP and MRI examinations during hospitalization. Patients were excluded if they met any of the following criteria: (1) concurrent severe stenosis in extracranial arteries; (2) the occurrence of an index ischemic event attributed to non-atherosclerotic intracranial stenosis (e.g., Moyamoya disease, vasculitis, or dissection); (3) evidence of potential cardioembolic stroke (e.g., atrial fibrillation); (4) presence of a known arteriovenous malformation or aneurysm; or (5) unstable vital signs, impaired consciousness, malignant tumors or severe organ dysfunction.

Patient demographics, cardiovascular risk factors, and laboratory test results were collected. The neurological severity of the index stroke was evaluated using the National Institutes of Health Stroke Scale (NIHSS). The location and luminal stenosis of the culprit ICAS were determined based on reconstructed CTA using the warfarin–aspirin symptomatic intracranial disease (WASID) method (12). The severity of stenosis was categorized as moderate (50%–69%) and severe (70%–99%) (13).

Multimodal CT examination and assessment of cerebral perfusion

All patients underwent a comprehensive CT scan using a 320-detector row, 640-slice cone-beam multidetector CT scanner (Aquilion One, Toshiba Medical Systems, Japan). A whole-brain non-contrast CT scan was performed in a wide-volume mode, with five rotations and a detector width of 4 cm. Following the non-contrast CT scan, CTP was acquired by administering 40 mL of the contrast agent (Ultravist 370, Bayer HealthCare, Berlin, Germany) intravenously at a rate of 5 mL/s, accompanied by 40 mL of saline. The CTP acquisition parameters were as follows: 120 kV, 112 mAs, and a total collimation width of 16 cm. The scan begins at 7 s after the contrast injection, employing a pulsed complete rotation technique with 19 time points acquired over 60 s. The 19 scans were divided into five parts: one scan at 7 s after contrast injection; three, six, and four scans with 2-s cycle time, respectively, starting at 11, 17, and 30 s; and five scans with 5-s cycle time starting at 40 s.

Perfusion parameters, including cerebral blood volume (CBV), cerebral blood flow (CBF), mean transit time (MTT), and Tmax, were automatically measured by the F-STROKE software version 1.0.18 (Neuroblem Ltd., Shanghai, China) in CTP source images. To offset the effects of inter-subject variations in absolute perfusion measures, we used relative perfusion measures in this study. Relative CBF (rCBF) was calculated as the ipsilesional CBF value divided by the CBF value in the contralesional MCA territory. Similarly, we calculated the relative MTT (rMTT) and relative Tmax (rTmax) of the ipsilesional MCA territory. The infarct core was defined as the ipsilesional brain region with CBF of <30%. The penumbra (the tissue at risk of ischemia) was defined with two thresholds in Tmax, that is, the area with Tmax of >6 s and of >4 s in the MCA territory. The penumbra-core mismatch

Abbreviations: CI, Confidence interval; CTP, CT perfusion; ICAS, Intracranial atherosclerotic stenosis; MCA, Middle cerebral artery; NIHSS, National Institutes of Health Stroke Scale; OR, Odds ratio; rCBF, Relative cerebral blood flow; rCBV, Relative cerebral blood volume; rMTT, Relative mean transit time; rTmax, Relative time to the maximum of residue function; sICAS, Symptomatic intracranial atherosclerotic stenosis.

volume was calculated by the penumbra volume minus the infarct core volume. An unfavorable perfusion pattern was defined as a penumbra-core mismatch volume of 15 mL or more.

Assessment of infarct topology

Two investigators (X. Xu and L. Lan) independently assessed and recorded the infarct topology of the index stroke on diffusion-weighted MR imaging, based on the published arterial supply templates (14), categorizing the infarcts into borderzone, perforator, territorial, and mixed patterns (Figure 1). The borderzone pattern referred to infarcts in the internal and external borderzone areas. The perforator pattern was defined with an isolated acute infarct in the penetrating artery territory adjacent to the stenosed intracranial artery. The territorial pattern was described as one or more cortical or subcortical infarct(s) lying entirely in the index diseased intracranial artery, without involvement of the borderzone areas. A mixed pattern refers to the coexistence of two or more of these patterns. In cases of disagreement, the two investigators met and achieved a consensus.

Outcome measure

The treatment strategy for the index ischemic stroke followed the latest clinical guidelines. A favorable early neurological outcome was defined as a decrease in NIHSS of ≥ 1 point at discharge compared with the score on admission (15), assessed by the neurologist in charge. The independent investigators (X. Xu and J. Yang) assessed the interrater reliability in scoring NIHSS in 20 randomly selected patients. The results showed substantial inter-rater reliabilities with an intraclass correlation coefficient of 0.982 (95% confidence interval [CI]: 0.955–0.993). In consideration of the influence of reperfusion therapies on the perfusion status and patients' outcomes, we excluded patients who received endovascular or intravenous reperfusion treatment from the analysis of the relationship between cerebral perfusion metrics and the outcome.

Statistical analyses

Data are presented as medians [interquartile range (IQR) or numbers (percentage)]. For comparison of the variables between groups with different infarct patterns, the Kruskal–Wallis test was used for continuous variables, and Pearson's chi-squared test or Fisher's exact method was used for categorical variables. The Benjamini–Krieger–Yekutieli two-stage procedure was used *post-hoc* to control the false discovery rate (FDR), with a q-value threshold set to 0.05. A comparison of variables between the groups with or without a favorable early neurological outcome was conducted using the Mann–Whitney U test for continuous variables and Pearson's chi-squared test or Fisher's exact method for categorical variables. Binary logistic regression analyses were employed to examine the association between

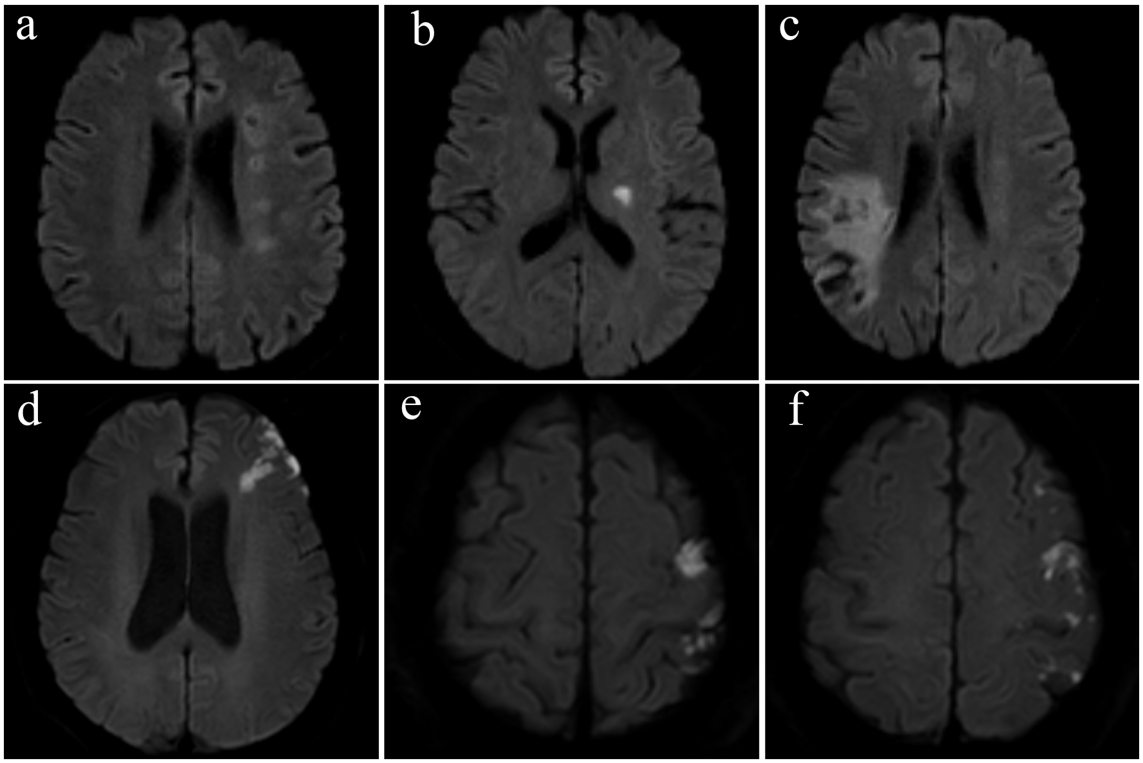

FIGURE 1
Representative examples of infarct patterns in four patients with symptomatic intracranial atherosclerotic stenosis. **(a)** Borderzone pattern, with chain-like, multiple infarcts in the internal borderzone, **(b)** perforator pattern, **(c)** territorial pattern, with wedge-shaped infarcts involving the cortical and subcortical territory of the inferior branch of the middle cerebral artery, and **(d–f)** a mixed pattern, with external borderzone infarcts shown in subpart **(d)** and multiple cortical infarcts shown in subparts **(e,f)**.

cerebral perfusion measures and the outcome. Odds ratio (OR) and 95% CIs were calculated for all models. In Model 1, adjustments were made for age, NIHSS score at admission, and other variables with a *p*-value of <0.05 in univariate comparisons. Model 2 included the onset to the CTP period based on Model 1. All statistical analyses were performed in SPSS (version 23.0, IBM, Inc., United States). The level of statistical significance was a *p*-value of <0.05 (two-sided).

Results

Patients' characteristics

A total of 144 acute stroke patients with sICAS were enrolled in the study (Figure 2), with a median age of 66 years and 61.8% being male. The median NIHSS at admission was 4 (IQR: 2–7). The most frequently observed infarct pattern was the mixed pattern, all having mixed borderzone and territorial patterns ($n = 55$; 38.2%), followed by the perforator pattern ($n = 37$; 25.7%). There was a higher percentage of smokers in the territorial and mixed pattern groups. The degree of stenosis in the perforator pattern group was lower than that in other groups. Other baseline characteristics were not significantly different among these groups (Table 1).

Cerebral perfusion features in different infarct patterns

The median interval between stroke onset and CTP examination was 3 (IQR: 1–7) days. On average, the perfusion time was prolonged (rMTT and rTmax of >1.0), and cerebral blood volume (rCBV > 1.0) was higher in the ipsilesional than the contralateral MCA territory to the sICAS. Figure 3 illustrates the cerebral perfusion characteristics in a patient with a borderzone infarct pattern. Perfusion imaging was able to detect the infarct core in 50 patients, with a median volume of 0 (IQR: 0–0.87) mL. The penumbra-core mismatch volume defined by Tmax of >4 s was 54.3 mL (IQR: 4.5–110.7) and Tmax of >6 s was 1.9 mL (IQR: 0–38.5).

Among patients with different infarct patterns, significant differences were observed in the cerebral perfusion parameters, including rCBV, rMTT, rTmax, infarct core volume, and mismatch volume (Table 2). In pairwise comparisons, the territorial pattern group presented a larger infarct core volume than all other patterns. The penumbra-core mismatch volume, defined by a Tmax delay of >4 s or of >6 s, was significantly smaller in patients with a perforator pattern compared to all other patterns. However, there was no statistically significant difference in penumbra-core mismatch volume between the borderzone and territorial pattern groups.

Cerebral perfusion and early neurological outcomes

As mentioned above, the 27 patients who received endovascular or intravenous reperfusion treatment were excluded from the analysis due to the relationship between cerebral perfusion metrics and the outcome, resulting in a total of 117 patients in such analyses. The median interval between the two assessments of the NIHSS (at admission and discharge) was 11 (IQR: 9–14) days. Among 117 patients, 71 (60.7%) demonstrated a favorable early neurological outcome. The baseline data and cerebral perfusion parameters were compared between those with the outcome and those without the outcome (Table 3). Patients' characteristics at baseline were not significantly different between the two groups. Notably, patients with a favorable early neurological outcome had less severe luminal stenosis in the sICAS lesion (medians 80% vs. 88%; $p = 0.038$). Regarding the

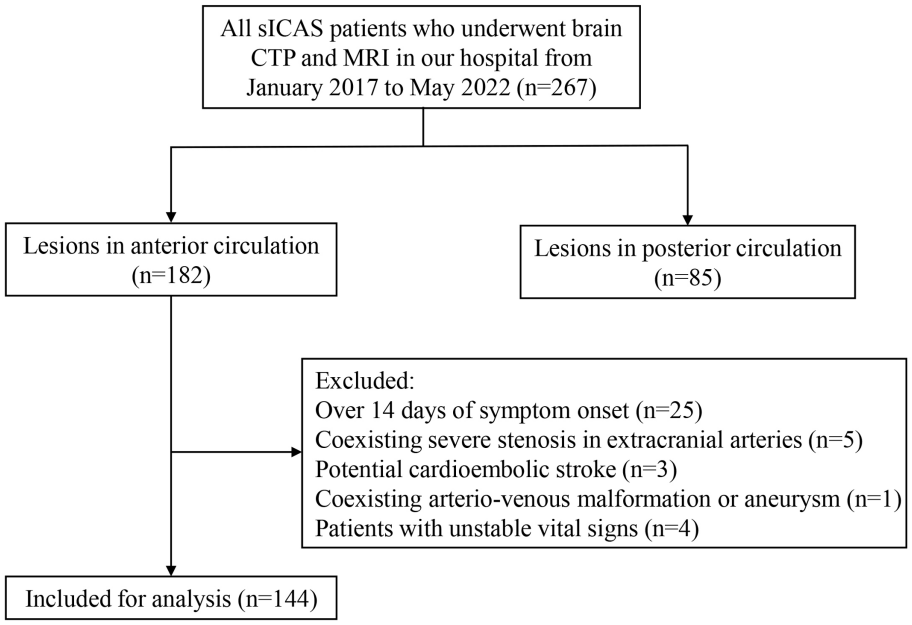

FIGURE 2
Flowchart of study patient enrollment. sICAS, symptomatic intracranial atherosclerotic stenosis; CTP, computed tomography (CT) perfusion.

TABLE 1 Baseline characteristics of patients with different infarct patterns.

Characteristics	All (*n* = 144)	Borderzone pattern (*n* = 28)	Perforator pattern (*n* = 37)	Territorial pattern (*n* = 24)	Mixed pattern (*n* = 55)	*p*-values
Age, years	66 (58–73)	68 (57–75)	66 (57–72)	64 (59–76)	66 (57.5–71.5)	0.944
Male	89 (61.8)	16 (57.1)	17 (45.9)	18 (75)	38 (69.1)	0.066
Vascular risk factors						
Smoking	65 (45.1)	8 (28.6)	13 (35.1)	14 (58.3)	30 (54.5)	0.041
Dyslipidemia	7 (4.9)	0 (0)	2 (5.4)	3 (12.5)	2 (3.6)	0.189
Hypertension	99 (68.8)	22 (78.6)	26 (70.3)	14 (58.3)	37 (67.3)	0.464
Diabetes mellitus	50 (34.7)	11 (39.3)	16 (43.2)	9 (37.5)	14 (25.5)	0.307
History of stroke/TIA	30 (20.8)	10 (35.7)	8 (21.6)	5 (20.8)	7 (12.7)	0.113
History of ischemic heart disease	6 (4.2)	1 (3.6)	2 (5.4)	0 (0)	3 (5.5)	0.837
SBP, mmHg	148 (130–167)	154 (132–175)	150 (134–180)	148 (123–162)	145 (126–163)	0.178
DBP, mmHg	86 (76–96)	85 (78–97)	89 (80–97)	81 (66–93)	85 (74–96)	0.117
Onset to admission, days	2 (1–5)	2 (2–7)	1 (0.5–4)	1.3 (0.38–4)	3 (1–5.5)	0.106
NIHSS at admission	4 (2–7)	4 (2–8)	4 (2–5)	4 (3–8)	4 (3–8)	0.209
NIHSS at admission >4	59 (41)	10 (35.7)	14 (37.8)	10 (41.7)	25 (45.5)	0.818
Laboratory test results						
Fasting Glucose, mmol/L	5.2 (4.6–7.4)	7.2 (4.8–8.2)	6.1 (4.6–7.4)	5.1 (4.6–7.4)	5.1 (4.6–6.4)	0.277
HbA1c, mmol/L	6.1 (5.5–7.7)	6.5 (5.7–8.1)	6.9 (5.5–8)	6.2 (5.5–6.7)	6 (5.4–7.0)	0.454
Triglyceride, mmol/L	1.3 (1–1.9)	1.7 (1.2–2.1)	1.4 (1.1–2.3)	1.1 (0.9–1.6)	1.3 (1–1.8)	0.24
HDL, mmol/L	1 (0.9–1.2)	1 (0.9–1.2)	1 (0.9–1.2)	1 (0.9–1.1)	1 (0.8–1.1)	0.498
LDL, mmol/L	2.8 (2.3–3.5)	3 (2.2–3.5)	2.8 (2.2–3.4)	2.7 (2.3–3.7)	2.7 (2.3–3.5)	0.97
Severity of sICAS						
Degree of stenosis	80 (62–99)	90 (70–99)	70 (50–90)	90 (70–99)	90 (69–99)	0.004
Severe stenosis (70–99%)	108 (75)	23 (82.1)	22 (59.5)	22 (91.7)	41 (74.5)	0.028
Recanalization therapy						
IV rtPA	3 (2.1)	0 (0)	2 (5.4)	0 (0)	1 (1.8)	0.837
EVT	24 (16.7)	7 (25)	4 (10.8)	4 (16.7)	9 (16.4)	0.116
Hospital stays, days	12 (9–14)	12 (8–17)	11 (8–14)	12 (8–15)	12 (9–14)	0.904

Data are median (IQR), or *n* (%). SBP, systolic blood pressure; DBP, diastolic blood pressure; NIHSS, National Institutes of Health Stroke Scale; TIA, transient ischemic attack; HbA1c, hemoglobin A1c; HDL, high-density lipoprotein cholesterol; LDL, low-density lipoprotein cholesterol; sICAS, symptomatic intracranial atherosclerotic stenosis; rtPA, recombinant tissue plasminogen activator; EVT, endovascular treatment.

cerebral perfusion parameters, no significant difference was observed in rCBV, rCBF, rMTT, rTmax, or infarct core volume between the two groups. However, the penumbra volume and penumbra-core mismatch volume were smaller, with fewer patients having an unfavorable perfusion pattern, defined with Tmax of >4 s or of 6 s, in patients with a favorable early neurological outcome than in those without.

A multivariate logistic regression analysis revealed that an unfavorable perfusion pattern defined with Tmax of >4 s was independently associated with lower odds of favorable early neurological outcomes, after adjusting for age, baseline NIHSS, stenosis degree of the sICAS lesion, and the onset to CTP time period (adjusted OR: 0.323; 95% CI: 0.121–0.866; $p = 0.03$). The unfavorable perfusion pattern defined with Tmax of >6 s was not significantly associated with the outcome (Table 4).

Discussion

This study revealed various cerebral perfusion characteristics among those with different infarct patterns in patients with acute ischemic stroke due to ICAS. Perfusion compromise was more likely to be observed in those with borderzone infarcts or territorial cortical/subcortical infarcts than in those with a single subcortical infarct in penetrating artery territory. Smaller volumes of penumbra (defined by Tmax > 4 s) and penumbra-infarct core mismatch at baseline were associated with a higher probability of achieving a favorable early neurological outcome upon discharge. This study reinforced cerebral perfusion compromise as an essential pathophysiological mechanism of stroke in ICAS, which may contribute to both borderzone and territorial infarcts and affect early outcomes of the patients.

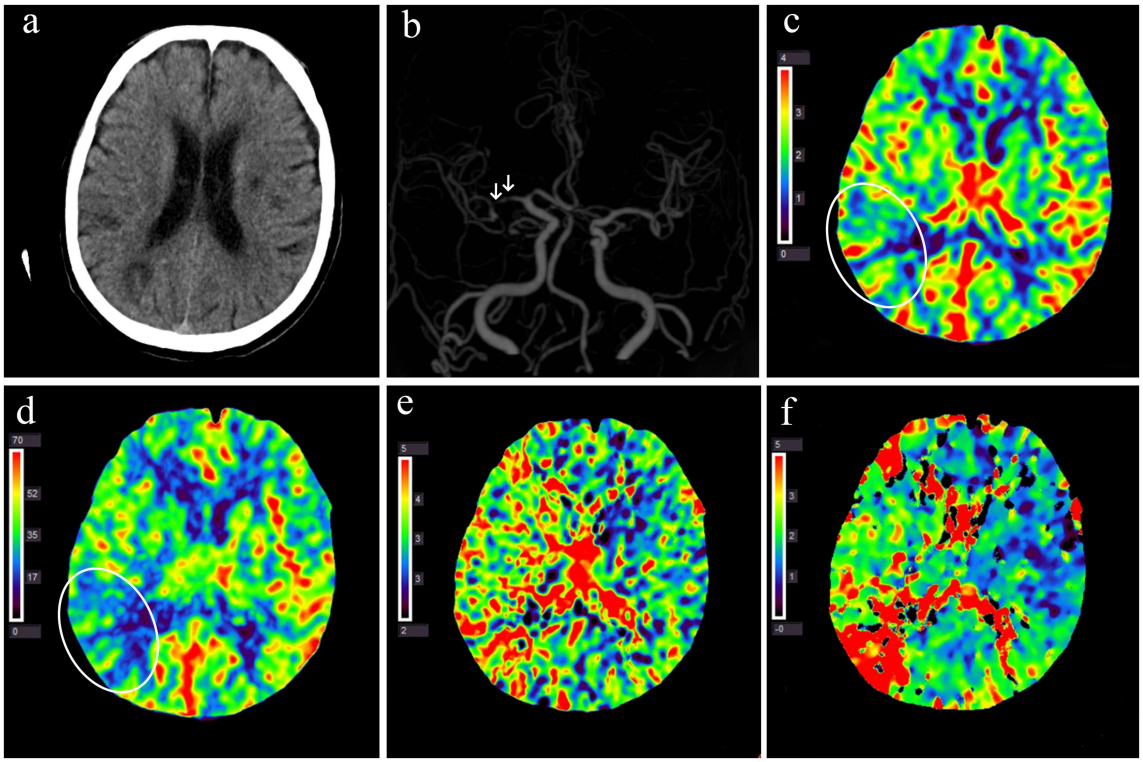

FIGURE 3
Multimodal CT examination of a patient with acute infarction at the right occipitoparietal junction 1 day after symptom onset. **(a)** Non-contrast CT shows multiple hypodense lesions in the right parieto-occipital lobe and bilateral basal ganglia. **(b)** CT angiography reveals multiple severe stenoses in the M1 segment of the right middle cerebral artery (white arrow). **(c–f)** Perfusion imaging demonstrates decreased CBV **(c)** and CBF **(d)** in the right occipitoparietal junction (white circles) and prolonged MTT **(e)** Tmax **(f)** in the right hemisphere. CBF, cerebral blood flow; CBV, cerebral blood volume; MTT, mean transit time; Tmax, the time to the maximum of residue function.

TABLE 2 Cerebral perfusion in patients with different infarct patterns.

Variable	All (*n* = 144)	Borderzone pattern (*n* = 28)	Perforator pattern (*n* = 37)	Territorial pattern (*n* = 24)	Mixed pattern (*n* = 55)	*p*-values
Onset to CTP, days	3 (1–7)	3 (2–7.8)	2 (0.5–6.5)	2 (0.4–6.8)	4 (1–8)	0.254
rCBF	1 (0.96–1.09)	1.05 (0.96–1.15)	1 (0.97–1.06)	1 (0.94–1.06)	1.02 (0.95–1.09)	0.6
rCBV	1.05 (0.99–1.15)	1.11 (1.01–1.26)	1.01 (0.97–1.09)	1.06 (1.02–1.12)	1.06 (0.99–1.18)	0.027
rMTT	1.05 (1.01–1.10)	1.07 (1.03–1.13)	1.01 (0.97–1.05)	1.08 (1.03–1.12)	1.05 (1.01–1.1)	<0.001
rTmax	1.36 (1.14–1.87)	1.5 (1.27–2.08)	1.2 (1.02–1.35)	1.6 (1.26–1.95)	1.5 (1.16–1.87)	0.001
Infarct core volume, mL	0 (0–0.87)	0 (0–0.25)	0 (0–0)	0.72 (0–7.17)	0 (0–1.04)	<0.001
Penumbra and mismatch defined with Tmax > 4 s						
Penumbra volume, mL	55.9 (4.6–112.2)	93.9 (41.1–142.8)	2.5 (0.5–19.4)	81.8 (50–111.1)	68.7 (12.8–124.2)	<0.001
Mismatch volume, mL	54.3 (4.5–110.7)	93.8 (40.5–142.2)	2.5 (0.5–19.4)	69.9 (44.4–107)	62.4 (12.8–124.2)	<0.001
Unfavorable perfusion pattern	94 (65.3%)	23 (82.1%)	9 (24.3%)	22 (91.7%)	40 (72.7%)	<0.001
Penumbra and mismatch defined with Tmax of >6 s						
Penumbra volume, mL	2.2 (0–45.2)	9.6 (0.2–63.3)	0 (0–0.05)	30.6 (1.3–57.9)	5.6 (0.1–54.8)	<0.001
Mismatch volume, mL	1.9 (0–38.5)	9.6 (0.2–63.3)	0 (0–0.05)	19.7 (1.2–44.4)	5.6 (0–54.5)	<0.001
Unfavorable perfusion pattern	53 (36.8%)	13 (46.4%)	3 (8.1%)	14 (58.3%)	23 (41.8%)	<0.001

Data are median (IQR), or *n* (%). CTP, CT perfusion; rCBF, relative cerebral blood flow; rCBV, relative cerebral blood volume; rMTT, relative mean transit time; rTmax, relative time to the maximum of residue function.

The relationship between impaired perfusion detected by non-invasive imaging and infarct patterns in patients with large artery occlusive disease has been investigated in previous studies (16–18). However, these earlier studies primarily focused on a specific infarct pattern, while data regarding the perfusion measures in those with different infarct patterns among patients with sICAS are scarce. This

TABLE 3 Characteristics of patients with and without a favorable early neurological outcome.

Characteristics	Favorable early neurological outcome (n = 71)	Otherwise (n = 46)	p-values
Age, years	65 (58–72)	67 (59–76)	0.401
Male sex	43 (60.6)	30 (65.2)	0.612
Vascular risk factors			
Smoking	30 (42.3)	24 (52.2)	0.293
Dyslipidemia	1 (1.4)	4 (8.7)	0.077
Hypertension	45 (63.4)	35 (76.1)	0.149
Diabetes mellitus	29 (40.8)	14 (30.4)	0.254
History of stroke/TIA	13 (18.3)	11 (23.9)	0.463
History of ischemic heart disease	1 (1.4)	3 (6.5)	0.298
SBP, mm Hg	150 (134–171)	151 (132–167)	0.953
DBP, mm Hg	88 (77–97)	88 (78–97)	0.643
Onset to admission, days	2 (1–5)	2 (1–6)	0.658
NIHSS at admission	4 (3–7)	3 (2–6)	0.105
Laboratory test			
Fasting glucose, mmol/L	5.3 (4.6–7.4)	5.2 (4.7–7.8)	0.526
HbA1c, mmol/L	6.2 (5.5–7.7)	6.1 (5.4–7)	0.559
Triglyceride, mmol/L	1.3 (1.0–2.1)	1.3 (1.1–1.8)	0.689
HDL, mmol/L	1 (0.9–1.2)	1 (0.8–1.1)	0.273
LDL, mmol/L	2.9 (2.3–3.7)	2.7 (2.2–3.5)	0.335
Severity of the sICAS			
Degree of stenosis	80 (58–90)	88 (68–99)	0.038
Severe stenosis (70–99%)	48 (67.6)	36 (78.3)	0.211
Hospital stays, days	11 (9–14)	11 (8–14)	0.754
Onset to CTP, days	3 (1–6)	5 (2–8.5)	0.084
rCBF	1.02 (0.97–1.09)	0.99 (0.96–1.07)	0.269
rCBV	1.05 (0.99–1.15)	1.04 (0.97–1.11)	0.584
rMTT	1.05 (1.00–1.08)	1.03 (1.00–1.10)	0.951
rTmax	1.2 (1.06–1.69)	1.4 (1.2–1.76)	0.142
Infarct core volume, mL	0 (0–0.27)	0 (0–0.57)	0.347
Penumbra and mismatch defined with Tmax of >4 s			
Penumbra volume, mL	23.2 (1.4–103)	76.5 (25.8–109.6)	0.041
Mismatch volume, mL	23.2 (1.4–100.5)	66.1 (25.8–100.2)	0.037
Unfavorable perfusion pattern	37 (52.1)	35 (76.1)	0.009
Penumbra and mismatch defined with Tmax > 6 s			
Penumbra volume, mL	0.13 (0–25.9)	5.8 (0.2–46.7)	0.012
Mismatch volume, mL	0.04 (0–18.8)	5.8 (0.01–39.1)	0.015
Unfavorable perfusion pattern	18 (25.4)	20 (43.5)	0.041

Data are median (IQR), or n (%). SBP, systolic blood pressure; DBP, diastolic blood pressure; NIHSS, National Institutes of Health Stroke Scale; CTP, CT perfusion; TIA, transient ischemic attack; HbA1c, hemoglobin A1c; HDL, high-density lipoprotein cholesterol; LDL, low-density lipoprotein cholesterol; rCBF, relative cerebral blood flow; rCBV, relative cerebral blood volume; rMTT, relative mean transit time; rTmax: relative time to the maximum of residue function.

study found that the penumbra-core mismatch volume, with the penumbra defined by the brain tissue with Tmax of >4 s or a Tmax delay of >6 s, was the smallest in the perforator infarct pattern group. This finding agrees with those of previous studies suggesting that a single subcortical infarct in the penetrating artery territory, in the presence of ICAS, represents a focal disease associated with the occlusion of a branch by the ICAS lesion, without global perfusion impairment (19, 20). In contrast, patients with borderzone infarct pattern displayed the most

TABLE 4 Results of multivariate logistic regression analysis on cerebral perfusion parameters in predicting a favorable early neurological outcome.

Variables	Model 1*		Model 2†	
	Adjusted OR (95% CI)	*p*	Adjusted OR (95% CI)	*p*
Mismatch volume defined by Tmax of >4 s, mL	0.993 (0.985–1.002)	0.13	0.993 (0.984–1.002)	0.12
Unfavorable perfusion pattern defined with Tmax of >4 s	0.354 (0.136–0.923)	0.03	0.323 (0.121–0.866)	0.03
Mismatch volume defined by Tmax of >6 s, mL	0.997 (0.983–1.011)	0.68	0.997 (0.983–1.012)	0.71
Unfavorable perfusion pattern defined with Tmax of >6 s	0.505 (0.203–1.258)	0.14	0.493 (0.195–1.248)	0.14

OR, odds ratio; CI, confidence interval. *Model 1: Multivariable binary logistic regression model after adjusting for age, NIHSS score at admission, and stenosis degree of the sICAS lesion. †Model 2: Model 1 after adjusting for the onset of the CTP time period.

significant hemodynamic compromise in CTP in this study, aligning with previous studies that have strongly associated internal borderzone infarctions to a hemodynamic mechanism (16). Another interesting finding of this study was the comparable penumbra and penumbra-core mismatch volumes in patients with territorial and borderzone infarct patterns. Artery-to-artery embolism due to a vulnerable atherosclerotic plaque's rupture has been generally considered an underlying mechanism of territorial cortical/subcortical infarcts in sICAS (21). This study provides additional evidence supporting the theory that hypoperfusion impairs the ability to clear small emboli stranded in distal territories (22). Hence, the affected patients may be more likely to have territorial infarcts (23).

Few studies investigated the relationships between cerebral perfusion metrics and early neurological outcomes in sICAS patients. In this study, univariate analyses demonstrated that patients with a smaller penumbra and a smaller penumbra-core mismatch volume, defined by Tmax of >4 s and of >6 s, were more likely to have a favorable early neurological outcome. Further multivariate logistic regression analysis showed that an unfavorable perfusion pattern defined with Tmax of >4 s, but not of >6 s, was independently associated with a favorable early neurological outcome after adjusting for age, baseline NIHSS, stenosis degree of the sICAS lesion, and the onset to CTP period. The finding differs from that of a previous study ($n = 26$), as mentioned above, which reported that a penumbra (defined using Tmax of >6 s or of >8 s)-core mismatch volume of >15 mL was associated with neurological deterioration at 30 days, but not when Tmax of >4 s was used in defining the penumbra (11). The inconsistency of the study findings could be attributed to various study populations (Chinese vs. mostly Caucasians), different sample sizes, or the more significant perfusion impairment in patients involved in the previous study (e.g., the median mismatch volumes defined by Tmax of >4 s in the two groups in this study were 23.2 and 66.1 mL; however, the median in the two groups in the previous study were 16.6 and 120 mL). In another recent study of sICAS patients ($n = 107$), the volume of the median Tmax of >6 s was 0 mL (IQR: 0–15) before angioplasty ± stenting therapy (comparable with the current study with a median of 2.2 mL), which was 0 (IQR: 0–0) after the endovascular treatment. However, the volume of the median Tmax of >4 s changed from 74 (IQR: 28–178) to 22 mL (IQR: 0–101) with angioplasty ± stenting therapy. Therefore, the study concluded that the volume of Tmax of >4 s may be more suitable than Tmax of >6 s to quantify perfusion compromise in sICAS patients (24). As these perfusion metrics were derived from hyperacute reperfusion therapy studies, further studies are needed to explore the optimal metrics and thresholds in assessing the perfusion status and predicting the outcomes in sICAS patients.

Our study provides valuable insights into the significance of penumbra-core mismatch on CT perfusion among patients with sICAS. We found that perfusion mismatch was associated not only with the borderzone infarct pattern but also with the territorial infarct pattern. Furthermore, a larger mismatch volume (defined by Tmax > 4 s) was less likely to be associated with a favorable early neurological outcome in sICAS patients. These findings underscore the significance of cerebral perfusion compromise in the risk stratification of sICAS patients and may further inform individualized treatment and secondary prevention. For instance, treatment strategies to restore cerebral perfusion, such as angioplasty ± stenting, may benefit patients with sICAS and hemodynamic compromise, which warrants further studies.

There were some limitations to this study. First, only patients with anterior-circulation stroke were included, as the infarct patterns in the posterior circulation differed and thus were challenging to group alongside anterior-circulation infarcts. Moreover, as mentioned above, the perfusion metrics measured in this study were mostly adopted from previous studies on hyperacute reperfusion therapy in ischemic stroke; it is unclear whether they are applicable or reliable in assessing the perfusion status in sICAS. The small infarct core and Tmax of >6 s volumes, as quantified in this and previous studies (11), may imply underestimation of the perfusion impairment based on these metrics in sICAS patients, which warrants validation with other imaging methods. Another limitation was that we used NIHSS reduction of ≥1 in defining the favorable early neurological outcome, with a cohort of patients with relatively mild neurological deficits (median admission NIHSS = 4; IQR: 2–7), but we demonstrated high inter-rater reliability in assessing the NIHSS score in this cohort. Furthermore, data were unavailable for the relationship between the cerebral perfusion metrics and long-term outcomes of the sICAS patients in this study, which warrants further investigation.

In conclusion, this study reinforced cerebral perfusion impairment as an important pathophysiological mechanism of stroke that was associated with borderzone and territorial cortical/subcortical infarcts in patients with sICAS. The penumbra-infarct core mismatch region in CTP, using Tmax of >4 s to define the penumbra, may represent the brain tissue at risk of ischemia in sICAS patients. This penumbra-core mismatch was associated with early neurological outcomes of sICAS patients.

Data availability statement

The raw data supporting the conclusions of this article will be made available by the authors upon reasonable request.

Ethics statement

The studies involving humans were approved by the First Affiliated Hospital of Sun Yat-sen University Clinical Research Ethics Committee. The studies were conducted in accordance with the local legislation and institutional requirements. The ethics committee/institutional review board waived the requirement of written informed consent for participation from the participants or the participants' legal guardians/next of kin due to the retrospective nature of the study.

Author contributions

XX: Conceptualization, Data curation, Formal analysis, Investigation, Methodology, Software, Visualization, Writing – original draft, Writing – review & editing. LL: Conceptualization, Data curation, Formal analysis, Funding acquisition, Investigation, Methodology, Supervision, Validation, Visualization, Writing – review & editing. ZL: Data curation, Resources, Software, Writing – review & editing. WZ: Data curation, Investigation, Writing – review & editing. JY: Data curation, Investigation, Writing – review & editing. XL: Conceptualization, Methodology, Project administration, Resources, Supervision, Validation, Writing – review & editing. YF: Conceptualization, Funding acquisition, Methodology, Project administration, Resources, Supervision, Validation, Writing – review & editing.

Funding

The author(s) declare financial support was received for the research and/or publication of this article. This study has received funding from the Young Scientists Fund (no. 81901187), the National Natural Science Foundation of China (no. 82071294), the Guangzhou Science-Brain Project (no. 2023A04J2193), and the Guangdong Basic and Applied Basic Research Project (Natural Science Foundation; no. 2314050003660).

Conflict of interest

The authors declare that the research was conducted in the absence of any commercial or financial relationships that could be construed as a potential conflict of interest.

The author(s) declared that they were an editorial board member of Frontiers, at the time of submission. This had no impact on the peer review process and the final decision.

Generative AI statement

The authors declare that no Gen AI was used in the creation of this manuscript.

Publisher's note

References

1. Wang Y, Zhao X, Liu L, Soo YOY, Pu Y, Pan Y, et al. Prevalence and outcomes of symptomatic intracranial large artery stenoses and occlusions in China: the Chinese intracranial atherosclerosis (CICAS) study. *Stroke*. (2014) 45:663–9. doi: 10.1161/STROKEAHA.113.003508

2. Ip B, Au L, Chan A, Fan F, Ip V, Ma SH, et al. Evolving ischemic stroke subtypes in 15 years: a hospital-based observational study. *Int J Stroke*. (2022) 17:444–54. doi: 10.1177/17474930211005953

3. Banerjee C, Chimowitz MI. Stroke caused by atherosclerosis of the major intracranial arteries. *Circ Res*. (2017) 120:502–13. doi: 10.1161/CIRCRESAHA.116.308441

4. Wong KS, Gao S, Chan YL, Hansberg T, Lam WWM, Droste DW, et al. Mechanisms of acute cerebral infarctions in patients with middle cerebral artery stenosis: a diffusion-weighted imaging and microemboli monitoring study. *Ann Neurol*. (2002) 52:74–81. doi: 10.1002/ana.10250

5. Schreiber S, Serdaroglu M, Schreiber F, Skalej M, Heinze HJ, Goertler M. Simultaneous occurrence and interaction of hypoperfusion and embolism in a patient with severe middle cerebral artery stenosis. *Stroke*. (2009) 40:e478–80. doi: 10.1161/STROKEAHA.109.549378

6. Amin-Hanjani S, Pandey DK, Rose-Finnell L, du X, Richardson DJ, Thulborn KR, et al. Effect of hemodynamics on stroke risk in symptomatic atherosclerotic Vertebrobasilar occlusive disease. *JAMA Neurol*. (2016) 73:178–85. doi: 10.1001/jamaneurol.2015.3772

7. Yamauchi H, Higashi T, Kagawa S, Nishii R, Kudo T, Sugimoto K, et al. Is misery perfusion still a predictor of stroke in symptomatic major cerebral artery disease? *Brain*. (2012) 135:2515–26. doi: 10.1093/brain/aws131

8. Liu Y, Li S, Tian X, Leung TW, Liu L, Liebeskind DS, et al. Cerebral haemodynamics in symptomatic intracranial atherosclerotic disease: a narrative review of the assessment methods and clinical implications. *Stroke Vasc Neurol*. (2023) 8:521–30. doi: 10.1136/svn-2023-002333

9. Dittrich TD, Sporns PB, Kriemler LF, Rudin S, Nguyen A, Zietz A, et al. Mechanical Thrombectomy versus best medical treatment in the late time window in non-DEFUSE-non-DAWN patients: a multicenter cohort study. *Stroke*. (2023) 54:722–30. doi: 10.1161/STROKEAHA.122.039793

10. Albers GW, Marks MP, Kemp S, Christensen S, Tsai JP, Ortega-Gutierrez S, et al. Thrombectomy for stroke at 6 to 16 hours with selection by perfusion imaging. *N Engl J Med*. (2018) 378:708–18. doi: 10.1056/NEJMoa1713973

11. Yaghi S, Khatri P, Prabhakaran S, Yeatts SD, Cutting S, Jayaraman M, et al. What threshold defines penumbral brain tissue in patients with symptomatic anterior circulation intracranial stenosis: an exploratory analysis. *J Neuroimaging*. (2019) 29:203–5. doi: 10.1111/jon.12577

12. Samuels OB, Joseph GJ, Lynn MJ, Smith HA, Chimowitz MI. A standardized method for measuring intracranial arterial stenosis. *AJNR Am J Neuroradiol*. (2000) 21:643–6.

13. Lan L, Leng X, Ip V, Soo Y, Abrigo J, Liu H, et al. Sustaining cerebral perfusion in intracranial atherosclerotic stenosis: the roles of antegrade residual flow and leptomeningeal collateral flow. *J Cereb Blood Flow Metab*. (2020) 40:126–34. doi: 10.1177/0271678X18805209

14. Tatu L, Moulin T, Bogousslavsky J, Duvernoy H. Arterial territories of the human brain: cerebral hemispheres. *Neurology*. (1998) 50:1699–708. doi: 10.1212/WNL.50.6.1699

15. Yang G, Hu R, Zhang C, Qian C, Luo QQ, Yung WH, et al. A combination of serum iron, ferritin and transferrin predicts outcome in patients with intracerebral hemorrhage. *Sci Rep*. (2016) 6:21970. doi: 10.1038/srep21970

16. Yong SW, Bang OY, Lee PH, Li WY. Internal and cortical border-zone infarction: clinical and diffusion-weighted imaging features. *Stroke*. (2006) 37:841–6. doi: 10.1161/01.STR.0000202590.75972.39

17. Li Y, Li M, Zhang X, Yang S, Fan H, Qin W, et al. Clinical features and the degree of cerebrovascular stenosis in different types and subtypes of cerebral watershed infarction. *BMC Neurol*. (2017) 17:166. doi: 10.1186/s12883-017-0947-6

18. Chaves CJ, Staroselskaya I, Linfante I, Llinas R, Caplan LR, Warach S. Patterns of perfusion-weighted imaging in patients with carotid artery occlusive disease. *Arch Neurol*. (2003) 60:237–42. doi: 10.1001/archneur.60.2.237

19. Caplan LR. Intracranial branch atheromatous disease: a neglected, understudied, and underused concept. *Neurology*. (1989) 39:1246–50. doi: 10.1212/WNL.39.9.1246

20. Baumgartner RW, Sidler C, Mosso M, Georgiadis D. Ischemic lacunar stroke in patients with and without potential mechanism other than small-artery disease. *Stroke*. (2003) 34:653–9. doi: 10.1161/01.STR.0000058486.68044.3B

21. Feng X, Chan KL, Lan L, Abrigo J, Liu J, Fang H, et al. Stroke mechanisms in symptomatic intracranial atherosclerotic disease: classification and clinical implications. *Stroke*. (2019) 50:2692–9. doi: 10.1161/STROKEAHA.119.025732

22. Caplan LR, Hennerici M. Impaired clearance of emboli (washout) is an important link between hypoperfusion, embolism, and ischemic stroke. *Arch Neurol*. (1998) 55:1475–82. doi: 10.1001/archneur.55.11.1475

23. Feng X, Fang H, Ip BYM, Chan KL, Li S, Tian X, et al. Cerebral hemodynamics underlying artery-to-artery embolism in symptomatic intracranial atherosclerotic disease. *Transl Stroke Res*. (2023) 15:572–9. doi: 10.1007/s12975-023-01146-4

24. Yan L, Hou Z, Fu W, Yu Y, Cui R, Miao Z, et al. Association of periprocedural perfusion non-improvement with recurrent stroke after endovascular treatment for intracranial atherosclerotic stenosis. *Ther Adv Neurol Disord*. (2022) 15:17562864221143178. doi: 10.1177/17562864221143178

frontiers | Frontiers in Neurology

TYPE Original Research
PUBLISHED 30 May 2025
DOI 10.3389/fneur.2025.1568401

OPEN ACCESS

EDITED BY
Haipeng Liu,
Coventry University, United Kingdom

REVIEWED BY
Nazareno Paolocci,
Johns Hopkins University, United States
Patricia Concepción García Suárez,
University of Kansas, United States
Maria Luisa Garo,
Mathsly Research, Italy
Abdur Raheem Khan,
Integral University, India

*CORRESPONDENCE
Birgit Vahlberg
✉ birgit.vahlberg@pubcare.uu.se
Sumonto Mitra
✉ Sumonto.mitra@ki.se

RECEIVED 10 March 2025
ACCEPTED 14 May 2025
PUBLISHED 30 May 2025

CITATION
Mitra S, Darreh-Shori T, Lundström E, Eriksson S, Cederholm T, Eriksdotter M and Vahlberg B (2025) Plasma cholinergic markers are associated with post-stroke walking recovery—revisiting the STROKEWALK study. *Front. Neurol.* 16:1568401. doi: 10.3389/fneur.2025.1568401

Plasma cholinergic markers are associated with post-stroke walking recovery—revisiting the STROKEWALK study

Sumonto Mitra[1]*, Taher Darreh-Shori[1], Erik Lundström[2], Staffan Eriksson[3,4,5], Tommy Cederholm[6], Maria Eriksdotter[1,7] and Birgit Vahlberg[3]*

[1]Division of Clinical Geriatrics, Department of Neurobiology, Care Sciences and Society (NVS), Karolinska Institutet, Center for Alzheimer Research, Huddinge, Sweden, [2]Department of Medical Sciences, Neurology, Uppsala University, Uppsala, Sweden, [3]Department of Public Health and Caring Sciences, Geriatrics, Uppsala University, Uppsala, Sweden, [4]Centre for Clinical Research, Sörmland, Uppsala University, Eskilstuna, Sweden, [5]Department of Community Medicine and Rehabilitation, Physiotherapy, Umeå University, Umeå, Sweden, [6]Department of Public Health and Caring Sciences, Clinical Nutrition and Metabolism, Uppsala University, Uppsala, Sweden, [7]Theme Inflammation and Aging, Karolinska University Hospital, Huddinge, Sweden

Introduction: Optimizing post-stroke rehabilitation strategies remains imperative for improving patient outcomes. Physical exercise, including outdoor walking, represents a promising intervention; however, its clinical efficacy, along with the utility of SMS-guided instructions to support adherence, requires further investigation. This study aims to elucidate the association of BDNF levels and cholinergic markers in the plasma of patients with previously reported post-stroke walking recovery (STROKEWALK study).

Methods: Post-stroke patients were randomly selected to receive SMS-guided exercise instructions (intervention group, n = 31) or not (control group, n = 31) at the time of stroke (baseline) and continued for the next 3 months. Plasma samples were collected at baseline (n = 28) and at 3-month follow-up (n = 28) and analyzed for Brain-Derived-Neurotrophic-Factor (BDNF) protein as a primary outcome. Secondary outcomes included enzyme activities of choline acetyltransferase (ChAT) and Butyrylcholinesterase (BChE), and the six-minute walking test (6MWT), which was assessed at the same time as the plasma sampling.

Results: A significant decline in BDNF was observed at 3 months in the total population (n = 56), primarily driven by the control group. Stratifying groups as intervention or control displayed no significant difference in BDNF protein levels, nor in ChAT or BChE activities at baseline or at 3-month follow-up, except for a significant correlation between BChE and Body-Mass Index (BMI). Patient stratification based on 6MWT performance displayed higher BDNF levels in the intervention group versus the control group, especially among females but not males. Females showed higher BChE than the males in the control group, but not in the intervention. Interestingly, the change in ChAT activity and cholinergic index (ChAT/BChE) from baseline to follow-up is significantly correlated with 6MWT performance.

Discussion: We conclude that SMS-guided exercise training improves post-stroke walking performance (6MWT) which attenuates the decline in BDNF levels. Cholinergic function correlates with improved walking performance and could be a useful marker to evaluate rehabilitation outcomes.

KEYWORDS

brain-derived neurotrophic factor (BDNF), stroke, cholinergic index, exercise, rehabilitation

1 Introduction

Stroke is a serious life-threatening medical condition and is the second most common cause of mortality and disability worldwide (1). Among various risk factors involved in later-life stroke incidence, several modifiable lifestyle factors have been reported recently (2). A sedentary lifestyle has been linked to both stroke incidence and outcome (3, 4), thus therapeutic programs including physical activity intervention are currently employed (5–7). Recently, great interest has been reported in utilizing web-based or mobile-based applications to support stroke patient's rehabilitation (8). Although physical exercise and activity may have meaningful benefits for stroke patients (9), more knowledge on underlying pathways is needed to evaluate their clinical benefits (10–12).

We have previously performed the STROKEWALK Study (13) where patients received text-message-guided physical exercise instructions for post-stroke training (treatment group) or not (control group). Between-group analysis revealed that 3 months of daily text messages (SMS) containing training instructions significantly improved walking performance (as measured by the six-minute walk test, 6MWT) and lower body strength in favor of the SMS treatment group (13, 14). The present study uses secondary analysis from the STROKEWALK study and aims to explore the molecular changes in plasma samples in the intervention and control groups.

Since physical exercise has been associated with increased plasma levels of brain-derived neurotrophic factor (BDNF) (15), which has neurotrophic effects in the brain (16), BDNF protein levels were estimated. Similarly, exercise is also associated with increased cholinergic input in the hippocampus and cortical regions of the brain (17), wherein cholinergic pathways modulate cognitive pathways (18). In addition, cholinergic pathways have important roles such as the anti-inflammatory and functional recovery of neurons (19, 20), and may aid in post-stroke recovery in the brain (21) and play crucial role in modulation neuromuscular junctions (22) in the periphery, which could be critical for post-stroke physical activity. Therefore, the plasma cholinergic markers choline acetyltransferase (ChAT) and butyrylcholinesterase (BChE) were analyzed. In this exploratory study, we aimed to study whether effects from the text messaging-guided training could induce changes in BDNF and cholinergic markers. We hypothesized that physical exercise would enhance walking performance and increase BDNF levels and that improvements in 6MWT outcomes would correlate with elevated cholinergic function in patient plasma.

2 Methods

2.1 Design and participants

Design, recruitment, determination of sample size, and intervention have been previously described (13). Recruitment started on November 1st, 2016; the last follow-up assessment was performed on December 19th, 2018. Briefly, this study included participants who were aged 18 or older, had a verified stroke (CT scan, infarction, or intracerebral hemorrhage with first or recurrent event), and were planning to be discharged home to independent living with access to a mobile phone. They also had no cognitive impairment (MoCA $\geq$ 23 points), a Modified Rankin scale of 2 or less, and could perform a six-minute walk test (6MWT) at discharge, with or without walking aids (13). Exclusion criteria included subarachnoid hemorrhage, uncontrolled hypertension, untreated arrhythmias, unstable cardiovascular conditions, dementia, severe aphasia, psychiatric issues, and difficulty understanding instructions. Randomization and allocation concealment were previously reported (13). Patients with a transient ischemic attack (TIA) were excluded from the present study.

Patients were classified into two subgroups for data analysis: (1) control or intervention group, based on whether they received SMS-guided training instructions; and (2) based on improvement in the 6MWT, categorized less than 34 m or 34 m or more, since a clinically significant improvement in physical recovery was observed in post-stroke patients who exceeded this threshold (13). Gender differences were also analyzed at multiple points to assess the potential role of sex in post-stroke recovery following our intervention (23). Individuals with stroke were included in the study a median of 5 days (IQR = 5) after hospital admission. Of these patients, 87.5% (n = 49) had a cerebral infarction (CI) and 12.5% (n = 7) had an intracerebral bleeding (ICH) [SMS group: CI: 89.3% (n = 25) and ICH: 10.7% (n = 3)].

Non-fasting blood samples were collected in heparinized vials at the hospital at the time of the stroke and during follow-up after 3 months. Plasma samples were collected at the same time as the 6MWT (meters) was assessed. The samples were frozen at −80°C until analysis.

This study is a secondary analysis of participants from a randomized controlled trial performed at the Uppsala University Hospital in Sweden. The original study was performed according to the Helsinki Declaration, and ethical approval was obtained from the regional Ethical Review Board of Uppsala University Hospital, Sweden: Dnr: 2015/550 and Dnr 2020/01087 for analyses of BDNF and cholinergic biomarkers. The study was registered with ClinicalTrials.gov (NCT 02902367).

2.2 Primary and secondary outcomes

The primary outcome variable in the present study was the concentration of brain-derived neurotrophic factor (BDNF), measured in the blood (plasma) at baseline and 3-month follow-up. Secondary outcomes were changes from the baseline and 3 months in butyrylcholinesterase (BChE) activity, Choline acetyltransferase (ChAT) activity, and the ChAT/BChE ratio (cholinergic index), measured in blood (plasma).

2.3 The intervention

The SMS-intervention group received daily cost-free text SMS[1] with simple instructions on what and how to exercise as an add-on to standard care for 3 months and comprised three different strategies: (1) 3 months of daily SMS-text messages, (2) training diaries, (3) pedometers for step counts during the first and last week of intervention (13). The text messaging gave instructions on how to exercise to increase outdoor walking performance and lower body strength, without the possibility of texting back for help or advice. The outdoor walking gradually increased

1 www.intime.nu

in walking time and the perceived/subjective intensity level increased from moderate to strenuous intensity by the third month. Moreover, the number of repetitions of the sit-to-stand exercise also gradually increased.

Control patients received standard care without any restrictions on physical activity, including exercise.

2.4 Randomization

The allocation to either intervention or control group was based on randomization, a 1:1 ratio, stratified by gender as previously reported (13).

2.5 Outcome assessments

2.5.1 Walking performance—the six-minute walking test

The maximal walking distance during 6 min over a 30-meter course was measured by the six-minute walking test (6MWT) and changes from baseline to three-month follow-ups were registered (24). The participants were instructed to walk at their maximum possible speed.

2.5.2 Estimation of plasma BDNF levels

Total BDNF levels were measured in plasma using the DuoSet BDNF ELISA kit (DY248, R&D Systems) following the manufacturer's protocol, with minor modifications wherein the detection system was replaced with alkaline phosphatase (prepared in reagent diluent, 1:10000; #11093266910, Roche Diagnostics) which was added for 2 h at RT. Samples were diluted 10 times in reagent diluent (1% BSA in PBS, 0.01% sodium azide, 0.22 µm filtered, pH 7.4) and measured twice in triplicates, to calculate the mean value. Absorbance data was kinetically read at 405 nm, every 5 min for a total duration of 1 h, using a spectrophotometer (Infinite M1000, Tecan).

2.5.3 Analysis of ChAT activity

Analysis of total ChAT activity was performed in 300 times diluted plasma samples as described previously (25). Briefly, plasma samples were prepared in dilution buffer (10 mM TBS, 0.05% Triton X-100, 1 mM EDTA, pH 7.4) and immediately processed. Each sample was applied in 384-well plates (#464718, Nunc MaxiSorp) in two formats in triplicates—native (10 µL/well of the actual sample) or denatured. The denatured sample was obtained by heating one aliquot of the actual diluted sample in a thermal cycler (3 × 8 min at 98°C), chilled briefly on ice, and centrifuged at 2,000 rpm for 2 min, and 10 µL supernatant was plated per well in triplicate.

Reaction was initiated on the native and denatured samples by adding 40 µL/well of cocktail A which contained 62.5 µM coenzyme-A lithium salt, 1.25 U/mL phosphotransacetylase, 14.78 mM lithium potassium acetyl-phosphate, 37.5 µM choline chloride and 0.075 mM eserine hemisulfate, prepared in dilution buffer. The plate was sealed and incubated at 38°C for 1 h. To calculate ChAT activity, a standard curve was prepared by serially diluting choline chloride starting from 100 µM to 0.78 µM prepared in dilution buffer and processed in triplicates (50 µL/well) in the same plate.

Subsequently, all the wells received 25 µL of cocktail B which was prepared in 50 mM PBS containing 0.93 U/mL choline oxidase, 1 U/5,000 µL Streptavidin-HRP, 3 mM 4-aminoantipyrine, 6.3 mM phenol, pH-7.6. Absorbance was immediately read at 500 nm for 1 h. ChAT activity was calculated by assessing the difference in choline concentration between denatured versus native samples as calculated using the choline chloride standard curve (pMole/min/mL samples).

2.5.4 Analysis of BChE activity

Analysis of the total BChE activity in the plasma samples was performed as previously described (26). Briefly, plasma samples (intervention and control groups) were diluted 400 times with dilution buffer containing 10 mM tris, 0.1% BSA, 1 mM EDTA, and 0.05% Triton X-100, pH 7.4. BChE activity was measured using 50 µL/well of samples which was then mixed with 25 µL/well of 3X master mix containing 15 mM butyrylthiocholine iodide, 1.2 mM 5,5′-dithiobis (2-nitrobenzoic acid) (DTNB), 1 µM of specific AChE inhibitor BW280C51, prepared in 50 mM sodium-potassium phosphate buffer, pH 7.4. The plates were immediately read in a spectrophotometer (Infinite M1000, Tecan) kinetically at 412 nm absorbance with 1 min intervals for a total duration of 20 min.

2.5.5 Calculation of cholinergic index

The cholinergic index was calculated as a ratio of the total ChAT activity (nMole/min/mL) to the total BChE activity (nMole/min/mL). Cholinergic index indicates the equilibrium of acetylcholine (ACh) availability which may influence various target pathways (22, 27).

2.5.6 Statistical analysis

No *a priori* power analysis was performed in this study and statistical analyses are based on complete case analysis. The baseline clinical characteristics were compared using Pearson's chi-squared test (χ^2). The plasma biomarker data were transformed using natural logarithms (Ln). The within-group changes over time were analyzed by the Wilcoxon signed-rank test. The differences between groups at baseline or the three-month follow-up and changes from baseline to follow-up were tested by the nonparametric Mann–Whitney U test. The use of non-parametric vs. parametric is a precautionary measure that we adopted to avoid any possible effect of outliers given the exploratory nature of the study and the relatively small number of subjects in the subgroups. All data are then illustrated as relative percentage change at follow-up compared to baseline using Notched Box Plots, where the notches represent a 95% confidence interval (CI) around the median. All other characteristics are the same as the conventional Box Plots.

The correlation analyses were performed using Spearman Rank correlation analyses and were visualized using simple regression analyses on Ln transformed data. In some cases, when deemed appropriate, we logarithmically (Ln) transformed the data to ensure their normal distribution. In these cases, we found that whether the Ln-transformed data were tested using parametric or non-parametric tests, there were no differences in the statistical tests results. Statistical significance was examined using a two-tailed test with a p value set at $p < 0.05$.

3 Results

3.1 Patient demographics and study outcomes

The inclusion and retention process of patients is shown as CONSORT mapping in Figure 1. Of 79 individuals participating in the

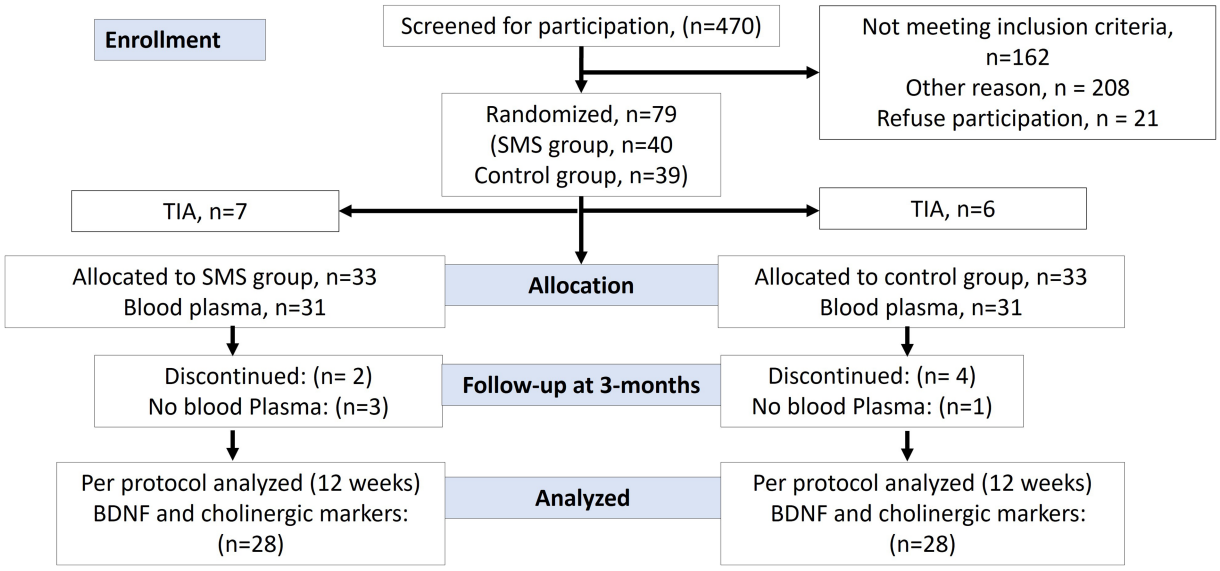

FIGURE 1
Flow chart of the study participants through the phases of the randomized controlled trial. Individuals were randomized within 1 week after baseline assessment. Data were collected at Uppsala University Hospital, Sweden between November 1st, 2016, and December 18th, 2018. Analysis of BDNF protein levels and cholinergic enzyme activity from plasma.

original study, 62 individuals with successful baseline plasma collection were randomized equally to the SMS intervention and the control group (13 TIA patients were excluded from the present analysis). Subsequently, in total 56 participants completed the study with successful plasma collection at 3-month follow-up, which was analyzed in this study ($n = 28$ in each group). Due to logistic reasons, some individuals were not able to provide the study with blood samples. The clinical characteristics at baseline are provided in Table 1. In total, the mean (SD) age was 64 (9.4) years, and 19 (33.9%) participants were women. Forty-nine individuals suffered an ischemic stroke (87.5%), and seven (12.5%) individuals suffered an intracerebral hemorrhage. According to the training diaries, adherence to the recommended SMS interventions ranged from 59 to 100% (13). The mean increase in steps per day was 2,084 (SD = 2,538). Among the 26 participants receiving the SMS, 6 experienced a decrease in their daily step count.

A significant post-stroke reduction in BDNF levels was observed ($p < 0.02$, 25% reduction) when all samples ($n = 56$, Ln data) were compared between baseline versus 3-month follow-up (Figure 2A). A sub-group analysis revealed a significant reduction in the control group (Ln, $p < 0.02$, 39% reduction), but not in the intervention group (Ln, $p < 0.40$, 12% reduction) (Figure 2B), signifying a positive role of physical exercise in resisting post-stroke decline in BDNF levels. There were no differences between the groups when analyzed on actual data (mean ± SD) (Table 2), except significant reduction in BDNF levels in the control group at 3-month follow-up as also shown in Figure 2B. There was no association between changes in BDNF and changes in the 6MWT at 3 months, $r = -0.16$, $p = 0.25$ (or any of the cholinergic markers) considering the intervention or control groups, respectively (Table 2).

At baseline, BChE concentration correlated with Body Mass Index (BMI), $r = 0.49$, $p < 0.0003$ (Supplementary Figure 1A). A similar correlation was observed at 3 months with $r = 0.54$ and $p < 0.0001$, including both the control and intervention groups, respectively (Supplementary Figure 1B).

3.2 Sub-group analysis showed increased plasma BDNF levels in the intervention group

We wanted to explore whether improvement in clinically meaningful walking capacity measured by 6MWT could be related to changes in the plasma biomarkers. We sub-grouped the patients based on changes in walking performance, i.e., 6MWT scores, in terms of their ability to walk over (≥34 m, *Improved group*) or below 34 m (<34 m, *Unchanged group*) compared to their baseline performance (Figure 3), based on previous observation (28).

Using this subgrouping, the SMS intervention group tended to have a higher plasma level of BDNF compared to the controls (Figure 4A, statistically not significant, $p < 0.07$) when it was analyzed among the *Improved group* (≥34 m). The corresponding changes among the *Unchanged group* (<34 m) were just numerically higher in the SMS intervention group (~23%, Figure 4A, $p < 0.34$).

Further analyses did not show any differences in relative levels of ChAT activity, BChE activity, or the estimated cholinergic index in plasma between the main groups or the treatment outcome subgroups (Figure 4A).

3.3 Gender differences in BDNF and cholinergic markers

The plasma level of BDNF tended to be higher among women in the SMS-intervention group (~18%) compared to women in the control group (Figure 4B, statistically not significant, $p < 0.07$).

There was also a 16% significant difference between the changes in the plasma BChE activity in men versus women in the control group (Figure 4B, $p < 0.04$), but no sex difference was observed in the SMS intervention group.

10.3389/fneur.2025.1568401

TABLE 1 Baseline clinical characteristics of the study population with minor stroke allocated to the text messaging or control group.

Variables	Missing value	Text messaging (n = 28)	Missing value	Control group (n = 28)
Gender, female, n (%)	0	11 (39.3)	0	8 (28.6)
Age (years), mean (SD)	0	63.3 (9.8)	0	64.6 (8.8)
Body mass index, kg/m^2, mean (SD)	0	27.5 (4.5)	0	26.7 (3.6)
Body mass index, kg/m^2, classes, n (%)				
Normal weight: <25	0	8 (28.6)	0	9 (32.1)
Overweight: 25–29.9	0	13 (46.4)	0	15 (53.6)
Obesity, class I: 30–35	0	5 (17.9)	0	3 (10.7)
Obesity class II: 35.1–39.9	0	2 (7.1)	0	1 (3.6)
Obesity, class III: ≥40	0		0	
Montreal cognitive assessment scale, Md (IQR)	3	27 (4)	5	26 (4)
Saltin-Grimby physical activity level, n (%)				
Sedentary	0	2 (7.1)	0	6 (21.4)
Light physical activity	0	18 (64.3)	0	17 (60.7)
Moderate/high physical activity	0	8 (28.6)	0	5 (17.9)
Modified Rankin scale, n (%)				
0	0	3 (10.7)	0	-
1	0	18 (64.3)	0	22 (78.6)
2	0	7 (25.0)	0	6 (21.4)
Six-minute walk test (6MWT), meters, mean (SD)	0	475 (99)	0	470 (125)
Cerebral infarction, n (%)	0	25 (89.3)	0	24 (85.7)
Intracerebral hemorrhage, n (%)	0	3 (10.7)	0	4 (14.3)
Thrombolysis, n (%)	0	2 (7.1)	0	1 (3.6)

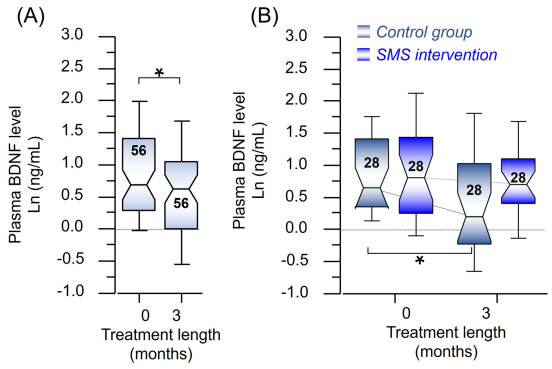

FIGURE 2
(A) Comparison of the level of BDNF between baseline and the follow-up in the whole study population (Ln, n = 56). **(B)** Time-dependent changes in the plasma BDNF levels when groups were stratified as control or intervention subgroups. The digits in the boxes represent the number of subjects in each subgroup. The notches of the boxes represent a 95% confidence interval around the median value. * All p values were <0.02.

Further analyses did not show any differences between men and women with regard to the changes in the 6MWT or the relative levels of the plasma ChAT activity or the estimated plasma cholinergic index (Figure 4B).

3.4 Plasma ChAT activity predicts and is correlated with post-stroke walking recovery

Analyses of the baseline data revealed no correlations between the actual 6MWT scores (Ln 6MWT) and levels of BDNF or BChE in the plasma baseline samples among the overall study population or the treatment arms of the study (i.e., the control vs. SMS intervention).

However, there was a positive correlation between the ChAT activity in plasma and 6MWT at baseline (rho = 0.35, $p < 0.05$, n = 32), among *the Improved group* who showed ≥34 m walking improvement as was defined in Figure 3. The correlation was reversed among *the Unchanged group* (i.e., patients who showed <34 m walking improvement) (rho = −0.39, $p < 0.05$, n = 28). A similar positive correlation was found regarding the plasma cholinergic index within *the Improved group* (rho = 0.36, $p < 0.05$, n = 32), but not among *the Unchanged group* (rho = −0.16, $p < 0.4$, n = 28).

Further analyses based on the SMS-intervention and the control subgroups among the *Unchanged group* revealed that the negative correlation between the plasma ChAT activity and the 6MWT results were significant among the SMS intervention group (rho = −0.70, $p < 0.04$, n = 10) but not Control (rho = −0.19, $p < 0.44$, n = 18). This relationship was reversed among *the Improved group,* i.e., the correlation was not significant among the

TABLE 2 Within-group and between-group differences of BDNF and plasma cholinergic markers in patients with minor stroke at the start of the intervention and after 3 months.

Stroke	Intervention group (n = 28)	n = 28	p-value	Control group (n = 28)	n = 28	p-value	Median estimate (95%CI)	p-value
	Baseline	3-month		Baseline	3-month		Between-group differences	
BDNF, ng/mL, mean (SD)	3.4 (3.0)	2.6 (1.7)	0.36	3.0 (2.6)	2.4 (2.4)	0.013	−0.3 (−1.3 to 1.1)	0.54
ChAT activity, nmol/min/mL, mean (SD)	278.5 (209.4)	253.5 (239.3)	0.43	247.2 (128.3)	245.0 (108.2)	0.83	29.8 (−56.3 to 120.5)	0.50
BChE, nmol/min/mL, mean (SD)	2384.7 (577.1)	2397.7 (576.6)	0.84	2208.7 (554.2)	2214.5 (493.0)	0.78	−29.3 (−266.8 to 186.3)	0.79
ChAT/BChE ratio, mean (SD)	0.119 (0.071)	0.108 (0.084)	0.54	0.118 (0.060)	0.116 (0.058)	0.94	0.012 (−0.03 to 0.06)	0.52

BDNF, brain-derived neurotrophic factor; BChE, butyrylcholinesterase; ChAT, Choline acetyltransferase; SD, Standard deviation.
The table displays actual data as mean ± SD. The within-group differences were analyzed with Wilcoxon's Signed Ranks Tests. Differences between groups (changes from baseline to follow-up) were analyzed by the Mann–Whitney U test. The median estimate was calculated using the Hodges-Lehmann test. CI indicates confidence interval.

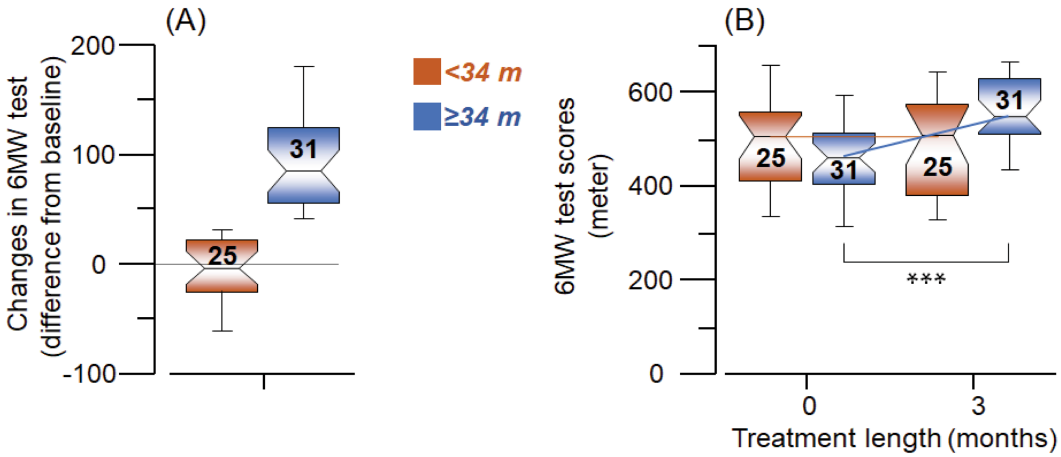

FIGURE 3
(A) Grouping the patients based on walking performance after 3 months of treatment assessed by scoring their ability to walk less than 34 meters (<34 m) and more than or equivalent to 34 meters (≥34 m), wherein the figure shows the extent of change from the baseline assessment to follow-up at 3 months. **(B)** The six-minute walking test (6MWT, meters) groups as defined in **(A)**, showing equivalent walking performance at baseline (red vs. blue) but a group of patients went on to improve their walking performance at follow-up (blue). The digits in the boxes represent the number of subjects. The notches of the boxes represent a 95% confidence interval around the median value. *** $p < 0.02$.

SMS intervention group (rho = 0.16, $p < 0.5$, $n = 19$) but instead was significant in *the Control* (rho = 0.73, $p < 0.02$, $n = 12$). Similar correlation analyses between the 6MWT results and the plasma cholinergic index showed the same relative relationships.

The correlation analyses between the absolute changes in 6MWT and the assessed plasma biomarkers at the completion of the study, i.e., the 3-month assessment did not show any significant findings. Nonetheless, analyses on the relative changes from baseline to the 3-month follow-up revealed a significant positive correlation among the *Improved group* between changes in the 6MWT distance and the changes in the activity of ChAT in plasma (Figure 5A). The analyses on the subgroups showed that the correlation was strongest among the SMS intervention group (Figure 5B).

3.5 Plasma cholinergic index is correlated with improved post-stroke walking performance

Like ChAT, changes in the cholinergic index showed a significant positive correlation with the changes in the 6MWT result among the Improved group (rho = 0.44, $p < 0.017$, $n = 31$) (Figure 5C). Further subgroup analysis showed that the correlation was strongest among the SMS intervention group (Figure 5D).

There was no significant correlation between changes in the 6MWT result and the changes in the BDNF levels or BChE activity in plasma. The subgroup analyses did not show any significant correlation among the subgroups.

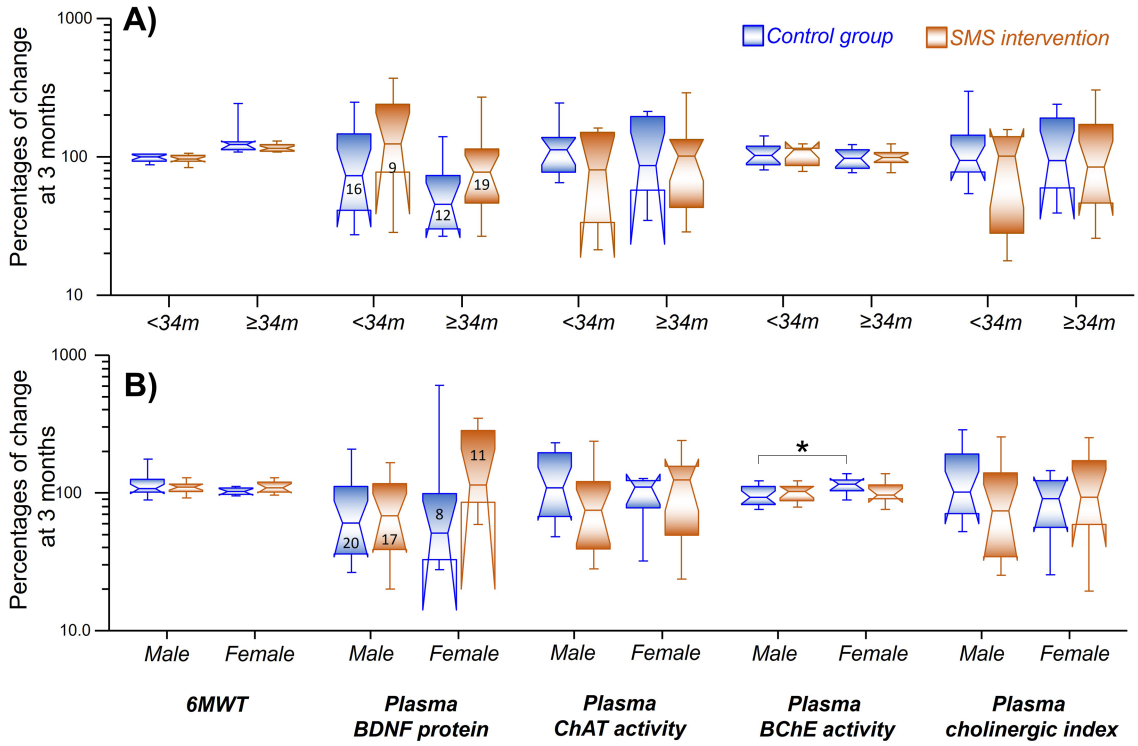

FIGURE 4
(A) Changes relative to baseline levels of the assessed biomarkers in relation to the treatment outcomes subgroups. Grouping was done as control (blue) or intervention (red), with subsequent stratification based on whether the outcomes on 6MWT (X-axis). **(B)** Changes in relative to baseline levels of the assessed biomarkers (X-axis), wherein the groups were stratified on the basis of gender (between men and women) among the treatment groups. *$p < 0.05$. The digits in the boxes represent the number of subjects applicable to all parameters. The notches of the boxes represent 95% confidence interval around the median value. The color coding applies to both the figures.

4 Discussion

This is one of the first studies to measure cholinergic index among post-stroke patients and we report an association of ChAT activity and cholinergic index with improved walking performance. Interestingly, the decline in BDNF levels post-stroke was significant in the control group but attenuated by the intervention, indicating a beneficial effect of exercise. A gender-specific change in total BDNF level was observed in females who showed increased BDNF in the SMS intervention group as compared to the control group, although they both showed improvement in 6MWT, respectively. However, due to the limited sample size, our findings represent exploratory findings.

Discrepancies remain about changes in BDNF levels at post-stroke follow-up in plasma/serum (29). We report that BDNF levels were significantly reduced post-stroke (Figure 2) until 3 months compared to the baseline but remain within the quantitative range as reported previously (30). BDNF was associated with various post-stroke outcomes, wherein some studies associate BDNF with a specific outcome while most did not find such an association (29, 31). This could be due to the different treatments provided to the patients in various studies included in a meta-analysis, and several technical aspects that might affect serum and plasma BDNF stability prior or during the estimation process (32).

Previous reports utilizing acute and long-term exercise have been reported to increase BDNF levels in the plasma and serum (15), which has a neurotrophic effect in the brain hippocampus (16). Although we did not observe any significant difference between the intervention and the control groups either at baseline or follow-up interval, the decrease in BDNF levels was significant in the control group but not in the intervention group, when compared to baseline levels (Table 2). Although an overall decrease in BDNF levels was observed post-stroke (Figure 2), stratifying post-stroke patients based on 6MWT performance displayed significantly higher BDNF levels in patients who improved most (i.e., ≥34 m) and received the intervention (Figure 4), probably signifying a beneficial role of exercise in reducing the decline in BDNF levels. Higher BDNF was more prominent in females than males when the intervention group was compared to control groups (Figure 4). Whether these improved plasma BDNF levels elevated brain function or affected other bodily functions (33), warrants further research.

Notably, recent studies have highlighted various physiological role of BDNF in the central and peripheral system [reviewed by Miranda et al. (34) and Ichimura-Shimizu et al. (35)]. Among others, cardiovascular risk factors are known to be crucial for exercise-induced secondary prevention strategies in stroke patients [reviewed by D'Isabella et al. (36)], wherein constitutive BDNF-mediated signaling was previously reported to be crucial for normal heart function (37). BDNF is critical in mediating the beneficial effects of exercise induced stress response and regulates myocardial cellular energetics (38) and contributes to reducing post-ischemic heart failure (39). Nonetheless, our data shows that BDNF levels are reduced post-stroke and physical activity could be a good tool to resist the reduction

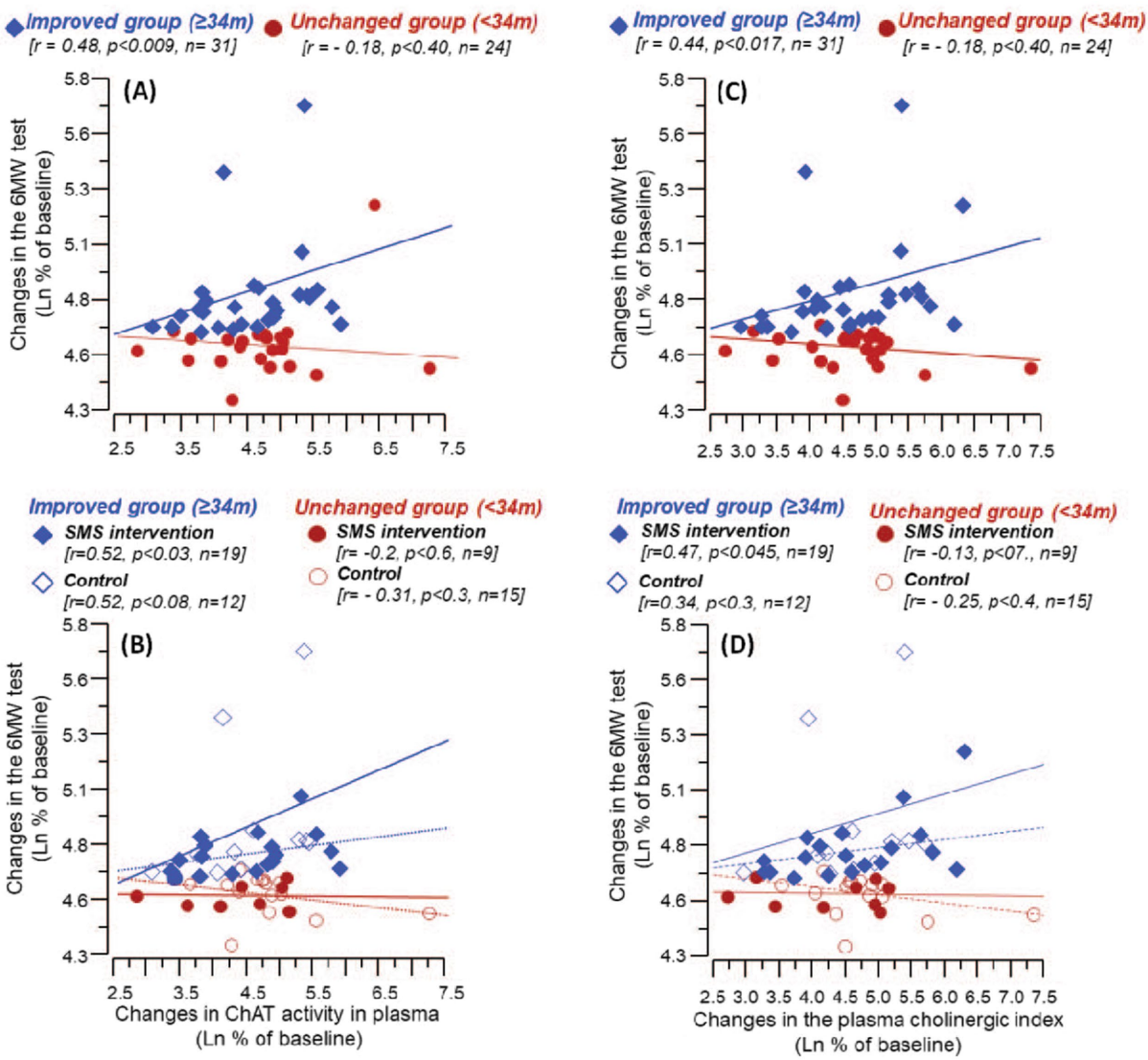

FIGURE 5
Correlation between changes from baseline levels till 3 months follow-up in 6MWT and the relative levels of ChAT activity and cholinergic index in plasma. **(A)** Shows the correlation between %changes in 6MWT and the plasma ChAT activity among *the Improved and the Unchanged groups (based on improvement on 6MWT at follow-up).* **(B)** Illustrates the corresponding correlations when the *Improved and the Unchanged groups* were further stratified based on the intervention (control or SMS-intervention). Similarly, **(C)** shows the correlation between %changes in 6MWT and the cholinergic index among *the Improved* and *the Unchanged groups*, whereas **(D)** illustrates the corresponding correlations among the intervention and control groups. In **(B)** and **(D)**, solid lines represent correlation among *the intervention group*, while the dashed lines among *the control group*.

of plasma BDNF levels which may counter post-stroke depression (40) along with cardioprotective effects.

Cholinergic pathways have been reported to be involved in post-stroke recovery in the brain (21) and improve memory function (41). This might be mediated via parasympathetic pathways (42), for which acetylcholine-mediated transmission is an important pre-requisite. Even though ChAT activity went down from baseline to 3-month follow-up in both groups, we found that change in ChAT activity from baseline to follow-up was significantly correlated with the improvement in 6MWT in the *Improved group*, indicating a role of cholinergic pathways in modulating the clinical outcomes (Figure 5). One of the plausible explanations could be the involvement of ACh in regulating inflammation, blood vessel constriction, muscle activity, etc. among many others (43, 44). Patients in our study were followed up to 1-year post-stroke, wherein none but one control patient died during this period.

We also measured the ACh degradative enzyme BChE in plasma, but did not find any difference in BChE activity between the intervention versus control groups at 3-month follow-up, nor when the samples were stratified based on 6MWT performance (Table 2, Figure 4A). We found a gender-specific differential activity, where females in the control group showed significantly increased BChE activity compared to males in the respective group. BChE activity was found to be increased at 3-month follow-up in the intervention group, whereas it decreased in the control group, without reaching any statistical significance when compared to baseline (Table 2). Increased post-stroke BChE has been previously reported to be associated with delirium, mortality prediction, and dementia (45–47). Although

BChE activity was found higher in the intervention group compared to the control group (Table 2), SMS intervention reduced BChE activity among females by the end of 3 months (Figure 4B).

Accumulating evidence indicates that ACh, besides its canonical function as a neurotransmitter, plays a key role in regulating various central and peripheral processes, including inflammatory responses and function of various organs (48). Given that stroke inevitably causes acute inflammatory responses which can affect various organs, the aforenoted positive correlation between changes in the clinical outcome and the ChAT activity suggests that the patients who were able to increase ChAT activity or their cholinergic index were successful in favorably modulating the outcome of the acute inflammatory responses, and thereby those patients were better able to clinically recuperate. Please note that in this study, the above mechanism may seem quite speculative. However, it should be noted that in stroke most often the BBB integrity becomes affected, allowing circulating immune cells to readily access the affected stroke sites, and ACh has been known to induce anti-inflammatory effect on immune cells (49).

Our mechanistic hypothesis concerns with an inherent capability of the patients in elevating ACh equilibrium state, most likely depending on the net outcome of a combination of feedback responses, one to acute inflammation as consequence of the stroke and the other to the treatment (physical activity) and/or the patient's physical condition. For example, we found a positive correlation between the patients' BMI and the plasma BChE activity both at the baseline and the follow-up (Supplementary material). This might negatively affect the cholinergic index in subjects with high BMI since BChE activity is in the denominator of the ratio of ChAT/BChE (i.e., because BChE degrades ACh). This in turn could reduce the efficacy of such patient's cholinergic anti-inflammatory response and thereby hamper effectively coping with consequences of an excessive inflammatory response. In addition, in patients with poorer physical condition the balance between the sympathetic and parasympathetic may become unfavorable with regard to a cholinergic anti-inflammatory response due to a reduced vagal input (required to raise the heartrate by sympathetic input). Nonetheless, this is a hypothetical explanation, which is quite speculative.

The calculation of the changes in the plasma cholinergic index involves determining percentages of two ratios between ChAT to BChE activities, at baseline and at the follow-up. This could result in some distortion of the data. However, this is unlikely to be a major issue in the current study given the close agreement between the data presented in Figure 5A vs. Figure 5C or between Figure 5B vs. Figure 5D. In addition, the cholinergic index calculations have been extensively assessed previously (25, 50–55). Stronger correlations of the cholinergic index with 6MWT were observed which is perhaps driven by ChAT activity, which was also found to correlate with 6MWT, respectively (Figure 5). This might be mediated through the anti-inflammatory function of ACh on other aspects of physiology including cardiovascular and vascular pathways, which need to be studied further (43, 44).

5 Conclusion

This study, summarized in Figure 6, shows the relevance and feasibility of using BDNF and cholinergic index as biomarkers for post-stroke recovery. Exercise could resist the decline in BDNF levels post-stroke. Whether cholinergic signaling plays a role in enhanced walking performance or increased walking elevates cholinergic function in post-stroke patients needs further validation.

6 Limitations and strengths

This study presents an exploratory analysis aimed at gaining insight into the potential interrelationships between stroke, brain-derived neurotrophic factor (BDNF), and the modulation of key components of the cholinergic system. We conducted a *post hoc* analysis on a small cohort of patients.

One of the main limitations of our study is the absence of brain MRI data, which restricts our ability to determine whether

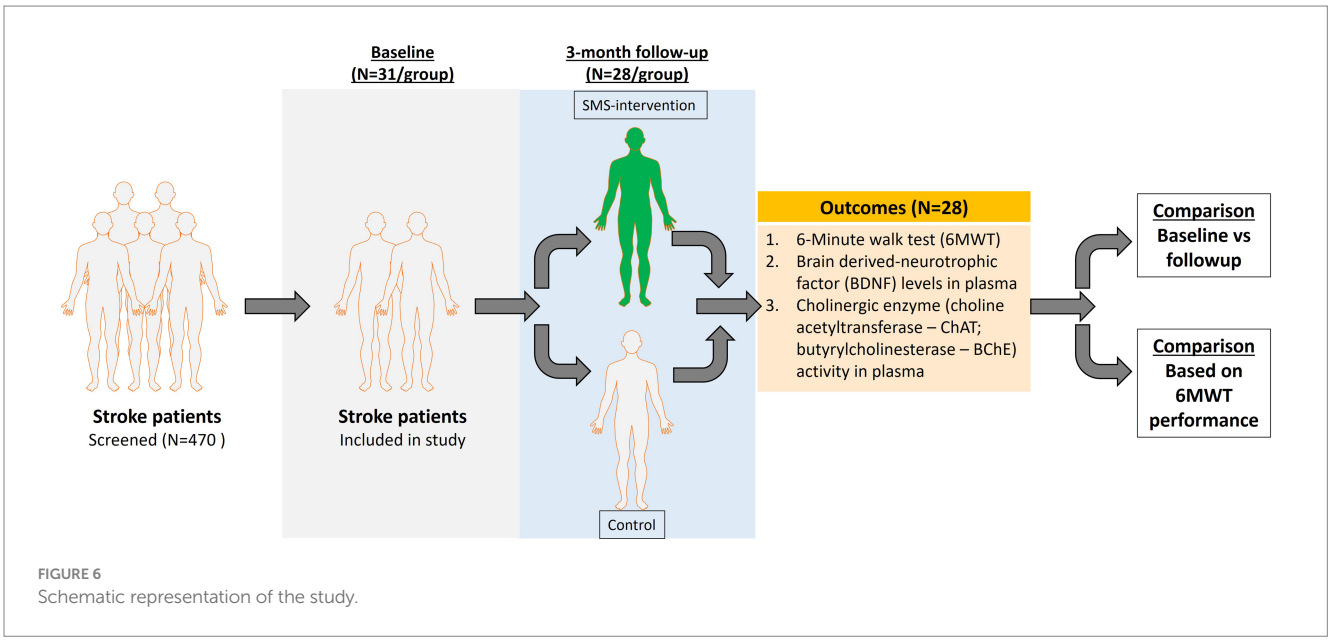

FIGURE 6
Schematic representation of the study.

improvements in the 6-min walk test (6MWT) and changes in the observed biomarkers are associated with structural brain recovery following the 3-month intervention period. Additionally, the relatively short duration of follow-up further limits the interpretation of long-term outcomes.

We could not establish whether patients not receiving the SMS instructions were devoid of exercise regimens other or similar than the ones recommended through the SMS instructions. Moreover, stratification based on 6MWT considers only the improvement of ≥34 m versus <34 m irrespective of whether they received SMS reminders or not, thereby only considering the clinical outcome with the parameters measured in this study.

Generalizability: This model of text messaging may not apply to individuals with more limited mobility after stroke, those with aphasia, or those with cognitive impairments who return home.

Potential bias: Random missing data, inability to fully maintain the assessor blinded at follow-up, challenges with using the training diary, and limited use of the pedometers.

Missing data can reduce statistical precision, increase standard error, and introduce bias if the missing data is not random. This makes it more difficult to draw valid conclusions and generalize the results to a broader population. Missing data in this study was random.

A key strength of this study is its randomized controlled design, combined with the use of real-world data. The intervention itself is also a notable advantage—it can be integrated alongside existing rehabilitation services, require no personnel, is easily accessible regardless of location, and is cost-effective. Additionally, the study included both men and women across a broad age range, enhancing the generalizability of the findings. Another strength is the lower-than-expected dropout rate, which supports the feasibility and acceptability of the intervention.

Data availability statement

The raw data supporting the conclusions of this article will be made available by the authors, without undue reservation.

Ethics statement

The studies involving humans were approved by the regional Ethical Review Board of Uppsala University Hospital, Sweden: Dnr: 2015/550 and Dnr 2020/01087. The studies were conducted in accordance with the local legislation and institutional requirements. The participants provided their written informed consent to participate in this study.

Author contributions

SM: Conceptualization, Data curation, Formal analysis, Funding acquisition, Investigation, Methodology, Project administration, Resources, Supervision, Validation, Writing – original draft. TD-S: Conceptualization, Data curation, Formal analysis, Funding acquisition, Resources, Validation, Visualization, Writing – review & editing. EL: Data curation, Methodology, Project administration, Resources, Writing – review & editing. SE: Data curation, Methodology, Project administration, Resources, Writing – review & editing. TC: Conceptualization, Data curation, Funding acquisition, Methodology, Project administration, Resources, Writing – review & editing. ME: Conceptualization, Data curation, Funding acquisition, Methodology, Project administration, Resources, Supervision, Writing – review & editing. BV: Conceptualization, Data curation, Formal analysis, Funding acquisition, Methodology, Project administration, Resources, Writing – review & editing.

Funding

The author(s) declare that financial support was received for the research and/or publication of this article. This work was supported by Medical Faculty at Uppsala University; the Swedish Stroke Association (Stroke-Riksförbundet); the Geriatric funding; the Swedish Associations of Physiotherapists, Neurology; Demensfonden; Olle Engkvist Byggmästare Foundation; Åhlén-Foundation; Gunvor and Josef Anérs Foundation; Magnus Bergvalls Foundation; Gun and Bertil Stohnes Foundation; Gamla Tjänarinnor; Tore Nilsons Foundation, the regional agreement on medical training and clinical research between the Stockholm County council and the Karolinska Institutet (ALF); Swedish Research council (#2020-02014); Swedish Order of St John, Karolinska Institutet Foundation grants; Foundation for Geriatric Diseases at Karolinska Institutet, Loo and Hans Osterman Foundation for Medical Research.

Conflict of interest

The authors declare that the research was conducted in the absence of any commercial or financial relationships that could be construed as a potential conflict of interest.

The author(s) declared that they were an editorial board member of Frontiers, at the time of submission. This had no impact on the peer review process and the final decision.

Generative AI statement

The authors declare that no Gen AI was used in the creation of this manuscript.

Publisher's note

Supplementary material

The Supplementary material for this article can be found online at: https://www.frontiersin.org/articles/10.3389/fneur.2025.1568401/full#supplementary-material

References

1. World Health Organization. *The top 10 causes of death* [Online]. (2020). Available online at: https://www.who.int/news-room/fact-sheets/detail/the-top-10-causes-of-death (Accessed June 11, 2024).

2. Harshfield EL, Georgakis MK, Malik R, Dichgans M, Markus HS. Modifiable lifestyle factors and risk of stroke: a Mendelian randomization analysis. *Stroke*. (2021) 52:931–6. doi: 10.1161/STROKEAHA.120.031710

3. Hall J, Morton S, Fitzsimons CF, Hall JF, Corepal R, English C, et al. Factors influencing sedentary behaviours after stroke: findings from qualitative observations and interviews with stroke survivors and their caregivers. *BMC Public Health*. (2020) 20:967. doi: 10.1186/s12889-020-09113-6

4. Wang Z, Jin X, Liu Y, Wang C, Li J, Tian L, et al. Sedentary behavior and the risk of stroke: a systematic review and dose-response meta-analysis. *Nutr Metab Cardiovasc Dis*. (2022) 32:2705–13. doi: 10.1016/j.numecd.2022.08.024

5. English C, Healy GN, Coates A, Lewis L, Olds T, Bernhardt J. Sitting and activity time in people with stroke. *Phys Ther*. (2016) 96:193–201. doi: 10.2522/ptj.20140522

6. Karklina A, Chen E, Berzina G, Stibrant Sunnerhagen K. Patients' physical activity in stroke units in Latvia and Sweden. *Brain Behav*. (2021) 11:e02110. doi: 10.1002/brb3.2110

7. Minet LR, Peterson E, Von Koch L, Ytterberg C. Healthcare utilization after stroke: a 1-year prospective study. *J Am Med Dir Assoc*. (2020) 21:1684–8. doi: 10.1016/j.jamda.2020.04.036

8. Irvine L, Morris JH, Dombrowski SU, Breckenridge JP, Farre A, Ozakinci G, et al. Keeping active with texting after stroke (KATS): development of a text message intervention to promote physical activity and exercise after stroke. *Pilot Feasibility Stud*. (2023) 9:105. doi: 10.1186/s40814-023-01326-x

9. Saunders DH, Greig CA, Mead GE. Physical activity and exercise after stroke: review of multiple meaningful benefits. *Stroke*. (2014) 45:3742–7. doi: 10.1161/STROKEAHA.114.004311

10. Boyne P, Billinger SA, Reisman DS, Awosika OO, Buckley S, Burson J, et al. Optimal intensity and duration of walking rehabilitation in patients with chronic stroke: a randomized clinical trial. *JAMA Neurol*. (2023) 80:342–51. doi: 10.1001/jamaneurol.2023.0033

11. Buvarp D, Viktorisson A, Axelsson F, Lehto E, Lindgren L, Lundstrom E, et al. Physical activity trajectories and functional recovery after acute stroke among adults in Sweden. *JAMA Netw Open*. (2023) 6:e2310919. doi: 10.1001/jamanetworkopen.2023.10919

12. English C, Manns PJ, Tucak C, Bernhardt J. Physical activity and sedentary behaviors in people with stroke living in the community: a systematic review. *Phys Ther*. (2014) 94:185–96. doi: 10.2522/ptj.20130175

13. Vahlberg B, Lundstrom E, Eriksson S, Holmback U, Cederholm T. Effects on walking performance and lower body strength by short message service guided training after stroke or transient ischemic attack (The STROKEWALK Study): a randomized controlled trial. *Clin Rehabil*. (2021) 35:276–87. doi: 10.1177/0269215520954346

14. Vahlberg BM, Lundstrom E, Eriksson S, Holmback U, Cederholm T. Potential effects on cardiometabolic risk factors and body composition by short message service (SMS)-guided training after recent minor stroke or transient ischaemic attack: post hoc analyses of the STROKEWALK randomised controlled trial. *BMJ Open*. (2021) 11:e054851. doi: 10.1136/bmjopen-2021-054851

15. Ribeiro D, Petrigna L, Pereira FC, Muscella A, Bianco A, Tavares P. The impact of physical exercise on the circulating levels of BDNF and NT 4/5: a review. *Int J Mol Sci*. (2021) 22. doi: 10.3390/ijms22168814

16. Liu PZ, Nusslock R. Exercise-mediated neurogenesis in the Hippocampus via BDNF. *Front Neurosci*. (2018) 12:52. doi: 10.3389/fnins.2018.00052

17. Zong B, Yu F, Zhang X, Zhao W, Sun P, Li S, et al. Understanding how physical exercise improves Alzheimer's disease: cholinergic and monoaminergic systems. *Front Aging Neurosci*. (2022) 14:869507. doi: 10.3389/fnagi.2022.869507

18. Hall JM, Savage LM. Exercise leads to the re-emergence of the cholinergic/nestin neuronal phenotype within the medial septum/diagonal band and subsequent rescue of both hippocampal ach efflux and spatial behavior. *Exp Neurol*. (2016) 278:62–75. doi: 10.1016/j.expneurol.2016.01.018

19. Conner JM, Chiba AA, Tuszynski MH. The basal forebrain cholinergic system is essential for cortical plasticity and functional recovery following brain injury. *Neuron*. (2005) 46:173–9. doi: 10.1016/j.neuron.2005.03.003

20. Martin A, Domercq M, Matute C. Inflammation in stroke: the role of cholinergic, purinergic and glutamatergic signaling. *Ther Adv Neurol Disord*. (2018) 11:1756286418774267. doi: 10.1177/1756286418774267

21. Geranmayeh F. Cholinergic neurotransmitter system: a potential marker for post-stroke cognitive recovery. *Brain*. (2022) 145:1576–8. doi: 10.1093/brain/awac142

22. Vaughan SK, Sutherland NM, Valdez G. Attenuating cholinergic transmission increases the number of satellite cells and preserves muscle mass in old age. *Front Aging Neurosci*. (2019) 11:262. doi: 10.3389/fnagi.2019.00262

23. Flansbjer UB, Holmback AM, Downham D, Patten C, Lexell J. Reliability of gait performance tests in men and women with hemiparesis after stroke. *J Rehabil Med*. (2005) 37:75–82. doi: 10.1080/16501970410017215

24. Brooks D, Solway S, Gibbons WJ. ATS statement on six-minute walk test. *Am J Respir Crit Care Med*. (2003) 167:1287. doi: 10.1164/ajrccm.167.9.950

25. Karami A, Darreh-Shori T, Schultzberg M, Eriksdotter M. CSF and plasma cholinergic markers in patients with cognitive impairment. *Front Aging Neurosci*. (2021) 13:704583. doi: 10.3389/fnagi.2021.704583

26. Darreh-Shori T, Vijayaraghavan S, Aeinehband S, Piehl F, Lindblom RP, Nilsson B, et al. Functional variability in butyrylcholinesterase activity regulates intrathecal cytokine and astroglial biomarker profiles in patients with Alzheimer's disease. *Neurobiol Aging*. (2013) 34:2465–81. doi: 10.1016/j.neurobiolaging.2013.04.027

27. Cisterna BA, Vargas AA, Puebla C, Fernandez P, Escamilla R, Lagos CF, et al. Active acetylcholine receptors prevent the atrophy of skeletal muscles and favor reinnervation. *Nat Commun*. (2020) 11:1073. doi: 10.1038/s41467-019-14063-8

28. Vahlberg B, Cederholm T, Lindmark B, Zetterberg L, Hellstrom K. Short-term and long-term effects of a progressive resistance and balance exercise program in individuals with chronic stroke: a randomized controlled trial. *Disabil Rehabil*. (2017) 39:1615–22. doi: 10.1080/09638288.2016.1206631

29. Karantali E, Kazis D, Papavasileiou V, Prevezianou A, Chatzikonstantinou S, Petridis F, et al. Serum BDNF levels in acute stroke: a systematic review and meta-analysis. *Medicina (Kaunas)*. (2021) 57:297. doi: 10.3390/medicina57030297

30. Yoshimura R, Sugita-Ikenouchi A, Hori H, Umene-Nakano W, Hayashi K, Katsuki A, et al. A close correlation between plasma and serum levels of brain-derived neurotrophic factor (BDNF) in healthy volunteers. *Int J Psychiatry Clin Pract*. (2010) 14:220–2. doi: 10.3109/13651501003748560

31. Chen G, Wu M, Chen J, Zhang C, Liu Q, Zhao Y, et al. Biomarkers associated with functional improvement after stroke rehabilitation: a systematic review and meta-analysis of randomized controlled trials. *Front Neurol*. (2023) 14:1241521. doi: 10.3389/fneur.2023.1241521

32. Gejl AK, Enevold C, Bugge A, Andersen MS, Nielsen CH, Andersen LB. Associations between serum and plasma brain-derived neurotrophic factor and influence of storage time and centrifugation strategy. *Sci Rep*. (2019) 9:9655. doi: 10.1038/s41598-019-45976-5

33. Marosi K, Mattson MP. BDNF mediates adaptive brain and body responses to energetic challenges. *Trends Endocrinol Metab*. (2014) 25:89–98. doi: 10.1016/j.tem.2013.10.006

34. Miranda M, Morici JF, Zanoni MB, Bekinschtein P. Brain-derived neurotrophic factor: a key molecule for memory in the healthy and the pathological brain. *Front Cell Neurosci*. (2019) 13:363. doi: 10.3389/fncel.2019.00363

35. Ichimura-Shimizu M, Kurrey K, Miyata M, Dezawa T, Tsuneyama K, Kojima M. Emerging insights into the role of BDNF on health and disease in periphery. *Biomolecules*. (2024) 14:444. doi: 10.3390/biom14040444

36. D'isabella NT, Shkredova DA, Richardson JA, Tang A. Effects of exercise on cardiovascular risk factors following stroke or transient ischemic attack: a systematic review and meta-analysis. *Clin Rehabil*. (2017) 31:1561–72. doi: 10.1177/0269215517709051

37. Feng N, Huke S, Zhu G, Tocchetti CG, Shi S, Aiba T, et al. Constitutive BDNF/TrkB signaling is required for normal cardiac contraction and relaxation. *Proc Natl Acad Sci USA*. (2015) 112:1880–5. doi: 10.1073/pnas.1417949112

38. Yang X, Zhang M, Xie B, Peng Z, Manning JR, Zimmerman R, et al. Myocardial brain-derived neurotrophic factor regulates cardiac bioenergetics through the transcription factor Yin Yang 1. *Cardiovasc Res*. (2023) 119:571–86. doi: 10.1093/cvr/cvac096

39. Cannavo A, Jun S, Rengo G, Marzano F, Agrimi J, Liccardo D, et al. beta3AR-dependent brain-derived neurotrophic factor (BDNF) generation limits chronic postischemic heart failure. *Circ Res*. (2023) 132:867–81. doi: 10.1161/CIRCRESAHA.122.321583

40. Zhang E, Liao P. Brain-derived neurotrophic factor and post-stroke depression. *J Neurosci Res*. (2020) 98:537–48. doi: 10.1002/jnr.24510

41. Kim JO, Lee SJ, Pyo JS. Effect of acetylcholinesterase inhibitors on post-stroke cognitive impairment and vascular dementia: a meta-analysis. *PLoS One*. (2020) 15:e0227820. doi: 10.1371/journal.pone.0227820

42. Cheyuo C, Jacob A, Wu R, Zhou M, Coppa GF, Wang P. The parasympathetic nervous system in the quest for stroke therapeutics. *J Cereb Blood Flow Metab*. (2011) 31:1187–95. doi: 10.1038/jcbfm.2011.24

43. Hamner JW, Tan CO, Tzeng YC, Taylor JA. Cholinergic control of the cerebral vasculature in humans. *J Physiol*. (2012) 590:6343–52. doi: 10.1113/jphysiol.2012.245100

44. Roy A, Guatimosim S, Prado VF, Gros R, Prado MA. Cholinergic activity as a new target in diseases of the heart. *Mol Med*. (2015) 20:527–37. doi: 10.2119/molmed.2014.00125

45. Ben Assayag E, Shenhar-Tsarfaty S, Ofek K, Soreq L, Bova I, Shopin L, et al. Serum cholinesterase activities distinguish between stroke patients and controls and predict 12-month mortality. *Mol Med*. (2010) 16:278–86. doi: 10.2119/molmed.2010.00015

46. Caeiro L, Novais F, Saldanha C, Pinho EMT, Canhao P, Ferro JM. The role of acetylcholinesterase and butyrylcholinesterase activity in the development of delirium in acute stroke. *Cereb Circ Cogn Behav*. (2021) 2:100017. doi: 10.1016/j.cccb.2021.100017

47. Chen YC, Chou WH, Fang CP, Liu TH, Tsou HH, Wang Y, et al. Serum level and activity of butylcholinesterase: a biomarker for post-stroke dementia. *J Clin Med*. (2019) 8:1778. doi: 10.3390/jcm8111778

48. Beckmann J, Lips KS. The non-neuronal cholinergic system in health and disease. *Pharmacology*. (2013) 92:286–302. doi: 10.1159/000355835

49. Kawashima K, Mashimo M, Nomura A, Fujii T. Contributions of non-neuronal cholinergic systems to the regulation of immune cell function, highlighting the role of alpha7 nicotinic acetylcholine receptors. *Int J Mol Sci*. (2024) 25. doi: 10.3390/ijms25084564

50. Darreh-Shori T, Hosseini SM, Nordberg A. Pharmacodynamics of cholinesterase inhibitors suggests add-on therapy with a low-dose carbamylating inhibitor in patients on long-term treatment with rapidly reversible inhibitors. *J Alzheimers Dis*. (2014) 39:423–40. doi: 10.3233/JAD-130845

51. Darreh-Shori T, Rezaeianyazdi S, Lana E, Mitra S, Gellerbring A, Karami A, et al. Increased active OMI/HTRA2 serine protease displays a positive correlation with cholinergic alterations in the Alzheimer's disease brain. *Mol Neurobiol*. (2019) 56:4601–19. doi: 10.1007/s12035-018-1383-3

52. Karami A, Eriksdotter M, Kadir A, Almkvist O, Nordberg A, Darreh-Shori T. CSF cholinergic index, a new biomeasure of treatment effect in patients with Alzheimer's disease. *Front Mol Neurosci*. (2019) 12:239. doi: 10.3389/fnmol.2019.00239

53. Karami A., Eyjólfsdóttir H., Vijayaraghavan S., Lind G., Almqvist P., Kadir A., et al. Changes in CSF cholinergic biomarkers in response to cell therapy with NGF in patients with Alzheimer's disease. 12th international Stockholm/Springfield symposium on advances in Alzheimer therapy, May 9–12, 2012 Stockholm, Sweden (2012).

54. Karami A, Eyjolfsdottir H, Vijayaraghavan S, Lind G, Almqvist P, Kadir A, et al. Changes in CSF cholinergic biomarkers in response to cell therapy with NGF in patients with Alzheimer's disease. *Alzheimers Dement*. (2015) 11:1316–28. doi: 10.1016/j.jalz.2014.11.008

55. Vijayaraghavan S, Karami A, Aeinehband S, Behbahani H, Grandien A, Nilsson B, et al. Regulated extracellular choline acetyltransferase activity – the plausible missing link of the distant action of acetylcholine in the cholinergic anti-inflammatory pathway. *PLoS One*. (2013) 8:e65936. doi: 10.1371/journal.pone.0065936

frontiers | Frontiers in Cell and Developmental Biology

TYPE Review
PUBLISHED 10 June 2025
DOI 10.3389/fcell.2025.1580479

OPEN ACCESS

EDITED BY
Haipeng Liu,
Coventry University, United Kingdom

REVIEWED BY
Samir Ranjan Panda,
University of California San Francisco, United States
Hongmei Yang,
Harvard Medical School, United States
Samar F. Darwish,
Badr University in Cairo, Egypt
Zhongmin Zou,
Army Medical University, China
Deep Yadav,
National Cancer Institute at Frederick (NIH), United States

*CORRESPONDENCE
Ming Xia,
xiaruibing2009@163.com
Jiwei Cheng,
chengjiwei1@126.com

†These authors have contributed equally to this work

RECEIVED 20 February 2025
ACCEPTED 28 May 2025
PUBLISHED 10 June 2025

CITATION
Yu L, Dong Y, Li M, Liu H, Yan C, Li X, Gu Y, Wang L, Xu C, Xu J, Yuan Z, Xia M and Cheng J (2025) Targeting microglia polarization with Chinese herb-derived natural compounds for neuroprotection in ischemic stroke. *Front. Cell Dev. Biol.* 13:1580479. doi: 10.3389/fcell.2025.1580479

Targeting microglia polarization with Chinese herb-derived natural compounds for neuroprotection in ischemic stroke

Lu Yu[1†], Yin Dong[1†], Mincheng Li[1†], Huifang Liu[2], Cuina Yan[1], Xiaoxian Li[3], Yuehua Gu[1], Liwei Wang[1], Chuan Xu[4], Jie Xu[1], Zhen Yuan[1], Ming Xia[1]* and Jiwei Cheng[1]*

[1]Comprehensive Department of Traditional Chinese Medicine, Department of Neurology, First Department of Integration, Putuo Hospital, Shanghai University of Traditional Chinese Medicine, Shanghai, China, [2]Department of Neurology, Shanghai Jinshan Hospital of Integrated Traditional Chinese and Western Medicine, Shanghai, China, [3]Department of Traditional Chinese Medicine, Xinqiao Community Health Service Center, Shanghai, China, [4]Department of Neurology, Yueyang Hospital of Integrated Traditional Chinese and Western Medicine, Shanghai University of Traditional Chinese Medicine, Shanghai, China

Given that ischemic stroke ranks as one of the most fatal diseases globally, it is imperative to develop clinically effective neuroprotective agents for stroke. Microglia serve as innate immune cells for maintaining brain homeostasis, and upon activation, they are well-known to be able to transform into two functional phenotypes, namely, the M1 and M2 types, which can convert each other and exert opposing effects on neurotoxicity and neuroprotection, respectively. Traditional Chinese medicine possesses a deep-rooted and profound history with rich theory in treating cerebrovascular disorders, and its natural compounds have been considered as promising adjunctive therapies. Recently, researchers have been devoting attention to the inflammation-suppressive properties of the compounds from Chinese herbs. These compounds are gradually emerging as adoptable therapeutic agents with wide application prospect for improving stroke outcomes, through regulating microglial polarization to attenuate neuroinflammation. Thereby, we reviewed the functions of microglial cells in inflammation and neuroprotection and explored the regulation of microglial activity by natural compounds to alleviate neuroinflammation and protect neural function after ischemic stroke. Collectively, using natural compounds to suppress the microglia-mediated detrimental inflammatory response, meanwhile enhancing their anti-inflammatory abilities to accelerate neuronal recovery, will be promising therapeutic approaches for ischemic stroke.

KEYWORDS

ischemic stroke, microglia, neuroinflammation, traditional Chinese herbs, natural compounds

1 Introduction

Stroke is the second leading cause of death worldwide and its morbidity rates continue escalating (Feigin et al., 2022). Ischemic stroke is the most common type of stroke, accounting for 87% of all cases (Saini et al., 2021), characterized by the formation of arterial thrombosis, which leads to blood flow interruption in a specific brain region, related to the responsible blood vessels (Jadhav et al., 2021), and in turn, triggers a cascade of neurological symptoms (Khoshnam et al., 2017). Currently, reperfusion therapies have been considered practical intervention strategies for ischemic stroke. However, their application remains limited due to the narrow therapeutic time window (Xiong et al., 2018). Thus, crucial problems existing in the management of ischemic stroke lie in discovering effective complementary methods to enhance therapeutic effects and improve stroke outcomes.

Microglia, the immune cells residing in the brain, serve as the initial responders when a cerebral ischemic attack occurs. They are activated within hours and remain active for several days after stroke (Ren et al., 2023). Microglia are renowned for exerting dual roles during the process of cerebral ischemic insult. It can transform from a resting state to an activated state, acquiring beneficial or detrimental bidirectional phenotypes (Ri et al., 2023). In this regard, microglia can regulate the progression of inflammation during brain ischemia by exerting either pro-inflammatory or anti-inflammatory effects (Paul and Candelario-Jalil, 2021; Var et al., 2021). Therefore, different measures aimed at regulating microglial responses to attenuate neuroinflammation can potentially rescue ischemia-damaged neurons.

In recent years, researchers have put emphasis on the redevelopment and utilization of traditional Chinese herbal medicine, which has been extensively applied as complementary and alternative therapies for cerebrovascular diseases under the guidance of theories of traditional Chinese medicine, with remarkable clinical effectiveness and few side effects. Natural compounds, isolated from Chinese herbs, are renowned for their multi-effective and multi-targeting properties (Yu et al., 2020). Emerging evidence has exhibited a broad application prospect of natural compounds in clinic, and the mechanisms of the actions of these compounds on cerebral ischemic injury have gradually been unveiled (Li X. H. et al., 2022; Yu et al., 2022a). The regulatory effects of natural compounds, as well as multi-component extracts, on microglial response have emerged as research hotspots. In this article, we will focus on the neuroprotective actions of natural compounds in cerebral ischemic insult and the regulatory effects of these compounds on microglia-mediated neuroinflammation, along with the related mechanisms involved.

2 Mechanisms of microglia in ischemic stroke

2.1 Ischemic stroke

Stroke can be classified into two major categories: ischemic and hemorrhagic, in which ischemic stroke represents over 80% of all occurrences (Feigin et al., 2022). In cases of ischemic stroke, circulating thrombi (or atherosclerotic plaques) obstruct cerebral blood vessels, such as the middle cerebral artery (MCA), leading to an interruption in blood and oxygen supply. This disruption results in neuronal necrosis, ultimately damaging brain structure and function (Liu H. W. et al., 2023). Consequently, it leads to a cascade of neurological symptoms, including loss of balance, hemiplegia, decreased sensory and vibratory perception, numbness, reduced or enhanced reflexes, ptosis,and visual field impairment, etc. (Khoshnam et al., 2017). The occurrence of brain ischemia initiates a sequence of detrimental events, including depletion of the ATP-dependent Na+/K+ pump, elevated levels of free cytosolic calcium, overaccumulation of glutamate outside the cell, excessive stimulation of N-methyl-D-aspartatic acid (NMDA) receptor, neuronal excitotoxicity, production of reactive oxygen species (ROS), oxidative stress, mitochondrial dysfunction, and inflammatory response (Jia et al., 2019) (Table 1). These pathological processes interact with each other, causing irreversible damage to neurons, glia and endothelial cells, which further bring about secondary brain injury, manifesting in apoptosis and autophagy/mitophagy in neuronal cells, blood-brain barrier (BBB) damage, hemorrhagic transformation, and vascular brain edema (Khoshnam et al., 2017). As the limited therapeutic time window of stroke, it is imperative to develop efficient complementary intervention methods to improve the clinical effects and the disease outcomes. Neuroinflammation elicited by the excessive activation of microglia is a key pathological process in the brain ischemia. Activated microglial cells are well known to polarize into bidirectional phenotypes, representing proinflammatory or anti-inflammatory action, depending on the specific activation signals they encounter. During the initial stage of brain ischemia, M1 subtype microglia induce neuroinflammation, which causes neuronal death and BBB damage, exacerbating brain ischemic insult. In the late stage of ischemic insult, M2 subtype microglia prompt the process of neuroprotection and neurorestoration, responsible for tissue repair and remodeling. Thus, modulating the equilibrium of microglial polarization to attenuate neuroinflammation might be a promising therapeutic method for treating ischemic stroke.

2.2 Morphology, structure, and physiological functions of microglia

Microglial cells are derived from myeloid progenitors originating in the yolk sac, and migrate into the brain during their initial stage of development before the blood brain barrier formation (Ginhoux et al., 2010; Waisman et al., 2015). They constitute a highly plastic group of neuroglia, accounting for 5%–15% of the total brain cells, and exhibiting varying proportions across diverse brain regions (Pelvig et al., 2008). Once microglia migrate into the brain, they mature into self-maintaining and renewing populations, without any contribution to peripheral surroundings (Ajami et al., 2007; Ajami et al., 2011). As a kind of resident immune cells, microglia, branched with multiple slender protrusions, constantly patrol, and scan the microenvironment in the brain using their motor branches, interacting with adjacent cells and factors, which is so called resting state of microglia. Evidence suggested that microglia in resting state are not entirely quiescent,

TABLE 1 Different pathological stages of brain ischemia.

Time course	Pathological mechanisms
Acute phase (minutes-hours)	• Decreased cerebral blood flow with inadequate oxygen/glucose delivery • Deprivation of ATP, depolarization of membrane and increased influx of intracellular ion • Accumulation of glutamate, overactivation of AMPA and NMDA • Release of neuromediators (excitotoxicity)
Subacute phase (hours-days)	• Generation of ROS and oxidative stress • Increased expression of cellular adhesion molecules • Activation of microglia and infiltration of leukocyte into the ischemic region • Secretion of pro-inflammatory mediators • Neuronal apoptosis • Autophagy/mitophagy • Dysfunction of BBB and endothelium
Delayed phase (days-weeks)	• Release of trophic factors (BDNF, IGF, GDNF) • Neurogenesis, angiogenesis, axonal remodeling, synaptogenesis • Proliferation of neuronal stem cells

but maintain a highly dynamic state (Li D. J. et al., 2018). When stimulated, microglia are rapidly converted into activated state (Cserép et al., 2021). Amoeboid-shaped microglia are observed to be abundant in the ischemic core area between 3 and 7 days in middle cerebral artery occlusion (MCAO) rats (Li Y. et al., 2021). On one hand, activated microglia fulfill their phagocytic function to eliminate pathogens, abnormal proteins, and cellular debris, including apoptotic cells and non-functional synapses, maintaining brain homeostasis (Nguyen et al., 2020). Phagocytic clearance of dead or dying cells by microglia is instrumental for inflammation resolution after stroke (Cai et al., 2019). On the other hand, they generate a huge number of signaling molecules, like pro-inflammatory cytokines, neurotransmitters, and extracellular matrix proteins, for modulating the activities of neurons and synapses (Nguyen et al., 2020). Besides, microglia perform a pivotal role in sustaining blood-brain barrier (BBB)'s integrity. In the early stage of ischemic stroke, microglia secrete pro-inflammatory factors, leading to a disruption in the BBB's structure and function; in the later stage, they safeguard BBB during neuroinflammation events by releasing anti-inflammatory mediators and engulfing immune cells (Qiu et al., 2021). Furthermore, microglia can stabilize synapses and orchestrate the development of neural circuit by regulating various neural elements, such as astrocytes, myelin and the extracellular matrix (Lukens and Eyo, 2022). However, microglia inadvertently generate ROS during the process of phagocytosis within phagosomes (Cheret et al., 2008). This ROS production can become detrimental in excessive amounts, contributing to oxidative stress, particularly in conditions like stroke (Zhang S. et al., 2024). Collectively, microglia exhibit remarkable phenotypic plasticity in response to destroyed brain homeostasis, such as ischemic condition. These various phenotypes can transform into each other based on changes in microglial morphology or the expression of cell surface antigens.

2.3 Activation of microglia after ischemic stroke

Microglia, the initial guardians of immune defense, promptly react to pathological alterations after brain ischemia occurs, maintaining an activated state for several months (Candelario-Jalil et al., 2022). In a transient ischemic stroke rat model, within 24 h after reperfusion, activated microglia become evident in the infarct core, reaching peak levels over a period of 4–7 days. In the peripheral region, microglia were detected to be accumulated within 3.5 h, with a peak at 7 days after reperfusion, which precedes the timing they appeared in the infarct area (Ito et al., 2001). Within the infarct core, microglial activation is initiated by excitotoxic signals that are triggered by brain ischemic insult. In contrast, in the penumbra region, microglial activation is closely tied to innate immune receptors, which are mediated by the release of neuromediators, damage-associated molecular patterns (DAMPs), high-mobility group box-1 (HMGB1) protein and reactive oxygen species (ROS), all originating from ischemia-damaged or -stressed neuronal cells (Khoshnam et al., 2017; Jurcau and Simion, 2022). The disruption of brain homeostasis induced by brain ischemia can trigger the activation of microglia, accompanied by morphological alterations (Ma et al., 2017). Once activated, microglial cells appear proliferated, migrate towards the ischemic-lesion site, and bring about diverse harmful effects, including releasing inflammatory cytokines and cytotoxic substances. They also generate inflammation-suppressive mediators, neurotrophic factors and growth factors that aid in tissue repair and eliminate cellular debris in the late stage of ischemic stroke (Ma et al., 2017). The roles of activated microglia, detrimental or beneficial, largely depend on their phenotypic polarization status after the onset of brain ischemia. Therefore, regulating the equilibrium of microglial phenotypic polarization is recognized as a hopeful therapeutic approach in treating ischemic stroke.

2.4 Microglial M1/M2 phenotypical polarization after ischemic stroke

The "detrimental" M1 type and "beneficial" M2 type are two subtypes of activated microglia, based on their distinct expression profiles of protein and cytokine (Lyu et al., 2021). After the occurrence of ischemia, the release of DAMPs from dead cells triggers microglial activation. Resting microglia are polarized into pro-inflammatory M1 phenotype. In stroke mice with MCAO, M1 microglia was found to secrete inflammatory cytokines, comprising tumor necrosis factor (TNF)-α, interleukin (IL)-1β, IL-6, IL-12, and IL-23, and enhance the levels of inducible nitric oxide synthase (iNOS) and proteolytic enzymes like MMP9 and MMP3 (Zhao et al., 2020; Zhu et al., 2021). M1 phenotype can be identified by detecting specific cell surface markers, like CD16, CD32, and CD86. Various phenotypic states of microglia can be interconverted through their specific activation pathways (Figure 1). In the polarization of the M1 phenotype, multiple signaling molecules interact to form the pro-inflammatory network. TLR4, an important immunorecognition receptor in the neuroinflammation cascade, can be transported to functional areas in the brain. When stimulated by ischemic injury, it recognizes DAMPs, leading to the activation of the

p65 subunit of downstream NF-κB pathway, which promotes the transcription of NLRP3 inflammasome components and further regulates inflammatory mediators (Luo et al., 2022; Chen et al., 2023). NLRP3 inflammasome, mainly observed in microglia, plays a crucial role in the inflammatory response following ischemic stroke. Its activation involves the recruitment of pro-caspase-1 to the NLRP3 receptor protein upon ischemia stimuli (Li X. et al., 2024). Suppressing the activation of NLRP3 inflammasome prevents the nuclear translocation of NF-κB p65, modulating microglial polarization and inhibiting microglial apoptosis, thus attenuating neuroinflammation induced by MCAO (Luo et al., 2022; Cai et al., 2024). The nuclear factor kappa B (NF-κB), an upstream signaling for the NLRP3 inflammasome, is capable of activating NLRP3 and inducing M1 microglial polarization (Barnabei et al., 2021; Chen Q. J. et al., 2021). During the acute stage of brain ischemia, the degradation of IκB was found to facilitate the nuclear translocation of NF-κB subunit p65, activating microglia and initiating the transcription of downstream proinflammatory genes (Bi et al., 2024). Notch signaling is activated through the interaction between Notch receptor and ligands, which causes nuclear translocation of intracellular Notch receptor domain (NICD). The NICD then binds to the effector molecules in the nucleus, thus activating the target genes, and subsequently inducing the transcriptional activation of NF-κB and regulating the transformation of microglia into M1 phenotype (Li X. H. et al., 2022). In the MCAO mouse model, the phosphorylation of signaling transducers and activators of transcription (STAT3) was observed to phosphorylate IκB and facilitate NF-κB nuclear translocation, leading to M1-like phenotype transformation (Liu Y. et al., 2024). Meanwhile, glycogen synthase kinase-3β, known as a serine/threonine kinase for controlling NF-κB signaling, dampens the activity of cAMP response element-binding protein (CREB) and increases the accumulation of intranuclear NF-κB induced by brain ischemia (Jover-Mengual et al., 2010). Prostaglandin E2 (PGE2), as a pro-inflammatory mediator, activates downstream signaling pathways through binding to different PGE2 receptors (EP) (Hosoi et al., 2013). Moreover, mTORC1, the contributor to the dysregulation of cellular function following brain ischemia, can mediate M0 microglia to polarize into pro-inflammatory M1 phenotype (Li et al., 2016). These molecules intricately interact with other pro-inflammatory signaling pathways, thus promoting or prolonging the polarization of the M1 phenotype and exacerbating neuroinflammation during the early stage of ischemic stroke (Figure 2).

A shift in microglia phenotype towards an anti-inflammatory M2 state represents a critical repair mechanism during brain ischemia. In contrast to the M1 phenotype, the M2 phenotype generates anti-inflammatory cytokines, such as transforming growth factor (TGF)-β, IL-4, IL-10 and IL-13, as well as increases the levels of growth factors, such as vascular endothelial growth factor (VEGF) and brain-derived neurotrophic factor (BDNF) for neuronal repair at the late stage of ischemic stroke (Qin et al., 2019; Lyu et al., 2021). M2 phenotype with anti-inflammation can be distinguished via some specific biomarkers like CD206 and arginase 1 (Arg1) (Lambertsen et al., 2019; Jurga et al., 2020) (Figure 1). Besides, the activated M2 phenotypes can further be categorized into M2a, M2b and M2c (Almolda et al., 2015). Among that, the M2a subtype is involved in reparative and regenerative processes; the M2b subtype, serving as an intermediate phenotype, is associated with inflammation modulation; M2c subtype participates in neuroprotection, including the clearance of cellular debris and tissue remodeling (Almolda et al., 2015). The polarization of M2 microglia is governed by several key signaling molecules. Peroxisome proliferation-activated receptor γ (PPARγ) serves as a transcription factor to control inflammation. It was found to orchestrate the polarization of microglia and promote the phagocytic ability of microglia, contributing to anti-inflammatory response in mice with tMCAO (Liu X. et al., 2024). Building on this, cAMP response element binding protein (CREB), cooperates with C/EBPβ to promote the expression of PGC-1α, which acts as a transcriptional coactivator to enhance the activity of PPARγ, thus increasing expressions of M2 phenotype-specific genes for maintaining microvascular integrity and ameliorating brain ischemic injury in MCAO rats (Ruffell et al., 2009; Ruan et al., 2019). Additionally, interferon regulatory factor-3 (IRF-3) can be activated through its upstream PI3K/AKT signaling pathway (Tarassishin, et al., 2011), in the form of phosphorylation, facilitating its dimerization and interaction with coactivators. The activated IRF-3 complex translocates into the nucleus and then modulates the transcription of target genes, thereby promoting M2 microglia polarization (Cho et al., 2016; Chistiakov et al., 2017). These signaling pathways collectively establish the functional characteristics of the M2 phenotype during the subacute to chronic phases of brain ischemia (Figure 3).

Notably, some studies pointed out the dichotomous nature of microglia, indicating that they exclusively transform into either M1 or M2 phenotype (Nguyen et al., 2020). However, these views are unable to entirely and accurately capture the intricate physiological characteristics and functions displayed by microglia. Morganti et al. reported that traumatic brain injury elicited a coexistence of different states of microglia, responsible for the production of inflammatory mediators (Morganti et al., 2016). Additionally, microglia were found to occupy a continuous expression spectrum ranging between the M1 and M2 subtypes in ischemia-induced damaged tissue (Hou et al., 2021). Furthermore, with the emergence of single-cell analysis technologies, microglia have been shown to exhibit specific subpopulations under inflammatory conditions that were distinct from neurodegenerative-associated phenotypes, indicating the heterogeneity in activation states of microglia and reflecting their specific functions in relevant environments (Sousa et al., 2018).

Various factors, including severity degrees of ischemic injury, different pathological stages during brain ischemia, the surrounding pathological environment, as well as aging, can influence the polarization of microglia at some extent (Ri et al., 2023). During the initial period of brain ischemia, microglia expressing the M1 phenotype can be detected in the ischemic core area (Subedi and Gaire, 2021; Zhang W. et al., 2021), whereas most microglial cells polarize towards the M2 phenotype in peri-infarct regions. However, a gradual transition towards the M1 phenotype occurs about 1 week after the brain insult, and lasts for weeks thereafter (Zhao et al., 2017; Lyu et al., 2021). The transformation of microglial phenotypes is contingent upon diverse signals they encounter or receive in the pathological environment. Thus, with the appropriate intervention measures, the M1 phenotype might be converted into the so-called protective M2 phenotype, thereby protecting against brain ischemic injury (Ye et al., 2019; Xu et al., 2021). Besides,

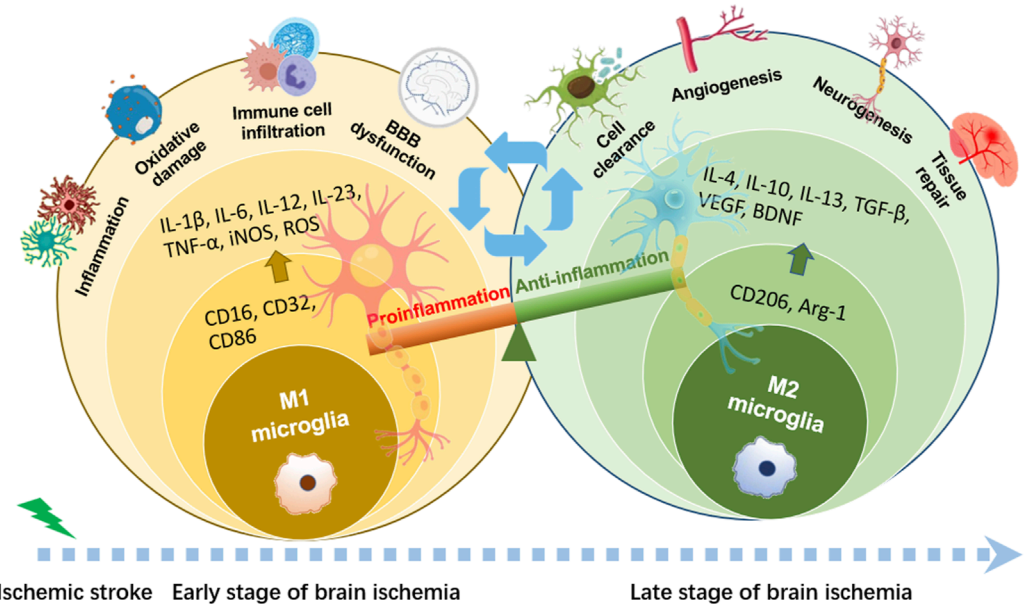

FIGURE 1
Phenotypic polarization of microglia. Once brain ischemia occurs, microglia rapidly switch from resting state to activated state with amoeboid-like phenotype in morphology. M1 phenotypic microglia mainly release the production of IL-1β, IL-6, IL-12, IL-23, TNF-α, iNOS and ROS, which have cytotoxic effects on neurons, resulting in inflammatory response and oxidative damage. M2 phenotypic microglia mainly secrete the production of IL-4, IL-10, IL-13, TGF-β, VEGF, BDNF, which can attenuate neuroinflammation and promote neurogenesis, for neuronal function recovery and injured tissue repair.

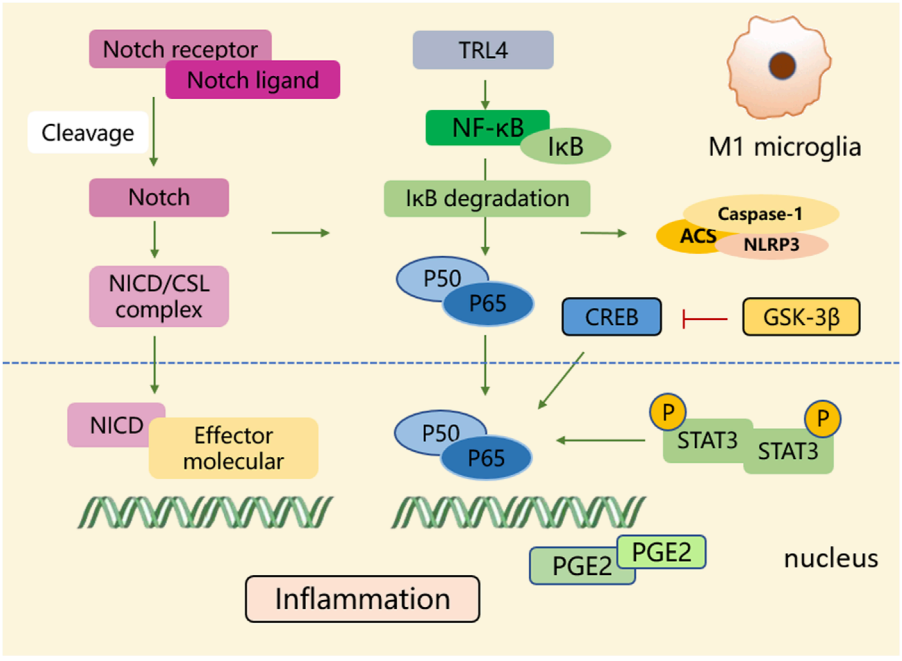

FIGURE 2
The polarization process of microglial M1 type. During the polarization process of the M1 phenotype, multiple signaling molecules construct a pro-inflammatory network. Signaling pathways such as NF-κB, Notch, STAT3, glycogen synthase kinase-3β, and PGE2 play crucial roles in activating transcriptional genes and downstream signaling cascades.

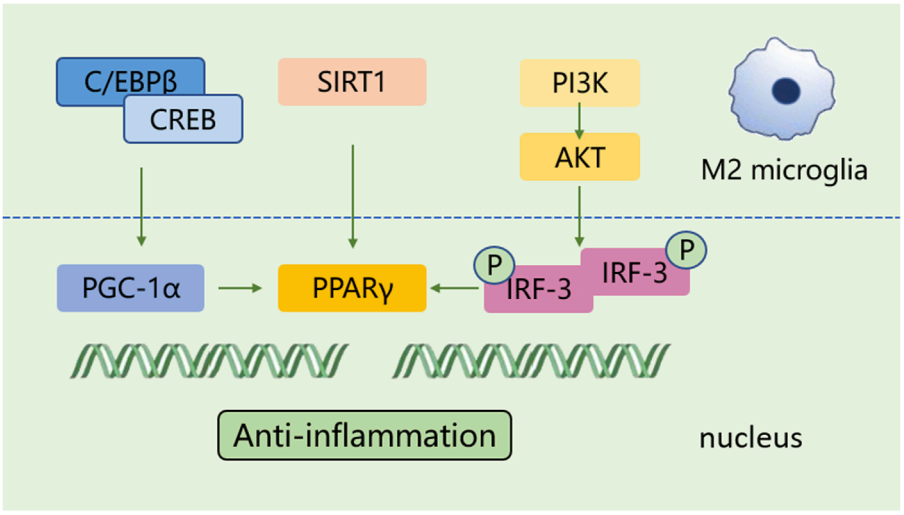

FIGURE 3
The polarization process of microglial M2 type. The polarization of M2 microglia is regulated by several key signaling molecules, such as PPARγ, CREB, and IRF-3, and others. These molecules control inflammation by regulating gene transcription and establish the functional characteristics of the M2 phenotype.

it has been found that diverse transcriptional mediators closely related to the M1/M2 polarization process represent differential expression patterns within the ischemic region, which serve as action targets for regulating the states of microglia (Holtman et al., 2017). Since M1 and M2 are commonly used to distinguish between distinct microglial phenotypes, the M1 phenotype is typically considered to mediate a pro-inflammatory response that exacerbates ischemic damage, conversely, the M2 phenotype participates in neuronal remodeling and repair processes during the delayed stage of brain ischemia. Therefore, developing therapeutic strategies for ischemic stroke, with the focus on regulating microglial polarization and facilitating their transformation into the neuroprotective M2 phenotype, has become a hotspot that attracts researchers' attention.

2.5 Microglia-mediated neuroinflammation and neuroprotection in ischemic stroke

The inflammatory response is regarded as a pivotal defensive mechanism partially mediated by microglia, tasked with eliminating cellular debris and facilitating tissue repair during the process of brain ischemia (Wei et al., 2020). Once ischemic stroke occurs, resident microglia can first sense and immediately react to danger signals (Lambertsen et al., 2019). They become activated by numerous ischemia-induced damage-associated molecular patterns (DAMPs) (Subedi and Gaire, 2021) and induce a significant inflammatory reaction. The overactivation of microglia generates inflammatory factors, such as IL-6, TNF-α, ROS, and NO, which further drive several types of cell death, including necrosis, apoptosis, and pyroptosis, mediated by the inflammasome and caspases (Xiong et al., 2016). Beyond that, inflammatory factors directly act on mitochondria, leading to abnormalities in their morphology and function. This in turn disrupts mitochondrial dynamics, which are characterized by continuous fusion and fission processes (Gan et al., 2025). The resulting mitochondrial dysfunction activates the NLRP3 inflammasome, promoting microglial M1 polarization. Meanwhile, the shift towards a proinflammatory M1 phenotype accelerates mitochondrial fission. This process leads to the release of damaged mitochondria, ultimately causing neuronal death (Gan et al., 2025). Damaged mitochondria transfer to neurons and fused with neuronal mitochondria, leading to elevated ROS production. The accumulation of ROS and the resultant oxidative stress injury triggers a vicious cycle involving microglial activation, aggregation, and hypersecretion of inflammatory factors (Zhang S. et al., 2024). These factors elicit the recruitment and infiltration of immune cells, including neutrophils, monocytes/macrophages, and T cells, towards the brain parenchyma, leading to a series of inflammatory reactions and subsequent disruption of the BBB, like increased permeability, diminished transport kinetics, and increased vulnerability to toxic or harmful molecules (Ronaldson and Davis, 2020; Zhang S. P. R. et al., 2021). A sequence of stroke-associated adverse outcomes is then followed, including vascular brain edema, hemorrhage transformation, and leakage of toxic substances from the BBB (Ma et al., 2017; Yang et al., 2019). Thereby, blocking the production of pro-inflammatory mediators from microglia to attenuate BBB disruption and tissue damage represents a hopeful therapeutic method for ischemic stroke (Lu et al., 2019; Liu et al., 2020b).

In contrast to M1 microglia, activated M2 microglial cells exhibit neuroprotective and neurorestorative functions during the delayed stage of brain ischemia (Miron et al., 2013). On one hand, M2 microglia produces numerous cytokines, releases various growth factors, and generates several neurotrophic factors, which provide significant assistance in suppressing inflammation, protecting neurons, and promoting tissue repair following ischemic insult (Wang Y. et al., 2022). For another, M2 microglia phagocytize cell debris and myelin fragments and initiate

the processes of synaptogenesis and neurogenesis, contributing to mitigating the harmful events and promoting tissue repair (Jia et al., 2021). Additionally, they phagocytize immune cells within damaged brain tissue when encountering special "eat me" signals emitted by endangered cells, thereby modulating inflammatory response (Yu F. et al., 2022). Moreover, M2 microglia promote the restoration of neuronal functions, encompassing neurogenesis, axonal regeneration, angiogenesis, oligodendrocyte production and remyelination, healing the injured tissue (Hu et al., 2015; Zhang S. P. R. et al., 2021). Beyond that, M2 microglia enhance the proliferation, differentiation, survival, and integration of neural progenitor cells (NPCs) in the ischemia-damaged brain (Deierborg et al., 2010). Elevating the number of insulin-like growth factor-1 (IGF-1)-expressed microglial cells following stroke can attenuate cellular apoptosis and facilitate the proliferation and differentiation of neural stem cells (NSCs) (Thored et al., 2009). Amplifying microglial reparative capabilities improves oligodendrocyte regeneration and remyelination during the late stage of ischemia (Shi et al., 2021). Moreover, microglia can stimulate vessel growth and angiogenesis directly or indirectly, representing their improvement effects on blood vessel reconstruction after stroke (Lyu et al., 2021). Apart from that, the polarization of M2 microglia enhances neural regeneration, leading to sustained neuroprotectiveness in the chronic phase of cerebral ischemia (Jin et al., 2014; Zhu J. et al., 2019; Shang et al., 2020).

Though detailed molecular mechanisms underlying the neuroprotective properties of microglial cells remain incompletely understood, numerous evidence supports their beneficial effects on neuronal recovery post stroke (Zhang W. et al., 2021). Altogether, regulating the activation and phenotypic transformation of microglia, to suppress M1-induced neuroinflammation and promote M2-associated neuronal recovery and tissue repair offers promising intervention strategies for ischemic stroke.

3 Regulatory effects of natural compounds from Chinese herbs on microglial response in ischemic stroke

Traditional Chinese herbal medicine has experienced a profound history in treating different diseases, including ischemic stroke. They have been demonstrated to possess remarkable efficacy with few side effects through extensive long-term clinical practices, such as honghua injection (Li L. et al., 2022), danhong injection (Wang et al., 2016), shuxuetong injection (Fang et al., 2020), and xuesaitong injection (Feng et al., 2021). Diverse natural compounds isolated from these Chinese herbs exhibit a wide range of pharmacological functions (Supplementary Table S1). Hence, it is necessary to elucidate the related mechanisms involved in pharmacological properties of the compounds. Substantial evidence indicates that natural compounds can effectively attenuate brain ischemic damage, foster neuronal recovery and improve prognosis by modulating the polarization of microglia. They regulate the signaling pathways and molecular targets to inhibit M1 microglial polarization and prompt M2 phenotypic transformation, thereby ameliorating inflammatory responses, maintaining BBB function, inhibiting neuronal apoptosis, attenuating oxidative stress, relieving neuronal excitoxicity, and promoting neurogenesis and angiogenesis.

Since activated microglia express mixed M1 and M2 markers with varying degrees in the damaged tissue, the modulation effects of natural compounds on microglia merits further reconsideration. It is rational to believe that the compounds possibly influence the equilibrium of microglial polarization, rather than directly induce exclusive activation of either M1 or M2 subtype (Ri et al., 2023). Herein, we will focus on various regulators engaged in the microglial response following cerebral ischemic injury, summarize their molecular mechanisms, and explain how representative natural compounds attenuate microglia-mediated neuroinflammation through these mechanisms.

3.1 Flavonoids

3.1.1 Wogonin

Wogonin is the main active constituent separated from *Scutellaria baicalensis* Georgi (Zhao et al., 2019). It has been demonstrated to possess an extensive spectrum of pharmacological actions, like anti-inflammation and anti-oxidation. Yeh et al. reported that wogonin could suppress the generation of PGE2 and nitric oxide (NO) in lipopolysaccharide (LPS)/interferon (IFN) γ-induced BV2 microglial cells through the modulation of the Src-MEK1/2-(ERK)1/2-NFκB signaling pathway, which was responsible for the alleviation effect of wogonin on neuroinflammation (Yeh et al., 2014).

3.1.2 Ginkgetin

Ginkgetin is a flavonoid dimer extracted from ginkgo, exhibiting anti-cancer, anti-inflammatory, anti-microbial, anti-adipogenic, and neuroprotective activities (Adnan et al., 2020). In recent years, it has been gradually discovered in more than 20 different plant species, most of which are well-known for their use in traditional medicine (Cankaya et al., 2023). PPARγ is a ligand-responsive nuclear transcription factor and has been identified to participate in various pathological processes, including regulating the transformation of microglia/macrophage to resolve inflammation and promote brain repair (Fang et al., 2024). Tang et al. reported that ginkgetin treatment shifted microglia from M1 towards M2 subtype, inhibited neuroinflammation, and exerted neuroprotective effects in OGD cellular model and in MCAO rats. However, the ginkgetin's effects were abolished by PPARγ antagonist GW9662, indicating that the promotion effect of ginkgetin on M2 microglial polarization was mediated through PPARγ signaling pathway (Tang T. et al., 2022).

3.1.3 Baicalin

Baicalin, a pleiotropic flavonoid ingredient, has attracted considerable interest for its neuroprotective effects on kinds of inflammatory and demyelinating diseases in central nervous system (Li Y. et al., 2020; Ai et al., 2022). Baicalin has been found to regulate the activation of microglia and astrocytes in the hippocampus of LPS-treated mice, resulting in neuroinflammation attenuation (Shah et al., 2020). Consistently, *in vitro* experiments using LPS-induced BV-2 microglial cells revealed that baicalin reduced the production of inflammatory mediators. Importantly, the inflammatory effects of baicalin were realized by blocking

toll-like receptor 4 (TLR4)-mediated signaling transduction through TLR4/MyD88/NF-κB and mitogen-activated protein kinases (MAPK) pathways (Li B. et al., 2022). In response to LPS-induced neuroinflammation in mice and microglial cell line, baicalin was evidenced to decrease microglia-mediated inflammation via downregulating HMGB1 level in a Sirtuin 1 (SIRT1)-dependent manner (Li Y. et al., 2020). These studies demonstrate that baicalin modulates microglia activation in LPS-induced neuroinflammatory models. Moreover, Xiao et al. set up a chronic cerebral hypoperfusion animal model and found that baicalin modified microglia polarization towards an anti-inflammatory phenotype and inhibited pro-inflammatory cytokines production (Xiao et al., 2023). In MCAO mice and OGD/R-induced BV2 cells, Wang et al. observed that baicalin inhibited microglia activation by upregulating the level of TREM2, thereby suppressing inflammatory responses (Wang H. et al., 2024).

3.1.4 Icariin

Icariin is a flavonoid constituent extracted from Chinese medicinal herb, Epimedium, which is commonly used to treat bone fracture and bone loss for thousands of years (Wang et al., 2018). Recently, icariin has captured more attention due to its multiple pharmacological properties, like anti-aging, anti-oxidation, and anti-inflammation (Liu et al., 2015). Current studies have validated neuroprotective actions of icariin against neurodegenerative diseases (Zheng et al., 2019). Nuclear factor erythroid 2 related factor 2 (Nrf2) serves as a key facilitator of endogenous inducible defense mechanisms, encoding diverse array of enzymes with anti-oxidative activities. Activated Nrf2 possesses the properties of anti-oxidation and anti-inflammation (Zheng et al., 2019). Zheng et al. pointed out that icariin modulated microglial polarization, effectively mitigating LPS-induced pro-inflammatory factors in microglia. Furthermore, the triggering of Nrf2 signaling pathway was evidenced to engage in icariin-mediated anti-inflammatory effects (Zheng et al., 2019). Additionally, in oxygen-glucose deprivation/reoxygenation (OGD/R)-damaged microglial cells, icariin downregulated the levels of IL-1β, IL-6 and TNF-α by the suppression of IRE1α-XBP1 signaling pathway, implying that its anti-inflammation effects could be achieved by mitigating endoplasmic reticulum stress (Mo et al., 2021).

3.1.5 Quercetin

Quercetin, existing in diverse traditional Chinese medicinal herbs, tea, fruits, and vegetables, is a common plant flavonoid with kinds of pharmacological effects, like anti-fibrosis, anti-virus, anti-cancer, anti-inflammation, as well as anti-oxidation (Russo et al., 2012). Quercetin has already been approved for clinical use owing to its suppressive effect on the activity of tyrosine kinase (Han et al., 2021). Han et al. reported that quercetin could regulate the LPS-induced proliferation and phagocytosis of primary microglia. Moreover, it suppressed inflammatory response in LPS-treated BV2 microglial cells without compromising their cellular viability. This suppression was likely attributed to its ability in reducing the expressions of NLR family, pyrin domain-containing 3 (NLRP3) inflammasome and pyroptosis-related proteins by promoting mitophagy (Han et al., 2021).

3.1.6 Hydroxysafflow yellow A

Hydroxysafflow yellow A (HSYA), a main bioactive compound extracted from *Carthami flos*, has been extensively used for cardio- and cerebrovascular diseases with its diverse biological functions, such as anti-oxidation, anti-inflammation, and anti-apoptosis, etc. (Yu et al., 2022b). It was reported that HSYA activated TLR9 in microglial cells of the ischemic cortex in rats with MCAO, and then blocked the pro-inflammatory NF-κB pathway from day 1 to day 7. However, its inflammation-suppressive action was abolished when silencing TLR9 in OGD/R-exposed primary microglial cells, indicating that the anti-inflammation effect of HSYA was tightly linked to reprograming the TLR9 signaling pathway (Gong et al., 2018). Similarly, in a Transwell co-culture system comprising microglia and neurons, HSYA treatment could suppress TLR4 expression in the LPS-activated microglia, resulting in reducing neuronal damage (Lv et al., 2016).

3.1.7 Schaftoside

Schaftoside exists in fruits, vegetables, nuts, seeds, herbs, spices, stems, flowers, as well as in tea and red wine (Romano et al., 2013). Zhou et al. reported that schaftoside could inhibit the generation of inflammation-promoting cytokines, like IL-1β, TNF-α and IL-6 in OGD/R-injured BV2 microglial cells through suppressing the activity of TLR4/MyD88 signaling pathway (Zhou et al., 2019). Mitochondria are critical organelles within microglia that regulate their functions. Mitochondrial dynamics, the balance between mitochondrial fission and fusion, are involved in numerous cellular pathways, including inflammation and apoptosis (Tabara et al., 2025). Dynamin-related protein 1 (Drp1) is a major modulator of mitochondrial fission, phosphorylation of Drp1 at the Ser616 site can speed up the fission of mitochondria (van der Bliek et al., 2013). Furthermore, schaftoside has been evidenced to inhibit expression level, phosphorylation, and translocation of Drp1 in OGD-conditioned BV2 microglial cells, hindering the fission of mitochondria and thereby counteracting neuroinflammatory response (Zhou et al., 2019).

3.2 Polyphenols

3.2.1 Gastrodin

Gastrodin, an effective polyphenol isolated from *Gastrodia elata*, possesses diverse neuroprotective effects, including attenuating brain ischemic damage (Zeng et al., 2006), ameliorating cytotoxicity mediated by hypoxia in cortex neurons (Xu et al., 2007), and safeguarding hippocampal neurons from neurotoxicity elicited by Aβ peptide (Zhao et al., 2012). Yao et al. pointed out that gastrodin could not only regulate the activation and the population size of microglia, but also suppress the LPS-induced inflammatory factors in both BV2 and primary microglial cells, as well as in three-day-old rats (Yao et al., 2019). Further study revealed that gastrodin inhibited inflammation and cell proliferation mainly through regulating the Wnt/β-catenin pathway (Yao et al., 2019). Interestingly, gastrodin was observed to hinder the release of pro-inflammatory mediators and concomitantly promoting the secretion of neurotrophic factors in OGD-stimulated BV2 microglia (Lv et al., 2021). The dual roles gastrodin performed in microglia might be due to its regulatory ability on MAPK signaling pathway

(Lv et al., 2021). Additionally, gastrodin exerted neuroprotective effects against the hypoxic-ischemia brain damage through the suppression of pro-inflammation mediators in activated microglia by the renin-angiotensin (RAS) system and the SIRT3 pathway (Liu S. J. et al., 2018). Moreover, it was found to block the migration of activated microglial cells through the Notch-1 pathway in LPS-stimulated BV2 microglia and postnatal rats (Yao et al., 2022). Most of these research findings have been observed in cellular models, indicating the inhibitory effects of gastrodin on microglial activation, proliferation, migration, and associated inflammation; however, validation in stroke animal models is still lacking.

3.2.2 Curcumin

Curcumin, a hydrophobic polyphenol separated from *Curcuma longa*, possesses a wide spectrum of therapeutic benefits, including inflammation-suppressive and antioxidative effects. Extensive studies have elucidated that curcumin could dampen the generation of reactive oxygen species and subsequently alleviate neuroinflammatory injury (Patel et al., 2020). Liu et al. reported that curcumin exhibited remarkable regulatory effects on microglia, facilitating M2 microglial polarization and inhibiting microglia-mediated inflammatory responses in mice subjected to dMCAO (Liu Z. et al., 2017). Similarly, curcumin was found to alleviate white matter lesions and reduce brain tissue loss at 21 days post stroke in MCAO mice. Cellular experiments further validated that curcumin could attenuate microglial pyroptosis induced by LPS and ATP, which is considered as a type of inflammatory programmed cell death (Ran et al., 2021). Emerging biomaterial-integrated drug delivery systems are employed to enhance the efficacy of natural compounds for ischemic stroke treatment, particularly focusing on modulating microglial inflammatory responses. Wang et al. prepared nanoparticles (NPs) using a single-emulsion method and encapsulated curcumin in mPEG-b-PLA block copolymer NPs to assess the intervention effects of NPcurcumin on brain ischemic insult (Wang Y. et al., 2019). The findings indicated that NPcurcumin was more efficient compared to curcumin alone in maintaining the integrity of BBB, dampening the activation of M1 microglia, and reducing the levels of inflammatory factors (Wang Y. et al., 2019). Moreover, for targeting the stroke cavity and ensuring sustained on-site drug release, Zhang et al. synthesized a curcumin-loaded injectable hydrogel with double ROS-scavenging effect. They found that curcumin loaded into hydrogels with enhanced ROS-scavenging capacity could facilitate anti-inflammatory microglia polarization through hindering the translocation of p47-*phox* and p67-*phox*, and subsequently enhancing neuroplasticity (Zhang S. et al., 2024).

3.2.3 Resveratrol

Resveratrol, a natural polyphenolic compound presenting in grapes, peanuts, plums, red wines, as well as other dietary sources, exhibits multiple biological activities, including anti-oxidation, anti-inflammation, anti-cancer, and neuroprotection (Zhang L. X. et al., 2021). Recently, resveratrol has been found to facilitate M2 microglia polarization for neuronal restoration following cerebral ischemia (Yang et al., 2017). Decreased expression of astroglial type-1 glutamate transporter (GLT-1) in the hippocampus after stroke leads to an increase in glutamate levels, which is considered as a key facilitator in neurotoxicity (Girbovan and Plamondon, 2015). Girbovan et al. reported that resveratrol could reverse the global ischemia-induced downregulation of GLT-1 level and inhibit the overexpression of CD11b/c and glial fibrillary acidic protein (GFAP), suggesting beneficial roles resveratrol performed in regulating microglial activation and attenuating excitotoxic cascade (Girbovan and Plamondon, 2015). Nrf2 is coupled with its cytoplasmic inhibitor, kelch-like ECH-associated protein 1 (KEAP1), functioning as an intracellular safeguard against oxidative insults (Chen S. et al., 2021). In the case of oxidative stress, Nrf2 dissociates from its inhibitor KEAP1, translocates towards the nucleus and interacts with the antioxidant response element, enhancing the activities of antioxidant enzymes (Kobayashi and Yamamoto, 2005). Since miR-450b-5p serves as a potential therapy target in inflammatory disorders (Luo et al., 2019), Liu et al. revealed that resveratrol could elevate Nrf2 level by modulating miR-450b-5p/KEAP1 axis, leading to the promotion of M2 microglial polarization, thus exerting neuroprotective effects against ischemic injury in MCAO rats (Liu J. et al., 2023).

The neuroprotective or neurotoxic roles NF-κB performed depends on biological functions of the subunits which compose the transcription factor. RelA (p65) and p50 are the subunits of NF-κB family, and p50/RelA complexes can be induced by neurotoxic stimuli (Inta et al., 2006). Since acetylation of RelA at the K310 site affects the function of p50/RelA complexes, Mota et al. combined class I histone deacetylase inhibitors (HDACi) MS-275 (20 μg/kg) with resveratrol (680 μg/kg) at low doses and found that the combination reduced infarct volume and neurological deficits in dMCAO mice, hindered the binding ability of RelA to the Nos2 promoter. Consequently, the combination reduced the levels of Nos2, IL-6, IL-1β, avoided leukocyte infiltration in the ischemic area, blunted the activation of microglia/macrophages, and weakened the immunoreactivity of iNOS and CD68 in Iba1-positive cells (Mota et al., 2020). All evidence suggested that the combination of MS-175 and resveratrol exerted anti-inflammation effects through directly inhibiting microglia/macrophage activation, achieving greater efficacy than either drug alone, even when the individual drugs were used at 100-fold higher doses.

3.2.4 6-shogaol

Zingiber officinale Roscoe (ginger), a Chinese medicinal herb, has long been applied for headaches, colds, nausea, and emesis, etc. (Mao et al., 2019). Many bioactive components containing in ginger have been identified, among which 6-shogaol is a pungent phenolic component with remarkable pharmacological properties (Mao et al., 2019). Han et al. reported that 6-shogaol elevated PPAR-γ level and subsequently reversed the enhanced activity of NF-κB to block the release of inflammatory mediators in LPS-treated BV2 microglial cells (Han et al., 2017). Gaire et al. reported consistent findings, which indicated that 6-shogaol could attenuate microglia-mediated neuroinflammation, and their animal study in MCAO mice further validated this effect (Gaire et al., 2015).

3.2.5 Paeonol

Paeonol, a major polyphenolic ingredient from *Paeonia Iactiflora* Pall., possesses various pharmacological properties, like anti-inflammation, anti-tumor, and neuroprotection (Zhang et al., 2019). Paeonal exerted anti-inflammation effects in LPS-activated N9 microglia cells, mainly via suppressing the TLR4 signaling

pathway (He et al., 2016). Moreover, paeonol was observed to inhibit inflammatory responses stimulated by LPS/IFN-γ and reduced ATP-induced enhanced migratory activity in BV2 microglia, which was attributed to its ability in modulating AMPK/GSK3 pathway. Improved rotarod performance and decreased microglial activation were observed in mice with systemic inflammation induced by LPS (Lin et al., 2015). However, studies on the regulation of microglia by paeonol in stroke animal models remain limited.

3.3 Terpenes

3.3.1 Triptolide

Triptolide, a kind of epoxidized diterpene lactone extracted from *Triprerygium*, exhibits favorable bioactivities in cancers and inflammatory and autoimmune disorders (Chen J. et al., 2022). Zhang et al. reported that triptolide held the ability to repress the synthesis of NO and iNOS in LPS-treated microglial cells and protected neuronal cells from microglia-mediated inflammation. Further, EP2/protein kinase A (PKA) pathway was evidenced to be a major contributor to suppressive effects of triptolide on NO production in microglia (Zhang et al., 2015). Zhou et al. found that triptolide could suppress the polarization of M1 microglia by modulating the CTSS/Fractalkine/CX3CR1 pathway, additionally, attenuate HT-22 cell apoptosis via crosstalk with BV-2 microglial cells (Zhou et al., 2024). Ki20227, a specific blocker of colony-stimulating factor 1 receptor (CSF1R), is responsible for modulating inflammatory response and neuronal synaptic plasticity (Jiang et al., 2022). Du et al. combined triptolide with Ki20227 to evaluate the neuroprotective action of this combination in mice with ischemic stroke. The combination was exhibited to upregulate the expression of synaptic proteins, improve the density of dendritic spines, especially, downregulate the expression of microglial marker Iba1 in stroke mice, which were achieved by inhibiting CSF1R signal and triggering BDNF-Akt and autophagy pathways (Du et al., 2020).

3.3.2 Ilexonin A

Ilexonin A, a pentacyclic triterpene existing in the medicinal herb *Ilex pubescens*, exhibits marked effects in cardiovascular disease, angina, and vasculitis (Luo et al., 1995). Ilexonin A promotes blood circulation for therapeutic actions through its anti-thrombotic and inflammation-suppressive properties (Xu et al., 2016). Xu et al. observed that ilexonin A elevated the number of GFAP-expressed astrocytes in the peri-infarct region after MCAO-induced ischemic injury at 1, 3, and 7 days. However, at 14 days, the number of these cells was decreased compared to the ischemia group. Besides, ilexonin A lowered the numbers of Iba-1 positive microglial cells at each time point (Xu et al., 2016). Another similar study suggested that the numbers of astrocytes in the hippocampal CA1 area promptly increased following ischemic stroke onset, and this augmentation was further amplified after ilexonin A treatment (Xu A. L. et al., 2020). On the other hand, microglial cells remained inactive after ischemia, but was observed to be activated following ilexonin A treatment (Xu A. L. et al., 2020), that were inconsistent with the previously mentioned findings. The reason behind the discrepancy may be that microglia in the CA1 area of hippocampus have not been immediately activated after the occurrence of ischemic insult, whereas those in the peri-infarction region have already been rapidly activated. The observation indicated that different injury regions can lead to varying degrees of activation and proliferation of astrocytes and microglia, and ilexonin A acted as a neuroprotective agent through regulating activities of astrocytes and microglia for attenuating inflammatory responses (Xu A. L. et al., 2020).

3.3.3 Artesunate

Artesunate is derived semi-synthetically from artemisinin and has anti-inflammatory properties. Okorji et al. found that artesunate could reverse the elevated levels of PGE2 stimulated by LPS + IFNγ in BV2 microglia, which was mediated by reduction in COX-2 and mPGES-1. Besides, it decreased the levels of inflammatory cytokines in activated BV2 microglial cells and its suppressive effects were obtained by interfering with p38 MAPK and NF-κB signaling (Okorji and Olajide, 2014). Further, Liu et al. reported artesunate's anti-inflammatory effects in mice subjected to distal middle cerebral artery occlusion (dMCAO). Artesunate could ameliorate inflammatory responses by reducing neutrophil infiltration, suppressing microglial activation, quenching the secretion of inflammatory cytokines, and restraining the triggering of the NF-κB signaling (Liu Y. et al., 2021).

3.4 Alkaloids

3.4.1 Berberine

Berberine is a bioactive isoquinoline alkaloid with extensive pharmacological properties in several central nervous system (CNS) disorders, such as ischemic stroke, Alzheimer's disease and Parkinson's disease (Lin and Zhang, 2018). Recent years, researchers put the hotspot on manipulating the peripheral environment or related factors to regulate microglia functions, rather than directly targeting microglia and neuroinflammation (Ni et al., 2022). Ni et al. investigated the contribution of gut-brain axis signals in the berberine-regulated microglia polarization after cerebral ischemia and found that berberine regulated the transformation of microglia and ameliorated inflammatory response in a microbiota-dependent manner. Importantly, the transmission of gut-brain axis signals mediated by berberine was mainly due to the stimulation of intestinal H_2S on vagal nerve activity, through the transient receptor potential vanilloid 1 (TRPV1) receptor (Ni et al., 2022). Additionally, berberine was shown to inhibit microglia polarization towards the M1 subtype and promote their shift towards the M2 subtype in mice subjected to tMCAO. These effects were validated to occur through AMP-activated protein kinase (AMPK)-dependent mechanisms (Zhu J. et al., 2019). Furthermore, Kim et al. suggested that berberine diminished global ischemia-induced cellular apoptosis by inhibiting the reactive astrogliosis and microglia activation via triggering the PI3K/Akt pathway (Kim et al., 2014).

3.4.2 Tetramethylpyrazine

Tetramethylpyrazine (TMP) is the major bioactive alkaloid separated from *Ligusticum chuanxiong* Hort (Lin et al., 2022) and commonly used in the treatment of cardiovascular, nervous, and digestive system conditions with its extensive physiological functions, including anti-oxidation, anti-inflammation, anti-apoptosis, angiogenesis regulation, and endothelial protection,

etc., (Lin et al., 2022). TMP has been reported to inhibit the LPS-induced overproduction of NO and iNOS in N9 microglial cells through restraining the activity of MAPK and PI3K/Akt signaling pathway (Liu et al., 2010). In a rat model of permanent cerebral ischemia, TMP was shown to decrease the percentage of activated macrophages and microglia and ameliorate pro-inflammatory responses after brain ischemia. Further, targeting macrophages/microglia by stimulating Nrf2/HO-1 pathway actively contributed to TMP-mediated neuroprotection (Kao et al., 2013). Moreover, TMP was observed to prevent demyelination and promote remyelination in rats with MCAO based on MRI-diffusion tensor imaging (DTI) and histopathology, and was further discovered to prompt the transformation of microglia towards M2 phenotype, acting through JAK2/STAT1/2 and GSK3-NFκB pathways (Feng et al., 2023).

3.5 Glycosides

3.5.1 Astragaloside IV

Astragaloside IV (AS-IV) is a cycloartane-type triterpene glycoside compound separated from Chinese herb *Astragalus mongholicus* Bunge (Zhang et al., 2020). AS-IV has been reported to attenuate behavioral and neurochemical deficits due to its antioxidant, anti-apoptotic, and anti-inflammatory properties in Alzheimer's disease, Parkinson's disease, cerebral ischemia, and autoimmune encephalomyelitis; additionally, it serves as a neuroprotector by reducing spontaneous neuronal excitability (Zhang et al., 2020). Li et al. suggested that AS-IV facilitated the shift of microglia/macrophage towards M2 subtype in a PPARγ-dependent manner, which contributed to enhancing neurogenesis, angiogenesis, and neurological functional recovery in rats with tMCAO (Li L. et al., 2021). Gao et al. constructed the molecular regulatory network of lncRNA/miRNA/mRNA to form the pyroptosis-associated competitive endogenous RNA (ceRNA) regulatory relationship specifically for NLRP3 molecules, and LOC10255978/miR-3584-5p/NLRP3 was included. In MCAO rats and OGD/D-treated primary rat microglial cells, AS-IV was found to inhibit microglia inflammatory reaction and pyroptosis by downregulating NLRP3 through LOC10255978, thereby exerting neuroprotective effects (Gao et al., 2024). Additionally, AS-IV was observed to suppress the activation of microglia and alleviate the secretion of inflammatory mediators through containing TLR4 signaling pathway and NLRP3 inflammasome overactivation, thereby restoring cognitive impairment in mice with bilateral common carotid artery occlusion (Li et al., 2017). Besides, AS-IV was displayed to decrease the levels of inflammatory mediators in BV2 and primary microglial cells, mainly mediated by stimulating nuclear factor erythropoietin-2-related factor 2 (Nrf2)/heme oxygenase-1 (HO-1) via the ERK pathway (Li C. et al., 2018). Moreover, it was reported to promote microglial polarization from M1 to M2 subtype in AMPK-dependent metabolic pathways after ischemic stroke (Li et al., 2024a). These findings were reciprocally validated through animal and cellular experimental models.

3.5.2 Cycloastragenol

Cycloastragenol (CAG), an activated derivative of astragaloside IV, is the hydrolysis product of astragaloside IV (Zhou et al., 2012), with pharmacological effects of activating telomerase and anti-aging (Yu et al., 2018). Chen et al. reported that CAG promoted M2 microglia and suppressed M1 polarization by activating Nrf2 signaling pathway and inhibiting NF-κB in LPS-stimulated BV-2 cells and ischemic mouse brain (Chen T. et al., 2022). In addition, it reduced the levels of pro-inflammatory cytokines and restrained the activation of microglia and astrocytes in ischemic brain, which was attributed to its actions on regulating SIRT1 expression, blunting p53 acetylation and inhibiting NF-κB activation (Li M. et al., 2020).

3.5.3 Salidroside

Salidroside, a phenylpropanoid glycoside separated from the root of *Rhodiola rasea* L. has various therapeutic effects in aging, cancer, inflammation, oxidative stress, and kinds of neurological disorders, like stroke and Alzheimer's disease (Magani et al., 2020). Using network pharmacology, transcriptome sequencing, macromolecular docking and molecular biology techniques, Zhang et al. revealed that salidroside inhibited the activation of microglia by inducing GSK3β phosphorylation, and in turn targeting downstream Nrf-2, facilitating β-catenin accumulation, and ultimately exerted protective effects against hypobaric hypoxia-induced brain injury (Zhang X. et al., 2024). Besides, Fan et al. simulated the hypoxic microenvironment in BV2 microglia, and investigated the change of cell metabolites using a cell microfluidic chip-mass spectrometry (CM-MS) system. The findings showed that microglial hypoxic inflammation was associated with cell energy metabolism, in which the process of metabolism changed from oxidative phosphorylation to glycolysis, and salidroside could reverse this change to further alleviate microglial hypoxic inflammatory injury (Fan et al., 2022). Although these studies did not employ stroke models directly, the hypoxia model shares numerous overlapping mechanisms with ischemic stroke, including energy depletion, BBB disruption, and neuroinflammation, thus allowing for cross-validating the underlying pathological pathways of ischemic stroke. Besides, salidroside was found to facilitate the polarization of M2 macrophage/microglia following ischemic injury, and initiate a shift from M1 towards M2 subtype in primary microglial cells. Moreover, it enhanced microglia phagocytic activity and attenuated microglia-mediated inflammatory cytokine release. When oligodendrocytes were cocultured with salidroside-treated M1 microglia, a marked acceleration in differentiation of oligodendrocyte was observed (Liu X. et al., 2018). Similarly, salidroside was found to block inflammatory responses in MCAO rats through the regulation of TLR4/NF-κB pathway (Liu J. et al., 2021) and PI3K/Akt pathway (Wei et al., 2017).

3.5.4 Ginsenoside Rd

Panax ginseng and *Panax notoginseng*, included in the Araliaceae family, are commonly utilized in clinical practice as functional herbs. They both contain crucial bioactive ingredients, like ginsenosides, which exhibit numerous pharmacological effects on the nervous system (Liu H. et al., 2020). Ginsenoside Rd, a kind of monomer, separated from these two traditional Chinese herbs (Tang K. et al., 2022), has long been applied in treating ischemic stroke with remarkable efficacies and few adverse reactions (Zhang G. et al., 2016). It has been reported to improve the outcome of ischemic stroke patients, and the therapeutic effect may result from its capacity of suppressing the

activity of proteasome in microglia, and sequential inflammatory responses (Zhang G. et al., 2016).

3.5.5 Ginsenoside Rb1

Ginsenoside Rb1 stands as another important active ingredient within ginsenosides, the bioactive saponins from *Panax ginseng* or *Panax notoginseng* (Liu H. et al., 2020). In recent years, more attention has been drawn for its remarkable properties in the nervous system (Gong et al., 2022). It could decrease the level of Iba1 and suppress microglial activation, thus attenuating neuroinflammation in mice with systemic LPS treatment (Lee et al., 2013). The findings in another cellular experiment were aligned with the observations mentioned above, indicating that ginsenoside Rb1 effectively maintained the morphology and structure of neural cells in a hypoxic-induced co-culture model with microglia, diminished cell apoptosis, and suppressed the generation of NO and superoxide as well (Ke et al., 2014). The major function of astrocyte is to safeguard neurons from glutamate-induced excitotoxicity by scavenging excessive excitatory glutamate. Astrocytes captured glutamate via the glutamate transporter-1 (GLT-1) and further converted it into glutamine through the enzymatic action of glutamine synthetase (GS) (Nangaku et al., 2021). Zhang et al. suggested that ginsenoside Rb1 markedly decreased the number of reactive microglia and ameliorated neuroinflammation in LPS-treated mice (Zhang H. et al., 2021). Crucially, ginsenoside Rb1 modulated the activities of astrocyte and microglia via the GLT-1/GS system by elevating GLT-1 level and reversing the LPS-induced decrease in GS level, thus avoiding glutamate excitotoxicity (Zhang H. et al., 2021). Notably, these studies employed LPS-induced systemic inflammation mouse models and hypoxic co-culture systems to mimic inflammation microenvironment in the brain for evaluating the effects of ginsenosides on microglia. However, ischemic stroke animal models are still lacking.

3.5.6 Paeoniflorin

Paeoniflorin, a water-soluble monoterpenoid glycoside separated from *Paeonia lactiflora* Pall., has extensive therapeutic effects, comprising anti-inflammation, anti-oxidation, anti-thrombosis, anti-convulsant, analgesic, neuroprotection, immunomodulation, and cognitive function enhancement (Zhou et al., 2020). Chen et al. found that paeoniflorin fostered the conversion of microglial phenotypes and reversed LPS-elicited inflammation, which were mediated by its regulatory actions on the NF-κB pathway (Chen et al., 2020). Tang et al. observed that paeoniflorin dampened the proliferation of microglia and produced a marked decrease in the generation of pro-inflammatory cytokines in rats with tMCAO. It also promoted neurogenesis and vasculogenesis after brain ischemic insult through suppressing JNK and NF-κB signaling pathways, thereby blocking inflammatory response and facilitating neurogenesis (Tang et al., 2021). In recent years, autophagy has been found to perform an essential role in normal cell function and homeostasis. Zhou et al. suggested that paeoniflorin attenuated neuroinflammation induced by microglia hyperactivation in LPS-treated BV2 microglia probably through reversing LPS-induced autophagy inhibition (Zhou et al., 2023).

3.6 Anthraquinones

3.6.1 Emodin

Emodin is a natural derivative of anthraquinone, presenting in kinds of Chinese medicinal herbs, like *Rheum officinale*. Extensive evidence points out that emodin possesses multiple pharmacological properties, such as anti-cancer, anti-inflammation, anti-oxidation and anti-microbial activities (Dong et al., 2016). Jiang et al. found that emodin alleviated LPS/adenosine triphosphate (ATP)-stimulated pyroptosis in BV2 microglial cells (Jiang et al., 2023). Since pyroptosis is triggered by the activation of NLRP3 inflammasome and the pyroptosis-executing protein GSDMD pathway (Li S. et al., 2021), the findings further underscored that the suppressive effects of emodin on neuronal pyroptosis stemmed from its abilities to prevent the activity of the NLRP3 inflammasome and the cleavage of GSDMD. When HT-22 neurons co-cultured with BV2 microglia, emodin was found to protect HT-22 neurons from BV2 microglia pyroptosis-mediated toxicity (Jiang et al., 2023). Similarly, the study conducted by Li et al. suggested that emodin inhibited microglial pyroptosis and prompted M1 to M2 subtype transformation through suppressing the activation of microglial NLRP3 inflammasome (Li X. et al., 2024). Besides, emodin blocked the generation of NO and PGE2, as well as iNOS and COX-2 induced by LPS in the primary microglial cells, which was mediated by the enhancement of HO-1 and NADPH quinone oxidoreductase 1 (NQO1) via regulating the AMPK/Nrf2 signaling pathway (Park et al., 2016).

3.6.2 Chrysophanol

Chrysophanol, the most common free anthraquinone species, is another important component separated from plants of the *Rheum genus*, exhibiting salutary effects in treating nervous system diseases (Su et al., 2020). Chrysophanol was found to hinder the generation of pro-inflammation mediators and cytokines in microglia through suppressing the activity of NF-κB and blocking the accumulative ROS. It also alleviated LPS-elicited mitochondrial fission via reducing dephosphorylation of dynamin-related protein 1 (DRP1) at the S637 site (Chae et al., 2017). Using a dMCAO mouse model and OGD or LPS-treated *in vitro* system, Liu et al. suggested that chrysophanol could regulate the polarization of microglia and blunt the expressions of inflammatory cytokines, thereby, enhancing the complexity of neurons and the density of neuronal spines. Further, the IL-6/STAT3 pathway was evidenced as a therapeutic target for anti-inflammation actions of chrysophanol (Liu X. et al., 2022).

3.7 Others

3.7.1 Arctigenin

Arctigenin, a lignan compound extracted from Chinese medicinal herb *Arctium lappa* L., is extensively applied in inflammatory diseases (Li et al., 2023). Yuan et al. demonstrated that arctigenin blunted the activity of glial cells and downregulated the levels of pro-inflammatory mediators in LPS-induced systemic inflammation mice. Importantly, arctigenin treatment inhibited the triggering of the inflammation-associated TLR-4/NF-κB pathway. Furthermore, in BV2 microglial cells, arctigenin was observed to

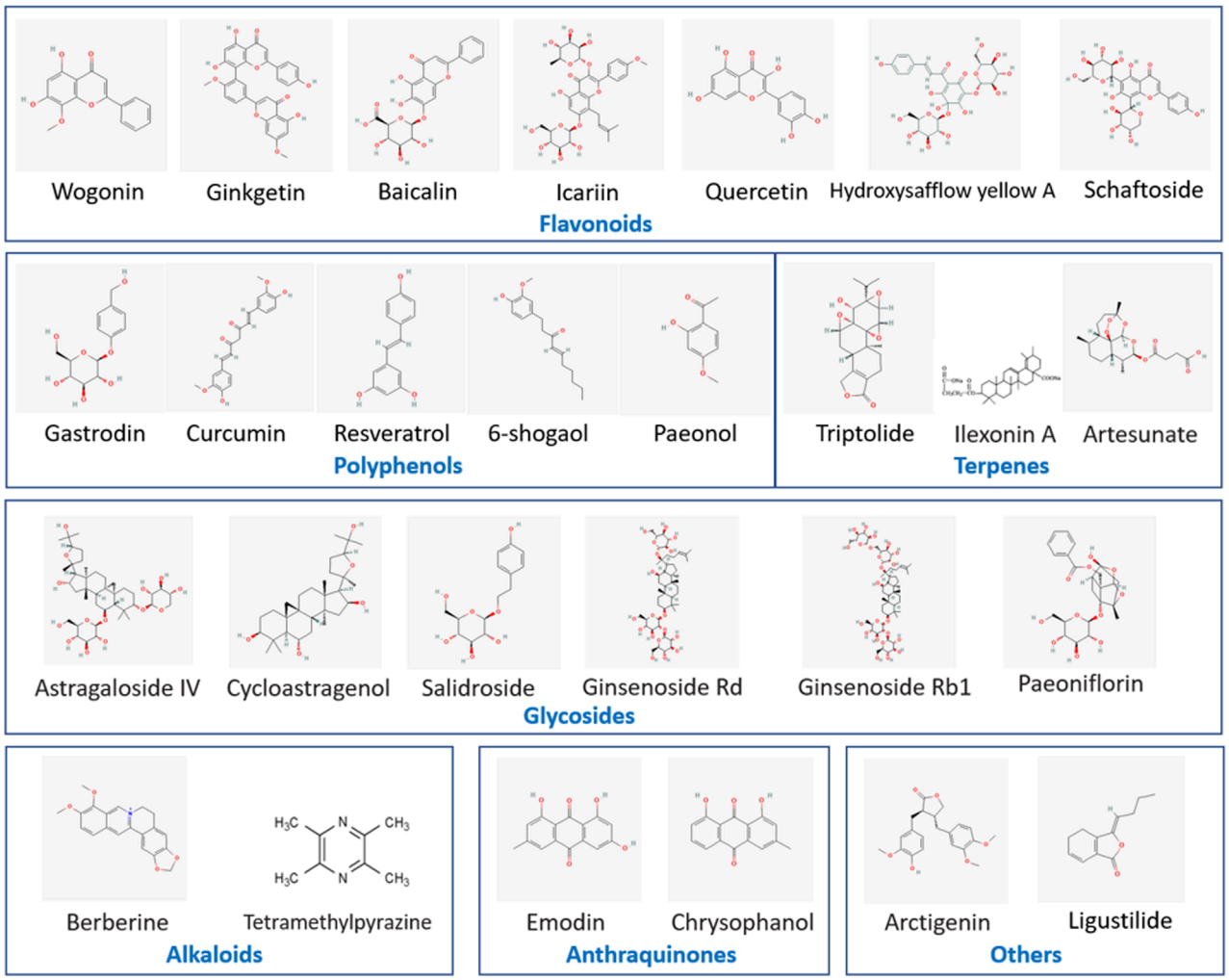

FIGURE 4
Chemical structural formulas of natural compounds in different categories. This figure lists the chemical structural formulas of natural compounds with the function of regulating microglial cell responses.

reverse the enhanced interaction between AdipoR1 and TLR4 and reduced the stability of the TLR4/CD14 complex, which in turn led to the suppression of TLR4-mediated signal transduction, thereby attenuating its downstream inflammatory response (Yuan et al., 2022).

3.7.2 Ligustilide

Ligustilide is a characteristic phthalide component of *Angelica sinensis* and *Ligusticum chuanxiongs* with multiple neuroprotective activities (Wu et al., 2022). Kuang et al. reported that ligustilide could suppress the activation of astrocyte and microglia/macrophages, limit the invasion of neutrophils and T-lymphocytes from periphery to brain parenchyma and reduce the production of inflammatory mediators in rats with MCAO. Its neuroprotective actions were attributed to the inhibitory effects on the TLR4/peroxiredoxin 6 (Prx6) signaling pathway (Kuang et al., 2014).

3.8 Herb extracts

3.8.1 Panax notoginseng saponins

Panax notoginseng saponins (PNS) are the major active compounds derived from herbal medicine *Panax notoginseng*, containing Ginsenoside Rb1, Ginsenoside Rg1, Notoginsenoside R1, Ginsenoside Rd and Ginsenoside Re (Huang et al., 2015), which have been extensively applied in treating cardiovascular and cerebrovascular disorders, especially stroke (Huang et al., 2015). Gao et al. reported that PNS suppressed the activation of microglia for ameliorating inflammatory response during the acute phase after stroke induced by photothrombosis. Moreover, PNS lowered the level of PKM2 in the nucleus of the activated microglia, concomitantly, blunted the hypoxia-inducible factor-1α (HIF-1α)/pyruvate kinase M2 (PKM2)/STAT3 pathway, which may underlie PNS's inflammation-inhibitory effect in stroke (Gao et al., 2022). Network pharmacology screening revealed that MAPK

TABLE 2 Neuroprotective effects of flavonoids on microglial responses after ischemic stroke.

Natural compound	Experimental models		The main regulatory effects on microglial response	Mechanisms	Ref.
	In vitro	*In vivo*			
Wogonin	LPS/INFγ-induced BV2 microglial cells		PGE2, NO, iNOS, COX-2↓	ERK1/2 pathway↓, MEK1/2↓, Srs activation↓	Yeh et al. (2014)
Ginkgetin	OGD/R-stimulated primary microglial cells	MCAO rats	M1 microglia (Iba1+, $CD16^+$)↓, M2 microglia (Iba1+, CD206+)↑, TNF-α, IL-1β↓, IL-4, IL-10↑	PPARγ signaling↑	Tang et al. (2022b)
Baicalin		LPS-induced neuroinflammatory mice	Microglia and astrocyte activation ($Iba\text{-}1^+$, $GFAP^+$)↓, IL-1β, TNF-α↓	NF-κB↓	Shah et al. (2020)
	LPS-induced BV2 microglial cells		NO, iNOS, IL-1β, COX-2 and PGE2↓	TLR4/MyD88/NF-κB and MAPK pathways↓, miR-155↓	Li et al. (2022a)
		BCCAO rats	Microglia activation ($Iba\text{-}1^+$) ↓, iNOS↓, Arg-1↑, IL-1β, TNF-α↓	Wnt/β-catenin↑, NF-κB signaling↓	Xiao et al. (2023)
	LPS-stimulated BV2 microglial cells	LPS-stimulated neuroinflammatory mice	Microglia and astrocyte activation ($Iba\text{-}1^+$, $GFAP^+$)↓, IL-1β, TNF-α↓	SIRT1↑, HMGB1↓	Li et al. (2020b)
	OGD/R-stimulated BV2 microglial cells	MCAO mice	ROS↓; TNF-α, iNOS, MMP9, IL-1β, CD16, CD86↓; Arg-1, CD206↑	TREM2↑	Wang et al. (2024a)
Icariin	LPS-induced BV2 microglial cells		Microglia activation ($Iba\text{-}1^+$) ↓, NO, IL-1β and IL-18↓	Nrf2↑, HO-1 and NQO1↑	Zheng et al. (2019)
	OGD/R-stimulated primary microglial cells		IL-1β, IL-6 and TNF-α↓	IRE1α/XBP1 pathway↓	Mo et al. (2021)
Quercetin	LPS/ATP-induced BV2 and primary microglial cells, dopaminergic neurons and hippocampal neurons cocultured with LPS and ATP stimulation		IL-1β, IL-6↓, microglial proliferation and phagocytosis↓, microglia activation ($Iba1^+$, $CD68^+$) ↓, ROS↓, pyroptosis↓, mitophagy↑	NF-κB↓, NLRP3 inflammasome↓, mitochondrial ROS stress↓	Han et al. (2021)
HSYA	OGD/R-stimulated primary microglial cells	MCAO rats	inflammation↓	TRL9↑, NF-κB pathway↓, IRF3↓	Gong et al. (2018)
	Microglial cells and primary neurons cocultured with LPS stimulation		microglia activation ($CD11b^+$)↓,morphological changes↓, IL-1β, TNF-α, NO↓, BDNF↑	TLR4 pathway↓, NF-κB/MAPK/cytokine signaling↓	Lv et al. (2016)
Schaftoside	OGD-stimulated BV2 microglial cells		IL-1β, TNF-α, and IL-6↓	TLR4/Myd88 pathway↓, Drp1↓, mitochondrial fission↓	Zhou et al. (2019)

TABLE 3 Neuroprotective effects of polyphenols on microglial responses after ischemic stroke.

Natural compound	Experimental models		The main regulatory effects on microglial response	Mechanisms	Ref.
	In vitro	*In vivo*			
Gastrodin	LPS-stimulated BV2 or primary microglia	Three-day postnatal rats treated with LPS	iNOS, TNF-α↓, cyclin-D1, Ki67↓, proliferation in BV2 microglia and brain microglia↓	GSK-3β↓, Wnt/β-catenin pathway↓	Yao et al. (2019)
	OGD-stimulated BV2 microglial cells		IL-1β, TNF-α↓, BDNF↑	MAPK↓	Lv et al. (2021)
	LPS-induced BV2 microglial cells	Postnatal rats with hypoxic-ischemia brain damage	NOX-2, iNOS and TNF-α↓	ACE, AT1↓, caspase-3↓, AT2 and SIRT3 pathway↑	Liu et al. (2018a)
	LPS-induced BV2 microglial cells	LPS-induced inflammation in postnatal rats	IL-1β, IL-6, IL-23, TNF-α and NO↓	Notch-1 pathway↓, MAPK↓	Yao et al. (2022)
Curcumin	LPS/IFN-γ-stimulated BV2 microglial cells	dMCAO mice	M1 microglia (Iba1+, $CD16^+$)↓, M2 microglia (Iba1+, CD206+)↑, TNF-α, IL-6, IL-12p70↓		Liu et al. (2017b)
	primary microglial cells treated with LPS and ATP	MCAO mice	GSDMD+, caspase-1+ in Iba1+ microglia/macorphage↓, cleaved caspase-1, NLRP3, IL-1β, IL-18↓	NF-κB/NLRP3 pathway↓	Ran et al. (2021)
NPcurcumin		tMCAO mice	M1 phenotype (Iba1+, $CD68^+$)↓, IL-1β, TNF-α↓, apoptosis↓, tight junction proteins↓		Wang et al. (2019b)
Curcumin gel	OGD-stimulated BV2 microglial cells	Photothrombic stroke model in mice	ROS↓; CD16, IL-1β↓; CD206, TGF-β↑; Iba-1/iNOS↓; Iba-1/CD206↑; PSD-95↑	ROS-NFκB pathway↓; p47-phox and p67-phox translocation↓	()
Resveratrol		Rats with 4-VO	Microglial activation (CD11b/c+)↓, astrocyte activation (GFAP+) ↓	GLT-1↑	Girbovan and Plamondon (2015)
		tMCAO rats	Micorglial activation (Iba1+)↓, M1 microglia (iNOS+)↓, M2 microglia (Ym1/2+, CD206+)↑	Nrf2↑, regulating miR-450b-5p/KEAP1 axis	Liu et al. (2023b)
MS275+resveratrol	Primary mixed glial cells exposed to NCM-OGD	pMCAO mice	Nos2, IL-1β, IL-6↓, Mrc1, Ym1, iNOS↓, CD68↓ 1 day after pMCAO, Ym1, Arg1, CD32↑ 7 days after pMCAO, microglia activation (Iba1+)↓, LDH↓	The binding of RelA to Nos2 promoter↓	Mota et al. (2020)
6-shogaol	LPS-induced BV2 microglial cells	MCAO mice	NO, iNOS↓, TNF-α, IL-6↓, microglial activation (Iba1+)↓		Gaire et al. (2015)

(Continued on the following page)

TABLE 3 (*Continued*) Neuroprotective effects of polyphenols on microglial responses after ischemic stroke.

Natural compound	Experimental models		The main regulatory effects on microglial response	Mechanisms	Ref.
	In vitro	*In vivo*			
	LPS-induced BV2 microglial cells		TNF-α, IL-1β, IL-6 and PGE2↓	NF-κB↓,PPAR-γ↑	Han et al. (2017)
Paenonal	BV2 microglial cells treated with LPS/IFN-γ	LPS-injected mice	NO, iNOS, COX-2, ROS↓, cell migratory activity↓, microglial activation (Iba1+)↓	AMPK/GSK3↑	Lin et al. (2015)
	LPS-induced N9 microglial cells		NO, iNOS↓, IL-1β, PGE2↓, COX-2↓	NF-κB↓, MAPK pathway↓, TLR4 pathway↓	He et al. (2016)

TABLE 4 Neuroprotective effects of terpenes on microglial responses after ischemic stroke.

Natural compound	Experimental models		The main regulatory effects on microglial response	Mechanisms	Ref.
	In vitro	*In vivo*			
Triptolide	LPS-stimulated primary rat microglial cells and BV2 cells, MN2D and SH-SY5Y cells treated with conditioned medium from LPS-induced microglia		NO and iNOS synthesis↓	EP2/PKA pathway↓	Zhang et al. (2015)
	LPS-stimulated BV-2 microglial cells	MCAO/R mice	IBA-1$^+$ and iNOS$^+$ cells↓; Arg-1$^+$ cells↑; TNF-α, IL-1β↓, HT-22 cell viability↑; HT-22 cell apoptosis↑	CTSS/Franctalkine/CX3CR1 signaling pathway↓	Zhou et al. (2024)
Triptolide + Ki20227		C57BL/6 mice with focal ischemic stroke induced by photochemical induction techniques	Synaptic protein expressions↑; dendritic spins density↑; microglia activation (Iba1$^+$) ↓	CSF1R signal↓; autophagy↑; BDNF-Akt pathway↑	Du et al. (2020)
Ilexonin A		MCAO rats	Microglia activation (Iba-1$^+$)↓ at each time point; astrocyte activation (GFAP$^+$)↑ at 1, 7 days, ↓at 14 days; VEGF, Flk-1, Nestin↑		Xu et al. (2016)
		MCAO rats	Microglia activation (Iba-1$^+$) and astrocyte activation (GFAP$^+$)↑ in the hippocampus; nestin↑; TNF-α, IL-1β↓		Xu et al. (2020a)
Artesunate	BV2 microglia treated with LPS + IFNγ		PGE2↓; mPGES-1, COX-2↓; TNF-α, IL-6 ↓	NK-κB and p38 MAPK signaling↓	Okorji and Olajide (2014)
		dMCAO mice	MPO↓; microglia activation (Iba-1$^+$)↓; TNF-α, IL-1β↓	NF-κB pathway↓	Liu et al. (2021b)

TABLE 5 Neuroprotective effects of alkloids on microglial responses after ischemic stroke.

Natural compound	Experimental models		The main regulatory effects on microglial response	Mechanisms	Ref.
	In vitro	*In vivo*			
Berberine		tMCAO rats	CD86-positive microglia↓; CD163-positive cells↑; IL-1, IL-6, TNF-α↓; IL-4, IL-10↑; vagal afferent nerve activity↑; intestinal H_2S production↑	TRPV1 receptors-dependent	Ni et al. (2022)
	LPS-induced BV2 microglial cells	tMCAO mice	M1 phenotype markers (IL-1β, CD32, TNF-α) ↓; M2 phenotype markers (CD206, Arg-1, Ym1/2) ↑; $CD16^+/Iba1^+$ microglia↓; $CD206^+/Iba1^+$ microglia↑; angiogenesis↑	AMPK↑	Zhu et al. (2019b)
		Gerbils with global ischemia	CD11b, GFAP↓; capase-3↓; apoptosis↓; cytochrome *c*↓	PI3K/Akt↑; Bax/Bcl-2↓	Kim et al. (2014)
Tetramithylpyrazine		Rats with permanent cerebral ischemia	Leukocyte intracerebral infiltration↓; activated macrophages/microglia ($CD45^+/CD11b^+$) ↓	JNK/AP-1 pathway↓; Nrf2, HO-1↑	Kao et al. (2013)
	LPS-induced N9 microglial cells		NO, iNOS↓; ROS↓	NF-κB↓; MAPK↓; Akt↓	Liu et al. (2010)
	LPS + IFN-γ-stimulated BV2 microglia	MCAO rats	$NG2^+$, $Ki67^+/NG2^+$, $CNPase^+$, $Ki67^+/CNPase^+$ cells↑; $Iba1^+$ and $Iba1^+/CD16^+$ cells↑; IL-6↓; IL-10↑	JAK2/STAT3 pathway↑; STAT1↓; GSK3/NFκB pathway↓	Feng et al. (2023)

signaling pathway was the key target pathway involved in the inhibitory effects of PNS on microglia-mediated inflammation. Molecular docking studies identified the binding sites of PNS to the MAPK pathway, revealing that PNS inhibited p39 and JNK activity and enhanced ERK1/2 phosphorylation through these interactions. These predictions were further validated in stroke animal models, providing experimental evidence to support the therapeutic potential of PNS for ischemic stroke (Duan et al., 2024).

3.8.2 Salvianolic acids for injection

Salvianolic acids for injection (SAFI) is primarily composed of water-soluble constituents of the roots of *Salvia miltiorrhiza* Bunge, comprising salvianolic acids (B, D, Y), rosmarinic acid and alkannic acid (Li W. et al., 2018). It is a lyophilized powder for intravenous injection which has been authorized by the Chinese FDA in treating ischemic stroke (Lyu et al., 2019). Numerous studies suggested that neuroprotective properties of SAFI against ischemic injury are probably attributed to its anti-inflammation ability (Zhang et al., 2017). Ma et al. proposed that the neuroprotective effects of SAFI were mediated by facilitating the polarization of microglia from M1 to M2 subtype and by blocking NLRP3 inflammasome/pyroptosis axis, as demonstrated in both MCAO rats and OGD/R cell systems (Ma et al., 2021). Similarly, Zhuang et al. pointed out SAFI treatment dampened activated microglia-induced neuroinflammation, partly by blunting the TLR4/NF-κB signaling pathway (Zhuang et al., 2017).

By collecting and analyzing relevant literature, we have identified the primary compounds isolated from traditional Chinese herbs that regulate microglia for stroke treatment as flavonoids, polyphenols, terpenes, alkaloids, glycosides, anthraquinones, and other herb extracts. Their chemical structural formulas are shown in Figure 4. Flavonoids, specific secondary metabolites from plants, are featured by two phenyl rings and a heterocyclic ring (Lu et al., 2024). The compounds that were evidenced to perform a beneficial role in microglial polarization include wogonin, ginkgetin, baicalin, icariin, quercetin, hydroxysafflow yellow A, and schaftoside (Table 2). Polyphenols, as natural antioxidants, possess a complex chemical structure with multiple hydroxyl groups on aromatic rings (Mamun et al., 2024). The presence of carboxyl and carbonyl groups determines their antioxidant activity (Li X. H. et al., 2022).

TABLE 6 Neuroprotective effects of glycosides on microglial responses after ischemic stroke.

Natural compound	Experimental models		The main regulatory effects on microglial response	Mechanisms	Ref.
	In vitro	*In vivo*			
Astragaloside IV		tMCAO rats	microglia activation ($Iba1^+$) ↓; M1 microglia ($CD86^+$, $CD16/32^+$, $iNOS^+$)↓; TNF-α, IL-1β, IL-6↓; M2 microglia ($Arg\text{-}1^+$, $YM1/2^+$, $CD206^+$)↑; IL-10, TGF-β↑; $BrdU^+/NeuN^+$ and $BrdU^+/GFAP^+$ cells↑; $BrdU^+/vWF^+$ cells↑; $CD206^+/BDNF^+$ and $CD206^+/IGF1^+$ cells↑; VEGF, IGF-1, BDNF↑	PPAR-γ pathway↑	Li et al. (2021a)
	OGD/R-induced primary rat microglia cells	MCAO rats	The survival rate of primary rat microglia cells↑; Iba-1↓	NLRP3 inflammasome pathway↓; LOC102555978↓; miR-3584-5p↑	Gao et al. (2024)
		BCCAO mice	microglia activation ($Iba1^+$) ↓; TNF-α, IL-1β↓; MDA, ROS↓; SOD↑	TLR4/NF-κB pathway↓; NLRP3 inflammasome↓; cleaved caspase-1↓	Li et al. (2017)
	LPS-stimulated BV2 and primary microglial cells		NO, IL-6, TNF-α↓	ERK↑; NRF2/HO-1 pathway↑	Li et al. (2018a)
	LPS + IFN-γ-stimulated BV2 microglial cells	MCAO rats	$C16^+/IBA1^+$ cells↓; $Arg1^+/IBA1^+$↑; CD16, CD86, iNOS, IL-1β, IL-6↓; CD206, BDNF, TGF-β1, IL-10↑; glycolytic key proteins↓	AMPK↑; mTOR/HIF-1α signaling pathway↓	Li et al. (2024a)
Cycloastragenol	LPS-stimulated BV-2 mouse microglial cells	MCAO mice	TNF-α, IL-1β, IL-6↓; iNOS, NO, COX-2↓; ROS↓; CD206↑; microglia activation ($Iba1^+$) ↓; M1 microglia ($CD16/32^+$)↓; M2 microglia ($CD206^+$)↑	NF-κB↓; Nrf2/HO-1 pathway↑	Chen et al. (2022b)
		MCAO mice	MMP9↓; ZO-1, occluding↑; BBB disruption↓; TNF-α, IL-1β↓; microglia activation ($Iba1^+$) ↓	SIRT1↑; p53 acetylation↓; Bax/Bcl-2 ratio↓; NF-κB↓	Li et al. (2020a)
Salidroside	BV-2 microglia cultured in hypoxia	Mice exposed to hypobaric hypoxia	Occluding, claudin-5↑; Iba-1↓; GSH↑; SOD, MDA↓; IL-18, IL-6, TNF-α↓	GSK3β↑, Nrf-2↑	Zhang et al. (2024b)
	Deferoxamine-stimulated BV2 microglial cells		LDH, ROS, HIF-1α, NF-κB p65, TNF-α, IL-1β, IL-6↓; inverting cell energy metabolism		Fan et al. (2022)

(Continued on the following page)

TABLE 6 (*Continued*) Neuroprotective effects of glycosides on microglial responses after ischemic stroke.

Natural compound	Experimental models		The main regulatory effects on microglial response	Mechanisms	Ref.
	In vitro	*In vivo*			
	Neuron-microglia cocultures exposed to OGD, microglia-oligodendrocyte cocultures, primary cortical neurons subjected to OGD	Mice with MCAO	Microglia activation ($Iba\text{-}1^+$)↓; M1 microglia/macrophages ($Iba\text{-}1^+$, $CD16/32^+$)↓; microglia/macrophages ($Iba\text{-}1^+$, $CD206^+$)↑; LDH↓; CD16 and iNOS↓; CD206 and Arg1↑; IL-1β, IL-2, IL-6, IL-8, TNFα↓; oligodendrocyte differentiation↑		Liu et al. (2018b)
	OGD/R-induced BV2 cells	MCAO rats	LDH↓; apoptosis↓; TNF-α, IL-6, IL-8↓	TLR4/NF-κB pathway↓; NLRP3 inflammasome↓	Liu et al. (2021a)
		MCAO rats	CD11b↓; CD14, CD44, TNF-α, IL-6, IL-1β, iNOS↓	PI3K/Akt pathway↑; HIF↑	Wei et al. (2017)
Ginsenoside Rd	OGD-, LPS-induced BV2, primary microglial cells		Microglia activation ($Iba\text{-}1^+$)↓; IL-1β, IL-6, IL-18, TNF-α, IFN-γ↓	NF-κB activation↓; proteasome activities↓	Zhang et al. (2016b)
Ginsenoside Rb1		Mice with systemic LPS-induced inflammation	Iba1↓; morphological activation of microglia↓; TNF-α, IL-6, IL-1β↓; COX-2↓		Lee et al. (2013)
	Cortical neuron-N9 microglia hypoxic coculture system		Neuronal apoptosis↓; caspase-3↓; TNF-α, NO, superoxide↓		Ke et al. (2014)
		Mice with LPS-induced inflammation	Microglia activation ($Iba\text{-}1^+$)↓; IL-1β↓	GLT-1, GS↑	Zhang et al. (2021a)
Paeoniflorin	OGD/R-induced BV-2 microglial cells	tMCAO rats	Microglial cell proliferation↓; Iba1↓; IL-1β, TNF-α, IL-6↓; microglial viability↓; neurogenesis and vasculogenesis↑	JNK/NF-κB signaling↓	Tang et al. (2021)
	LPS-induced BV-2 microglial cells		TNF-α, IL-1β, IL-6, IFNγ↓; IL-4, IL-10↑, SOD, GSH↑; ROS, MDA↓; M1 microglia ($iNOS^+$, $CD32^+$)↓; M2 microglia ($Ym1^+$)↑	NF-κB pathway↓	Chen et al. (2020)
	LPS-induced BV-2 microglial cells		LC3-II↑; p62↓; IL-1β, TNF-α↓		Zhou et al. (2023)

In this article, the major polyphenolic compounds that exert anti-inflammatory effects through regulating microglia comprise gastrodin, curcumin, resveratrol, 6-shogaol, and paeonol (Table 3). Terpenes are the most abundant group of secondary metabolites in plants, including triptolide, Ilexonin A, artesunate, and others (Table 4). Their basic structure is made up of isoprene units. Based on the number of isoprene units, terpenes can be divided into monoterpenes, sesquiterpenes, diterpenes, triterpenes, and tetraterpenes (Araruna et al., 2020). Alkaloids are a common class of nitrogen-containing organic compounds, such as berberine and tetramethylpyrazine, which exist in various Chinese herbal medicines (Table 5). The compounds are characterized by complex ring structures with nitrogen elements, which serve as the key active group for alkaloids in treating ischemic stroke (Fan et al.,

TABLE 7 Neuroprotective effects of anthraquinones on microglial responses after ischemic stroke.

Natural compound	Experimental models		The main regulatory effects on microglial response	Mechanisms	Ref.
	In vitro	*In vivo*			
Emodin	LPS/ATP-induced BV2 microglial cells, BV2 and HT-22 cocultures stimulated by LPS/ATP		Pyroptosis↓; TNF-α, IL-1β, IL-18↓	NLRP3 inflammasome, GSDMD↓	Jiang et al. (2023)
	OGD/R-induced BV-2 microglial cells	tMCAO rats	M1 microglia ($CD32^+/Iba1^+$)↓; M2 microglia ($CD206^+/Iba1^+$)↑; CD16, CD32, iNOS↓; CD206, Arg1, CCL-22↑; GSDMD↓	NLRP3 inflammasome↓	Li et al. (2024c)
	LPS-induced primary microglia		HO-1, NQO1↑; NO, PGE2↓; iNOS, COX-2↓; TNF-α, IL-6↓	AMPK/Nrf-2↑; NF-κB↓	Park et al. (2016)
Chrysophanol	LPS-induced BV2 microglial cells	dMCAO mice	Microglia activation ($Iba\text{-}1^+$)↓; pro-inflammatory phenotype marker (CD16/32)↓; IL-6↓; the neuron complexity and the spine density	IL-6/JAK/STAT3 pathway↓	Liu et al. (2022b)
	LPS-induced BV-2 murine microglial cells		NO, IL-1β, IL-6, TNF-α↓; ROS↓; NF-κB↓; mitochondrial fission↓	Regulating MAPK and NF-κB pathway; Drp1 dephosphorylation↓	Chae et al. (2017)

TABLE 8 Neuroprotective effects of other compounds and herb extracts on microglial responses after ischemic stroke.

Natural compound	Experimental models		The main regulatory effects on microglial response	Mechanisms	Ref.
	In vitro	*In vivo*			
Other compounds					
Arctigenin	LPS-induced BV-2 microglial cells	Mice with LPS-induced inflammation	Synaptic density↑; Iba-1, GFAP↓; TNF-α, IL-1β, IL-6↓	AdipoR1↓; NF-κB↓; TLR4/CD14↓	Yuan et al. (2022)
Ligustilide		MCAO rats	TNF-α, IL-1β, ICAM-1, MMP-9, IFN-γ, IL-17↓; IL-10↑	Prx6↓; TLR4 signaling↓	Kuang et al. (2014)
Herb extracts					
Panax notoginseng saponins		Mice with photothrombotic stroke	Microglia activation ($Iba\text{-}1^+$)↓; TNF-α, IL-1β↓	PKM2↓; HIF-1α/PKM2/STAT3 signaling↓	Gao et al. (2022)
		MCAO rats	iNOS, TNF-α, IL-1β↓	P38, JNK↓; ERK1/2 phosphorylation↑	Duan et al. (2024)
Salvianolic Acids for Injection	Primary neurons and primary microglia cocultures stimulated by OGD/R	MCAO/R rats	$Iba\text{-}1^+/CD16^+$ cells↓; $Iba\text{-}1^+/CD206^+$ cells↑; caspase-1, IL-1β↓	NLRP3 inflammasome/pyroptosis axis↓	Ma et al. (2021)
	LPS-stimulated BV-2 microglia	MCAO rats	Microglia activation ($Iba\text{-}1^+$)↓; IL-1β, IL-6, TNF-α, NO↓	TLR4/NF-κB↓	Zhuang et al. (2017)

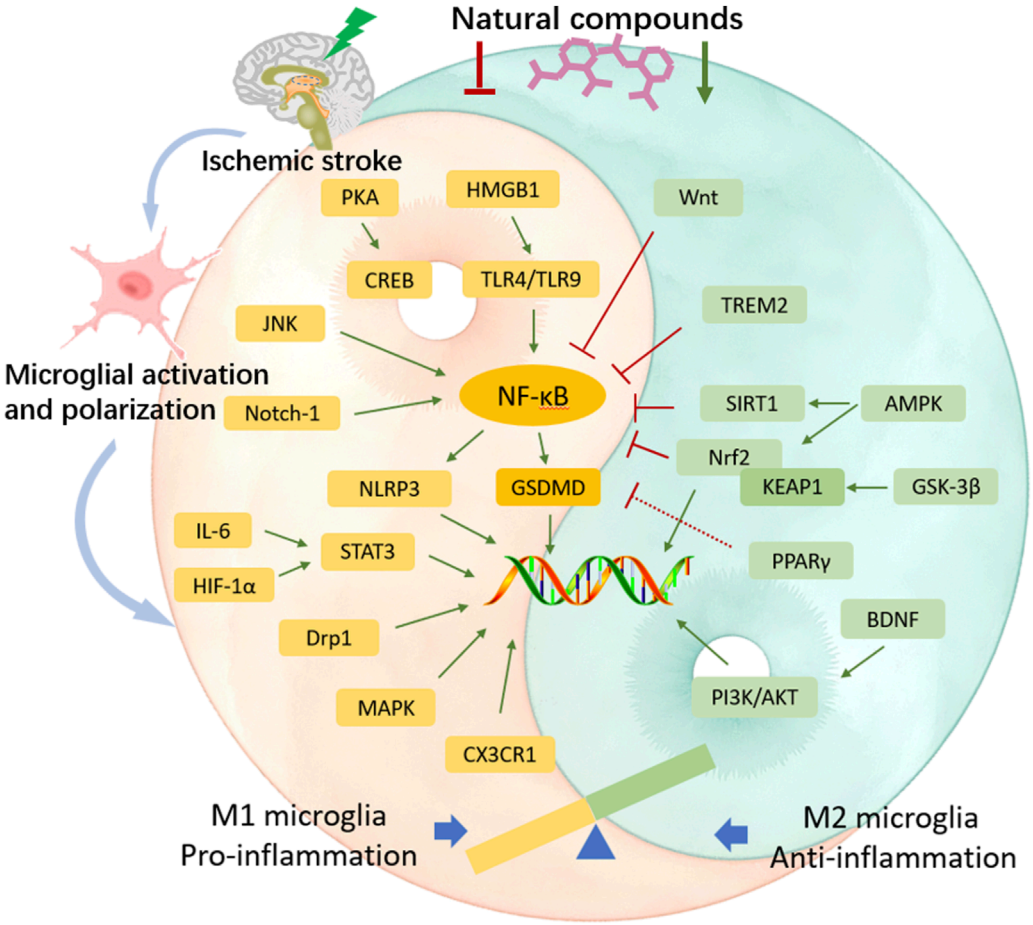

FIGURE 5
The regulatory effects of natural compounds from Chinere herbs on microglial activation after cerebral ischemia. After cerebral ischemic injury, microglia undergo rapid activation and polarization into two distinct phenotypes. M1-polarized microglia exacerbate the inflammatory response, causing further damage to brain tissue; whereas M2-polarized microglia exert anti-inflammatory effects and promote neuronal repair. Natural compounds can inhibit M1 phenotype-related pro-inflammatory signaling pathways, trigger M2 phenotype-related anti-inflammatory signaling pathways, to suppress the inflammatory response and ameliorate cerebral ischemic injury.

2024). Glycosides are sugar-containing compounds formed by an aglycone linked to one or more sugar moieties. Saponins are a common class of glycosides. The monosaccharide composition and the arrangement of sugar chains within the structure of glycosides can influence their diverse bioactivities (Thuan et al., 2024). Many glycosides have been validated to regulate microglia-associated neuroinflammation, including astragaloside IV, cycloastragenol, salidroside, ginsenoside Rd, ginsenoside Rb1, and paeoniflorin, and others. (Table 6). Anthraquinones, such as emodin and chrysophanol, are polycyclic compounds characterized by a 9,10-anthraquinone structure with three rings of A, B, and C. The side groups can be converted into the substitution patterns of hydroxyl groups, which provides anthraquinones with diverse biological activities (Wang P. et al., 2024) (Table 7). Arctigenin is a dibenzyl butyrolactone lignan from the medicinal plant *A. lappa*, and ligustilide is a natural phthalide existing in Angelica sinensis. Beyond that, herb extracts commonly used in the clinic, such as panax notoginseng saponins and salvianolic acids for injection, have remarkable anti-inflammatory effects (Table 8). Aforementioned compounds can regulate microglial response to ameliorate ischemia-induced inflammatory response through various signaling molecules and transduction pathways. These pathways are primarily associated with neuroinflammation, oxidative stress, endoplasmic reticulum stress, mitophagy, mitochondrial fission, neurotoxicity, the RAS system, embryo development, neurogenesis, angiogenesis, gut microbiota, and pyroptosis, which are critical processes in the pathogenesis of ischemic stroke (Figure 5). Moreover, changing the drug form of the compounds, using biomaterial-integrated drug delivery systems, and combining with some other small molecular drugs might exhibit superior efficiency in alleviating ischemic insults.

4 Clinical application of natural compounds that modulate microglial response

In recent years, numerous clinical trials have been conducted on ischemic stroke, focusing on the therapeutic effectiveness

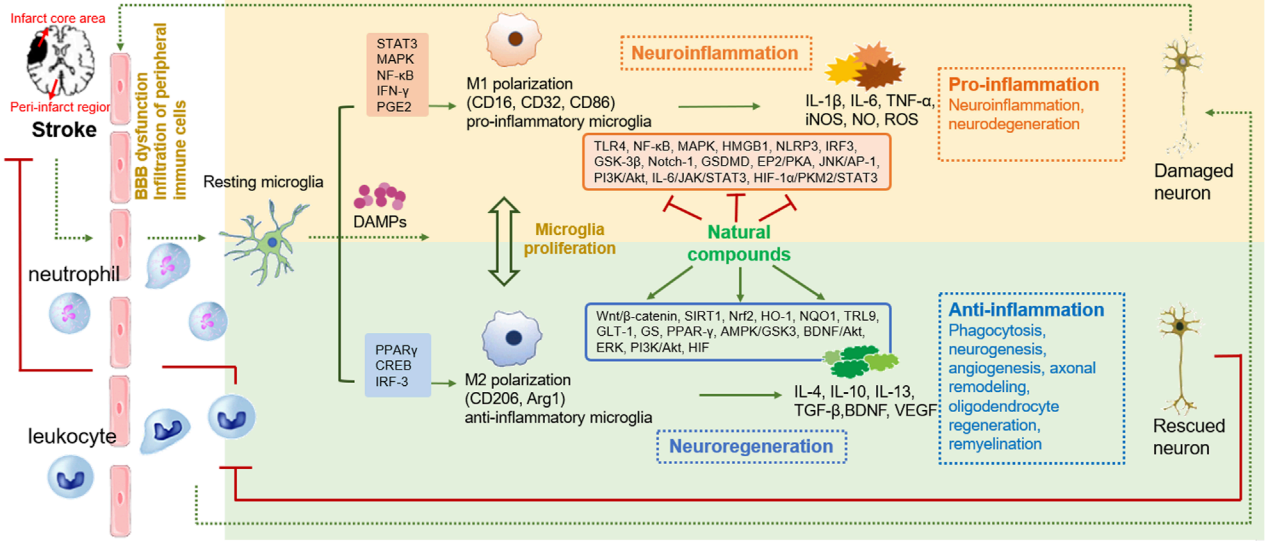

FIGURE 6
The effects of natural compounds on microglial activation and polarization in ischemic stroke. After the onset of brain ischemia, resting microglia become activated and change their morphology in the amoeboid shape. Activated microglia may be polarized into pro-inflammatory M1 phenotype or anti-inflammatory M2 phenotype. The polarization of M1 state is mediated by STAT3, MAPK, NF-κB, IFN-γ and PGE2 signaling, etc., and leads to the production of pro-inflammatory cytokines. The polarization of M2 state involves PPARγ, CREB and IRF-3 signaling, etc. Natural compounds could inhibit the activation, proliferation and M1 phenotypic polarization of microglia, while promote M2 phenotypic polarization to mitigate inflammatory response for protecting brain blood barrier, resulting in neuroprotection and neurorestoration.

and safety of the compounds isolated from traditional Chinese herbs. These compounds have been proven to participate in the regulation of microglial response in preclinical studies. A meta-analysis included a total of 14 randomized control trials (RCTs), comprising 1309 individuals suffering from acute ischemic stroke, showed that the combination of injectable salvianolic acids with the conventional treatment demonstrated superior therapeutic outcomes compared to the conventional treatment alone (Lyu et al., 2019). This superiority was embodied in the enhanced total effective rate and the recovery in neurological impairments, as well as the improvement in activities of daily living. Drug side effects in all studies were minor and transient, and the symptoms were disappeared quickly upon discontinuation of the medication (Lyu et al., 2019). For assessing the therapeutic effectiveness and safety profile of ginsenoside Rd in clinical practices, Zhang et al. carried out a pooled analysis (Zhang G. et al., 2016). The data collection process comprised two phases. In the first phase, data were gathered from 199 cases with acute ischemic stroke, and in the second phase, data were from 390 cases. By applying modified Rankin Scale (mRS) score on day 90 following stroke, the findings revealed that ginsenoside Rd effectively alleviated the degrees of disability in patients, and by applying NIH Stroke Scale (NIHSS) and Barthel Index (BI) scores on days 15 and 90 following stroke, ginsenoside Rd exhibited an improvement in neurological deficits (Zhang G. et al., 2016). A total 47 adverse events were recorded in the ginsenoside Rd group, indicating its low incidence of adverse reactions in clinical practices (Zhang G. et al., 2016). Luo et al. conducted a meta-analysis including 17 clinical studies, involving 1670 individuals with acute ischemic stroke, to assess the therapeutic effects of berberine (Luo et al., 2023). The findings revealed that berberine held suppression abilities on neuroinflammation and could be applied as an adjuvant agent for ischemic stroke. And berberine in combination with the conventional treatment exhibited superior outcomes to the only conventional treatment (Luo et al., 2023). These positive outcomes were manifested in the improvements in inflammatory markers, indicators of immune function, related biomarkers and atherosclerosis of the carotid artery (Luo et al., 2023). Available clinical data suggested that modulating microglia-driven inflammatory responses using natural compounds might be an innovative option for ischemic stroke. Since microglia perform essential roles in modulating the innate immune response (Xu S. et al., 2020), it is necessary to note that inappropriate or excessive inhibition of their activation may potentially influence or destroy other defensive mechanisms in the immune system. Owing to the intricacy of the immune system and the fact that natural compounds possess multiple action targets, it is plausible that compounds may cause some unanticipated adverse reactions during the management of ischemic stroke. Herein, conducting large-scale, long-term, and well-designed clinical trials with rigorous follow-up is imperative for further investigating safety profiles of these compounds. Such trials must evaluate not only the therapeutic benefits but also the toxicities and side effects of the compounds to ensure that any potential benefits outweigh the risks.

5 Conclusion and perspectives

Strategies that inhibit microglia-mediated detrimental inflammatory response while enhancing their inflammation-suppressive abilities serve as effective therapy methods against

ischemic stroke. Regulating microglial polarization by natural compounds from traditional Chinese herbs is considered as a crucial aspect in attenuating ischemic injury (Figure 6). Although natural compounds hold great potential to ameliorate neuroinflammatory response after stroke, research on microglia and their regulation in ischemic stroke still has limitations. For instance, cell surface markers used to distinguish between M1 subtype and M2 subtype can also be expressed by other immune cells. This overlap complicates the specific identification and isolation of microglial phenotypes. Appropriate methods and optimized technologies for segregating two subtypes of microglia would facilitate further differentiation of their pro- or anti-inflammatory characteristics. In addition, multiple factors are involved in brain ischemia and reperfusion injury, including the severity of the ischemic episode, the timing of therapeutic intervention, the approach for reperfusion treatment, as well as the presence of complications, especially the duration of the ischemic period. It is imperative to closely mimic the pathological conditions associated with these factors. Notably, animal models and related *in vivo* studies are still insufficiently designed to simulate the ischemic stroke conditions specific to elderly patients. For better addressing the aforementioned issues, the utilization of single-cell analysis, omics-based technology, and cerebral imaging methods is needed to detect and identify more sensitive microglial markers and specific targets for drugs. Besides, various influencing factors and pathological states should be considered when studying effects of natural compounds on microglia. Moreover, developing optimized animal-based and cellular stroke models simulating the intricate cerebral microenvironment is urgently needed. Further, when using natural compounds to treat stroke, it is essential to remain vigilant about potential unexpected adverse reactions, as these could interact with other pathological processes or signaling networks, thus influencing therapeutic effects and the judgement of outcomes.

Though large number of preclinical studies have been conducted on the treatment of ischemic stroke with natural compounds, their clinical applications still encounter challenges. On one hand, unclear mechanisms and action targets of compounds in brain ischemia restrict new drugs development. Proper *in vivo* methods need to be established for finding drug targets directly in the real physiological environment (Zhang et al., 2025). On the other hand, complex chemical components contained in Chinese herbal extracts pose difficulties for the isolation of monomer components with pharmacological activity and quality control of drugs (Zhu et al., 2022). Diverse factors, like sources of herbs, cultivation processes, collection and processing will affect the content of the active components within the medicinal herbs. Besides, significant first-pass effect, drug stability, and inappropriate administration routes may reduce the bioavailability of natural plant drugs. Novel drug delivery methods, such as nasal drug delivery (Rajput et al., 2022), biosynthetic drug delivery systems, such as nanoparticle encapsulation (Wang Y. et al., 2019), change in drug dosage forms, and drug purification processes, will be enable drugs to target the brain more precisely and improve their bioavailability. Importantly, issues regarding the toxic and side effects of natural compounds remain to be addressed before clinical practices. For example, excessive use of glycyrrhizic acid (GA) and glycyrrhetinic acid (GRA) may cause corticosteroid-like adverse reactions (Makino, 2021). Saikosaponins, the main active components of bupleurum chenense, have been reported to induce hepatotoxicity, neurotoxicity, hemolysis, and cardiotoxicity (Zhou et al., 2021). Besides, the potential adverse reactions arising from the interactions between natural compounds and other drugs need to be taken seriously. Herein, future investigations of natural compounds require the verification of long-term effects and a deeper exploration on pharmacological effects, including bioavailability, safety and toxicity, biosynthesis, drug delivery systems, and potential synergistic effects when combined with other compounds or Western medicine. Classical Chinese medicine formulas are widely applied in clinical practice. In recent years, there have been numerous reports on the regulation of microglial polarization by classical formulas to relieve cerebral ischemia. For instance, Buyang Huanwu Decoction suppressed microglia M1 polarization while simultaneously promoting microglia M2 polarization via AMPK pathways-mediated energy transporters and NF-Kb/CREB pathways (Li et al., 2024b). Huangqi Guizhi Wuwu Decoction modulated M2 microglia polarization and synaptic plasticity via regulating SIRT1/NF-κB/NLRP3 pathway (Ou et al., 2023). However, the components of Chinese herbal decoctions are complex, containing a variety of chemical substances, making it difficult to accurately analyze all of them, which affects the determination of quality control standards and the identification of the action targets of their active components.

It is worth noting that emerging evidence shows that exosome from different sources can regulate microglia polarization, which is mediated by exosomal miRNA cargo. Given the ability of exosomes to cross the blood-brain barrier, the use of endogenous exosomes or exosomes as carriers to transport some drug molecules to promote M2 polarization during brain ischemia offers new opportunities for stroke treatment (Wan et al., 2022). Recent study reported that M2 microglia-derived exosomes promoted the communication between M2 microglia and oligodendrocyte precursor cells, suggesting a promising therapeutic strategy for white matter repair in stroke (Li Y. et al., 2022). However, the precise number of exosomes transferred into the brain, the distribution and metabolism of exosomes, and key techniques for enhancing exosome targeting efficiency, are important issues that require deeper investigation (Li Y. et al., 2022; Ikeda et al., 2024). Considering the intricate pathogenesis of ischemic stroke, as well as the multi-targeting and multi-effecting properties of natural compounds, further studies on microglial biological properties and the regulation of microglial polarization in cerebral ischemia are not only necessary to identify novel natural compounds with optimal neuroprotective effects, but also to provide evidence that supports new clinical drug development targeting microglia-mediated neuroinflammation for ischemic stroke.

Author contributions

LY: Funding acquisition, Writing – original draft, Conceptualization. YD: Writing – original draft. ML: Writing – original draft. HL: Writing – review and editing. CY: Writing – review and editing. XL: Writing – review and editing. YG: Visualization, Writing – review and editing. LW: Visualization, Writing – review and editing. CX: Visualization, Writing – review and editing. JX: Validation, Writing – review and editing. ZY:

Validation, Writing – review and editing. MX: Funding acquisition, Supervision, Writing – review and editing. JC: Funding acquisition, Supervision, Writing – review and editing, Conceptualization.

Funding

The author(s) declare that financial support was received for the research and/or publication of this article. This work was supported by Shanghai "14th Five-Year Plan" Project for TCM Characteristic Specialty Incubation (ZYTSZK2-8), Shanghai Famous Traditional Chinese Medicine Putuo Inheritance Studio Construction Project (ptzygzs2411), Shanghai District-level General Hospital's Specialty Capability Enhancement Project for Integrated Traditional Chinese and Western Medicine (QJZXYJK-202411), Project for TCM Clinical Key Specialty Construction of Putuo District (ptzyzk2406). Project for Capacity Promotion of Putuo District Clinical Special Disease (2023tszb04). Science and Technology Innovation Project of Putuo District Health System (ptkwws202301).

Conflict of interest

The authors declare that the research was conducted in the absence of any commercial or financial relationships that could be construed as a potential conflict of interest.

Generative AI statement

The author(s) declare that no Generative AI was used in the creation of this manuscript.

Publisher's note

Supplementary material

The Supplementary Material for this article can be found online at: https://www.frontiersin.org/articles/10.3389/fcell.2025.1580479/full#supplementary-material

References

Adnan, M., Rasul, A., Hussain, G., Shah, M. A., Zahoor, M. K., Anwar, H., et al. (2020). Ginkgetin: a natural biflavone with versatile pharmacological activities. *Food Chem. Toxicol.* 145, 111642. doi:10.1016/j.fct.2020.111642

Ai, R. S., Xing, K., Deng, X., Han, J. J., Hao, D. X., Qi, W. H., et al. (2022). Baicalin promotes CNS remyelination via PPARγ signal pathway. *Neurol. Neuroimmunol. Neuroinflamm.* 9, e1142. doi:10.1212/NXI.0000000000001142

Ajami, B., Bennett, J. L., Krieger, C., McNagny, K. M., and Rossi, F. M. V. (2011). Infiltrating monocytes trigger EAE progression, but do not contribute to the resident microglia pool. *Nat. Neurosci.* 14, 1142–1149. doi:10.1038/nn.2887

Ajami, B., Bennett, J. L., Krieger, C., Tetzlaff, W., and Rossi, F. M. V. (2007). Local self-renewal can sustain CNS microglia maintenance and function throughout adult life. *Nat. Neurosci.* 10, 1538–1543. doi:10.1038/nn2014

Almolda, B., de Labra, C., Barrera, I., Gruart, A., Delgado-Garcia, J. M., Villacampa, N., et al. (2015). Alterations in microglial phenotype and hippocampal neuronal function in transgenic mice with astrocyte-targeted production of interleukin-10. *Brain Behav. Immun.* 45, 80–97. doi:10.1016/j.bbi.2014.10.015

Araruna, M. E., Serafim, C., Alves Junior, E., Hiruma-Lima, C., Diniz, M., and Batista, L. (2020). Intestinal anti-inflammatory activity of terpenes in experimental models (2010-2020): a review. *Molecules* 25, 5430. doi:10.3390/molecules25225430

Barnabei, L., Laplantine, E., Mbongo, W., Rieux-Laucat, F., and Weil, R. (2021). NF-κB: at the borders of autoimmunity and inflammation. *Front. Immunol.* 12, 716469. doi:10.3389/fimmu.2021.716469

Bi, Y., Xie, Z., Cao, X., Ni, H., Xia, S., Bao, X., et al. (2024). Cedrol attenuates acute ischemic injury through inhibition of microglia-associated neuroinflammation via ERβ-NF-κB signaling pathways. *Brain Res. Bull.* 218, 111102. doi:10.1016/j.brainresbull.2024.111102

Cai, Q., Zhao, C., Xu, Y., Lin, H., Jia, B., Huang, B., et al. (2024). Qingda granule alleviates cerebral ischemia/reperfusion injury by inhibiting TLR4/NF-κB/NLRP3 signaling in microglia. *J. Ethnopharmacol.* 324, 117712. doi:10.1016/j.jep.2024.117712

Cai, W., Dai, X., Chen, J., Zhao, J., Xu, M., Zhang, L., et al. (2019). STAT6/Arg1 promotes microglia/macrophage efferocytosis and inflammation resolution in stroke mice. *JCI Insight* 4, e131355. doi:10.1172/jci.insight.131355

Cai, Y., Huang, C., Zhou, M., Xu, S., Xie, Y., Gao, S., et al. (2022). Role of curcumin in the treatment of acute kidney injury: research challenges and opportunities. *Phytomedicine* 104, 154306. doi:10.1016/j.phymed.2022.154306

Candelario-Jalil, E., Dijkhuizen, R. M., and Magnus, T. (2022). Neuroinflammation, stroke, blood-brain barrier dysfunction, and imaging modalities. *Stroke* 53, 1473–1486. doi:10.1161/STROKEAHA.122.036946

Cankaya, I. I. T., Devkota, H. P., Zengin, G., and Samec, D. (2023). Neuroprotective potential of *biflavone ginkgetin*: a review. *Life (Basel)* 13, 562. doi:10.3390/life13020562

Chae, U., Min, J. S., Lee, H., Song, K. S., Lee, H. S., Lee, H. J., et al. (2017). Chrysophanol suppresses pro-inflammatory response in microglia via regulation of Drp1-dependent mitochondrial fission. *Immunopharmacol. Immunotoxicol.* 39, 268–275. doi:10.1080/08923973.2017.1344988

Chen, H. D., Jiang, M. Z., Zhao, Y. Y., Li, X., Lan, H., Yang, W. Q., et al. (2023). Effects of breviscapine on cerebral ischemia-reperfusion injury and intestinal flora imbalance by regulating the TLR4/MyD88/NF-κB signaling pathway in rats. *J. Ethnopharmacol.* 300, 115691. doi:10.1016/j.jep.2022.115691

Chen, J., Xue, Y., Shuai, X., Ni, C., Fang, Z., Ye, L., et al. (2022a). Effect of major components of Tripterygium wilfordii Hook. f on the uptake function of organic anion transporting polypeptide 1B1. *Toxicol. Appl. Pharmacol.* 435, 115848. doi:10.1016/j.taap.2021.115848

Chen, Q., Liu, Y., Zhang, Y., Jiang, X., Zhang, Y., and Asakawa, T. (2020). An *in vitro* verification of the effects of paeoniflorin on lipopolysaccharide-exposed microglia. *Evid. Based Complement. Altern. Med.* 2020, 5801453. doi:10.1155/2020/5801453

Chen, Q. J., Ohta, S., Sheu, K. M., Spreafico, R., Adelaja, A., Taylor, B., et al. (2021a). NF-κB dynamics determine the stimulus specificity of epigenomic reprogramming in macrophages. *Science* 372, 1349–1353. doi:10.1126/science.abc0269

Chen, S., Zhou, H., Zhang, B., and Hu, Q. (2021b). Exosomal miR-512-3p derived from mesenchymal stem cells inhibits oxidized low-density lipoprotein-induced vascular endothelial cells dysfunction via regulating Keap1. *J. Biochem. Mol. Toxicol.* 35, 1–11. doi:10.1002/jbt.22767

Chen, S. R., Dai, Y., Zhao, J., Lin, L., Wang, Y., and Wang, Y. (2018). A mechanistic overview of triptolide and celastrol, natural products from tripterygium wilfordii hook F. *Front. Pharmacol.* 9, 104. doi:10.3389/fphar.2018.00104

Chen, T., Li, Z., Li, S., Zou, Y., Gao, X., Shu, S., et al. (2022b). Cycloastragenol suppresses M1 and promotes M2 polarization in LPS-stimulated BV-2 cells and ischemic stroke mice. *Int. Immunopharmacol.* 113, 109290. doi:10.1016/j.intimp.2022.109290

Chen, Y. Y., Liu, Q. P., An, P., Jia, M., Luan, X., Tang, J. Y., et al. (2022c). Ginsenoside Rd: a promising natural neuroprotective agent. *Phytomedicine* 95, 153883. doi:10.1016/j.phymed.2021.153883

Cheret, C., Gervais, A., Lelli, A., Colin, C., Amar, L., Ravassard, P., et al. (2008). Neurotoxic activation of microglia is promoted by a nox1-dependent NADPH oxidase. *J. Neurosci.* 28, 12039–12051. doi:10.1523/JNEUROSCI.3568-08.2008

Chistiakov, D. A., Myasoedova, V. A., Revin, V. V., Orekhov, A. N., and Bobryshev, Y. V. (2017). The impact of interferon-regulatory factors to macrophage differentiation and polarization into M1 and M2. *Immunobiology* 223, 101–111. doi:10.1016/j.imbio.2017.10.005

Cho, D. Y., Ko, H. M., Kim, J., Kim, B. W., Yun, Y. S., Park, J. I., et al. (2016). Scoparone inhibits LPS-simulated inflammatory response by suppressing IRF3 and ERK in BV-2 microglial cells. *Molecules* 21, 1718. doi:10.3390/molecules21121718

Cserép, C., Pósfai, B., and Dénes, A. (2021). Shaping neuronal fate: functional heterogeneity of direct microglia-neuron interactions. *Neuron* 109, 222–240. doi:10.1016/j.neuron.2020.11.007

Deierborg, T., Roybon, L., Inacio, A. R., Pesic, J., and Brundin, P. (2010). Brain injury activates microglia that induce neural stem cell proliferation *ex vivo* and promote differentiation of neurosphere-derived cells into neurons and oligodendrocytes. *Neuroscience* 171, 1386–1396. doi:10.1016/j.neuroscience.2010.09.045

Dong, Q., Li, Z., Zhang, Q., Hu, Y., Liang, H., and Xiong, L. (2022). Astragalus mongholicus Bunge (fabaceae): bioactive compounds and potential therapeutic mechanisms against alzheimer's disease. *Front. Pharmacol.* 13, 924429. doi:10.3389/fphar.2022.924429

Dong, X., Fu, J., Yin, X., Cao, S., Li, X., Lin, L., et al. (2016). Emodin: a review of its pharmacology, toxicity and pharmacokinetics. *Phytother. Res.* 30, 1207–1218. doi:10.1002/ptr.5631

Du, X., Gao, F., Chen, S., Botchway, B. O. A., Amin, N., Hu, Z., et al. (2020). Combinational pretreatment of colony-stimulating factor 1 receptor inhibitor and triptolide upregulates BDNF-akt and autophagic pathways to improve cerebral ischemia. *Mediat. Inflamm.* 2020, 8796103. doi:10.1155/2020/8796103

Duan, Z., Jia, W., Wang, J., Xu, D., Yang, Y., Qi, Z., et al. (2024). Exploring the mechanism of Panax notoginseng saponin in inhibiting the inflammatory response of microglia in cerebral ischemia based on network pharmacology. *Acta. Biochim. Biophys. Sin. (Shanghai).* 56, 1566–1570. doi:10.3724/abbs.2024114

Fan, B., Guo, Q., and Wang, S. (2024). The application of alkaloids in ferroptosis: a review. *Biomed. Pharmacother.* 178, 117232. doi:10.1016/j.biopha.2024.117232

Fan, F., Xu, N., Sun, Y., Li, X., Gao, X., Yi, X., et al. (2022). Uncovering the metabolic mechanism of salidroside alleviating microglial hypoxia inflammation based on microfluidic chip-mass spectrometry. *J. Proteome. Res.* 21, 921–929. doi:10.1021/acs.jproteome.1c00647

Fan, F., Yang, L., Li, R., Zou, X., Li, N., Meng, X., et al. (2020). Salidroside as a potential neuroprotective agent for ischemic stroke: a review of sources, pharmacokinetics, mechanism and safety. *Biomed. Pharmacother.* 129, 110458. doi:10.1016/j.biopha.2020.110458

Fang, H., Zhou, H., Zhang, J., Li, Z., Chen, Z., Yuan, R., et al. (2020). Effects of shuxuetong injection for cerebral infarction: a protocol for systematic review and meta-analysis. *Med. Baltim.* 99, e21929. doi:10.1097/MD.0000000000021929

Fang, M., Yu, Q., Ou, J., Lou, J., Zhu, J., and Lin, Z. (2024). The neuroprotective mechanisms of PPAR- γ: inhibition of microglia- mediated neuroinflammation and oxidative stress in a neonatal mouse model of hypoxic- ischemic white matter injury. *CNS Neurosci. Ther.* 30, e70081. doi:10.1111/cns.70081

Feigin, V. L., Brainin, M., Norrving, B., Martins, S., Sacco, R. L., Hacke, W., et al. (2022). World stroke organization (WSO): global stroke fact sheet 2022. *Int. J. Stroke* 17, 18–29. doi:10.1177/17474930211065917

Feng, L., Wu, X. J., Cao, T., and Wu, B. (2021). The efficacy and safety of Xuesaitong injection combined with western medicines in the treatment of ischemic stroke: an updated systematic review and meta-analysis. *Ann. Palliat. Med.* 10, 9523–9534. doi:10.21037/apm-21-1828

Feng, X., Li, M., Lin, Z., Lu, Y., Zhuang, Y., Lei, J., et al. (2023). Tetramethylpyrazine promotes axonal remodeling and modulates microglial polarization via JAK2-STAT1/3 and GSK3-NFκB pathways in ischemic stroke. *Neurochem. Int.* 170, 105607. doi:10.1016/j.neuint.2023.105607

Gaire, B. P., Kwon, O. W., Park, S. H., Chun, K. H., Kim, S. Y., Shin, D. Y., et al. (2015). Neuroprotective effect of 6-paradol in focal cerebral ischemia involves the attenuation of neuroinflammatory responses in activated microglia. *PLoS One* 10, e0120203. doi:10.1371/journal.pone.0120203

Gan, J., Yang, X., Wu, J., Liu, P., Chen, Z., Hu, Y., et al. (2025). Neuroprotective mechanisms of microglia in ischemic stroke: a review focused on mitochondria. *Mol. Biol. Rep.* 52, 355. doi:10.1007/s11033-025-10469-4

Gao, J., Yao, M., Zhang, W., Yang, B., Yuan, G., Liu, J. X., et al. (2022). Panax notoginseng saponins alleviates inflammation induced by microglial activation and protects against ischemic brain injury via inhibiting HIF-1α/PKM2/STAT3 signaling. *Biomed. Pharmacother.* 155, 113479. doi:10.1016/j.biopha.2022.113479

Gao, P., Shi, H., Jin, X., Guo, S., Zhou, X., and Gao, W. (2024). Mechanism of astragaloside IV regulating NLRP3 through LOC102555978 to attenuate cerebral ischemia reperfusion induced microglia pyroptosis. *Int. Immunopharmacol.* 131, 111862. doi:10.1016/j.intimp.2024.111862

Giacomelli, N., Yongping, Y., Huber, F. K., Ankli, A., and Weckerle, C. S. (2017). Angelica sinensis (oliv.) diels: influence of value chain on quality criteria and marker compounds ferulic acid and Z-ligustilide. *Med. (Basel)* 4, 14. doi:10.3390/medicines4010014

Ginhoux, F., Greter, M., Leboeuf, M., Nandi, S., See, P., Gokhan, S., et al. (2010). Fate mapping analysis reveals that adult microglia derive from primitive macrophages. *Science* 330, 841–845. doi:10.1126/science.1194637

Girbovan, C., and Plamondon, H. (2015). Resveratrol downregulates type-1 glutamate transporter expression and microglia activation in the hippocampus following cerebral ischemia reperfusion in rats. *Brain Res.* 1608, 203–214. doi:10.1016/j.brainres.2015.02.038

Gong, L., Yin, J., Zhang, Y., Huang, R., Lou, Y., Jiang, H., et al. (2022). Neuroprotective mechanisms of ginsenoside Rb1 in central nervous system diseases. *Front. Pharmacol.* 13, 914352. doi:10.3389/fphar.2022.914352

Gong, Z., Pan, J., Li, X., Wang, H., He, L., and Peng, Y. (2018). Hydroxysafflor yellow A reprograms TLR9 signalling pathway in ischaemic cortex after cerebral ischaemia and reperfusion. *CNS Neurol. Disord. Drug Targets* 17, 370–382. doi:10.2174/1871527317666180502110205

Gu, M., Zhou, Y., Liao, N., Wei, Q., Bai, Z., Bao, N., et al. (2022). Chrysophanol, a main anthraquinone from Rheum palmatum L. (rhubarb), protects against renal fibrosis by suppressing NKD2/NF-κB pathway. *Phytomedicine* 105, 154381. doi:10.1016/j.phymed.2022.154381

Guglietti, B., Sivasankar, S., Mustafa, S., Corrigan, F., and Collins-Praino, L. E. (2021). Fyn kinase activity and its role in neurodegenerative disease pathology: a potential universal target? *Mol. Neurobiol.* 58, 5986–6005. doi:10.1007/s12035-021-02518-3

Han, Q., Yuan, Q., Meng, X., Huo, J., Bao, Y., and Xie, G. (2017). 6-Shogaol attenuates LPS-induced inflammation in BV2 microglia cells by activating PPAR-γ. *Oncotarget* 8, 42001–42006. doi:10.18632/oncotarget.16719

Han, X., Xu, T., Fang, Q., Zhang, H., Yue, L., Hu, G., et al. (2021). Quercetin hinders microglial activation to alleviate neurotoxicity via the interplay between NLRP3 inflammasome and mitophagy. *Redox Biol.* 44, 102010. doi:10.1016/j.redox.2021.102010

He, L. X., Tong, X., Zeng, J., Tu, Y., Wu, S., Li, M., et al. (2016). Paeonol suppresses neuroinflammatory responses in LPS-activated microglia cells. *Inflammation* 39, 1904–1917. doi:10.1007/s10753-016-0426-z

Holtman, I. R., Skola, D., and Glass, C. K. (2017). Transcriptional control of microglia phenotypes in health and disease. *J. Clin. Investig.* 127, 3220–3229. doi:10.1172/JCI90604

Hong, L., Chen, W., He, L., Tan, H., Peng, D., Zhao, G., et al. (2021). Effect of Naoluoxintong on the NogoA/RhoA/ROCK pathway by down-regulating DNA methylation in MCAO rats. *J. Ethnopharmacol.* 281, 114559. doi:10.1016/j.jep.2021.114559

Hosoi, T., Honda, M., Oba, T., and Ozawa, K. (2013). ER stress upregulated PGE_2/IFNγ-induced IL-6 expression and down-regulated iNOS expression in glial cells. *Sci. Rep.* 3, 3388. doi:10.1038/srep03388

Hou, K., Li, G. C., Yu, J. L., Xu, K., and Wu, W. (2021). Receptors, channel proteins, and enzymes involved in microglia-mediated neuroinflammation and treatments by targeting microglia in ischemic stroke. *Neuroscience* 460, 167–180. doi:10.1016/j.neuroscience.2021.02.018

Hu, X., Leak, R. K., Shi, Y., Suenaga, J., Gao, Y., Zheng, P., et al. (2015). Microglial and macrophage polarization-new prospects for brain repair. *Nat. Rev. Neurol.* 11, 56–64. doi:10.1038/nrneurol.2014.207

Huang, X. P., Ding, H., Lu, J. D., Tang, Y. H., Deng, B. X., and Deng, C. Q. (2015). Effects of the combination of the main active components of Astragalus and panax notoginseng on inflammation and apoptosis of nerve cell after cerebral ischemia-reperfusion. *Am. J. Chin. Med.* 43, 1419–1438. doi:10.1142/S0192415X15500809

Ikeda, T., Kawabori, M., Zheng, Y., Yamaguchi, S., Gotoh, S., Nakahara, Y., et al. (2024). Intranasal administration of mesenchymal stem cell-derived exosome alleviates hypoxic-ischemic brain injury. *Pharmaceutics* 16, 446. doi:10.3390/pharmaceutics16040446

Inta, I., Paxian, S., Maegele, I., Zhang, W., Pizzi, M., Spano, P., et al. (2006). Bim and Noxa are candidates to mediate the deleterious effect of the NF-kappa B subunit RelA in cerebral ischemia. *J. Neurosci.* 26, 12896–12903. doi:10.1523/JNEUROSCI.3670-06.2006

Ito, D., Tanaka, K., Suzuki, S., Dembo, T., and Fukuuchi, Y. (2001). Enhanced expression of Iba1, ionized calcium-binding adapter molecule 1, after transient focal cerebral ischemia in rat brain. *Stroke* 32, 1208–1215. doi:10.1161/01.str.32.5.1208

Jadhav, A. P., Desai, S. M., and Jovin, T. G. (2021). Indications for mechanical thrombectomy for acute ischemic stroke current guidelines and beyond. *Neurology* 97, S126–S136. doi:10.1212/WNL.0000000000012801

Jia, J., Yang, L., Chen, Y., Zheng, L., Chen, Y., Xu, Y., et al. (2021). The role of microglial phagocytosis in ischemic stroke. *Front. Immunol.* 12, 790201. doi:10.3389/fimmu.2021.790201

Jia, W. J., Yuan, Y., and Wu, C. Y. (2019). Therapeutic effects of herbal compounds in cerebral ischemia with special reference to suppression of microglia activation implicated in neurodegeneration. *Histol. Histopathol.* 34, 965–983. doi:10.14670/HH-18-103

Jiang, C., Wang, Z. N., Kang, Y. C., Chen, Y., Lu, W. X., Ren, H. J., et al.(2022). Ki20227 aggravates apoptosis, inflammatory response, and oxidative stress after focal cerebral ischemia injury. *Neural. Regen. Res.* 17(1), 137–143. doi:10.4103/1673-5374.314318

Jiang, S., Cui, H., Wu, P., Liu, Z., and Zhao, Z. (2019). Botany, traditional uses, phytochemistry, pharmacology and toxicology of Ilex pubescens Hook et Arn. *J. Ethnopharmacol.* 245, 112147. doi:10.1016/j.jep.2019.112147

Jiang, W., Liu, Z., Wu, S., Meng, T., Xu, L. L., Liu, J. F., et al. (2023). Neuroprotection of emodin by inhibition of microglial NLRP3 inflammasome-mediated pyroptosis. *J. Integr. Neurosci.* 22, 48. doi:10.31083/j.jin2202048

Jin, Q., Cheng, J., Liu, Y., Wu, J., Wang, X., Wei, S., et al. (2014). Improvement of functional recovery by chronic metformin treatment is associated with enhanced alternative activation of microglia/macrophages and increased angiogenesis and neurogenesis following experimental stroke. *Brain Behav. Immun.* 40, 131–142. doi:10.1016/j.bbi.2014.03.003

Jin, X., Liu, S., Chen, S., Wang, L., Cui, Y., He, J., et al. (2023). A systematic review on botany, ethnopharmacology, quality control, phytochemistry, pharmacology and toxicity of Arctium lappa L. fruit. *J. Ethnopharmacol.* 308, 116223. doi:10.1016/j.jep.2023.116223

Jover-Mengual, T., Miyawaki, T., Latuszek, A., Alborch, E., Zukin, R. S., and Etgen, A. M. (2010). Acute estradiol protects CA1 neurons from ischemia-induced apoptotic cell death via the PI3K/Akt pathway. *Brain Res.* 1321, 1–12. doi:10.1016/j.brainres.2010.01.046

Jurcau, A., and Simion, A. (2022). Neuroinflammation in cerebral ischemia and ischemia/reperfusion injuries: from pathophysiology to therapeutic strategies. *Int. J. Mol. Sci.* 23, 14. doi:10.3390/ijms23010014

Jurga, A. M., Paleczna, M., and Kuter, K. Z. (2020). Overview of general and discriminating markers of differential microglia phenotypes. *Front. Cell. Neurosci.* 14, 198. doi:10.3389/fncel.2020.00198

Kao, T. K., Chang, C. Y., Ou, Y. C., Chen, W. Y., Kuan, Y. H., Pan, H. C., et al. (2013). Tetramethylpyrazine reduces cellular inflammatory response following permanent focal cerebral ischemia in rats. *Exp. Neurol.* 247, 188–201. doi:10.1016/j.expneurol.2013.04.010

Ke, L., Guo, W., Xu, J., Zhang, G., Wang, W., and Huang, W. (2014). Ginsenoside Rb1 attenuates activated microglia-induced neuronal damage. *Neural. Regen. Res.* 9, 252–259. doi:10.4103/1673-5374.128217

Khoshnam, S. E., Winlow, W., Farzaneh, M., Farbood, Y., and Moghaddam, H. F. (2017). Pathogenic mechanisms following ischemic stroke. *Neurol. Sci.* 38, 1167–1186. doi:10.1007/s10072-017-2938-1

Kim, M., Shin, M. S., Lee, J. M., Cho, H. S., Kim, C. J., Kim, Y. J., et al. (2014). Inhibitory effects of isoquinoline alkaloid berberine on ischemia-induced apoptosis via activation of phosphoinositide 3-kinase/protein kinase B signaling pathway. *Int. Neurourol. J.* 18, 115–125. doi:10.5213/inj.2014.18.3.115

Kobayashi, M., and Yamamoto, M. (2005). Molecular mechanisms activating the Nrf2-Keap1 pathway of antioxidant gene regulation. *Antioxid. Redox Signal.* 7, 385–394. doi:10.1089/ars.2005.7.385

Kuang, X., Wang, L. F., Yu, L., Li, Y. J., Wang, Y. N., He, Q., et al. (2014). Ligustilide ameliorates neuroinflammation and brain injury in focal cerebral ischemia/reperfusion rats: involvement of inhibition of TLR4/peroxiredoxin 6 signaling. *Free Radic. Biol. Med.* 71, 165–175. doi:10.1016/j.freeradbiomed.2014.03.028

Lambertsen, K. L., Finsen, B., and Clausen, B. H. (2019). Post-stroke inflammation-target or tool for therapy? *Acta. Neuropathol.* 137, 693–714. doi:10.1007/s00401-018-1930-z

Lee, J. S., Song, J. H., Sohn, N. W., and Shin, J. W. (2013). Inhibitory effects of ginsenoside Rb1 on neuroinflammation following systemic lipopolysaccharide treatment in mice. *Phytother. Res.* 27, 1270–1276. doi:10.1002/ptr.4852

Li, B., Wang, M., Chen, S., Li, M., Zeng, J., Wu, S., et al. (2022a). Baicalin mitigates the neuroinflammation through the TLR4/MyD88/NF-κB and MAPK pathways in LPS-stimulated BV-2 microglia. *Biomed. Res. Int.* 2022, 3263446. doi:10.1155/2022/3263446

Li, C., Yang, F., Liu, F., Li, D., and Yang, T. (2018a). NRF2/HO-1 activation via ERK pathway involved in the anti-neuroinflammatory effect of Astragaloside IV in LPS induced microglial cells. *Neurosci. Lett.* 666, 104–110. doi:10.1016/j.neulet.2017.12.039

Li, D., Wang, C., Yao, Y., Chen, L., Liu, G., Zhang, R., et al. (2016). mTORC1 pathway disruption ameliorates brain inflammation following stroke via a shift in microglia phenotype from M1 type to M2 type. *FASEB J.* 30, 3388–3399. doi:10.1096/fj.201600495R

Li, D. J., Lang, W. J., Zhou, C., Wu, C., Zhang, F., Liu, Q., et al. (2018b). Upregulation of microglial ZEB1 ameliorates brain damage after acute ischemic stroke. *Cell. Rep.* 22, 3574–3586. doi:10.1016/j.celrep.2018.03.011

Li, L., Gan, H., Jin, H., Fang, Y., Yang, Y., Zhang, J., et al. (2021a). Astragaloside IV promotes microglia/macrophages M2 polarization and enhances neurogenesis and angiogenesis through PPARγ pathway after cerebral ischemia/reperfusion injury in rats. *Int. Immunopharmacol.* 92, 107335. doi:10.1016/j.intimp.2020.107335

Li, L., Shao, C., Liu, Z., Wu, X., Yang, J., and Wan, H. (2022b). Comparative efficacy of Honghua class injections for treating acute ischemic stroke: a Bayesian network meta-analysis of randomized controlled trials. *Front. Pharmacol.* 13, 1010533. doi:10.3389/fphar.2022.1010533

Li, M., Jiang, H., Wang, Y., Xu, Z., Xu, H., Chen, Y., et al. (2023). Effect of arctigenin on neurological diseases: a review. *J. Ethnopharmacol.* 315, 116642. doi:10.1016/j.jep.2023.116642

Li, M., Li, H., Fang, F., Deng, X., and Ma, S. (2017). Astragaloside IV attenuates cognitive impairments induced by transient cerebral ischemia and reperfusion in mice via anti-inflammatory mechanisms. *Neurosci. Lett.* 639, 114–119. doi:10.1016/j.neulet.2016.12.046

Li, M., Li, S. C., Dou, B. K., Zou, Y. X., Han, H. Z., Liu, D. X., et al. (2020a). Cycloastragenol upregulates SIRT1 expression, attenuates apoptosis and suppresses neuroinflammation after brain ischemia. *Acta. Pharmacol. Sin.* 41, 1025–1032. doi:10.1038/s41401-020-0386-6

Li, M. C., Jia, J. T., Wang, Y. X., Zhuang, Y. M., Wang, H. Y., Lin, Z. Y., et al. (2024a). Astragaloside IV promotes cerebral tissue restoration through activating AMPK- mediated microglia polarization in ischemic stroke rats. *J. Ethnopharmacol.* 334, 118532. doi:10.1016/j.jep.2024.118532

Li, M. C., Li, M. Z., Lin, Z. Y., Zhuang, Y. M., Wang, H. Y., Jia, J. T., et al. (2024b). Buyang Huanwu Decoction promotes neurovascular remodeling by modulating astrocyte and microglia polarization in ischemic stroke rats. *J. Ethnopharmacol.* 323, 117620. doi:10.1016/j.jep.2023.117620

Li, S., Sun, Y., Song, M., Song, Y., Fang, Y., Zhang, Q., et al. (2021b). NLRP3/caspase-1/GSDMD-mediated pyroptosis exerts a crucial role in astrocyte pathological injury in mouse model of depression. *JCI Insight* 6, e146852. doi:10.1172/jci.insight.146852

Li, W., Polachi, N., Wang, X., Chu, Y., Wang, Y., Tian, M., et al. (2018c). A quality marker study on salvianolic acids for injection. *Phytomedicine* 44, 138–147. doi:10.1016/j.phymed.2018.02.003

Li, X., Yao, M., Li, L., Ma, H., Sun, Y., Lu, X., et al. (2024c). Aloe-emodin alleviates cerebral ischemia-reperfusion injury by regulating microglial polarization and pyroptosis through inhibition of NLRP3 inflammasome activation. *Phytomedicine* 129, 155578. doi:10.1016/j.phymed.2024.155578

Li, X. H., Yin, F. T., Zhou, X. H., Zhang, A. H., Sun, H., Yan, G. L., et al. (2022c). The signaling pathways and targets of natural compounds from traditional Chinese medicine in treating ischemic stroke. *Molecules* 27, 3099. doi:10.3390/molecules27103099

Li, Y., Dong, Y., Ran, Y., Zhang, Y., Wu, B., Xie, J., et al. (2021c). Three-dimensional cultured mesenchymal stem cells enhance repair of ischemic stroke through inhibition of microglia. *Stem Cell. Res. Ther.* 12, 358. doi:10.1186/s13287-021-02416-4

Li, Y., Liu, T., Li, Y., Han, D., Hong, J., Yang, N., et al. (2020b). Baicalin ameliorates cognitive impairment and protects microglia from LPS-induced neuroinflammation via the SIRT1/HMGB1 pathway. *Oxid. Med. Cell. Longev.* 2020, 4751349. doi:10.1155/2020/4751349

Li, Y., Liu, Z., Song, Y., Pan, J., Jiang, Y., Shi, X., et al. (2022d). M2 microglia-derived extracellular vesicles promote white matter repair and functional recovery via miR-23a-5p after cerebral ischemia in mice. *Theranostics* 12, 3553–3573. doi:10.7150/thno.68895

Liao, H., Ye, J., Gao, L., and Liu, Y. (2021). The main bioactive compounds of Scutellaria baicalensis Georgi. for alleviation of inflammatory cytokines: a comprehensive review. *Biomed. Pharmacother.* 133, 110917. doi:10.1016/j.biopha.2020.110917

Lin, C., Lin, H. Y., Chen, J. H., Tseng, W. P., Ko, P. Y., Liu, Y. S., et al. (2015). Effects of paeonol on anti-neuroinflammatory responses in microglial cells. *Int. J. Mol. Sci.* 16, 8844–8860. doi:10.3390/ijms16048844

Lin, J., Wang, Q., Zhou, S., Xu, S., and Yao, K. (2022). Tetramethylpyrazine: a review on its mechanisms and functions. *Biomed. Pharmacother.* 150, 113005. doi:10.1016/j.biopha.2022.113005

Lin, X., and Zhang, N. (2018). Berberine: pathways to protect neurons. *Phytother. Res.* 32, 1501–1510. doi:10.1002/ptr.6107

Liu, B., Xu, C., Wu, X., Liu, F., Du, Y., Sun, J., et al. (2015). Icariin exerts an antidepressant effect in an unpredictable chronic mild stress model of depression in rats and is associated with the regulation of hippocampal neuroinflammation. *Neuroscience* 294, 193–205. doi:10.1016/j.neuroscience.2015.02.053

Liu, H., Lu, X., Hu, Y., and Fan, X. (2020a). Chemical constituents of Panax ginseng and Panax notoginseng explain why they differ in therapeutic efficacy. *Pharmacol. Res.* 161, 105263. doi:10.1016/j.phrs.2020.105263

Liu, H., Zhu, L., Chen, L., and Li, L. (2022a). Therapeutic potential of traditional Chinese medicine in atherosclerosis: a review. *Phytother. Res.* 36, 4080–4100. doi:10.1002/ptr.7590

Liu, H. T., Du, Y. G., He, J. L., Chen, W. J., Li, W. M., Yang, Z., et al. (2010). Tetramethylpyrazine inhibits production of nitric oxide and inducible nitric oxide synthase in lipopolysaccharide-induced N9 microglial cells through blockade of MAPK and PI3K/Akt signaling pathways, and suppression of intracellular reactive oxygen species. *J. Ethnopharmacol.* 129, 335–343. doi:10.1016/j.jep.2010.03.037

Liu, H. W., Gong, L. N., Lai, K., Yu, X. F., Liu, Z. Q., Li, M. X., et al. (2023a). Bilirubin gates the TRPM2 channel as a direct agonist to exacerbate ischemic brain damage. *Neuron* 111, 1609–1625.e6. doi:10.1016/j.neuron.2023.02.022

Liu, J., Chen, J., Zhang, J., Fan, Y., Zhao, S., Wang, B., et al. (2023b). Mechanism of resveratrol improving ischemia-reperfusion injury by regulating microglial function through microRNA-450b-5p/KEAP1/nrf2 pathway. *Mol. Biotechnol.* 65, 1498–1507. doi:10.1007/s12033-022-00646-2

Liu, J., Ma, W., Zang, C. H., Wang, G. D., Zhang, S. J., Wu, H. J., et al. (2021a). Salidroside inhibits NLRP3 inflammasome activation and apoptosis in microglia induced by cerebral ischemia/reperfusion injury by inhibiting the TLR4/NF-κB signaling pathway. *Ann. Transl. Med.* 9, 1694. doi:10.21037/atm-21-5752

Liu, M., Liu, C., Chen, H., Huang, X., Zeng, X., Zhou, J., et al. (2017a). Prevention of cholesterol gallstone disease by schaftoside in lithogenic diet-induced C57BL/6 mouse model. *Eur. J. Pharmacol.* 815, 1–9. doi:10.1016/j.ejphar.2017.10.003

Liu, M., Xu, Z., Wang, L., Zhang, L., Liu, Y., Cao, J., et al. (2020b). Cottonseed oil alleviates ischemic stroke injury by inhibiting the inflammatory activation of microglia and astrocyte. *J. Neuroinflammation* 17, 270. doi:10.1186/s12974-020-01946-7

Liu, M., Zhang, G., Wu, S., Song, M., Wang, J., Cai, W., et al. (2020c). Schaftoside alleviates HFD-induced hepatic lipid accumulation in mice via upregulating farnesoid X receptor. *J. Ethnopharmacol.* 255, 112776. doi:10.1016/j.jep.2020.112776

Liu, S. J., Liu, X. Y., Li, J. H., Guo, J., Li, F., Gui, Y., et al. (2018a). Gastrodin attenuates microglia activation through renin-angiotensin system and Sirtuin3 pathway. *Neurochem. Int.* 120, 49–63. doi:10.1016/j.neuint.2018.07.012

Liu, X., Wang, J., Jin, J., Hu, Q., Zhao, T., Wang, J., et al. (2024a). S100A9 deletion in microglia/macrophages ameliorates brain injury through the STAT6/PPARγ pathway in ischemic stroke. *CNX Neurosci. Ther.* 30, e14881. doi:10.1111/cns.14881

Liu, X., Wen, S., Yan, F., Liu, K., Liu, L., Wang, L., et al. (2018b). Salidroside provides neuroprotection by modulating microglial polarization after cerebral ischemia. *J. Neuroinflammation* 15, 39. doi:10.1186/s12974-018-1081-0

Liu, X., Zhang, X., Chen, J., Song, D., Zhang, C., Chen, R., et al. (2022b). Chrysophanol facilitates long-term neurological recovery through limiting microglia-mediated neuroinflammation after ischemic stroke in mice. *Int. Immunopharmacol.* 112, 109220. doi:10.1016/j.intimp.2022.109220

Liu, Y., Dang, W., Zhang, S., Wang, L., and Zhang, X. (2021b). Artesunate attenuates inflammatory injury and inhibits the NF-κB pathway in a mouse model of cerebral ischemia. *J. Int. Med. Res.* 49, 3000605211053549. doi:10.1177/03000605211053549

Liu, Y., Leng, C., Li, Y., Zhou, M., Ye, X., Li, C., et al. (2024b). A novel p55PIK signaling peptide inhibitor alleviates neuroinflammation via the STAT3/NF-kB signaling pathway in experimental stroke. *J. Stroke Cerebrovasc. Dis.* 33, 107736. doi:10.1016/j.jstrokecerebrovasdis.2024.107736

Liu, Y., Xin, H., Zhang, Y., Che, F., Shen, N., and Cui, Y. (2022c). Leaves, seeds and exocarp of Ginkgo biloba L. (Ginkgoaceae): a Comprehensive Review of Traditional Uses, phytochemistry, pharmacology, resource utilization and toxicity. *J. Ethnopharmacol.* 298, 115645. doi:10.1016/j.jep.2022.115645

Liu, Z., Ran, Y., Huang, S., Wen, S., Zhang, W., Liu, X., et al. (2017b). Curcumin protects against ischemic stroke by titrating microglia/macrophage polarization. *Front. Aging Neurosci.* 9, 233. doi:10.3389/fnagi.2017.00233

Lu, D., Shen, L., Mai, H., Zang, J., Liu, Y., Tsang, C. K., et al. (2019). HMG-CoA reductase inhibitors attenuate neuronal damage by suppressing oxygen glucose deprivation-induced activated microglial cells. *Neural. Plast.* 2019, 7675496. doi:10.1155/2019/7675496

Lu, W., Chen, Z., and Wen, J. (2024). Flavonoids and ischemic stroke-induced neuroinflammation: focus on the glial cells. *Biomed. Pharmacother.* 170, 115847. doi:10.1016/j.biopha.2023.115847

Lukens, J. R., and Eyo, U. B. (2022). Microglia and neurodevelopmental disorders. *Annu. Rev. Neurosci.* 45, 425–445. doi:10.1146/annurev-neuro-110920-023056

Luo, D., Yu, B., Sun, S., Chen, B., Harkare, H. V., Wang, L., et al. (2023). Effects of adjuvant berberine therapy on acute ischemic stroke: a meta-analysis. *Phytother. Res.* 37, 3820–3838. doi:10.1002/ptr.7920

Luo, L., Liu, M., Fan, Y., Zhang, J., Liu, L., Li, Y., et al. (2022). Intermittent theta-burst stimulation improves motor function by inhibiting neuronal pyroptosis and regulating microglial polarization via TLR4/NFκB/NLRP3 signaling pathway in cerebral ischemic mice. *J. Neuroinflammation* 19, 141. doi:10.1186/s12974-022-02501-2

Luo, R. J., Chen, J. W., Quan, Z. L., Li, C., Liang, J. K., Feng, C. C., et al. (1995). Effects of Ilexonin A on circulatory neuroregulation. *Adv. Exp. Med. Biol.* 363, 143–154. doi:10.1007/978-1-4615-1857-0_16

Luo, X., Wang, W., Li, D., Xu, C., Liao, B., Li, F., et al. (2019). Plasma exosomal miR-450b-5p as a possible biomarker and therapeutic target for transient ischaemic attacks in rats. *J. Mol. Neurosci.* 69, 516–526. doi:10.1007/s12031-019-01341-9

Lv, Y., Cao, H., Chu, L., Peng, H., Shen, X., and Yang, H. (2021). Effects of Gastrodin on BV2 cells under oxygen-glucose deprivation and its mechanism. *Gene* 766, 145152. doi:10.1016/j.gene.2020.145152

Lv, Y., Qian, Y., Ou-Yang, A., and Fu, L. (2016). Hydroxysafflor yellow A attenuates neuron damage by suppressing the lipopolysaccharide-induced TLR4 pathway in activated microglial cells. *Cell. Mol. Neurobiol.* 36, 1241–1256. doi:10.1007/s10571-015-0322-3

Lyu, J., Xie, Y., Wang, Z., and Wang, L. (2019). Salvianolic acids for injection combined with conventional treatment for patients with acute cerebral infarction: a systematic review and meta-analysis of randomized controlled trials. *Med. Sci. Monit.* 25, 7914–7927. doi:10.12659/MSM.917421

Lyu, J. X., Xie, D., Bhatia, T. N., Leak, R. K., Hu, X. M., and Jiang, X. Y. (2021). Microglial/Macrophage polarization and function in brain injury and repair after stroke. *CNS Neurosci. Ther.* 27, 515–527. doi:10.1111/cns.13620

Ma, D. C., Zhang, N. N., Zhang, Y. N., and Chen, H. S. (2021). Salvianolic Acids for Injection alleviates cerebral ischemia/reperfusion injury by switching M1/M2 phenotypes and inhibiting NLRP3 inflammasome/pyroptosis axis in microglia *in vivo* and *in vitro*. *J. Ethnopharmacol.* 270, 113776. doi:10.1016/j.jep.2021.113776

Ma, Y. Y., Wang, J. X., Wang, Y. T., and Yang, G. Y. (2017). The biphasic function of microglia in ischemic stroke. *Prog. Neurobiol.* 157, 247–272. doi:10.1016/j.pneurobio.2016.01.005

Magani, S. K. J., Mupparthi, S. D., Gollapalli, B. P., Shukla, D., Tiwari, A. K., Gorantala, J., et al. (2020). Salidroside - can it be a multifunctional drug? *Curr. Drug Metab.* 21, 512–524. doi:10.2174/1389200221666200610172105

Makino, T. (2021). Exploration for the real causative agents of licorice-induced pseudoaldosteronism. *J. Nat. Med.* 75, 275–283. doi:10.1007/s11418-021-01484-3

Mamun, A. A., Shao, C., Geng, P., Wang, S., and Xiao, J. (2024). Polyphenols targeting NF-kappaB pathway in neurological disorders: what we know so far? *Int. J. Biol. Sci.* 20, 1332–1355. doi:10.7150/ijbs.90982

Mao, Q. Q., Xu, X. Y., Cao, S. Y., Gan, R. Y., Corke, H., Beta, T., et al. (2019). Bioactive compounds and bioactivities of ginger (zingiber officinale Roscoe). *Foods* 8, 185. doi:10.3390/foods8060185

Miron, V. E., Boyd, A., Zhao, J. W., Yuen, T. J., Ruckh, J. M., Shadrach, J. L., et al. (2013). M2 microglia and macrophages drive oligodendrocyte differentiation during CNS remyelination. *Nat. Neurosci.* 16, 1211–1218. doi:10.1038/nn.3469

Mo, Z. T., Zheng, J., and Liao, Y. L. (2021). Icariin inhibits the expression of IL-1β, IL-6 and TNF-α induced by OGD/R through the IRE1/XBP1s pathway in microglia. *Pharm. Biol.* 59, 1473–1479. doi:10.1080/13880209.2021.1991959

Morganti, J. M., Riparip, L. K., and Rosi, S. (2016). Call off the dog(ma): M1/M2 polarization is concurrent following traumatic brain injury. *Plos One* 11, e0148001. doi:10.1371/journal.pone.0148001

Mota, M., Porrini, V., Parrella, E., Benarese, M., Bellucci, A., Rhein, S., et al. (2020). Neuroprotective epi-drugs quench the inflammatory response and microglial/macrophage activation in a mouse model of permanent brain ischemia. *J. Neuroinflammation* 17, 361. doi:10.1186/s12974-020-02028-4

Nangaku, M., Yoshino, K., Oda, Y., Kimura, M., Kimura, H., Hirose, Y., et al. (2021). Astroglial glutamate transporter 1 and glutamine synthetase of the nucleus accumbens are involved in the antidepressant-like effects of allopregnanolone in learned helplessness rats. *Behav. Brain Res.* 401, 113092. doi:10.1016/j.bbr.2020.113092

Naz, S., Imran, M., Rauf, A., Orhan, I. E., Shariati, M. A., Iahtisham Ul, H., et al. (2019). Chrysin: pharmacological and therapeutic properties. *Life Sci.* 235, 116797. doi:10.1016/j.lfs.2019.116797

Nguyen, P. T., Dorman, L. C., Pan, S., Vainchtein, I. D., Han, R. T., Nakao-Inoue, H., et al. (2020). Microglial remodeling of the extracellular matrix promotes synapse plasticity. *Cell.* 182, 388–403. doi:10.1016/j.cell.2020.05.050

Ni, S. J., Yao, Z. Y., Wei, X., Heng, X., Qu, S. Y., Zhao, X., et al. (2022). Vagus nerve stimulated by microbiota-derived hydrogen sulfide mediates the regulation of berberine on microglia in transient middle cerebral artery occlusion rats. *Phytother. Res.* 36, 2964–2981. doi:10.1002/ptr.7490

Okorji, U. P., and Olajide, O. A. (2014). A semi-synthetic derivative of artemisinin, artesunate inhibits prostaglandin E2 production in LPS/IFNγ-activated BV2 microglia. *Bioorg. Med. Chem.* 22, 4726–4734. doi:10.1016/j.bmc.2014.07.007

Ou, Z., Zhao, M., Xu, Y., Wu, Y., Qin, L., Fang, L., et al. (2023). Huangqi Guizhi Wuwu decoction promotes M2 microglia polarization and synaptic plasticity via Sirt1/NF-κB/NLRP3 pathway in MCAO rats. *Aging (Albany NY)* 15, 10031–10056. doi:10.18632/aging.204989

Park, S. Y., Jin, M. L., Ko, M. J., Park, G., and Choi, Y. W. (2016). Anti-neuroinflammatory effect of emodin in LPS-stimulated microglia: involvement of AMPK/Nrf2 activation. *Neurochem. Res.* 41, 2981–2992. doi:10.1007/s11064-016-2018-6

Patel, S. S., Acharya, A., Ray, R. S., Agrawal, R., Raghuwanshi, R., and Jain, P. (2020). Cellular and molecular mechanisms of curcumin in prevention and treatment of disease. *Crit. Rev. Food Sci. Nutr.* 60, 887–939. doi:10.1080/10408398.2018.1552244

Paul, S., and Candelario-Jalil, E. (2021). Emerging neuroprotective strategies for the treatment of ischemic stroke: an overview of clinical and preclinical studies. *Exp. Neurol.* 335, 113518. doi:10.1016/j.expneurol.2020.113518

Pelvig, D. P., Pakkenberg, H., Stark, A. K., and Pakkenberg, B. (2008). Neocortical glial cell numbers in human brains. *Neurobiol. Aging* 29, 1754–1762. doi:10.1016/j.neurobiolaging.2007.04.013

Pu, W. L., Zhang, M. Y., Bai, R. Y., Sun, L. K., Li, W. H., Yu, Y. L., et al. (2020). Anti-inflammatory effects of Rhodiola rosea L.: a review. *Biomed. Pharmacother.* 121, 109552. doi:10.1016/j.biopha.2019.109552

Qin, C., Zhou, L. Q., Ma, X. T., Hu, Z. W., Yang, S., Chen, M., et al. (2019). Dual functions of microglia in ischemic stroke. *Neurosci. Bull.* 35, 921–933. doi:10.1007/s12264-019-00388-3

Qiu, Y. M., Zhang, C. L., Chen, A. Q., Wang, H. L., Zhou, Y. F., Li, Y. N., et al. (2021). Immune cells in the BBB disruption after acute ischemic stroke: targets for immune therapy? *Front. Immunol.* 12, 678744. doi:10.3389/fimmu.2021.678744

Rajput, A., Pingale, P., and Dhapte-Pawar, W. (2022). Nasal delivery of neurotherapeutics via nanocarriers: facets, aspects, and prospects. *Front. Pharmacol.* 13, 979682. doi:10.3389/fphar.2022.979682

Ran, Y., Su, W., Gao, F., Ding, Z., Yang, S., Ye, L., et al. (2021). Curcumin ameliorates white matter injury after ischemic stroke by inhibiting microglia/macrophage pyroptosis through NF-κB suppression and NLRP3 inflammasome inhibition. *Oxid. Med. Cell. Longev.* 2021, 1552127. doi:10.1155/2021/1552127

Ren, H. L., Pan, Y., Wang, D. N., Hao, H. Y., Han, R. R., Qi, C. Y., et al. (2023). CD22 blockade modulates microglia activity to suppress neuroinflammation following intracerebral hemorrhage. *Pharmacol. Res.* 196, 106912. doi:10.1016/j.phrs.2023.106912

Ri, M. H., Xing, Y., Zuo, H. X., Li, M. Y., Jin, H. L., Ma, J., et al. (2023). Regulatory mechanisms of natural compounds from traditional Chinese herbal medicines on the microglial response in ischemic stroke. *Phytomedicine* 116, 154889. doi:10.1016/j.phymed.2023.154889

Romano, B., Pagano, E., Montanaro, V., Fortunato, A. L., Milic, N., and Borrelli, F. (2013). Novel insights into the pharmacology of flavonoids. *Phytother. Res.* 27, 1588–1596. doi:10.1002/ptr.5023

Ronaldson, P. T., and Davis, T. P. (2020). Regulation of blood-brain barrier integrity by microglia in health and disease: a therapeutic opportunity. *J. Cereb. Blood Flow. Metab.* 40, S6–S24. doi:10.1177/0271678X20951995

Ruan, W., Li, J., Xu, Y., Wang, Y., Zhao, F., Yang, X., et al. (2019). MALAT1 up-regulator polydatin protects brain microvascular integrity and ameliorates stroke through C/EBPβ/MALAT1/CREB/PGC-1α/PPARγ pathway. *Cell. Mol. Neurobiol.* 39, 265–286. doi:10.1007/s10571-018-00646-4

Ruffell, D., Mourkioti, F., Gambardella, A., Kirstetter, P., Lopez, R. G., Rosenthal, N., et al. (2009). A CREB-C/EBPbeta cascade induces M2 macrophage-specific gene expression and promotes muscle injury repair. *Proc. Natl. Acad. Sci. U. S. A.* 106, 17475–17480. doi:10.1073/pnas.0908641106

Russo, M., Spagnuolo, C., Tedesco, I., Bilotto, S., and Russo, G. L. (2012). The flavonoid quercetin in disease prevention and therapy: facts and fancies. *Biochem. Pharmacol.* 83, 6–15. doi:10.1016/j.bcp.2011.08.010

Saini, V., Guada, L., and Yavagal, D. R. (2021). Global epidemiology of stroke and access to acute ischemic stroke interventions. *Neurology* 97, S6–S16. doi:10.1212/WNL.0000000000012781

Shah, M. A., Park, D. J., Kang, J. B., Kim, M. O., and Koh, P. O. (2020). Baicalin alleviates lipopolysaccharide-induced neuroglial activation and inflammatory factors activation in hippocampus of adult mice. *Lab. Anim. Res.* 36, 32. doi:10.1186/s42826-020-00058-w

Shang, K., He, J., Zou, J., Qin, C., Lin, L., Zhou, L. Q., et al. (2020). Fingolimod promotes angiogenesis and attenuates ischemic brain damage via modulating microglial polarization. *Brain Res.* 1726, 146509. doi:10.1016/j.brainres.2019.146509

Shi, L., Sun, Z., Su, W., Xu, F., Xie, D., Zhang, Q., et al. (2021). Treg cell-derived osteopontin promotes microglia-mediated white matter repair after ischemic stroke. *Immunity* 54, 1527–1542.e8. doi:10.1016/j.immuni.2021.04.022

Sousa, C., Golebiewska, A., Poovathingal, S. K., Kaoma, T., Pires-Afonso, Y., Martina, S., et al. (2018). Single-cell transcriptomics reveals distinct inflammation-induced microglia signatures. *EMBO Rep.* 19, e46171. doi:10.15252/embr.201846171

Su, S., Wu, J., Gao, Y., Luo, Y., Yang, D., and Wang, P. (2020). The pharmacological properties of chrysophanol, the recent advances. *Biomed. Pharmacother.* 125, 110002. doi:10.1016/j.biopha.2020.110002

Subedi, L., and Gaire, B. P. (2021). Phytochemicals as regulators of microglia/macrophages activation in cerebral ischemia. *Pharmacol. Res.* 165, 105419. doi:10.1016/j.phrs.2021.105419

Sun, X., Jia, B., Sun, J., Lin, J., Lu, B., Duan, J., et al. (2023). Gastrodia elata Blume: a review of its mechanisms and functions on cardiovascular systems. *Fitoterapia* 167, 105511. doi:10.1016/j.fitote.2023.105511

Tabara, L., Segawa, M., and Prudent, J. (2025). Molecular mechanisms of mitochondrial dynamics. *Nat. Rev. Mol. Cell. Biol.* 26, 123–146. doi:10.1038/s41580-024-00785-1

Tang, H., Wu, L., Chen, X., Li, H., Huang, B., Huang, Z., et al. (2021). Paeoniflorin improves functional recovery through repressing neuroinflammation and facilitating neurogenesis in rat stroke model. *PeerJ* 9, e10921. doi:10.7717/peerj.10921

Tang, K., Qin, W., Wei, R., Jiang, Y., Fan, L., Wang, Z., et al. (2022a). Ginsenoside Rd ameliorates high glucose-induced retinal endothelial injury through AMPK-STRT1 interdependence. *Pharmacol. Res.* 179, 106123. doi:10.1016/j.phrs.2022.106123

Tang, T., Wang, X., Qi, E., Li, S., and Sun, H. (2022b). Ginkgetin promotes M2 polarization of microglia and exert neuroprotection in ischemic stroke via modulation of PPARγ pathway. *Neurochem. Res.* 47, 2963–2974. doi:10.1007/s11064-022-03583-3

Tarassishin, L., Suh, H., and Lee, S. C. (2011). Interferon regulatory factor 3 plays an anti-inflammatory role in microglia by activating the PI3K/Akt pathway. *J. Neuroinflammation* 8, 187. doi:10.1186/1742-2094-8-187

Thored, P., Heldmann, U., Gomes-Leal, W., Gisler, R., Darsalia, V., Taneera, J., et al. (2009). Long-term accumulation of microglia with proneurogenic phenotype concomitant with persistent neurogenesis in adult subventricular zone after stroke. *Glia* 57, 835–849. doi:10.1002/glia.20810

Thuan, N. H., Huong, Q. T. T., Lam, B. D., Tam, H. T., Thu, P. T., Canh, N. X., et al. (2024). Advances in glycosyltransferase-mediated glycodiversification of small molecules. *3 Biotech.* 14, 209. doi:10.1007/s13205-024-04044-0

van der Bliek, A. M., Shen, Q., and Kawajiri, S. (2013). Mechanisms of mitochondrial fission and fusion. *Cold Spring Harb. Perspect. Biol.* 5, a011072. doi:10.1101/cshperspect.a011072

Var, S. R., Shetty, A. V., Grande, A. W., Low, W. C., and Cheeran, M. C. (2021). Microglia and macrophages in neuroprotection, neurogenesis, and emerging therapies for stroke. *Cells* 10, 3555. doi:10.3390/cells10123555

Waisman, A., Ginhoux, F., Greter, M., and Bruttger, J. (2015). Homeostasis of microglia in the adult brain: review of novel microglia depletion systems. *Trends Immunol.* 36, 625–636. doi:10.1016/j.it.2015.08.005

Wan, T., Huang, Y., Gao, X., Wu, W., and Guo, W. (2022). Microglia polarization: a novel target of exosome for stroke treatment. *Front. Cell. Dev. Biol.* 10, 842320. doi:10.3389/fcell.2022.842320

Wang, H., Ma, J., Li, X., Peng, Y., and Wang, M. (2024a). FDA compound library screening Baicalin upregulates TREM2 for the treatment of cerebral ischemia-reperfusion injury. *Eur. J. Pharmacol.* 969, 176427. doi:10.1016/j.ejphar.2024.176427

Wang, H., Ren, S., Liu, C., and Zhang, X. (2016). An overview of systematic reviews of danhong injection for ischemic stroke. *Evid. Based Complement. Altern. Med.* 2016, 8949835. doi:10.1155/2016/8949835

Wang, J., Wang, L., Lou, G. H., Zeng, H. R., Hu, J., Huang, Q. W., et al. (2019a). Coptidis Rhizoma: a comprehensive review of its traditional uses, botany, phytochemistry, pharmacology and toxicology. *Pharm. Biol.* 57, 193–225. doi:10.1080/13880209.2019.1577466

Wang, L., Ma, R., Liu, C., Liu, H., Zhu, R., Guo, S., et al. (2017). Salvia miltiorrhiza: a potential red light to the development of cardiovascular diseases. *Curr. Pharm. Des.* 23, 1077–1097. doi:10.2174/1381612822666161010105242

Wang, P., Wei, J., Hua, X., Dong, G., Dziedzic, K., Wahab, A. T., et al. (2024b). Plant anthraquinones: classification, distribution, biosynthesis, and regulation. *J. Cell. Physiol.* 239, e31063. doi:10.1002/jcp.31063

Wang, Q., Yang, Z., Wu, X., Zhang, X., Geng, F., Wang, Q., et al. (2022a). Chrysin alleviates lipopolysaccharide-induced neuron damage and behavioral deficits in mice through inhibition of Fyn. *Int. Immunopharmacol.* 111, 109118. doi:10.1016/j.intimp.2022.109118

Wang, X., Sun, W., Fang, S., Dong, B., Li, J., Lv, Z., et al. (2023). AaWRKY6 contributes to artemisinin accumulation during growth in Artemisia annua. *Plant Sci.* 335, 111789. doi:10.1016/j.plantsci.2023.111789

Wang, X. L., Feng, S. T., Wang, Y. T., Chen, N. H., Wang, Z. Z., and Zhang, Y. (2021). Paeoniflorin: a neuroprotective monoterpenoid glycoside with promising anti-depressive properties. *Phytomedicine* 90, 153669. doi:10.1016/j.phymed.2021.153669

Wang, Y., Leak, R. K., and Cao, G. (2022b). Microglia-mediated neuroinflammation and neuroplasticity after stroke. *Front. Cell. Neurosci.* 16, 980722. doi:10.3389/fncel.2022.980722

Wang, Y., Luo, J., and Li, S. Y. (2019b). Nano-curcumin simultaneously protects the blood-brain barrier and reduces M1 microglial activation during cerebral ischemia-reperfusion injury. *ACS Appl. Mater. Interfaces.* 11, 3763–3770. doi:10.1021/acsami.8b20594

Wang, Z., Wang, D., Yang, D., Zhen, W., Zhang, J., and Peng, S. (2018). The effect of icariin on bone metabolism and its potential clinical application. *Osteoporos. Int.* 29, 535–544. doi:10.1007/s00198-017-4255-1

Wei, J., Chen, P., Gupta, P., Ott, M., Zamler, D., Kassab, C., et al. (2020). Immune biology of glioma-associated macrophages and microglia: functional and therapeutic implications. *Neuro. Oncol.* 22, 180–194. doi:10.1093/neuonc/noz212

Wei, Y., Hong, H., Zhang, X., Lai, W., Wang, Y., Chu, K., et al. (2017). Salidroside inhibits inflammation through PI3K/akt/HIF signaling after focal cerebral ischemia in rats. *Inflammation* 40, 1297–1309. doi:10.1007/s10753-017-0573-x

Weng, W., and Goel, A. (2022). Curcumin and colorectal cancer: an update and current perspective on this natural medicine. *Semin. Cancer. Biol.* 80, 73–86. doi:10.1016/j.semcancer.2020.02.011

Wu, Q., Liu, J., Mao, Z., Tian, L., Wang, N., Wang, G., et al. (2022). Ligustilide attenuates ischemic stroke injury by promoting Drp1-mediated mitochondrial fission via activation of AMPK. *Phytomedicine* 95, 153884. doi:10.1016/j.phymed.2021.153884

Xiao, Y., Guan, T., Yang, X., Xu, J., Zhang, J., Qi, Q., et al. (2023). Baicalin facilitates remyelination and suppresses neuroinflammation in rats with chronic

cerebral hypoperfusion by activating Wnt/β-catenin and inhibiting NF-κB signaling. *Behav. Brain Res.* 442, 114301. doi:10.1016/j.bbr.2023.114301

Xiong, X. Y., Liu, L., and Yang, Q. W. (2016). Functions and mechanisms of microglia/macrophages in neuroinflammation and neurogenesis after stroke. *Prog. Neurobiol.* 142, 23–44. doi:10.1016/j.pneurobio.2016.05.001

Xiong, X. Y., Liu, L., and Yang, Q. W. (2018). Refocusing neuroprotection in cerebral reperfusion era: new challenges and strategies. *Front. Neurol.* 9, 249. doi:10.3389/fneur.2018.00249

Xu, A. L., Zheng, G. Y., Wang, Z. J., Chen, X. D., and Jiang, Q. (2016). Neuroprotective effects of Ilexonin A following transient focal cerebral ischemia in rats. *Mol. Med. Rep.* 13, 2957–2966. doi:10.3892/mmr.2016.4921

Xu, A. L., Zheng, G. Y., Ye, H. Y., Chen, X. D., and Jiang, Q. (2020a). Characterization of astrocytes and microglial cells in the hippocampal CA1 region after transient focal cerebral ischemia in rats treated with Ilexonin A. *Neural. Regen. Res.* 15, 78–85. doi:10.4103/1673-5374.264465

Xu, S., Lu, J., Shao, A., Zhang, J. H., and Zhang, J. (2020b). Glial cells: role of the immune response in ischemic stroke. *Front. Immunol.* 11, 294. doi:10.3389/fimmu.2020.00294

Xu, X., Gao, W., Li, L., Hao, J., Yang, B., Wang, T., et al. (2021). Annexin A1 protects against cerebral ischemia-reperfusion injury by modulating microglia/macrophage polarization via FPR2/ALX-dependent AMPK-mTOR pathway. *J. Neuroinflammation* 18, 119. doi:10.1186/s12974-021-02174-3

Xu, X., Lu, Y., and Bie, X. (2007). Protective effects of gastrodin on hypoxia-induced toxicity in primary cultures of rat cortical neurons. *Planta. Med.* 73, 650–654. doi:10.1055/s-2007-981523

Yang, C., Hawkins, K. E., Dore, S., and Candelario-Jalil, E. (2019). Neuroinflammatory mechanisms of blood-brain barrier damage in ischemic stroke. *Am. J. Physiol. Cell. Physiol.* 316, C135–C153. doi:10.1152/ajpcell.00136.2018

Yang, X., Xu, S., Qian, Y., and Xiao, Q. (2017). Resveratrol regulates microglia M1/M2 polarization via PGC-1α in conditions of neuroinflammatory injury. *Brain Behav. Immun.* 64, 162–172. doi:10.1016/j.bbi.2017.03.003

Yang, Y., Xu, J., Tu, J., Sun, Y., Zhang, C., Qiu, Z., et al. (2024). Polygonum cuspidatum Sieb. et Zucc. Extracts improve sepsis-associated acute kidney injury by inhibiting NF-κB-mediated inflammation and pyroptosis. *J. Ethnopharmacol.* 319, 117101. doi:10.1016/j.jep.2023.117101

Yao, Y. Y., Bian, L. G., Yang, P., Sui, Y., Li, R., Chen, Y. L., et al. (2019). Gastrodin attenuates proliferation and inflammatory responses in activated microglia through Wnt/β-catenin signaling pathway. *Brain Res.* 1717, 190–203. doi:10.1016/j.brainres.2019.04.025

Yao, Y. Y., Li, R., Guo, Y. J., Zhao, Y., Guo, J. Z., Ai, Q. L., et al. (2022). Gastrodin attenuates lipopolysaccharide-induced inflammatory response and migration via the notch-1 signaling pathway in activated microglia. *Neuromolecular Med.* 24, 139–154. doi:10.1007/s12017-021-08671-1

Ye, Y., Jin, T., Zhang, X., Zeng, Z., Ye, B., Wang, J., et al. (2019). Meisoindigo protects against focal cerebral ischemia-reperfusion injury by inhibiting NLRP3 inflammasome activation and regulating microglia/macrophage polarization via TLR4/NF-κB signaling pathway. *Front. Cell. Neurosci.* 13, 553. doi:10.3389/fncel.2019.00553

Yeh, C. H., Yang, M. L., Lee, C. Y., Yang, C. P., Li, Y. C., Chen, C. J., et al. (2014). Wogonin attenuates endotoxin-induced prostaglandin E2 and nitric oxide production via Src-ERK1/2-NFκB pathway in BV-2 microglial cells. *Environ. Toxicol.* 29, 1162–1170. doi:10.1002/tox.21847

Yu, F., Wang, Y., Stetler, A. R., Leak, R. K., Hu, X., and Chen, J. (2022a). Phagocytic microglia and macrophages in brain injury and repair. *CNS Neurosci. Ther.* 28, 1279–1293. doi:10.1111/cns.13899

Yu, L., Jin, Z., Li, M., Liu, H., Tao, J., Xu, C., et al. (2022b). Protective potential of hydroxysafflor yellow A in cerebral ischemia and reperfusion injury: an overview of evidence from experimental studies. *Front. Pharmacol.* 13, 1063035. doi:10.3389/fphar.2022.1063035

Yu, L., Tao, J., Zhao, Q., Xu, C., and Zhang, Q. J. (2020). Confirmation of potential neuroprotective effects of natural bioactive compounds from traditional medicinal herbs in cerebral ischemia treatment. *J. Integr. Neurosci.* 19, 373–384. doi:10.31083/j.jin.2020.02.63

Yu, S., Peng, W., Qiu, F., and Zhang, G. (2022c). Research progress of astragaloside IV in the treatment of atopic diseases. *Biomed. Pharmacother.* 156, 113989. doi:10.1016/j.biopha.2022.113989

Yu, Y., Zhou, L., Yang, Y., and Liu, Y. (2018). Cycloastragenol: an exciting novel candidate for age-associated diseases. *Exp. Ther. Med.* 16, 2175–2182. doi:10.3892/etm.2018.6501

Yuan, Q., Wu, Y., Wang, G., Zhou, X., Dong, X., Lou, Z., et al. (2022). Preventive effects of arctigenin from Arctium lappa L against LPS-induced neuroinflammation and cognitive impairments in mice. *Metab. Brain Dis.* 37, 2039–2052. doi:10.1007/s11011-022-01031-3

Zeng, X., Zhang, S., Zhang, L., Zhang, K., and Zheng, X. (2006). A study of the neuroprotective effect of the phenolic glucoside gastrodin during cerebral ischemia *in vivo* and *in vitro*. *Planta. Med.* 72, 1359–1365. doi:10.1055/s-2006-951709

Zhang, A., Liu, X., Li, X., Duan, N., and Huang, B. (2025). A narrative review on the role of traditional Chinese medicine (TCM) in treating coronary artery disease. *J. Pak. Med. Assoc.* 75, 462–468. doi:10.47391/JPMA.11610

Zhang, B. Q., Zheng, G. Y., Han, Y., Chen, X. D., and Jiang, Q. (2016a). Ilexonin A promotes neuronal proliferation and regeneration via activation of the canonical Wnt signaling pathway after cerebral ischemia reperfusion in rats. *Evid. Based Complement. Altern. Med.* 2016, 9753189. doi:10.1155/2016/9753189

Zhang, G., Xia, F., Zhang, Y., Zhang, X., Cao, Y., Wang, L., et al. (2016b). Ginsenoside Rd is efficacious against acute ischemic stroke by suppressing microglial proteasome-mediated inflammation. *Mol. Neurobiol.* 53, 2529–2540. doi:10.1007/s12035-015-9261-8

Zhang, H., Chen, X., Wang, X., Liu, Y., Sands, C. D., and Tang, M. (2021a). Ginsenoside Rb1 attenuates lipopolysaccharide-induced neural damage in the brain of mice via regulating the dysfunction of microglia and astrocytes. *J. Integr. Neurosci.* 20, 813–823. doi:10.31083/j.jin2004084

Zhang, J., Fan, F., Liu, A., Zhang, C., Li, Q., Zhang, C., et al. (2022). Icariin: a potential molecule for treatment of knee osteoarthritis. *Front. Pharmacol.* 13, 811808. doi:10.3389/fphar.2022.811808

Zhang, J., Wu, C., Gao, L., Du, G., and Qin, X. (2020). Astragaloside IV derived from Astragalus membranaceus: a research review on the pharmacological effects. *Adv. Pharmacol.* 87, 89–112. doi:10.1016/bs.apha.2019.08.002

Zhang, L., Li, D. C., and Liu, L. F. (2019). Paeonol: pharmacological effects and mechanisms of action. *Immunopharmacol* 72, 413–421. doi:10.1016/j.intimp.2019.04.033

Zhang, L. L., Tian, K., Tang, Z. H., Chen, X. J., Bian, Z. X., Wang, Y. T., et al. (2016c). Phytochemistry and pharmacology of Carthamus tinctorius L. *Am. J. Chin. Med.* 44, 197–226. doi:10.1142/S0192415X16500130

Zhang, L. X., Li, C. X., Kakar, M. U., Khan, M. S., Wu, P. F., Amir, R. M., et al. (2021b). Resveratrol (RV): a pharmacological review and call for further research. *Biomed. Pharmacother.* 143, 112164. doi:10.1016/j.biopha.2021.112164

Zhang, S., Ran, Y., Tuolhen, Y., Wang, Y., Tian, G., Xi, J., et al. (2024a). Curcumin loaded hydrogel with double ROS-scavenging effect regulates microglia polarization to promote poststroke rehabilitation. *Mater. Today. bio.* 28, 101177. doi:10.1016/j.mtbio.2024.101177

Zhang, S. P. R., Phan, T. G., and Sobey, C. G. (2021c). Targeting the immune system for ischemic stroke. *Trends Pharmacol. Sci.* 42, 96–105. doi:10.1016/j.tips.2020.11.010

Zhang, T., Gong, X., Hu, G., and Wang, X. (2015). EP2-PKA signaling is suppressed by triptolide in lipopolysaccharide-induced microglia activation. *J. Neuroinflammation* 12, 50. doi:10.1186/s12974-015-0275-y

Zhang, W., Tian, T., Gong, S. X., Huang, W. Q., Zhou, Q. Y., Wang, A. P., et al. (2021d). Microglia-associated neuroinflammation is a potential therapeutic target for ischemic stroke. *Neural. Regen. Res.* 16, 6–11. doi:10.4103/1673-5374.286954

Zhang, X., Zhang, H., Liu, Z., Huang, T., Yi, R., Ma, Z., et al. (2024b). Salidroside improves blood-brain barrier integrity and cognitive function in hypobaric hypoxia mice by inhibiting microglia activation through GSK3β. *Phytother. Res.* 39, 1808–1825. doi:10.1002/ptr.8264

Zhang, Y., Zhang, X., Cui, L., Chen, R., Zhang, C., Li, Y., et al. (2017). Salvianolic Acids for Injection (SAFI) promotes functional recovery and neurogenesis via sonic hedgehog pathway after stroke in mice. *Neurochem. Int.* 110, 38–48. doi:10.1016/j.neuint.2017.09.001

Zhao, S. C., Ma, L. S., Chu, Z. H., Xu, H., Wu, W. Q., and Liu, F. D. (2017). Regulation of microglial activation in stroke. *Acta. Pharmacol. Sin.* 38, 445–458. doi:10.1038/aps.2016.162

Zhao, T., Tang, H., Xie, L., Zheng, Y., Ma, Z., Sun, Q., et al. (2019). Scutellaria baicalensis Georgi. (Lamiaceae): a review of its traditional uses, botany, phytochemistry, pharmacology and toxicology. *J. Pharm. Pharmacol.* 71, 1353–1369. doi:10.1111/jphp.13129

Zhao, X., Zou, Y., Xu, H., Fan, L., Guo, H., Li, X., et al. (2012). Gastrodin protect primary cultured rat hippocampal neurons against amyloid-beta peptide-induced neurotoxicity via ERK1/2-Nrf2 pathway. *Brain Res.* 1482, 13–21. doi:10.1016/j.brainres.2012.09.010

Zhao, Y., Wei, Z. Z., Lee, J. H., Gu, X., Sun, J., Dix, T. A., et al. (2020). Pharmacological hypothermia induced neurovascular protection after severe stroke of transient middle cerebral artery occlusion in mice. *Exp. Neurol.* 325, 113133. doi:10.1016/j.expneurol.2019.113133

Zheng, Y., Zhu, G., He, J., Wang, G., Li, D., and Zhang, F. (2019). Icariin targets Nrf2 signaling to inhibit microglia-mediated neuroinflammation. *Int. Immunopharmacol.* 73, 304–311. doi:10.1016/j.intimp.2019.05.033

Zhou, J., Ye, W., Chen, L., Li, J., Zhou, Y., Bai, C., et al. (2024). Triptolide alleviates cerebral ischemia/reperfusion injury via regulating the Fractalkine/CX3CR1 signaling pathway. *Brain Res. Bull.* 211, 110939. doi:10.1016/j.brainresbull.2024.110939

Zhou, K., Wu, J., Chen, J., Zhou, Y., Chen, X., Wu, Q., et al. (2019). Schaftoside ameliorates oxygen glucose deprivation-induced inflammation associated with the TLR4/Myd88/Drp1-related mitochondrial fission in BV2 microglia cells. *J. Pharmacol. Sci.* 139, 15–22. doi:10.1016/j.jphs.2018.10.012

Zhou, P., Shi, W., He, X. Y., Du, Q. Y., Wang, F., and Guo, J. (2021). Saikosaponin D: review on the antitumour effects, toxicity and pharmacokinetics. *Pharm. Biol.* 59, 1480–1489. doi:10.1080/13880209.2021.1992448

Zhou, R. N., Song, Y. L., Ruan, J. Q., Wang, Y. T., and Yan, R. (2012). Pharmacokinetic evidence on the contribution of intestinal bacterial conversion to beneficial effects of astragaloside IV, a marker compound of astragali radix, in traditional oral use of the herb. *Drug Metab. Pharmacokinet.* 27, 586–597. doi:10.2133/dmpk.dmpk-11-rg-160

Zhou, X., Chen, X., Cheng, X., Lin, L., Quan, S., Li, S., et al. (2023). Paeoniflorin, ferulic acid, and atractylenolide III improved LPS-induced neuroinflammation of BV2 microglia cells by enhancing autophagy. *J. Pharmacol. Sci.* 152, 151–161. doi:10.1016/j.jphs.2023.04.007

Zhou, Y. X., Gong, X. H., Zhang, H., and Peng, C. (2020). A review on the pharmacokinetics of paeoniflorin and its anti-inflammatory and immunomodulatory effects. *Biomed. Pharmacother.* 130, 110505. doi:10.1016/j.biopha.2020.110505

Zhu, H., Jian, Z., Zhong, Y., Ye, Y., Zhang, Y., Hu, X., et al. (2021). Janus kinase inhibition ameliorates ischemic stroke injury and neuroinflammation through reducing NLRP3 inflammasome activation *via* JAK2/STAT3 pathway inhibition. *Front. Immunol.* 12, 714943. doi:10.3389/fimmu.2021.714943

Zhu, H., Liu, C., Hou, J., Long, H., Wang, B., Guo, D., et al. (2019a). Gastrodia elata blume polysaccharides: a review of their acquisition, analysis, modification, and pharmacological activities. *Molecules* 24, 2436. doi:10.3390/molecules24132436

Zhu, J., Cao, D., Guo, C., Liu, M., Tao, Y., Zhou, J., et al. (2019b). Berberine facilitates angiogenesis against ischemic stroke through modulating microglial polarization via AMPK signaling. *Cell. Mo.l Neurobiol.* 39, 751–768. doi:10.1007/s10571-019-00675-7

Zhu, Y., Ouyang, Z., Du, H., Wang, M., Wang, J., Sun, H., et al. (2022). New opportunities and challenges of natural products research: when target identification meets single-cell multiomics. *Acta. Pharm. Sin. B* 12, 4011–4039. doi:10.1016/j.apsb.2022.08.022

Zhuang, P., Wan, Y., Geng, S., He, Y., Feng, B., Ye, Z., et al. (2017). Salvianolic Acids for Injection (SAFI) suppresses inflammatory responses in activated microglia to attenuate brain damage in focal cerebral ischemia. *J. Ethnopharmacol.* 198, 194–204. doi:10.1016/j.jep.2016.11.052

frontiers | Frontiers in Neurology

TYPE Original Research
PUBLISHED 16 July 2025
DOI 10.3389/fneur.2025.1583982

OPEN ACCESS

EDITED BY
Hao Yu,
Zhejiang University, China

REVIEWED BY
Alejandro A. Canales-Aguirre,
CONACYT Centro de Investigación y Asistencia en Tecnología y Diseño del Estado de Jalisco (CIATEJ), Mexico
Stanislaw Szlufik,
Medical University of Warsaw, Poland
Eiichiro Nagata,
Tokai University Isehara Hospital, Japan
Xiaohuan Sun,
Drexel University, United States

*CORRESPONDENCE
Guo-Yuan Yang
✉ gyyang0626@163.com
Xinkai Qu
✉ qxkchest@126.com
Wenshi Wei
✉ wenshiwei1999@163.com

RECEIVED 26 February 2025
ACCEPTED 07 July 2025
PUBLISHED 16 July 2025

CITATION
Wang L-P, Liu C, Ma Y, Yan A, Yang G-Y, Qu X and Wei W (2025) Oligodendrocyte precursor cell transplantation attenuates inflammation after ischemic stroke in mice. *Front. Neurol.* 16:1583982. doi: 10.3389/fneur.2025.1583982

Oligodendrocyte precursor cell transplantation attenuates inflammation after ischemic stroke in mice

Li-Ping Wang[1,2], Chang Liu[3], Yuanyuan Ma[4], Aijuan Yan[1], Guo-Yuan Yang[3]*, Xinkai Qu[2]* and Wenshi Wei[1]*

[1]Department of Neurology, Huadong Hospital, Fudan University, Shanghai, China, [2]Department of Geriatric Medicine, Huadong Hospital, Fudan University, Shanghai, China, [3]School of Biomedical Engineering and Med-X Research Institute, Shanghai Jiao Tong University, Shanghai, China, [4]Department of Neurology, Zhongshan Hospital, Fudan University, Shanghai, China

Background: Disruption of blood–brain barrier and neuroinflammation are critical pathological features in the acute phase of ischemic stroke. This study investigates whether oligodendrocyte precursor cell transplantation can downregulate inflammation to attenuate blood–brain barrier disruption following ischemic brain injury.

Methods: Adult male Institute of Cancer Research mice (n = 60) underwent transient middle cerebral artery occlusion. Post ischemic assault, these mice received a stereotactic injection of oligodendrocyte precursor cells (6×10^5). Neurobehavioral outcomes, infarct volume, inflammatory cytokines, myeloperoxidase, and tight junction protein levels were measured following ischemia.

Results: Oligodendrocyte precursor cell transplantation reduced infarct volume, alleviated anxiety and depression, and promoted neurological recovery after ischemic stroke. Compared to the control group, oligodendrocyte precursor cell treated mice exhibited reduced levels of inflammatory cytokines IL-1β, IL-6, and TNF-α, reduced neutrophil infiltration, and diminished loss of tight junction protein. Oligodendrocyte precursor cells alleviated inflammation by increasing β-catenin expression. The administration of β-catenin inhibitor blocked the beneficial effects of oligodendrocyte precursor cell transplantation on neuroinflammation and blood–brain barrier permeability.

Conclusion: This study demonstrates that oligodendrocyte precursor cell transplantation attenuates neuroinflammation and protectes blood–brain barrier in the acute phase of ischemic stroke. Our findings indicate that oligodendrocyte precursor cell transplantation is a promising therapeutic approach for ischemic stroke.

KEYWORDS

blood–brain barrier, inflammation, ischemic stroke, oligodendrocyte precursor cell, transplantation

Introduction

Ischemic stroke is one of the leading causes of death and disability in the world (1, 2). Currently, thrombolysis and endovascular interventional therapy are the most effective treatment strategies in the early stage after ischemic stroke, but the time windows for both treatments are limited (3, 4). Many pathological processes, including blood–brain barrier (BBB) dysfunction, inflammation, excitotoxicity, oxidative stress, neuronal loss, and glial activation, are involved in stroke progression (5).

BBB disruption and neuroinflammation are critical pathological features in the acute phase of cerebral ischemia (6, 7). BBB is comprised of brain endothelial cells with their tight junctions, the basement membrane, pericytes, and astrocyte end-feet (8). Brain endothelial cells express high levels of tight junction proteins, which determine BBB integrity (8, 9). After ischemic stroke, inflammatory responses at the blood-endothelial interface of brain capillaries are the basis of ischemic tissue damage (10). Post-ischemic inflammation is associated with acute BBB disruption, vasogenic edema, hemorrhagic transformation, and worse neurological outcomes in animals and humans (11). The proinflammatory signals from immune mediators activate resident cells and influence infiltration of inflammatory cells into the ischemic region, exacerbating brain damage (12). Neutrophils migrate through the endothelial vessel wall and are attracted towards the ischemic area (13). Neutrophils cause secondary injury by releasing proinflammatory factors, reactive oxygen species (ROS), proteases, and matrix metalloproteinases (MMPs) (12). Therefore, targeting neuroinflammation may be a promising therapeutic approach for the treatment of ischemic stroke.

Oligodendrocyte precursor cells (OPCs) are derived from the ventricular zone in the embryo and migrated widely through the central nervous system (14). OPCs could maintain BBB integrity during development and mediate the remyelination process after brain injury (15). OPC transplantation showed a promising potential for ischemic stroke therapy (16–18). In our previous study, OPC transplantation could attenuate tight junction disruption in brain endothelial cells in the acute phase of ischemic stroke and promote angiogenesis and remyelination in the chronic phase of ischemic stroke via activating the Wnt/β-catenin pathway. As neuroinflammation is closely related to BBB integrity, we hypothesize that the protective role of OPC transplantation on BBB is achieved through attenuating neuroinflammation in ischemic stroke.

In this study, we use a mouse model of transient middle cerebral artery occlusion (tMCAO) to explore whether OPC transplantation downregulates inflammation to attenuate BBB disruption after ischemic brain injury.

Materials and methods

Experimental protocol

Animal procedures and protocols were approved by the Institutional Animal Care and Use Committee (IACUC) of Fudan University, Shanghai, China. Animal studies were reported according to ARRIVE 2.0 guidelines. Adult male Institute of Cancer Research mice ($n = 60$) weighing 28–30 g (JSJ, Shanghai, China) were used in the study. Animals were housed with free access to water and food. Mice were randomly divided into four groups: sham group, phosphate buffered saline (PBS) treated group, OPC-treated group, and OPC-treated plus β-catenin inhibitor (XAV-939) group, $n = 10$–16 per group.

OPC isolation and identification

The brain cortex was dissected from P1 Sprague–Dawley rat pups as described (19, 20). Brain tissue was dissociated into a single-cell suspension and was filtered with a 70-μm filter. Then cells were seeded on poly-d-lysine (PDL, Sigma, St. Louis, MO) coated culture flasks in DMEM (Gibco, Carlsbad, CA) with 10% fetal calf serum (Gibco). Eight days later, the microglia were separated from glia cell mixtures after 30 min of culture by a 220-rpm shake and then OPCs were collected by 20 h of culture by a 200-rpm shake. Collected cells were injected into the mouse or seeded on a PDL-coated culture dish in Neurobasal-A (Gibco) containing 2% B27 (Gibco), 10 ng/mL PDGF-AA (Gibco), 10 ng/mL bFGF (Peprotech, Rocky Hill, NJ) and 2 mmoL/L glutamine (Gibco).

For identification, OPCs were incubated with primary antibodies against NG2 (1:200, Millipore, Bedford, MA), GAFP (1:200, Millipore), MBP (1:200, Abcam, Cambridge, United Kingdom), NeuN (1:200, Millipore), and Iba-1 (1:200, WAKO, Osaka, Japan) at 4°C overnight. Then cells were incubated with the fluorescence conjugated second antibodies at 37°C for 1 h.

Establishing a mouse model of tMCAO

The mouse model of tMCAO was performed as described previously (21). Mice were anesthetized with 1.5% isoflurane (RWD Life Science, Shenzhen, China) and placed supine. After the isolation of the left common carotid artery, external carotid artery, and internal carotid artery, the origin of the middle cerebral artery was occluded by a silicone-coated 6-0 suture (Covidien, Mansfield, MA). The suture was withdrawn after 90 min of tMCAO. The success of occlusion was assessed by the laser Doppler flowmetry (Moor Instruments, Devon, United Kingdom) with a decrease of cerebral blood flow at least 80% of the baseline. Sham mice were conducted in the same procedure except for the insertion of suture.

Transplantation of OPCs

OPCs were injected at 24 h after tMCAO (Figure 1E). Before transplantation, OPCs were labeled with carboxyfluorescein diacetate-succinimidyl ester (CFDA-SE, Beyotime, Shanghai, China) for tracking. The mice after tMCAO were anesthetized and received stereotaxic transplantation. A microsurgical drill made a small skull hole 2 mm lateral to the bregma. An amount of 6×10^5 OPCs was suspected in 5 μL PBS and slowly injected into the left striatum at 2 mm lateral to the bregma and 3 mm under the dura (AP = 0 mm, ML = 2 mm, DV = 3 mm) at a rate of 1 μL/min by the 10 μL Hamilton syringe (Hamilton, Bonaduz, Switzerland) (17, 18, 22, 23). The same amount of PBS was injected as control (16).

Abbreviations: BBB, Blood–brain barrier; tMCAO, Transient middle cerebral artery occlusion; MMP, Matrix metalloproteinase; mNSS, Modified neurological severity score; OPCs, Oligodendrocyte precursor cells.

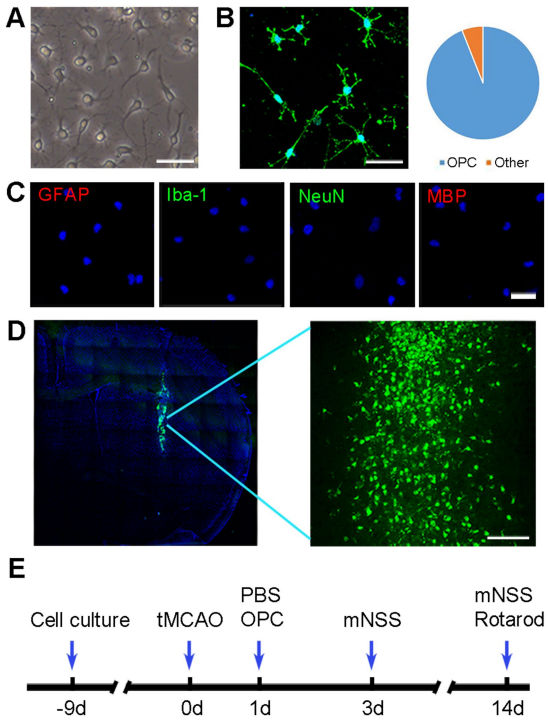

FIGURE 1
OPC identification and transplantation. **(A)** Morphology of cultured cells under phase-contrast microscopy. Scale bar = 50 μm. **(B)** Representative image of NG2 in cultured cells. Scale bar = 50 μm. **(C)** Immunofluorescence staining showed that cultured cells were negative for GFAP, Iba-1, NeuN, and MBP. Scale bar = 50 μm. **(D)** Green fluorescent OPCs (CFDA-SE stained) were located in the ischemic hemisphere. Scale bar = 100 μm. **(E)** Diagram of experimental design.

Administration of drugs

The mice were injected i.p. daily with cyclosporine A (5 mg/kg, Sigma) for immunosuppression after cell transplantation. The PBS group and sham group were administered cyclosporine A as well. For the OPC plus XAV-939 group, the β-catenin inhibitor XAV-939 (40 mg/kg, MCE, Monmouth Junction, NJ) was injected intraperitoneally once a day (16, 24).

Neurobehavioral assessment

The modified neurological severity score (mNSS) was performed by an investigator who was blinded to the experimental treatment to evaluate the neurological function at 3 and 14 days after tMCAO. The mNSS ranged from 0 to 14 and included motor, sensory, balance, and reflex tests (25).

Rotarod test was performed at 7 and 14 days after tMCAO to test the motor coordination and balance. Briefly, Mice were trained on a rotating rod at 20 rpm for 3 consecutive days before tMCAO. Mice were placed on the rod for adaption, after which the rod was continuously accelerated to 40 rpm. The mice were monitored, and the time mice stayed on the rod (latency to fall) was recorded (17).

The novel object recognition test is used to test cognition behavior. The apparatus is a box 45 cm × 45 cm× 45 cm in size. The first 3 days are for adaption. Each mouse was placed in the apparatus and allowed to explore freely for 10 min. On the inspection day, two objects of the same shape, size, and color are placed on the bottom of the box. Each mouse is placed inside the instrument and allowed to explore freely for 10 min. One hour later, one of the objects is replaced by a novel object with different shapes and colors. Each mouse is put back into the apparatus and allowed to explore freely for 5 min. The novel object preference index is time spent exploring novel objects/total time to explore novel and familiar objects (26, 27).

The tail suspension test is a test for the antidepressant activity (17). In the test, the tail of the mouse is suspended on a lever with tape, and a camera is used to record its behavior. The mouse struggles to escape for a period of time and then adopt a posture of immobility. After 2 min of induction time, the time for each mouse to keep immobility and the total time are recorded within left 4 min. Depression can decrease the frequency and duration of locomotor activity.

The elevated plus maze test is used to evaluate anxiety-related behaviors which is based on the test animals' aversion to open spaces when feeling anxious (20). The equipment consists of a "+"-shaped maze elevated above the ground with 2 opposite closed arms, 2 opposite open arms, and a central area. Choice behavior was observed for 10 min. The number of entries to the open arms were counted and the time in the open arms were recorded by a video camera installed above the maze.

Brain infarct volume measurement

Mice were sacrificed at 3 days after tMCAO, and brains were cut into a series of 20 μm thick coronal sections. The cresyl violet staining (Sigma) was performed to measure the brain infarct volume. Infarct volume was calculated using ImageJ software (National Institutes of Health, Bethesda, MD) as described previously (5).

Immunofluorescence staining

Brain slices were fixed with methanol at 4°C for 10 min and blocked with diluted donkey serum (Jackson ImmunoResearch, West Grove, PA) for 60 min at room temperature. Slides were incubated with primary antibodies of MPO (1:200, R&D system, Minneapolis, MN), Iba-1 (1:200, NB100-1028, Novusbio, CO), CD31 (1:200, R&D system), occludin (1:200, Invitrogen, Carlsbad, CA), ZO-1 (1:100, Invitrogen) overnight at 4°C. After rinsing three times with PBS, brain slices were incubated with the fluorescence conjugated second antibodies for 1 h at room temperature. Immunofluorescence photos were collected by a confocal microscope (Leica, Solms, Germany). We measured the vessel length and gap by ImageJ software (National Institutes of Health). Gap length was presented as a percentage (%) of gap length in the whole vessel (16).

Real-time PCR analysis

Regional brain tissues from the infarct hemisphere of ischemic mice, including cortex and striatum, were isolated for real-time PCR. The real-time PCR assay was performed as described previously (28). The two-stage RT-PCR amplification parameters were 95°C for 30 s followed by 40 cycles of 95°C for 5 s and 60°C for 30 s. The

mRNA expression level was normalized to reference gene GAPDH and displayed as relative expression of mRNA by $2^{-\Delta\Delta Ct}$ method.

Western blot analysis

Western blot was performed as described previously (17, 29). The membranes were blocked with 5% skim milk and incubated with primary antibodies against β-catenin (1:500, Abcam) and GAPDH (1:1000, Abcam) overnight at 4°C. After washing with TBST buffer, the membranes were incubated with HRP-conjugated secondary antibody.

Statistical analysis

The sample size was determined according to our previous publications for similar outcomes (17, 20). For immunohistochical images, we adopted the manual fluorescence positive cell counting or software to measure the length of linear expression (21, 22). Analysis was performed by Prizm Graphpad 9. Multiple comparisons were analyzed using one-way ANOVA followed by Tukey's post-hoc test for normally distributed data. Comparisons between the two groups were carried out using Student's *t*-test. Data were expressed as mean ± SD. A probability value of less than 0.05 was considered significant.

Results

OPC identification and transplantation

Cultured OPCs showed a bipolar or multipolar morphology under phase contrast microscope (Figure 1A). The cultured OPCs were identified by immunofluorescence 10 days after isolating from P1 rat brains. Immunofluorescent staining showed that the percentage of $NG2^+$ cells was 94% (Figure 1B). Very few cells expressed GFAP, Iba-1, NeuN or MBP (Figure 1C). Transplanted OPCs were labeled with CFDA-SE for *in vivo* cell tracking. The results demonstrated that a considerable number of transplanted OPCs could survive at 3 days after tMCAO (Figure 1D).

OPC transplantation reduced infarct volume, alleviated anxiety and depression, and improved neurobehavioral recovery after tMCAO

The brain infarct volume was evaluated using cresyl violet staining. Results showed that infarct volume was significantly decreased in the OPC-treated mice compared to the control (PBS) mice at 3 days after tMCAO (Figures 2A,B, $p < 0.05$).

The novel object recognition test was performed to detect the memory and cognition. OPC transplantation increased the new object exploring time at 14 days after tMCAO which indicating better memory and cognitive abilities (Figure 2C, $p < 0.05$).

The mNSS and rotarod test were performed to evaluate the neurological function. OPC transplantation significantly decreased neurological scores at 3 and 14 days after tMCAO (Figure 2D, $p < 0.05$). The rotarod test demonstrated that the time staying on the rotarod was prolonged in OPC-treated mice compared to control mice at 7 and 14 days after tMCAO (Figure 2E, $p < 0.05$). The OPC-treated group attenuated the neurobehavioral deficiency compared to the control group.

The tail suspension test was performed to assess the depression-like behavior. The induction time and freezing time indicated depression level. The decrease of the induction time or the increase of the freezing time represented that the mice tended to be more depressed. Our test showed that there was no difference in the induction time. The freezing time significantly decreased in OPC-treated mice compared to the PBS-treated mice (Figure 2F, $p < 0.05$). This result indicated that OPC transplantation could alleviate post-stroke depression.

The plus maze test was performed to estimate the anxiety behavior of mice. The number of entries to the open zone and the time in the open zone of OPC-treated mice were increased compared to the control (Figure 2G, $p < 0.05$). This indicated that OPC transplantation could attenuate anxious behavior.

OPC transplantation downregulated the expression of inflammatory factors after tMCAO

Inflammatory factors IL-1β, IL-6, and TNF-α were upregulated at 3 days after tMCAO. However, OPC transplantation reduced IL-1β, IL-6, and TNF-α expression compared to the control group (Figure 3A, $p < 0.05$). Besides, OPC transplantation downregulated the NF-κB pathway related to inflammatory factors (Figure 3A, $p < 0.05$).

OPC transplantation alleviated the leukocyte infiltration and increase of microglia after tMCAO

Neutrophils are the primary inflammatory cell type that responds to the inflammatory stimulus following ischemic stroke (30). To determine whether OPC transplantation alleviated leukocyte infiltration after tMCAO, we conducted immunostaining to examine the number of MPO^+ cells. We found that OPC transplantation reduced the number of MPO^+ cells in the ipsilateral brain at 3 days after tMCAO (Figure 3B, $p < 0.05$). It was noted that neutrophil infiltration was greatly reduced in the OPC-transplanted mice after tMCAO.

Microglia are resident immune cells in the central nervous system. To detect whether OPC transplantation affected the number of microglia, we conducted immunostaining to examine the number of $Iba\text{-}1^+$ cells. We found that OPC transplantation reduced the number of $Iba\text{-}1^+$ cells in the ipsilateral brain at 3 days after tMCAO (Figure 3C, $p < 0.05$). So, OPC transplantation alleviated the increase of microglia after tMCAO.

OPC transplantation attenuated BBB disruption after tMCAO

Occludin and ZO-1 expression presented a gap in the endothelial cell margin of the cerebral microvessel after ischemic injury. CD31/

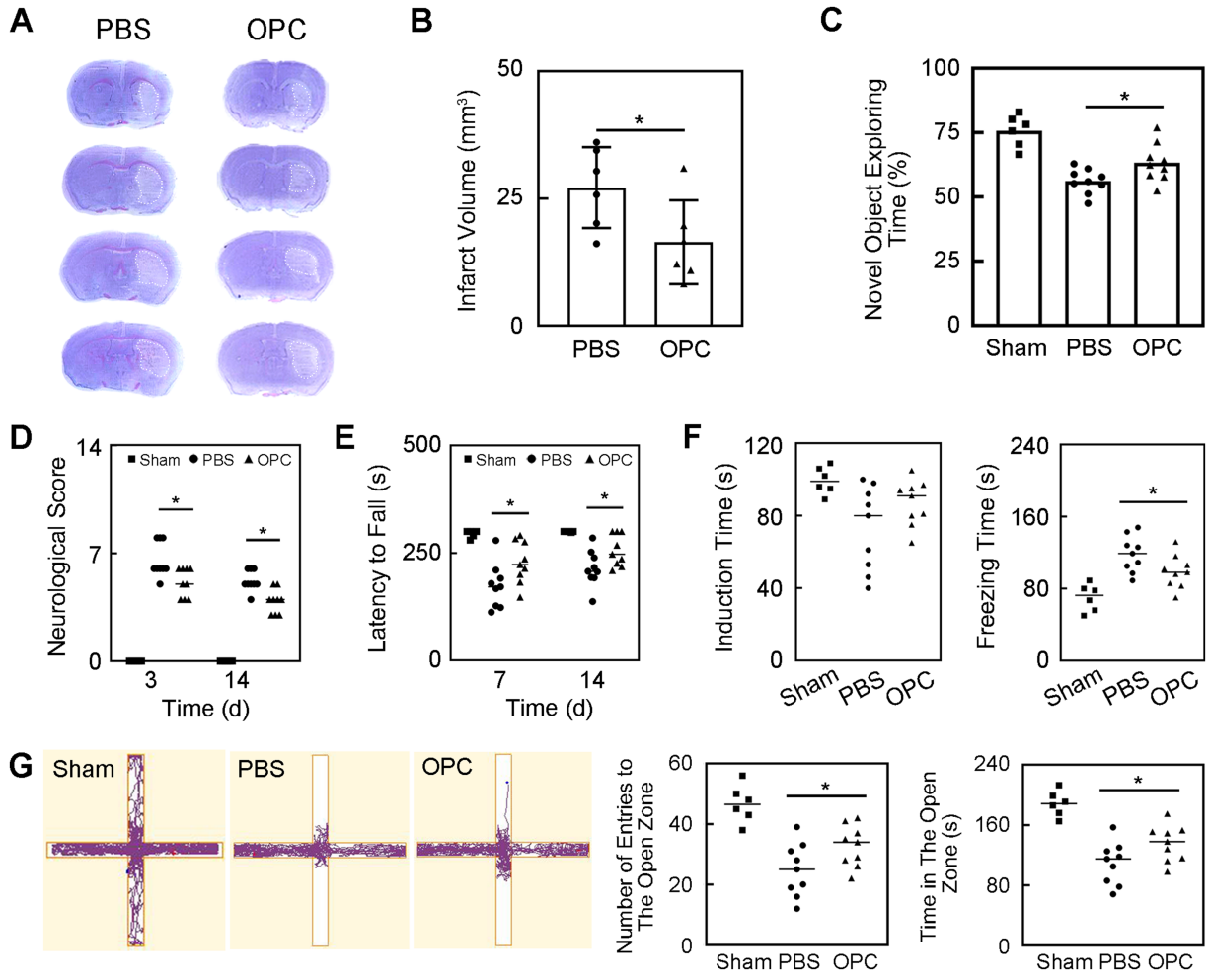

FIGURE 2
OPC transplantation reduced infarct volume and improved neurobehavioral recovery after tMCAO. **(A)** Cresyl violet staining showed the infarction after tMCAO in PBS and OPC groups. **(B)** Bar graph indicated that OPC transplantation reduced infarct volume. $N = 6$ per group. **(C)** Bar graph of novel object exploring time in the novel object recognition test. $N = 6–9$ per group. **(D)** Bar graph of neurological scores. $N = 6–9$ per group. **(E)** Bar graph of latency to fall. $N = 6–9$ per group. **(F)** Bar graphs of induction time and freezing time in the tail suspension test. $N = 6–9$ per group. **(G)** The track plot and bar graphs of number of entries to the open zone and time in the open zone in the plus maze test. $N = 6–9$ per group. Data are mean ± SD, $^*p < 0.05$.

occludin double staining results showed that OPC transplantation alleviated the disruption of occludin (Figure 4A, $p < 0.001$). CD31/ZO-1 double staining results suggested that OPC transplantation alleviated the disruption of ZO-1 (Figure 4B, $p < 0.05$). OPC transplantation significantly reduced gap formation after tMCAO.

Inhibition of β-catenin aggravated inflammation and BBB disruption

OPC transplantation enhanced β-catenin expression in the ipsilateral hemisphere compared to the control (Figure 5, $p < 0.05$). As we supposed that the downregulated inflammation caused by OPC transplantation was related to the enhanced β-catenin expression, we used XAV-939 to inhibit the β-catenin. The β-catenin inhibitor XAV-939 administration could suppress the β-catenin expression which was enhanced by OPC transplantation (Figure 5, $p < 0.05$). To further examine whether β-catenin was involved in the beneficial role of OPCs after tMCAO, β-catenin inhibitor XAV-939 was injected in OPC-treated ischemic mice. We found that XAV-939 could upregulate the expression of inflammatory factors and increase neutrophil infiltration after tMCAO (Figures 6A,B, $p < 0.05$). Besides, the inhibition of β-catenin downregulated the NF-κB pathway (Figure 6A, $p < 0.05$). The endothelial gap formation was increased after XAV-939 administration (Figure 6C, $p < 0.05$). XAV-939 treatment reversed the protective role of OPC transplantation on the integrity of BBB.

Discussion

Our study demonstrated that OPC transplantation reduced inflammation, attenuated tight junction disruption of BBB, and improved neurobehavioral outcomes in ischemic mice. The Wnt/β-catenin pathway activated by OPC treatment might contribute to the downregulation of neuroinflammation after ischemic stroke.

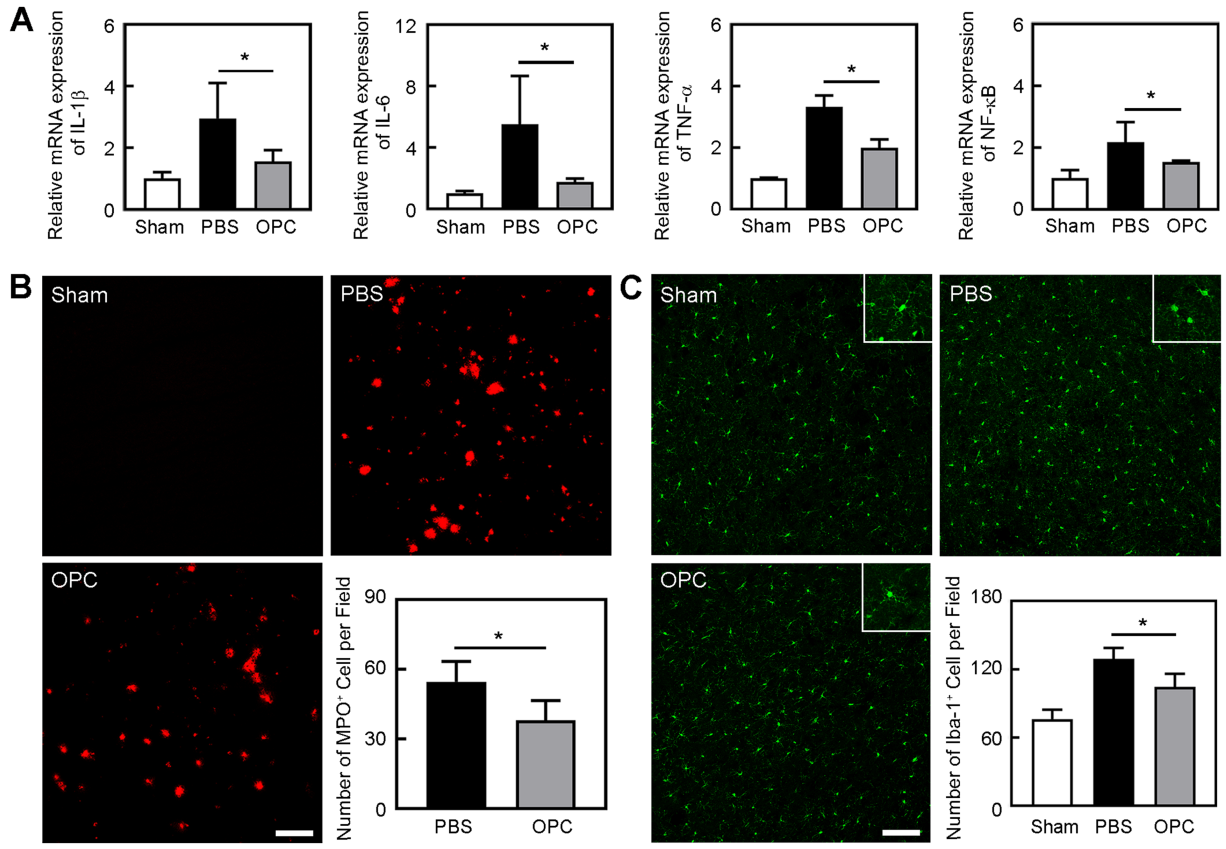

FIGURE 3
OPC transplantation reduced inflammation after tMCAO. **(A)** Bar graphs showed the mRNA level of IL-1β, IL-6, TNF-α, and NF-κB in the sham, PBS, and OPC groups at 3 days after tMCAO. *N* = 4 per group. **(B)** Representative images of MPO staining in the peri-infarct area at 3 days after tMCAO. Bar graph showed the quantification of MPO$^+$ cells. Scale bar = 100 μm. *N* = 6 per group. **(C)** Representative images of Iba-1 staining in the peri-infarct area at 3 days after tMCAO. Bar graph showed the quantification of Iba-1$^+$ cells. Scale bar = 100 μm. *N* = 6 per group. Data are mean ± SD, **p* < 0.05.

Inflammation could exacerbate ischemic tissue damage and worsen clinical outcome in patients with stroke (31). The intense neuroinflammation occurring during the acute phase of stroke is associated with BBB breakdown, neuronal injury, and worse neurological outcomes. Inflammation-driven injury mechanisms in stroke include oxidative stress, increased MMPs production, microglial activation, and infiltration of peripheral immune cells into the ischemic tissue (32). Many types of stem cells can potentially treat ischemic stroke (33). Mesenchymal stem cell therapy could reduce inflammation and attenuate BBB disruption in mice after ischemia (22). Our data showed that OPC transplantation significantly attenuated inflammation after ischemia. Inflammatory cytokines IL-1β, IL-6, and TNF-α and neutrophil infiltration were reduced in OPC-treated mice compared to the control group. The suppression of inflammation of OPC transplantation ameliorated neurobehavioral deficiency.

Inflammatory interactions at the blood-endothelial interface include cytokines, chemokines, adhesion molecules, and white blood cells, which are crucial for the pathogenesis of cerebral infarction (34). Proinflammatory intracellular signaling cascades and transcription factors, for example, NF-κB, ROS, MMPs, and the release of proinflammatory cytokines, especially IL-1β, IL-6, and TNF-α, are associated with BBB dysfunction after stroke (32). Our results showed that OPC transplantation reduced tight junction protein degradation after ischemia. The protective effect on BBB of OPC transplantation could be through the downregulation of inflammation.

The Wnt/β-catenin pathway is involved in cellular proliferation, survival, differentiation, migration, angiogenesis, and vascular maturation (35). Research indicated that enhancing cerebrovascular Wnt/β-catenin activity would offer protection against BBB permeability and neuroinflammation in acute infection (36). Previous studies reported that reactivation of Wnt/β-catenin signaling in vessels during experimental autoimmune encephalomyelitis/multiple sclerosis partially restored functional BBB integrity and limited immune cell infiltration into the brain (37). In our study, OPC transplantation increased the level of β-catenin and downregulated the mRNA level of NF-κB. Furthermore, the inhibition of β-catenin reversed the inflammation inhibition by OPC transplantation and aggravated tight junction protein disruption.

Wnt/β-catenin signaling exerts the anti-inflammatory function partially due to repressing the NF-κB pathway (38). Previous research suggested the negative regulation of NF-κB-mediated inflammatory responses by β-catenin in intestinal epithelial cells (39). Wnt/β-catenin pathway components modulate inflammatory and immune responses via the interaction with NF-κB (40). Our results demonstrated that the level of NF-κB had a negative correlation with that of β-catenin. Therefore, we supposed that OPC transplantation attenuated

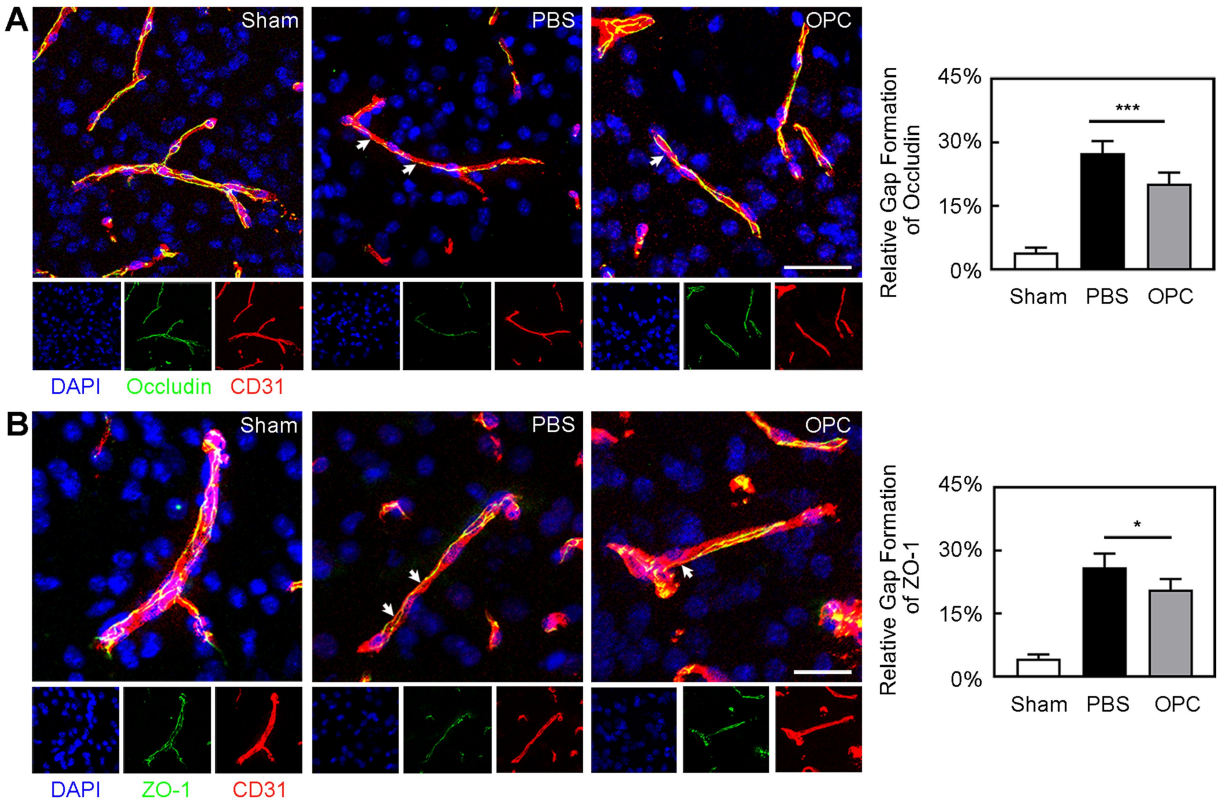

FIGURE 4
OPC transplantation attenuated the breakage of occludin and ZO-1 after tMCAO. **(A)** Three-dimension reconstruction confocal microscopy images of occludin (green), endothelial marker CD31 (red) and DAPI (blue) at 3 days after tMCAO in three groups. The white arrows indicated the gap formation of occludin. Bar graph showed the quantification of gap formation of occludin. Scale bar = 50 μm. **(B)** Three-dimension reconstruction confocal microscopy images of ZO-1 (green), CD31 (red), and DAPI (blue) at 3 days after tMCAO in three groups. The white arrows indicated the gap formation of ZO-1. Bar graph showed the quantification of gap formation of ZO-1. Scale bar = 25 μm. Data are mean ± SD, $N = 6$ per group, $^{*}p < 0.05$ and $^{***}p < 0.001$.

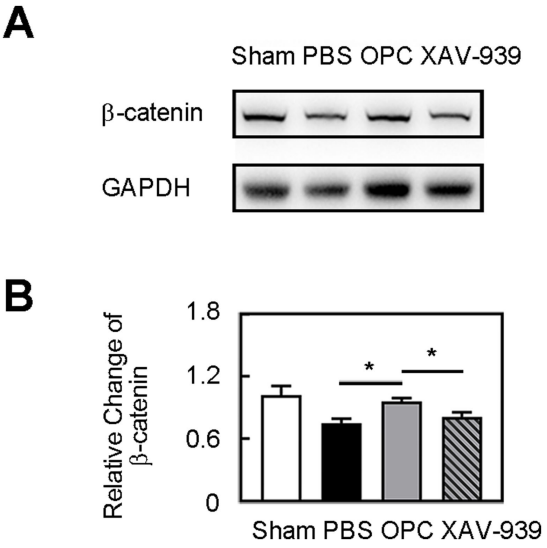

FIGURE 5
OPC transplantation increased β-catenin level. **(A)** Western blot of β-catenin expression in sham, PBS, OPC, and OPC plus XAV-939 groups at 3 days after tMCAO. **(B)** Bar graph of relative expression of β-catenin. $N = 4$ per group. Data are mean ± SD, $^{*}p < 0.05$.

inflammation by β-catenin and the downstream pathway might be NF-κB.

In our previous study, some transplanted OPCs differentiate into oligodendrocyte which expressed MBP around the myelin at 28 days after tMCAO (17). We found OPCs could secret Wnt7a which activated endothelial cells (16). Besides Wnt7a, OPCs could secret trophic factors, providing trophic signals to neighboring cells. Based on other basic researches on stem cell transplantation, like mesenchymal stem cell and endothelial progenitor cell, we tended to believe that factors released by OPCs were crucial for the beneficial effects of OPC transplantation following ischemic stroke (21, 33, 41).

We previously proved that OPC transplantation's chronic effects on angiogenesis and remyelination after ischemic stroke. OPC transplantation reduced BBB permeability which indicated the better vascular maturity (17). But we did not focus on the chronic effects on the tight junction proteins in the endothelial cells. The long-term impact needs to be assessed. We ever injected OPCs 7 days after tMCAO and found improved behavior recovery and reduced brain atrophy volume at 28 days after OPC transplantation (18). The delayed OPC transplantation could enhance endogenous oligodendrogenesis, neurite growth, and synaptogenesis.

There were some limitations in our study. Conditional knock-out mice of β-catenin are needed to show a larger certainty of the underlying

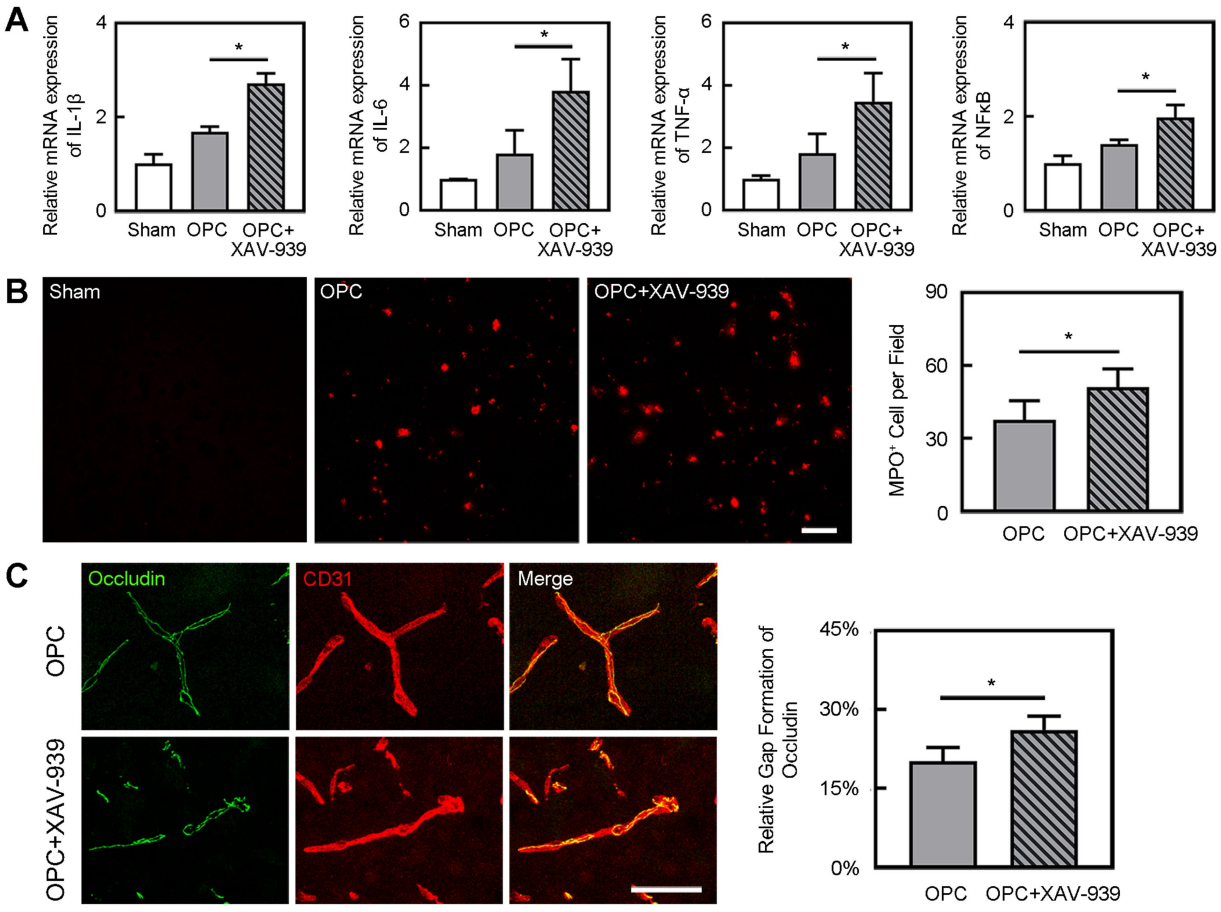

FIGURE 6
Inhibition of β-catenin aggravated inflammation and BBB disruption. **(A)** Bar graphs showed the mRNA level of IL-1β, IL-6, TNF-α, and NF-κB in the sham, OPC, and OPC plus XAV-939 groups at 3 days after tMCAO. *N* = 4 per group. **(B)** Representative images of MPO staining in the peri-infarct area at 3 days after tMCAO in sham, OPC, and OPC plus XAV-939 groups. Bar graph showed the quantification of MPO+ cells. Scale bar = 100 μm. *N* = 6 per group. **(C)** Three-dimension reconstruction confocal microscopy images of occludin (green) and CD31 (red) at 3 days after tMCAO in OPC and OPC plus XAV-939 groups. Bar graph showed the quantification of gap formation of occludin. Scale bar = 50 μm. *N* = 6 per group. Data are mean ± SD, $^*p < 0.05$.

mechanism. The β-catenin activation in different type of cells in the central nervous system, for example, microglial and astrocyte, should be further explored. A previous study showed that activation of Wnt/β-catenin signaling attenuated ICAM-1/VCAM-1-mediated adhesion of both macrophages and neutrophils to alveolar epithelial cells (42). So other targets need to be studied in future.

In this study, we demonstrated that OPC transplantation attenuated inflammation, which protected BBB, decreased brain infarct volume and improved neurological outcomes after ischemic stroke in mice. This anti-inflammatory function of OPC transplantation might be via activating β-catenin and then affecting NF-κB. OPC transplantation is a promising approach for the ischemic stroke therapy.

Data availability statement

The raw data supporting the conclusions of this article will be made available by the authors, without undue reservation.

Ethics statement

The animal study was approved by Institutional Animal Care and Use Committee (IACUC) of Fudan University. The study was conducted in accordance with the local legislation and institutional requirements.

Author contributions

L-PW: Conceptualization, Funding acquisition, Project administration, Writing – original draft. CL: Investigation, Methodology, Writing – original draft. YM: Data curation, Formal analysis, Writing – original draft. AY: Methodology, Project administration, Writing – original draft. G-YY: Conceptualization, Writing – review & editing. XQ: Supervision, Writing – review & editing. WW: Formal analysis, Writing – review & editing.

Funding

The author(s) declare that financial support was received for the research and/or publication of this article. This study was supported by grant from the National Natural Science Foundation of China (82001228, L-PW).

Conflict of interest

The authors declare that the research was conducted in the absence of any commercial or financial relationships that could be construed as a potential conflict of interest.

Generative AI statement

The authors declare that no Gen AI was used in the creation of this manuscript.

Publisher's note

References

1. Benjamin EJ, Blaha MJ, Chiuve SE, Cushman M, Das SR, Deo R, et al. Heart disease and stroke statistics-2017 update: a report from the American Heart Association. *Circulation*. (2017) 135:e146–603. doi: 10.1161/CIR.0000000000000485

2. Ma Y, Liu Z, Jiang L, Wang L, Li Y, Liu Y, et al. Endothelial progenitor cell transplantation attenuates synaptic loss associated with enhancing complement receptor 3-dependent microglial/macrophage phagocytosis in ischemic mice. *J Cereb Blood Flow Metab*. (2023) 43:379–92. doi: 10.1177/0271678X221135841

3. Li S, Xing X, Wang L, Xu J, Ren C, Li Y, et al. Remote ischemic conditioning reduces adverse events in patients with acute ischemic stroke complicating acute myocardial infarction: a randomized controlled trial. *Crit Care*. (2024) 28:5. doi: 10.1186/s13054-023-04786-y

4. Luo Y, Shen H, Liu HS, Yu SJ, Reiner DJ, Harvey BK, et al. CART peptide induces neuroregeneration in stroke rats. *J Cereb Blood Flow Metab*. (2013) 33:300–10. doi: 10.1038/jcbfm.2012.172

5. Zhang Q, Liu C, Shi R, Zhou S, Shan H, Deng L, et al. Blocking C3d$^+$/GFAP$^+$ A1 astrocyte conversion with semaglutide attenuates blood-brain barrier disruption in mice after ischemic stroke. *Aging Dis*. (2022) 13:943–59. doi: 10.14336/AD.2021.1029

6. Chang J, Mancuso MR, Maier C, Liang X, Yuki K, Yang L, et al. Gpr124 is essential for blood-brain barrier integrity in central nervous system disease. *Nat Med*. (2017) 23:450–60. doi: 10.1038/nm.4309

7. Pan JJ, Qi L, Wang L, Liu C, Song Y, Mamtilahun M, et al. M2 microglial extracellular vesicles attenuated blood-brain barrier disruption via MiR-23a-5p in cerebral ischemic mice. *Aging Dis*. (2024) 15:1344–56. doi: 10.14336/AD.2023.0714

8. Obermeier B, Daneman R, Ransohoff RM. Development, maintenance and disruption of the blood-brain barrier. *Nat Med*. (2013) 19:1584–96. doi: 10.1038/nm.3407

9. Lv J, Hu W, Yang Z, Li T, Jiang S, Ma Z, et al. Focusing on claudin-5: a promising candidate in the regulation of BBB to treat ischemic stroke. *Prog Neurobiol*. (2017) 161:79–96. doi: 10.1016/j.pneurobio.2017.12.001

10. Zhu H, Hu S, Li Y, Sun Y, Xiong X, Hu X, et al. Interleukins and ischemic stroke. *Front Immunol*. (2022) 13:828447. doi: 10.3389/fimmu.2022.828447

11. Candelario-Jalil E, Dijkhuizen RM, Magnus T. Neuroinflammation, stroke, blood-brain barrier dysfunction, and imaging modalities. *Stroke*. (2022) 53:1473–86. doi: 10.1161/STROKEAHA.122.036946

12. Jayaraj RL, Azimullah S, Beiram R, Jalal FY, Rosenberg GA. Neuroinflammation: friend and foe for ischemic stroke. *J Neuroinflammation*. (2019) 16:142. doi: 10.1186/s12974-019-1516-2

13. Wang Y, Jin H, Wang Y, Yao Y, Yang C, Meng J, et al. Sult2b1 deficiency exacerbates ischemic stroke by promoting pro-inflammatory macrophage polarization in mice. *Theranostics*. (2021) 11:10074–90. doi: 10.7150/thno.61646

14. Tsai HH, Niu J, Munji R, Davalos D, Chang J, Zhang H, et al. Oligodendrocyte precursors migrate along vasculature in the developing nervous system. *Science*. (2016) 351:379–84. doi: 10.1126/science.aad3839

15. Watzlawik J, Warrington AE, Rodriguez M. Importance of oligodendrocyte protection, BBB breakdown and inflammation for remyelination. *Expert Rev Neurother*. (2010) 10:441–57. doi: 10.1586/ern.10.13

16. Wang L, Geng J, Qu M, Yuan F, Wang Y, Pan J, et al. Oligodendrocyte precursor cells transplantation protects blood-brain barrier in a mouse model of brain ischemia via Wnt/beta-catenin signaling. *Cell Death Dis*. (2020) 11:9. doi: 10.1038/s41419-019-2206-9

17. Wang LP, Pan J, Li Y, Geng J, Liu C, Zhang LY, et al. Oligodendrocyte precursor cell transplantation promotes angiogenesis and remyelination via Wnt/beta-catenin pathway in a mouse model of middle cerebral artery occlusion. *J Cereb Blood Flow Metab*. (2022) 42:757–70. doi: 10.1177/0271678X211065391

18. Li W, He T, Shi R, Song Y, Wang L, Zhang Z, et al. Oligodendrocyte precursor cells transplantation improves stroke recovery via oligodendrogenesis, neurite growth and synaptogenesis. *Aging Dis*. (2021) 12:2096–112. doi: 10.14336/AD.2021.0416

19. Chen Y, Balasubramaniyan V, Peng J, Hurlock EC, Tallquist M, Li J, et al. Isolation and culture of rat and mouse oligodendrocyte precursor cells. *Nat Protoc*. (2007) 2:1044–51. doi: 10.1038/nprot.2007.149

20. Wang LP, Geng J, Liu C, Wang Y, Zhang Z, Yang GY. Diabetes mellitus-related neurobehavioral deficits in mice are associated with oligodendrocyte precursor cell dysfunction. *Front Aging Neurosci*. (2022) 14:846739. doi: 10.3389/fnagi.2022.846739

21. Geng J, Wang L, Qu M, Song Y, Lin X, Chen Y, et al. Endothelial progenitor cells transplantation attenuated blood-brain barrier damage after ischemia in diabetic mice via HIF-1α. *Stem Cell Res Ther*. (2017) 8:163. doi: 10.1186/s13287-017-0605-3

22. Cheng Z, Wang L, Qu M, Liang H, Li W, Li Y, et al. Mesenchymal stem cells attenuate blood-brain barrier leakage after cerebral ischemia in mice. *J Neuroinflammation*. (2018) 15:135. doi: 10.1186/s12974-018-1153-1

23. Ma Y, Jiang L, Wang L, Li Y, Liu Y, Lu W, et al. Endothelial progenitor cell transplantation alleviated ischemic brain injury via inhibiting C3/C3aR pathway in mice. *J Cereb Blood Flow Metab*. (2020) 40:2374–86. doi: 10.1177/0271678X19892777

24. Yuen TJ, Silbereis JC, Griveau A, Chang SM, Daneman R, Fancy SPJ, et al. Oligodendrocyte-encoded HIF function couples postnatal myelination and white matter angiogenesis. *Cell*. (2014) 158:383–96. doi: 10.1016/j.cell.2014.04.052

25. Li Y, Huang J, He X, Tang G, Tang YH, Liu Y, et al. Postacute stromal cell-derived factor-1alpha expression promotes neurovascular recovery in ischemic mice. *Stroke*. (2014) 45:1822–9. doi: 10.1161/STROKEAHA.114.005078

26. Liu S, Fan M, Xu JX, Yang LJ, Qi CC, Xia QR, et al. Exosomes derived from bone-marrow mesenchymal stem cells alleviate cognitive decline in AD-like mice by improving BDNF-related neuropathology. *J Neuroinflammation*. (2022) 19:35. doi: 10.1186/s12974-022-02393-2

27. Zheng L, Jia J, Chen Y, Liu R, Cao R, Duan M, et al. Pentoxifylline alleviates ischemic white matter injury through up-regulating Mertk-mediated myelin clearance. *J Neuroinflammation*. (2022) 19:128. doi: 10.1186/s12974-022-02480-4

28. Pan J, Qu M, Li Y, Wang L, Zhang L, Wang Y, et al. MicroRNA-126-3p/-5p overexpression attenuates blood-brain barrier disruption in a mouse model of middle cerebral artery occlusion. *Stroke*. (2020) 51:619–27. doi: 10.1161/STROKEAHA.119.027531

29. Zhou PT, Wang LP, Qu MJ, Shen H, Zheng HR, Deng LD, et al. Dl-3-N-butylphthalide promotes angiogenesis and upregulates sonic hedgehog expression after cerebral ischemia in rats. *CNS Neurosci Ther*. (2019) 25:748–58. doi: 10.1111/cns.13104

30. Tang Y, Xu H, Du X, Lit L, Walker W, Lu A, et al. Gene expression in blood changes rapidly in neutrophils and monocytes after ischemic stroke in humans: a microarray study. *J Cereb Blood Flow Metab*. (2006) 26:1089–102. doi: 10.1038/sj.jcbfm.9600264

31. Gelderblom M, Gallizioli M, Ludewig P, Thom V, Arunachalam P, Rissiek B, et al. IL-23 (interleukin-23)-producing conventional dendritic cells control the detrimental IL-17 (interleukin-17) response in stroke. *Stroke*. (2018) 49:155–64. doi: 10.1161/STROKEAHA.117.019101

32. Gulke E, Gelderblom M, Magnus T. Danger signals in stroke and their role on microglia activation after ischemia. *Ther Adv Neurol Disord*. (2018) 11:1756286418774254. doi: 10.1177/1756286418774254

33. Tang YH, Ma YY, Zhang ZJ, Wang YT, Yang GY. Opportunities and challenges: stem cell-based therapy for the treatment of ischemic stroke. *CNS Neurosci Ther*. (2015) 21:337–47. doi: 10.1111/cns.12386

34. Al-Bahrani A, Taha S, Shaath H, Bakhiet M. TNF-alpha and IL-8 in acute stroke and the modulation of these cytokines by antiplatelet agents. *Curr Neurovasc Res*. (2007) 4:31–7. doi: 10.2174/156720207779940716

35. Cho C, Smallwood PM, Nathans J. Reck and Gpr124 are essential receptor cofactors for Wnt7a/Wnt7b-specific signaling in mammalian CNS angiogenesis and blood-brain barrier regulation. *Neuron*. (2017) 95:1221–5. doi: 10.1016/j.neuron.2017.08.032

36. Trevino TN, Fogel AB, Otkiran G, Niladhuri SB, Sanborn MA, Class J, et al. Engineered Wnt7a ligands rescue blood-brain barrier and cognitive deficits in a COVID-19 mouse model. *Brain*. (2024) 147:1636–43. doi: 10.1093/brain/awae031

37. Lengfeld JE, Lutz SE, Smith JR, Diaconu C, Scott C, Kofman SB, et al. Endothelial Wnt/beta-catenin signaling reduces immune cell infiltration in multiple sclerosis. *Proc Natl Acad Sci USA*. (2017) 114:E1168–77. doi: 10.1073/pnas.1609905114

38. Ma B, Hottiger MO. Crosstalk between Wnt/beta-catenin and NF-kappaB signaling pathway during inflammation. *Front Immunol*. (2016) 7:378. doi: 10.3389/fimmu.2016.00378

39. Jeon JI, Ko SH, Kim JM. Intestinal epithelial cells exposed to *Bacteroides fragilis* enterotoxin regulate NF-κB activation and inflammatory responses through beta-catenin expression. *Infect Immun*. (2019) 87:e00312-19. doi: 10.1128/IAI.00312-19

40. Nejak-Bowen K, Kikuchi A, Monga SP. Beta-catenin-NF-κB interactions in murine hepatocytes: a complex to die for. *Hepatology*. (2013) 57:763–74. doi: 10.1002/hep.26042

41. Tang Y, Zhang C, Wang J, Lin X, Zhang L, Yang Y, et al. MRI/SPECT/fluorescent tri-modal probe for evaluating the homing and therapeutic efficacy of transplanted mesenchymal stem cells in a rat ischemic stroke model. *Adv Funct Mater*. (2015) 25:1024–34. doi: 10.1002/adfm.201402930

42. Guo Y, Mishra A, Howland E, Zhao C, Shukla D, Weng T, et al. Platelet-derived Wnt antagonist Dickkopf-1 is implicated in ICAM-1/VCAM-1-mediated neutrophilic acute lung inflammation. *Blood*. (2015) 126:2220–9. doi: 10.1182/blood-2015-02-622233

frontiers | Frontiers in Neurology

TYPE Methods
PUBLISHED 23 July 2025
DOI 10.3389/fneur.2025.1595379

OPEN ACCESS

EDITED BY
Haipeng Liu,
Coventry University, United Kingdom

REVIEWED BY
Dwijendra K. Gupta,
Allahabad University, India
Stanislaw Szlufik,
Medical University of Warsaw, Poland
Koteswara Rao Nalamolu,
California Health Sciences University, United States
Michela Giulii Capponi,
Santo Spirito in Sassia Hospital, Italy
Jeremy Man Ho Hui,
The University of Hong Kong, Hong Kong SAR, China

*CORRESPONDENCE
Xiaofang Ding
✉ 254787416@qq.com
Guoying Zou
✉ zouwanshan75@163.com

RECEIVED 24 March 2025
ACCEPTED 10 July 2025
PUBLISHED 23 July 2025

CITATION
Ding X, Zou G, Ma N, Tang X and Zhou J (2025) Knowledge mapping of exosomes in ischemic stroke: a bibliometric analysis.
Front. Neurol. 16:1595379.
doi: 10.3389/fneur.2025.1595379

Knowledge mapping of exosomes in ischemic stroke: a bibliometric analysis

Xiaofang Ding*, Guoying Zou*, Nuoya Ma, Xudong Tang and Jia Zhou

Department of Clinical Laboratory, The Second People's Hospital of Hunan Province (Brain Hospital of Hunan Province), Changsha, China

Background: Ischemic stroke is a disease in which local ischemia and hypoxia of brain tissues are caused by obstruction of blood vessels in the brain, which in turn triggers brain tissue damage and neurological dysfunction. Recent studies have made significant progress in understanding the role of exosomes in ischemic stroke. Exosomes exhibit anti-inflammatory, immunomodulatory, anti-apoptotic, angiogenic, and neuroregenerative effects, as well as glial scar reduction and drug delivery effects in ischemic stroke. However, there is a notable gap in bibliometric analyses that focus specifically on this subject. This study systematically evaluated the current knowledge and identified emerging research trends regarding exosomes in ischemic stroke through a bibliometric analysis.

Methods: We retrieved research articles on the role of exosomes in ischemic stroke published between 2004 and 2023 from the Web of Science Core Collection (WoSCC) database and then conducted a bibliometric analysis using VOSviewer, CiteSpace, and the bibliometrix package in the R programming environment.

Results: A comprehensive analysis of 374 publications from 38 countries revealed a steady increase in research focused on exosomes in ischemic stroke. This analysis significantly emphasized the contributions of researchers from China and the United States. Key research institutions in this field include Henry Ford Health System, Henry Ford Hospital, and Shanghai Jiao Tong University. The *International Journal of Molecular Sciences* is the top journal in terms of publication output, and Stroke is the most frequently co-cited journal. This extensive study involved 468 authors, the most prolific of whom are Michael Chopp, Zhengbiao Zhang, and Liang Zhao, Hongqi Xin is the most frequently co-cited researcher. The primary areas of investigation are the role of endogenous exosomes in initiating and progressing ischemic stroke, as well as the potential therapeutic applications of exogenous exosomes.

Conclusion: In the context of ischemic stroke, a recent bibliometric evaluation provided a comprehensive analysis of research trends and developments related to exosomes. The findings of this study highlight current research frontiers and identify significant emerging trends. These findings offer a crucial resource for researchers focusing on exploring exosomes.

KEYWORDS

bibliometrics, exosomes, ischemic stroke, CiteSpace, VOSviewer

Introduction

Ischemic stroke significantly contributes to global mortality and disability (1). Treatment options are limited, primarily because effective interventions must occur within a short timeframe. This often results in suboptimal post-treatment outcomes. Therefore, it is crucial to investigate management strategies requiring immediate, comprehensive care. Current treatment options for ischemic stroke include thrombolytic therapy, mechanical thrombectomy, angioplasty, anticoagulant and antiplatelet medication use. In addition, various interventional techniques, such as stent placement and surgical revascularization, have been employed in clinical practice (2). However, it's important to acknowledge that these surgical and interventional methods carry risks, and long-term medication use can result in side effects. Therefore, there is an urgent need to develop safer and more effective alternative treatments. It is particularly crucial to explore new strategies for managing ischemic stroke because timely intervention and a collaborative approach are essential for improving patient outcomes. Exosomes are small, 30- to 150-nanometer-sized vesicles released by various cell types into body fluids, such as blood, urine, saliva, and cerebrospinal fluid, they are formed by the fusion of endosomes with the plasma membrane, allowing the vesicles to enter the extracellular space. Exosomes carry a variety of important biomolecules, including lipids, proteins, RNA (especially microRNA and messenger RNA), and DNA fragments, all of which are essential for cellular communication and many biological processes (3). Almost all cell types can produce exosomes, which are characterized by low immunogenicity and tumorigenicity, efficient drug delivery, and blood–brain barrier crossing (4). Recent studies have shown that exosome therapy has neuroprotective and reparative effects in ischemic stroke, suggesting that it may be an effective new therapeutic strategy. Meanwhile, studies on using exosomes as diagnostic markers and using engineered exosomes as drug carriers are emerging. However, there is a gap between animal experiments and clinical translation, as well as between laboratory results and bedside applications. This paper uses bibliometrics to grasp the overall development of exosomes in ischemic stroke, reveal research hotspots, predict future research trends, accurately locate innovation breakthroughs, and provide "discipline navigation" and "cutting-edge insight" for the field, this information provides smarter decision support for the research ecology.

Methods

Search strategy

A systematic literature search was performed in the Web of Science Core Collection (WoSCC),[1] using the following query: ((TS = "Exosomes") AND TS = "ischemic stroke") AND LA = "English," with filters applied for "articles" and "reviews" (Figure 1).

1 https://webofscience_clarivate_cn.hnucm.opac.vip/wos/woscc/basic-search

Data analysis

VOSviewer (version 1.6.19) is bibliometric analysis software that extracts key information from numerous publications. It is commonly used to construct networks of collaboration, co-citation, and co-occurrence. In this study, the software performed the following analyses: journal and co-cited journal analysis, co-cited author analysis, country and institution analysis, and keyword co-occurrence analysis. In VOSviewer maps, nodes represent items such as countries, institutions, journals, and authors. The size and color of the nodes indicate the quantity and classification of these items, respectively. The thickness of the lines between nodes reflects the degree of collaboration or co-citation between items. In our study, CiteSpace was used to plot biplot overlays of journals and to analyze references using citation bursts. The R package "Bibliometrix" (version 4.3.2) was used for thematic evolution analysis and to construct a global distribution network of exosomes in ischemic stroke. Additionally, we analyzed the annual publication volume of papers using Microsoft Office Excel 2021.

Results

Quantitative analysis of publication

Our investigation identified 358 studies related to exosomes in the context of ischemic stroke published over the last two decades. This collection comprises 271 original research articles and 87 review papers. The data indicate that from 2012 to 2017, the number of publications was relatively low, averaging just 5.1 articles per year, which suggests that this research area was still in its early stages of development. In contrast, from 2018 to 2023, there was a remarkable increase in the publication frequency, with an average of 54 articles published annually. Notably, in 2020, 53 articles were published, 1.8-fold increase compared to previous years. The total number of publications reached 92 by 2023, demonstrating a consistent upward trend in research output since 2018, especially compared with earlier years.

Country and institutional analysis

A total of 36 countries and 199 academic institutions have conducted research on the role of exosomes in ischemic stroke. A significant portion of this research originates from Asia, with notable contributions from three European countries (Table 1). China was the leading contributor, producing 229 publications, accounting for 59.48% of the total output. The United States was the second-largest contributor, with 85 publications (22.07%), Germany and Italy added 18 (4.6%) and 9 (2.3%) publications, respectively. China and the United States together constitute 81.6% of the total publication volume, an analysis of collaborative networks among 48 countries reveals strong partnerships, particularly between the two countries. Additionally, notable collaborations involve Germany and China, as well as Australia partnering with both (Figure 2).

The leading institutions in this field are primarily located in three countries, with China accounting for 60% of them. Notable contributors include the Henry Ford Health System, Henry Ford Hospital, Shanghai Jiao Tong University, and Oakland University.

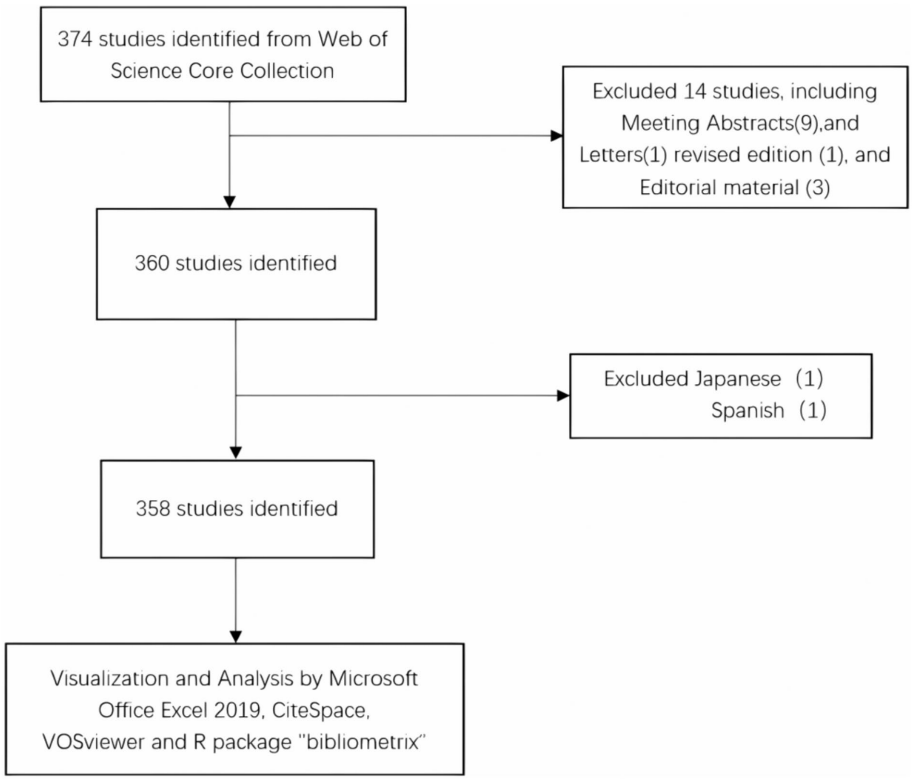

FIGURE 1
Publications screening flowchart.

TABLE 1 Top 10 countries and institutions on research on exosomes in ischemic stroke.

Rank	Country (region)	Publication counts	Institution	Publication counts (%)
1	China (Asia)	229	Henry Ford Health System (US)	20 (13.07%)
2	USA (North America)	85	Henry Ford Hospital (US)	20 (13.07%)
3	Germany (Europe)	18	Shanghai Jiao Tong University (China)	20 (13.07%)
4	Italy (Europe)	9	Oakland University (US)	19 (12.41%)
5	Romania (Europe)	9	Central South University (China)	15 (9.80%)
6	South Korea (Asia)	9	University System of Ohio (US)	13 (8.49%)
7	Iran (Asia)	8	Fudan University (China)	12 (7.84%)
8	Australia (Oceania)	6	Jinzhou Medical University (China)	12 (7.84%)
9	India (Asia)	6	Capital Medical University (China)	11 (7.18%)
10	Japan (Asia)	6	Nanjing Medical University (China)	11 (7.18%)

Each institution is responsible for about 13% of the total publications. This research focus resulted in the formation of a collaborative network of 62 institutions, each of which has published at least three papers, this highlights the significant cooperative efforts within this area. Key partnerships were formed between Shanghai Jiao Tong University, Fudan University, Tongji University, and Central South University. Additionally, Auckland University has established partnerships with Tianjin Medical University, Harvard Medical School, and Massachusetts General Hospital, highlighting the interconnected nature of research initiatives in this field (Figure 3).

Journals and co-cited journals

A thorough examination revealed that 178 scholarly journals published research on exosomes in the context of ischemic stroke.

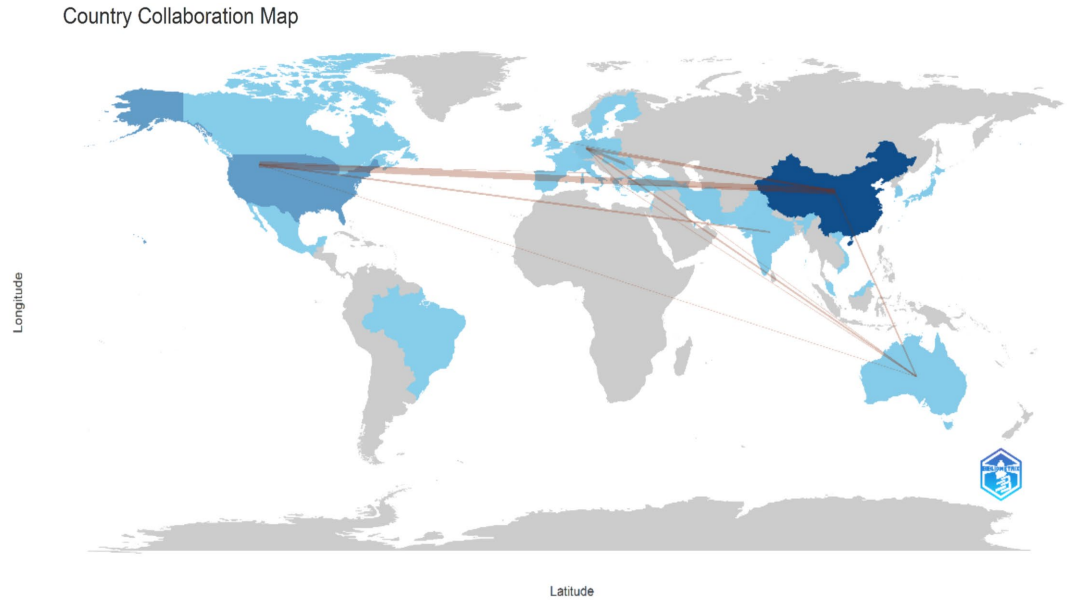

FIGURE 2
Geographical distribution of exosome research on ischemic stroke.

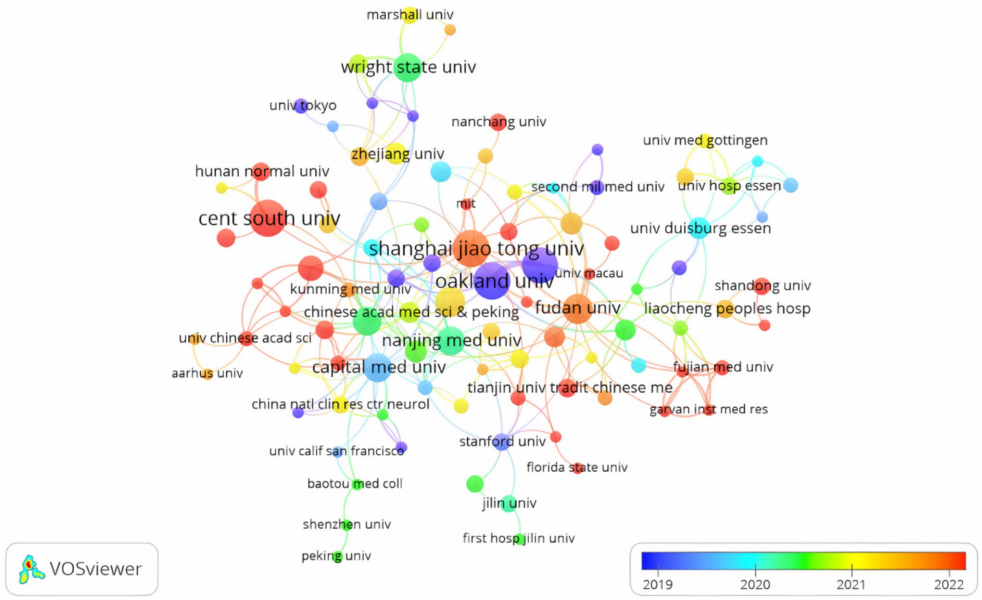

FIGURE 3
Visualization of institutions for research on exosomes in ischemic stroke.

The *International Journal of Molecular Sciences* was the leading publication, accounting for 8.42% of the total output with 15 articles. *Stem Cell Research & Therapy* published 9 articles (5.05%), while *Stroke* and *Translational Stroke Research* contributed 8 (4.49%) and 7 articles (3.93%), respectively. Among the top 10 journals, the *Journal of Nanobiotechnology* had the highest impact factor at 10.6, closely followed by the *Journal of Controlled Release* at 10.5. A detailed literature review identified 27 journals, each with at least two relevant publications, which facilitated the creation of a citation network map (Figure 4A). This figure shows that leading international journals in the field of molecular science, such as *Stroke*, the *Journal of Cerebral Blood Flow and Metabolism*, and the *International Journal of Molecular Sciences*, demonstrate significant citation interactions within the established network. As shown in Table 2, four of the 10 most frequently cited journals surpassed 400 citations. Notably, *Stroke* leads the list with a co-citation count of 1,042, followed by the *Journal of Cerebral Blood Flow and Metabolism* (co-citations = 475), *PLoS One* (co-citations = 436), and the *Journal of Extracellular Vesicles* (co-citations = 408). In addition, *the Journal of Extracellular Vesicles* had the highest impact factor (IF = 15.5),

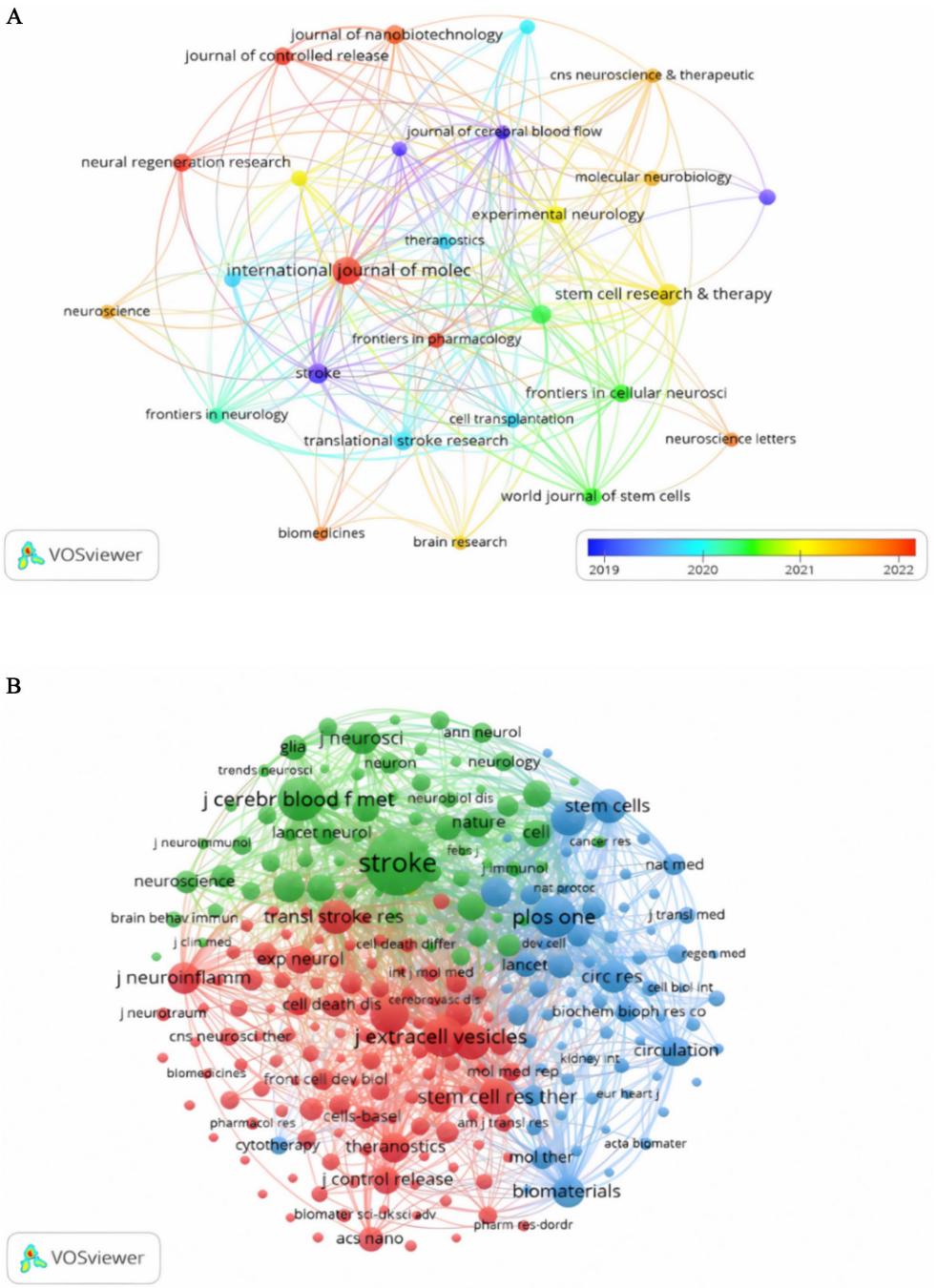

FIGURE 4
Visualization of journals **(A)** and co-cited journals **(B)** on research on exosomes in ischemic stroke.

followed by *the Proceedings of the National Academy of Sciences of the United States of America* (IF = 9.4). As shown in Figure 4B, *Stroke* exhibits positive co-citation associations with *the Journal of Cerebral Blood Flow and Metabolism*, *PLOS One*, *and the Journal of Extracellular Vesicles*, among others. This reflects the trend toward interdisciplinary cooperation and technological integration. The dual-map overlay of academic journals illustrates citation trends, with cited journals positioned on the left and co-cited journals on the right (5). The main citation path indicated by the orange line, reveals that research in the areas of *Molecular/Biology/Immunology* primarily references works from the *Molecular/Biology/Genetics* field (Figure 5).

Co-cited authors and co-cited references

A total of 2,271 researchers have studied exosomes in the context of ischemic stroke. The top 10 authors among these contributors published 18, 10, 10, 10, and 10 articles, respectively (Table 3). Through the co-citation analysis, 13,032 authors were identified. Five

TABLE 2 Top 10 journals and co-cited journals for research of exosomes in ischemic stroke.

Rank	Journal	Publication counts	Impact factor (IF)	JCR	Co-cited journal	Co-citation counts	Impact factor (IF)	JCR
1	International Journal of Molecular Sciences	15	4.9	Q2	Stroke	1,042	7.8	Q1
2	Stem Cell Research & Therapy	9	7.1	Q2	Journal of Cerebral Blood Flow and Metabolism	475	4.9	Q2
3	Stroke	8	7.8	Q1	PLoS One	436	2.9	Q3
4	Translational Stroke Research	7	3.8	Q2	Journal of Extracellular Vesicles	408	15.5	Q1
5	Frontiers in Neuroscience	7	3.2	Q3	International Journal of Molecular Sciences	346	4.9	Q2
6	Journal of Nanobiotechnology	7	10.6	Q1	Scientific Reports	335	3.8	Q3
7	Experimental Neurology	6	4.6	Q2	Stem Cell Research & Therapy	325	7.1	Q2
8	World Journal of Stem Cells	6	3.6	Q3	Stem Cells	299	4	Q2
9	Frontiers in Cellular Neuroscience	6	4.2	Q3	Translational Stroke Research	282	3.8	Q2
10	Journal of Controlled Release	6	10.5	Q1	Proceedings of the National Academy of Sciences of the United States of America	280	9.4	Q1

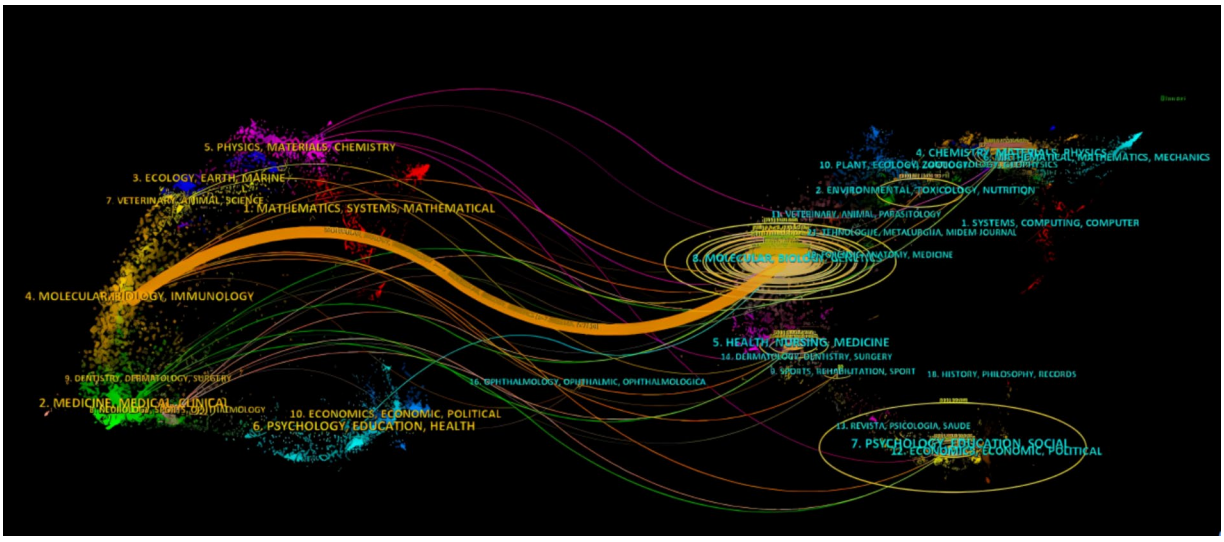

FIGURE 5
Dual-map overlay of journals on research on exosomes in ischemic stroke.

of these authors had a co-citation frequency of more than 100 (Table 3). Leading this count was Xin H. Q., who received an impressive total of 367 citations, following Xin H. Q. was Zhang Z. G. with 129 citations, and Chen J. L. closely trailed with 124 citations. Furthermore, a co-citation network was established for authors cited at least 30 times (Figure 6B). This network highlights significant collaborative relationships, particularly between Xin H. Q. and Chen J. L., and between Xin H. Q. and Zhang Z. G.

Over the last 20 years, researchers have identified 17,271 co-cited studies pertaining to exosomes in the context of ischemic stroke. Within the top 10 most frequently co-cited references (Table 4), each publication received a minimum of 47 citations, with one reference surpassing 90 citations. These 10 articles demonstrate a changing research trend on exosomes: research on exosome is shifting from basic studies (existence, composition) to applications in disease treatment (e.g., stroke). This reflects basic research moving to clinical

TABLE 3 Top 10 authors and co-cited authors on research of exosomes in ischemic stroke.

Rank	Authors	Publication counts	Co-cited authors	Co-citation counts
1	Chopp, Michael	18	Xin, H. Q.	367
2	Zhang, Zheng Gang	10	Zhang, Z. G.	129
3	Hermann, Dirk M.	10	Chen, J. L.	124
4	Liang, Jia	10	Doeppner, T. R.	105
5	Zhao, Liang	10	Thery, C.	101
6	Yang, Guo-Yuan	9	Otero-Ortega, L.	88
7	Shi, Yijie	9	Zhang, Y.	80
8	Chen, Yanfang	8	Tian, T.	68
9	Zhang, Zhijun	8	Li, Y.	65
10	Xin, Hongqi	7	Yang, J. L.	63

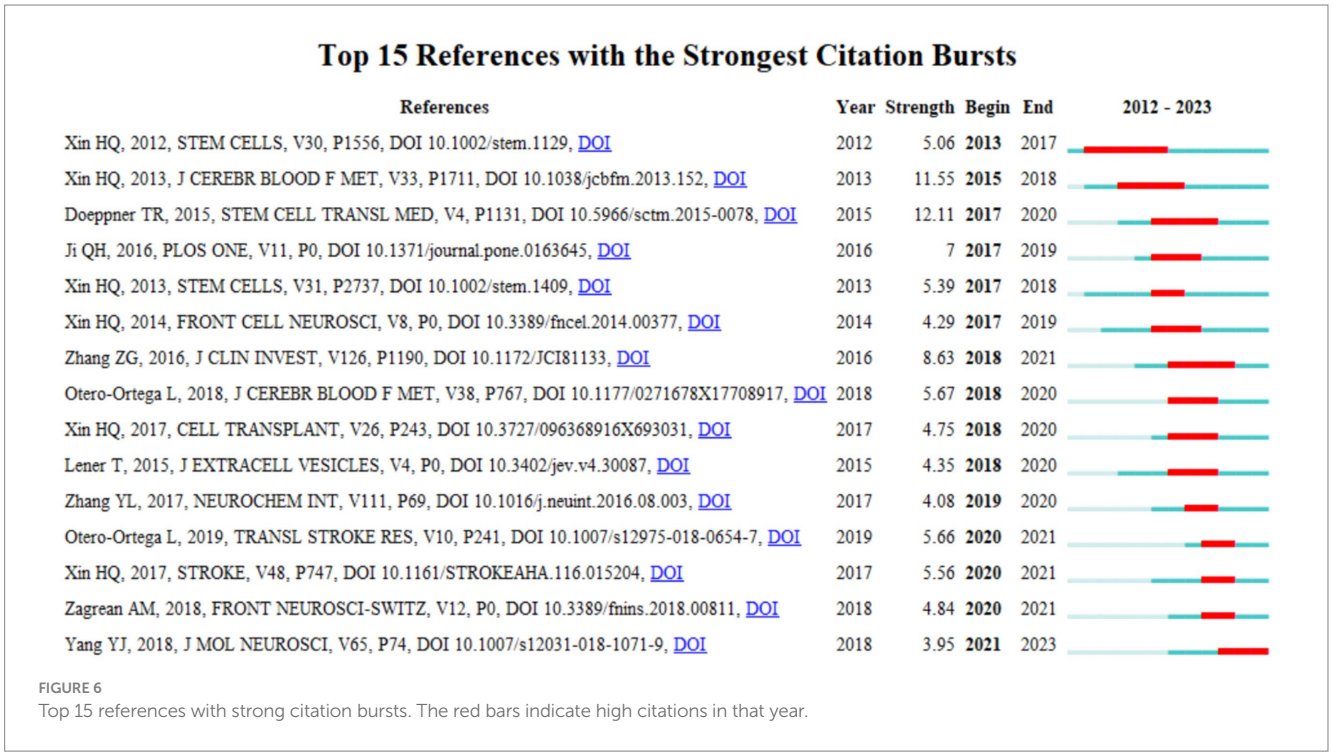

FIGURE 6
Top 15 references with strong citation bursts. The red bars indicate high citations in that year.

TABLE 4 Top 10 co-cited references on research of exosomes in ischemic stroke.

Rank	Co-cited reference	Citations
1	Xin H. Q., 2013, J Cerebr Blood F Met, v33, p. 1711	93
2	Doeppner T. R., 2015, Stem Cell Transl Med, v4, p. 1131	73
3	Xin H. Q., 2017, Stroke, v48, p. 747	72
4	Valadi H., 2007, Nat Cell Biol, v9, p654	61
5	Xin H. Q., 2013, Stem Cells, v31, p. 2737	58
6	Tian T., 2018, Biomaterials, v150, p. 137	52
7	Zhang Z. G., 2019, Nat Rev Neurol, v15, p. 193	49
8	Xin H. Q., 2012, Stem Cells, v30, p. 1556	48
9	Yang J. L., 2017, Mol Ther-Nucl Acids, v7, p. 278	47
10	Song Y. Y., 2019, Theranostics, v9, p. 2910	47

applications. Initially focused on cell biology, research on exosome involves neuroscience, material science, clinical medicine, and other disciplines, reflecting a transformation from a single field to multidisciplinary cross-fertilization.

Reference with citation bursts

This study used CiteSpace to identify 15 pivotal publications characterized by citation bursts, which are notable spikes in citations within a specific period of time (Figure 6). The red bars in the figure denote the periods of increased citation activity that transpired from 2012 to 2021. The paper by Doeppner T. R. et al., regarding extracellular vesicles and their role in stroke recovery exhibited the most pronounced citation burst from 2017–2020, with an intensity of 12.11, proposing standardized protocols or efficacy enhancement strategies for stem cell transplantation that will serve as technical benchmarks for subsequent studies. A study by Xin et al., conducted from 2015 to 2018, focusing on exosomes and neurovascular plasticity post-stroke, recorded the second highest burst intensity of 11.55. The five high-bursts of literature published by Xin H. Q.'s team between 2012–2017 (e.g., Stem Cells, 2012) all focused on the mechanisms of stem cell transplantation for the repair of cerebral ischemia, suggesting that this direction was an early research hotspot. After 2018, the studies were more inclined to clinical validation (e.g., Otero-Ortega L., 2018) and molecular mechanisms (e.g., Zhang T. L., 2017), reflecting the transition of the field from fundamentals to applications.

Hotspots and frontiers

The analysis of co-occurring keywords highlights key research trends. Table 5 shows that "extracellular vesicles" and "mesenchymal stem cells" were the most cited keywords, each referenced more than 30 times, indicating their importance in ischemic stroke research. A study of keywords mentioned five or more times using VOSviewer (Figure 7A) revealed six clusters: the green cluster included extracellular vesicles, mesenchymal stem cells, microglia, angiogenesis, and stem cells; the red cluster covered exosomes, stroke, microRNA, and the blood–brain barrier; the blue cluster featured exosomes, angiogenesis, and neuroprotection; the yellow cluster consisted of ischemic stroke, microglia, inflammation, and neurogenesis; the purple cluster related to cerebral ischemia, miRNAs, and pyroptosis; and the cyan cluster involved autophagy, apoptosis, and oxidative stress. The trend analysis in Figure 7B shows that, from 2004 to 2019, research primarily focused on functional recovery and ischemic conditions. In contrast, after 2021, the focus has shifted to understanding the pathogenesis and therapeutic potential of exosomes, especially in aging, extracellular vesicles, and neural stem cells.

Discussion

General information

Between 2004 and 2011, there were no publications concerning exosomes in the context of ischemic stroke (Figure 8). The immaturity of exosome isolation and purification technology, as well as the insufficient sensitivity of detection technology, makes it difficult to study the mechanism of action in depth. During the period when the biological function of exosomes was not well understood in academia, research hotspots did not focus on the application of exosomes in ischemic stroke. Insufficient multidisciplinary cross-fertilization and difficulties in clinical translation limited the research and application of exosomes in this field, indicating that there is an obvious gap in research linking these two fields during this period. From 2012 to 2017, the output of academic papers remained modest, with an average of about 5.1 publications per year, suggesting that exosome research is still in its infancy in this particular field. From 2012 to 2017, the number of academic papers published annually averaged about 5.1, suggesting that exosome research is still in its infancy. In contrast, from 2018 to 2023, there is a significant increase in published academic papers, averaging about 54 papers per year. A notable peak occurred in 2020, with 53 papers published, an 80% increase compared with 2019. Additionally, the number of published papers increased significantly to 92 in 2023. Over the past 6 years, the annual growth rate of research on exosomes and ischemic stroke has continued to increase, indicating a growing interest in this area that portends significant progress and increased academic attention.

The exploration of exosomes in the field of ischemic stroke, starting from the discovery of intercellular communication carriers

TABLE 5 Top 20 keywords on research of exosomes in ischemic stroke.

Rank	Keywords	Counts	Rank	Keywords	Counts
1	Exosomes	128	11	Inflammation	16
2	Ischemic stroke	104	12	Neuroinflammation	16
3	Stroke	74	13	Neurogenesis	13
4	Exosome	61	14	Blood–brain barrier	13
5	Extracellular vesicles	51	15	miRNA	12
6	Mesenchymal stem cells	31	16	Neuroprotection	11
7	MicroRNA	25	17	Biomarkers	11
8	Angiogenesis	25	18	Acute ischemic stroke	11
9	Microglia	20	19	Microvesicles	10
10	Stem cells	17	20	Oxidative stress	10

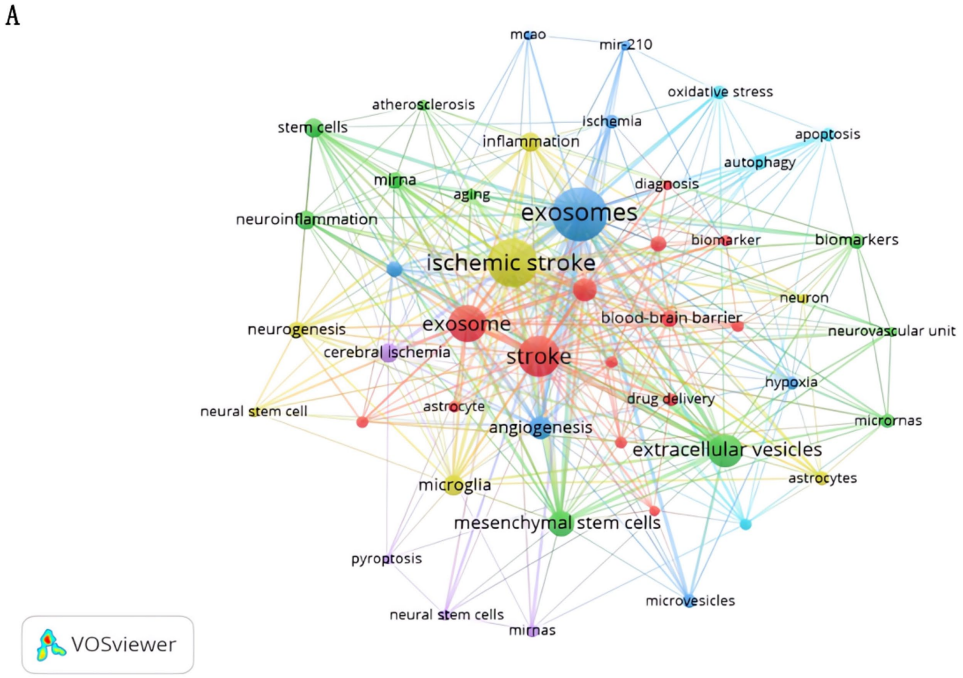

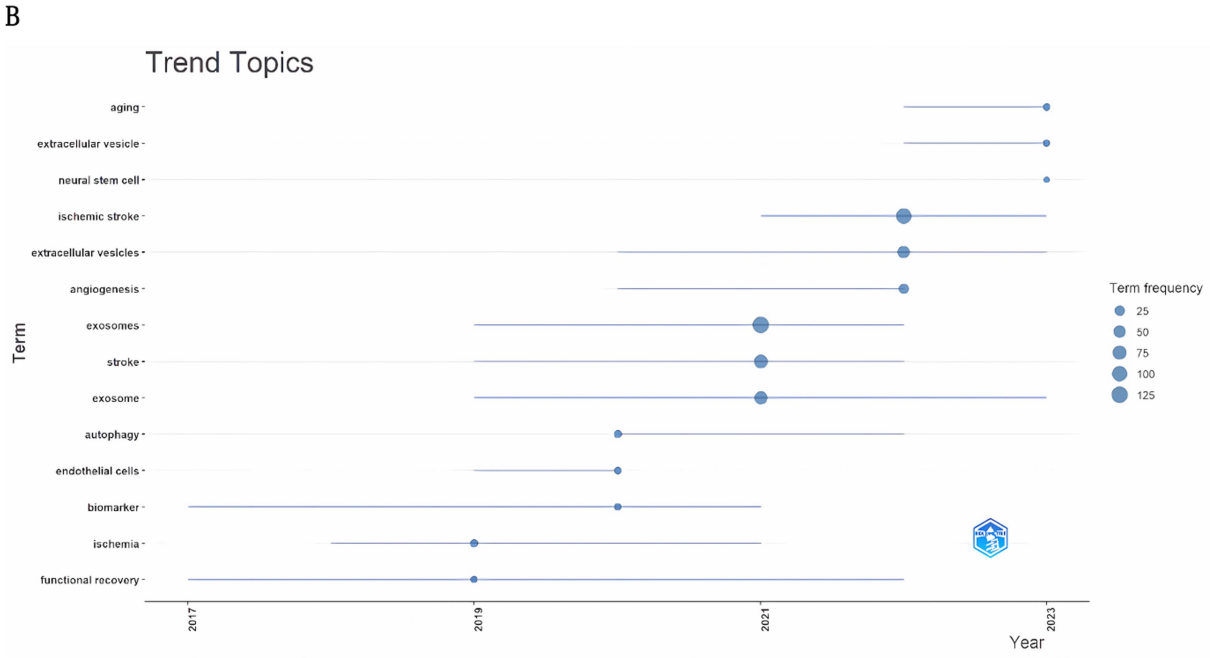

FIGURE 7
Keyword cluster analysis **(A)** and trend topic analysis **(B)**.

and gradually revealing their multi-mechanism roles, has opened new avenues for the treatment of ischemic stroke, demonstrating the potential for clinical translation and moving towards clinical application. Since the discovery of the neurorestorative mechanism of exosomes in the early 2010s, research on exosomes in the treatment of ischemic stroke has gone through several phases of elucidation of molecular mechanisms, validation of animal models, and recent preliminary exploration in early-stage clinical trials, making exosomes a very promising option for therapeutic applications, especially in the treatment of ischemic stroke (Figure 9). As shown in Figure 8, the number of articles published each year about exosomes in ischemic stroke increased suddenly from 2019 to 2020. This increase is related to the outbreak of the novel coronavirus epidemic, which accelerated the application of exosomes in ischemic stroke therapy by promoting demand for mRNA delivery technology. This accelerated the research of inflammatory mechanisms and clinical translation, pushing exosome research from "basic exploration" to "clinical translation," especially in the field of ischemic stroke, this has led to an upgrade in treatment concepts and technical tools. Technological breakthroughs and resource reorganization driven by crises can lead to

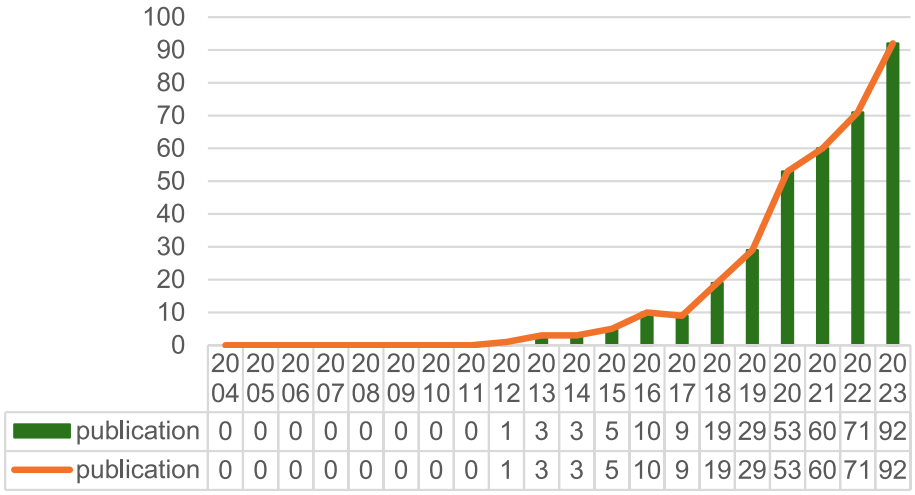

FIGURE 8
Annual output of research of exosomes in ischemic stroke.

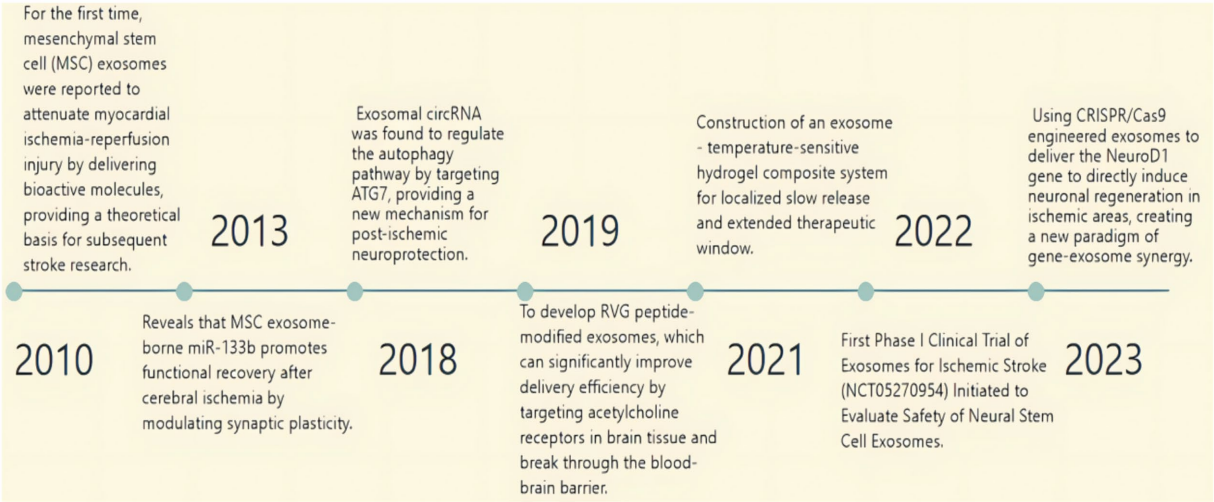

FIGURE 9
The evolution of exosomes in ischemic stroke applications.

interdisciplinary changes. To transform emergencies into sustainable drivers of innovation, there is a need for interdisciplinary collaboration, clinical orientation, and the development of a resilient research ecology. China and the United States are leaders in exosome research focused on ischemic stroke, with China ranking among the top countries in this field. Among the top 10 research organizations, 52.91% are in China, followed by the United States (34.63%) and New Zealand (12.41%). China and the United States dominate exosome research in ischemic stroke due to their significant advantages in basic research, technological innovation, clinical application, interdisciplinary cooperation, resource integration, policy support, and financial investment. Notably, China has significant collaborations with both the United States and Germany. Australia has also collaborated with both Germany and China.

Shanghai Jiao Tong University, Fudan University, Tongji University, and Central South University are among the research institutions that have formed strong partnerships. Institutions such as Auckland University, Tianjin Medical University, Harvard Medical School, and Massachusetts General Hospital have maintained active international partnerships. Despite the sizable number of papers from Central South University, its collaborative network is limited, highlighting the need for greater international cooperation. Therefore, to accelerate exosome research related to ischemic stroke, research institutions around the world should strengthen their collaboration.

A significant portion of the literature concerning exosomes in the context of ischemic stroke has been published in the *International Journal of Molecular Sciences* (IF = 4.9, Q1), highlighting their significance within this research domain. Among the journals with the highest impact factors, the *Journal of Nanobiotechnology* (IF = 10.6, Q1) holds the leading position, closely followed by the *Journal of Controlled Release* (IF = 10.5, Q1). Co-citation analysis revealed that the most cited journals were high-impact Q1 publications,

underscoring the quality and global recognition of research in this field. The majority of published studies are found in journals dedicated to molecular biology and related fields, whereas clinical research journals feature relatively few articles. This suggests that the investigation of exosomes in the context of ischemic stroke is predominantly at the fundamental research level.

Chopp, Michael is the most published authors with 18 articles, closely followed by Zhang, Zheng Gang, Hermann, Dirk M and Liang, Jia, who each published 10 articles. Notably, 9 of the 18 articles authored by Chopp, Michael were devoted to the therapeutic significance of microRNAs (miRNAs) and various bioactive compounds found in exosomes in promoting stroke recovery. Their research showed that miR-27a, which is found in exosomes or small extracellular vesicles (sEVs) from cerebral endothelial cells (CEC-sEVs) in ischemic brain tissue, plays a crucial role in promoting axon growth and aiding brain remodeling. Additionally, a collaborative review by Zhang et al. highlighted the essential role of miRNAs in brain repair via exosome-mediated cellular communication. The review suggests that exosomes play a vital role in brain remodeling and offer promising opportunities for treating ischemic brain injury and improving neurological function. Dirk M. Hermann's article titled "New Light on the Horizon" in Stroke describes how extracellular vesicles (EVs) in the blood can be a diagnostic tool for transient ischemic attack (TIA) and stroke. Liang and Jia highlighted the neuroprotective effects and functional improvements associated with exosomes, demonstrating their potential as a therapeutic option for ischemic stroke through specific antioxidant pathways.

In summary, the studies mentioned above have mainly discussed the pathogenesis, diagnosis, and therapeutic role of exosomes in ischemic stroke.

MSC-exos

Mesenchymal stem cells (MSCs) have recently received significant attention due to their impressive tissue regeneration and immunomodulation capabilities, especially in ischemic stroke treatment. This increased interest stems from the ability of MSC-derived exosomes to cross the blood–brain barrier, their low immunogenic profile, and their minimal toxicity (6). Consequently, MSCs are being increasingly integrated into clinical trials focused on managing ischemic stroke, with numerous studies reporting favorable therapeutic outcomes. Consistent evidence shows that MSC-based treatments substantially improve recovery following ischemic stroke (7–9). MSCs can easily be isolated from various sources, such as the umbilical cord, bone marrow, and peripheral blood (10). These stem cell-derived exosomes exhibit characteristics such as low immunogenicity, reduced risk of tumor formation, high transport efficiency, inherent stability, and the capacity to traverse the blood–brain barrier (11, 12). Exosome-based therapies are still in the early stages of clinical application, but they have shown promising therapeutic effects in animal models of ischemic cerebrovascular accidents (CVAs) (13). Research indicates that exosomes from bone marrow mesenchymal stem cells (BMMSCs) can significantly alleviate systemic immune suppression 4 weeks after ischemia, they can also promote neurovascular regeneration and enhance motor function (14). Additionally, studies have shown that exosomes extracted from adipose-derived mesenchymal stem cells (ADMSCs) can reduce infarct size, promote neurological recovery, enhance corticospinal tract integrity, and promote white matter repair in rat stroke models (15). Furthermore, it has been shown that exosomes from BMMSCs are effective in reversing peripheral immunosuppression after ischemia, thereby promoting infarct neurovascular regeneration (16, 17). Exosomes derived from neural stem cells reduce volume and enhance recovery following stroke (18). In addition to MSC-derived exosomes, exosomes from other cell types have also been found to contribute to neuroprotection after stroke (19). Webb et al. (18) discovered that astrocyte-derived exosomes inhibited the expression of TNF-α, IL-6, and IL-1β, which attenuated neuronal damage by inhibiting autophagy.

Exosomes and biomarkers

Exosomes are vesicles derived from body fluids, such as serum, plasma, and urine. Among their components, miRNAs are among the most widely studied (20). Exosomes contain various functional RNA molecules, including miRNAs, which reflect the physiological and pathological characteristics of the originating cells (21, 22). By transferring mature miRNAs to recipient cells, exosomes can modulate gene expression and affect various cellular and molecular pathways (23). Recent studies have highlighted the role of exosomal miRNAs in modulating physiological and pathological processes after ischemic stroke, as well as their contribution to brain remodeling by enhancing substance transport (24). Therefore, exosomes are considered promising biomarkers for early diagnosis and prognosis of stroke, as well as potential drug candidates for stroke therapy (25, 26).

Exosomal miRNAs are more stable than free miRNAs because they are shielded from enzymes and RNases in biological fluids, making them less likely to break down (27). The increased stability of exosomal miRNAs has made it possible to identify changes in their expression over time during disease progression. Additionally, it allows these microRNAs to promote sustained cellular signaling associated with disease (28, 29). Some researchers have investigated whether the transfer of miRNAs via exosomes creates a new mechanism of cell-to-cell communication (30). Exosomal miRNAs from the central nervous system may carry information from their parent cells. In contrast, exosomal miRNAs from injured neuroblasts can monitor the condition of brain cells and tissues directly (31–33). Recent experiments have revealed substantial changes in the synthesis, secretion, and composition of exosomes, suggesting potential new targets for disease treatment (34, 35). Exosomes are rich in miRNAs, which are more accessible than cellular miRNAs. Deep sequencing results indicate that the percentage of miRNAs present in serum exosomes is three to four times higher than that in pure serum (36). Consequently, exosomes obtained from biological fluids, along with their miRNA content, are increasingly recognized as important targets for biomarker analysis (37–39). Research suggests that in diseases of the central nervous system such as stroke, the sorting mechanisms of miRNAs during exosome biogenesis may be disrupted, which in turn affects both disease pathogenesis and neuroregeneration (40). Consequently, exosomal miRNAs may exhibit greater disease specificity than cellular or free miRNAs, they are considered superior biomarkers for stroke due to their sensitivity and specificity (41–43).

Therapeutic and neuroprotective roles of exosomes

Exosomes can cross the blood–brain barrier (BBB) or choroid plexus, allowing information exchange between the central nervous system (CNS) and the peripheral circulation (44). The primary mechanism through which exosomes exert their therapeutic effects is molecular delivery, specifically via miRNA transfer (45). Exosomes facilitate communication between cells and tissues by delivering proteins and miRNAs (46). Exosomes regulate gene expression and various cellular and molecular pathways by releasing mature microRNAs (miRNAs) into recipient cells (47). The unique characteristics of miRNAs in exosomes allow them to serve as effective drug carriers, they can target the CNS specifically and modulate gene expression related to disease. This could guide the development of new therapeutic strategies for CNS disorders (48, 49). Exosomes can be administered via several routes, such as nasal, intravenous, intraperitoneal, and intracranial, to deliver proteins and RNA to the brain (50). This flexibility makes exosome-based drug delivery a promising method for treating central nervous system (CNS) diseases (51, 52).

Brain recovery after an ischemic stroke is achieved through various interconnected processes, such as the formation of new blood vessels and neurons, the production of cells that support myelin, the activation of mechanisms that prevent cell death, and the engagement of the immune response (53, 54). These processes work together to enhance the reconstruction of the neurovascular units and restore neurological function (55, 56). Research indicates that enhancing miR-126 significantly increases the therapeutic effectiveness of exosomes obtained from endothelial progenitor cells (EPCs) (57, 58). After an ischemic stroke, an insufficient blood supply can cause miR-126 to target vascular cell adhesion protein 1 (VCAM-1), thereby regulating EPC function and angiogenesis (59). Adipose-derived stem cell exosomes are rich in microRNA-181b-5p, which regulates angiogenesis after a stroke by inhibiting transient receptor potential melastatin 7 (TRPM7) (60). Neuronal exosomes can carry microRNA-132 (miRNA-132) to endothelial cells, which helps maintain the integrity of the blood–brain barrier (BBB) (61). Additionally, exosomes from human microvascular endothelial cells contain the Dll4 protein, which regulates angiogenesis. The Dll4-Notch signaling pathway, which occurs in both endothelial cells and pericytes, is essential for angiogenesis and for maintaining the integrity of the blood–brain barrier (62).

Neural regeneration and angiogenesis are key processes in recovery from ischemic stroke. Research on exosomal miRNAs is advancing rapidly, particularly in the field of nerve regeneration. Recent studies have demonstrated the ability of exosomal miRNAs to positively impact nerve injury by modulating apoptosis, the inflammatory response, and regenerative processes in nerve cells. These small RNA molecules are important cell-to-cell signaling molecules that regulate the growth, survival, and regeneration of neurons. Recent studies have shown that, in addition to serving as carriers for drug delivery, exosomes regulate signaling pathways related to nerve regeneration through the miRNAs they contain. For instance, researchers discovered that exosomes from adipose-derived stem cells promote Schwann cell proliferation and migration by delivering miRNA-22-3p, thereby accelerating the repair of peripheral nerve injuries (63). Additionally, another study demonstrated that Schwann cell-derived exosomes promote nerve regeneration and functional recovery via microRNA-21 (64). Studies have shown that exosomes containing miRNA-124 reduce ischemic injury by converting neural progenitor cells into neurons (65, 66). Mesenchymal stem cell (MSC) exosomes deliver microRNA-133b (miRNA-133b) to neurons and astrocytes, this leads to the downregulation of connective tissue growth factor (CTGF) and the secondary release of astrocyte exosomes, which promote synaptic growth (67). This action reduces PTEN levels and increases Akt and mTOR phosphorylation by activating TLR7 and NF-κB/MAPK pathways, ultimately promoting neurogenesis, neuroplasticity, and oligodendrocytopoiesis after ischemic brain injury (68, 69).

Inflammation is a key pathogenic mechanism of post-ischemic brain injury and a trigger of secondary injury. Exosomes derived from MSCs can ameliorate inflammation after acute ischemia or ischemia–reperfusion injury by modulating anti-inflammatory molecules (IL-4 and IL-10) and pro-inflammatory cytokines (IL-6, TNF-α, and IL-1β), and inhibiting microglia activation (70). Exosomes enriched with miR-138-5p or miR-1906 inhibit inflammatory signaling pathways and reduce inflammation, thereby enhancing recovery after stroke (71–73). Wang et al. (74) reported that Fxr2 in ADSC-derived exosomes alleviated iron-induced ferroptosis in M2 microglial cells by regulating the expression of Atf3/Slc7a11, which suppressed the inflammatory microenvironment and improved neurological recovery from brain I/R injury. Research shows that exosomes from bone marrow-derived mesenchymal stem cells (BMMSCs) can reduce ischemia–reperfusion injury by inhibiting inflammation and apoptosis mediated by the NLRP3 inflammasome (75, 76).

There are many challenges with using exosomes for the treatment and diagnosis of ischemic stroke. In terms of cell source, extraction, and purification, various cell types have different advantages and disadvantages. The extraction methods are time-consuming, costly, and complicated. Research on the mechanism of action is insufficient, and the synergistic effect is unknown (77). In clinical application, it is difficult to guarantee yield quality, and targeting is insufficient, affected by individual differences, safety and efficacy need to be verified (78, 79). In the future, it's necessary to analyze the heterogeneity in conjunction with new technologies, conduct clinical trials to validate them and promote their use.

Conclusion

Ischemic stroke is a serious neurological disease with an extremely complex pathogenesis, and its core pathology includes multisystem disorders such as inflammatory response, apoptosis, oxidative stress, and blood–brain barrier disruption. In recent years, exosomes have emerged in ischemic stroke research due to their unique intercellular communication function.

As nanoscale membrane-structured vesicles, exosomes are rich in active molecules such as proteins, lipids, and nucleic acids, and different sources of exosomes exhibit different modes of action in the stroke process. Neurogenic exosomes carry neurotrophic factors and precisely regulate inflammatory and apoptotic pathways to achieve neuronal repair and regeneration, while immunogenic exosomes play dual roles in early inflammatory amplification and late immune remodeling. In

addition, the specific molecular markers carried by exosomes are expected to overcome the traditional diagnostic limitations due to their high specificity and sensitivity, opening a new window for early and accurate diagnosis and dynamic monitoring of ischemic stroke. However, there are still many bottlenecks in current research: the isolation and purification technology needs to be innovated to meet the needs of clinical translation; the metabolism and molecular regulation mechanism of exosomes in the brain needs to be thoroughly analyzed; and the stability, targeting, and safety of exosomes as therapeutic carriers need to be verified in large-scale clinical trials.

Although exosomes have the potential to serve as biomarkers and therapeutic vehicles in the diagnosis and treatment of ischemic stroke, their clinical translation still faces challenges. These challenges include standardization, targeted delivery, and large-scale production. In order to transition from laboratory research to clinical application, multidisciplinary innovation and rigorous, evidence-based validation are necessary.

Data availability statement

The raw data supporting the conclusions of this article will be made available by the authors, without undue reservation.

Ethics statement

The studies involving humans were approved by the Second People's Hospital of Hunan Province (Brain Hospital of Hunan Province). The studies were conducted in accordance with the local legislation and institutional requirements. The ethics committee/institutional review board waived the requirement of written informed consent for participation from the participants or the participants' legal guardians/next of kin because this paper is a bibliometric study with no human samples. The requirement of ethical approval was waived by the Second People's Hospital of Hunan Province (Brain Hospital of Hunan Province) for the studies involving animals because no animal samples were used.

Author contributions

XD: Conceptualization, Data curation, Formal analysis, Investigation, Methodology, Software, Visualization, Writing – original draft, Writing – review & editing. GZ: Formal analysis, Investigation, Supervision, Validation, Writing – review & editing. NM: Conceptualization, Investigation, Software, Writing – original draft. XT: Data curation, Investigation, Methodology, Software, Writing – original draft. JZ: Conceptualization, Data curation, Methodology, Writing – original draft.

Funding

The author(s) declare that financial support was received for the research and/or publication of this article. This work was supported by the Hunan University of Chinese Medicine Joint University–Hospital Research Fund (grant number 2024YXLH240).

Conflict of interest

The authors declare that the research was conducted in the absence of any commercial or financial relationships that could be construed as a potential conflict of interest.

Generative AI statement

The authors declare that no Gen AI was used in the creation of this manuscript.

Publisher's note

References

1. Feske SK. Ischemic stroke. *Am J Med*. (2021) 134:1457–64. doi: 10.1016/j.amjmed.2021.07.027

2. Herpich F, Rincon F. Management of acute ischemic stroke. *Crit Care Med*. (2020) 48:1654–63. doi: 10.1097/CCM.0000000000004597

3. Lee EC, Ha TW, Lee DH, Hong DY, Park SW, Lee JY, et al. Utility of exosomes in ischemic and hemorrhagic stroke diagnosis and treatment. *Int J Mol Sci*. (2022) 23:8367. doi: 10.3390/ijms23158367

4. Chen N, Wang YL, Sun HF, Wang ZY, Zhang Q, Fan FY, et al. Potential regulatory effects of stem cell exosomes on inflammatory response in ischemic stroke treatment. *World J Stem Cells*. (2023) 15:561–75. doi: 10.4252/wjsc.v15.i6.561

5. Chen C, Song M. Visualizing a field of research: a methodology of systematic scientometric reviews. *PLoS One*. (2019) 14:e0223994. doi: 10.1371/journal.pone.0223994

6. Waseem A, Saudamini, Haque R, Janowski M, Raza SS. Mesenchymal stem cell-derived exosomes: shaping the next era of stroke treatment. *Neuroprotection*. (2023) 1:99–116. doi: 10.1002/nep3.30

7. Chen Y, Peng D, Li J, Zhang L, Chen J, Wang L, et al. A comparative study of different doses of bone marrow-derived mesenchymal stem cells improve post-stroke neurological outcomes via intravenous transplantation. *Brain Res*. (2023) 1798:148161. doi: 10.1016/j.brainres.2022.148161

8. Zhuo Y, Chen W, Li W, Huang Y, Duan D, Ge L, et al. Ischemic-hypoxic preconditioning enhances the mitochondrial function recovery of transplanted olfactory mucosa mesenchymal stem cells via miR-181a signaling in ischemic stroke. *Aging*. (2021) 13:11234–56. doi: 10.18632/aging.202807

9. Cunningham CJ, Wong R, Barrington J, Tamburrano S, Pinteaux E, Allan SM. Systemic conditioned medium treatment from interleukin-1 primed mesenchymal stem cells promotes recovery after stroke. *Stem Cell Res Ther*. (2020) 11:32. doi: 10.1186/s13287-020-1560-y

10. Watson JT, Foo T, Wu J, Moed BR, Thorpe M, Schon L, et al. CD271 as a marker for mesenchymal stem cells in bone marrow versus umbilical cord blood. *Cells Tissues Organs*. (2013) 197:496–504. doi: 10.1159/000348794

11. Zhu X, Badawi M, Pomeroy S, Sutaria DS, Xie Z, Baek A, et al. Comprehensive toxicity and immunogenicity studies reveal minimal effects in mice following sustained dosing of extracellular vesicles derived from HEK293T cells. *J Extracell Vesicles*. (2017) 6:1324730. doi: 10.1080/20013078.2017.1324730

12. Gowen A, Shahjin F, Chand S, Odegaard KE, Yelamanchili SV. Mesenchymal stem cell-derived extracellular vesicles: challenges in clinical applications. *Front Cell Dev Biol*. (2020) 8:149. doi: 10.3389/fcell.2020.00149

13. Huang M, Hong Z, Xiao C, Li L, Chen L, Cheng S, et al. Effects of exosomes on neurological function recovery for ischemic stroke in pre-clinical studies: a meta-analysis. *Front Cell Neurosci*. (2020) 14:593130. doi: 10.3389/fncel.2020.593130

14. Doeppner TR, Herz J, Görgens A, Schlechter J, Ludwig AK, Radtke S, et al. Extracellular vesicles improve post-stroke neuroregeneration and prevent postischemic immunosuppression. *Stem Cells Transl Med*. (2015) 4:1131–43. doi: 10.5966/sctm.2015-0078

15. Chen KH, Chen CH, Wallace CG, Yuen CM, Kao GS, Chen YL, et al. Intravenous administration of xenogenic adipose-derived mesenchymal stem cells (ADMSC) and ADMSC-derived exosomes markedly reduced brain infarct volume and preserved neurological function in rat after acute ischemic stroke. *Oncotarget*. (2016) 7:74537–56. doi: 10.18632/oncotarget.12902

16. Huang CW, Hsueh YY, Huang WC, Patel S, Li S. Multipotent vascular stem cells contribute to neurovascular regeneration of peripheral nerve. *Stem Cell Res Ther*. (2019) 10:234. doi: 10.1186/s13287-019-1317-7

17. Li R, Zhao K, Ruan Q, Meng C, Yin F. Bone marrow mesenchymal stem cell-derived exosomal microRNA-124-3p attenuates neurological damage in spinal cord ischemia-reperfusion injury by downregulating Ern1 and promoting M2 macrophage polarization. *Arthritis Res Ther*. (2020) 22:75. doi: 10.1186/s13075-020-2146-x

18. Webb RL, Kaiser EE, Scoville SL, Thompson TA, Fatima S, Pandya C, et al. Human neural stem cell extracellular vesicles improve tissue and functional recovery in the murine thromboembolic stroke model. *Transl Stroke Res*. (2018) 9:530–9. doi: 10.1007/s12975-017-0599-2

19. Pei X, Li Y, Zhu L, Zhou Z. Astrocyte-derived exosomes suppress autophagy and ameliorate neuronal damage in experimental ischemic stroke. *Exp Cell Res*. (2019) 382:111474. doi: 10.1016/j.yexcr.2019.06.019

20. Ma X, Liao X, Liu J, Wang Y, Wang X, Chen Y, et al. Circulating endothelial microvesicles and their carried miR-125a-5p: potential biomarkers for ischemic stroke. *Stroke Vasc Neurol*. (2023) 8:89–102. doi: 10.1136/svn-2021-001476

21. Zhou X, Xu C, Chao D, Chen Z, Li S, Shi M, et al. Acute cerebral ischemia increases a set of brain-specific miRNAs in serum small extracellular vesicles. *Front Mol Neurosci*. (2022) 15:874903. doi: 10.3389/fnmol.2022.874903

22. Pir GJ, Zahid MA, Akhtar N, Ayadathil R, Pananchikkal SV, Joseph S, et al. Differentially expressed miRNA profiles of serum derived extracellular vesicles from patients with acute ischemic stroke. *Brain Res*. (2024) 1845:149171. doi: 10.1016/j.brainres.2024.149171

23. Tsang EK, Abell NS, Li X, Anaya V, Karczewski KJ, Knowles DA, et al. Small RNA sequencing in cells and exosomes identifies eQTLs and 14q32 as a region of active export. *G3*. (2017) 7:31–9. doi: 10.1534/g3.116.036137

24. Yang J, Zhang X, Chen X, Wang L, Yang G. Exosome mediated delivery of miR-124 promotes neurogenesis after ischemia. *Mol Ther Nucleic Acids*. (2017) 7:278–87. doi: 10.1016/j.omtn.2017.04.010

25. Yang J, Cao LL, Wang XP, Guo W, Guo RB, Sun YQ, et al. Neuronal extracellular vesicle derived miR-98 prevents salvageable neurons from microglial phagocytosis in acute ischemic stroke. *Cell Death Dis*. (2021) 12:23. doi: 10.1038/s41419-020-03310-2

26. Shetgaonkar GG, Marques SM, DCruz CEM, Vibhavari RJA, Kumar L, Shirodkar RK. Exosomes as cell-derivative carriers in the diagnosis and treatment of central nervous system diseases. *Drug Deliv Transl Res*. (2022) 12:1047–79. doi: 10.1007/s13346-021-01026-0

27. Yousif G, Qadri S, Haik M, Haik Y, Parray AS, Shuaib A. Circulating exosomes of neuronal origin as potential early biomarkers for development of stroke. *Mol Diagn Ther*. (2021) 25:163–80. doi: 10.1007/s40291-020-00508-0

28. Xiao PP, Wan QQ, Liao T, Tu JY, Zhang GJ, Sun ZY. Peptide nucleic acid-functionalized nanochannel biosensor for the highly sensitive detection of tumor exosomal microRNA. *Anal Chem*. (2021) 93:10966–73. doi: 10.1021/acs.analchem.1c01898

29. Lee JU, Kim WH, Lee HS, Park KH, Sim SJ. Quantitative and specific detection of exosomal miRNAs for accurate diagnosis of breast cancer using a surface-enhanced Raman scattering sensor based on plasmonic head-flocked gold nanopillars. *Small*. (2019) 15:e1804968. doi: 10.1002/smll.201804968

30. Almujally H, Abuharfeil N, Sharaireh A. Novel exosomal miRNA expression in irradiated human keratinocytes. *Int J Mol Sci*. (2024) 25:12477. doi: 10.3390/ijms252212477

31. Zhang X, Sai B, Wang F, Wang L, Wang Y, Zheng L, et al. Hypoxic BMSC-derived exosomal miRNAs promote metastasis of lung cancer cells via STAT3-induced EMT. *Mol Cancer*. (2019) 18:40. doi: 10.1186/s12943-019-0959-5

32. Li Q, Li H, Liang J, Mei J, Cao Z, Zhang L, et al. Sertoli cell-derived exosomal microRNA-486-5p regulates differentiation of spermatogonial stem cell through PTEN in mice. *J Cell Mol Med*. (2021) 25:3950–62. doi: 10.1111/jcmm.16347

33. Xia X, Wang Y, Huang Y, Zhang H, Lu H, Zheng JC. Exosomal miRNAs in central nervous system diseases: biomarkers, pathological mediators, protective factors and therapeutic agents. *Prog Neurobiol*. (2019) 183:101694. doi: 10.1016/j.pneurobio.2019.101694

34. Gomes AR, Sangani NB, Fernandes TG, Diogo MM, Curfs LMG, Reutelingsperger CP. Extracellular vesicles in CNS developmental disorders. *Int J Mol Sci*. (2020) 21:9428. doi: 10.3390/ijms21249428

35. Huang Y, Liu Z, Li N, Tian C, Yang H, Huo Y, et al. Parkinson's disease derived exosomes aggravate neuropathology in SNCA*A53T mice. *Ann Neurol*. (2022) 92:230–45. doi: 10.1002/ana.26421

36. Wu Q, Yu L, Lin X, Zheng Q, Zhang S, Chen D, et al. Combination of serum miRNAs with serum exosomal miRNAs in early diagnosis for non-small-cell lung cancer. *Cancer Manag Res*. (2020) 12:485–95. doi: 10.2147/CMAR.S232383

37. Shi Y, Zhuang Y, Zhang J, Chen M, Wu S. Four circulating exosomal miRNAs as novel potential biomarkers for the early diagnosis of human colorectal cancer. *Tissue Cell*. (2021) 70:101499. doi: 10.1016/j.tice.2021.101499

38. Wang C, Wang J, Cui W, Liu Y, Zhou H, Wang Y, et al. Serum exosomal miRNA-1226 as potential biomarker of pancreatic ductal adenocarcinoma. *Onco Targets Ther*. (2021) 14:1441–51. doi: 10.2147/OTT.S296816

39. Hwang S, Yang YM. Exosomal microRNAs as diagnostic and therapeutic biomarkers in non-malignant liver diseases. *Arch Pharm Res*. (2021) 44:574–87. doi: 10.1007/s12272-021-01338-2

40. Chen Y, Song Y, Huang J, Qu M, Zhang Y, Geng J, et al. Increased circulating exosomal miRNA-223 is associated with acute ischemic stroke. *Front Neurol*. (2017) 8:57. doi: 10.3389/fneur.2017.00057

41. Bang OY, Kim EH, Oh MJ, Yoo J, Oh GS, Chung JW, et al. Circulating extracellular-vesicle-incorporated microRNAs as potential biomarkers for ischemic stroke in patients with cancer. *J Stroke*. (2023) 25:251–65. doi: 10.5853/jos.2022.02327

42. Tan PPS, Hall D, Chilian WM, Chia YC, Mohd Zain S, Lim HM, et al. Exosomal microRNAs in the development of essential hypertension and its potential as biomarkers. *Am J Physiol Heart Circ Physiol*. (2021) 320:H1486–97. doi: 10.1152/ajpheart.00888.2020

43. Wang L, Zhang L. Circulating exosomal miRNA as diagnostic biomarkers of neurodegenerative diseases. *Front Mol Neurosci*. (2020) 13:53. doi: 10.3389/fnmol.2020.00053

44. Gonçalves RA, De Felice FG. The crosstalk between brain and periphery: implications for brain health and disease. *Neuropharmacology*. (2021) 197:108728. doi: 10.1016/j.neuropharm.2021.108728

45. Kang JY, Park H, Kim H, Mun D, Park H, Yun N, et al. Human peripheral blood-derived exosomes for microRNA delivery. *Int J Mol Med*. (2019) 43:2319–28. doi: 10.3892/ijmm.2019.4150

46. Pegtel DM, Peferoen L, Amor S. Extracellular vesicles as modulators of cell-to-cell communication in the healthy and diseased brain. *Philos Trans R Soc B*. (2014) 369:20130516. doi: 10.1098/rstb.2013.0516

47. Czernek L, Düchler M. Functions of cancer-derived extracellular vesicles in immunosuppression. *Arch Immunol Ther Exp*. (2017) 65:311–23. doi: 10.1007/s00005-016-0453-3

48. Yu Y, Hou K, Ji T, Wang X, Liu Y, Zheng Y, et al. The role of exosomal microRNAs in central nervous system diseases. *Mol Cell Biochem*. (2021) 476:2111–24. doi: 10.1007/s11010-021-04053-0

49. Wang ZY, Wen ZJ, Xu HM, Zhang Y, Zhang YF. Exosomal noncoding RNAs in central nervous system diseases: biological functions and potential clinical applications. *Front Mol Neurosci*. (2022) 15:1004221. doi: 10.3389/fnmol.2022.1004221

50. Fan Y, Chen M, Zhang J, Maincent P, Xia X, Wu W. Updated progress of nanocarrier-based intranasal drug delivery systems for treatment of brain diseases. *Crit Rev Ther Drug Carrier Syst*. (2018) 35:433–67. doi: 10.1615/CritRevTherDrugCarrierSyst.2018024697

51. Li J, Peng H, Zhang W, Li M, Wang N, Peng C, et al. Enhanced nose-to-brain delivery of combined small interfering RNAs using lesion-recognizing nanoparticles for the synergistic therapy of Alzheimer's disease. *ACS Appl Mater Interfaces*. (2023) 15:53177–88. doi: 10.1021/acsami.3c08756

52. Sarkar SN, Corbin D, Simpkins JW. Brain-wide transgene expression in mice by systemic injection of genetically engineered exosomes: CAP-exosomes. *Pharmaceuticals*. (2024) 17:270. doi: 10.3390/ph17030270

53. Khan SU, Khan MI, Khan MU, Khan NM, Bungau S, Hassan SSU. Applications of extracellular vesicles in nervous system disorders: an overview of recent advances. *Bioengineering*. (2022) 10:51. doi: 10.3390/bioengineering10010051

54. He T, Yang GY, Zhang Z. Crosstalk of astrocytes and other cells during ischemic stroke. *Life*. (2022) 12:910. doi: 10.3390/life12060910

55. Zhu T, Wang L, Xie W, Meng X, Feng Y, Sun G, et al. Notoginsenoside R1 improves cerebral ischemia/reperfusion injury by promoting neurogenesis via the BDNF/Akt/CREB pathway. *Front Pharmacol*. (2021) 12:615998. doi: 10.3389/fphar.2021.615998

56. Kang L, Yu H, Yang X, Zhu Y, Bai X, Wang R, et al. Neutrophil extracellular traps released by neutrophils impair revascularization and vascular remodeling after stroke. *Nat Commun*. (2020) 11:2488. doi: 10.1038/s41467-020-16191-y

57. Wang J, Chen S, Zhang W, Chen Y, Bihl JC. Exosomes from miRNA-126-modified endothelial progenitor cells alleviate brain injury and promote functional recovery after stroke. *CNS Neurosci Ther*. (2020) 26:1255–65. doi: 10.1111/cns.13455

58. Ma C, Wang J, Liu H, Chen Y, Ma X, Chen S, et al. Moderate exercise enhances endothelial progenitor cell exosomes release and function. *Med Sci Sports Exerc*. (2018) 50:2024–32. doi: 10.1249/MSS.0000000000001672

59. Pan Q, Zheng J, Du D, Liao X, Ma C, Yang Y, et al. MicroRNA-126 priming enhances functions of endothelial progenitor cells under physiological and hypoxic conditions and their therapeutic efficacy in cerebral ischemic damage. *Stem Cells Int*. (2018) 2018:2912347. doi: 10.1155/2018/2912347

60. Yang Y, Cai Y, Zhang Y, Liu J, Xu Z. Exosomes secreted by adipose-derived stem cells contribute to angiogenesis of brain microvascular endothelial cells following oxygen-glucose deprivation *in vitro* through microRNA-181b/TRPM7 axis. *J Mol Neurosci*. (2018) 65:74–83. doi: 10.1007/s12031-018-1071-9

61. Xu B, Zhang Y, Du XF, Li J, Zi HX, Bu JW, et al. Neurons secrete miR-132-containing exosomes to regulate brain vascular integrity. *Cell Res*. (2017) 27:882–97. doi: 10.1038/cr.2017.62

62. Deng SL, Fu Q, Liu Q, Huang FJ, Zhang M, Zhou X. Modulating endothelial cell dynamics in fat grafting: the impact of DLL4 siRNA via adipose stem cell extracellular vesicles. *Am J Physiol Cell Physiol*. (2024) 327:C929–45. doi: 10.1152/ajpcell.00186.2024

63. Yang J, Wang B, Wang Y, Feng C, Chen L, Liu Y, et al. Exosomes derived from adipose mesenchymal stem cells carrying miRNA-22-3p promote Schwann cells proliferation and migration through downregulation of PTEN. *Dis Markers*. (2022) 2022:7071877. doi: 10.1155/2022/7071877

64. Liu YP, Yang YD, Mou FF, Zhu J, Li H, Zhao TT, et al. Exosome-mediated miR-21 was involved in the promotion of structural and functional recovery effect produced by electroacupuncture in sciatic nerve injury. *Oxid Med Cell Longev*. (2022) 2022:7530102. doi: 10.1155/2022/7530102

65. Ji Q, Ji Y, Peng J, Zhou X, Chen X, Zhao H, et al. Increased brain-specific MiR-9 and MiR-124 in the serum exosomes of acute ischemic stroke patients. *PLoS One*. (2016) 11:e0163645. doi: 10.1371/journal.pone.0163645

66. Yang Y, Ye Y, Kong C, Su X, Zhang X, Bai W, et al. MiR-124 enriched exosomes promoted the M2 polarization of microglia and enhanced Hippocampus neurogenesis after traumatic brain injury by inhibiting TLR4 pathway. *Neurochem Res*. (2019) 44:811–28. doi: 10.1007/s11064-018-02714-z

67. Xin H, Li Y, Buller B, Katakowski M, Zhang Y, Wang X, et al. Exosome-mediated transfer of miR-133b from multipotent mesenchymal stromal cells to neural cells contributes to neurite outgrowth. *Stem Cells*. (2012) 30:1556–64. doi: 10.1002/stem.1129

68. Xin H, Wang F, Li Y, Lu QE, Cheung WL, Zhang Y, et al. Secondary release of exosomes from astrocytes contributes to the increase in neural plasticity and improvement of functional recovery after stroke in rats treated with exosomes harvested from microRNA 133b-overexpressing multipotent mesenchymal stromal cells. *Cell Transplant*. (2017) 26:243–57. doi: 10.3727/096368916X693031

69. Wu W, Liu J, Yang C, Xu Z, Huang J, Lin J. Astrocyte-derived exosome-transported microRNA-34c is neuroprotective against cerebral ischemia/reperfusion injury via TLR7 and the NF-κB/MAPK pathways. *Brain Res Bull*. (2020) 163:84–94. doi: 10.1016/j.brainresbull.2020.07.013

70. Zhao Y, Gan Y, Xu G, Yin G, Liu D. MSCs-derived exosomes attenuate acute brain injury and inhibit microglial inflammation by reversing CysLT2R-ERK1/2 mediated microglia M1 polarization. *Neurochem Res*. (2020) 45:1180–90. doi: 10.1007/s11064-020-02998-0

71. Lu W, Si YI, Ding J, Chen X, Zhang X, Dong Z, et al. Mesenchymal stem cells attenuate acute ischemia-reperfusion injury in a rat model. *Exp Ther Med*. (2015) 10:2131–7. doi: 10.3892/etm.2015.2806

72. Jiang M, Wang H, Jin M, Yang X, Ji H, Jiang Y, et al. Exosomes from MiR-30d-5p-ADSCs reverse acute ischemic stroke-induced, autophagy-mediated brain injury by promoting M2 microglial/macrophage polarization. *Cell Physiol Biochem*. (2018) 47:864–78. doi: 10.1159/000490078

73. Haupt M, Zheng X, Kuang Y, Lieschke S, Janssen L, Bosche B, et al. Lithium modulates miR-1906 levels of mesenchymal stem cell-derived extracellular vesicles contributing to poststroke neuroprotection by toll-like receptor 4 regulation. *Stem Cells Transl Med*. (2021) 10:357–73. doi: 10.1002/sctm.20-0086

74. Wang Y, Liu Z, Li L, Zhang Z, Zhang K, Chu M, et al. Anti-ferroptosis exosomes engineered for targeting M2 microglia to improve neurological function in ischemic stroke. *J Nanobiotechnology*. (2024) 22:291. doi: 10.1186/s12951-024-02560-y

75. Liu X, Zhang M, Liu H, Zhu R, He H, Zhou Y, et al. Bone marrow mesenchymal stem cell-derived exosomes attenuate cerebral ischemia-reperfusion injury-induced neuroinflammation and pyroptosis by modulating microglia M1/M2 phenotypes. *Exp Neurol*. (2021) 341:113700. doi: 10.1016/j.expneurol.2021.113700

76. Deng J, Zhang T, Li M, Cao G, Wei H, Zhang Z, et al. Irisin-pretreated BMMSCs secrete exosomes to alleviate cardiomyocytes pyroptosis and oxidative stress to hypoxia/reoxygenation injury. *Curr Stem Cell Res Ther*. (2023) 18:843–52. doi: 10.2174/1574888X18666221117111829

77. Aghadavod E, Zarghami N, Farzadi L, Zare M, Barzegari A, Movassaghpour AA, et al. Isolation of granulosa cells from follicular fluid; applications in biomedical and molecular biology experiments. *Adv Biomed Res*. (2015) 4:250. doi: 10.4103/2277-9175.170675

78. Jønsson AB, Krogh S, Laursen HS, Aagaard P, Kasch H, Nielsen JF. Safety and efficacy of blood flow restriction exercise in individuals with neurological disorders: a systematic review. *Scand J Med Sci Sports*. (2024) 34:e14561. doi: 10.1111/sms.14561

79. Lian J, Wang J, Li X, Yang S, Li H, Zhong Y, et al. Different dosage regimens of tanezumab for the treatment of chronic low back pain: a meta-analysis of randomized controlled trials. *Clin Neuropharmacol*. (2023) 46:6–16. doi: 10.1097/WNF.0000000000000530

Frontiers in Neurology

Explores neurological illness to improve patient care

The third most-cited clinical neurology journal explores the diagnosis, causes, treatment, and public health aspects of neurological illnesses. Its ultimate aim is to inform improvements in patient care.

Discover the latest Research Topics

See more →

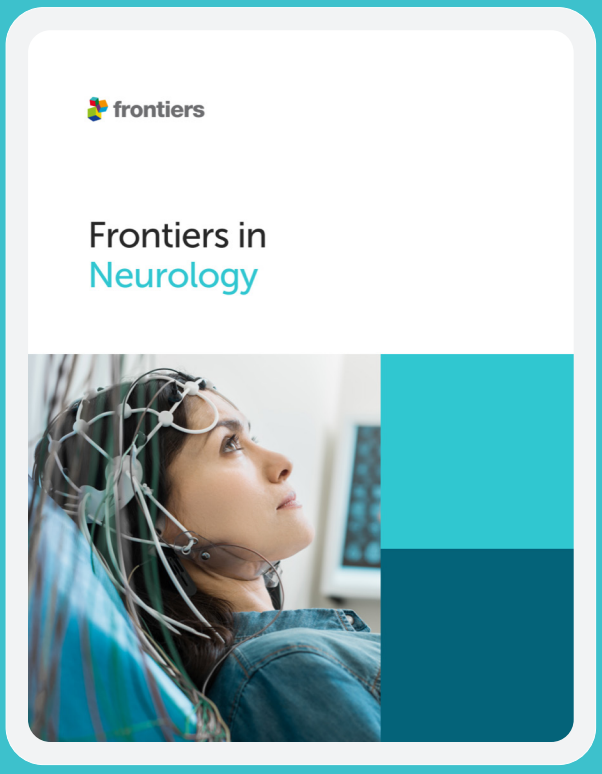

Frontiers

Avenue du Tribunal-Fédéral 34
1005 Lausanne, Switzerland
frontiersin.org

Contact us

+41 (0)21 510 17 00
frontiersin.org/about/contact